THE HIP JOINT CAPSULE

MECHANICAL PROPERTIES AND CONTRIBUTION TO JOINT STABILITY IN TOTAL HIP REPLACEMENT

By

Dimitrios P. APATSIDIS

MEng, MSc

This thesis is submitted in accordance with the regulations governing the award of the degree of Doctor of Philosophy in Bioengineering

Bioengineering Unit

University of Strathclyde

Glasgow

United Kingdom

October 2002

I would like to dedicate this thesis to my beloved parents for enabling me accomplish all my dreams. You have always been my driving force and source of empowerment. Thank you.

Θα ήθελα να αφιερώσω τη διδακτορική διατριβή μου στους αγαπητούς μου γονείς, στους οποίους οφείλω την εκπλήρωση όλων των ονείρων μου. Είσαστε η κινητήρια δύναμή μου και πηγή της απόδοσής μου.
Σας ευχαριστώ.

ACKNOWLEDGEMENTS

First of all I would like to thank my supervisor Prof. Sandy Nicol for all the guidance throughout this project and for his unique way of making me give my best. Thank you Sandy for introducing me to the fascinating world of Orthopaedic Biomechanics. Working with you has opened many doors for me, I will always appreciate this.

My sincere words of appreciation also go to Prof. Barbenel without whom I would never have had the opportunity to experience the Bioengineering Unit. Thank you for your trust in me and for the excellent advise and mentoring you always gave me. Having been your student fills me with pride. I shall always honour your kind friendship.

I would like to acknowledge the generous financial support that was provided by DePuy International Ltd, Leeds, UK. In particular, my thanks go to Ian Revie for entrusting me with this prestigious project and to Stefano Alfonsi for facilitating many and very fruitful meetings with other biomechanics researchers.

I am deeply indebted to the people of the Biomechanics Group at the Technical University in Hamburg-Harburg, Germany. In particular I wish to thank Prof. Michael Morlock for making his lab available, but also Kay Selenschloh and Thomas Kruppa for their help with the experiments and for creating such an amazing atmosphere in the lab.

I am grateful to Dr. John Shaw-Dunn from the Human Anatomy Department of Glasgow University, for his unlimited help in familiarising me with the human hip joint. Many thanks also to my friend Davie Robb, who again succeeded in defeating time restraints and building the test rig in a very short time without sacrificing quality.

I would like to thank Prof. Paul for taking time to comment on my thesis and for briefing me into the process of defending my research findings effectively.

My penultimate words are to all my friends in the Bioengineering Unit and in Glasgow generally. I enjoyed some memorable occasions in your pleasant company.

My final words go to my fiancé Mekala, who is the most valuable 'item' I am taking away from the Bioengineering Unit. Everything I have experienced during the last years has been so much nicer because of your presence.

ABSTRACT

The hip joint capsule is a complex soft tissue structure that comprises a number of ligaments with different thickness and strength respectively, as well as a thinner membrane-like part that provides the structural integrity for the capsule. The role of the capsule is twofold, forming a closed environment around the joint surfaces, in which the synovial fluids are retained, but also providing a passive joint resistance that acts in addition to the surrounding muscles and mainly in extreme limb positions and in unexpected limb loading. Despite its important role, the capsule is commonly removed in Total Hip Replacement (THR), either fully or partially, to clear the view to the joint.

The little existing knowledge on the mechanical properties of the capsule and its performance *in situ* during various walking activities makes it difficult to argue for its preservation and repair following THR, especially due to the additional efforts that this brings along for the surgical team. This project is an attempt to provide this required information and to highlight any changes in joint resistance that occur as a result of a complete or partial removal of the hip joint capsule.

A cadaveric approach was used at first, in which complete human hip joints with intact capsules were tested. A sequential removal of the capsular ligaments was carried out, in order to reveal the total contribution to joint resistive moments of the individual ligaments. Anterior ligaments were distinguished from posterior ones and the tests were carried out in those limb positions in which the joint would be least stable under absence of the respective ligaments. Partial damage of the posterior aspects of the capsule showed increased risk for posterior joint dislocation when the limb was in flexion and internal rotation compared to the effects of an anteriorly damaged capsule.

A 3-D computer model of the hip joint with its capsular ligaments was created, in order to confirm the findings from the cadaveric study, but also for the purpose of simulating effects in post-operative anatomies. Different methods of creating the geometric model were attempted and it was achieved to create a model that would be used to simulate the resistive moments produced by the individual ligaments. For simplicity, the ligament action was simulated by linear spring elements. The findings of the cadaveric experiments could not be reproduced, because of the way the ligament forces were modelled, which does not consider the viscoelastic properties of soft biological tissues. However, it was still possible to draw valuable conclusions on the effect that various prosthetic component attributes have on the total joint moments. Recommendations were made for the optimal approach to the capsule in THR.

CONTENTS

Chapter 1- Aims and Objectives

1.1 Introduction

Altius, citius, fortius or swifter, higher, stronger. The motto of the Olympic games states what in modern times is a statement of life. The so-called high performance society in which we are living demands highest performance from everyone for a long period of time. However, the human body has a set expiry date, beyond which certain functions can no longer be performed satisfactorily. Reduced performance, loss of life quality and pain are the consequence. The hip joint and its diseases that lead to the termination of its function are one such example. Since Professor Sir John Charnley performed the first hip resurfacing operations in the early 1950's, many things have changed in Total Hip Replacement (THR) surgery. Designs have evolved, materials selection is much more sophisticated and also surgical techniques have seen various modifications, depending on the individual surgeon's preferences. The presently available prostheses show in general good survival rates, with the Charnley type presenting up to 97.2% survivorship at 30 years after implantation (Wroblewski et al, 1999). Does this mean that hip implants have reached complete maturity and can provide a guarantee for excellent performance forever? Is there no room for further improvement and development? The answer to this is of course no. The majority of the available designs were developed having one target in mind, namely the relief of pain. Since this could be provided in the above mentioned reliable manner, the next demand from a prosthetic device appeared to be the minimisation of restrictions in daily activities. This request came about mainly by the younger patient group aged between 20 and 55 years that required THR. In these groups the demand for a better life quality despite a prosthetic hip, led to further development of new designs that would be able to handle increased loads at their interface with the biological host environment and at their articulating surfaces. Higher and more intense loading would usually lead to reduced survival rates, which for younger patients would mean one or more revision operations (Goldsmith et al, 2001) within their lifetime. Bone stock preservation during the primary THR for this patient group is therefore essential, to enable the surgeon to fit an implant in the

remaining part of the femur in the revision surgery. Thus, frequently surgeons prefer smaller prostheses for use in younger patients very often combined with small femoral head component sizes. However, stability of the artificial joint is affected by the femoral head component size and tends to result in less stable assemblies as the size reduces. It is therefore of extreme importance to consider a good balance between the components' size and other stabilising structures that are around the hip joint.

One of these structures is the hip joint capsule, which surrounds the joint surfaces much like a protective sleeve that also forms an enclosed volume for the synovial fluids. Despite its apparent importance, the hip joint capsule is very commonly sacrificed in THR surgery for the benefit of an improved accessibility to the diseased joint surfaces. There are no studies, though, that could assist in determining the role of the capsule and studying its relevance in stabilising the hip joint.

1.2 Aims and Objectives

It is the aim of the present study to investigate the material properties and the mechanics of the capsule and its role in stabilising the hip joint in the healthy anatomy and in the replaced hip joint. A computational model is employed in order to make it possible to study different situations- mainly of post-operative anatomy- that could prove critical. Further, it is the aim to develop a 3-D computer model and to validate it against the cadaver models. A cadaver study of anatomically intact human hip joints is of assistance in the efforts undertaken to characterise the mechanical properties of the capsule. Conclusions are reached on the role of the capsule and on the effects of its absence in a replaced hip joint, in relation to prosthetic component sizes. Possible future applications of the computer model are discussed that will help to further improve the understanding of the hip joint capsule.

1.3 Thesis Outline

Chapter 2 of this thesis gives a review of how much work has been done in the past regarding the hip joint capsule both by means of histological and anatomical work, but also in relation to is role and function within the human body. Also presented are other factors relating to hip joint stability after THR and a summary on how these factors correlate.

Chapter 3 outlines various approaches that were investigated for the characterisation of the materials properties of the capsular tissues. The devices that were considered are reviewed and explanations are given as to why they were rejected. Finally, the test set-up of choice is presented and the design and manufacture of the required equipment is illustrated.

Chapter 4 describes tests that were done on cadaveric human hip joint specimens including the hip joint capsule. The capsule's mechanical behaviour during human locomotion and in extreme limb positions is presented, both for intact joints and for joints with damaged capsular ligaments as they would result from cuts during THR surgery.

Chapter 5 deals with the details and techniques that needed to be considered in the development of the three-dimensional (3-D) computer model of the hip joint and its capsule. The different visualisation modalities that were employed are explained and all file format types that were necessary for the further utilisation of the model are explained.

Chapter 6 contains all numerical analysis work that was done on the computer model of the hip joint. Thereby, a special Finite Element Analysis (FEA) software was used. The numerical approach includes studies of the effect of prosthetic component sizes on stability and on the role of the individual capsular ligaments.

The overall conclusions from the present study are summarised in chapter 7 and indications for necessary further work are given.

Chapter 2- Background and Literature Review

2.1 Anatomy of the Hip Joint Capsule

The hip joint is a ball and socket joint lying deep under several layers of soft tissues, including skin, fat, connective tissues and various muscles. It is mainly these muscles that contribute to the stabilisation of the joint by acting through the joint interface compressing the two bones of the joint thereby holding them firmly together. Figures 2.1 and 2.2 show the two main parts of the hip joint, namely the pelvis and the femur.

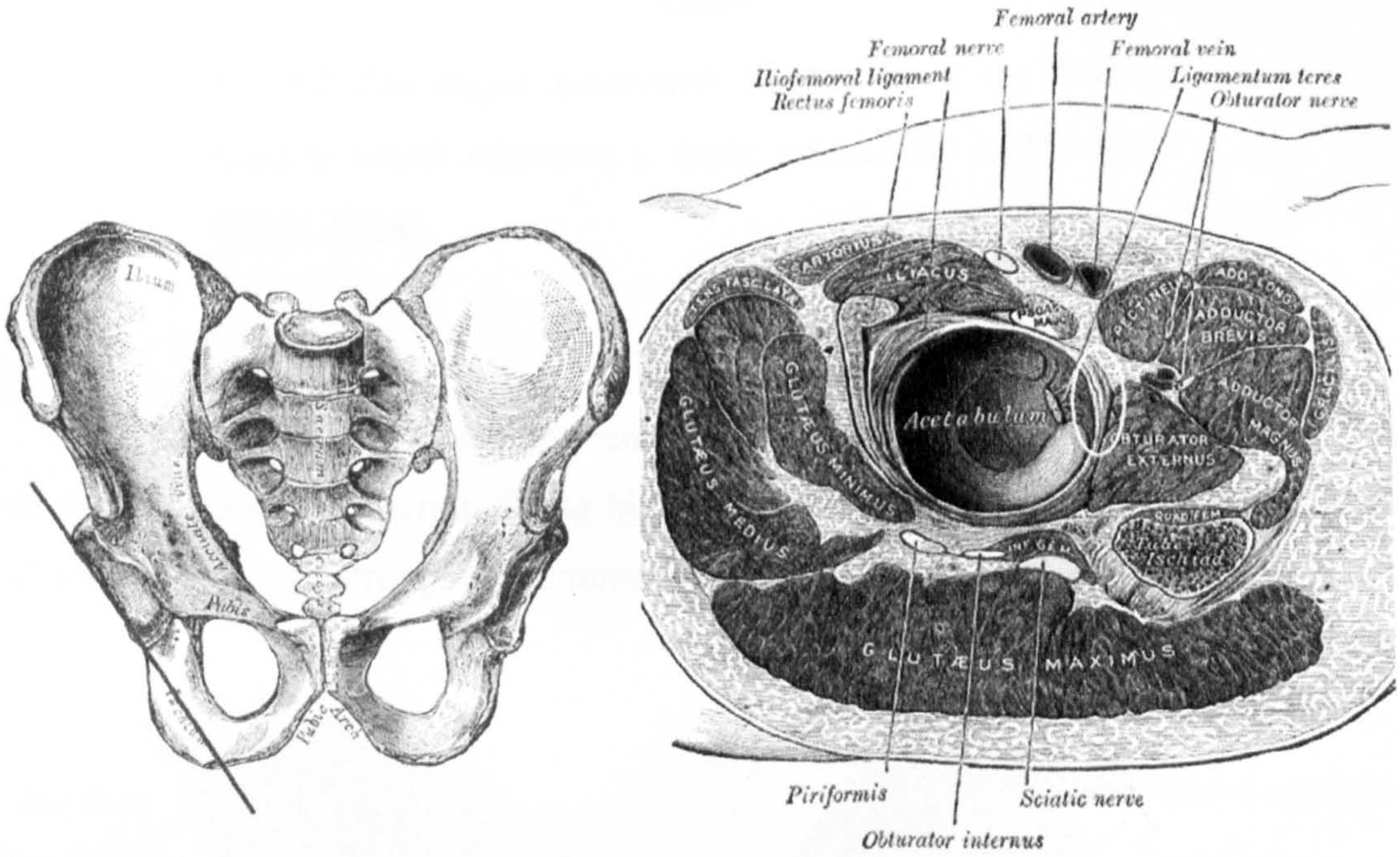

Fig 2.1 Anterior aspect of the complete pelvic bone and section through the acetabular level of the hip joint with the femur reflected (Gray, 1918).

An interesting aspect of the acetabulum is the semi-lunar cartilage, against which the femoral head is sliding during gait. The red line in figure 2.1 shows the orientation of the section plane that is illustrated on the right part of figure 2.1. The ligamentum teres originates in the femoral head and connects to the acetabular notch, blending in with the transverse ligament (yellow ellipse in figure 2.1).

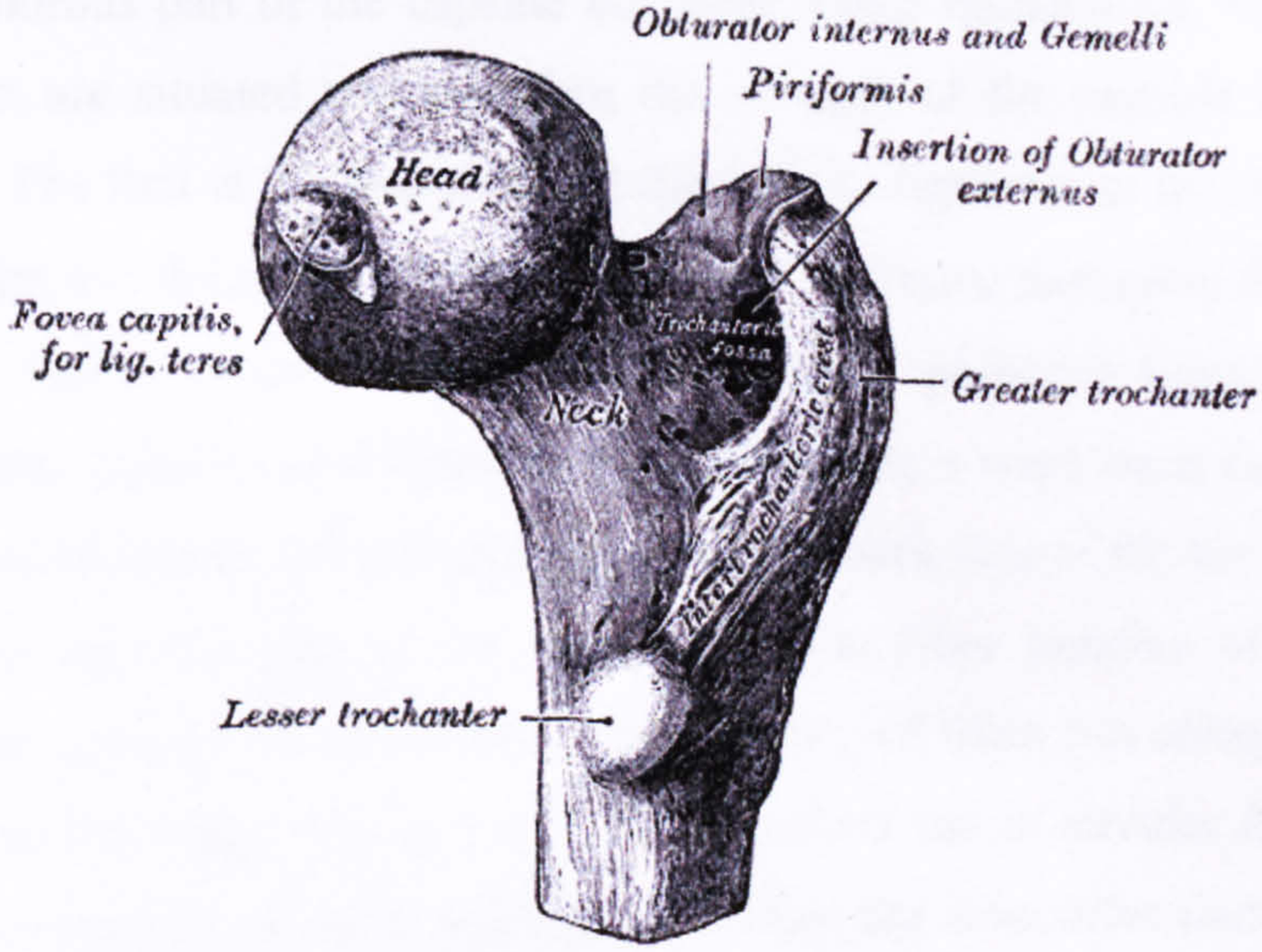

Fig 2.2 The major anatomical landmarks of the femoral bone to which reference is made extensively in this thesis (Gray, 1918).

The capsule might also be seen as the connecting link between the pelvic and the femoral bones. It surrounds the hip joint generally like a protective sleeve from all sides and is very strong in its anterior aspect.

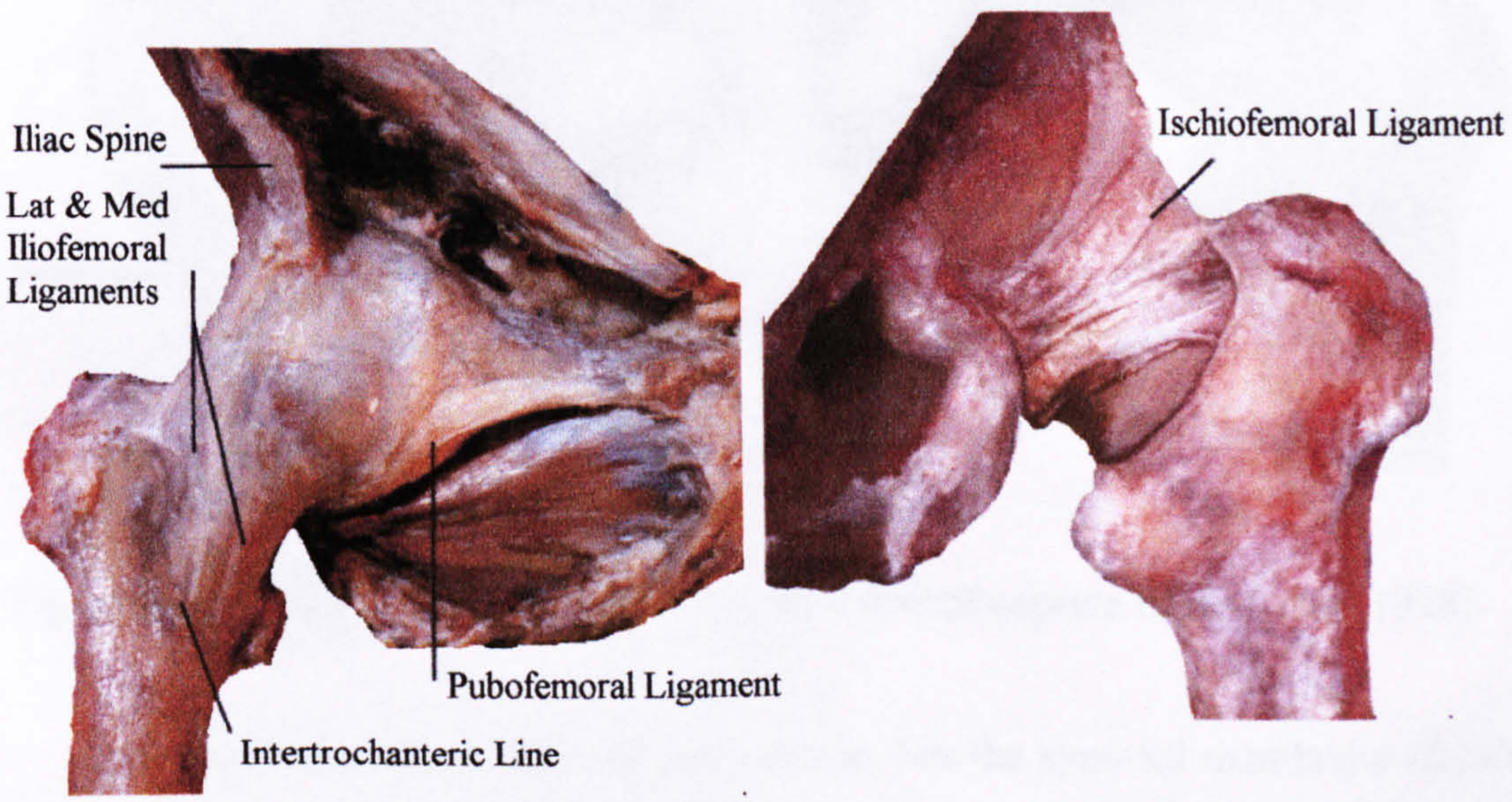

Fig 2.3 Ligaments of the hip joint capsule at the anterior and posterior aspects.

The fibrous part of the capsule has three major thickenings, which is where the ligaments are situated and therefore the strength of the capsule is the highest (figure 2.3). The first is the two-stranded iliofemoral ligament at the anterior aspect of the hip joint and the second is the pubofemoral ligament that spans from the pubic bone to the region of the lesser trochanter. On the posterior aspect of the joint capsule lies the ischiofemoral ligament that is basically a weak band that arises from the ischium at the acetabular rim and surrounds the back side of the femoral neck and inserts at the superior part of the trochanter. The fibre bundles of the capsular ligaments run in two main directions. The majority of them run obliquely from the acetabulum to the femur (figure 2.4), whereas others run in circular fashion almost parallel to the margins of the acetabulum and form the zona orbicularis (figure 2.5). It has been stated that the direction of fibres relates directly to loads they are subjected to (Ralphs and Benjamin, 1994). To judge by the shape and fibre orientation of the zona, it can be stated that its role comprises preventing twisting of the capsule and also strengthening the synovial membrane's boundaries.

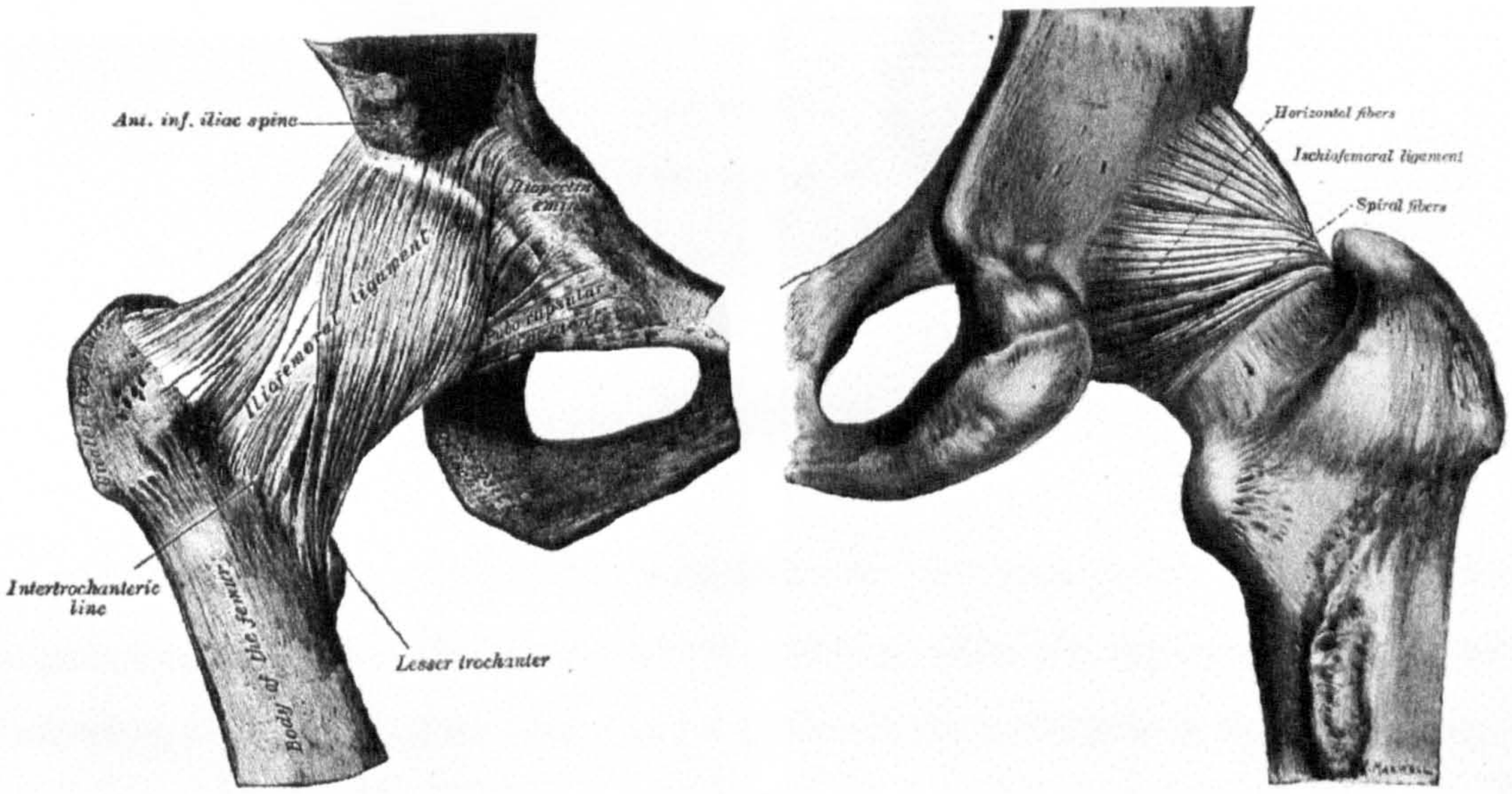

Figure 2.4 Anterior (left) and posterior (right) views of capsule fibres (Gray, 1918).

Beneath the strong fibres of the capsule, lies the synovial membrane (figure 2.5), which forms the inner lining of the capsule, into which the ligaments are embedded in a kind of mesh. The synovial membrane ensures that the synovial fluids

are retained within it, providing sufficient lubrication for the cartilaginous joint surfaces. Frequently, the synovial membrane is referred to as the capsule, separating it from the ligaments of the hip joint. However, since the synovial membrane and the hip joint ligaments are blended into each other, it has become more common that researchers refer to the complete construct of membrane and ligaments as the capsule (Zuckermann, 1963).

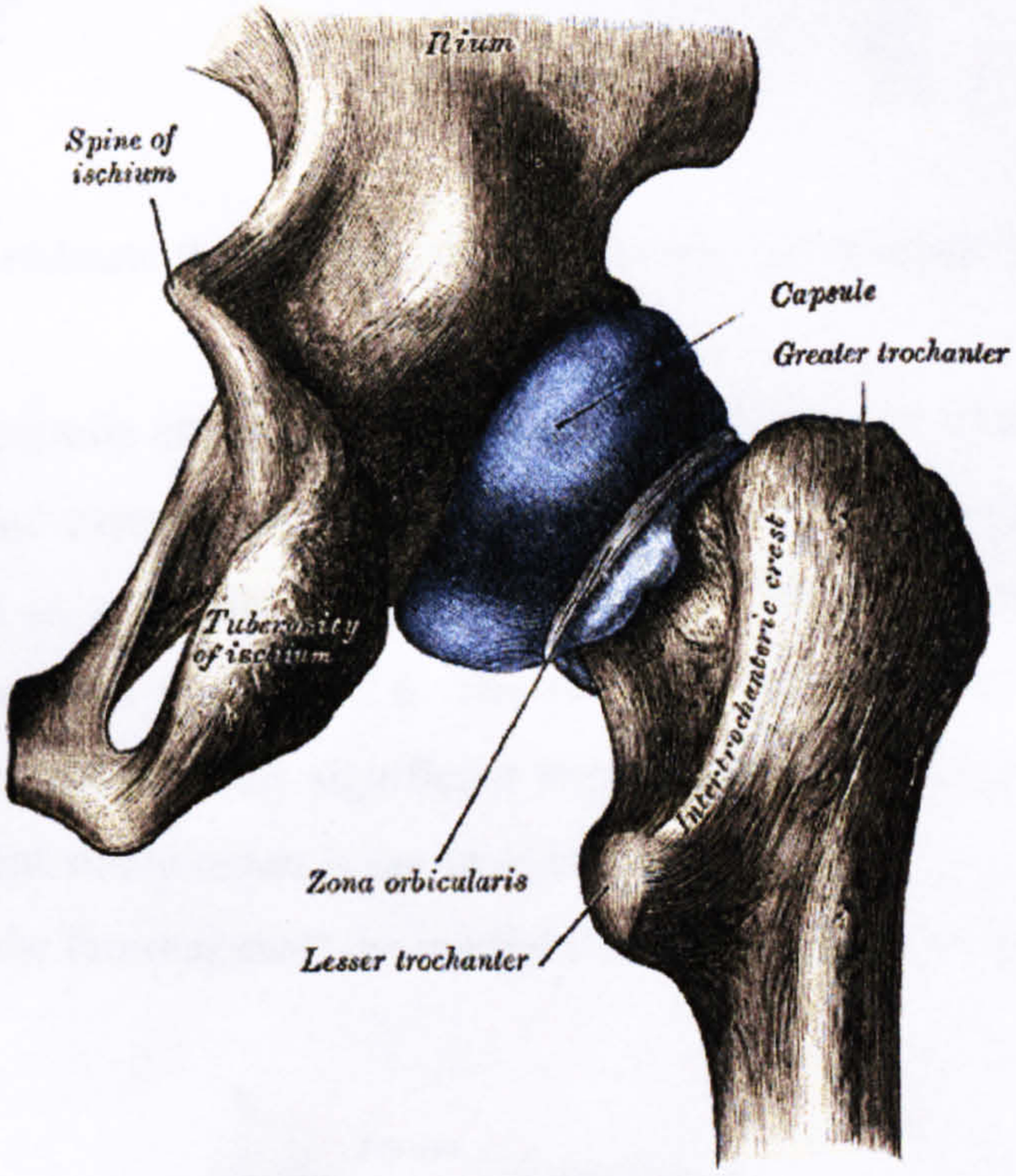

Fig 2.5 The posterior synovial membrane (Gray, 1918).

The synovial membrane originates at the semi-lunar surface of the acetabulum and passes the acetabular rim, running under the capsular ligaments and extending to the neck of the femur as far as the cartilage margins of the femoral head (Romanes, 1977). The synovial membrane also encloses the ligamentum teres femoris.

It has already been mentioned that proximally, the individual capsular ligaments originate along the acetabular rim, but in what concerns their insertion into the femur things are a little more complex.

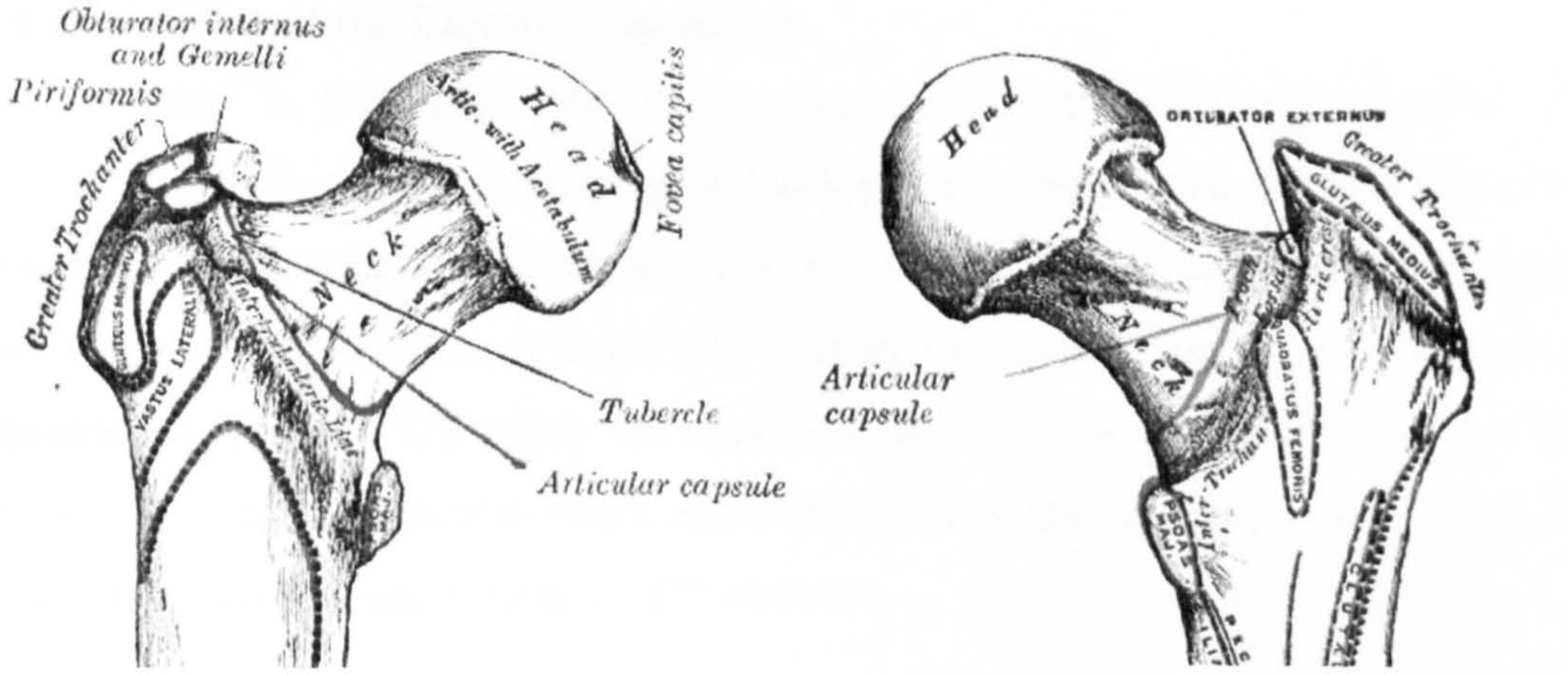

Figure 2.6 Blue lines indicate the margins of femoral capsular insertion (Gray, 1918).

Distally, the capsule attaches to the femur along the intertrochanteric line at the anterior aspect and extends not quite as far as the intertrochanteric crest at the posterior aspect and is generally weak (Zuckermann, 1963). The insertions are highlighted with blue lines in figure 2.6. The red lines indicate insertion areas of muscles, but that does not bear any significant importance within this project, as the role of muscles in joint stabilisation is not investigated in this work. It is noteworthy how far down along the femoral shaft the medial iliofemoral ligament extends (figure 2.7).

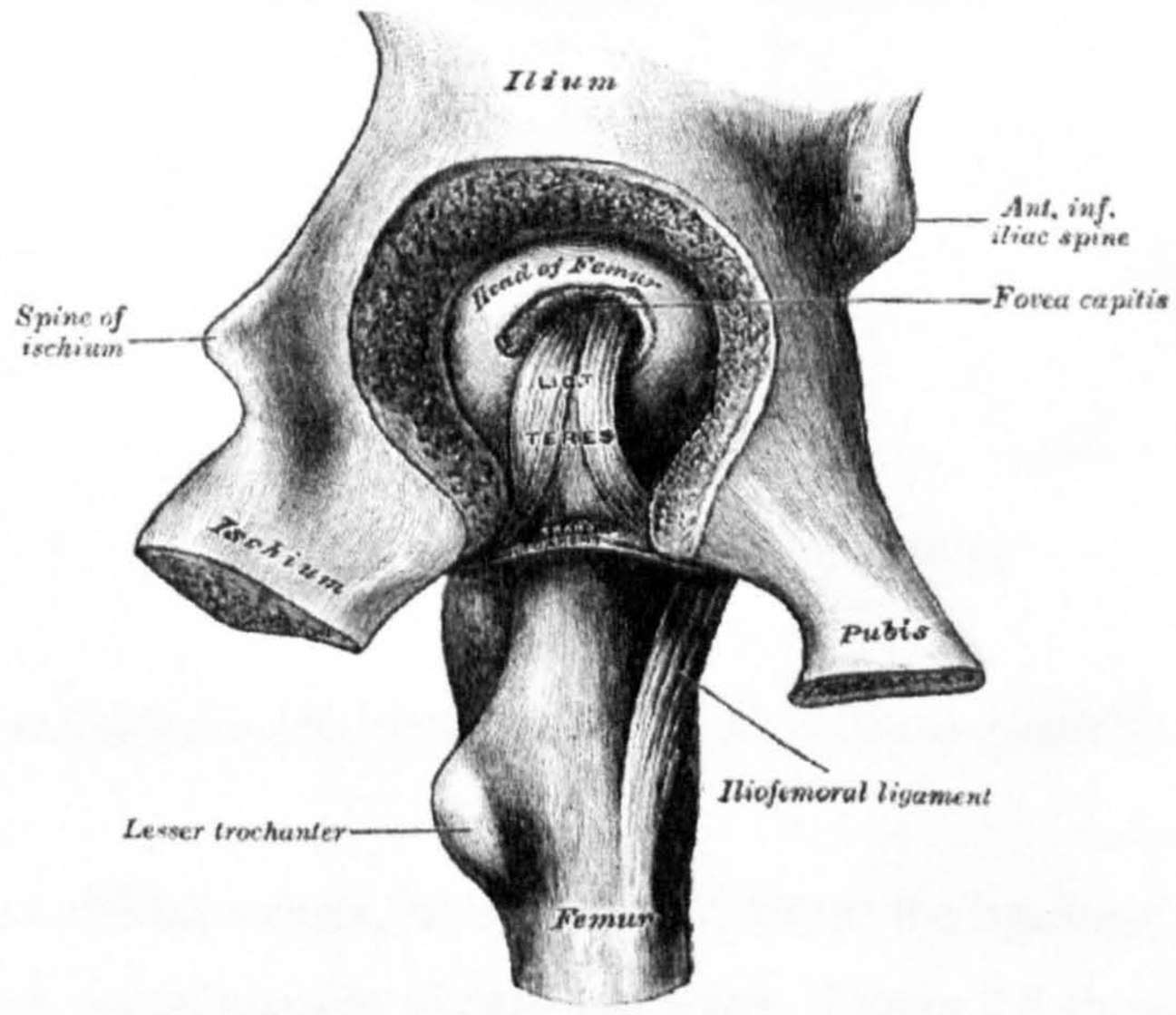

Fig 2.7 Removed acetabular floor viewed from inside (Gray, 1918).

2.2 Composition of the Capsule Ligaments

'Ligare' is the Latin word for connecting, which is the main purpose of ligaments. They connect the two bones of articulating joints and ensure that they stay connected, maintaining in this way the joint's stability. Further, ligaments guide joint movement and therefore play a major role in extremely mobile joints i.e. those with a wide range of motion. Therefore, the expected characteristics of ligaments are high deformability, but also great strength and fast and complete recovery to their original shape. These requirements apply to all ligaments.

2.2.1 Cellular and Extra-Cellular Histology

Ligament composition can be divided into cellular and extra-cellular components (Binkley, 1989). The cellular component includes fibroblasts, macrophages and plasma. Fibroblasts are in charge of regulating the extra-cellular environment based on the external stimuli. They produce collagen and ensure it is replaced in case of microscopic damage. Therefore, despite their small numbers fibroblasts play an important role for ligaments (Nigg and Herzog, 1999).

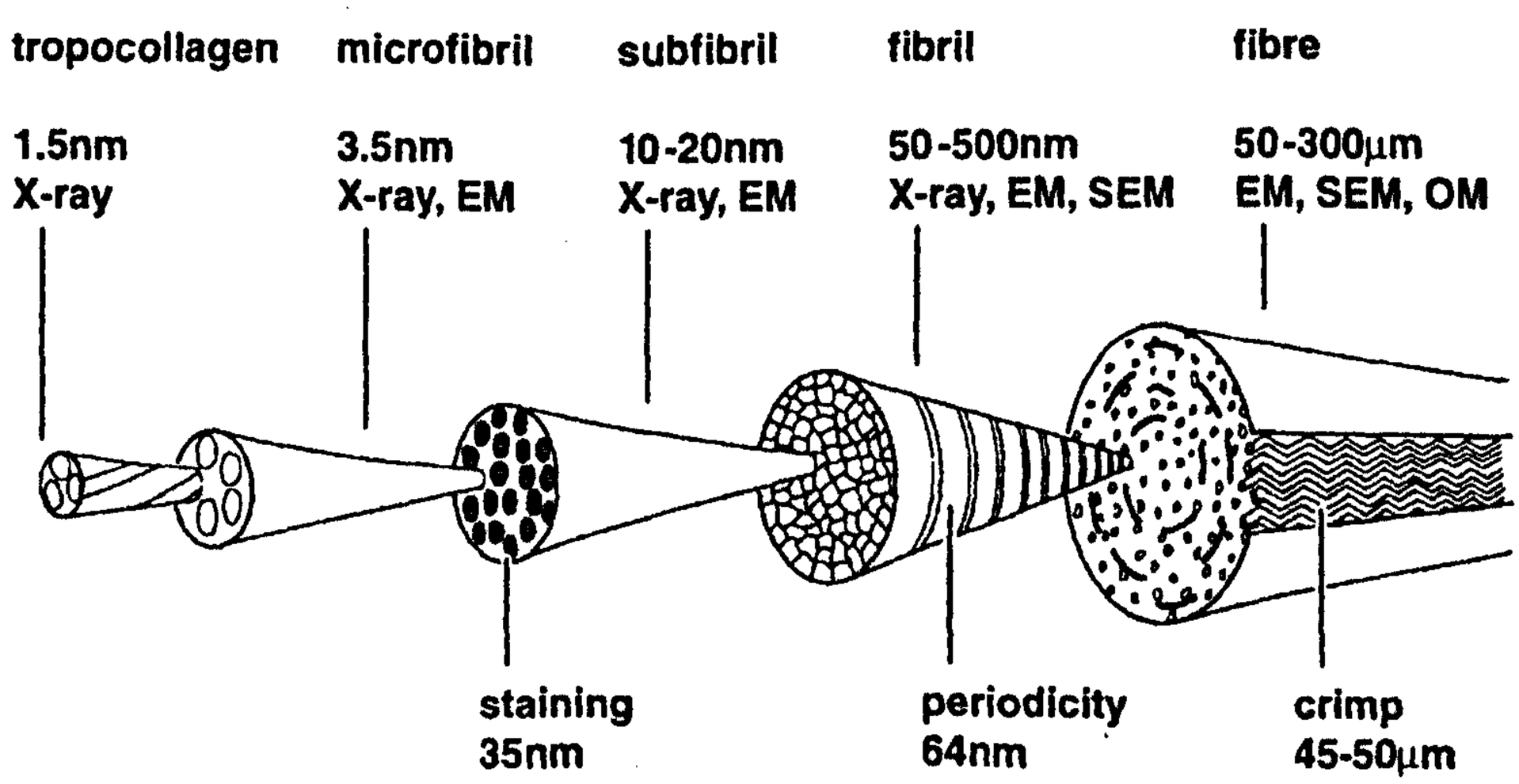

Fig 2.8 Macro- and microscopic structure of ligament fibres (Kastelic et al, 1978).

The extra cellular matrix, which basically forms the ligament's body, is made up from collagen, proteoglycans, elastin and water. Figure 2.8 shows an illustration of the fibres that compose ligament tissues based on the elemental protein collagen.

Collagen fibrils have a 'zig-zag' crimp form that is straightened when tensile load is applied on the tissue. Collagen fibres vary in size and are typically within the range of 10-1500 nm (Nigg and Herzog, 1999), depending mainly on age. The larger their size the greater the loads that the tissue can withstand. Externally enforced relative movement of collagen fibres reduces viscosity of the capsular ligaments and allows easier stretching of the tissue. This behaviour depends largely on the strain rate (figure 2.9). Slow strain rates mean that there is enough time for interstitial fluids to flow within the ligament's body without providing great resistance to the applied deformation. At higher strain rates fluid pressure resists deformation more. However, for large strains the elastic effects of the stretched-out collagen fibres gain importance over the fluid effects that are predominant at low total strains.

The purpose of proteoglycans in ligaments is only speculated. It is believed that their main role is in controlling the viscoelastic behaviour of the ligament by regulating the amount and movement of water within the matrix (thixotropy), based on its hydrophilic nature. Apart from influencing the thixotropy of the ligament matrix, water has the additional role of providing lubrication for inter-fascicular sliding (Nigg and Herzog, 1999) and also to carry nutrients to the fibroblasts whilst also removing waste substances. Finally, elastin plays the role of restoring the initial length of ligaments after removal of a tensile load. Elastin can do that by remaining in a coiled shape when the ligament is in unloaded condition. Presumably, some of the ligament's strength results from the presence of elastin (Nigg and Herzog, 1999).

2.2.2 Factors Affecting Ligamentous Histology

It is known that age, sex hormones, activity and diet are factors that play a role in the biochemical composition of soft connective tissues like the capsule and its ligaments (Nigg and Herzog, 1999). In young age, tissue is in an immature state and as it reaches maturation an increase in the size of collagen fibres is observed as well as a rise in number of cross-links. With ageing this process is reversed and therefore its strength diminishes. Estrogen- a sex hormone predominant in female- was shown to influence the strength of the capsular tissues beneficially by increasing the diameter of the elastic fibres (Shikata et al, 1979). This means that in mature females,

estrogen affects the tissue properties. Furthermore, it has been stated that lack of activity leads to reduced range of joint motion (Binkley,1989) as a result of the changing material properties of the tissues that occur. Thereby, it has been postulated that these changes are due to altered water contents of the extra-cellular matrix that results from the joint immobilisation and causes the increase of viscoelasticity and shortening of the ligament and capsule tissue. This theory is more commonly accepted amongst physiotherapists, but an alternative explanation for the increased joint stiffness following immobilisation, has to do more with the shrinking number of collagen fibres that comprise the ligament (Akeson, 1961). My feeling is that the number of collagen fibres reduces due to the absent ligament loading in immobilised joints, without being able to reject the opinion of Binkley (1989) regarding the water content's effects on ligament strength. In any case the observation following joint immobilisation is that the passive joint stiffness is increased, which means that a greater torque is required to move the limb into a certain position compared to prior of joint immobilisation. The complex composition and diverse interaction of all the ligamentous components makes it extremely important to select an appropriate method for defining its mechanical properties, as they will be influenced by the condition of all the living components.

2.3 Function of the Hip Joint Capsule

The vital importance of the hip joint capsule is the result of the numerous functions that this tissue has. As was already mentioned briefly, the capsule provides a seal for the lubricating synovial fluids and also contributes passively to joint stability, which means that they ascertain the correct joint movement whilst securing its structural integrity. Reduced joint stability could in extreme cases result in the dislocation of the hip joint, which means that the femoral bone would end up being displaced out of the acetabulum.

2.3.1 Alternative Roles of the Hip Joint Capsule

Beyond that, though, it has been proposed that it might also play a role in the proprioception via its nerve endings (Eldred et al, 1998). This would mean that by removing or damaging the capsule partly or completely during THR surgery, would

cause a disturbance to the proprioceptive perception of the limb position and could place an additional risk to joint stability at extreme limb positions, because important information would not be passed on to the surrounding stabilising musculature (Kennedy et al, 1982). The absence of strengthening capsular ligaments would add to the limited stabilising joint forces.

Wingstrand et al (1990) have reported on the importance of the hip joint capsule in providing additional stability to the hip joint not only due to the mechanical forces produced by the ligaments, but also because of the intracapsular pressure. On the cadaver model they inserted a steel axis through the greater trochanter and along the neck of the femur, enabling them to apply extension or flexion angles to the hip joint by externally turning that axis. Thereby, the changes of pressure in the joint capsule that occurred with every change of rotational orientation of the femur were recorded, using a piezoelectric pressure transducer connected to a saline-filled pressure resistant tube. The findings of this research showed that even at normal intracapsular pressure levels, a rise in pressure occurred when rotating the femur into positions of extreme extension and flexion of the joint. This increased intracapsular pressure contributes- even if only marginally- to the stability of the hip joint, in particular in the critical joint positions of full extension or flexion. This would suggest that when a capsule is damaged or excised during THR, this additional intracapsular pressure becomes redundant, increasing the risk for hip dislocation. It is therefore proposed, that this factor should also be considered when performing THR surgery and cutting through the joint capsule. The effect of intracapsular pressure on joint stability is not accepted by all researchers, because it is not clear to what extent the intracapsular pressure comes into action, before the ligaments begin to produce resistance moments.

2.3.2 The Role of the Capsule in Hip Joint Stiffness

Nevertheless, in this work the weight is placed on the investigation of the mechanical action of the hip joint capsule ligaments. The way the different ligaments are positioned within this capsular meshwork, predisposes their role in producing resistance moments around the hip joint. According to the anatomical observations of

Fuss and Bacher (1991) the following restrictions are produced by the individual ligaments:

Pubofemoral ligament- restricts abduction independent of flexion-extension and internal-external rotation

Ischiofemoral ligament- restricts inward rotation with its superior fibre bundles, unless the limb is in extreme adduction combined with full flexion or extension. It also restricts flexion, regardless of the presence of internal or external rotation.

Medial iliofemoral ligament- restricts extension if no adduction is present. This is independent of internal or external rotation present.

Lateral iliofemoral ligament- partly restricts extension of the limb, but only if the limb is not abducted beyond half of its range. This restriction is obviously carried by the medial bundles of the lateral iliofemoral ligament. On the contrary, the lateral bundles restrict outward rotation when the limb is in flexion, but without the presence of severe adduction.

Flexion is less restricted than other limb movements. However, it is restricted by the thigh bone contacting the trunk and also by the resistance that the inferior bundles of the ischiofemoral ligament apply in extreme flexion. The above described ligament actions are of great importance when trying to estimate the effect that capsular excision during THR surgery has on the stability of the post-operative hip joint. These actions are also matter of discussion in chapters 4 and 6. The above observations are based exclusively on the anatomical location of the individual ligaments, but the impression gained during the course of the cadaver work that is described in chapter 4, is that rather than having exclusive roles, each of the ligaments has a contribution to total resistive moments in more than one limb movement. This fact is also confirmed in the numerical analysis that is presented in chapter 6, where the individual resistive moments from the different ligaments are shown individually for the various simulated limb positions.

2.4 Previous Research on Hip Joint Capsule Biomechanics

Ahlers et al (1978) attempted to determine the mechanical properties of the hip joint capsule by comparing ten specimens that were removed intra-operatively from patients with coxarthrosis, which is a chronic degenerative disease of the hip joint, undergoing primary THR to ten specimens from the capsule of patients undergoing revision THR (i.e. where a neocapsule or pseudocapsule had already formed after the primary operation). The result of this study showed that almost all figures that describe the properties of a tissue are similar in both types of capsule. Only in terms of tensile strength the neocapsule could take almost twice the load of the diseased coxarthrosis capsule (table 2.1). Any capsule harvested from donors with coxarthrosis would have undergone certain degeneration as a result of the disease, which explains the reduced strength of that these specimens experienced.

	Original Capsule	**Neocapsule**
Tensile Strength [MPa]	1.77	3.26
Max Strain [%]	119	125
Elastic Modulus (10% strain) [MPa]	2.05	2.2
Transition Point [% of l_0]	11	9.9

Table 2.1 Properties of original capsule and neocapsule (Ahlers et al 1978).

Transition point in table 2.1 describes at what percentage of elongation relative to the initial length of the specimen (l_0) the shift from the initial toe region of a stress-strain curve to the linear region occurs. The modulus of elasticity is derived graphically by drawing a tangential line on the stress-strain curve at the interposition of 10% strain. One aspect of this work that gives reason for concern on the reliability of the findings is the way the samples were excised out of the complete hip joint capsule. In fact, their efforts concentrated on creating standard sizes and in particular sizes of $10\times2\times2$ (mm^3) and not in ensuring that individual ligaments were excised from the capsular mesh. It is possible that lack of knowledge at the present time led to the acceptance of such a limitation.

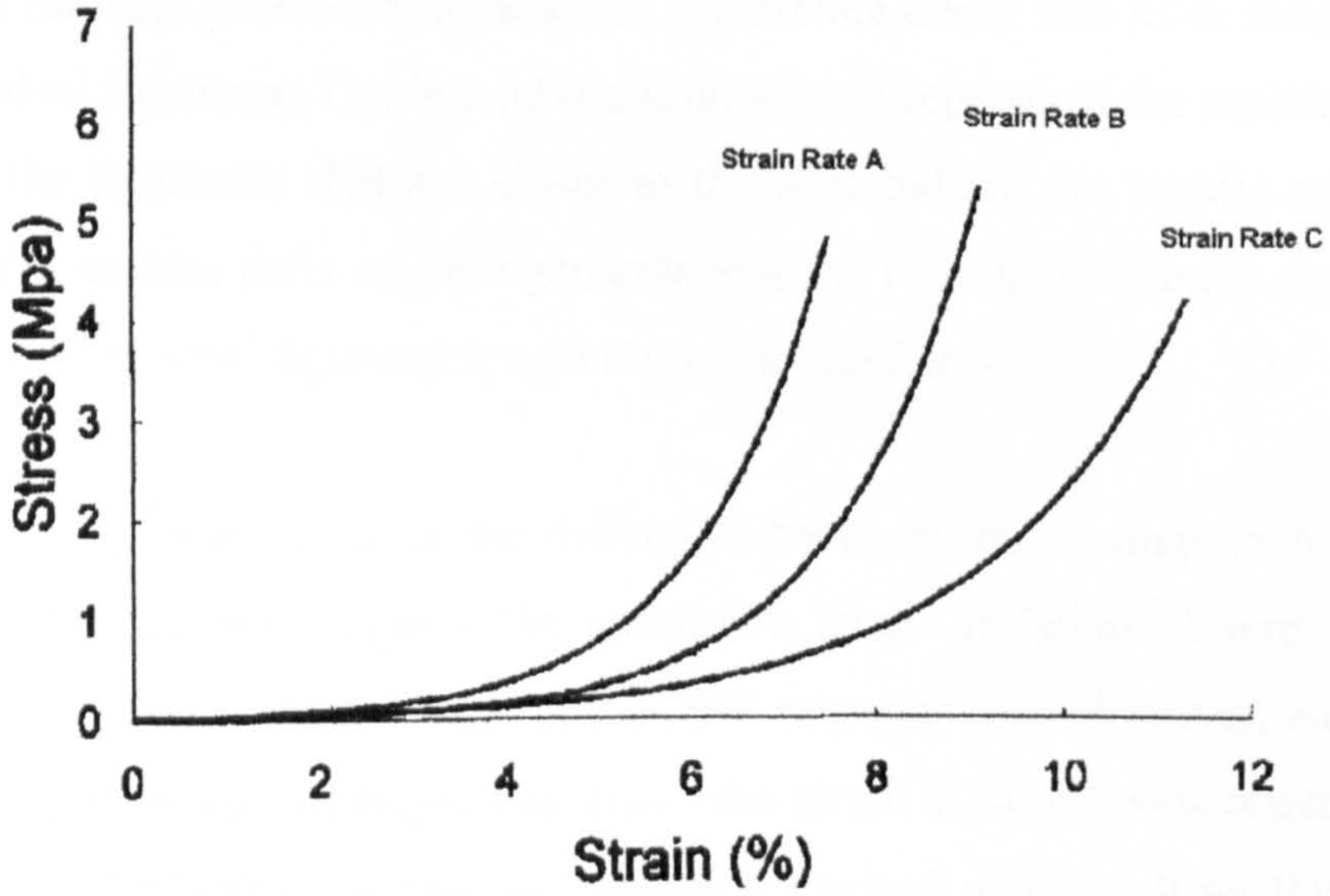

Fig 2.9 Stress-strain curves for different strain rates (A, B and C). Greater strain rates result in faster stress response (A>B>C).

Another more recent research involving the hip joint capsule made an advance by excising the various individual ligaments that are part of the capsular mesh and subjecting them to tensile tests (Hewitt et al, 2001 and 2002). The findings of this research group are of great relevance to the present research and are part of a comparison that is done within the present work. For this reason the review will not be too extensive at this point, as a more detailed description of Hewitt et al's findings is given under paragraph 3.6.1 of this thesis. However, the main findings are summarised in this paragraph as a means of comparison to the findings reported by Ahlers et al (1978) and presented in table 2.2.

	Lat Ilio Lig			**Med Ilio Lig**			**Ischio Lig**		
Tensile Strength [MPa]	3.3	2.7	2.7	6.1	6.2	6.1	2.4	2.0	3.5
Max Strain [%]	8.5	6.2	13.3	11.6	10.4	11.4	7.8	8.1	25.3
Elastic Modulus (10% strain) [MPa]	3.2	1.9	1.0	3.0	3.3	2.2	4.8	3.9	2.1
Rupture Force (N)	320.3 ±267.7			351.3 ±159.4			136.0 ±74.6		

Table 2.2 Properties of individual ligaments from hip capsule (Hewitt et al 2001).

The findings presented in table 2.2 are broken down into three subgroups for each individual ligament. The left sub-column always represents the results for those regions of the ligaments that are closer to the acetabulum, the middle sub-column stands for the middle parts of the ligaments and the right sub-columns contain data for the third of the total ligament length closest to the femur.

A striking observation is the difference between the findings in Ahlers' and Hewitt's studies in what regards the maximum strain at failure. There is a large inconsistency between them (120% and 6-25% respectively). However, Ahlers et al (1978) state that in case of aligned fascicles the strain at failure was observed to be much less (20-30%) than in case of randomly excised samples from the capsular tissue, as was done in their study. This is a conclusive evidence that the available techniques in 1978 were a limitation in the detailed study of the behaviour of specialised soft hydrated tissues, like the capsular ligaments.

2.5 Biomechanics Research on Other Ligaments

The joint ligaments, on which the greatest literature has been accumulated dealing with their biomechanical properties, are those of the knee joint. A brief summary on the findings by various researchers regarding their biomechanical properties is given in the following paragraph. The findings by different researchers reveal generally significant deviations, depending on the condition of the specimen and on the applied testing techniques. Claes (1983) has summarised the results reported by various researchers, which are presented in table 2.3.

It is mentioned in the same work that it is of great importance to measure rupture forces on a fresh cadaver rather than as an isolated separate tissue, because of the better approximation with in vivo ruptures, which happen at the insertion points more than at the central region of a ligament. This is in accordance to the findings reported by Hewitt et al (2001) on the hip joint ligaments, where the maximum strain at failure was shown to be smaller at central regions of the ligaments rather than at the insertion points into the bones. Therefore, it is probably more appropriate to test

ligaments as part of a bone-ligament-bone sample and not as isolated ligamentous strands.

	Collateral Ligaments			Cruciate Ligaments		
	Medial	Lateral	Author	Ant	Post	Author
Stiffness (N/mm)	72	62	Trent et al (1976)	141	183	Trent et al (1976)
	93.9	47.4	Claes (1983)	129/182	-	Noyes et al (1976)
Rupture Force (N)	526	384	Trent et al (1976)	633	571	Trent et al (1976)
	654	354	Claes (1983)	734/1730	-	Noyes et al (1976)
Maximum Strain [%]	18.15	20.89	Claes (1983)	44.3/30	-	Noyes et al (1976)
	23	-	Kennedy et al (1976)	30.8	28.3	Kennedy et al (1976)

Table 2.3 Properties of knee joint ligaments by various researchers (Claes, 1983).

Stiffness in table 2.3 was defined as the ratio: $S= \Delta F/\Delta l$ (N/mm), which is the load difference over the resulting elongation in the linear region of the stress-strain curves. Noyes and Grood (1976) have compared anterior cruciate ligaments of both older and younger subjects and both findings are listed in the right column of table 2.3. Thereby, the number before the slash refers to the older subject group and after the slash to the younger subjects. An interesting observation on the summarised data reported on the collateral and cruciate ligaments by the various researchers listed in table 2.3 is that based on the data of rupture force and maximum strain at failure, it is obvious that the knee ligaments are capable of withstanding much greater loads than the ligaments of the hip joint. This was somehow to be expected, as the knee joint is a much less stable joint than the hip both in terms of its bone elements (femur and tibia) and also the surrounding musculature.

Binkley (1989) has also reported values for the medial collateral ligaments of the knee joint and compared normal post mortem rat medial collateral knee ligaments samples to those with previous immobilisation. The values are illustrated in table 2.4. Even though there is very little point in comparing these findings to the data on human knee and hip ligaments, it is interesting to see the effect that immobilisation has on the mechanical properties of ligaments. It is therefore important to assure that

when testing ligaments in tension no previous immobilisation and presumably any other influencing state was imposed upon the donor subject from where the samples were derived.

	Normal	Immobilised
Tensile Strength [MPa]	7.65	1.95
Max Strain [%]	114	113
Elastic Modulus (10% strain) [MPa]	2.86	1
Transition Point [% of l_0]	6	9

Table 2.4 Effect of immobilisation on medial collateral ligaments (Binkley, 1989).

In summary, it has been of great benefit looking at the mechanical properties of other joint ligaments as it gives an estimate of the value of any findings on the ligaments under investigation. In particular, the absence of any useful data on the mechanical properties of the hip joint capsule and its ligaments until recently, made it a valuable comparative means. Since adaptation is a great part of the evolutionary process of human anatomy every part of it, including the hip ligaments, have such properties that enable them to at least perform under normal conditions, but also allow them to function under occasional excessive loads.

2.6 Risk for Hip Dislocation

A hip dislocation is a very dramatic event involving immense pain, regardless of whether it occurs in an apparently healthy hip joint or one that had previously received a prosthetic replacement. The occurrence in a normal hip is by far more rare than it is after THR. However, the capsule plays a role in both cases and for this reason two individual sections are dedicated for each case below. Hip dislocation can be split into two groups:

- Posterior dislocation, which is caused by flexion, adduction, and internal rotation. Such dislocations are most commonly observed in case of posterior approach in surgery.

- Anterior dislocation, which is caused by extension, adduction, and external rotation. This type of dislocation is most frequently encountered in case of damage to the anterior aspects of the hip capsule. Such damage occurs in case of an anterolateral surgical approach.

2.6.1 Dislocation Without THR

The hip is generally considered a stable joint as a result of its shape that is often referred to as a ball and socket joint and dislocations do not usually occur, unless a pathology is present. Common pathological disturbances that can lead to hip dislocations are a spastic hip, where the spasticity of muscles wrapping the hip joint can cause subluxating dislocations (figure 2.10). Another pathologic reason for dislocation is coxa saltans (latin for snapping hip), which is a spastic imbalance of the muscles that surround the hip joint that can lead to joint dislocation. Bellabarba et al (1998) report on five patients without prior trauma. In this study they confirm previous findings of Massie and Howorth (1954), regarding the progressive development of subluxation and hip dysplasia in patients with joint capsule laxity. Thereby the proposed postulation is that the clinical finding of a capsular laxity usually results in subluxation or hip dysplasia in later life.

Fig. 2.10 Subluxation of a normal hip.

Further, a dislocated hip can also result from impact. Hamilton and Broughton (1998) presented 18 cases, the majority of which involved posterior dislocation, which could be due to the direction of the impact, but might also be indicative of a difference in strength between the anterior and posterior joint capsule. In support of this Graham and Lapp (1990) showed evidence of a patient who had a posteriorly dislocated hip as a result of having brought the limb into internal rotation combined with adduction and slight flexion. The recurrent dislocation showed to have been the result of a lax posterior capsule that resulted from the initial dislocation. The joint became stable only after surgical capsulorrhaphy (i.e. stitching of the capsule). Weber and Ganz (1997) have presented further support for the theory that damage to the hip joint capsule- like a partial rupture- can be a reason for recurrent dislocations.

The above clinical observations highlight the important role of the joint capsule in stabilising the joint, especially when there is not sufficient time for the surrounding muscles to activate and tighten the joint. In these situations the capsule plays the role of a 'safety-belt' that acts passively. Also it was shown that in a lax capsule, which could be compared to an incised or even excised capsule, the absent capsular restraint forces can allow dislocation, even without extra-ordinary external forces.

2.6.2 Dislocation After THR

The postoperative dislocation after THR is regarded as one of the typical early complications with an average occurrence ratio from 1.7% to 3.6% as was stated in articles published by Yuan and Shih (1999), Hedlundh et al (1996), Scifert et al (1998) and Bickels et al (2000). Other sources refer to an incidence ratio of about 1% (McCollum and Gray, 1990). However, it appears that the risk for multiple dislocation is elevated in patients with a revision THR or in patients who have experienced previous complications of the hip. It has been reported (Dorr et al, 1983) that 74% of patients who experience multiple dislocations had previous hip surgery whereas only 47% of those with a single dislocation had hip surgery before. This means that patients with previous surgery of the hip are more likely to suffer

recurrent dislocation than just a single case. Williams and Gottesmann (1982) reported a 20% dislocation rate in patients who prior to THR had some kind of hip surgery in contrast to those patients without, where the rate was at 0.6%.

2.6.3 Predisposing Factors in Post-THR Dislocation

Regardless of the real incidence of hip dislocation occurrence, it is necessary to improve the rates and to try and improve stability as much as possible, because of the severity of complications that it can initiate, ranging from thrombo-embolic disease to nerve palsy. Therefore, it is vital to understand the various factors that may lead to dislocation. In the literature, the following reasons have been identified:

- Extreme incision into the capsule and the abductor muscles or complete excision of capsule. In this case an imbalance of soft tissues is enforced on the joint. This means that agonist and antagonist muscles result in imbalance.

- Inadequate size of the head, socket and neck of the prosthesis (Scifert et al, 1998). Amstutz and Markolf (1974) showed with in vitro studies that a smaller head size means that the distraction that is required to cause a dislocation, i.e. to pull the head out of the socket is smaller than in case of a larger head size. This can also be seen graphically in figure 2.11, where the horizontal blue line is parallel to the ground, and the other blue line, which is under an angle, is tangential to the acetabular rim. The red line is tangential to the femoral head component for a 32-mm size, whereas the green line is tangential to the femoral head of a 22-mm size component. Both the red and the green line are parallel to the blue line that is tangential to the acetabular rim. The respective distances between the red or green lines to the blue line mark the distance that the femoral head component needs to move as to result in a dislocation. This effect depends also on the shape of the acetabular cup.

- Mal-positioning of the prosthetic components relative to the pre-operative planning, have been identified as a major cause for dislocation (McCollum and Gray, 1990). In this work, this cause of dislocation is not studied further.

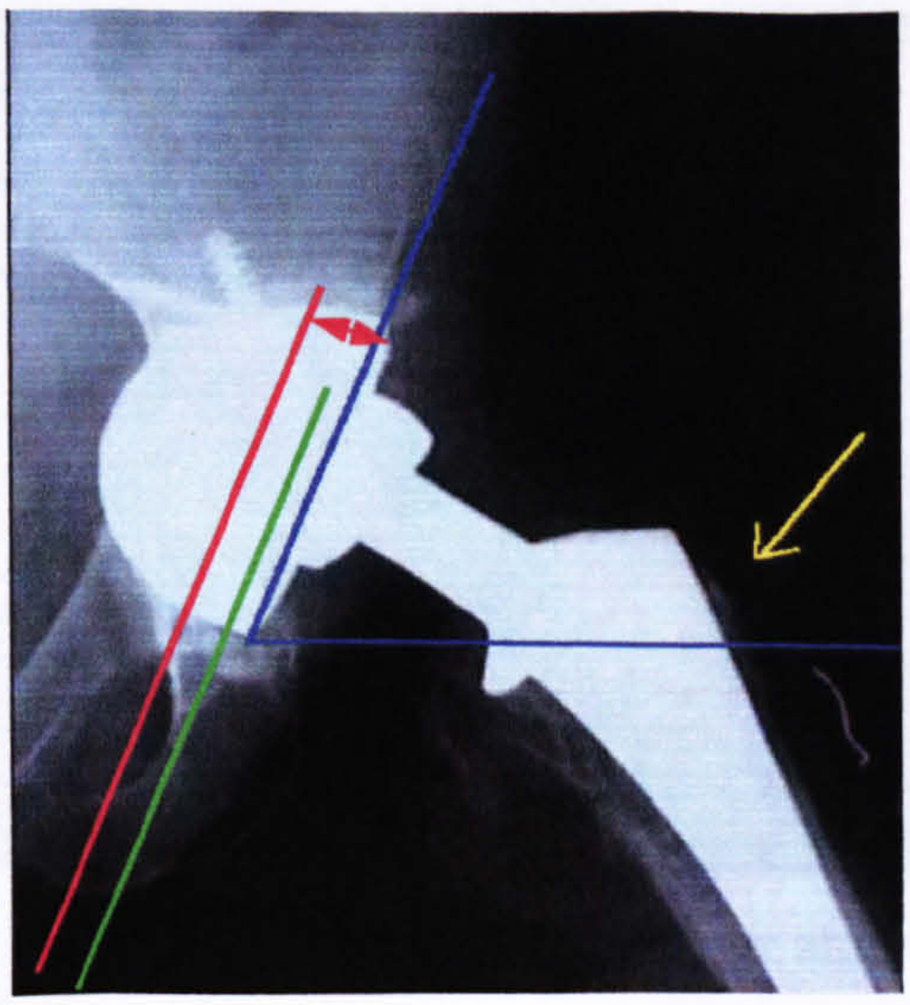

Fig 2.11 Difference in lengths that a 22mm and 32mm femoral head has to travel in order to exit the socket.

- Inappropriate combination of prosthetic neck length and width. A wider neck reduces the range of motion and increases the risk for dislocation from impingement (figure 2.12), because of the contact between neck and cup.

- Too early post-operative weight-bearing can be a reason for dislocation due to the non-healed soft tissues, but mobilisation with protected weight bearing assists in the healing process of the wound.

In more detail, Kelley et al (1998) proved that stability is greater the larger the head size, without reducing or negatively affecting the range of motion of the joint. Similar results were presented by Scifert et al (1998) mentioning a constant head-neck ratio to be the method to maintain a sufficient range of motion without causing an early impingement. Yuan and Shih (1999) reported that in a comparison between the 26-mm and 32-mm femoral head sizes the prosthesis with the smaller head was resulting in single and recurrent hip dislocations at significantly higher rates than the larger head. Hedlundh et al (1996) state that there was no difference in the incidence of early dislocations (<1 year) between the 22-mm and the 32-mm head sizes included in this study. Dislocation rates for both prostheses were about 2.4%.

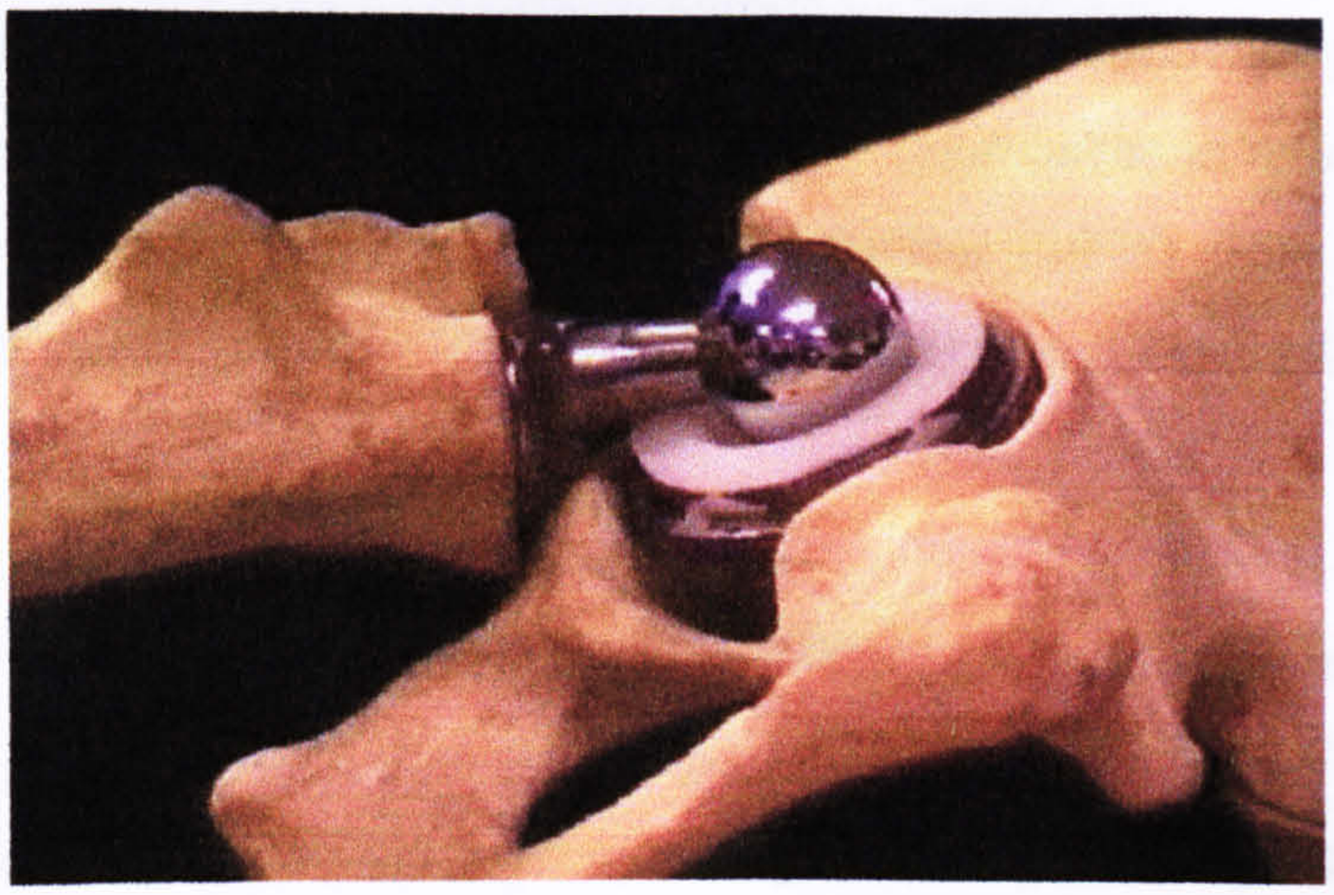

Fig 2.12 Impingement of prosthetic neck and socket in position of extreme abduction in a skeletal model.

2.7 Surgical Approaches to the Hip Joint

The surgical approach that is taken in the surgeon's efforts to reach the diseased hip joint surfaces, depends very much on individual preferences and experience of senior clinical staff that supervised the individual surgeon. Various researchers have found that there is a significant effect of the surgical technique on the dislocation rate of the post THR hip. Morrey (1992) states that the use of a posterior approach to hip joint replacement led to a significantly higher rate of dislocation (5.8% for 685 reviewed cases) when compared to an anterior (2.3% for 770 reviewed cases) or lateral (3.1% for 1898 reviewed cases) approach.

It is of interest to investigate four commonly applied techniques and to look into their individual characteristics. This can be of help in identifying any potential relation with possible damage that is done to the hip joint capsule. The surgical technique is closely related with the individual prostheses that are to be implanted and therefore is subject to modifications depending on the needs during implantation of the various components. Thereby, the main concerns of the surgeon are to keep blood loss during surgery low and to minimise the duration in theatre, which both help to reduce post-operative complications. A quick recovery after surgery is another key aspect for each surgeon. Depending on the approach that is chosen by the surgeon, there will be an effect on the capsular incision and the review of the

different surgical approaches is done under this aspect. The following paragraphs are an attempt to give an overview of various surgical approaches in relation to the hip joint capsule, based on the THR manual of Eftekhar (1978) from where all the surgical illustrations depicted in the following paragraphs were also taken.

2.7.1 Anterior and Anterolateral Approaches

Despite the most logical body position (flat supine) that is taken by the patient during the surgical procedure (similar to figure 2.13), the actual anterior approach to the hip joint articulation has never gained any particular popularity. This was mainly due to the immense time and invasiveness that is required to detach the various muscles, which is necessary in order to create sufficient insight into the articulation.

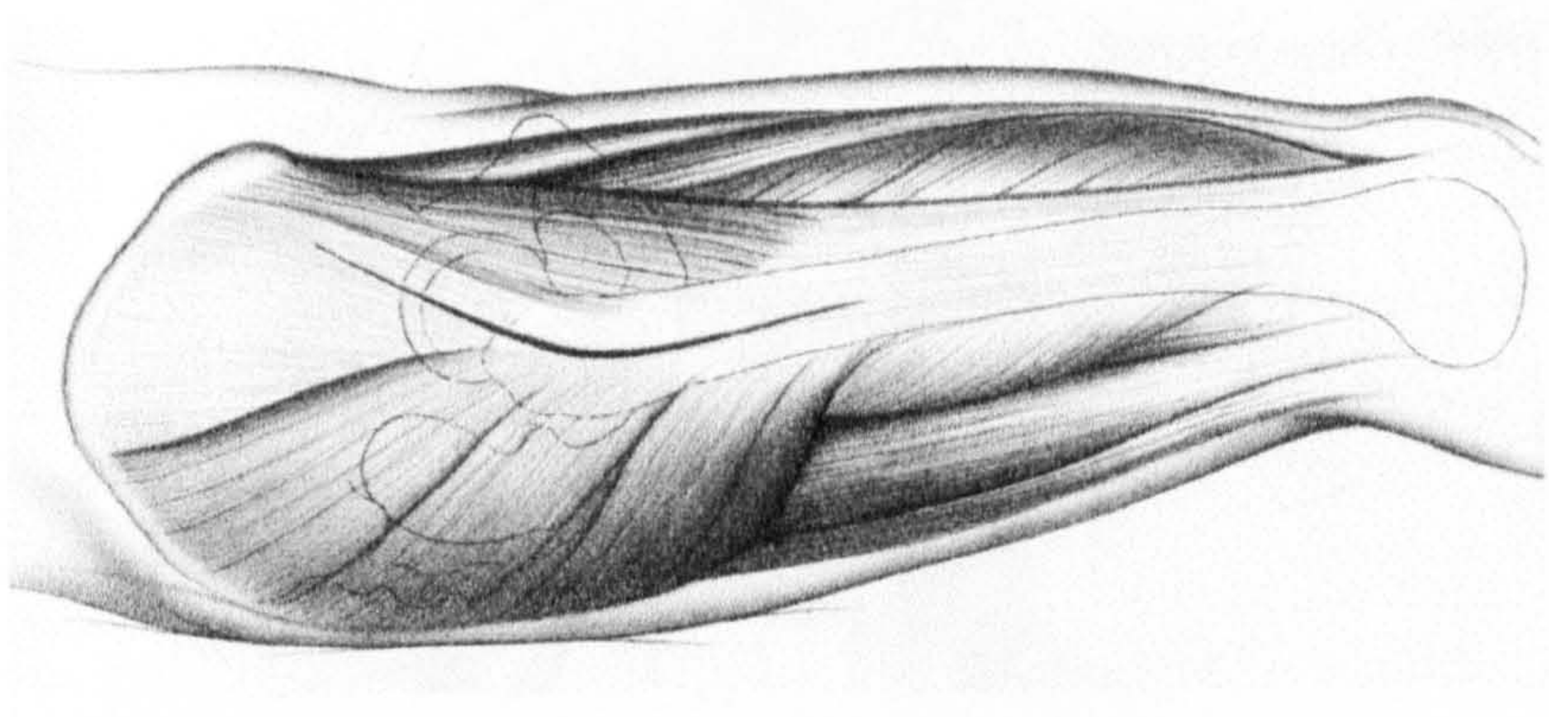

Fig 2.13 Supine position of patient in anterolateral approach to the hip joint. Black curve over femoral neck marks the incision line.

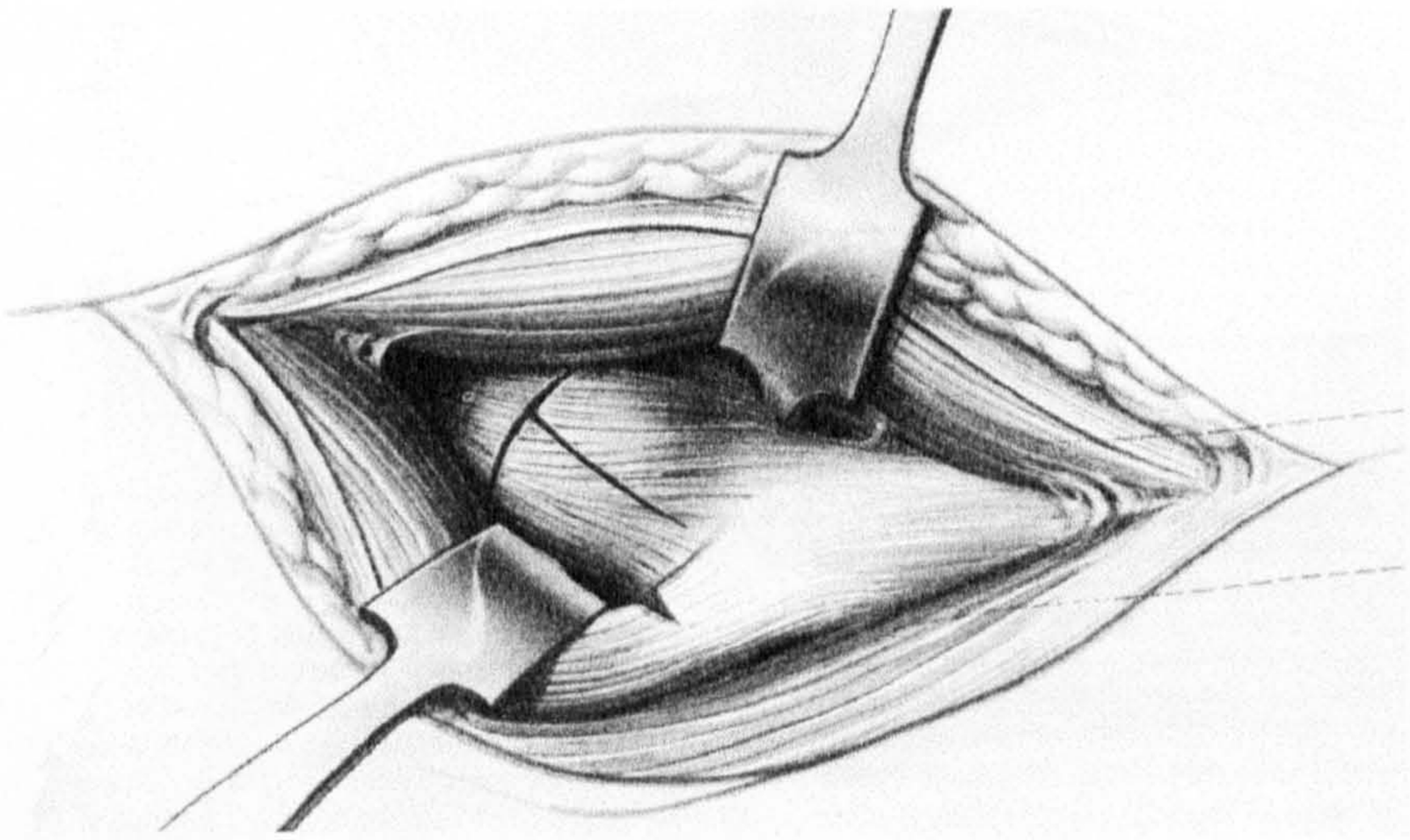

Fig 2.14 Retractors opening access to the joint capsule after incision (v-cut) in the tensor fascia femoris provides some tension relief.

With a strictly anterior approach, an increased risk to vital structures such as the femoral nerve and artery is present, which makes this approach unpopular. In contrast to the purely anterior approach, a more common method has been the anterolateral approach as it was first described by Watson-Jones (1936) and widely spread by McKee (1970) and Müller (1970). Thereby the patient is again in supine position and the gluteal muscles are retracted widely. The greater trochanter is not detached, which might make it necessary to cut through the tensor fascia femoris in order to provide more space with the lower retractor, enabling easier access to the joint capsule (figure 2.14).

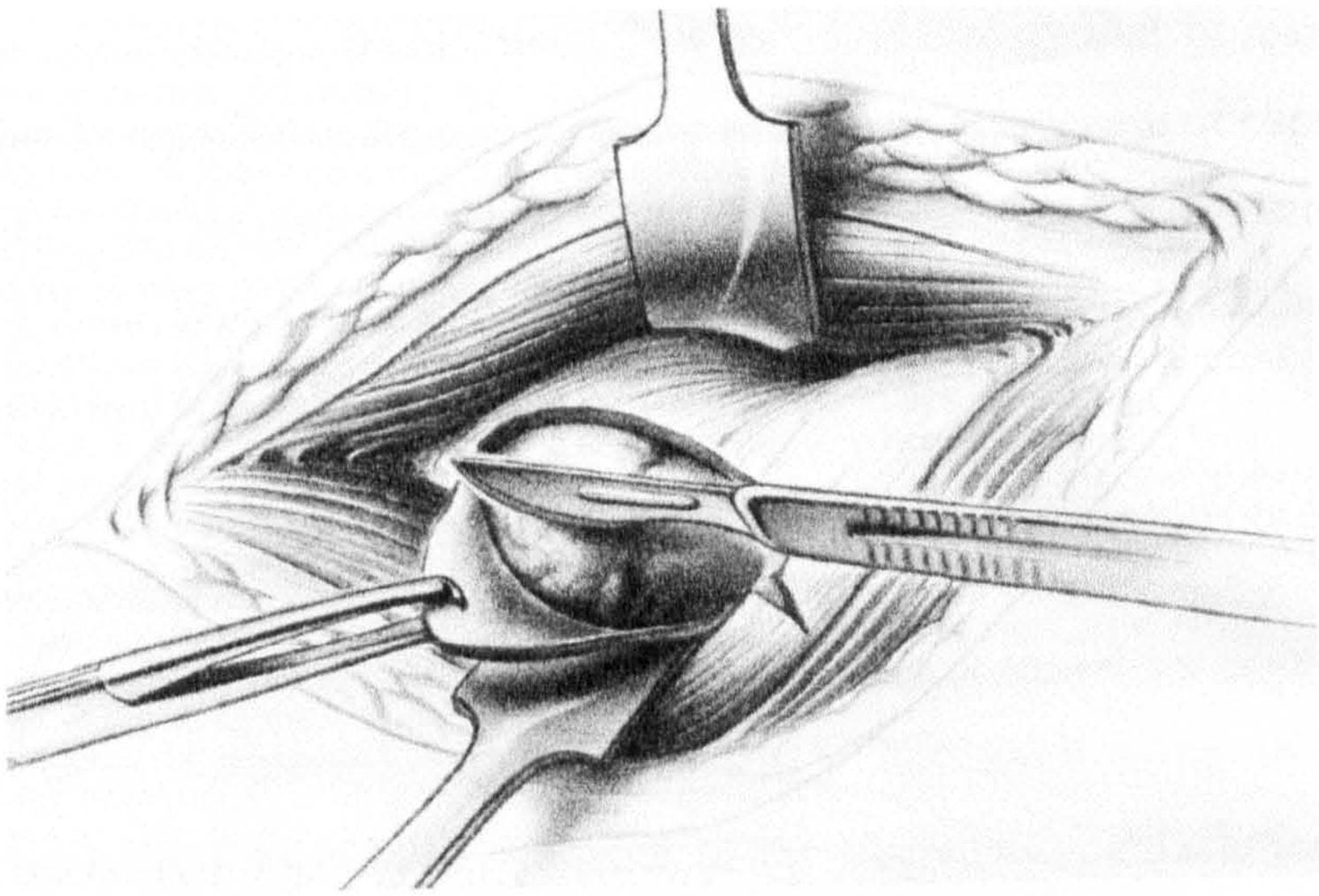

Fig 2.15 Capsular excision for easier femoral head dislocation.

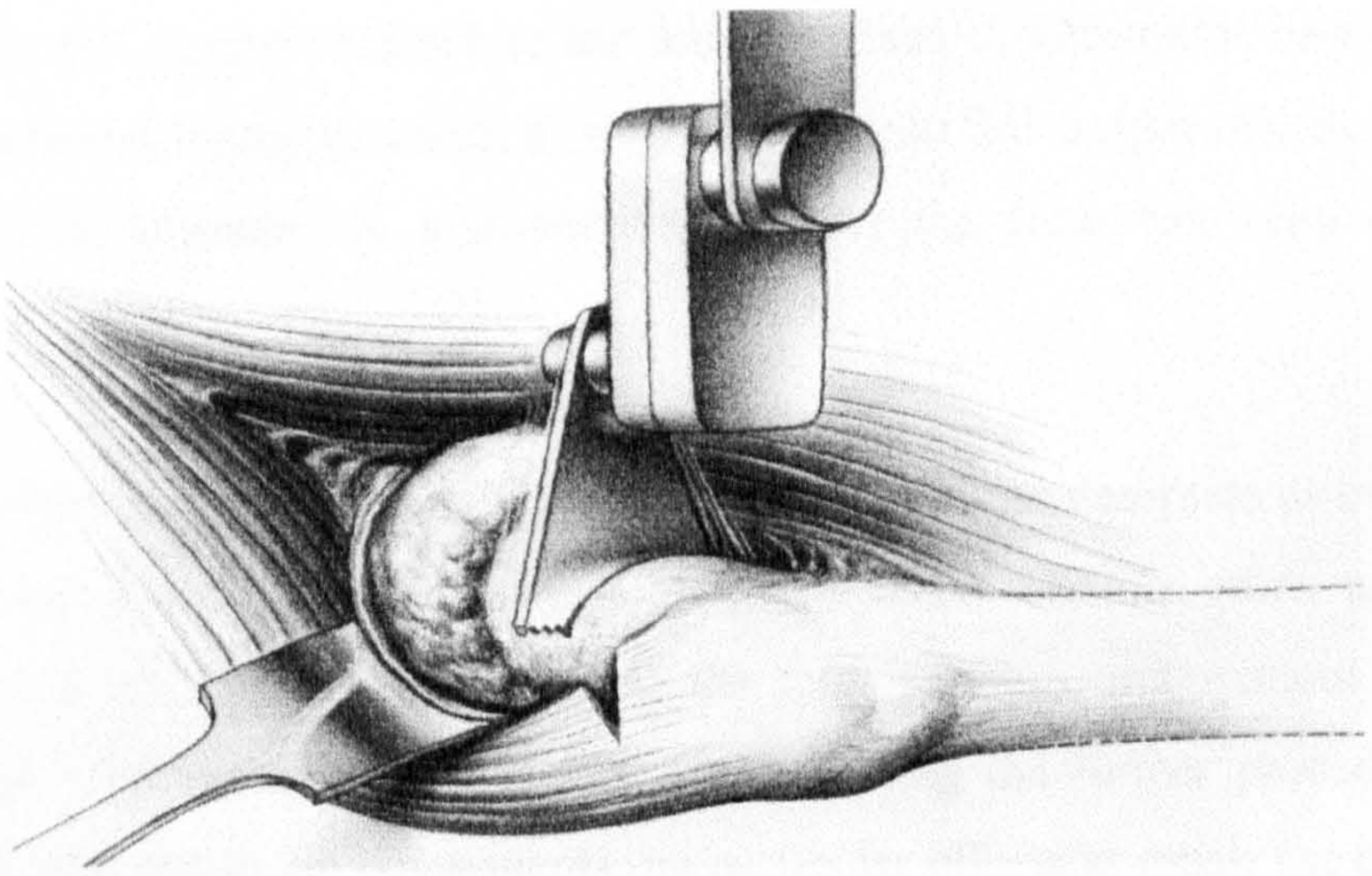

Fig 2.16 Removal of femoral head with an oscillating saw after completion of the soft tissue preparation.

The common anterolateral approach as it is described in the textbooks recommends at this stage a complete capsulectomy in order to allow for satisfactory anterior dislocation of the femoral head (figure 2.15). The final stage of this type of approach to the joint surfaces comprises the femoral head removal, using an oscillating saw as shown in figure 2.16.

It has always been clearly described in textbooks for orthopaedic surgeons and has also always been the subject of oral communication in operating theatres that in case of use of an anterior or anterolateral approach it would be advisable to incise the capsular tissues to 'clear the view'. It is self explanatory that in many cases of patients undergoing THR there will be some with an affected state of capsular tissue health as a result of the pathology that led to the THR. However, it has been common practice to excise even healthy tissue as part of a standardised procedure, without even knowing the importance and role of it.

2.7.2 Lateral or Trans-Trochanteric Approaches

The lateral or trans-trochanteric approach has acquired its popularity from one of its strict followers. Sir John Charnley has been using this approach extensively and has always been in favour of the trochanteric detachment, which is an inseparable part of this procedure. Amongst the advantages of this method, is that it does not cause any interference with any nerves and arteries as the muscles are separated in the attempt to reach to the joint interface. Additionally, because of the greater trochanter being detached, it is possible to gain full insight into the complete acetabulum both anteriorly and posteriorly after the limb has been dislocated (Eftekhar, 1978).

Another main advantage of this technique is that no complete or even partial capsulectomy is required. A common approach to the capsule when using these techniques, is an incision for access to the joint surfaces, but without having to remove the resulting flaps, unless they are disturbing the further procedure. After insertion of the prosthetic components, no particular efforts to repair the capsule are suggested, even though there is the potential for such intervention.

2.7.3 Posterior and Posterolateral Approaches

The posterior approach has first been described by von Langenbeck (1878), but modified several times by various researchers. One popular modification of this approach is the 'southern exposure' described by Moore (1957), which is widely used for femoral head replacement surgery. The incision is placed rather posteriorly, and in parallel with the muscle fibres of the gluteus maximus muscle, as indicated by line A of figure 2.17. This method is not generally considered adequate for THR, because of the low incision, which does not allow good vision to the upper femur.

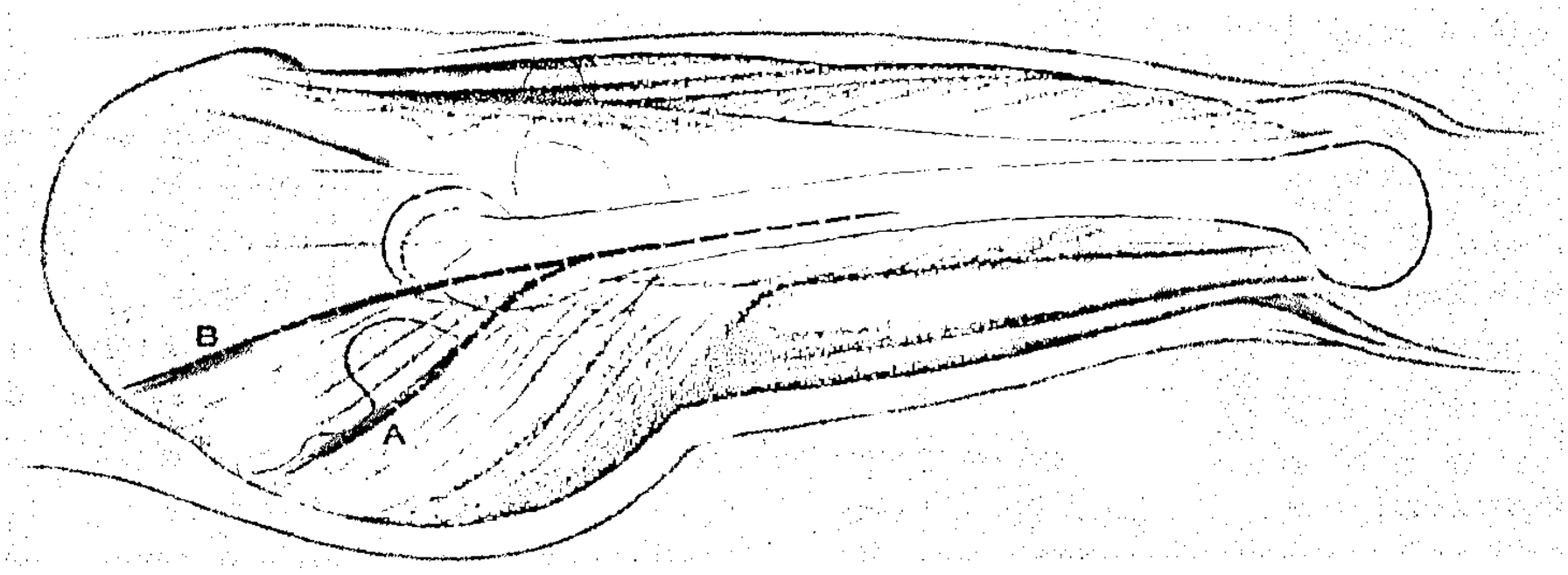

Fig 2.17 Incisions for posterior (A) and posterolateral (B) approaches.

A more appropriate method for THR surgery is the posterolateral approach that follows the incision pattern highlighted by line B of figure 2.17. This incision is performed on the patient lying laterally on the operating table. The sciatic nerve is not a risk for the surgeon, as the incisions occur too far lateral in the anatomy.

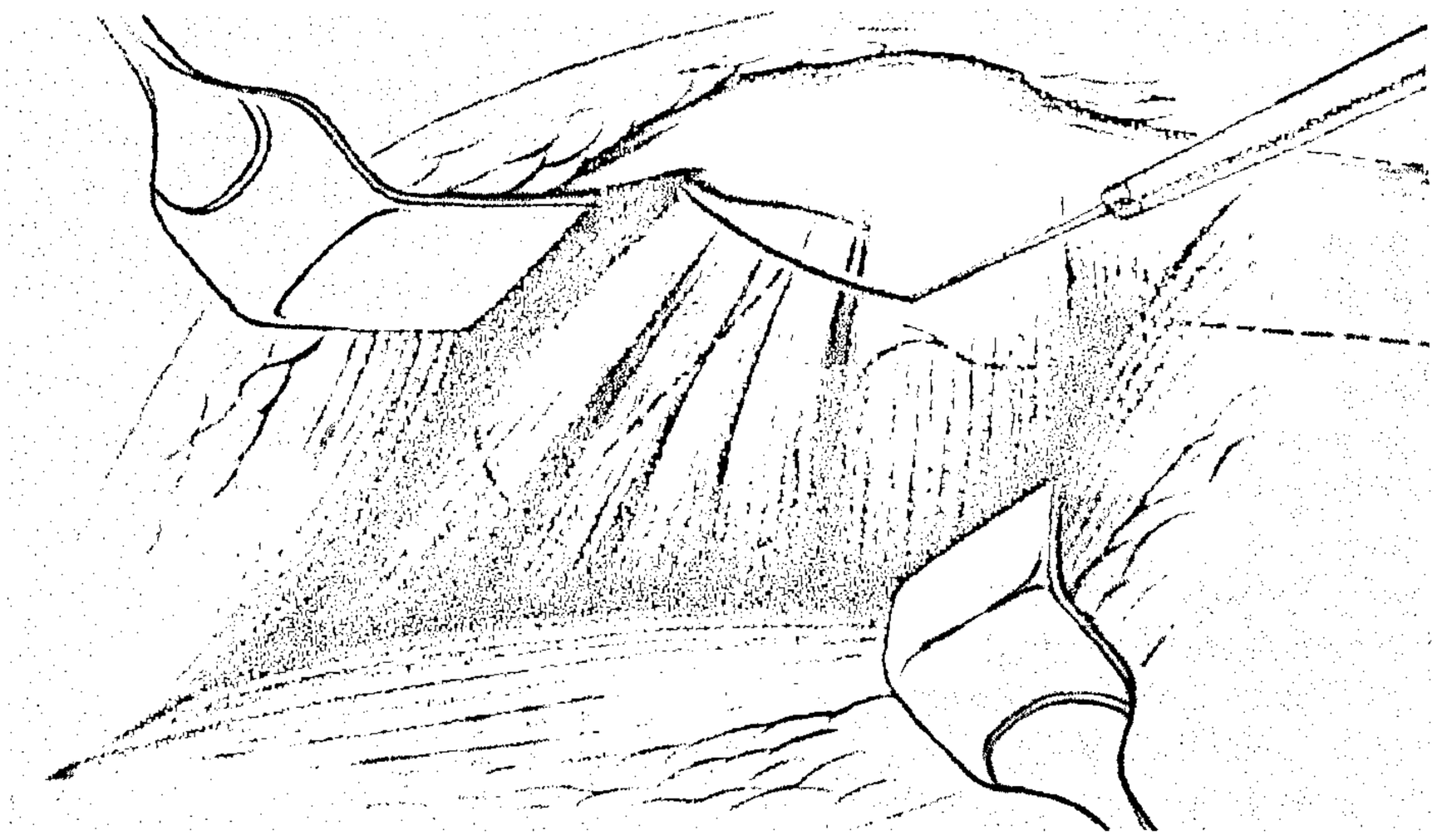

Fig. 2.18 Line of incision through the short rotators and the underlying posterior capsule following the posterolateral approach.

After retracting the gluteal muscles, the short rotators together with the posterior parts of the capsule (ischiofemoral ligament) that attach to the posterior aspect of the greater trochanter are detached with the use of a diathermic knife (figure 2.18).

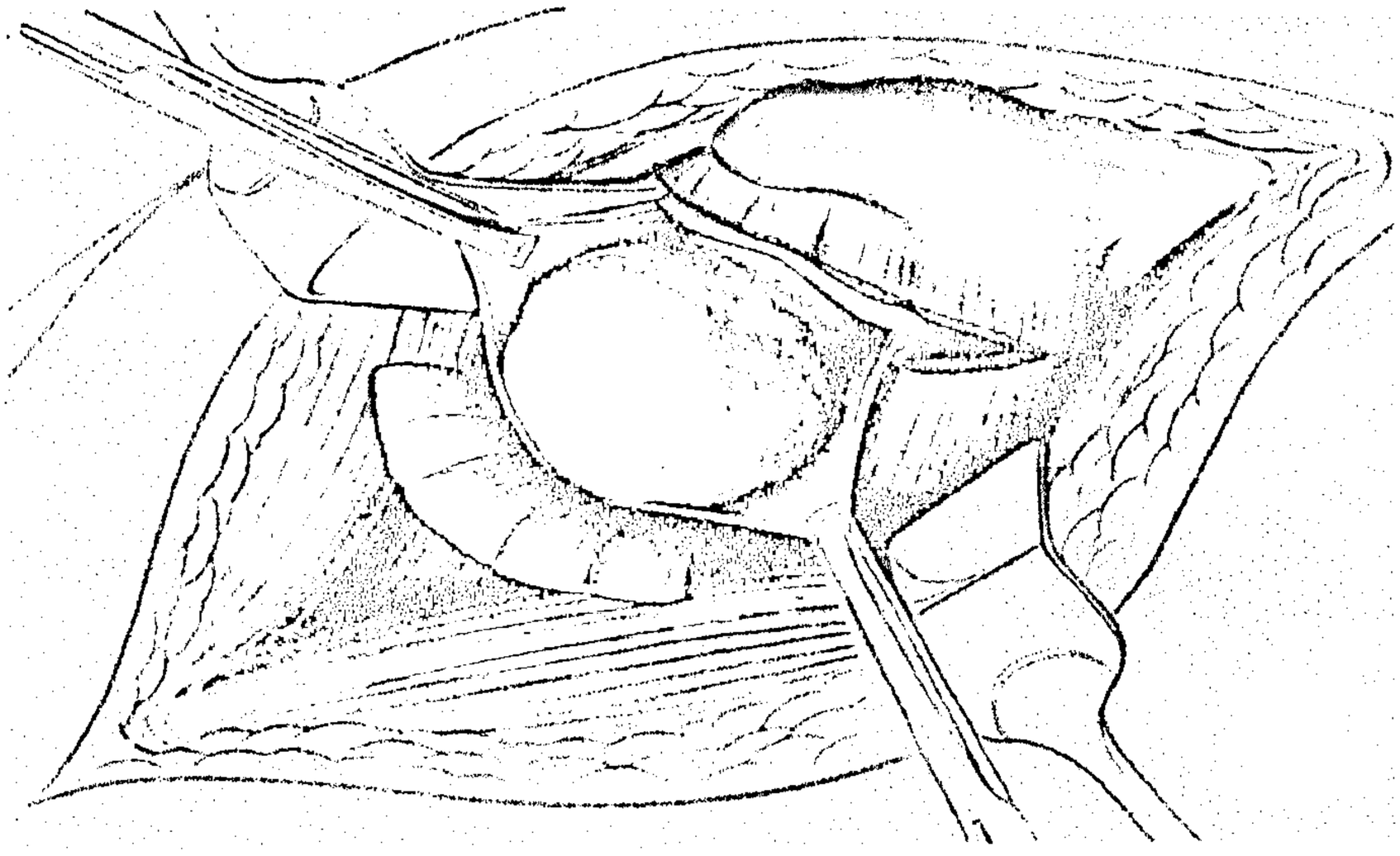

Fig. 2.19 Dislocating femoral head after excision of posterior capsule.

The posterior aspect of the capsule is commonly excised thoroughly, ensuring that all parts of it have been carefully removed in order to facilitate the dislocation of the femoral head posteriorly (figure 2.19). The only parts of the capsule that are preserved in the presently described methodology, are the anterior parts.

One characteristic that all the above described approaches have in common is that none of them takes the capsule into consideration. It is widely accepted practice to remove the joint capsule, whether it is diseased or healthy. The reasons for this practice in surgery is that capsular repair requires additional time in the operating theatre, which brings along all associated risks, such as increased blood loss, prolonged exposure of the wound to the air, longer time under anaesthesia and of course above all reduced access to the joint surfaces. No scientific evidence resulting from organised studies using perhaps numerical methods has been presented to surgeons so far, which in a way explains their behaviour. Only recently and in certain clinical environments orthopaedic surgeons have started asking themselves the question, whether it is worthwhile to accept all the previously mentioned drawbacks

for the purpose of an improved post-operative recovery. First follow-up studies are now available and seem to be strengthening more and more surgeons in this belief. It is to the engineers now to provide them with sufficient mechanical evidence that this undertaking is worthwhile. Following is a review on the current state of capsular repair in THR and its first beneficial results.

2.7.4 Surgery With Capsular Repair

Recently, a few surgeons have started to take a different approach to capsular repair under the scope of reports on the capsule's contribution to hip joint stability as presented in paragraph 2.6. One of the surgical teams that has documented their approach and have reported on the results of their capsular repair technique is De Buttet and Pasquier (1999). Their surgical approach is documented with the following sketches in figures 2.20 to 2.22.

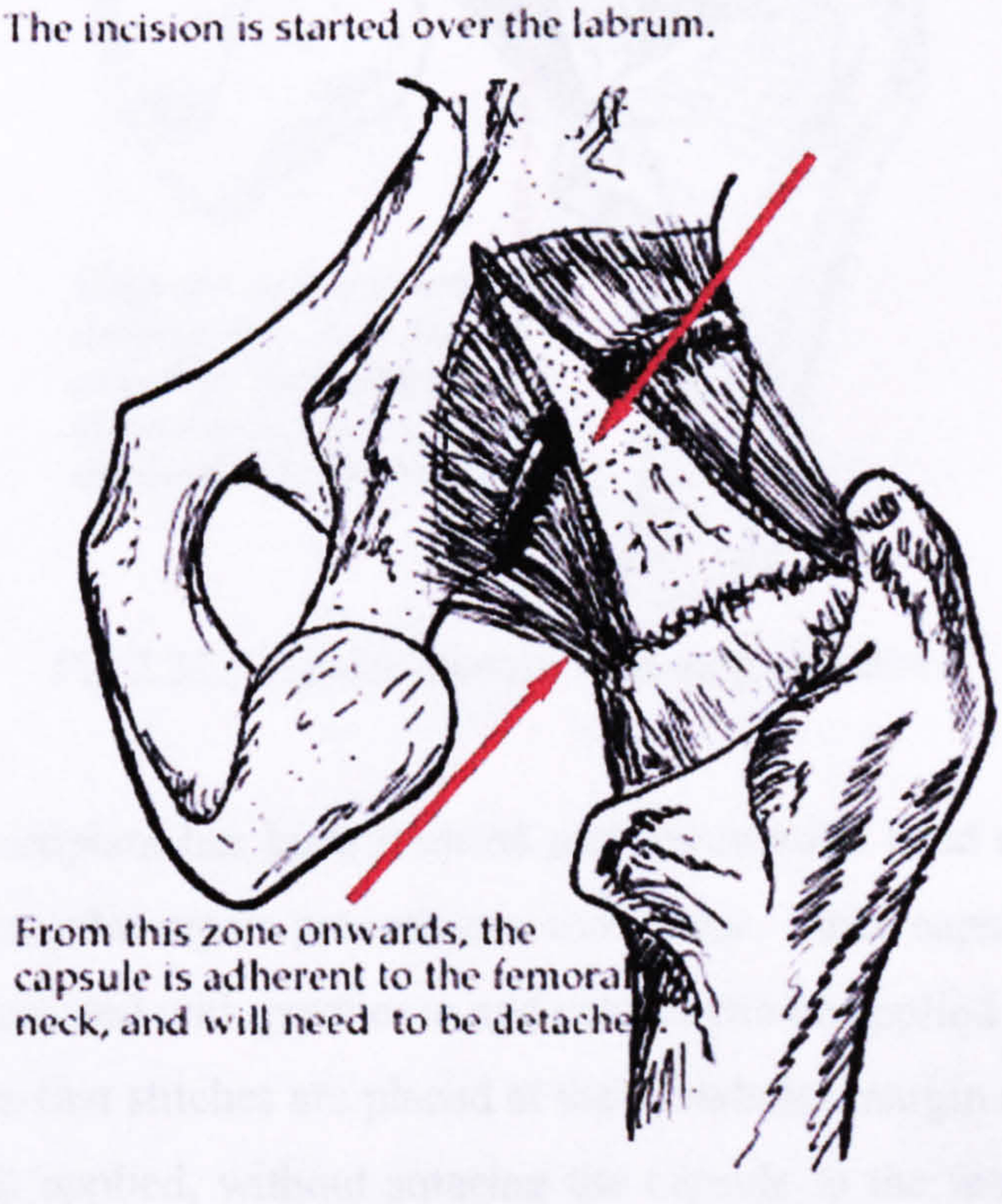

Fig 2.20 Posterior capsular incision along the neck.

The approach used by De Buttet and Pasquier (1999) is the posterolateral in precisely the same way as was described in paragraph 2.7.3. The incision is placed on the posterior aspect of the femur and longitudinally along the midline of the femoral neck. This long cut extends from the acetabular margin (incising the labrum) down to the intertrochanteric line and along its margins, as shown in figure 2.20. The resulting flaps are held away from the incision line with the use of retractors without any risk for tissue damage.

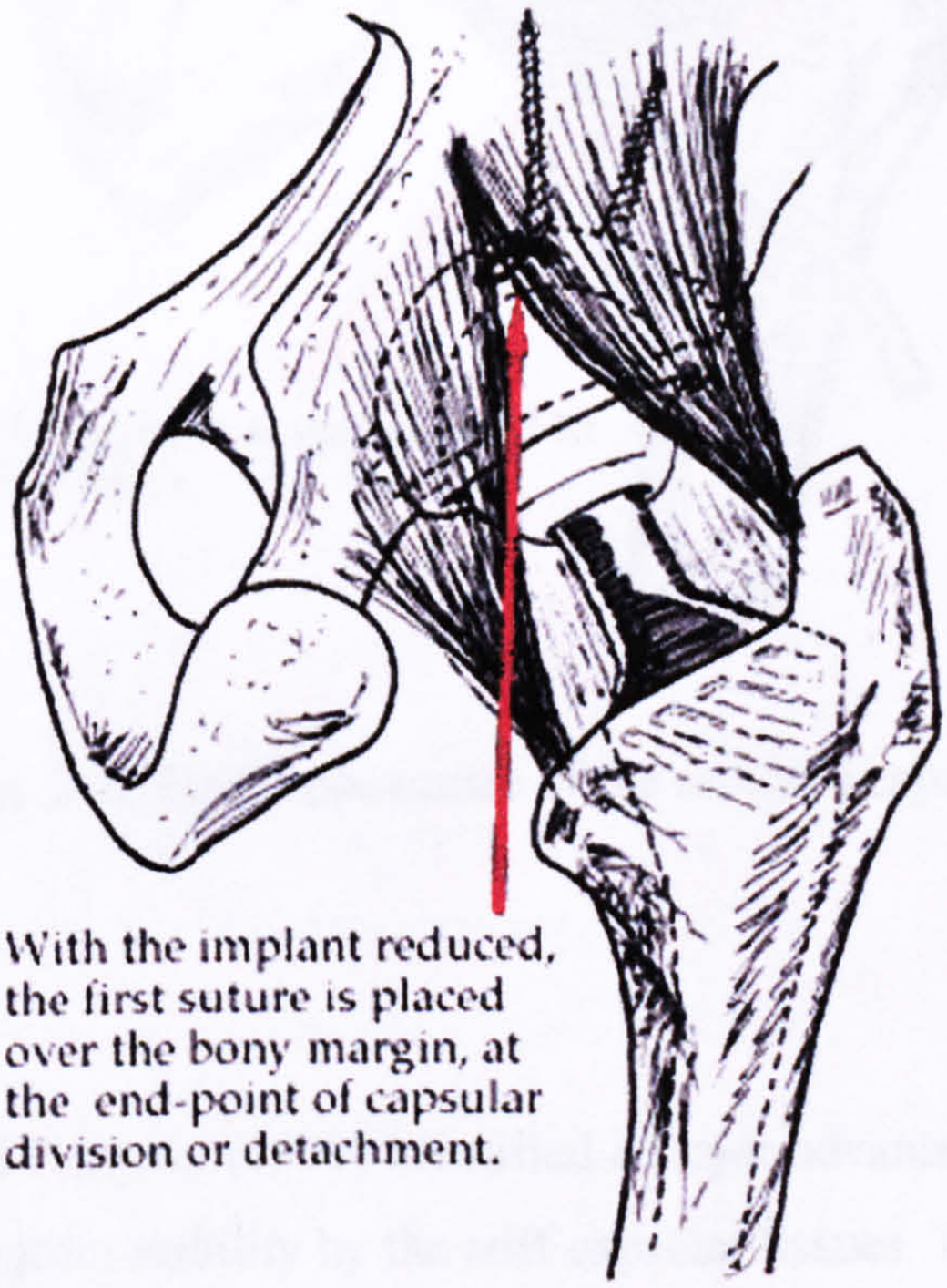

Fig 2.21 Capsular closure with surgical suture.

After the implant has been inserted and the femoral head reduced back into the socket, the capsular repair process can commence. Since capsular tissue is very strong it can be handled with great ease and sutures can be applied without problems (figure 2.21). The first stitches are placed at the acetabular margin and a total of four to five stitches is applied, without suturing the capsule to the femur and leaving a small drain through the suture line (figure 2.22). The recovery process that is involved with this approach is similar to that of any other posterolateral approach and the only adaptation of the patient should be to avoid certain movements until the soft tissues have healed.

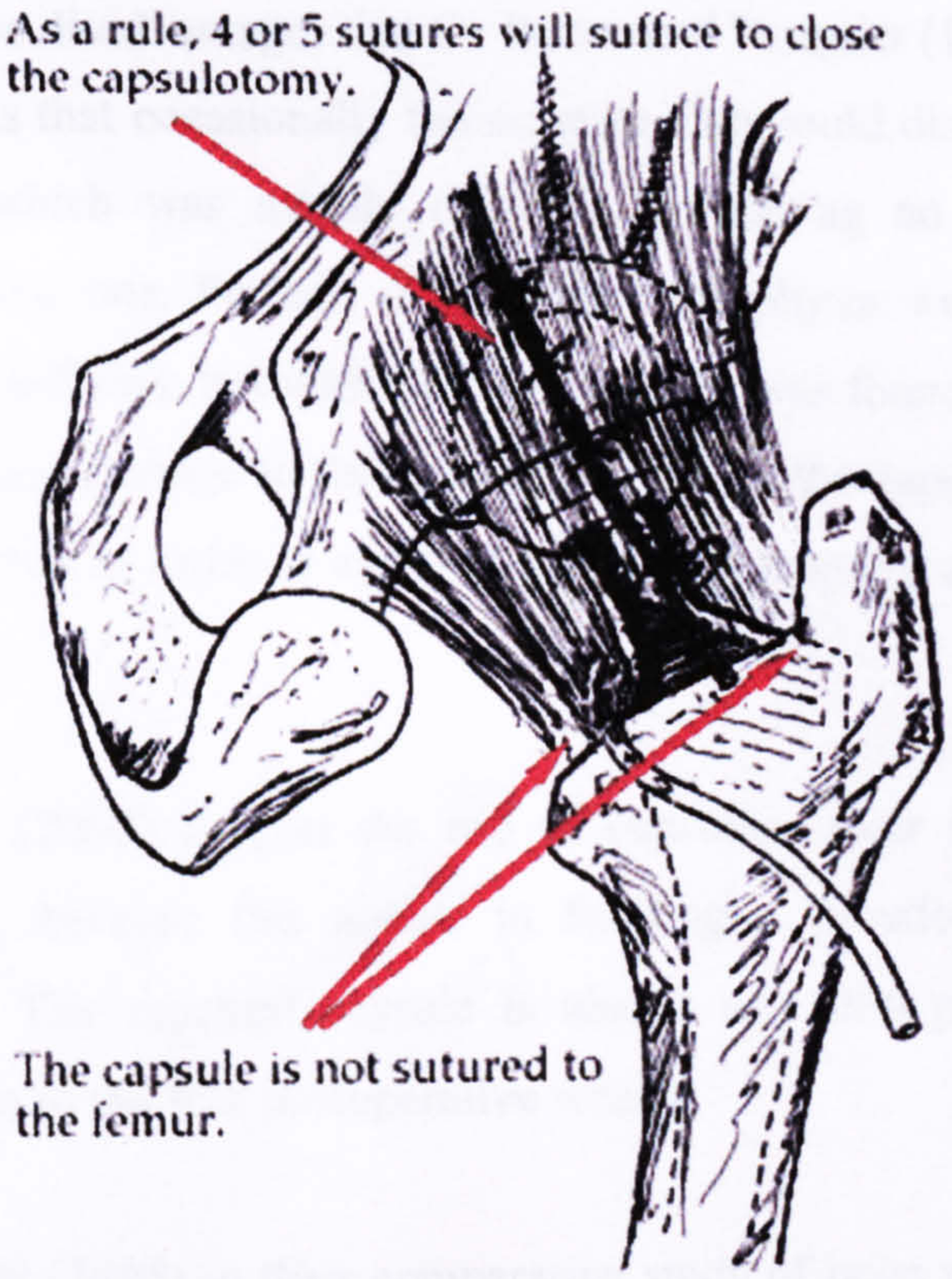

Fig. 2.22 Final appearance of the repaired capsule.

DeButtet and Pasquier (1999) identified a major advantage of capsular repair in the support of the joint stability by the stiff capsular tissues. The good tolerance of the reamers and retractors by the capsular tissues was another motivating aspect they observed, supporting capsular repair. The total dislocations that De Buttet and Pasquier (1999) recorded were in 22 cases of 186 that were performed without capsular repair compared to only one in 174 cases where capsular repair was performed with the above described method. The difference was significant ($p<0.001$). Similar findings were also reported by White et al (2001) with a dislocation rate of 4.8% for the cases where they had completely excised the posterior capsule and only 0.7% in case of a posterior capsular repair.

Amongst the disadvantages that De Buttet and Pasquier (1999) identified with capsular repair was that occasionally the superior flap could disturb clear view into the acetabulum, which was usually resolved by placing an additional incision vertically to the first one. Further, if posterior osteophytes were present, the cup insertion could be difficult, but with additional care it was found possible to remove them without causing damage to the capsule. However, the capsular flaps had to be always well protected in order to avoid injury during reaming and preparing of the acetabulum.

Chiu et al (2000) support the use of capsular repair in case of posterior surgical approach, because this assists in forming a pseudocapsule around the prosthetic device. The repaired capsule is also a soft stop preventing excessive flexion and rotation in the first postoperative weeks.

Lejman et al (1995) in their comparative study of open reduction techniques including capsulorrhaphy and capsulectomy found no significant differences both in the range of motion and stability. An anterior approach was used for the reduction of dislocated hips of children with developmental dysplasia. As a reason for the higher number of re-dislocation in the capsulorrhaphy group it was stated that an anterior tightening of the hip capsule could increase the risk for posterior dislocation. Indeed, if the capsular repair is not done precisely along the incision line, but somehow further, the repaired capsule becomes tighter and affects the range of motion increasing at the same time the risk for posterior dislocation. De Buttet and Pasquier (1999) also proposed that cutting parallel to the capsular fibres, as shown in figure 2.20 could reduce risk of damaging pain-transmitting nerves that were identified in synovial membranes (Grönblad et al, 1985).

2.8 Summary

In this chapter the function and importance of the hip joint capsule to joint stability has been emphasised. This need is now more current than it has ever been with the rising awareness of surgeons to preserve as much bone stock as possible- especially in younger patients- during primary THR. Bone stock preservation means

that ever smaller prosthetic components need to be brought on the market, that facilitate both surgical implantation and also require more conservative bone resection. The more of the original bone anatomy a surgeon wants to preserve the smaller the utilised prosthesis and its components have to be. Such a device is shown in figure 2.23- the Sulzer Thrust Plate®.

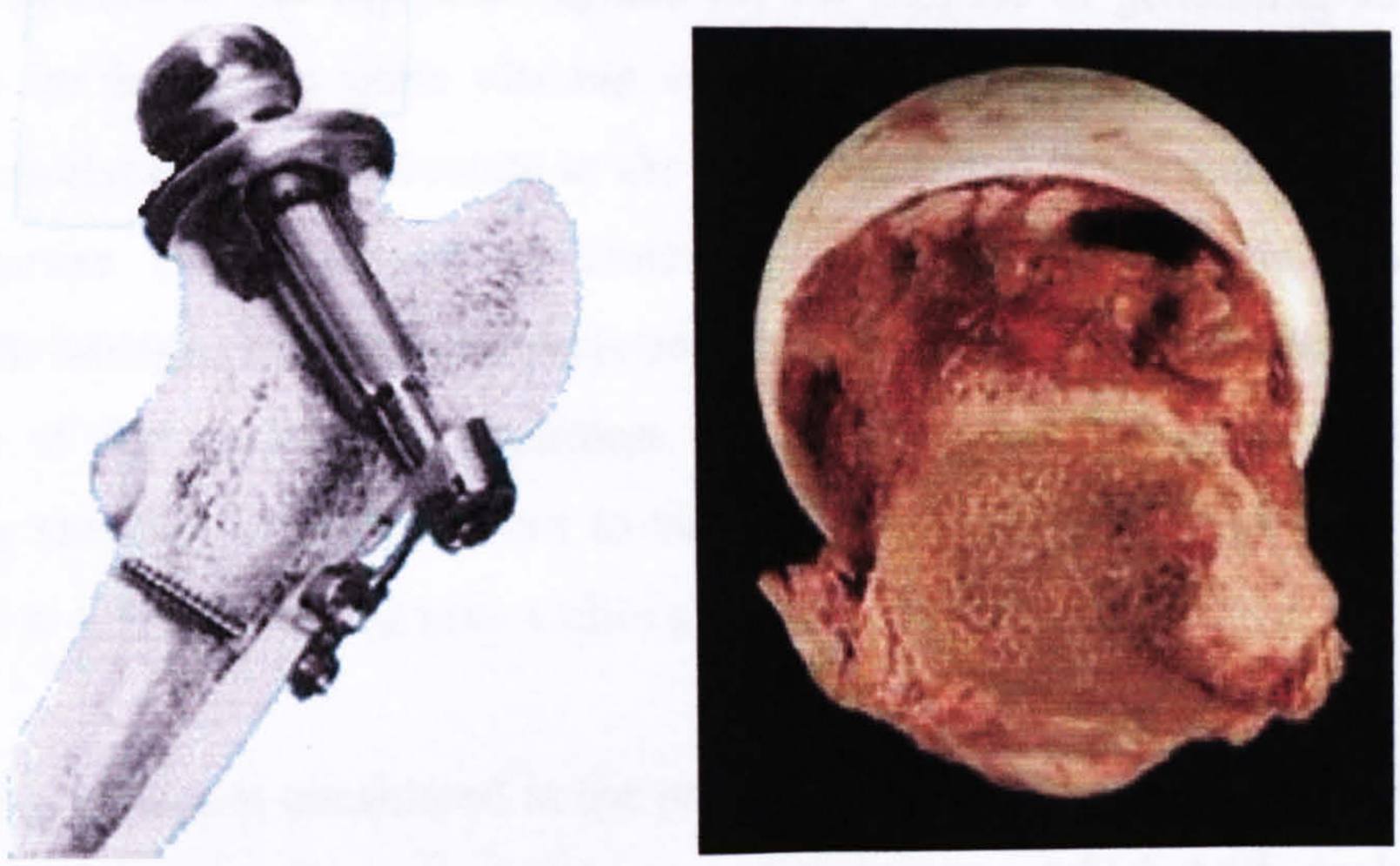

Fig 2.23 The Sulzer Thrust Plate® (left) is a bone stock preserving approach to Total Hip Arthroplasty. An alternative to that is the Birmingham hip resurfacing approach (right).

However, as the size of the prosthetic components reduces, the need for additional mechanical support- like for example from the joint capsule- becomes more apparent. After all it has been shown in the previous paragraphs that smaller head sizes have a higher risk for dislocation, but are often preferred for the smaller amount of wear they produce. This is the undertaking in the next chapters, namely to quantify how much the capsule can contribute to joint stability and how femoral head component size and other prosthesis factors can influence this role.

Chapter 3- Methods of Identifying Tissue Properties

3.1 Introduction

As previously mentioned, the aim of the present study is to determine the mechanical properties of the hip joint capsule for the purpose of generating some information to be fed into a finite element analysis (FEA) program. Every finite element analysis can only be as accurate as the model itself and the definition of the material properties of all critical structures that comprise the model under investigation. In biological or anatomical systems this represents a limiting factor for the credibility of the model and- regardless of the computational power that is employed- one sacrifice or the other has to be made in the characterisation of the model in order to keep processing time within acceptable limits.

In the model that is considered in the present study, there are only two kinds of non-engineering materials present, bones and ligaments, which both include interstitial fluids. Cartilage at the joint interface is of no importance, because contact forces are not part of the intended calculations in the finite element analysis. However, the material properties of the capsular ligaments need to be defined with great accuracy and with a realistic approach, since the calculation of internal loads in each ligament is the main purpose of creating a finite element model of the hip joint. Bone is a much harder and stiffer tissue than ligament and it can be considered as a uniform solid, ignoring its viscoelastic behaviour.

The following paragraphs describe the main characteristics of the above tissues in more detail and give an overview of different approaches for collecting information on their mechanical properties as they were considered for the purpose of this work. Finally, the methodology of choice for data collection in this work is described and defended at the end of the present chapter.

3.2 Parameters of Mechanical Properties

In this paragraph an outline is given of the parameters that define the mechanical properties of a material, such as the ligamentous structures of the capsule. These parameters were determined by the requirements that are set by the FEA software. The software that was used for the simulation- as is described in chapter 6 of this thesis- is IDEAS-8 Master Series of Electronic Data Systems (Plano, Texas, USA). The most commonly required material properties in establishing a materials library for a new material within this software are modulus of elasticity (also referred to as Young's modulus), Poisson's ratio or simply the stress-strain curve.

The elastic or Young's modulus is the ratio of a tensile or compressive stress applied to a sample material over the linear strain due to the applied load. Linear strain can simply be defined as the ratio of length change of a material under uniaxial tensile or compressive load divided by its original length. Shear strain is another dimension that describes the response to shear loads on a material. Shear strain is defined as the ratio of the displacement in the principal load axis over the initial dimension in a direction vertical to the principal load axis. Poisson's ratio (ν) is the negative ratio of lateral to axial strain under uniaxial load applications. For metallic engineering materials this tends to be in the range of 0.28 to 0.32 (Lardner, 1994). However, for soft hydrated tissues (i.e. those tissues that have a high content in water) this value has been estimated at ν=0.5 (Krouskop et al, 1987 and Bilgen and Insana, 1996) as it tends to be volumetrically almost incompressible as a result of the high water content. However, only recently there have been reports that include actual data that was recorded for hip joint capsular ligaments and show a Poisson's ratio of between ν=1.1 and ν=2.0 (Hewitt et al, 2001), which is due to the anisotropy of the ligament tissues. These figures may at first seem excessive, but considering that ligaments are in fact biphasic materials, as is explained in greater detail in paragraph 3.3.4 and that means that apart from the elastic deformation that occurs in the solid part of the tissue matrix, there is an additional volume change resulting from the displacement of interstitial fluid, which forms the fluid phase of the ligament. These combined volume changes result in such a big Poisson's ratio.

The materials that would need to be defined, because they are not included in the software's existing materials library, are both the ligamentous materials of the capsule as well as the bone materials for the femur and the acetabulum. The cartilage material can be disregarded for the particular study, because of its absence in hip joints that have undergone THR. The modulus of elasticity for bone material- Nigg and Herzog (1999) report 1GPa for trabecular bone and 20GPa for compact bone- in relation to those of capsular ligaments (Hewitt et al state 0.1Gpa in their 2001 publication) is greater by orders of magnitude. This allows the assumption that bone can be simulated as a linear and homogeneous engineering material, with an elastic modulus the order of magnitude of up to 20GPa. This assumption is justified, because the loads that are applied by the ligaments during the numerical analysis are so small. In reality it would be the muscle forces that act around the hip joint, which would produce sufficient moments to cause a deflection of the bones they insert into. However, muscle forces are not considered in the present model and therefore, deformation of the bone structures can be ignored. The fact that basic engineering materials are assumed to have no viscoelastic properties presents no limitation either, since the duration of load application in the simulation is not enough to cause any viscoelastic effects on the bone tissues. Also, the limited effect of the load that is to be applied on the joint model, allows the assumption of bones being homogeneous. Therefore bones can be modelled as uniform solids, without distinguishing between compact and trabecular bone. All assumptions that were made for the simulation of the bone material are also discussed in more detail in chapter 6.

A good approximation of the ligamentous material properties- in the contrary- is of great importance, because the loads transferred by the ligaments depend on these properties, and further, because the quality of ligament simulation determines to a great extent the effect that can be observed in the numerical analysis. The following paragraphs outline the current state of research in the determination and simulation of the materials properties of ligaments and also describe the efforts made within the present project to find a suitable method of defining the properties of the hip joint capsule ligaments.

3.3 Theories in Soft Tissue Mechanics

Biological tissues in contrast to engineering materials cannot be described mathematically with quite the same ease. That is, because they are time and moisture dependent and also undergo metabolic changes that affect their mechanical properties and that relate to sex, age and levels of activity of the humans they are excised from. Various research centres have produced numerous approaches for the simplification of ligament material properties for use in finite element analysis software packages, without altering their basic behaviour under load excessively. Thereby, the main features of soft biological tissues are the main consideration. These features of soft biological tissues, and indeed all biological tissues- indicate that none of them can be described as Hookean solids for the following reasons:

Biological tissues are viscoelastic, anisotropic and non-homogeneous materials, unlike most common engineering materials. This means that they undergo stress-relaxation, creep and hysteresis and that their structure is not the same in all directions. Furthermore, strain history and rate of load application influences the performance of viscoelastic materials and can only be simulated with great difficulty. These features represent the major difficulty when studying a biological model in a computer simulation such as FE analysis. Hence, simplifications of the mechanical properties of soft tissues are necessary, as to reduce the immense calculating power that is otherwise required from a computer.

Simulating viscoelastic behaviour in a desktop application is a tremendously difficult objective that sets high requirements for the computational power and was beyond the possibilities of the present work. However, even when simulating material properties as not time dependent, it is the linearity or non-linearity that places further restrictions on the computational power as well as the isotropy or anisotropy of the materials. Based on the current computational standards it is only possible to either simulate material properties of ligaments as:

- Non-linear elastic and isotropic or
- Linear elastic and anisotropic

3.3.1 Linearity and Isotropy

The following analysis, which was proposed by Saada (1974) aims to describe a simplification for ligament materials and treats biological tissue as a Hookean elastic solid. The stress- strain relation is given by the following equation:

$$\sigma_i = c_{ij} e_j \qquad (3.1)$$

σ_i is the stress tensor and e_j the strain tensor. Both i and j can take values between 1 and 6, because the stress equations are proportional to all six strain components. This results in the extended formulation that is shown in equation 3.2. C_{ij} is a tensor of elastic constants that are unique for each material and independent of stress or strain. It turns out that due to symmetry $C_{12} = C_{21}$, $C_{13} = C_{31}$ etc. This means that the initially 36 elastic variables reduce to only 21. The elastic tensor C_{ij} can be simplified even further, if the material under consideration can be considered orthotropic. In that case the constants can be reduced to 9 and the elastic tensor becomes as shown in equation 3.2b. Thereby $C_{14}=C_{15}=C_{16}=C_{24}=C_{25}=C_{26}=C_{34}=C_{35}=C_{36}=C_{45}=C_{46}=C_{56}=0$.

$$\begin{bmatrix}\sigma_1\\ \sigma_2\\ \sigma_3\\ \sigma_4\\ \sigma_5\\ \sigma_6\end{bmatrix} = \begin{bmatrix}C_{11} & C_{12} & C_{13} & C_{14} & C_{15} & C_{16}\\ C_{21} & C_{22} & C_{23} & C_{24} & C_{25} & C_{26}\\ C_{31} & C_{32} & C_{33} & C_{34} & C_{35} & C_{36}\\ C_{41} & C_{42} & C_{43} & C_{44} & C_{45} & C_{46}\\ C_{51} & C_{52} & C_{53} & C_{54} & C_{55} & C_{56}\\ C_{61} & C_{62} & C_{63} & C_{64} & C_{65} & C_{66}\end{bmatrix}\begin{bmatrix}\varepsilon_1\\ \varepsilon_2\\ \varepsilon_3\\ \varepsilon_4\\ \varepsilon_5\\ \varepsilon_6\end{bmatrix} \qquad (3.2)$$

This is because an orthotropic material has by definition two orthogonal planes of symmetry, where material properties are independent of direction within each plane. The 9 elastic constants in orthotropic constitutive equations comprise three Young's moduli Ex, Ey, Ez, the three Poisson's ratios ν_{yz}, ν_{zx}, ν_{xy}, and the three shear moduli Gyz, Gzx, Gxy. Isotropic materials have a further reduced array of elastic constants and the tensor can be expressed quite simply as a function of only two elastic constants E (elastic modulus) and G (shear modulus). These elastic constants are in the following relation to each other: $E = 2G(1+\nu)$.

Considering the structure of ligaments (figure 3.1) it is easy to accept that ligaments can be described as transversely isotropic as has been proposed among others by Hearmon (1961) as well as Almeida and Spilker (1998). This means that the materials properties of ligaments are substantially similar along the two axes that run perpendicular to their long axis that is along the collagen fibres (see arrows in figure 3.1). Therefore the assumption that ligaments are isotropic materials can be made with greater ease than assuming they were characterised by linear behaviour. Hence, the preferred ligament material characterisation between those proposed in paragraph 3.3 would be as an isotropic and non-linear elastic material.

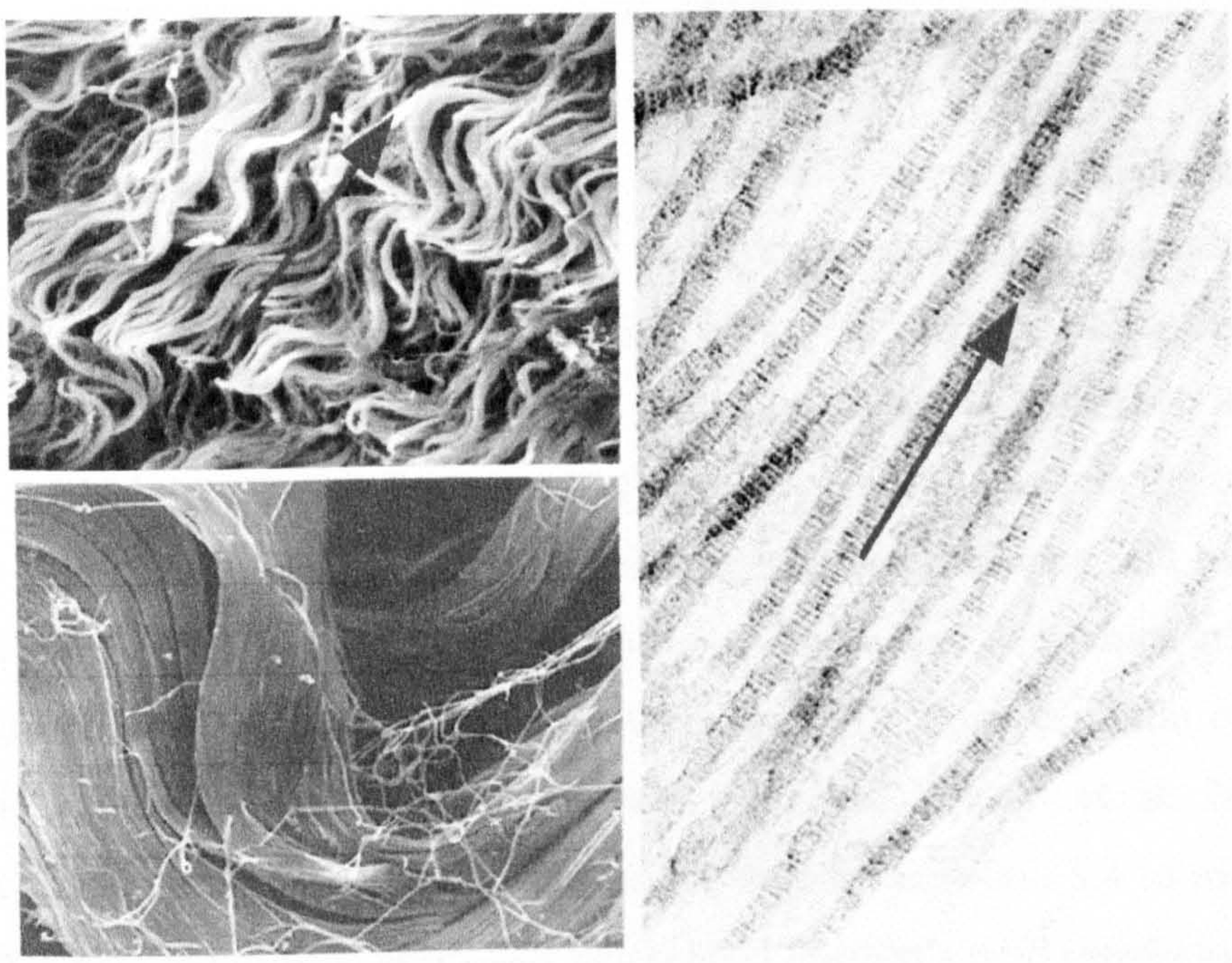

Fig 3.1 The distribution of the collagen fibres is along a single axis as indicated by the arrows.

As will be demonstrated in the following paragraphs a number of both invasive and non-invasive methods for determining mechanical tissue properties were reviewed. Both methodologies involve compression tests in their approach, which means they yield data somewhat different from that commonly produced in ordinary tensile material tests. Therefore it is necessary to establish a connection between the materials properties in vertical and longitudinal direction of the tested

ligaments. This link could be established by using the relation that exists between the shear modulus and the elastic modulus (also called Young's modulus)

$$G = \frac{E}{2(1+\nu)} \qquad (3.3)$$

where G is shear modulus, E the elastic modulus and ν Poisson's ratio, which could be taken as 0.5 for the case of soft hydrated (that means high concentration of water) biological tissues. This would result in the following equation:

$$G = \frac{E}{3} \qquad (3.4)$$

This means that Young's modulus can be established, as long as the shear modulus can be calculated by using any of the methods that are outlined further below. In particular, for the case of using ultrasonic methods to determine the velocity of shear waves within the tissue under investigation, technically the shear modulus could be produced. Equation (3.4), however, is valid only in the case of an isotropic solid, which means that this assumption or generalisation will have to be accepted in order to allow for a 'squeeze' or compression test to produce information on the elasticity of a material. Furthermore, in case of a Poisson's ratio other than 0.5, which in more recent studies has been proposed (Hewitt et al, 2001), the equation would change accordingly. This means that for equation 3.4 to maintain its validity it is required to have previously determined Poisson's ratio satisfactorily.

3.3.2 Quasi-Linear Viscoelasticity

Another description for simplification of viscoelastic material properties was proposed by Viidik (1996) and sustained by Fung (1993). This approach- labelled quasi-linear viscoelasticity (QLV)- is based on a series of linear Kelvin type models (third and fourth row in figure 3.2). The participating springs in this model increase as the total strain rises, much in the same way in which an increasing number of collagen fibres would participate in the resistance as strain was progressing. Therefore in the QLV model, the spring elements' stiffness is non-linear, as it

depends on the total deformation, which again depends on the number of springs that are placed under tension at any given time. In the case of very small or quasi static deformations, the model can be described by a linear viscoelastic function. In the contrary, for larger deformations, as they occur in joint ligaments during limb movement, the non-linear stress-strain properties of living tissues gain more importance. This explains the principles of QLV, which depends on the individual spring elements' extent of deformation.

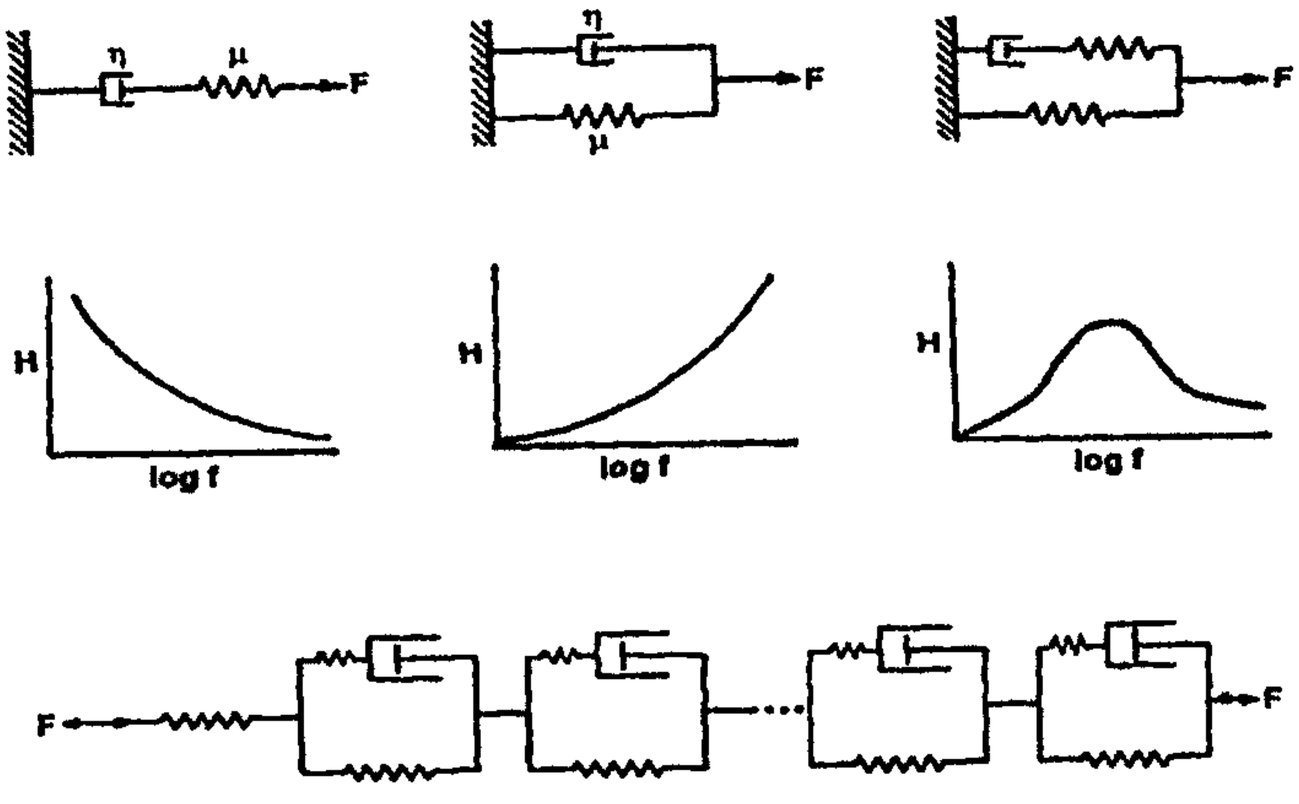

Fig 3.2 Rows 1 and 2 show various viscoelastic models. On the left is a Maxwell model, in the centre a Voigt model and on the right is a Kelvin model. In row 3 is the spring and dashpot model for viscoelastic biological tissues (Fung, 1993).

The fundamental justification of the quasi-linear viscoelasticity theory lies in the fact that the result of the individual spring units' (collagen fibres) loading and unloading cycles add up to a total hysteresis response. This effect is due to the fact that the elastic component of a neighbouring spring element acts faster than the relaxation of its counterpart damping element. In this way the time dependent response to externally applied loads can be achieved in the model, which is in accordance with the observed behaviour of soft tissues.

3.3.3 Pseudo Elasticity

The theory of pseudo elasticity is another attempt to further simplify the constitutive equation that describes the behaviour of any given tissue in mathematical terms. It can be considered the next step to the quasi-linear viscoelasticity theory. To apply this theory to a tissue it is necessary to assume that it is in a preconditioned state. This means that the tissue must have previously been loaded and unloaded in a sufficient number of cycles. This assumption is generally valid, when considering capsular ligaments, where a preconditioning occurs after the first few cycles of loading have been performed during the first cycles of walking. The preconditioning effect subsides thereafter, only if a long resting period of the ligaments in neutral position is taken. However, once the tissues have been preconditioned it is generally observable that the stress-strain curves between loading and unloading come closer together than in the first few cycles (figure 3.3). This is the result of stress relaxation that occurs with all viscoelastic materials.

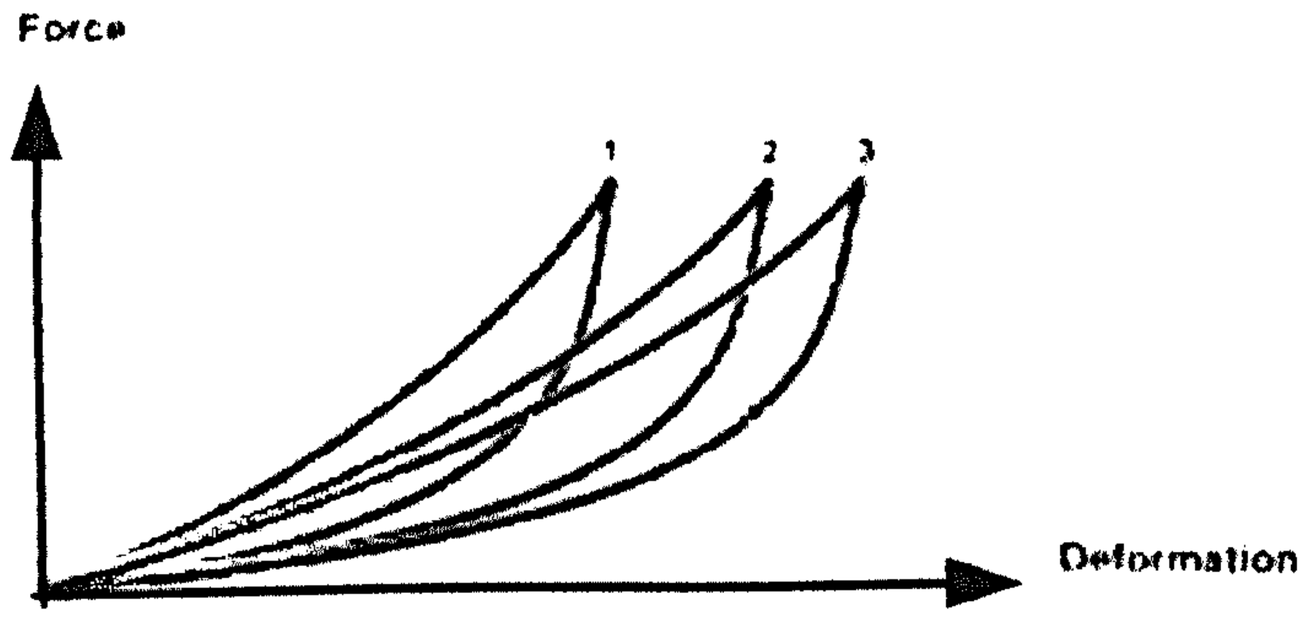

Fig 3.3 Force-deformation graphs after repeated loading-unloading cycles (Nigg and Herzog, 1999).

Based on the assumptions of the pseudo-elasticity theory it is possible to apply two individual material properties for each of the ligaments, one for the loading cycle and another during unloading. That would mean that the same individual ligaments can be treated as two different materials, based on the loading situation. Each of these individual materials can be then treated as elastic. Attention has to be paid to whether a ligament is loaded or unloaded when simulating limb movements in the numerical software environment, distinguishing loading from unloading.

From the review of the pseudo elasticity theory it arises that this is a convenient simplification of the complicated viscoelastic formulation of soft tissues into a simpler elastic formulation. The conclusion is that an easy approach for the numerical simulation of ligaments is to characterise them as non-linear elastic isotropic materials. Still, the modelling of non-linear material properties of soft tissues is a complex matter to be applied in a computer model, and various efforts have been made in the past to overcome this without resulting in a commonly accepted methodology.

3.3.4 Biphasic Theory

The theory of biphasic tissues was first described by Mow et al (1980) and involves modelling of the tissues as a mixture of fluid (interstitial ligamentous fluids) and non-compressible solid, which mainly represents the protein composites of the tissue. The time dependent response of this composite material to load, is achieved by the resistance to the flow of the fluid component within the porous structure of the composite. Apart from the fluid part of the composite it is also assumed that the solid component is incompressible, but that it is linear elastic in tension. By applying appropriate boundary conditions the directions of fluid flow can be manipulated in such way that a desired friction with the porous solid matrix can be achieved, producing the required time dependence.

Under consideration of the computational restrictions that exist, and because of the existing models that simulate the soft tissue behaviour, it seems easiest to model soft tissues as isotropic and non-linear elastic materials within the FEA software.

3.4 Non-Invasive Methods

The advantages of using a non-invasive method for determining mechanical properties of the ligaments, are two-fold. Firstly, there is no risk of infections involved resulting from cuts that are necessary to access the usually deep lying ligaments. Secondly, the ethics involved in non-invasive procedures are much simpler as there are no permanent effects from applying this technique on volunteers. The required ethical approval for using such technique would be much simpler and

the chances of getting consent from volunteers would be higher. Thus, it seems that a non-invasive method would be the approach of choice, however, the feasibility, usefulness and accuracy of such an approach has certain limitations. A number of non-invasive techniques that were reviewed for their suitability in the characterisation of the capsule ligaments are presented in the following paragraphs.

3.4.1 Mechanical Indentation

One of the major complications and restrictions in the challenge to develop an appropriate method for determination of the mechanical properties of the hip joint capsule, is the fact that it is a deep lying tissue. A vast volume of muscle bulk and other soft connective tissue is overlying it and make an external procedure very difficult (figure 3.4). It is obvious that any externally provoked mechanical indentation would have the fate of losing its effect when reaching the depth of the capsule due to effects of dissipation in the surrounding tissues. It is extremely difficult to calculate what ratio of the externally applied load would eventually reach the surface of the capsular ligaments. For this reason there have been mathematical algorithms developed to help calculating the local load (Ponnekanti et al, 1992), but they tend to be rather vague.

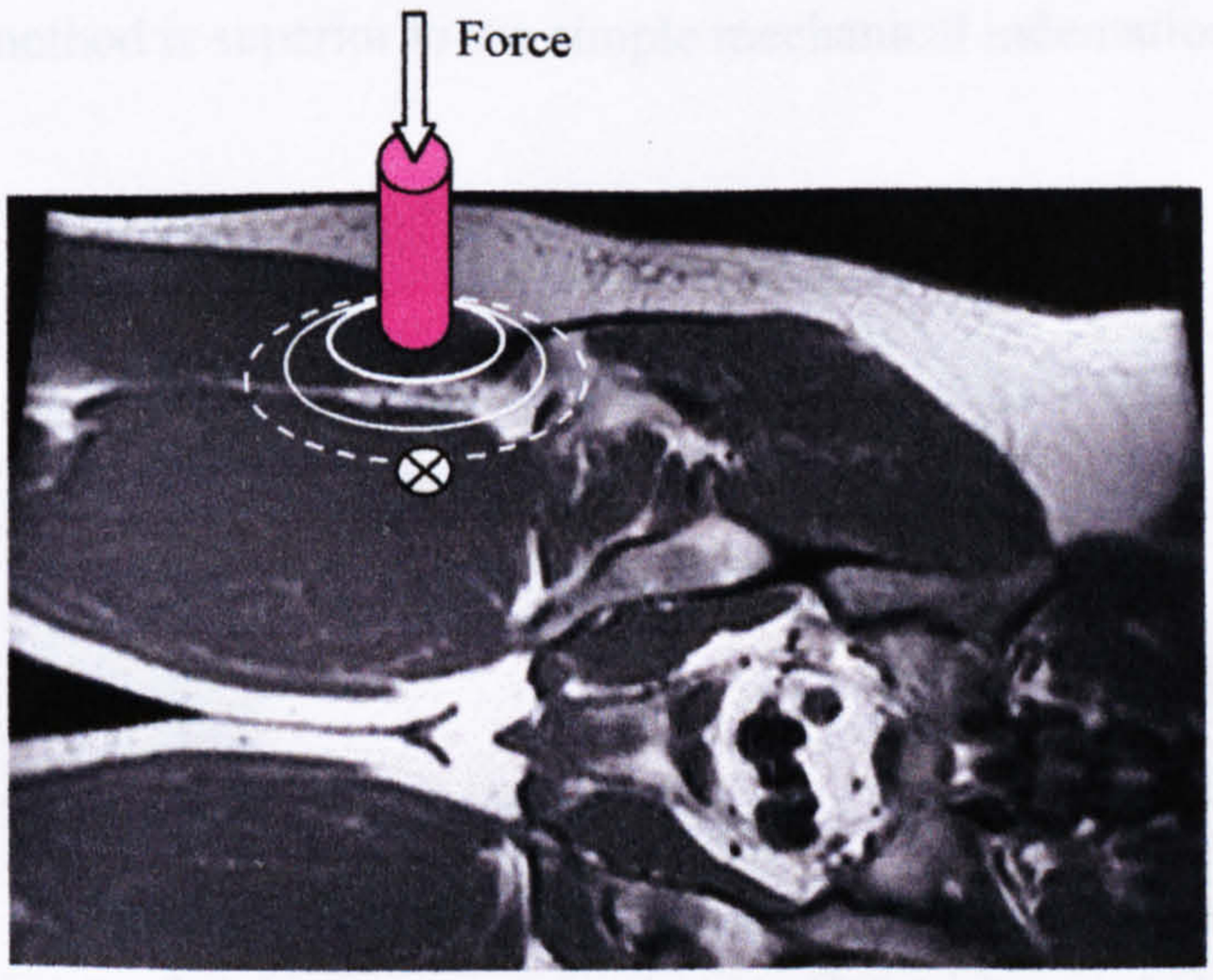

Fig 3.4 Force applied over the area of the hip joint capsule, thereby depressing skin, fat and muscle tissues as well, scattering the external load randomly.

Torres-Moreno (1991) described a mechanical indentation device for use in residual limbs of amputees. The mechanical indenter in that study was used to determine the mechanical properties of the underlying tissues as a composite mix structure. However, for the mechanical properties of the capsule ligaments, this represents an unacceptable approximation, because it fails to accurately determine the strain that is induced on the capsule ligaments by the external load. Instead, strain is taken as equal to the displacement of the indenter that is observed externally, ignoring phenomena of displacement dissipation within the various underlying tissue layers. The use of such simple mechanical indentation device for the purpose of determining the elastic moduli of the capsular ligaments was subsequently discarded, because both stress and strain could not be characterised satisfactorily.

3.4.2 Ultrasonic Elastography

Ultrasonic elastography is based upon the theory that the elastic properties of any material are dependent on its ultrasonic properties like the velocity at which sound waves are propagating within it (Maaß and Kühnapfel, 1999). Thereby the determination of the mechanical properties can be achieved by applying some kind of external stimulus of known extent and by recording the resulting internal tissue motions at the site of interest by using ultrasonic transducers (figures 3.5 and 3.6). Therefore this method is superior to the simple mechanical indentation technique.

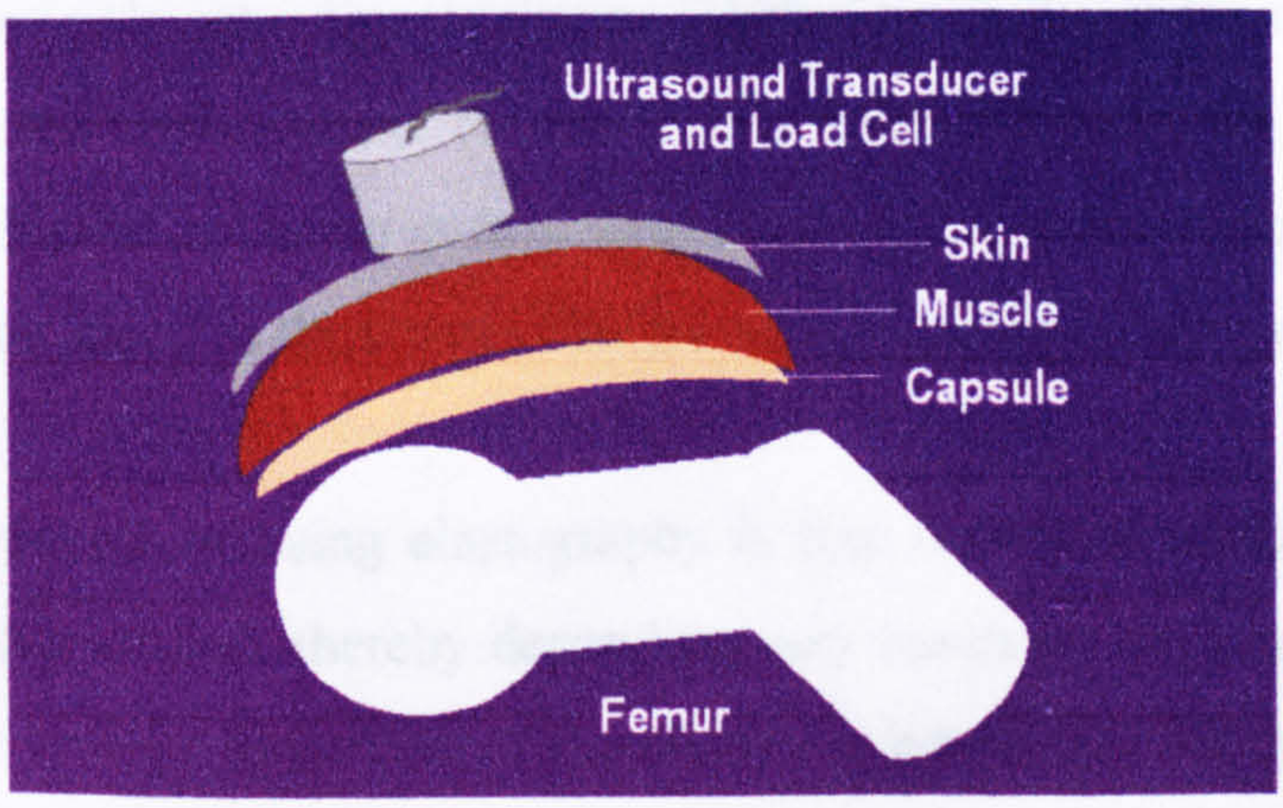

Figure 3.5 The external load is applied and recorded by the load cell and can be picked up by the ultrasound transducer for each tissue layer separately.

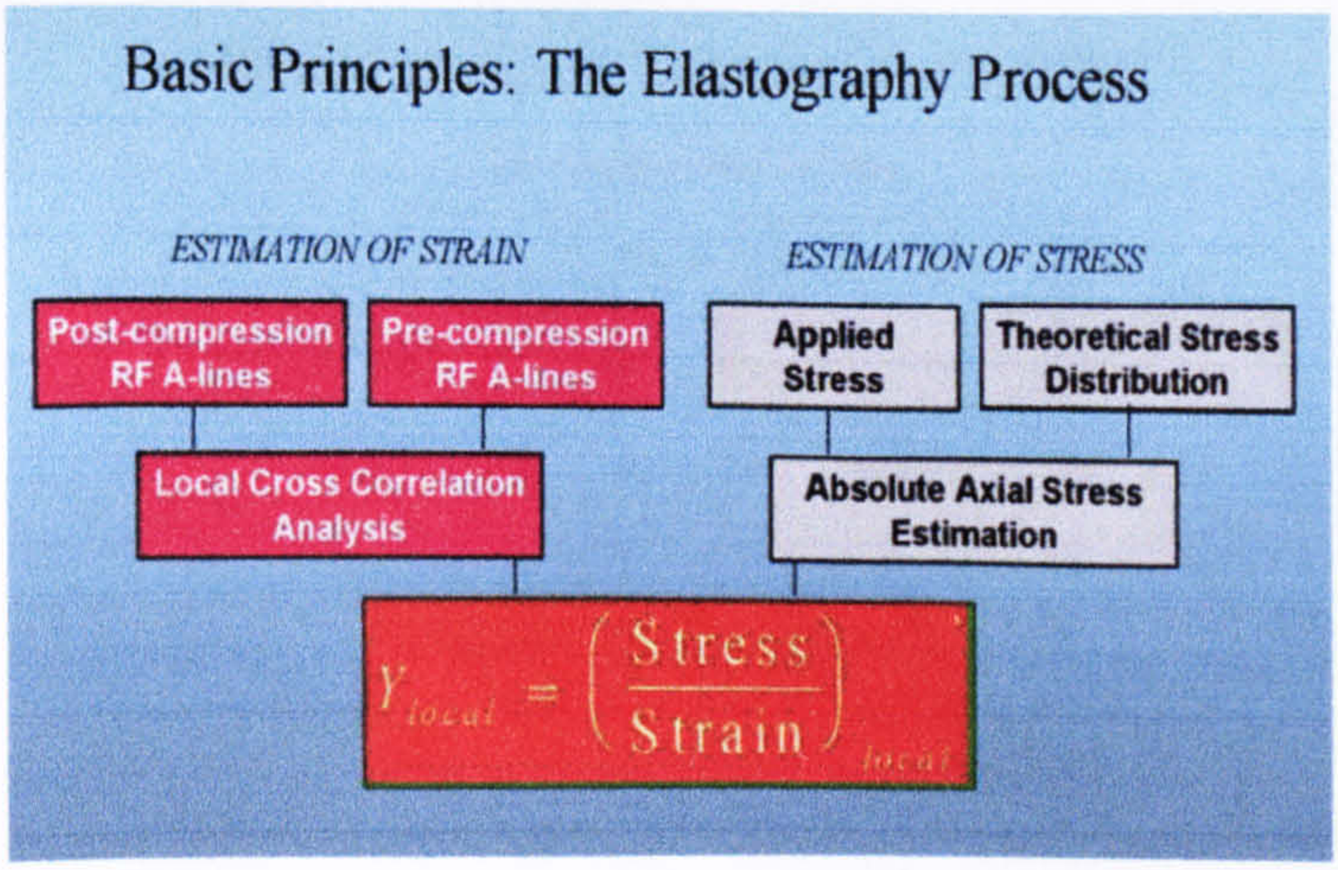

Figure 3.6 Stress and strain estimation and calculation of local elastic modulus in elastography.

Several methods of propagating an external mechanical stimulus to the internal tissue structures under investigation have been proposed in the past. These can be grouped into two basic categories. In the first category, the tissues are compressed quasi-statically and the resulting strains are calculated using ultrasonic techniques as has been described by Ophir et al (1991). In the second category the tissue deformation is achieved by applying a low frequency vibration to the tissues of interest and subsequently registering their behaviour. This technique has been described extensively by Yamakoshi et al (1990). The strain that is induced by applying quasi-static compressions is estimated by calculating time delays between the A-mode ultrasonic echo signals that are picked up in the states of pre and post-application of the deformation (figure 3.7). Strain imaging for low-frequency vibrations is achieved by using colour Doppler imaging methods to measure shear wave propagation speed in the tissues that are set in vibration (Ophir et al, 1996).

The advantage of using elastography is that local mechanical properties of tissues can be determined, thereby depending very much on the size of the utilised ultrasonic probe and the dispersion of the ultrasonic waves into the overlying tissues. Another important advantage of this method is that the load application can be kept very brief, thereby reducing the viscous effect of the tissue and only considering the elastic proportion of its resistance.

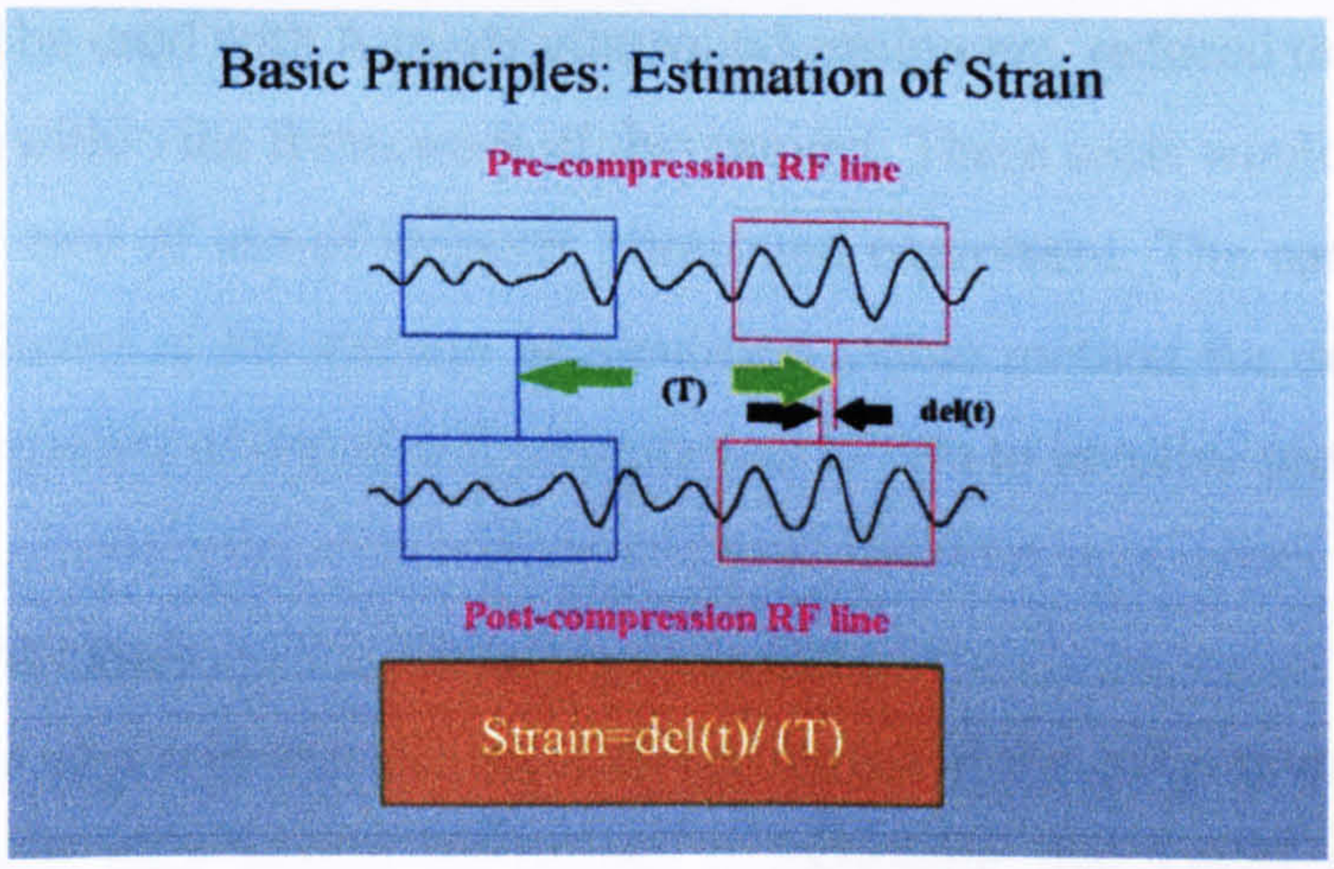

Fig 3.7 Explanation of strain estimation in elastography.

The disadvantages of this method include the limitation that only 'squeeze-tests' can be applied, which is a common procedure in impact testing for material hardness, but does not represent common practice in elasticity testing (Maaß and Kühnapfel, 1999). This would mean that the approximation expressed in equation (3.4) would be necessary for producing the elastic modulus, which reduces the accuracy of this method. The accuracy of the tracking system that is used to determine the tissue site that is set into vibration externally is another limiting factor of this technique. As the calculation of the induced strain relies on ultrasonic image representations of the investigated tissues, they are often subjected to the presence of imaging artefacts and heavily rely on the quality of applied image processing techniques. The determination of stress largely depends on the use of mathematical algorithms as it is largely unknown how the externally applied load disperses within the various tissue layers (Ponnekanti et al, 1992).

3.4.3 Limitations of Non-Invasive Methods

It has been explained that elastography has a greater potential to produce reliable data on the mechanical properties- elastic moduli in particular- of capsular ligaments, when compared to the mechanical indentation technique that was presented in the previous paragraph. Nonetheless, the need for theoretical models for the estimation of the absolute local stress at the capsular ligaments (figure 3.6) means that this technique is still subject to modelling errors. Additionally, the costs that are involved in developing a probe comprising the ultrasonic transducer and the load cell

that could then be used with A-mode ultrasound equipment, reduced the applicability of this method within the framework of this project. These costs would be, naturally, even higher in case of use of Doppler ultrasound equipment. The natural next step that was considered in the attempt to identify a viable method for determining the mechanical properties of capsular ligaments was to turn to invasive methods.

3.5 Invasive Methods

It seems apparent that the most direct approach for collecting useful *in vivo* force-deformation data would be to use a technique that could perform these measurements at the direct site of interest, i.e. the hip joint capsule. The sole possibility that exists to have the capsular construct exposed *in vivo* would be during total hip replacement surgery, immediately prior to its removal that is required to allow access to the diseased joint. Care would need to be taken that the capsule itself was not affected by any disease. The following paragraphs outline possible methods that the author identified during the course of his research for the collection of purposeful data on the mechanical properties of the capsule.

3.5.1 Intra-operative Elastography

The proposed method that was described in paragraph 3.4.2 forms the basis of this technique, which was considered as an evolution of non-invasive ultrasonic elastography. The problem of applying algorithms for the estimation of local stress at the capsule site, but also to simplify the strain recording, making RF echo pattern analysis (figure 3.7) redundant.

3.5.2 Impression Technique and Tactile Sensors

This method is based on the shift in resonance frequency that occurs to a vibrating rod when it comes into contact with another object under the application of a force:

$$F(t) = F_{st} + F_a \sin \omega t \qquad (3.5)$$

with a static component F_{st} and an alternating component $F_a \sin \omega t$, which brings the cylindrical rod into oscillation at the resonance frequency (Kleesattel and Gladwell, 1968).

The degree of resonance shift has been found to be related to the material properties of the object that comes into contact with the rod (Omata and Terunuma, 1992). In particular it is surface hardness that is determined by this frequency shift, whereby a soft surface causes a higher frequency shift than a hard surface. The advantage of using tactile sensors, rather than strain gauges and resistive sensor devices is that even very soft tissues cause some change in vibration frequency as soon as they get into contact with the indenter, without the need of large deflections.

3.5.2.1 Function of the Tactile Sensors

The configuration of such a tactile sensor system has been described by Lindahl et al (1998) and consists primarily of a ceramic piezoelectric transducer made of lead zirconate titanate (PZT) and a vibration pickup (figure 3.8). Applying an alternating voltage causes the PZT to vibrate in a free manner. The vibration pickup records the frequency of the vibration and feeds this information back to the circuit, which then regulates the vibration frequency to equal the resonance frequency (f_0) of the tactile sensor. When the end of the transducer is pressed against another object the vibration frequency changes. The magnitude of this shift depends on the acoustic impedance of the object in contact (Ingard, 1988). One use of this shift of frequency has been proposed by Lindahl and Omata (1995) (see appendix I):

$$z_x = \frac{force}{velocity} = \alpha + j\beta \qquad (3.6)$$

where z_x represents the acoustic impedance of the object in contact with the sensor, comprising a real part α (acoustic resistance) and an imaginary part β (acoustic reactance). The shift in frequency (Δf) may also be represented as:

$$\Delta f = f_x - f_0 = f_x - \frac{\omega_0}{2\pi} = - \frac{u_0 \beta}{2\pi d z_0} \qquad (3.7)$$

where u_0: equivalent sound velocity in the sensor, l: the length of the PZT rod and z_0: the equivalent impedance of the complete sensor. Reactance (β), however, according to Eklund et al (1999) comprises a mass load part (ωm) and a stiffness part ($\frac{k}{\omega}$):

$$\beta = \omega m - \frac{k}{\omega} \qquad (3.8)$$

with ω being the angular frequency of the sensor's oscillation, m the mass load and k the stiffness. These values can be represented as:

$$m = \frac{\rho \pi^{3/2}}{10(1-\nu)} h^3 \qquad (3.9)$$

$$k_x = \frac{2E}{(1-\nu^2)} h \qquad (3.10)$$

In the equations (3.9) and (3.10), h is the penetration depth of the transducer tip (with a radius of r) into the contact object (figure 3.8), ρ is the object's material density, ν its Poisson's ratio and, finally, E its Young's modulus.

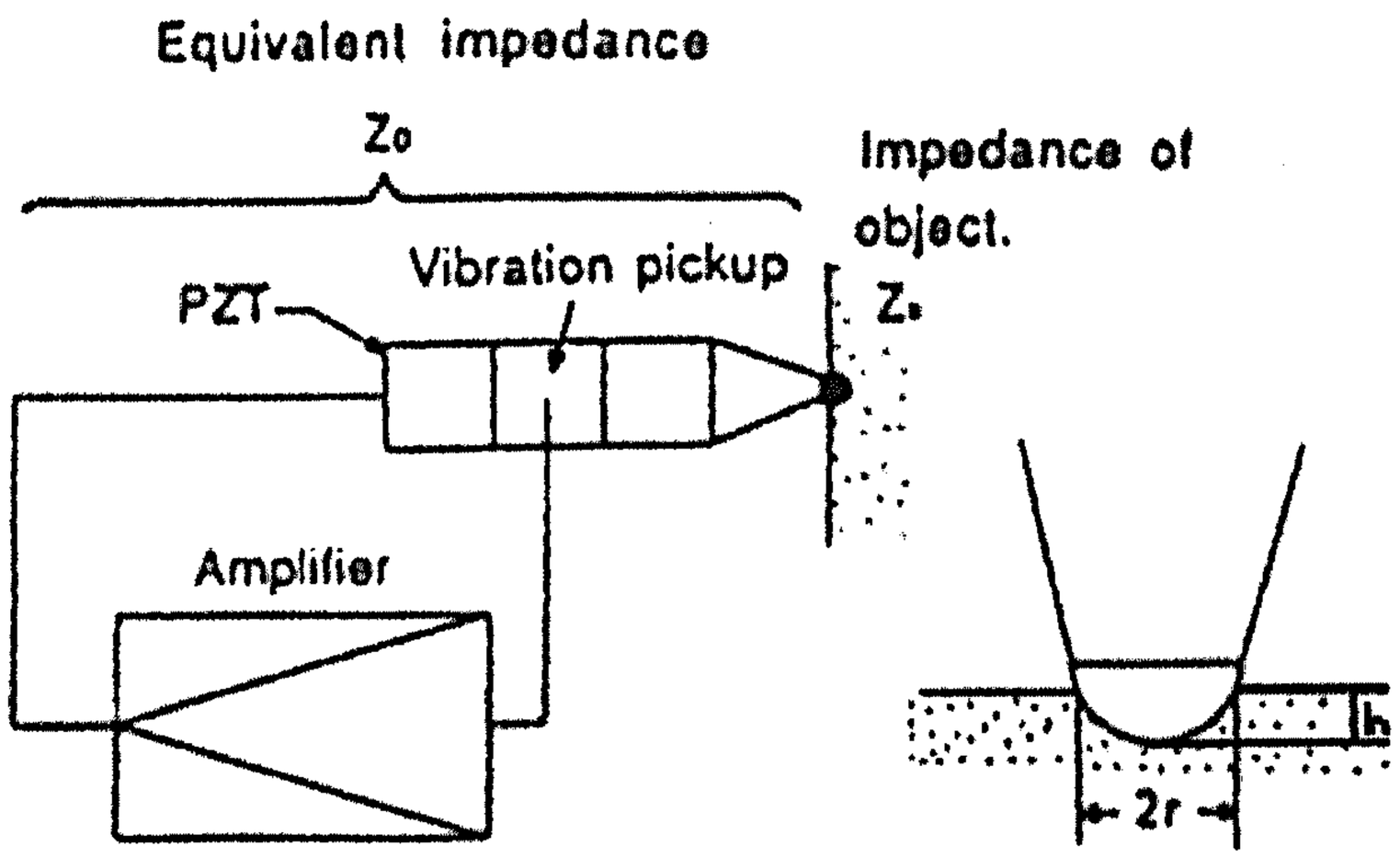

Fig 3.8 Explanation of the tactile sensor showing dependence on acoustic impedance. The sensor tip's penetration depth into the tissue (Lindahl and Omata, 1995).

Depending on the hardness of a tissue, the penetration depth of the sensor tip into the tissue is small. If this penetration depth can be kept such that h<<r , then the effect of the mass loading part (m) remains small, because h is in a cubic power in equation (3.9), but the effect of stiffness (k_x) loading increases based on equation (3.10). In extreme cases Lindahl and Omata (1995) considered that m→0. In that case the resonance frequency shift is described by:

$$\Delta f = \frac{1}{2\pi^2}\left(\frac{k_\chi}{z_0}\right) \qquad (3.11)$$

by substituting equation (3.10) for k_x in equation (3.11) and solving for elastic modulus (E) equation (3.12) is the result

$$E = \frac{\omega \cdot \pi \cdot l(1-\nu^2) \cdot z_0 \cdot \Delta f}{h} \qquad (3.12)$$

By looking at equation (3.12) one realises that utilising the tactile sensor is capable of producing information on local Young's modulus, depending on the frequency shift recordings. However, a major drawback in this method is the requirement that h<<r, for equation (3.12) to be valid. Otherwise, it is not possible to produce Young's moduli as frequency shift in that case is solely depending on mass loading effects, which in turn do not depend on Young's modulus. Determining whether or not h is much smaller than r is very subjective and represents a potential source of error. Furthermore, it means that an additional instrumentation is required that can measure the value of h.

3.5.2.2 Different Designs

The individual needs of the various researchers have lead Axiom (Axiom Co Ltd, Koriyama, Japan) to release numerous different types of their tactile sensors, each one with another key feature. For the present work two designs were considered, namely the Venustron™ (figure 3.9a) and the Pen-Type™ (figure 3.9b). The reason why the Pen-Type was considered initially, was due to its advantageous

shape, which would allow access to the hip joint capsule through the very limited space that is available through the bulk of muscle tissues. Also, the neatness of its design that includes all the electronic wiring within a metal casing, would easily make it possible to be encapsulated in a sterile bag. However, the absence of a pressure sensor meant that this design could only be used for identifying differences between two measurements qualitatively. A quantitative evaluation of the displacement recordings could thus not be achieved with this system type. In particular, the absence of pressure recordings meant that a fundamental feature for the determination of the elastic modulus- namely stress- remained unknown. Therefore, despite its suitable design that would enable a relatively accurate placement of the sensor over the capsular ligaments immediately prior to the surgeons incision to the capsule, it was discarded for use in this study.

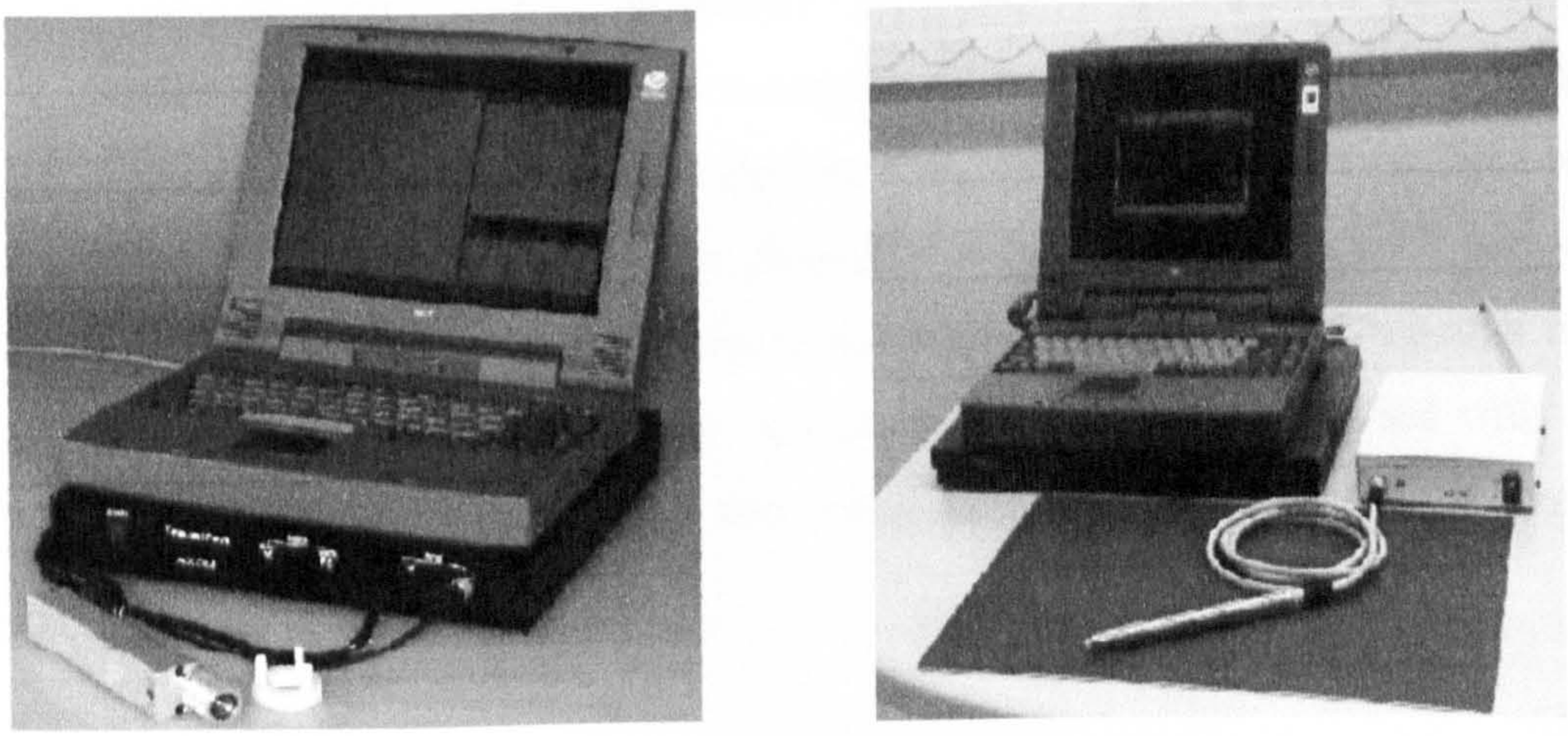

Figure 3.9a and b The Venustron™ and Pen-Type™ Axiom tactile sensors.

In contrast to the Pen-Type™ system a pressure sensor is incorporated in the probe of the Venustron™ system (figure 3.10). The depression sensor can record displacement in [mm] whereas the pressure sensor records the applied load in units of mass [g], which is the equivalent to a 10^4 Pa pressure applied on a 1 mm^2 area of load application. Whichever the system of choice would be, all Axiom sensors carry the burden of a very high acquisition price, even beyond the cost of an ultrasonic elasticity set-up.

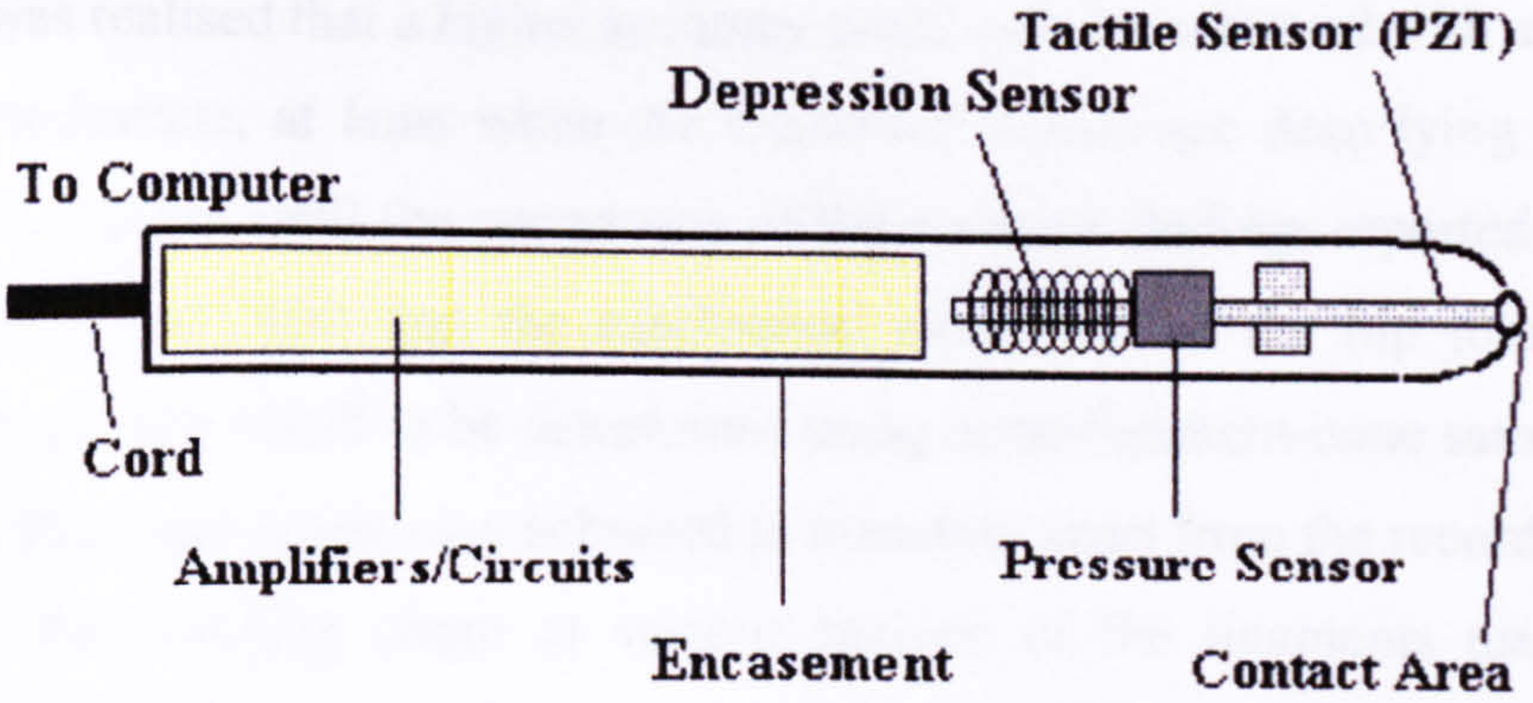

Fig 3.10 The set-up of the Venustron™ probe with pressure sensor.

3.5.3 Limitations of Invasive Methods

For both invasive elastography as well as for the tactile method the main limitation is involved with the difficulty in obtaining ethical approval for performing tests on patients during surgery in theatre, even though it had been possible by previous researchers (Crisp, 1972). Furthermore, it is difficult to convince surgeons to participate in these experiments and also the risk involved in performing them was a rather high one to take as part of this project. The costs involved in extra surgical time required as well as the expenses for acquisition of the equipment, whether it is the ultrasonic modalities or the tactile systems could also not be justified with the technical benefit they would provide and strengthened the decision of abandoning them.

3.6 Cadaver Method

The above described methodologies for invasive and non-invasive determination of soft tissue mechanical properties revealed that the location and anatomical structure of the hip joint capsule and its ligaments places restrictions that cannot be overcome sufficiently with the currently available technologies. Local elastic moduli are calculated in a direction perpendicular to their long axis, in which ligaments actually work under tension. This requires a further assumption to be made, namely that the estimated local elastic modulus in compression is a third of that along the long axis of the ligament's body. However, this is only the case for isotropic materials, but applies mainly to tensile moduli, rather than compressive.

It was realised that a higher accuracy could only be achieved with an external, cadaveric technique, at least when the examined tissues are deep lying ligaments. However, it was not until the occurrence of the research findings reported by Hewitt et al in 2001 and 2002 that the mechanical properties of the hip joint capsular ligaments were attempted to be determined using bone-ligament-bone samples under tension. In that work it was also achieved to measure- apart from the recorded applied load- also the resulting strain at various regions of the ligaments using optical methods. Nonetheless, it was felt that this study was suffering from the limitation that it collected data from ligament samples that were dissected from their location within the capsular mesh. This means that their anatomical and structural role was ignored and that the role of their orientation around the hip joint was not considered. A major concern with using excised ligaments in the author's opinion is the difficulty to identify the precise borders along the ligaments' length as well as the exact location of their bone insertion into the acetabulum and femur.

Even so, the findings of Hewitt et al (2001 and 2002) carry a significant weight and are the only data available at present on the mechanical properties of the hip joint capsular ligaments. It was therefore considered to be appropriate to try and confirm these findings by using a different approach to the biomechanics of the hip joint capsule. A 3-D computer model of the hip joint as presented in chapter 5 of this thesis- comprising the acetabular region, part of the femur and all the capsular ligaments- would act as a tool to compare any findings from the cadaver study with those results. Thereby, the data of Hewitt et al (2001 and 2002) would be used in the numerical analysis software and a sequence of limb movements would be simulated within this software. The resulting moments around the hip joint centre would be then recorded together with the flexion/extension, abduction/adduction and external/internal rotation angles of the joint. The moments for the same locations would then also be recorded by using complete cadaveric hip joints mounted on a rig that would be specially designed for this purpose. This test rig will be presented in more detail in the following paragraphs. In this way it would be possible to confirm the findings of Hewitt et al (2001 and 2002) and to verify the utilised 3-D computer model.

3.6.1 Tensile Tests on Freshly Excised Samples

From the previous paragraph it becomes apparent that the studies by Hewitt et al (2001 and 2002) have a certain importance in the present work. Therefore, this paragraph provides a brief review of the findings on the material properties of the hip capsule's ligaments. The two strands of the iliofemoral ligament as well as the ischiofemoral ligament were included in their study, which involved tensile tests of bone-ligament-bone samples and digital video analysis of strain development in the body of the ligaments. The findings of this study are summarised in the following graph (figure 3.11) and table 3.1.

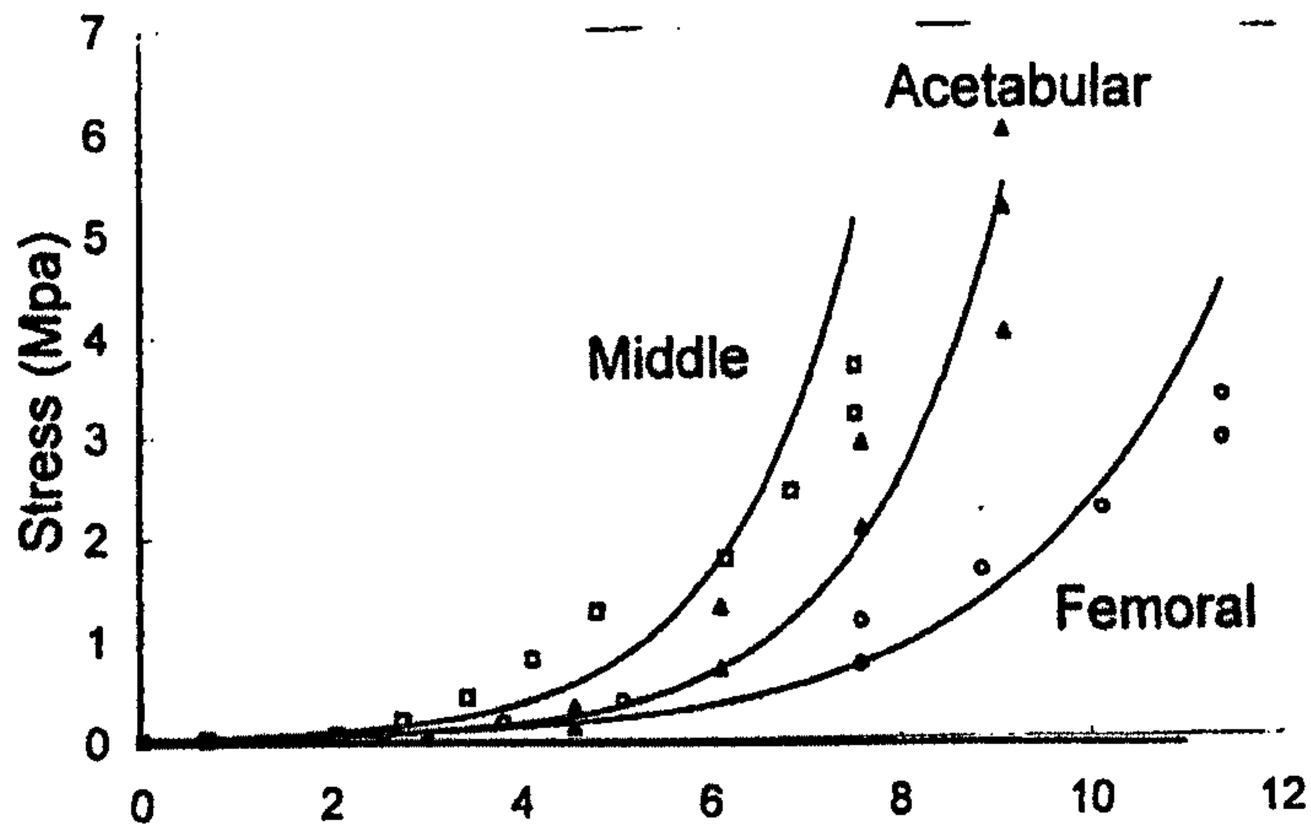

Fig 3.11 Stress-strain curves for different regions of an iliofemoral ligament (Hewitt et al, 2001).

It is in the femoral area that the greatest strain occurs and this is also reflected in table 3.1 under strain at failure. This could be down to changes in biochemical composition of various areas of ligaments and might be the result of biological adaptation, due to increased movement of those parts of the ligaments closest to the femoral bone, which has the greatest range of movement within the hip joint during gait.

	Lateral Iliofemoral	Medial Iliofemoral	Ischiofemoral Ligament
Strain at failure			
Acetabular Region	8.5%	11.6%	7.8%
Middle Region	6.2%	10.4%	8.1%
Femoral Region	13.3%	11.4%	25.3%
Elastic Modulus at 80% of failure (MPa)			
Acetabular Region	112.9	285.8	80.9
Middle Region	113.3	242.2	99.5
Femoral Region	76.1	139.3	82.1
Average Poisson's ratio			
65-90% failure strain	1.3	1.4	1.4

Table 3.1 Regional material properties of capsule ligaments (Hewitt et al, 2001).

As can be seen in table 3.1 Poisson's ratio has been recorded to be in the range of ν=1.3-1.4. In the past, though, it has quite commonly been accepted as ν=0.5, based on the assumption that as a highly hydrated tissue it would be almost incompressible. Also for other tissues there have been reports of higher Poisson's ratios, like for articular cartilage (ν=2.2), by Elliott et al (1999) and meniscus (ν=1.6-2.3), by Setton et al (1999). This is, because of the dependency of Poisson's ratio on the anisotropy within a material. Therefore, it is necessary to collect enough information when attempting to include this information on a biological tissue into a simulation software. The outcome of this simulation depends largely on the accuracy of the approximation of Poisson's ratio. The effect of selecting a Poisson's ratio as ν=0.5 versus ν=1.3-1.4 as recorded by Hewitt et al (2001) will be shown in chapter 6 as part of the FE modelling of the joint.

Finally, the displacement rate that was applied in Hewitt's study was rather low (0.04 mm/s) avoiding viscoelastic effects of ligaments. However, it was shown in other studies that an increased displacement rate results in higher ligament stiffness (Woo et al, 1990). This means that at higher gait speeds the ligaments *in vivo* would present greater stiffness. This was an issue that needed to be addressed in

the cadaver study, too. Therefore the angular displacement rate of the joint on the mechanical test rig was selected to be as close as possible to physiological, in particular it was chosen at 25 deg/s as is also described in the following chapter.

3.7 Test Rig for Cadaver Method

The design of the mechanical test rig that was to be used for collecting data on the mechanical behaviour of both intact and dissected cadaver hip capsules in several limb positions, depended largely on the angles of the limb position that was to be achieved in the simulation. In the present cadaver study it was decided that the joint should be brought into angles that would approximate those limb positions that place the highest risk for either anterior or posterior dislocation when a not fully intact capsule is present, as would be the case after THR surgery. This meant that the following angles of the joint had to be adjustable, each on a single plane of reference:

- Flexion and Extension
- Internal and External Rotation, and
- Abduction and Adduction

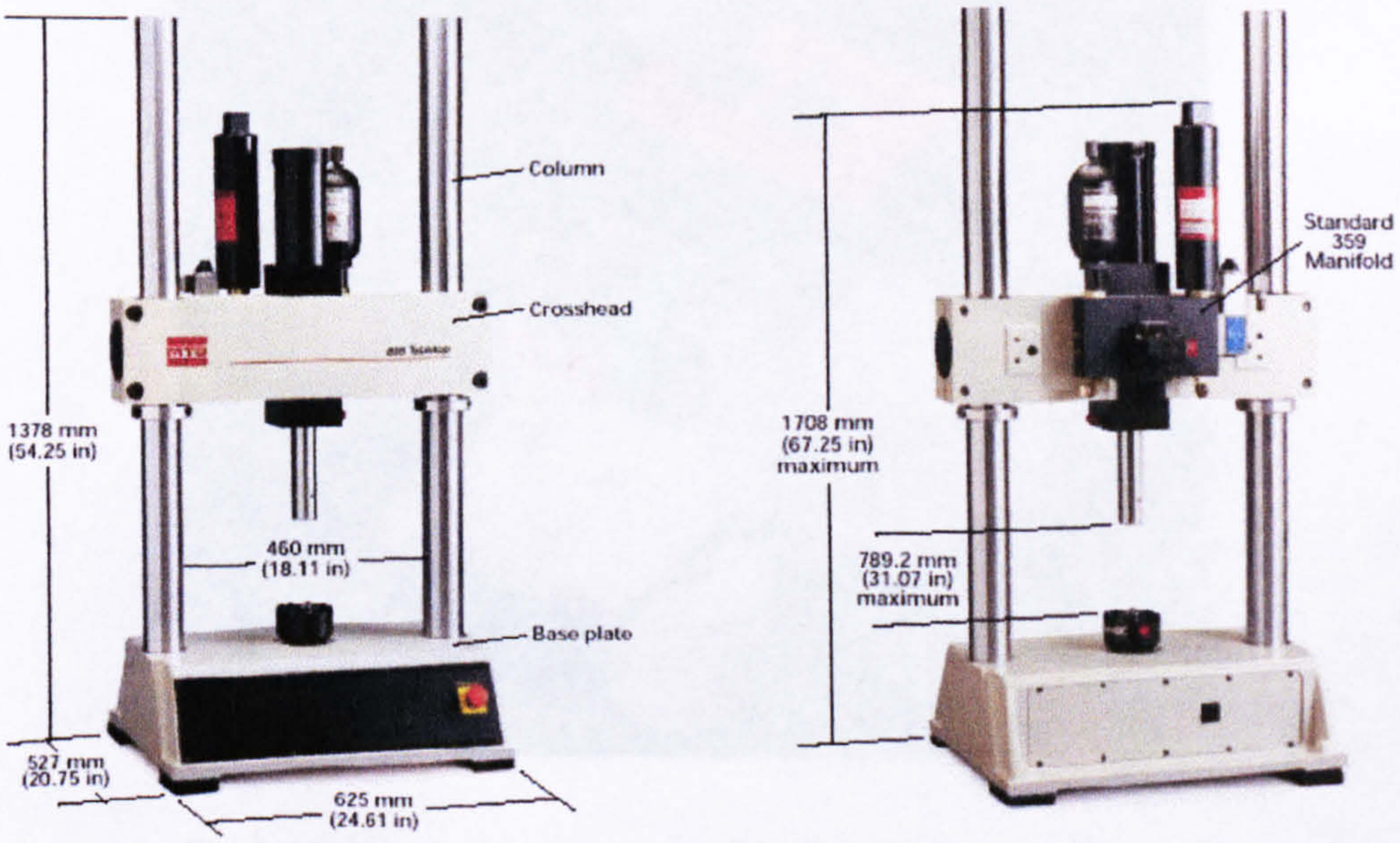

Fig 3.12 The frame of the MTS Bionix and its dimensional restrictions.

Furthermore, since the width between the two pillars of the utilised MTS Bionix 858.2 (MTS Systems Corporation, Eden Prairie, Minnesota, USA) shown in figure 3.12 was limited to 460 mm, the design of the rig would have to be kept compact to avoid collisions during the simulated limb movement. To accomplish this design aim, the decision was made to develop the rig in such way that its femoral component (i.e. that part that would carry the femoral part of the hip joint) would be the one driven by the cross-head of the MTS Bionix in a rotational movement.

The bottom part, which would be carrying the acetabular component of the cadaveric hip joint, would need to include all the mechanisms that are required for adjusting all joint angles that would want to be achieved. The femoral component of the rig would also be adjustable, but only for the purpose of setting up the joint within the rig in such way, that an ideal alignment could be achieved between the actual hip joint centre of rotation with the centre of the MTS rotating cross-head and the equivalent load cell at the bottom of the MTS. Considering all the above restrictions and requirements the following design concept was developed.

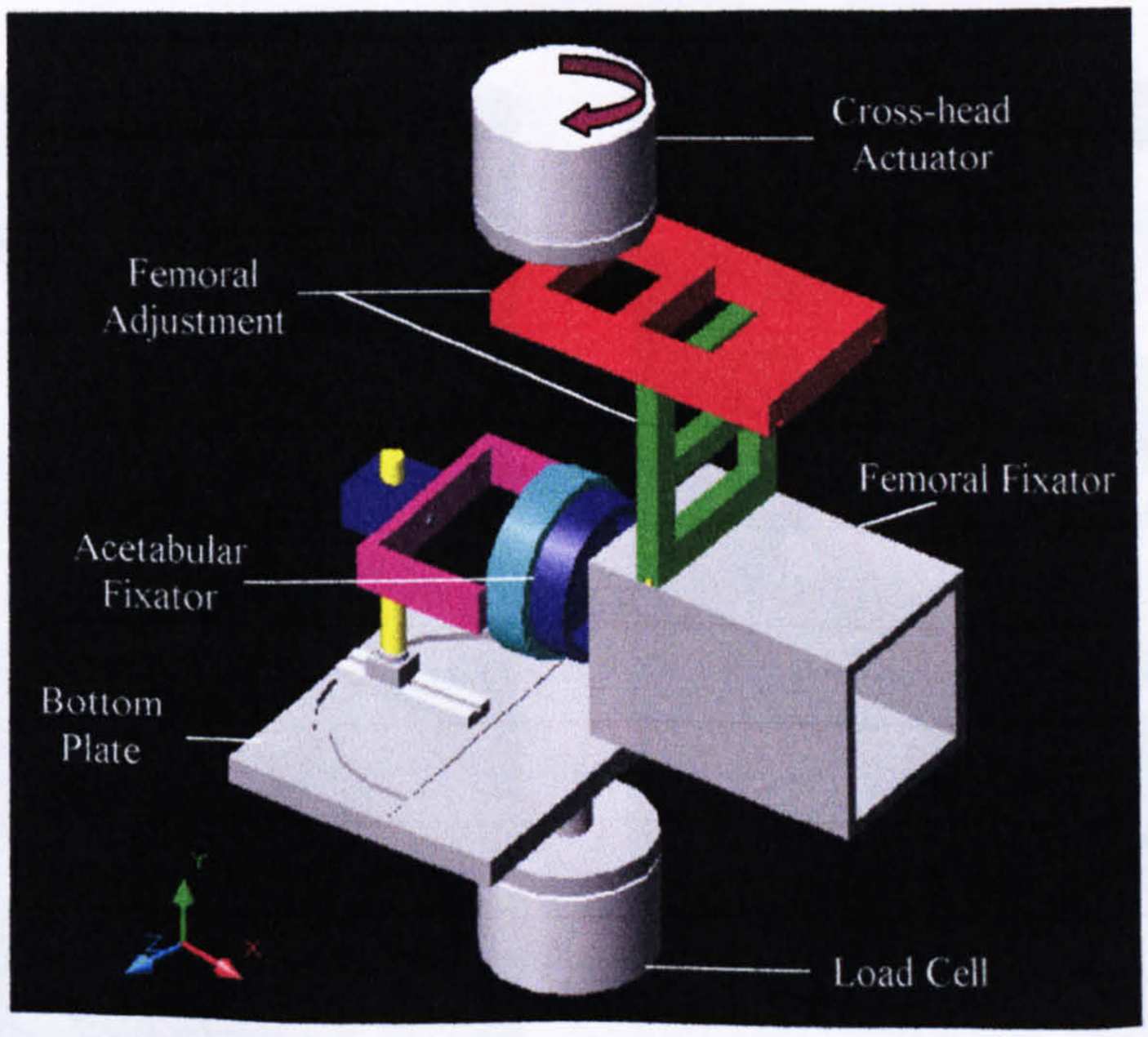

Fig 3.13 The design concept with all its components.

Aluminium was the material of choice in order to keep the total weight of the rig to a minimum. This was particularly important as the femoral component was to be moved at an angular speed of 25 deg/s and high inertial forces disturbing the sensitive load cell could result from an increased mass of the rig. Portability of the rig was also considered when selecting the material. This was of particular importance, because the rig was to be carried to Professor Michael Morlock's biomechanics lab at the Technical University of Hamburg-Harburg, Germany, where the MTS test set-up was available and cadaver tests could be carried out. The following paragraphs describe the mechanisms of the test rig.

3.7.1 Femoral Fixator

In the development of the femoral fixator the main consideration was that the actual hip joint centre of rotation could be aligned with the centres of the cross-head and load cell of the MTS. For this reason the upper parts of the femoral component of the rig had to be adjustable along the x- and z-axis of the coordinate system of figure 3.13 as shown in figure 3.14.

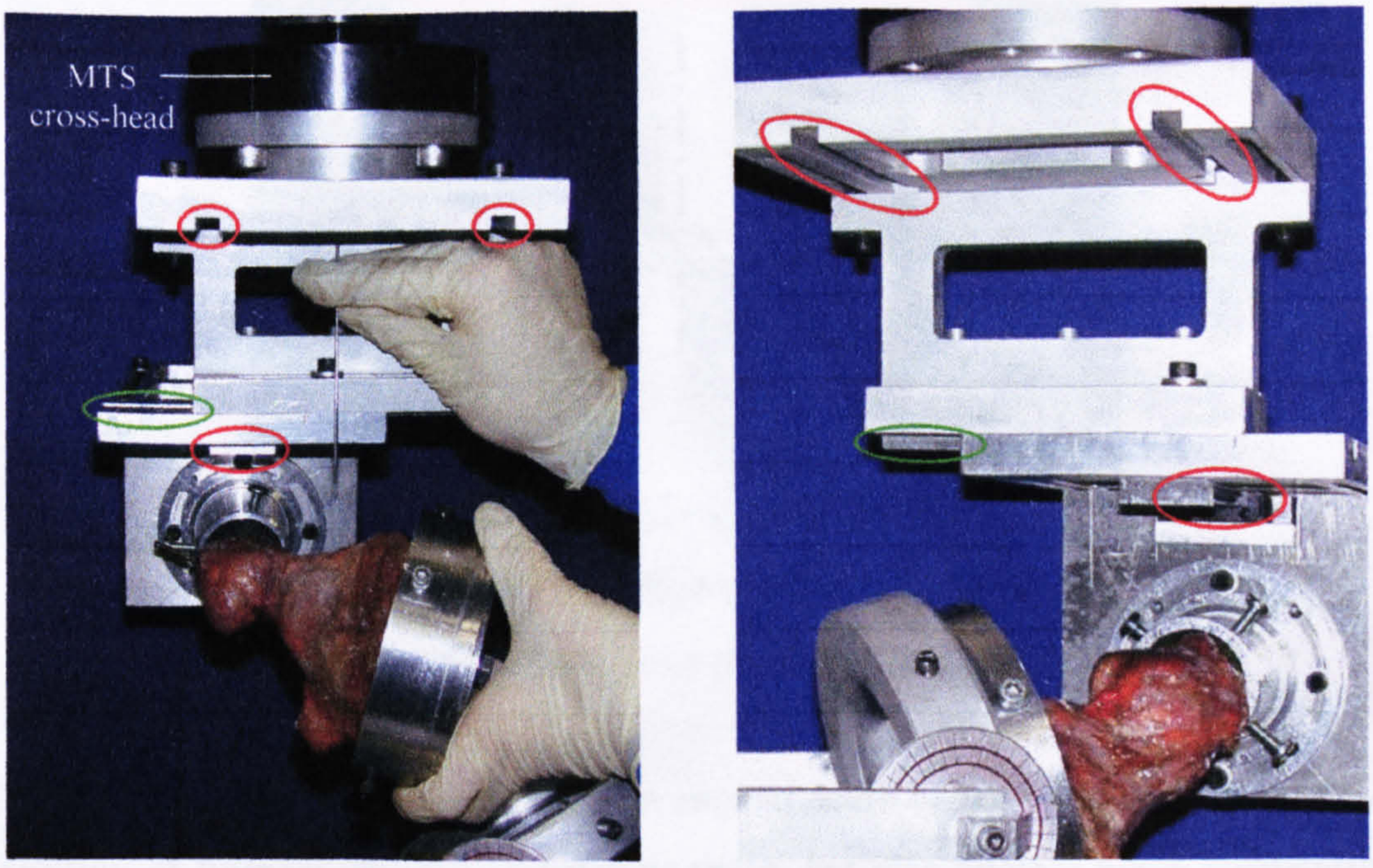

Fig 3.14 Red markings indicate adjustability of the femoral fixator along the femur's long axis. Green markers refer to adjustability transverse to the long axis.

The grooves and slides indicated in figure 3.14 have been included considering that the femur's long axis is parallel to the long axis of its cementing pot. Otherwise it would mean that any adjustment performed along those axes, would translate the hip joint centre of rotation from its ideal location even further.

3.7.2 Acetabular Fixator

The acetabular fixator had to be of such design, that it would be fairly simple to adjust the other two joint angles that were to be, namely internal and external rotation and flexion or extension. For this purpose a pot within another pot system was designed. The first pot would be used for cementing the joint, thereby ascertaining that its centre would be in alignment with the imaginary acetabular centre (figure 3.15). This was done, so that by just rotating the cementing pot within the second pot, it would be possible to alternate the angle of internal and external rotation (figure 3.16).

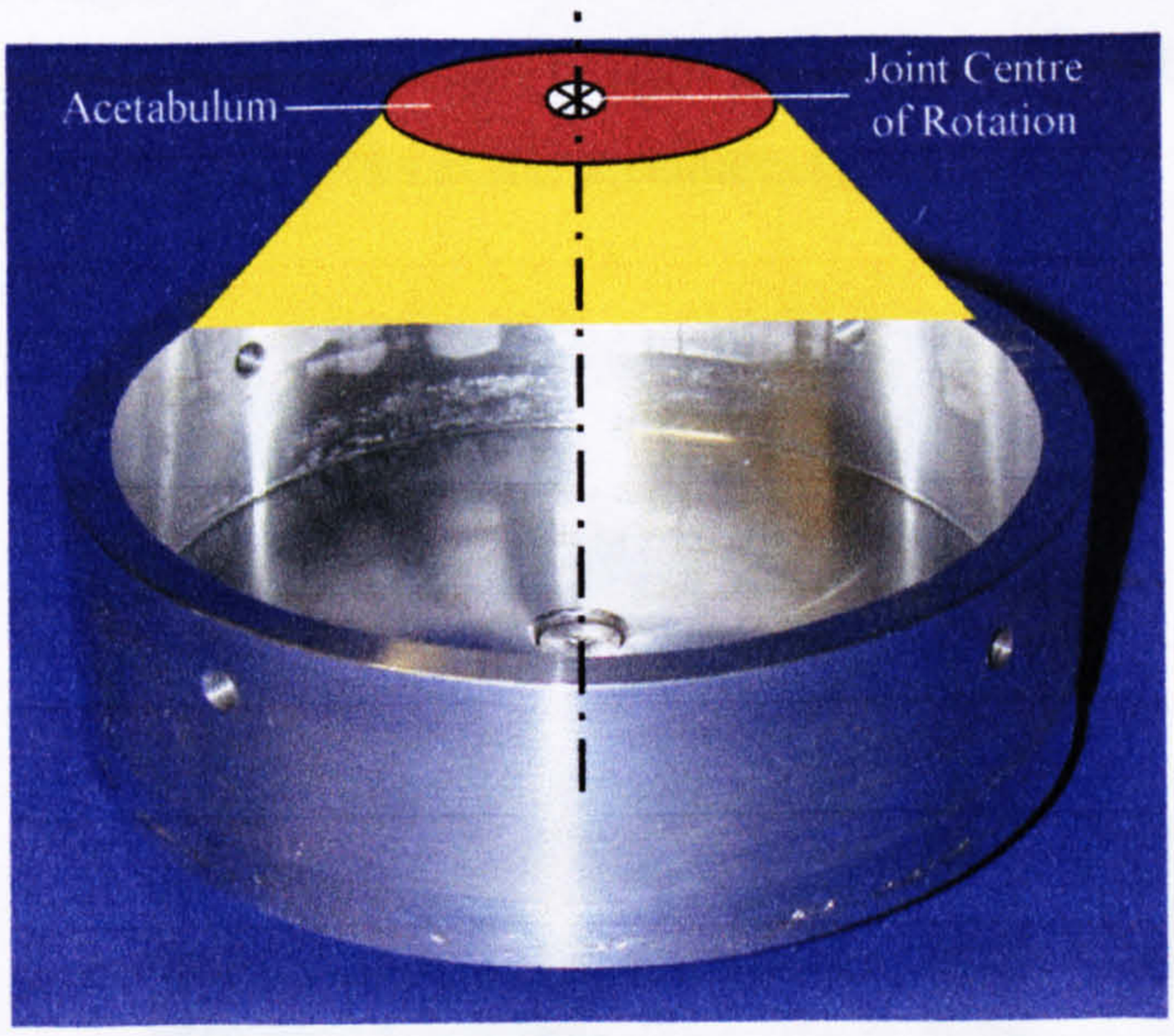

Fig 3.15 Aligning the hip joint centre of rotation with the centre of the cementing pot was very important.

On the back of the cementing pot is an angular scale of 360° which facilitates the selection of internal or external rotation angle, but also another hinge mechanism with angular scale plate for choosing flexion or extension angles (figure 3.16).

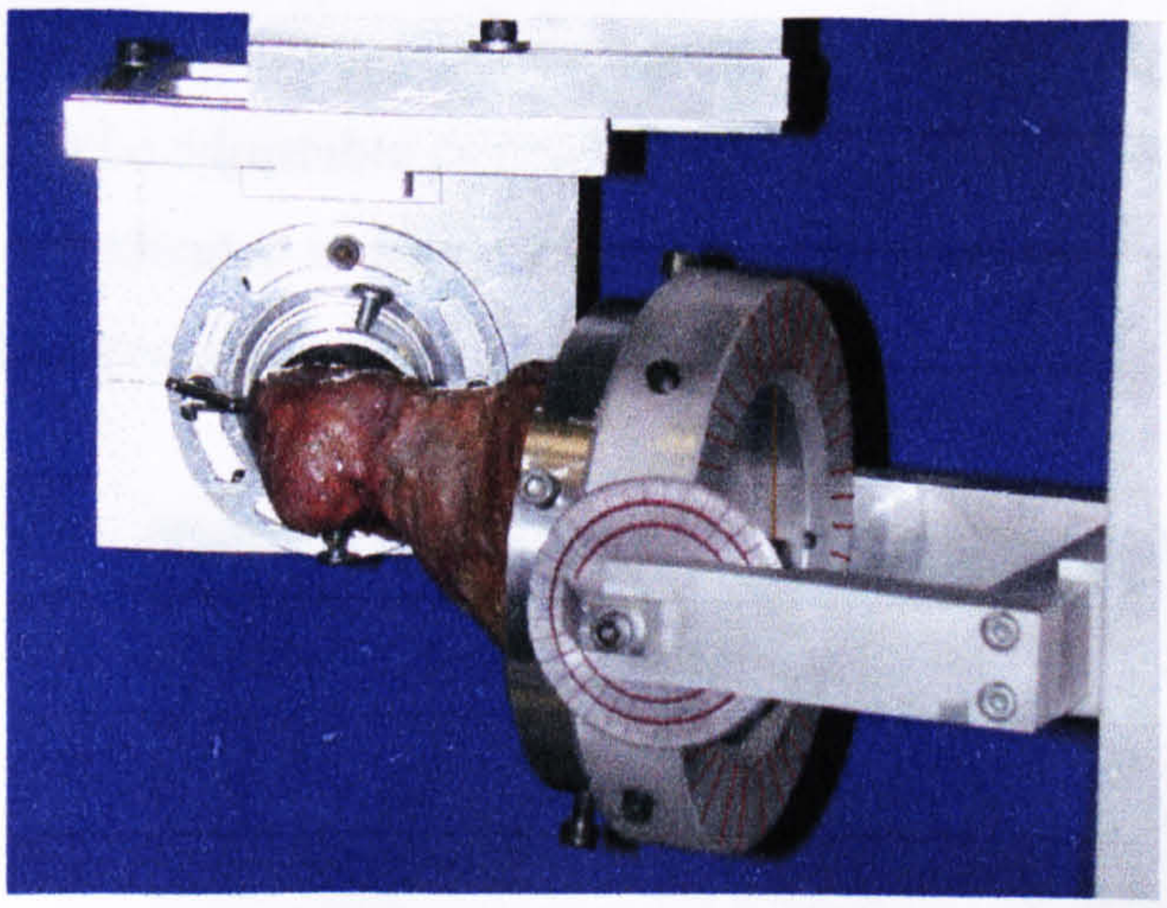

Fig 3.16 Angular scales of the acetabular fixator.

3.7.3 Acetabular Adjustability

It was already mentioned that after having aligned the hip joint centre of rotation with the cross-head and load cell of the MTS the femoral fixator would be locked and not re-adjusted throughout the course of all the tests on each individual specimen. Thus, the joint configuration in each test could be reproduced accurately by using the aforementioned scales of the acetabular fixator.

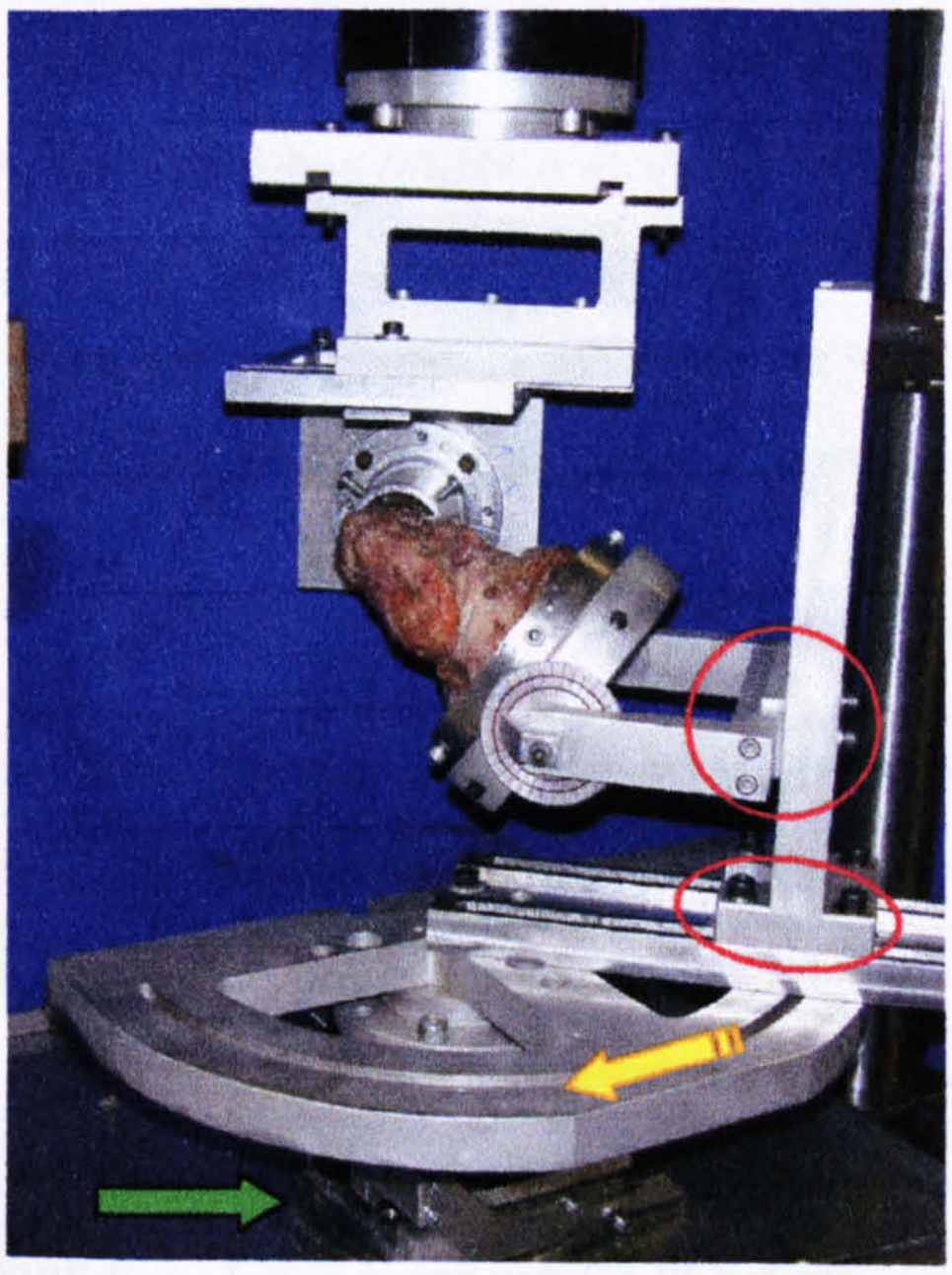

Fig 3.17 Adjustability of acetabular pot.

However, in the attempt to produce flexion or extension angles, the acetabular fixator would need to be adjustable in height and also length (i.e. along the x- and y–axes respectively, as indicated in figure 3.13). These adjustments are shown in figure 3.17 and indicated by the red circles.

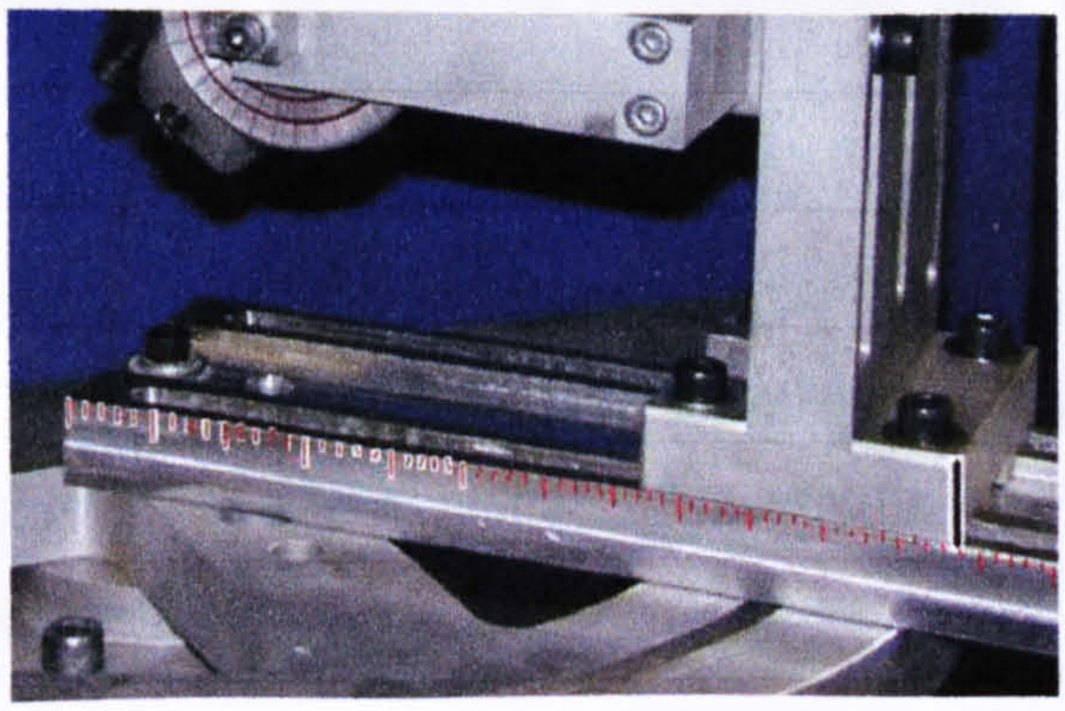

Fig 3.18 Linear scales attached to the test rig.

In order to be able to accommodate both left and right specimens, but also to allow for adjustability of anatomical discrepancies in what concerns the varus angles of the different femora, the bottom plate was designed in such way as to allow for 180° of rotation as indicated by the yellow arrow in figure 3.17. All angular adjustments on the acetabular part could be locked after setting the joint up and reproduced at any time by using the circular and linear scales (figure 3.18) for the x- and y- axis adjustment. The complete mechanical rig was mounted on a so-called 'x-y table' (green arrow in figure 3.17), which allows for a ±3.5cm movement in both the x- and z-axis when referring to the coordinates of figure 3.13).

3.8 Summary

A large number of both invasive and non-invasive methods was reviewed and analysed under the scope of their possible employment within this study. It was concluded after considering the available technologies, that the most appropriate approach would be to use complete cadaveric joints on a rig specifically designed for this purpose. These results will then be compared to the existing data of Hewitt et al (2001 and 2002), by using a 3-D computer model in a numerical analysis. The results of the cadaver tests performed with the test rig are presented in the following chapter.

Chapter 4- Hip Joint Capsule and Joint Stiffness

4.1 Introduction

The following paragraphs describe the methodology that was followed to utilise the test rig that was described in the previous chapter. It is explained in detail how the tests were set up and executed. All observations from the tests and any errors are presented and evaluated. A comparison with the findings of other researchers is done and the different approaches are discussed. Finally, a reference to the pitfalls of the applied methods is made and suggestions are made for the improvement of the acquired results.

The justification and necessity for the present chapter and the work described therein lies in the need for evaluation of the computational model that was applied for studying the contribution of the capsule and its ligaments to hip stability. The use of this computational model in simulating and evaluating critical situations of hip stability in THR is described and discussed in more detail in chapter 6, where the results of the numerical analysis are presented. However, the idea and structure of this chapter resulted from the need to verify the very little data on the mechanical properties of the capsular ligaments that was available (Hewitt et al, 2001). There was no comparative data by other researchers and it was unclear as to how the data, which resulted from excised ligament bands under tensile tension, would relate to the computational model. However, by testing the mechanical properties of the capsular ligaments in the cadaveric model allows both drawing immediate conclusions from the results of the study and also enables an evaluation of the 3-D computer model. This could be achieved by using the data that were produced by Hewitt et al (2001) in the numerical analysis software. Thereafter the hip joint could be moved into the same positions into which they were also moved in the cadaver experiments. The package would calculate the developing moments around the hip joint centre of rotation resulting from the capsular ligament bands resisting the femoral displacement. These moments could then be compared to the actual moments recorded in the cadaver experiments.

4.2 Methods

In order for an *ex vivo* study to produce the expected results it is necessary to ensure that all input parameters are appropriately selected and prepared. In the present case it was the effect of the individual capsular ligaments that was to be studied without the presence of any other soft tissues, in order for the cadaveric model to be matching the computational model. Therefore, it was necessary to ensure that the specimens were prepared in such way that no other tissues, like muscle and tendon were in place, thereby contributing to the overall resistance erroneously.

4.2.1 Specimen Preparation

Initially the specimens were received from the forensic department with the majority of the muscle tissue having been removed. As for the pelvis it was cut in such a way that no risk to the capsule would arise when cutting the bones. The way of resecting the pelvic bone is much the same as is done in triple osteotomy (Fig 4.1). The femoral bone was resected at 3-4 centimetres below the lesser trochanter.

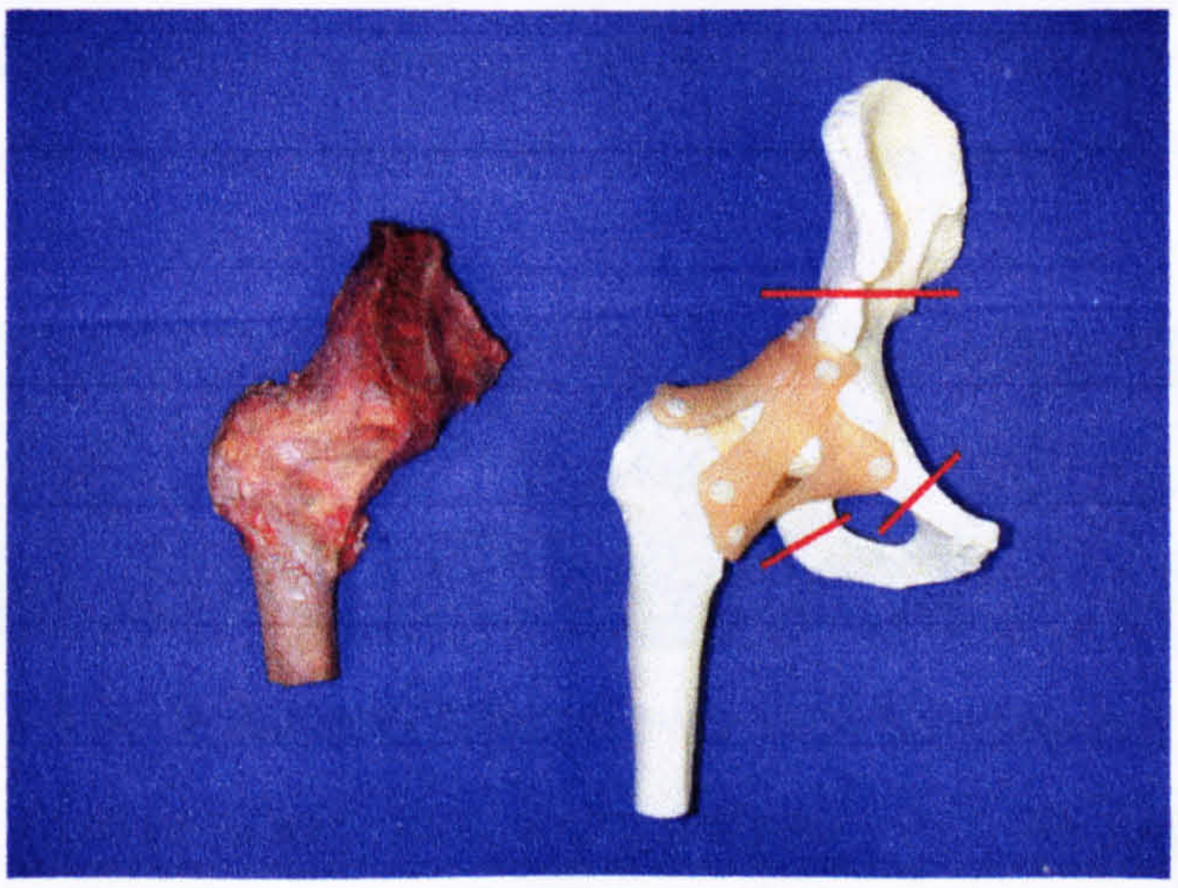

Fig 4.1 Red lines indicate the location of the applied resections for the triple osteotomy. Left is the triple osteotomy of the cadaver specimen.

The initial task was to remove any excessive muscle bulk from the specimens to ensure that no tissues other than those forming the capsule would contribute to the

recorded resistance. At first the main existing muscle bulks were split into muscle groups and carefully removed, using the tools pictured in figure 4.2.

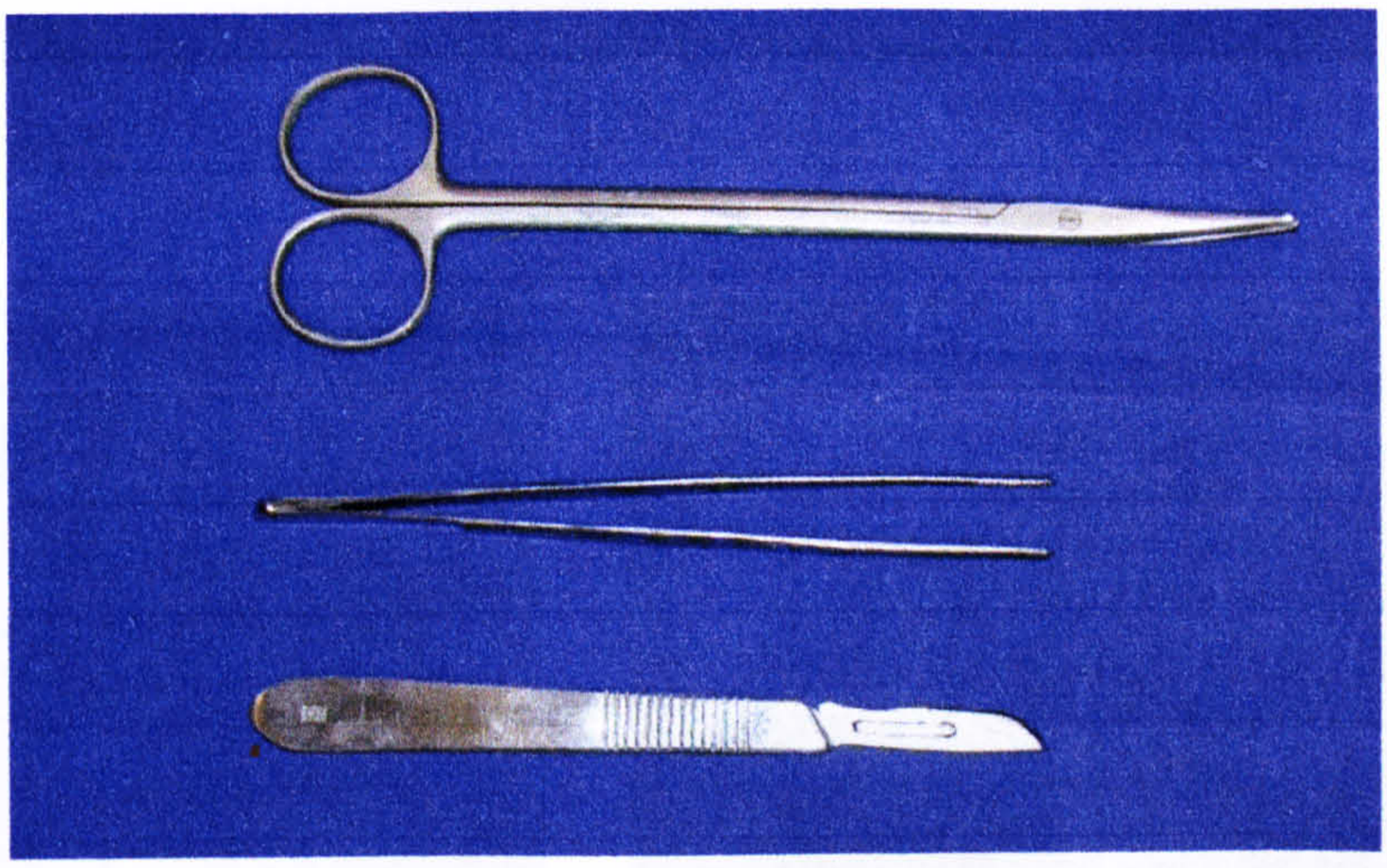

Fig 4.2 Tools that were used for removing bulk muscle tissue included curved scissors, surgical forceps and scalpel.

When approaching the deeper layers, much more care needed to be taken in order to avoid damaging the capsular tissues that are merged with the deeper muscle fascia. For this task the only tool used was a Volkmann's spoon, shown in figure 4.3.

Fig 4.3 The Volkmann's spoon was used for scraping away small muscle fibres that were merged with the capsular tissues.

As soon as the excessive tissues were removed to the examiner's satisfaction and nothing but capsular tissue was surrounding the joint, the joint surfaces were investigated further by using x-ray, which was available at the site of the tissue preparation laboratory. It was considered extremely important to ascertain that no deformities of the cartilage or calcifications of the capsular tissues were present. Care was also taken that no damage or abnormality of the bone was there. These

investigations were simply an additional precaution in order to avoid any effects on the recorded resistance measurements resulting from anomalies. However, a full history of the specimen was available from the forensic department that also supplied the cadaveric bones. Below are photographic and x-ray sets of all specimen that were used in this study.

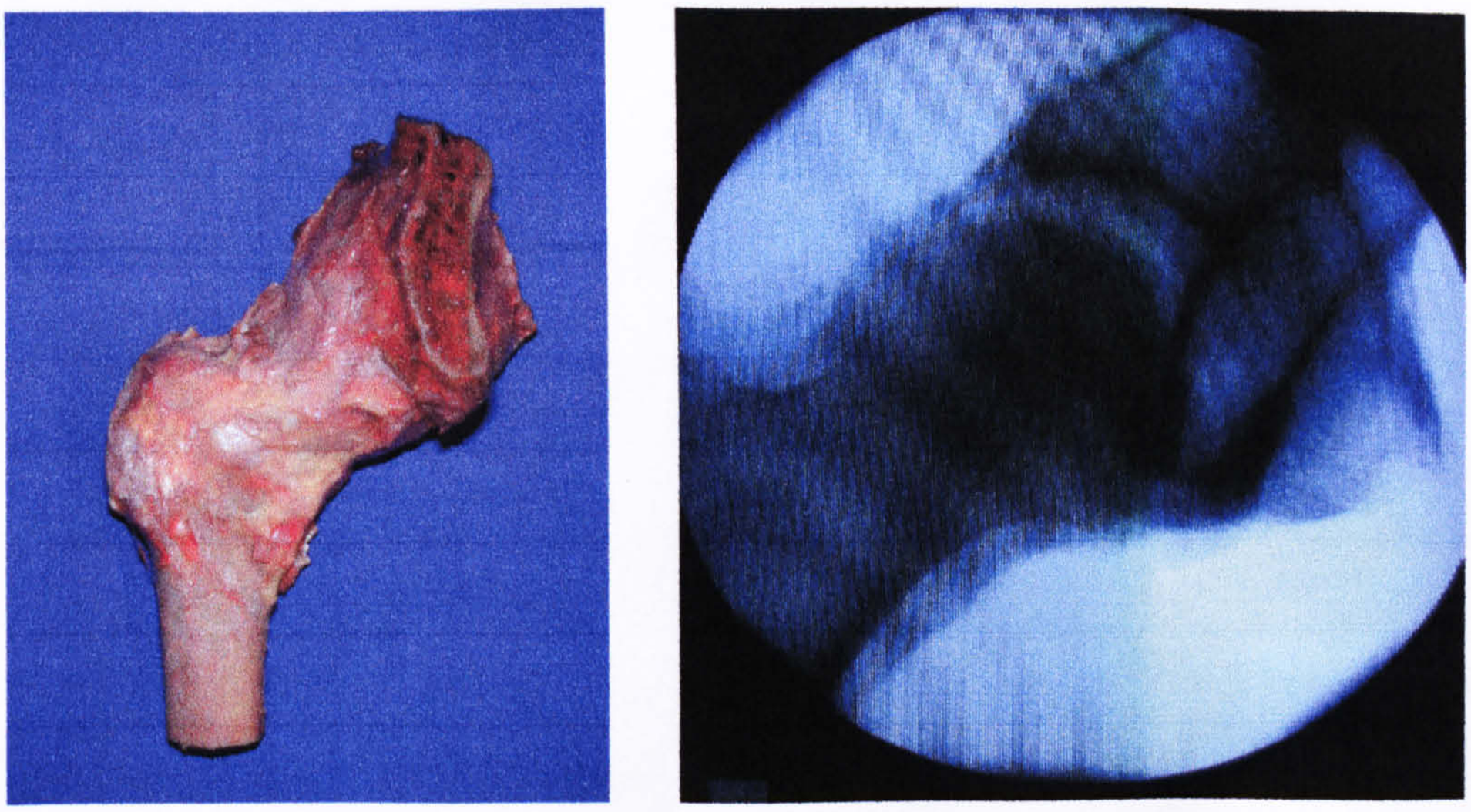

Fig 4.4 a and b The final appearance of cadaveric specimen 1 on the left and its equivalent x-ray.

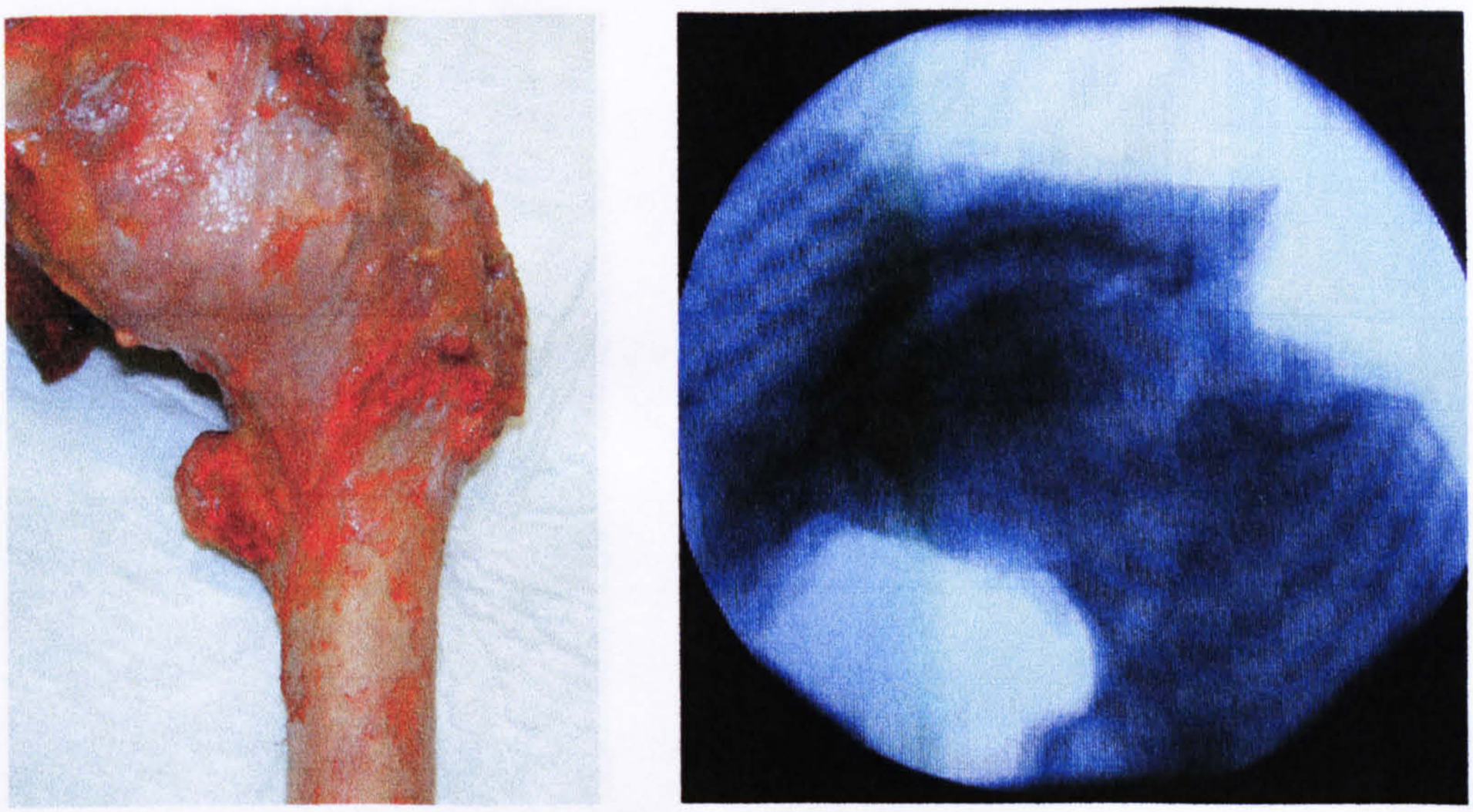

Fig 4.5 a and b Similar images for specimen 2.

Specimen 1, which is shown in figure 4.4a, was a right hip joint and it was excised from a 60-year old male. Specimen 2 (figure 4.5a) was from a left hip joint and it was excised from a 73-year old male. As can be seen in figures 4.4b and 4.5b no obvious damages to the joint surfaces, like possible results of arthritis could be seen, nor any distinct marks on the capsular tissues.

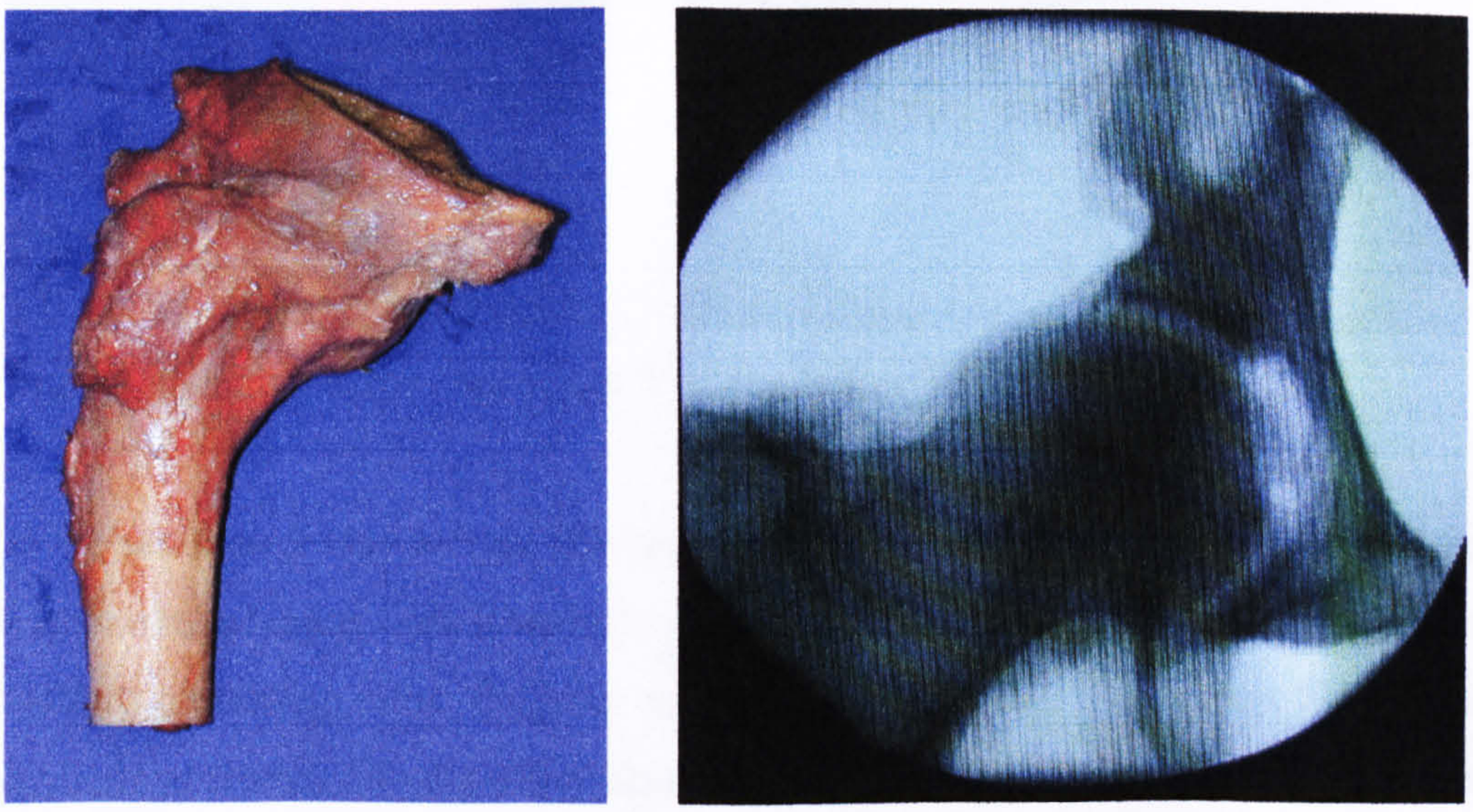

Fig 4.6 a and b Images for specimen 3.

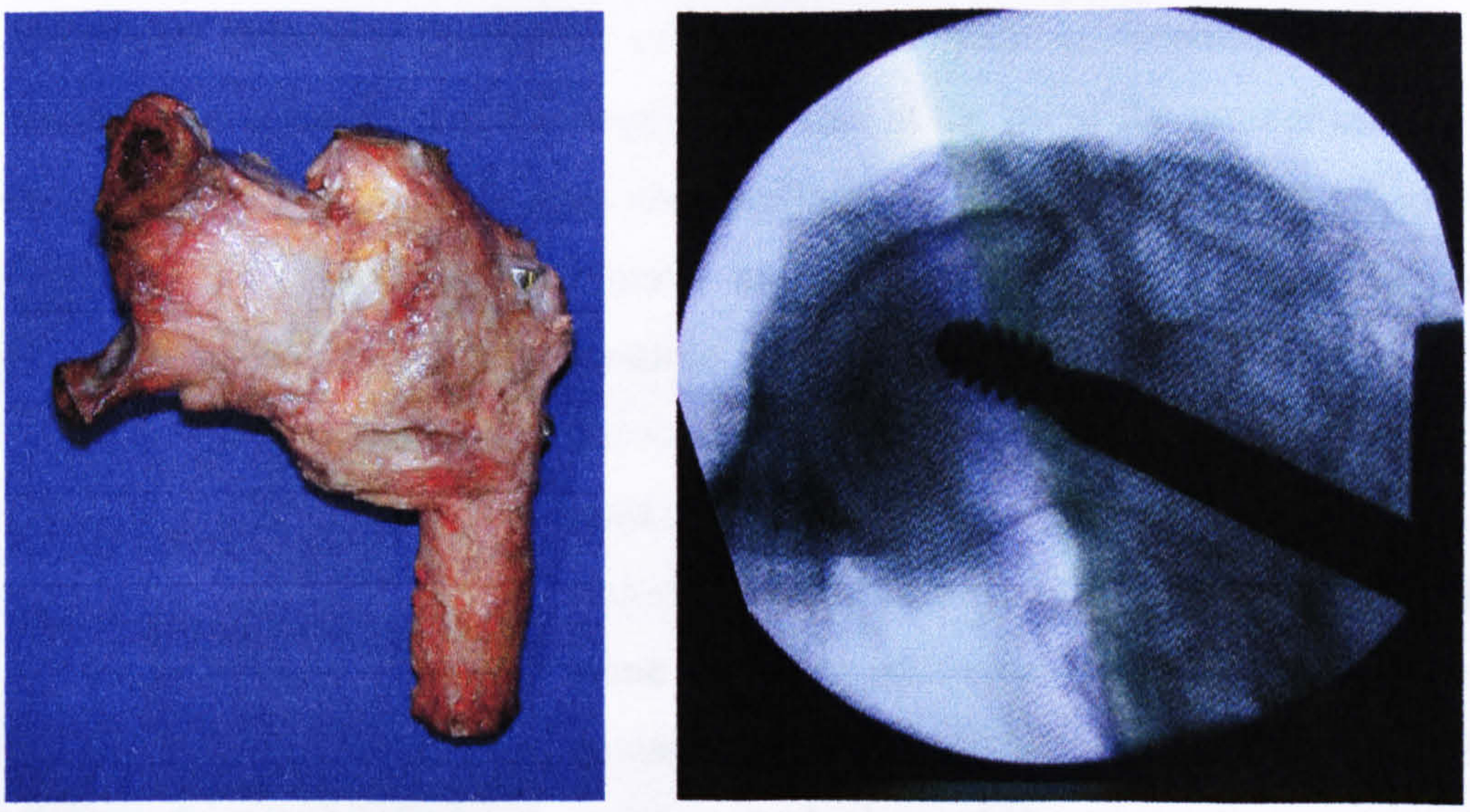

Fig 4.7 a and b Specimen 4 with the γ-nail inserted into the femur. Severe exostoses resulted from the fracture healing, reducing the range of movement.

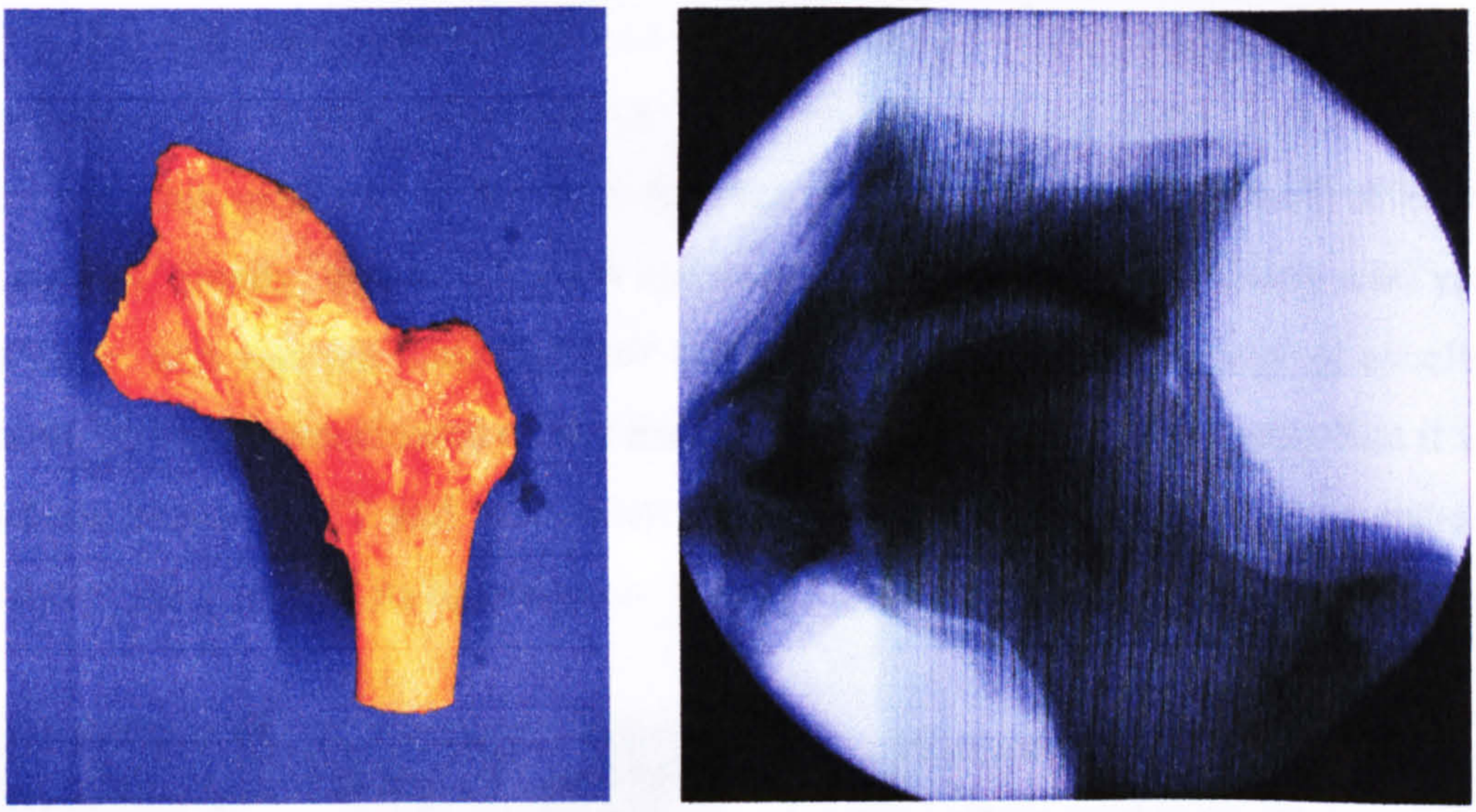

Fig 4.8 a and b Cadaver specimen 5 on the left and its equivalent x-ray.

Specimen 3 was a right hip joint that was excised from a 73-year old male and is shown in figure 4.6a. It was the matching pair of specimen 2 and there were no anomalies present on either the joint surfaces or the soft capsular tissues. Specimen 4 was obtained from a 54 year old male and is shown in figures 4.7. Several exostoses are evident as a result of the presence of an intramedullary γ-nail that had been used in the past to repair a fracture of the femoral neck. The fractured bone appears to have healed very irregularly along the diaphysis of the femur (figure 4.9) and seems to have also caused a shortening of the femoral neck in combination with an increased bone deposition at this region, but also at the tip of the greater and lesser trochanter. Even though blade saws and oscillating saws were used in the attempt to remove most of the excessive bone, it was not possible to bring the present specimen into an acceptable condition that would be suitable to be used for this test. The fear was that the range of abduction-adduction would be too limited and that some exostoses within the capsule could come into contact and contribute to the total recorded resistance, which would be an artefact.

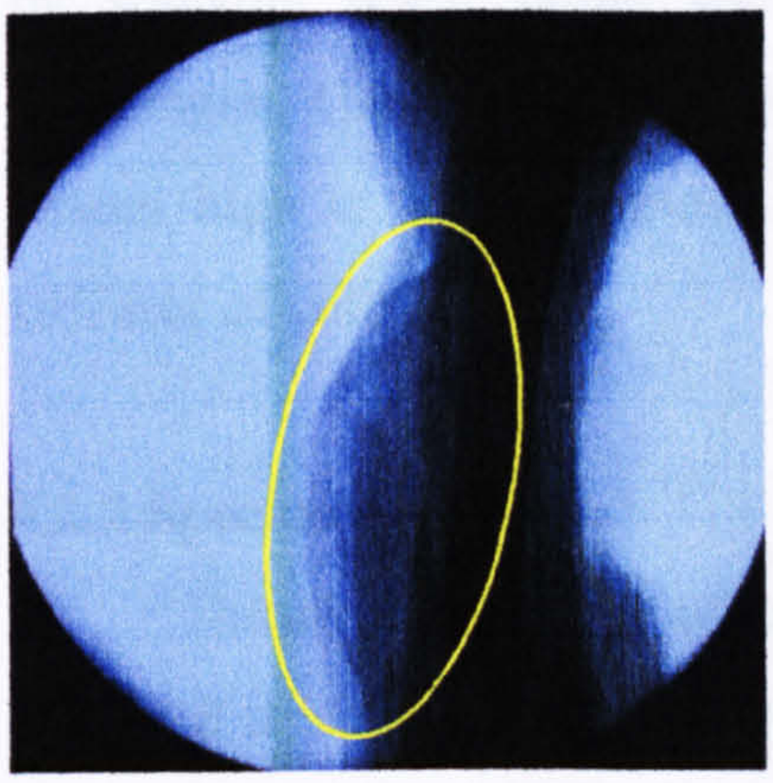

Fig 4.9 X-ray for specimen 4.

For the above reasons it was decided not to include the findings on this specimen in the results. However, an attempt was still made to produce recordings even with this specimen in the hope that none of the abnormalities would affect the recordings. Finally, figures 4.8 show specimen 5, which was excised from a 60 years old male and was the matching pair of specimen 1. Specimen 5 was an excellent sample that had been cleared of any excessive muscle fibres in such a way that it was used for obtaining CT and MRI scans for later use in creating a three dimensional model of the joint and its ligamentous structures, as it is outlined in chapter 5.

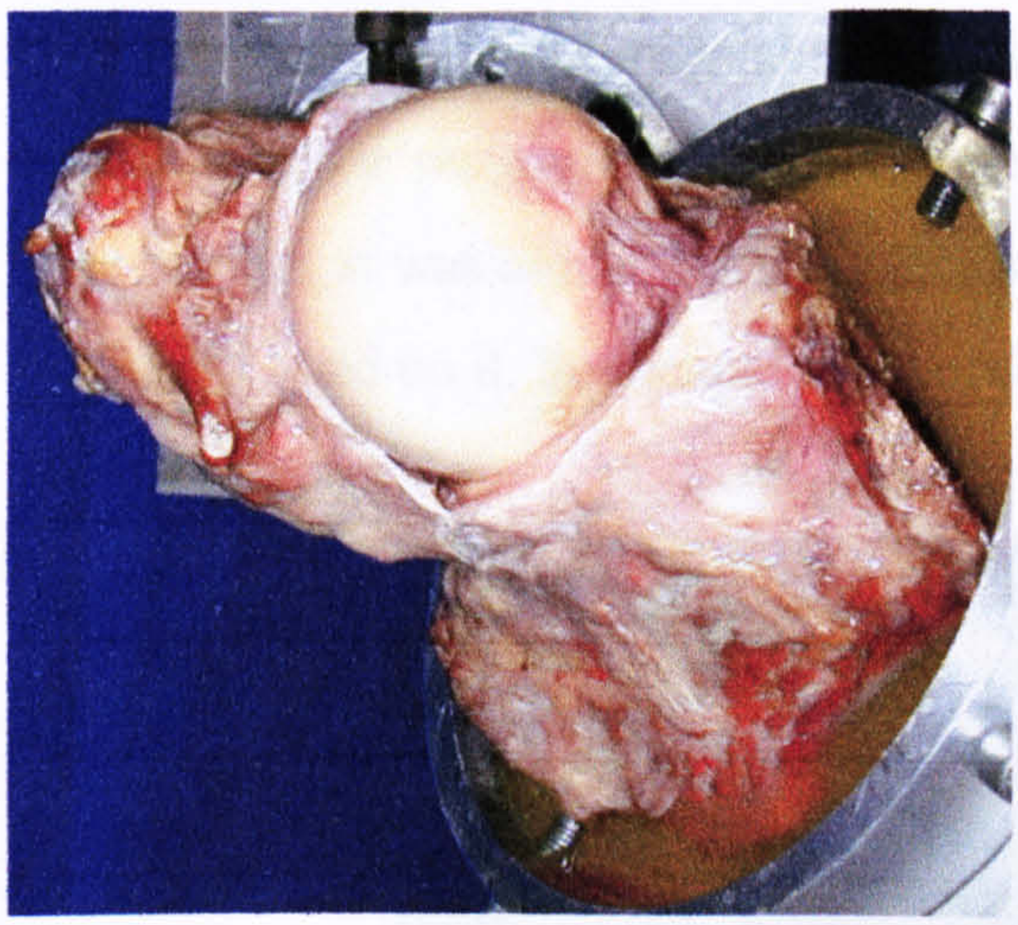

The indications from the x-ray were always confirmed after the completion of the testing procedure, by visual examination of the tissues, since a good insight into the joint capsule was possible after the transsection of a substantial part of it (figure 4.10). None of the joint surfaces presented any anomalies or damaged cartilage.

Fig 4.10 Final joint surface inspection.

Throughout the complete procedure of the dissection and specimen preparation, as well as during the test execution, the capsular tissues were kept moist by spraying 0.9% saline solution (Firma B Braun, Melsungen AG, D-34209 Melsungen, Germany). It has been shown that keeping the water content of soft tissues high is very important (Nigg and Herzog, 1999), as water determines the stiffness of collagen.

4.2.2 Specimen Fixation

During the testing of cadaveric specimens there are several issues to be observed in order to avoid damaging the specimen and also to ensure that the links between the biological specimen and the engineered test rig are strong enough and will withstand the external loads applied during the test. The way the specimens were

mounted within the rig is described in this paragraph and the quality and pitfalls of this method are discussed.

Initially, cancellous bone was resected from areas that were planned to be immersed into the bone cement in the utilised pots. For this purpose a bone rongeur was used (figure 4.11). Subsequently, cotton balls and paper were inserted between the compact bone walls after removal of cancellous bone, in the attempt to dry the surface as much as possible and to ensure in this way that the bone cement would bond better with the bone. Additionally, a few holes were drilled through the compact bone walls of the acetabulum to allow for an anchoring of the bone with the cement. On the remaining compact bone surfaces, which were to be immersed in bone cement, it was ensured that all periosteum layers were removed, as bone cement would not bond on it. Sandpaper was used to make the surface rougher.

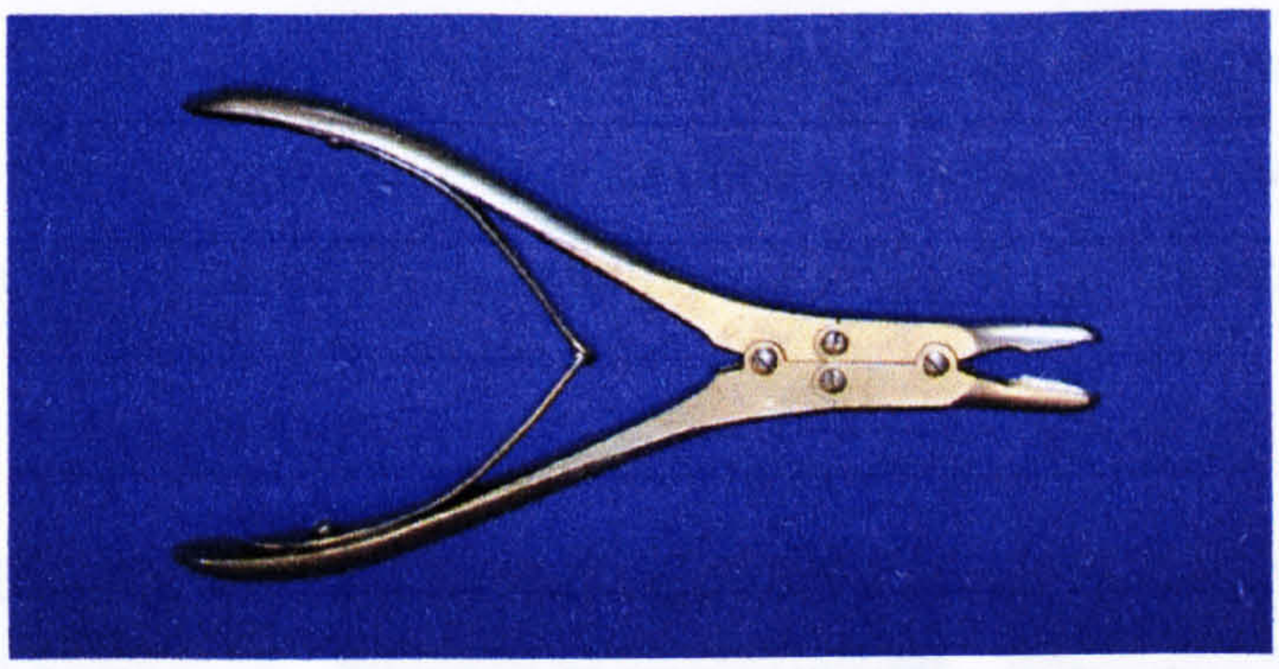

Fig 4.11 The bone rongeur was used to nibble off cancellous bone from the pelvic part for better cement flow and stronger bond with the cement pot.

The next step towards a strong and properly aligned fixation of the specimens was the use of two Kirschner wires that were drilled into the femoral bone. An x-ray C-Arm was used for navigation of the drills that were opening the holes for the wires to be placed (figure 4.12a). Very low force and rotational speed was applied on the air drill (figure 4.12b) and new x-rays were taken on two different planes in regular intervals, ensuring that the holes were drilled in correct orientation (figure 4.13).

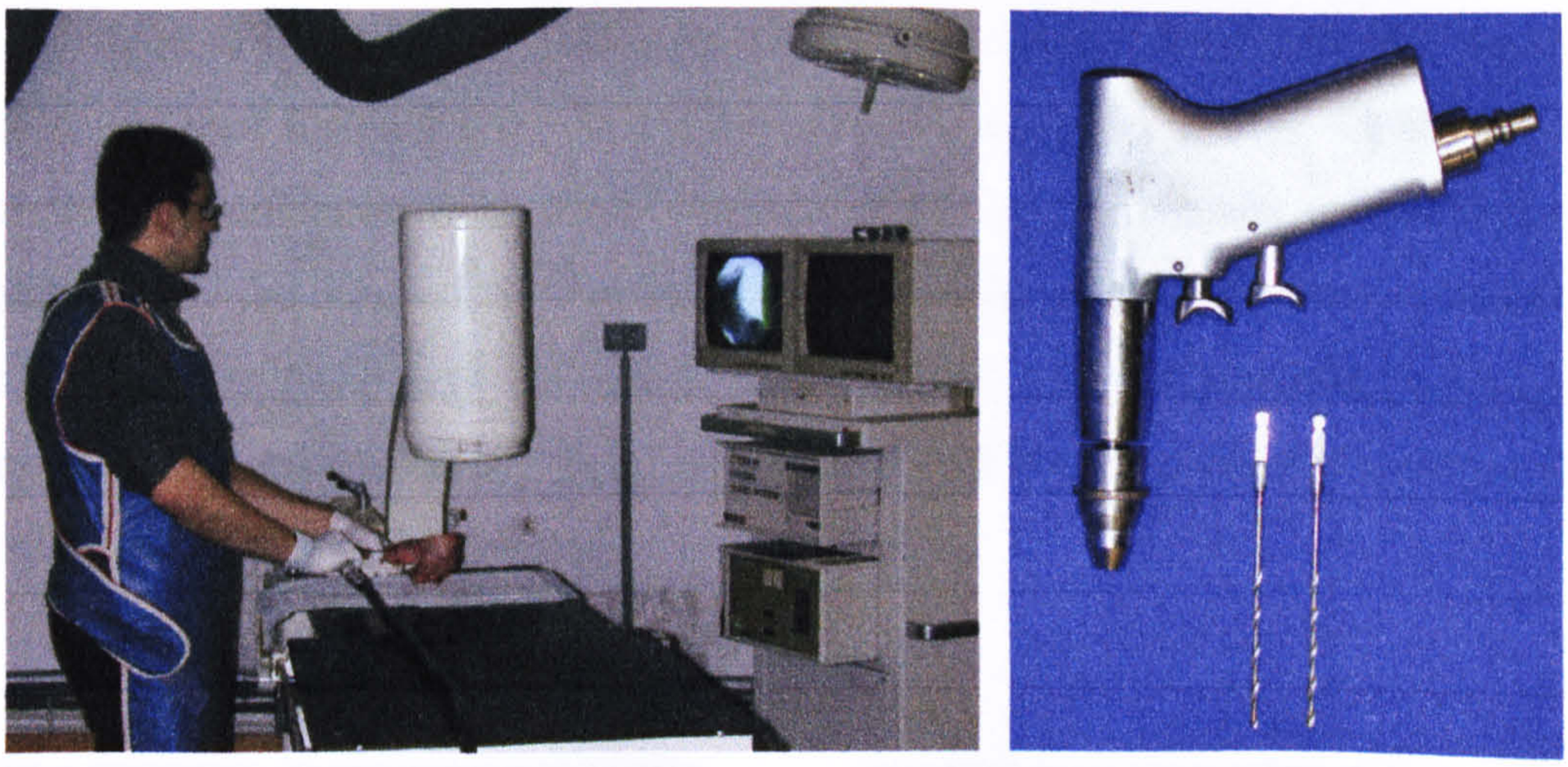

Fig 4.12 a and b Kirschner wires were inserted into the bone with x-ray visualisation. Pneumatic drills were used for opening the holes in the femur.

In particular, the first wire was inserted parallel to the femoral shaft's main axis, to assist the parallel alignment of the femur with the long axis of the femoral cementing pot. The other wire was inserted parallel to the femoral neck's main axis as an assistance when trying to align the specimen on the test rig in such a way that it would allow for a 7° anteversion in relation to the test rig's horizontal table (figure 4.13).

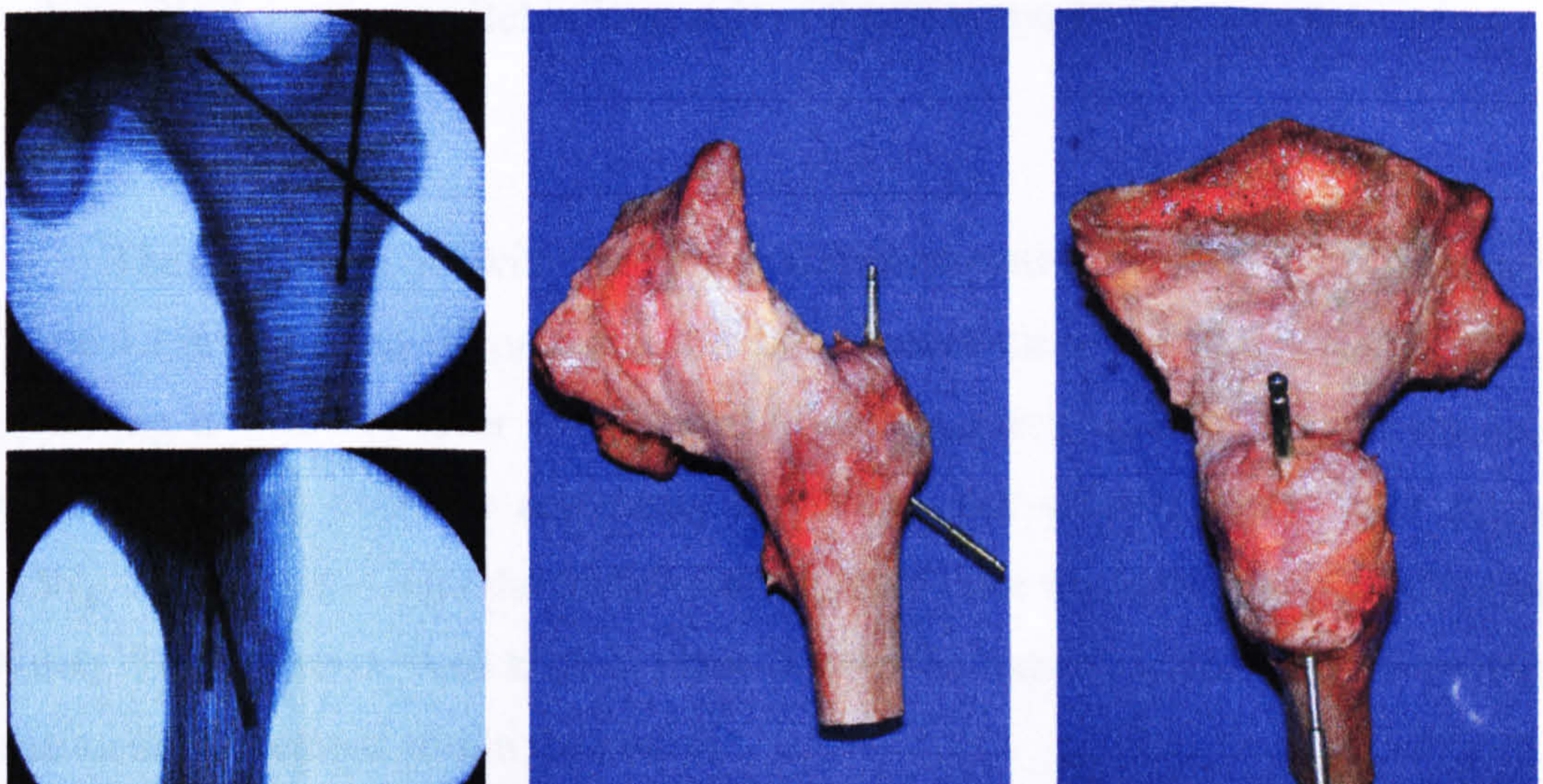

Fig 4.13 X-rays of anterior and lateral aspect of the specimen after having inserted wires that would help aligning them in the cementing pots and on the rig.

After all necessary works on the tissues were completed, the femoral component was inserted into the cylindrical cementing pot (figure 4.14a) making sure that no contact between the bone and any part of the pot was made. This was guaranteed by the screws that were inserted in the walls of the pot, which would hold the specimen in place until the cement would harden when they would be removed. Care had to be taken that the long axis of the femur was in parallel alignment with the long axis of the cylindrical pot.

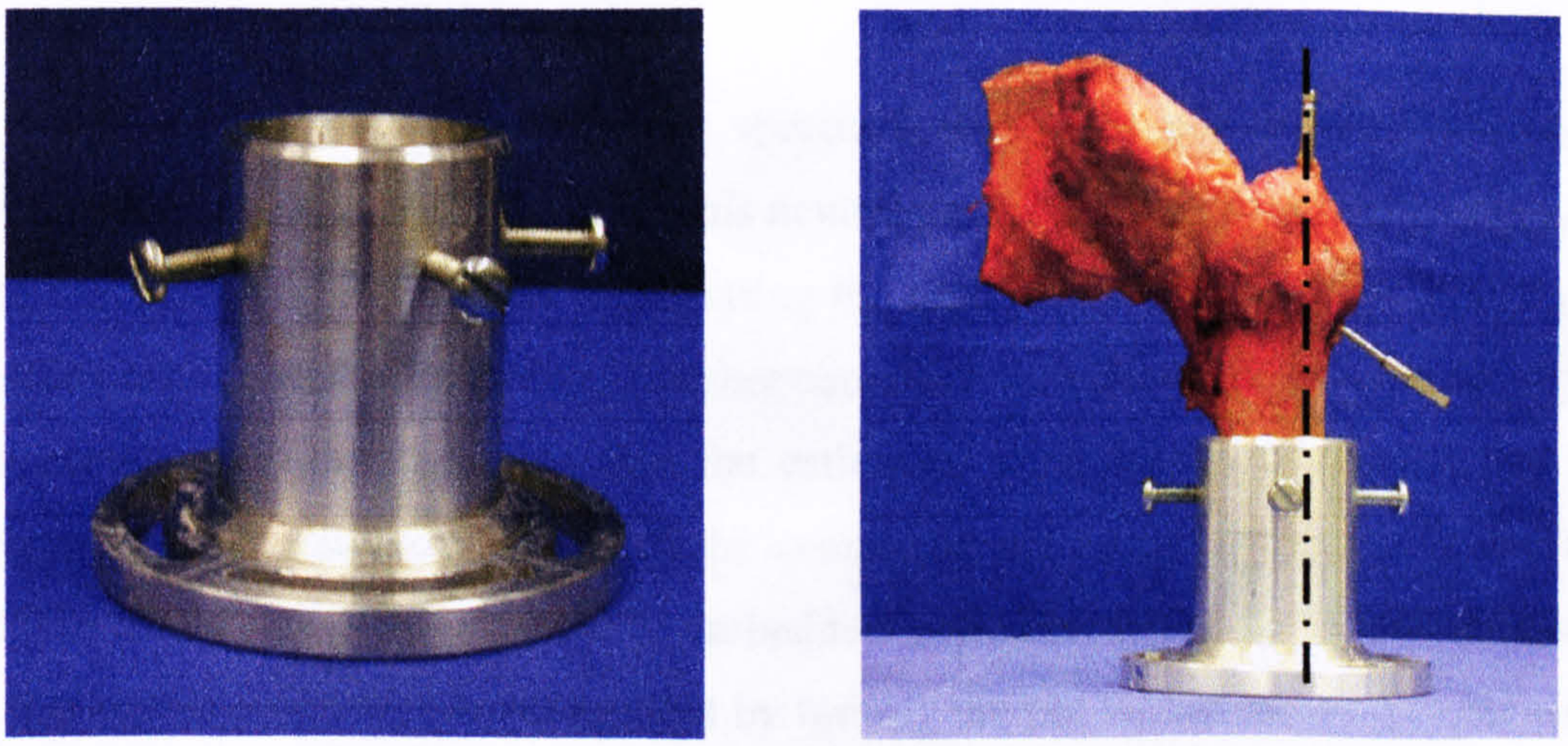

Fig 4.14 a and b The femoral cementing pot. The femur is held by screws in place. Black line is parallel to long axis of femur as marked by Kirschner wires

The cementing pot with the joint was then mounted onto the cementing frame (figure 4.15a). The way of mounting the femoral cementing pot on this frame was by supporting it with the lever arm in such way that the acetabular part of the joint would be placed over the acetabular cementing pot without touching it (figure 4.15b). Small screws held the acetabulum in place once the appropriate position was chosen. These screws were kept in place during the tests as a resistance to possible rotation of the cement within the pot.

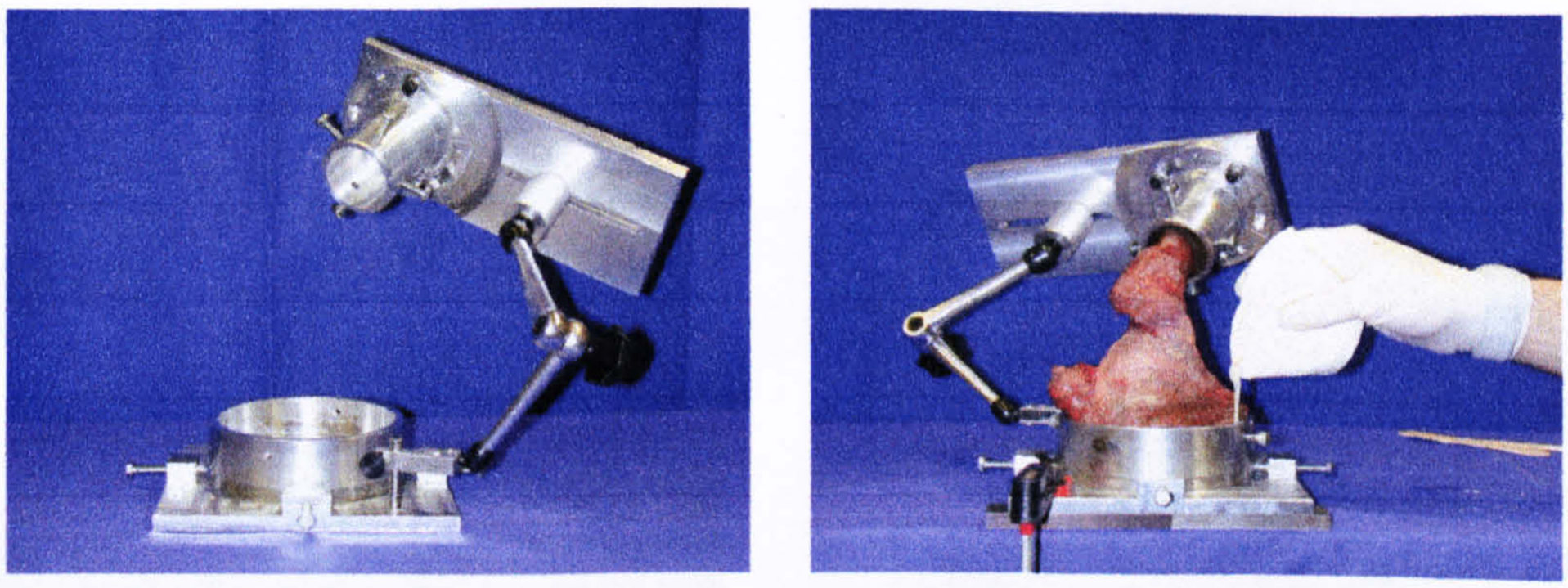

Fig 4.15 a and b The cementing frame with its two cementing pots. (b) Joint kept in neutral position during cementing.

The cementing frame held the specimen within the pots in a position that simulated the neutral joint position. This neutral position was approximately the one that was also used in the tests representing the limb position of a person lying in a supine position on a hard surface. Another necessary restriction prior to cementing of the acetabular component was that the estimated joint centre of rotation should overlap with the diameter centre of the cementing pot as closely as possible. The surface of the acetabulum should be embedded in parallel to the pot's surface. Only in this way it could be guaranteed that by turning the pot within the acetabular sub-assembly a movement of flexion or extension would be simulated.

Once the joint elements were aligned appropriately within the cementing pots, the inner walls of the pots were covered with silicone spray to facilitate removal of the specimen out of the cementing pots after the test procedure. The cement mix that was used for bonding the specimen with the cementing pots (figure 4.16) was composed of a powder and a liquid form (mix ratio 2:1) of a substance containing methyl metacrylate (Technovit®, Heraeus Kulzer GmbH & Co KG, D-61273 Wehrheim/Ts, Germany). The required hardening time was approximately 5 minutes.

Fig 4.16 The cement components.

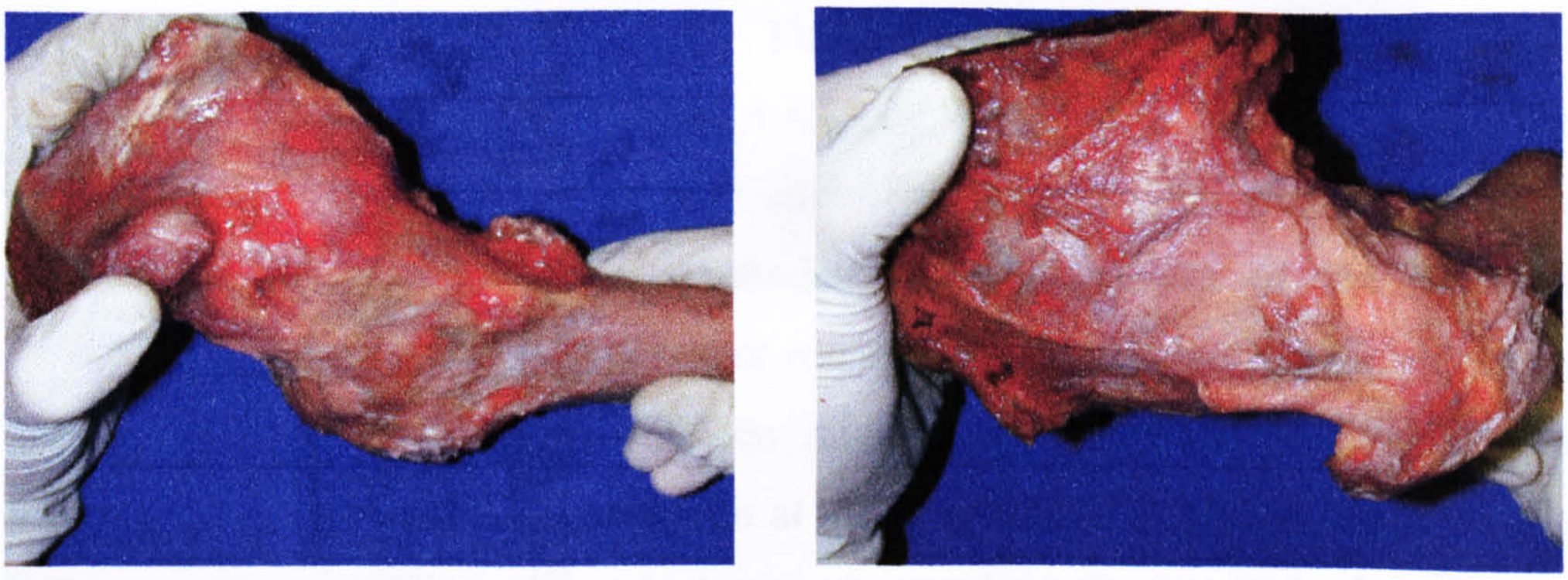

Fig 4.17 a and b The ligamentous structures of the capsule under tension.

It was noticed that the way the specimen were prepared it could very easily have happened that some of the actual ligament strands were embedded partly within the cement. This could have lead to erroneous recordings in the tests. Therefore, prior to choosing the final position of the specimen within the pots the individual ligament strands were identified by tensing the joint into its extremes of motion (figure 4.17 a and b). While the cement was dispensed into the pots it had to be taken care of that none of these strands was accidentally embedded in the cement.

4.2.3 Test Set-up

After the specimen was completely embedded in the bone cement, they were transferred to the test rig- described in paragraph 3.7- that was mounted on the MTS Bionix 858 (MTS Systems Corporation, Eden Prairie, Minnesota, USA) test machine. The angles that could be adjusted and locked by turning certain components of the rig, were: flexion/extension and internal/external rotation of the femoral bone relative to the acetabulum. These adjustments could be achieved by turning parts of the rig as well as by moving other parts linearly. The only angle that can not be adjusted on the rig is abduction/adduction, because that is what the MTS records for the purpose of this study at a sampling rate of 10Hz. The angular velocity of the cross-head was selected at 25 deg/s, where both the viscous and elastic behaviour of the ligaments contribute. This is about the average angular velocity at which the leg swings in normal to brisk walking. The angular velocity is not actually constant throughout the complete swing phase, but reaches a peak in mid-swing and decelerates towards the extremes of swing phase, i.e. near full flexion and extension.

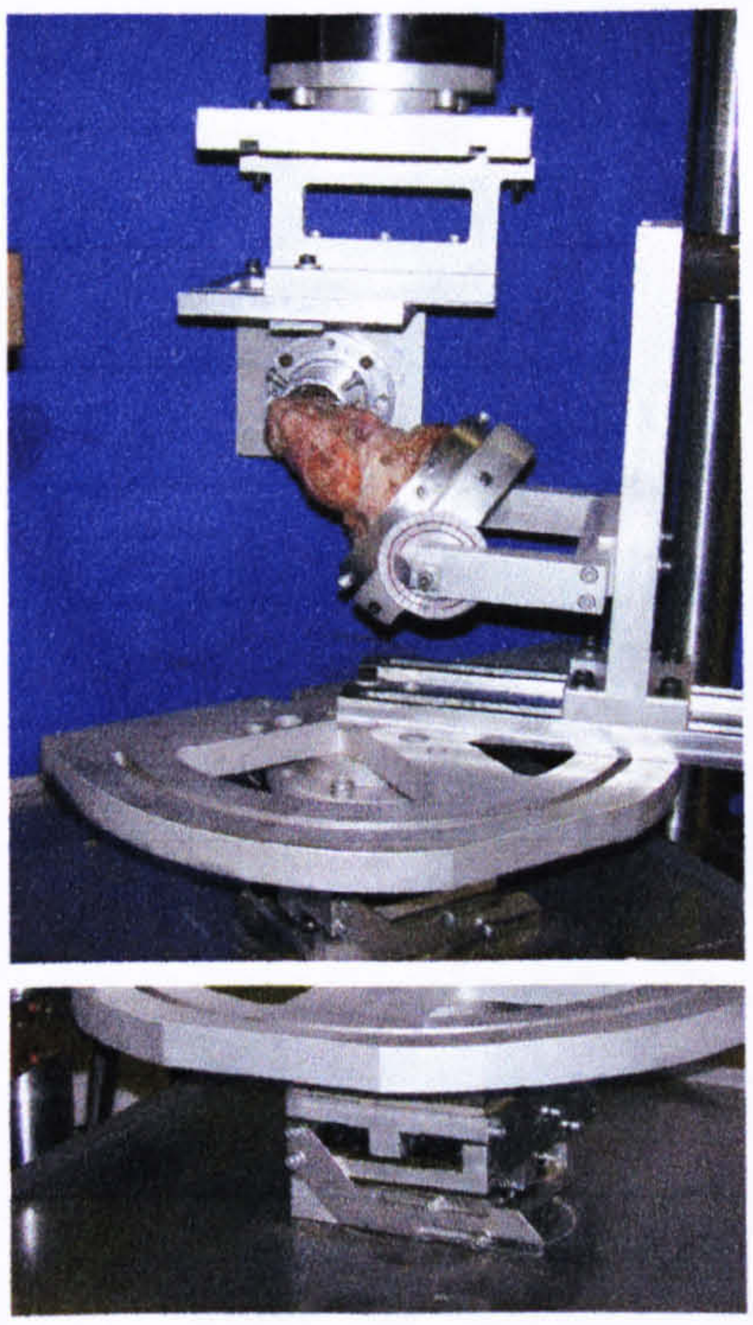

Fig 4.18 The x-y table.

The complete rig was based on a x-y table (figure 4.18) that was capable of moving by ±3.5cm in both axes. These movements were necessary to accommodate a self-alignment of the hip joint centre of rotation. This centre has to be in alignment with the adaptor of the MTS machine on the actuator at the crossbar and the flange of the test rig, which was mounted on the x-y table. In this way, even if the alignment was not maintained during the applied rotational movement, the x-y table would allow a certain amount of movement that can prevent the build-up of external stresses, disturbing the data acquisition.

A Kirschner wire was used to indicate the axis of rotation, which had to be in alignment with the joint centre of rotation of the MTS adaptors (figure 4.19). The yellow 'bull's-eye' indicates the estimated joint centre of rotation as it was identified by the investigator after moving the acetabulum in relation to the femoral head in all the directions. Depending on the initial location of the joint centre of rotation it was possible to adjust the position of the femur in the x and y direction and keep it locked there throughout the test procedure. All necessary adjustments would then be done by moving the acetabular joint part into different angles, thus simulating the required test positions (i.e. neutral, full flexion, full extension etc.). These adjustments could be monitored and recorded for reproduction after the dissection of another capsular ligament, with the assistance of different scales.

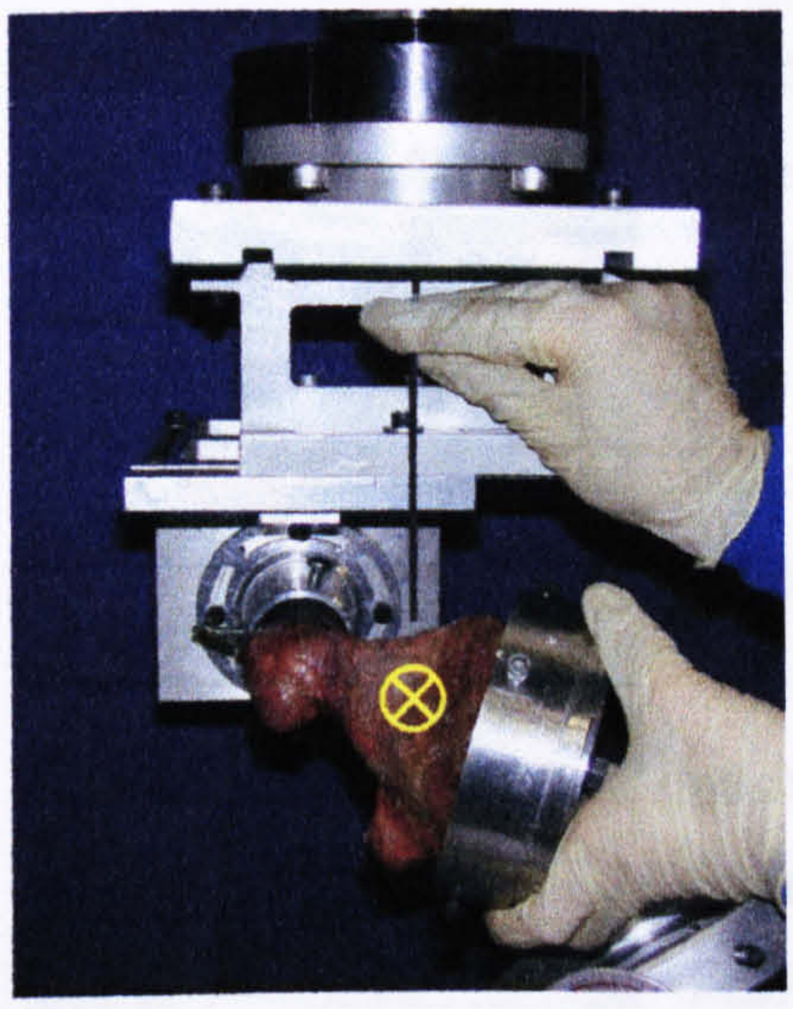

Fig 4.19 Aligning the joint centre.

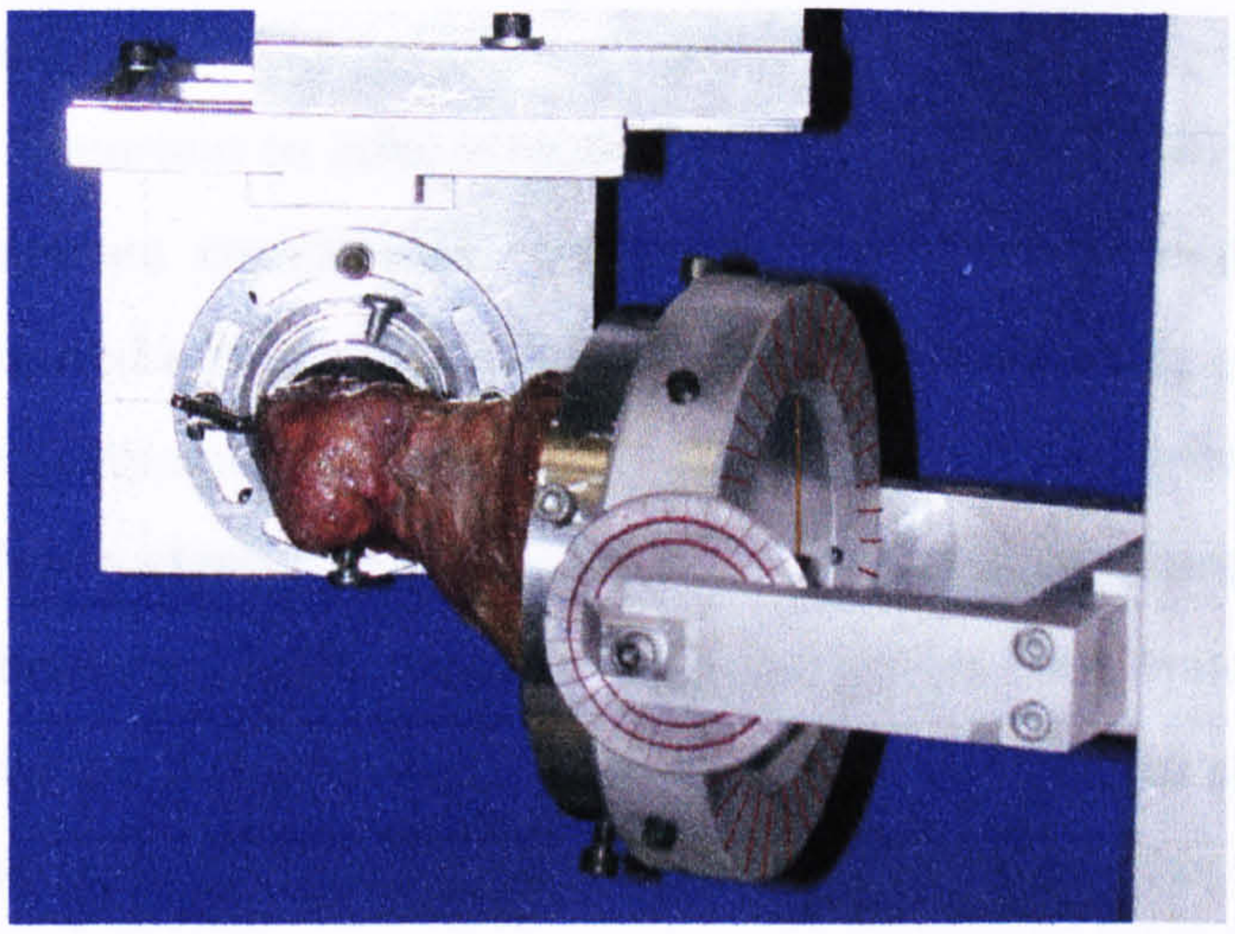

Fig 4.20 The adjustment of the acetabulum with the help of circular scales.

Since the acetabular cementing pot was the only part of the joint that was altered between the test stages, it was only for these apertures that adjustment scales were placed. In particular, there were two circular scales engraved on the acetabular sub-assembly (figure 4.20). The larger disc shows increments of 10°, which were relevant for adjustments of flexion and extension by moving the acetabulum. That is also the reason why it was considered to be so important to have the plane of the acetabulum parallel with the cementing pot's bottom. The smaller disc at the side of the sub-assembly was of assistance when adjusting the degree of internal or external rotation. Clearly, the use of a potentiometer instead of an analogue display would have been more accurate and might have resulted in a smaller error. However, in addition to the circular scales and for the purpose of higher accuracy, linear scales were attached to the sides of the linear slides of the rig- marked with orange in figure 4.21. After all positions had been recorded with an intact capsule, the same positions could be reproduced using both the scales in figure 4.20 and 4.21, for the cases of additionally divided ligaments.

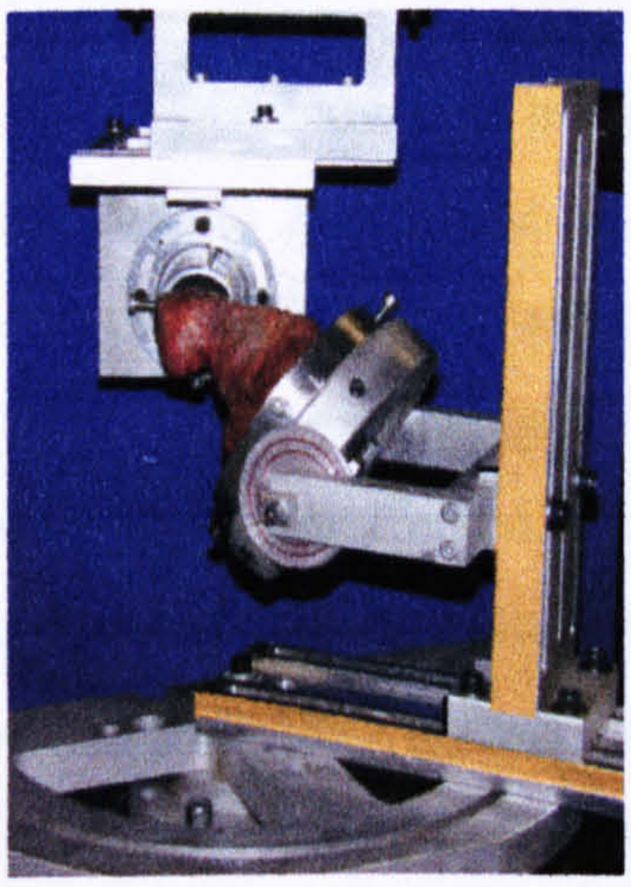

Fig 4.21 The linear scales.

4.2.4 Test Protocol

It is very important to adhere to a certain testing protocol in order to ensure that all recordings are comparable. This study on complete cadaveric hip joint specimens was carried out in order to improve our understanding of the function of the capsular ligaments and their individual importance to hip joint stability. These effects are not shown clearly in models of excised individual strands that are tested under tension. However, as the capsule really comprises four major ligaments that strengthen it in various movements, it was considered necessary to study the effect of each of them, but instead of doing so in a random fashion it was decided to study their effect simulating a real situation. A real situation could be the case of a THR where the capsule is most commonly damaged to allow access to the joint surfaces. In particular, depending on the approach of surgery, it is either the anterior or posterior as well as the lateral capsular ligaments that are damaged.

The anterior and anterolateral approaches require a complete anterior exposure of the joint, which in turn would make a complete excision of the medial and lateral iliofemoral ligaments necessary (Eftekhar, 1978). In the contrary to that, posterior and posterolateral approaches require a complete division of the posterior capsular ligament and usually also the lateral iliofemoral ligament. The posterolateral approach involves division of the ischiofemoral ligament as well as the lateral iliofemoral ligament.

In Charnley's preferred method of the lateral or transtrochanteric approach, the medial and lateral iliofemoral ligaments are kept intact and only the posterior capsule is divided in order to allow the joint to be dislocated. However, even in this "least capsule damaging" approach the lateral iliofemoral ligament is not left completely unaffected, as its distal insertion point- the greater trochanter- is detached for the purpose of surgery and re-attached thereafter. Only if no effect from re-connecting the greater trochanter can be assumed, will the lateral iliofemoral ligament be considered unaffected.

Whichever the selected approach, two ligaments are damaged- namely either both ischiofemoral and lateral iliofemoral ligaments or both medial and lateral iliofemoral ligaments. For this reason it was decided to proceed with the cadaveric tests by dissecting the same combinations of ligaments, in the hope to identify from the results, which of the two combinations would place the least burden on the post-operative rehabilitation and range of motion.

For the above reasons it was decided to test three specimens for risk of posterior dislocation- which is higher in case of a posterior or posterolateral approach where the posterior and lateral ligaments are removed and two specimens for risk of anterior dislocation, which is more evident when anterior ligaments are removed i.e. during anterior and anterolateral surgical procedures. The situations that were simulated in both cases were limb positions that enhance risk for posterior and anterior dislocation equivalently (Scifert et al, 1998 and Romanes, 1977).

Posterior Dislocation

Four situations were simulated in this trial

- Neutral Position
- Full Flexion
- Full Flexion and Internal Rotation
- Full Internal Rotation

Anterior Dislocation

Again four situations were simulated in this trial

- Neutral Position
- Full Extension
- Full Extension and External Rotation
- Full External Rotation

These situations were recorded for the case of an intact hip joint capsule and then repeated at the same locations for the cases of a dissected ischiofemoral ligament and again for the case of an additionally dissected lateral iliofemoral

ligament. For the case of the anterior dislocation study the situations that were simulated were for a removed medial iliofemoral ligament and again for an additionally removed lateral iliofemoral ligament. Figures 4.22a and b show how the ligament was divided, while the specimen remained mounted on the test rig.

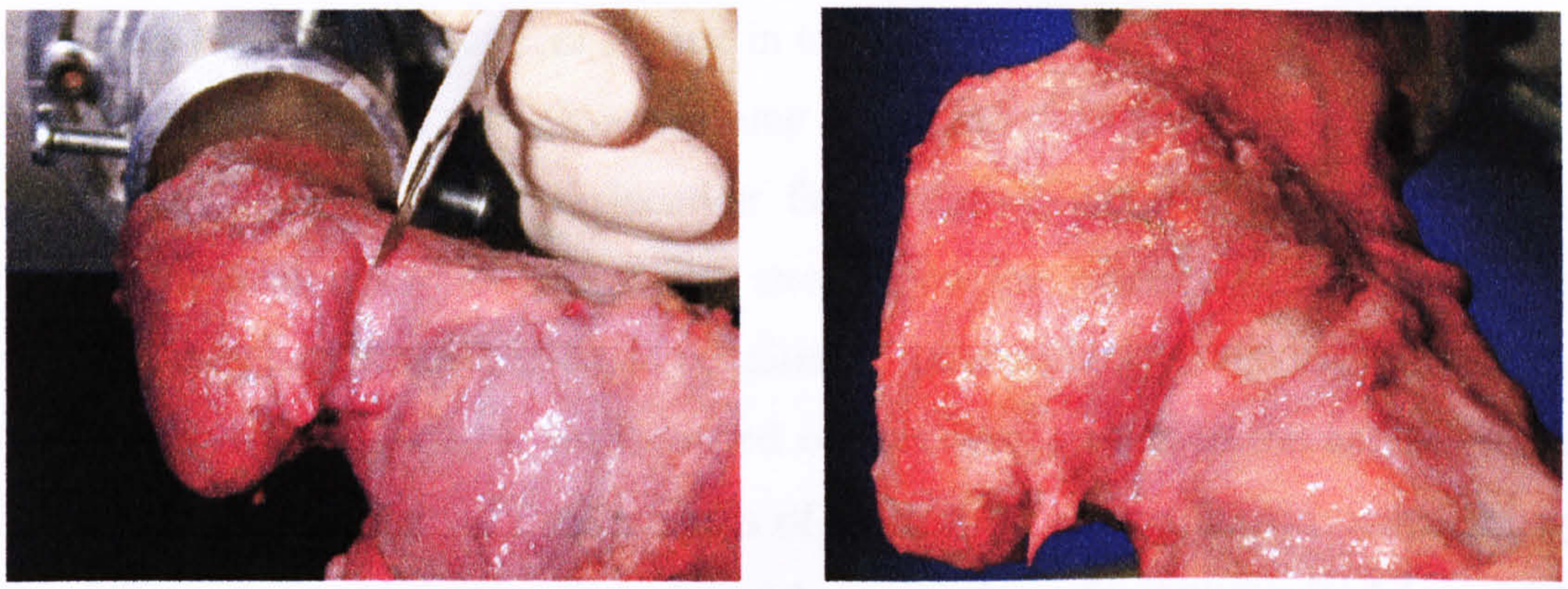

Fig 4.22 a and b The targeted ligament was divided under tension. (b) After the cut.

4.2.5 Data Processing

The final stage of the cadaveric study comprises the data processing in such a way that the findings can be presented in a clear and comprehensible way. A correct and sound data processing assists also in the statistical calculations, which is vital for the detection of any significant effects of the division of certain capsular ligaments. Since the actual recordings by the MTS were for the abduction/adduction angle, the collected data sets included negative angles and moment recordings as well as positive ones. Between those peaks was a region of almost zero moment. In most cases the moments within this region were between –0.3 Nm and +0.3 Nm. Next to these border values was the start of the stiffness curve, given that the following recording would show a 50% change from it i.e. be ±0.45 Nm. Somewhere within this region must be the neutral position, where the limb is neither in abduction nor in adduction. In a cadaver comprising only bone and ligaments it is extremely difficult to decide where this neutral position would be. In the absence of a better method it was decided to adopt the observations of Gerhardt and Rippstein (1990) that a ratio of 45°:35° (or equivalently: 56.25% : 43.75%) exists between abduction and adduction. This ratio was then applied to that near zero region between –0.3Nm and +0.3Nm of recordings.

4.3 Effects of Individual Ligaments on Joint Stiffness

In the following paragraphs it is presented how the various ligaments of the hip joint capsule contribute to the total resistance to rotation of the joint. This effect is analysed with regard to changing limb positions as simulated by moving the femoral joint part in relation to the acetabular part whilst they were kept mounted on the test rig. There were three specimens for use in tests for posterior dislocation risk and two for anterior dislocation risk. However, one of the specimens that were used for the study of risk for posterior dislocation failed during the test procedure due to inadvertent loading, which raised the stresses on the ligaments excessively, and therefore only part of the data could be utilised. An additional test specimen was used for preliminary tests, which were carried out six weeks prior to the actual tests in order to highlight eventual design errors of the test rig and the experimental set up. The following graphs feature the relation between the moments required (y-axis) to drive the femoral joint part into the various angles as they were recorded versus the actual angles (x-axis).

4.3.1 Joint Stiffness and Posterior and Lateral Ligaments

In the following pages are the graphs for those specimen that were tested for risk of posterior dislocation. They have been classified based on the limb position that was simulated by adjusting the femoral part to the acetabular part. This presentation assists in understanding the effect that a ligament excision had on the stiffness of the hip joint. Straight after the presentation of the graphs is a selection of tables that show the proportional effect of the ligament excision on the overall joint resistance. The statistical results follow thereafter and give an impression on the significance of the individual findings.

The way the graphs have been designed is to include the abduction/adduction angles on the x-axis and the respective moment recordings on the y-axis. Thereby, the labels in the corners of each graph indicate whether the joint was in abduction or adduction. The title of each graph refers to the angle that was selected during the particular recording, which was kept fixed throughout the respective data acquisition. This angle, of course, is different from the recorded angle of abduction/adduction.

Neutral Position

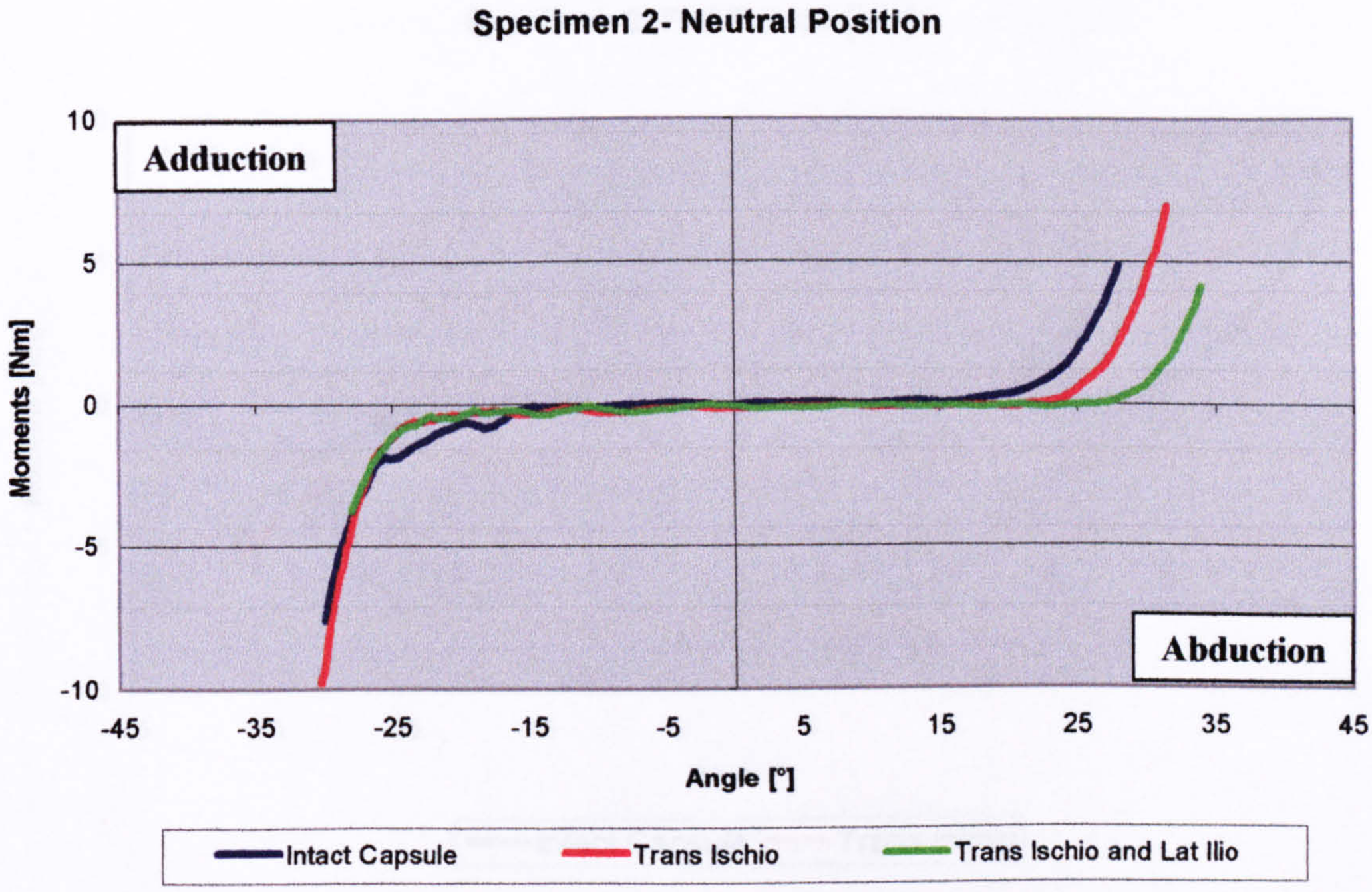

Figure 4.23a The joint resistance to abduction-adduction motion.

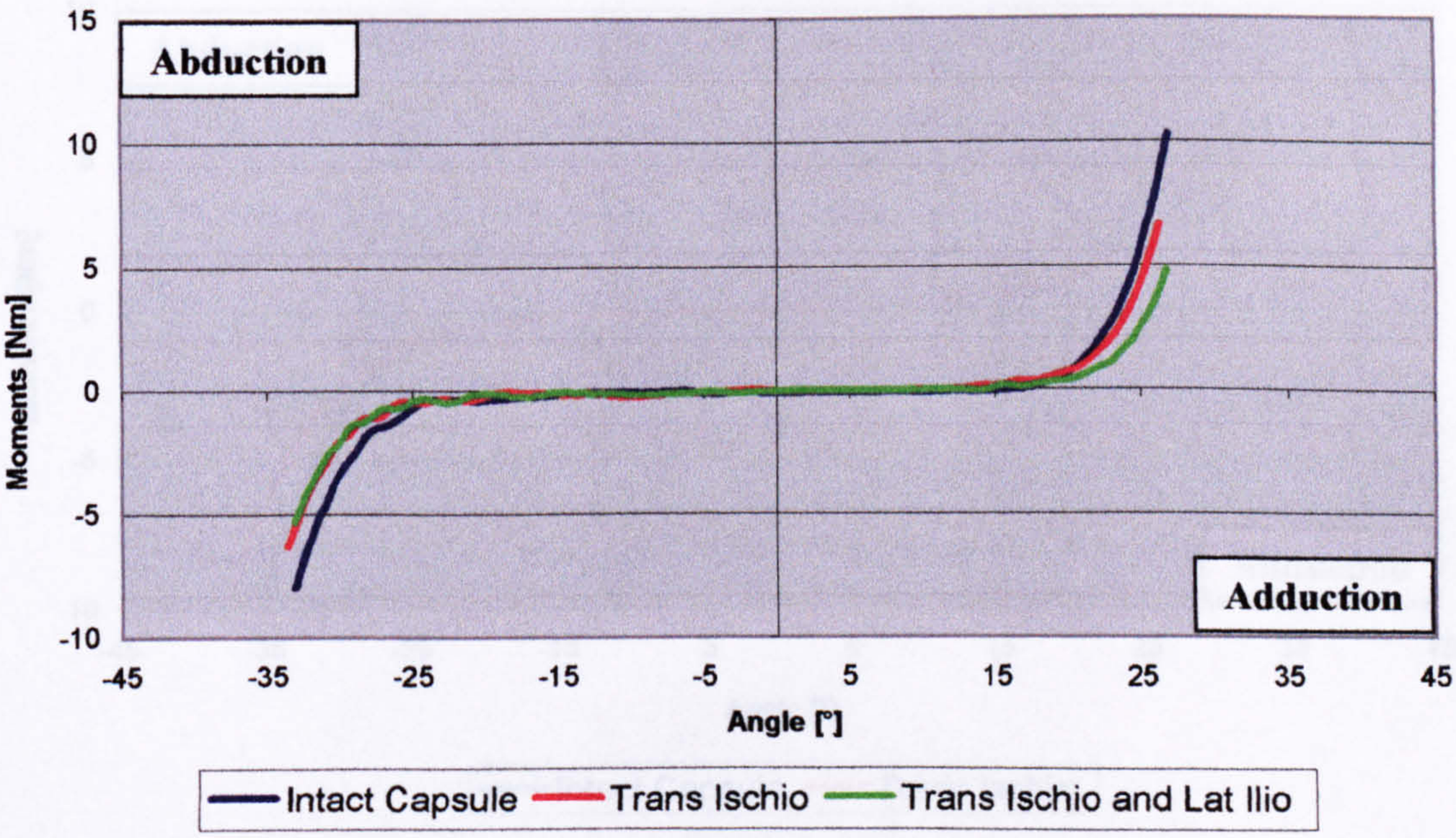

Figure 4.23b The joint resistance to abduction-adduction motion.

Full Flexion

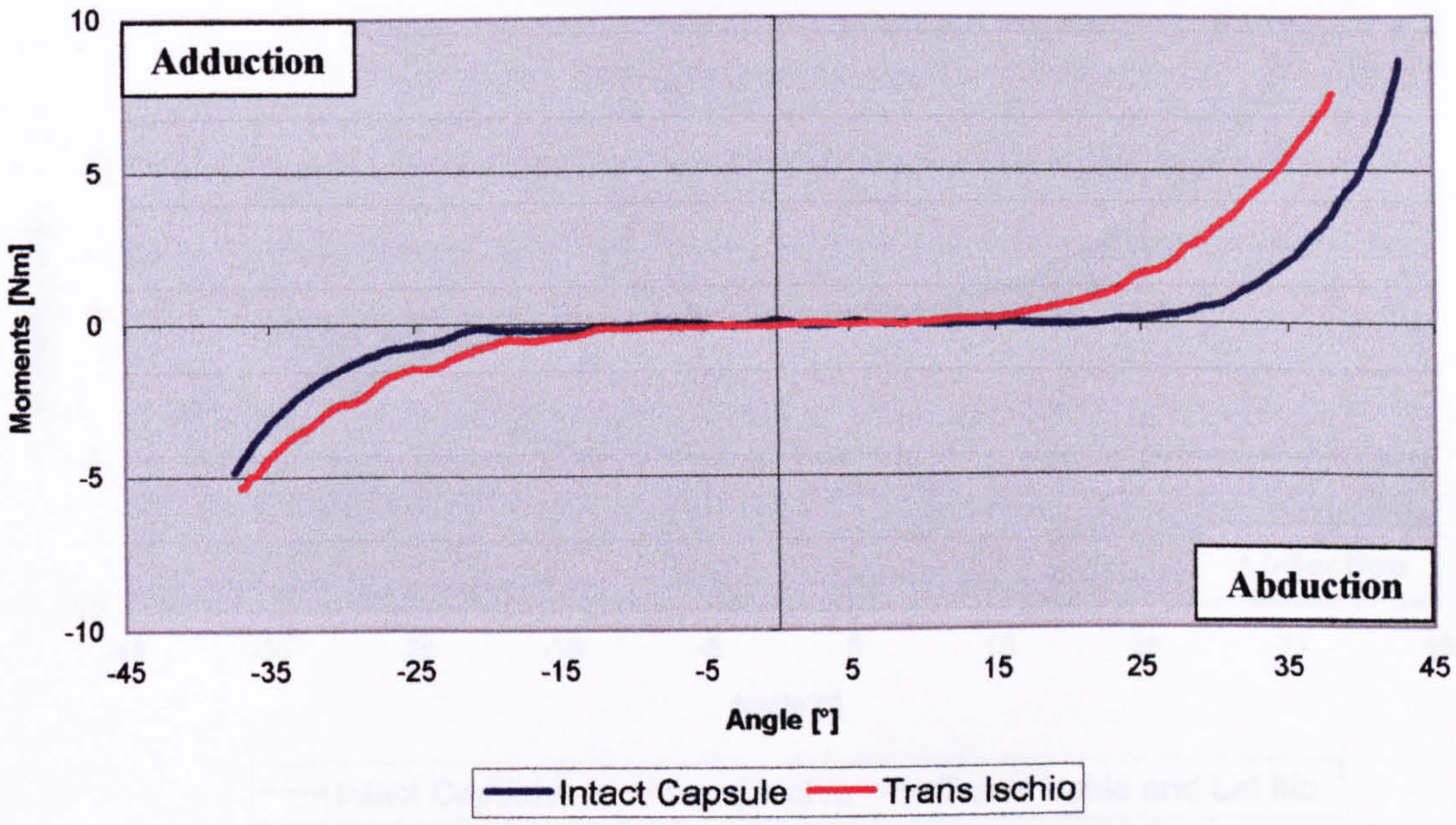

Figure 4.24a The joint resistance to abduction-adduction motion.

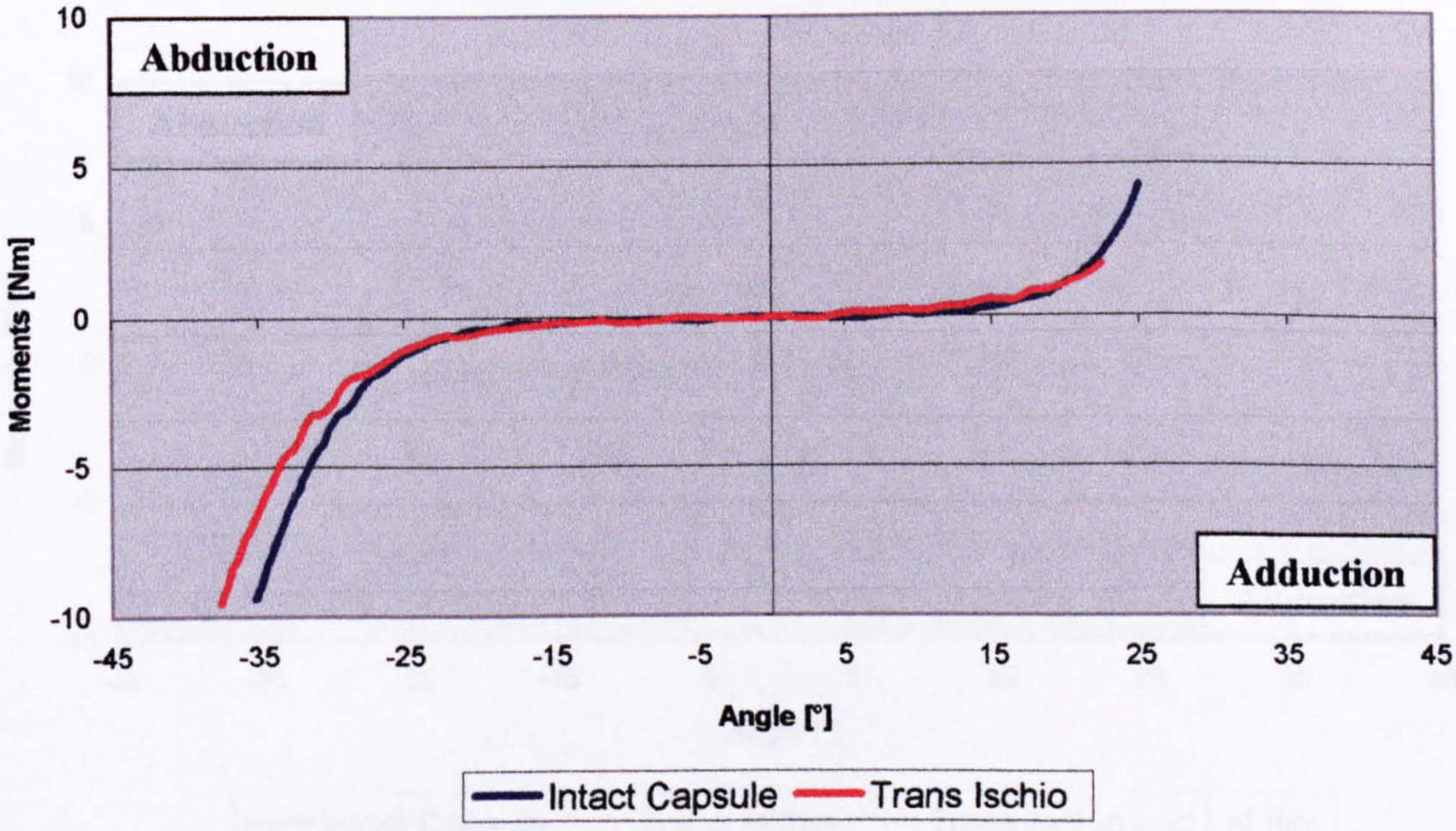

Figure 4.24b The joint resistance to abduction-adduction motion.

Full Flexion and Internal Rotation

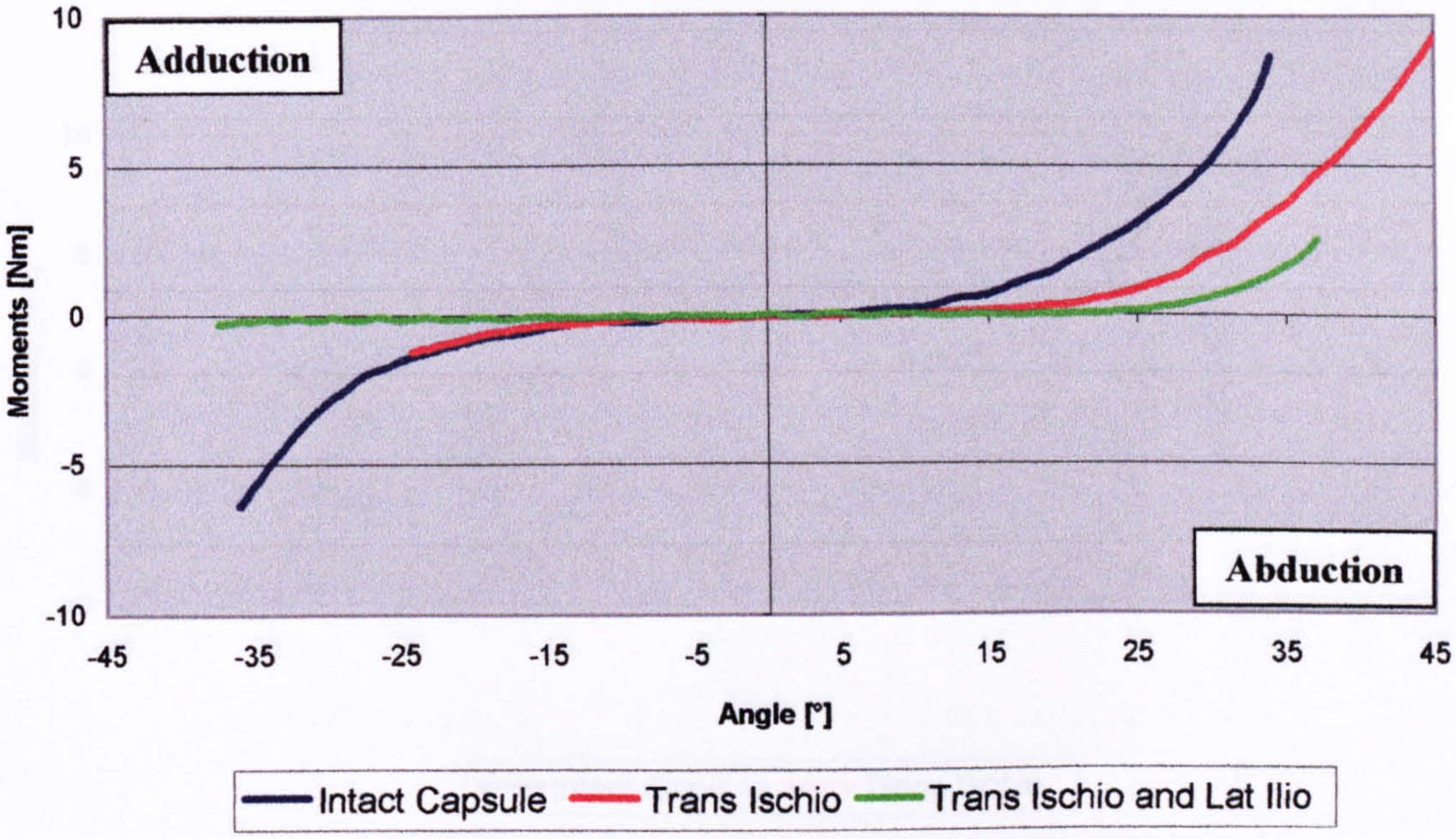

Figure 4.25a The joint resistance in abduction-adduction motion.

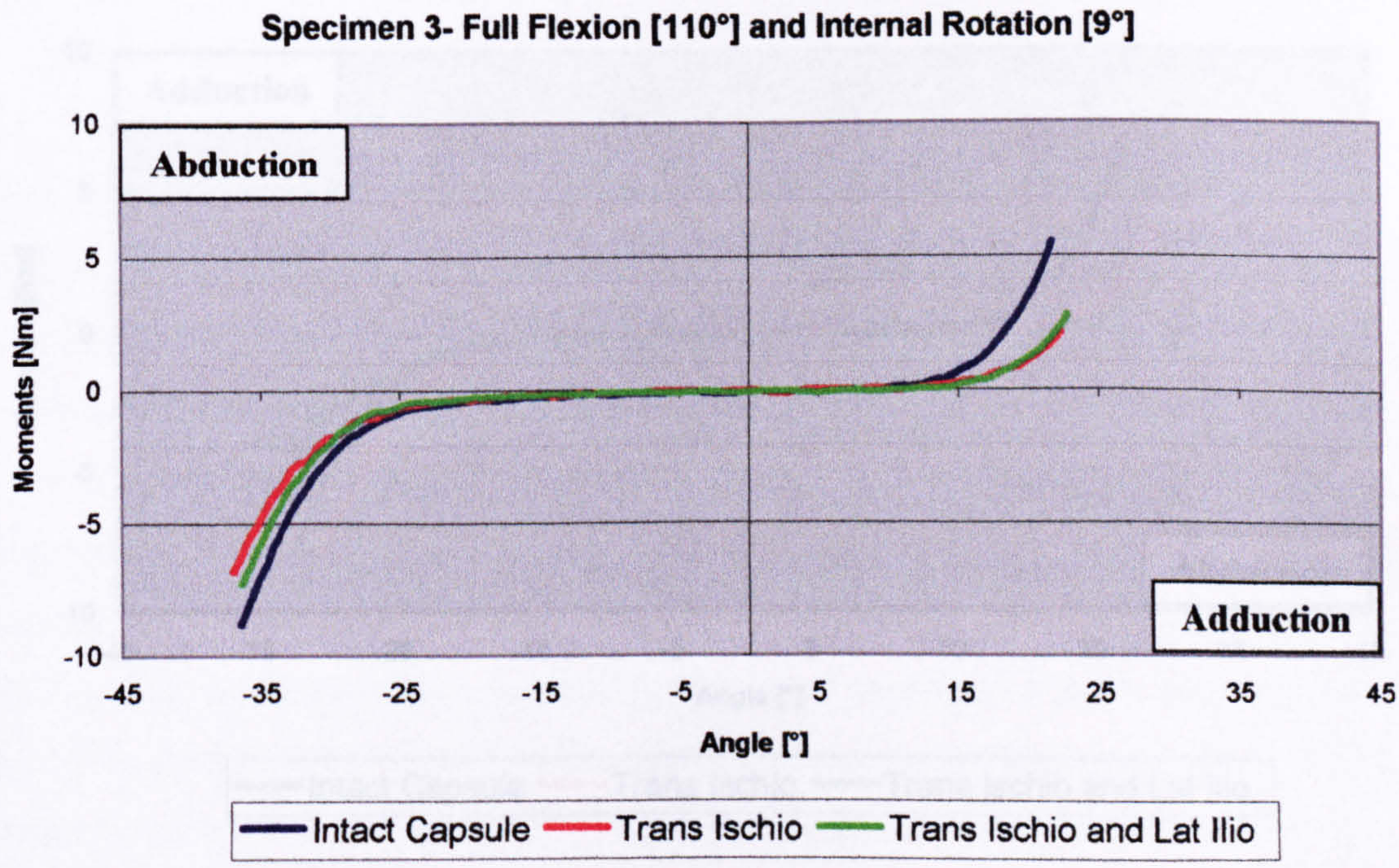

Figure 4.25b The joint resistance to abduction-adduction.

Full Internal Rotation

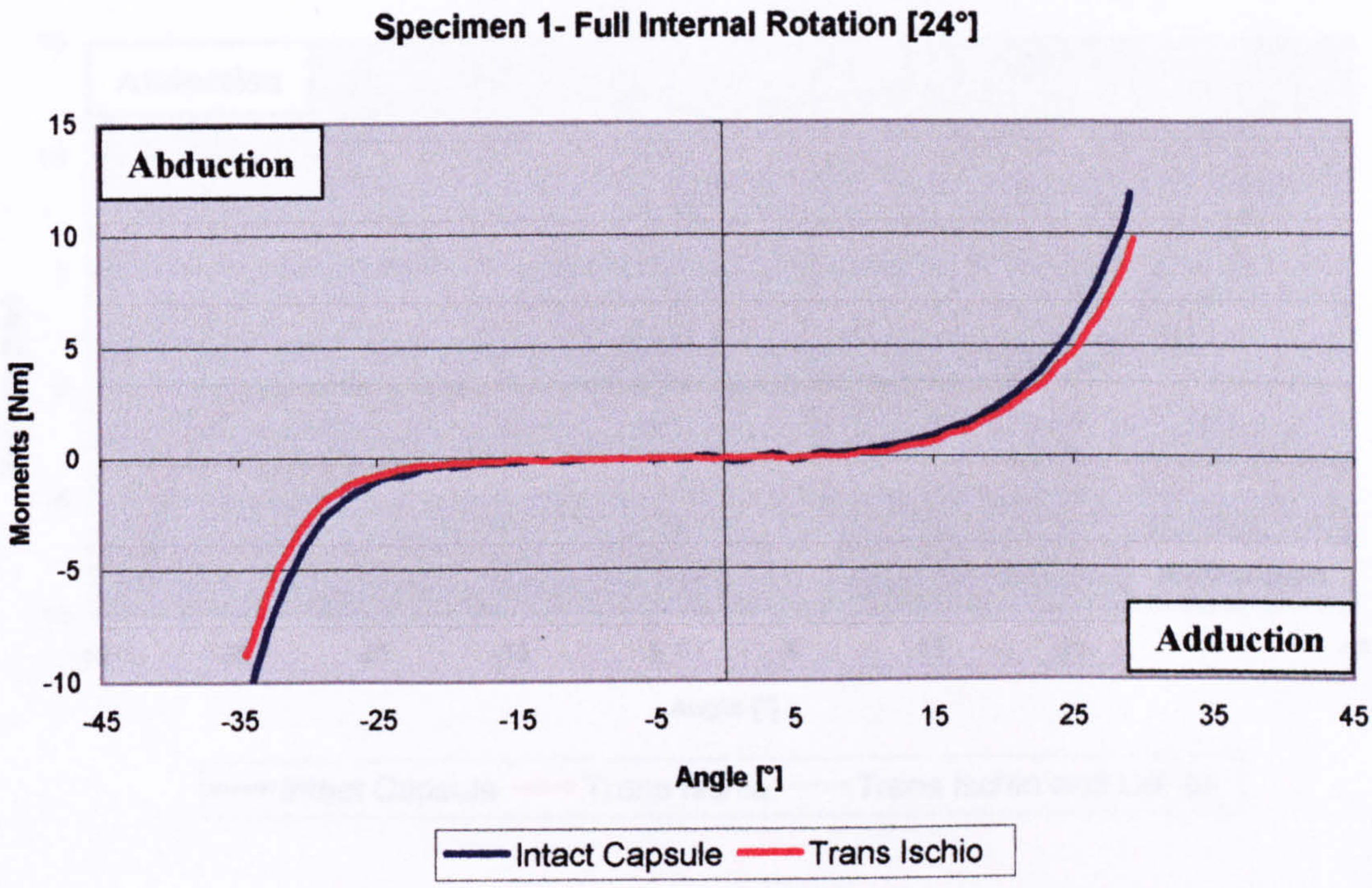

Figure 4.26a The joint resistance to abduction-adduction motion.

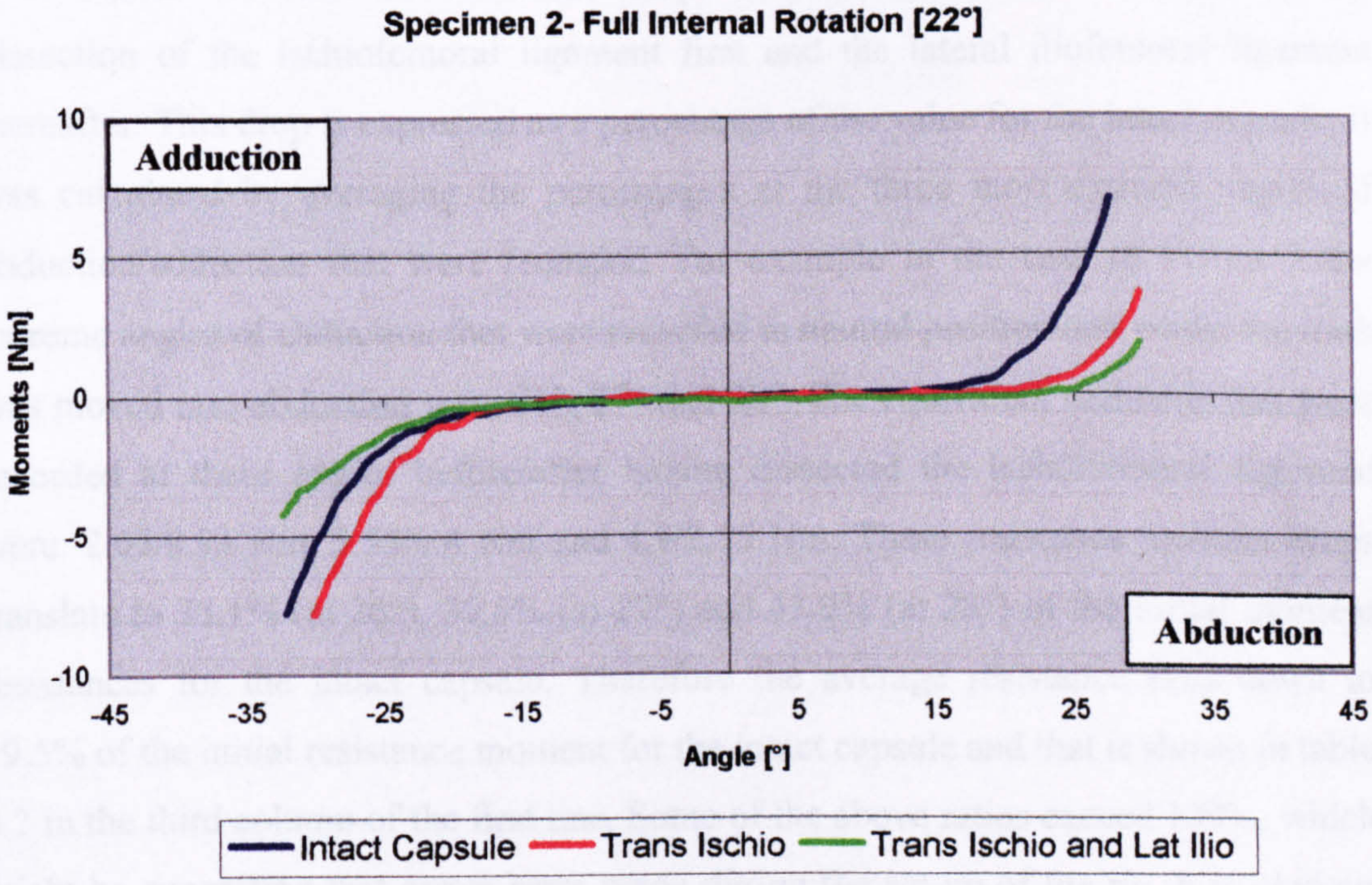

Figure 4.26b The joint resistance to abduction-adduction motion.

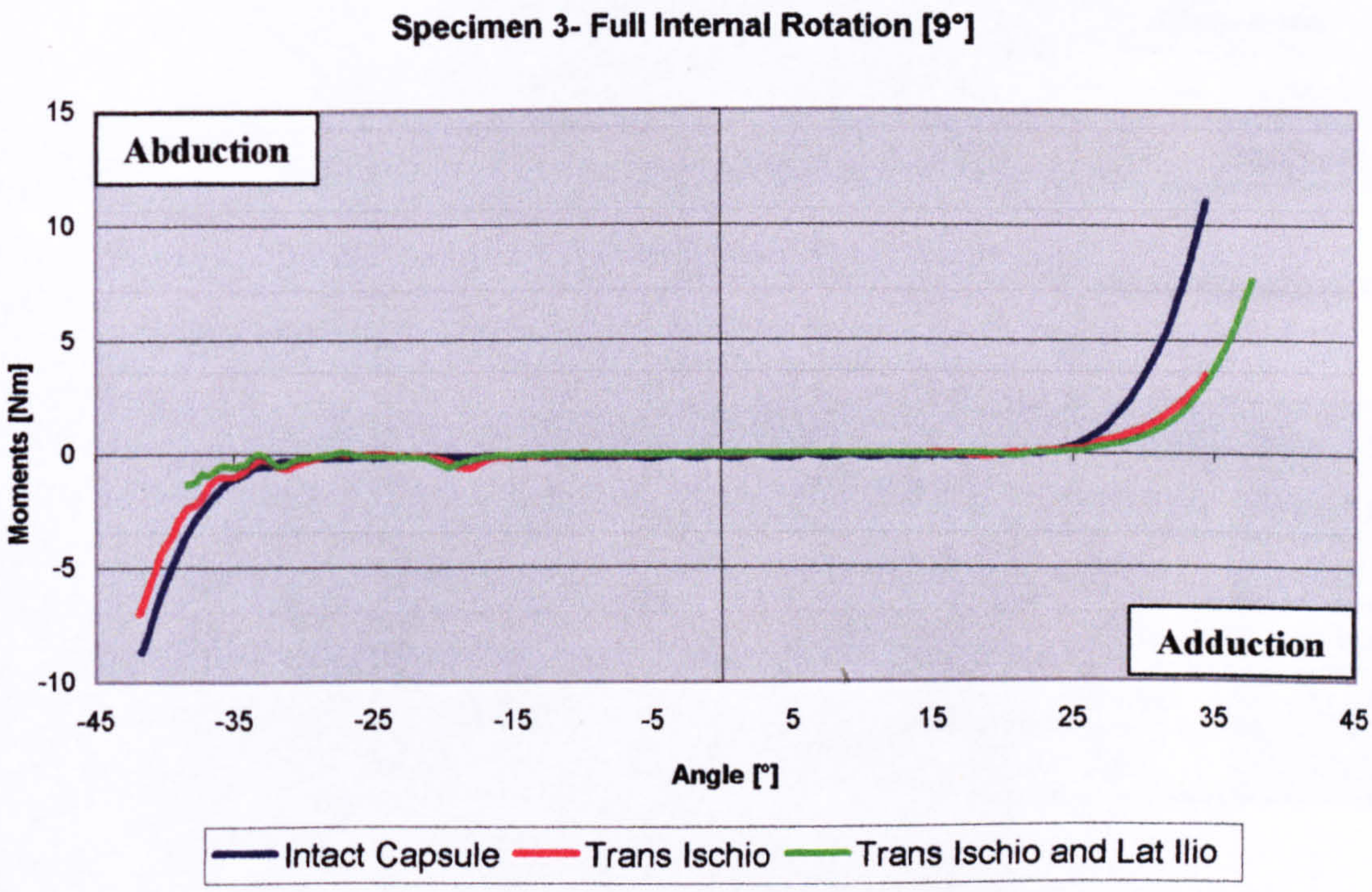

Figure 4.26c The joint resistance to abduction-adduction motion.

Tables 4.1 and 4.2 show the drops in capsule resistance caused by the dissection of the ischiofemoral ligament first and the lateral iliofemoral ligament thereafter. This drop is expressed as a percentage of the value for the intact capsule. It was calculated by averaging the percentages at the three most extreme angles of abduction/adduction that were recorded. For example in the case of Femur 2 the extreme angles of abduction that were recorded in neutral position and whilst the limb was moved into abduction were 26°, 27° and 28°. The equivalent moments that were recorded at these angles before/after having dissected the ischiofemoral ligament were: 2.65/0.93 Nm, 3.55/1.4 Nm and 4.9/2.15 Nm. These resistance moment drops translate to 35.1% (at 26°), 39.5% (at 27°) and 43.9% (at 28°) of the initial moment resistances for the intact capsule. Therefore the average resistance falls down to 39.5% of the initial resistance moment for the intact capsule and that is shown in table 4.2 in the third column of the first line. Some of the above ratios exceed 100%, which might be suggesting that errors were made during the set-up of the rig. It is obvious that the results for these limb positions can not be taken into account, as that would lead to wrong interpretations.

SPECIMEN 1	Adduction		Abduction	
	Trans Ischio	Trans Lat Ilio	Trans Ischio	Trans Lat Ilio
Full Internal Rotation	79.5%	specimen failed	78.2%	specimen failed

Table 4.1 Stiffness reduction ratios of the hip joint capsule after sequential dissection.

SPECIMEN 2	Adduction		Abduction	
	Trans Ischio	Trans Lat Ilio	Trans Ischio	Trans Lat Ilio
Neutral Position	no change	no change	39.5%	1.3%
Full Flexion	**145%**	not tested	**245%**	not tested
Full Flexion and Internal Rotation	89.5%	12.1%	39.1%	13.5%
Full Internal Rotation	**160%**	66.9%	19%	4.1%

Table 4.2 The equivalent ratios of reduction for Specimen 2.

SPECIMEN 3	Adduction		Abduction	
	Trans Ischio	Trans Lat Ilio	Trans Ischio	Trans Lat Ilio
Neutral Position	74.5%	44.7%	63%	59.1%
Full Flexion	96.4%	not tested	70.8%	not tested
Full Flexion and Internal Rotation	32%	31.5%	68.9%	81.4%
Full Internal Rotation	32.2%	25.2%	74.1%	40.7%

Table 4.3 The equivalent ratios of reduction for Specimen 3.

4.3.2 Joint Stiffness and Anterior and Lateral Ligaments

Following are the graphs of the tests for risk of anterior dislocation and the equivalent results in percent. The difference compared to the graphs of posterior dislocation risk is that now the medial and the lateral iliofemoral ligaments of the hip capsule were sequentially dissected. It is brought into the reader's attention once more that in specimen 4 an intramedullary fracture fixator was discovered unexpectedly, which resulted in several bone deformities to be present. The conclusions from those graphs should be drawn conservatively as for the purpose of the statistical analysis they are not taken into consideration.

Neutral Position

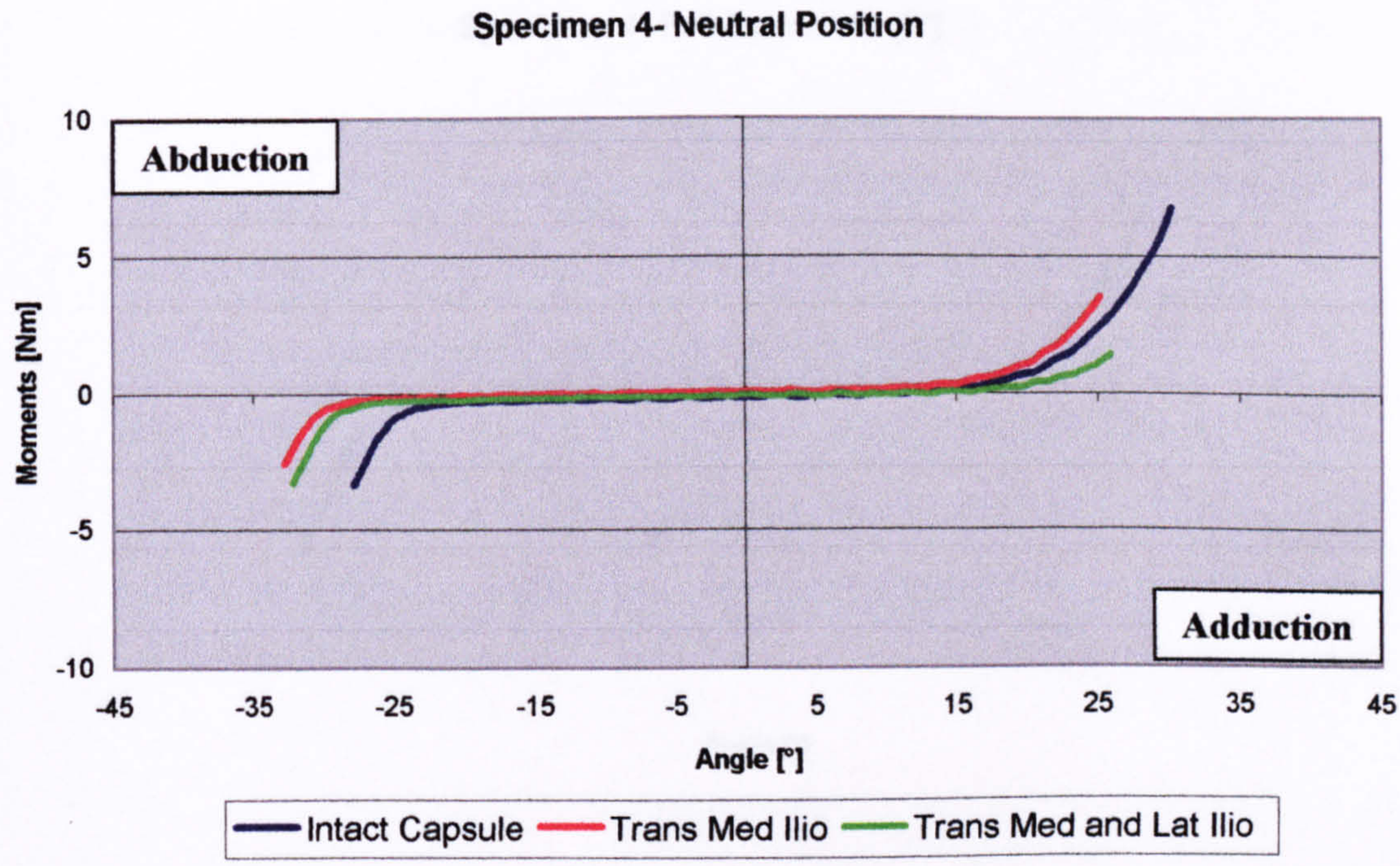

Figure 4.27a The joint resistance to abduction-adduction motion.

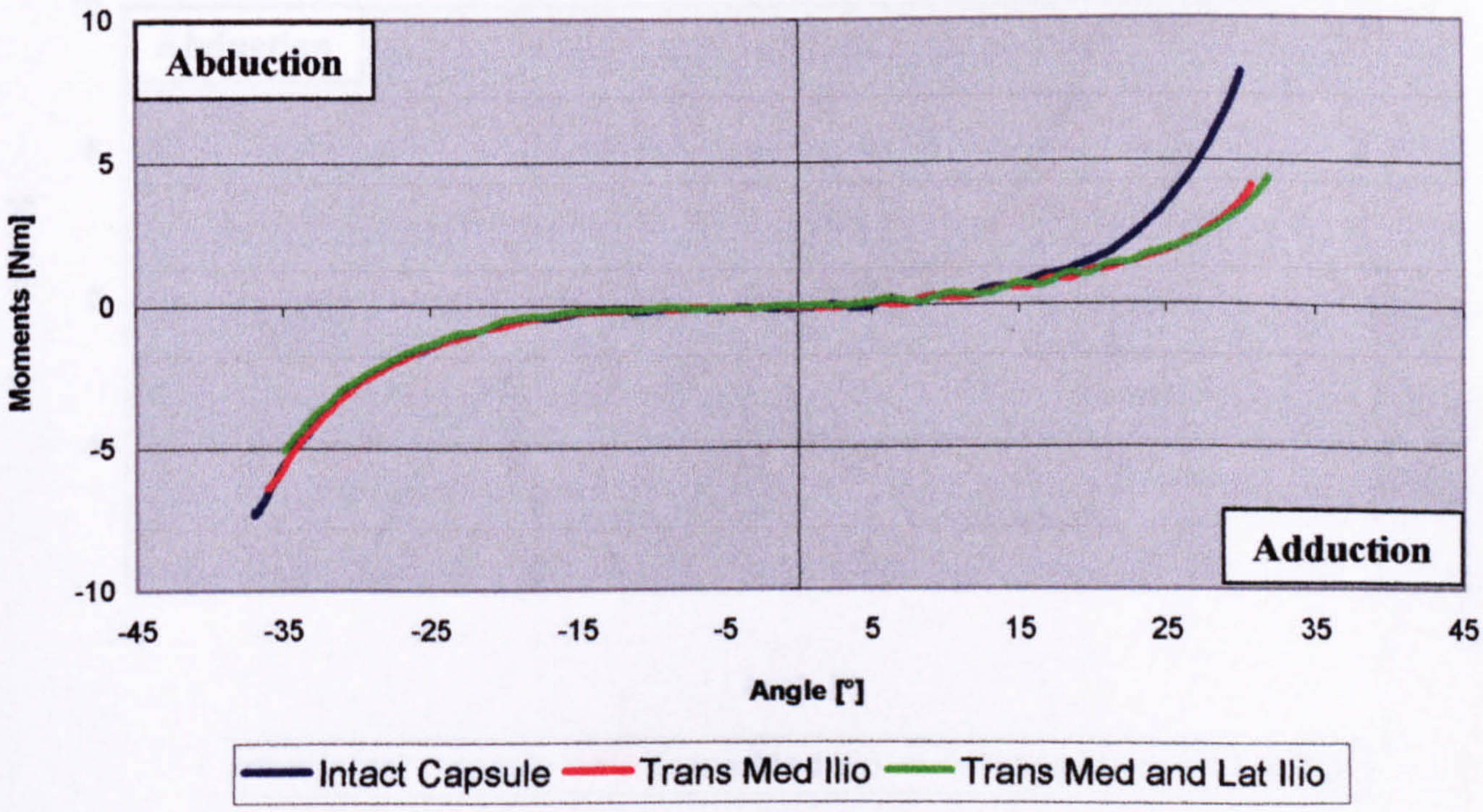

Figure 4.27b The joint resistance in abduction-adduction motion.

Full Extension

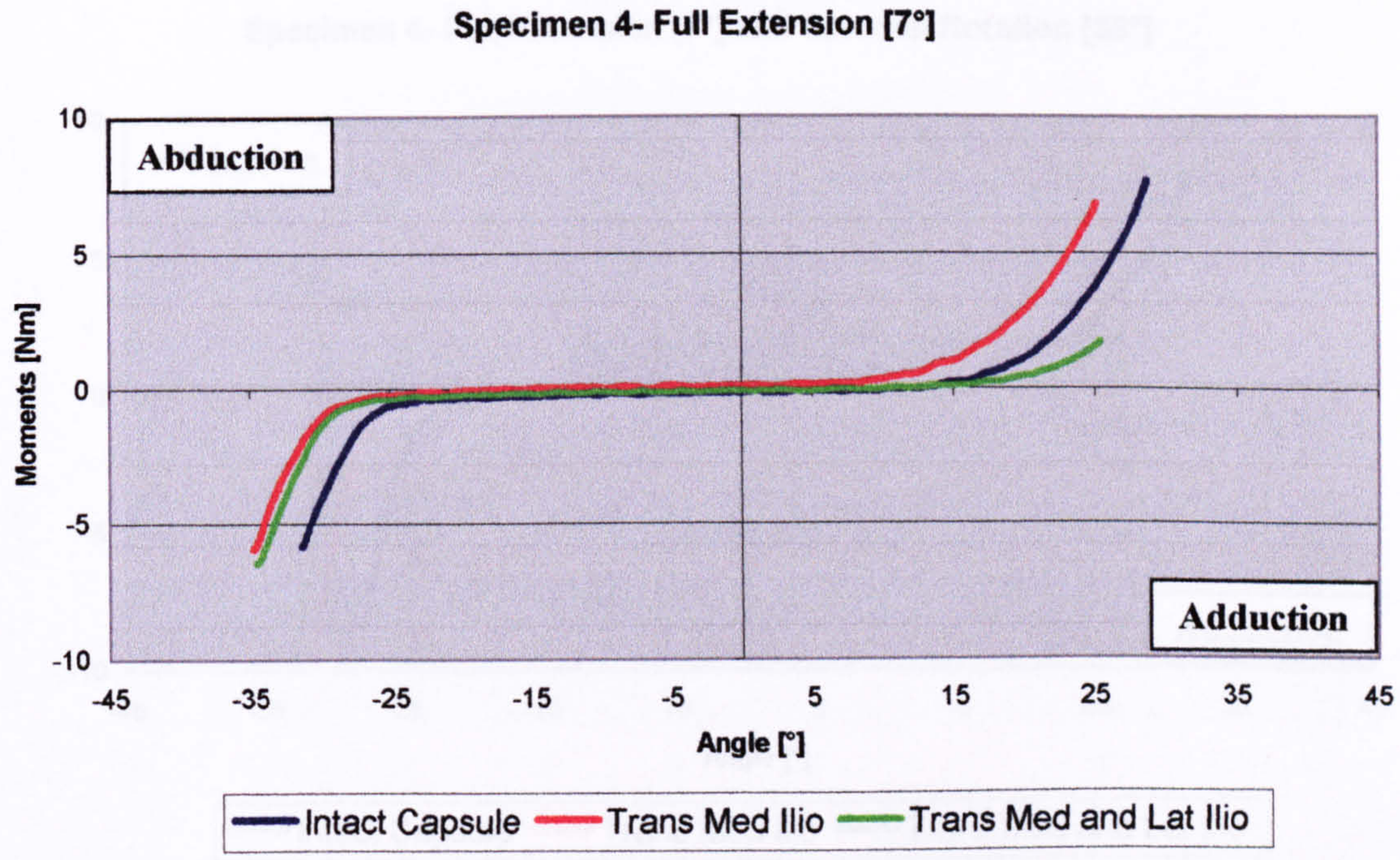

Figure 4.28a The joint resistance in abduction-adduction motion.

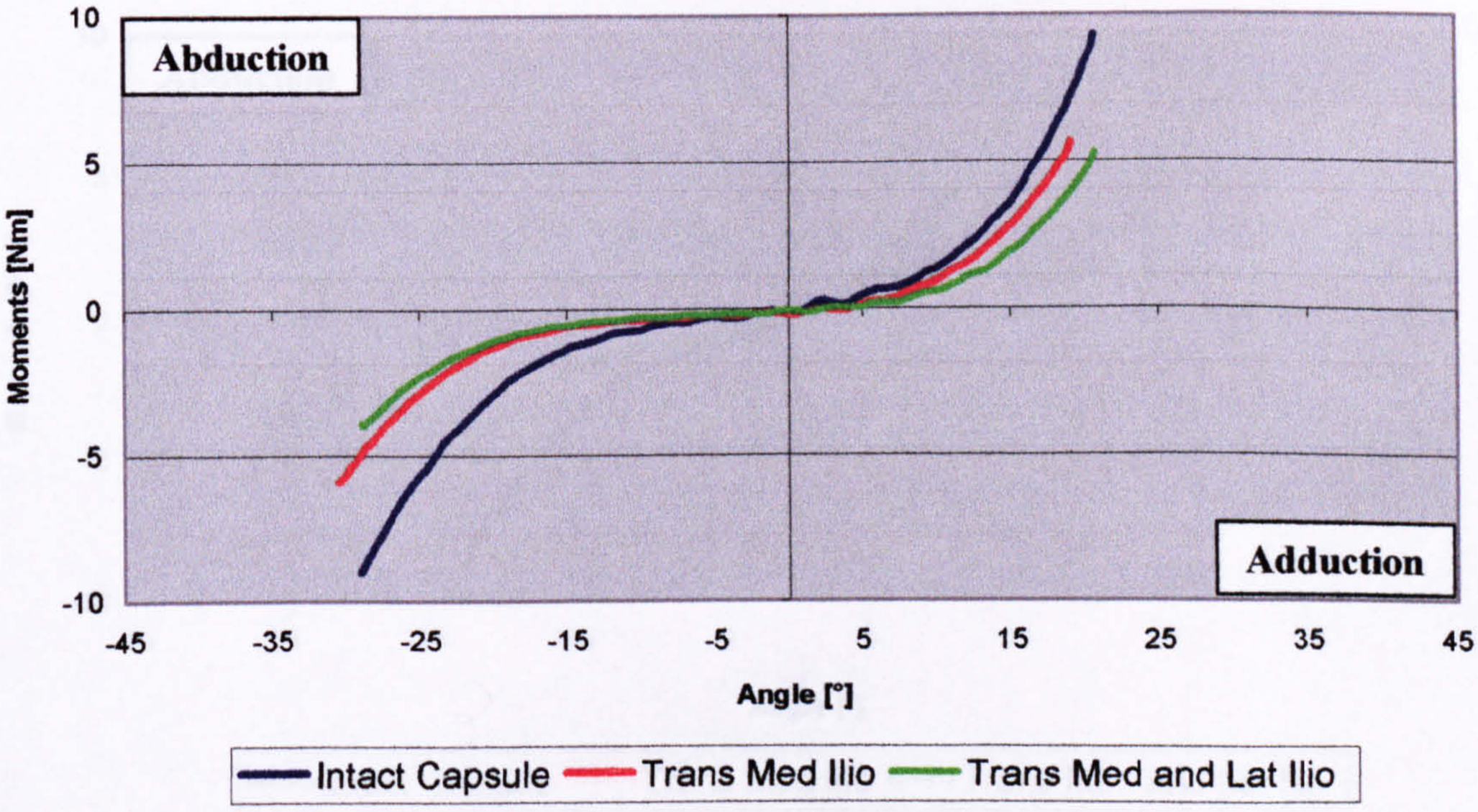

Figure 4.28b The joint resistance in abduction-adduction motion.

Full Extension and External Rotation

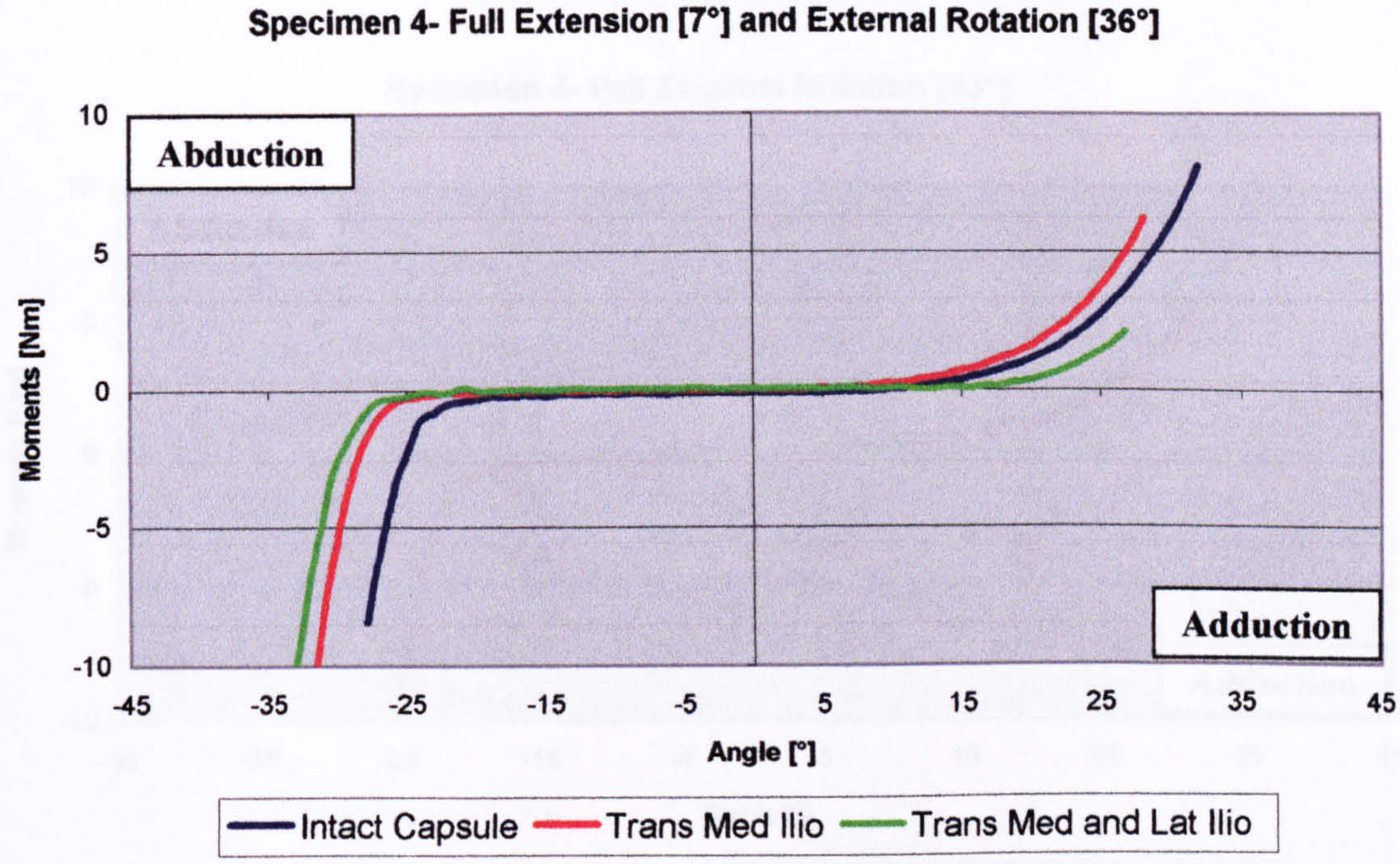

Figure 4.29a The joint resistance in abduction-adduction motion.

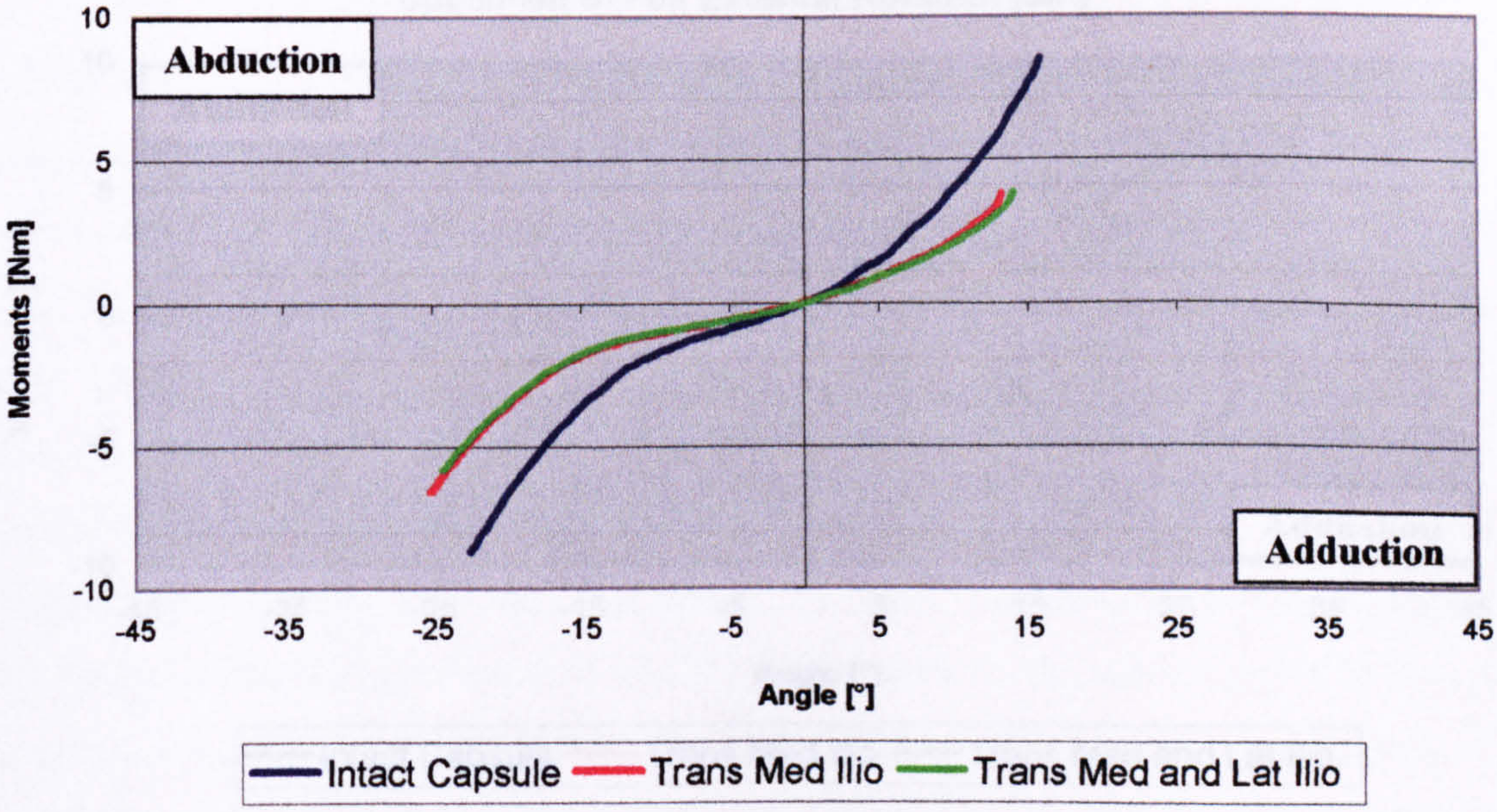

Figure 4.29b The joint resistance in abduction-adduction motion.

Full External Rotation

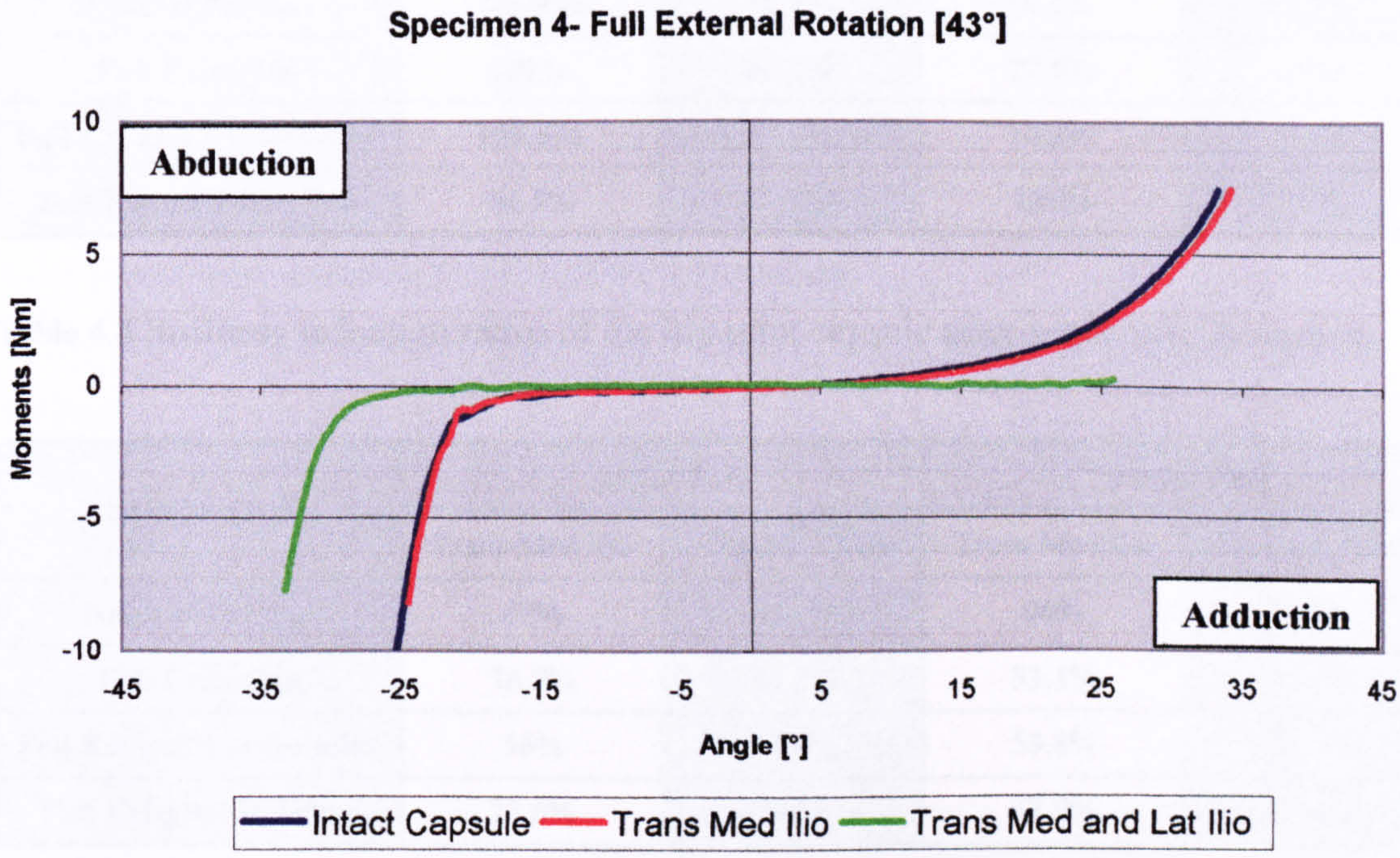

Figure 4.30a The joint resistance in abduction-adduction motion.

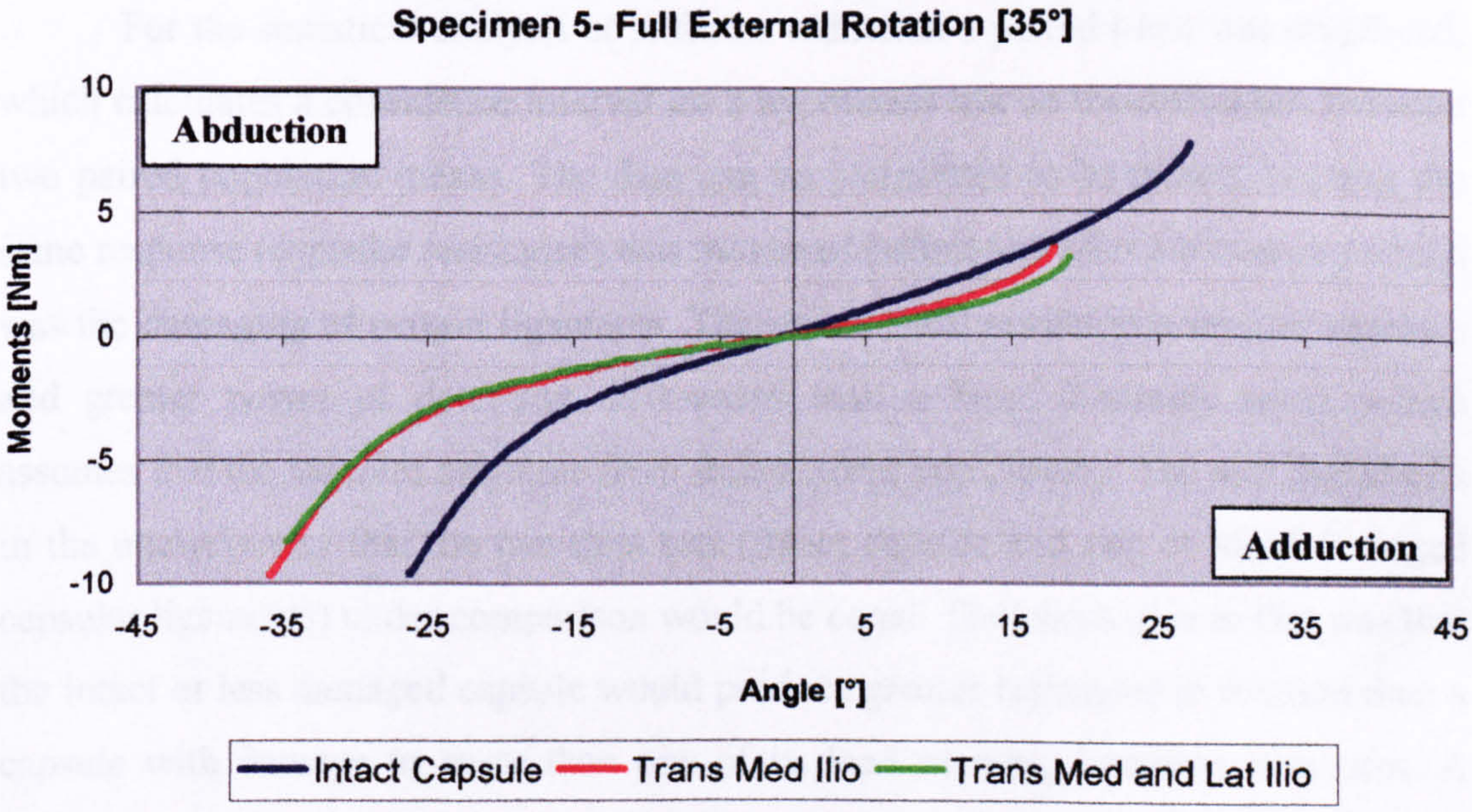

Figure 4.30b The joint resistance in abduction-adduction motion.

SPECIMEN 4	Adduction		Abduction	
	Trans Med Ilio	Trans Lat Ilio	Trans Med Ilio	Trans Lat Ilio
Neutral Position	**146.9%**	42.7%	20.5%	17.1%
Full Extension	**200%**	38.2%	27.5%	38%
Full Ext and Ext Rotation	**135.6%**	47.3%	19.3%	9.1%
Full External Rotation	86.5%	5.6%	100%	5.1%

Table 4.4 Stiffness reduction ratios of the hip joint capsule after sequential dissection.

SPECIMEN 5	Adduction		Abduction	
	Trans Med Ilio	Trans Lat Ilio	Trans Med Ilio	Trans Lat Ilio
Neutral Position	47%	45.3%	99%	90.8%
Full Extension	76.7%	54.3%	53.1%	42.6%
Full Ext and Ext Rotation	56%	52.4%	53.8%	52.3%
Full External Rotation	78.6%	58%	37.9%	36.6%

Table 4.5 The equivalent ratios of reduction for Specimen 5.

4.4 Statistical Significance of Stiffness Reduction

For the statistical analysis of stiffness reduction a paired t-test was employed, which calculates a confidence interval for a hypothesis test on the difference between two paired population means. The data can be considered to be paired, because the same response (capsular resistance) was measured before and after a treatment, which was the damaging of certain ligaments. The paired t-test results in a smaller variance and greater power of detecting differences than a basic 2-sample t-test, which assumes that the samples originate from independent populations. The null hypothesis in the analysis was that the two data sets (intact capsule and one or more damaged capsular ligaments) under comparison would be equal. The alternative to that was that the intact or less damaged capsule would produce greater resistance in rotation than a capsule with damage to more than one of its load carrying ligament structures. A confidence interval that does not include zero would suggest that the null hypothesis is not valid. In combination with a very small p-value (<0.05) this would mean that the alternative hypothesis is the case. However, a large p-value (>0.05) in

combination with zero being included in the confidence interval means that the null hypothesis is valid and that there is no important difference between the two data sets. The paired t-test procedure requires that the data are paired and the paired differences follow a normal distribution. These normality tests are presented in appendix II and III.

4.4.1 Results for Posterior and Lateral Ligaments

It is brought into mind again that the datasets that were used for the statistical analysis comprised six values for each capsule state (i.e. intact, with one or two dissected ligaments). Three of the values were from the recordings in abduction and another three from the adduction recordings. Each of the three was paired by the same angle of abduction or adduction for all capsule states.

Specimen 1

FULL INTERNAL ROTATION	Trans Ischiofemoral		Trans Ischio and Lat Ilio	
	Adduction	Abduction	Adduction	Abduction
Intact Capsule	> (p=0.021)*	> (p=0.017)*	Specimen Failed	Specimen Failed
Trans Ischiofemoral	---	---	Specimen Failed	Specimen Failed

Table 4.6 Paired t-test results for specimen 1 (Full Internal Rotation).

Specimen 2

NEUTRAL POSITION	Trans Ischiofemoral		Trans Ischio and Lat Ilio	
	Adduction	Abduction	Adduction	Abduction
Intact Capsule	Equal	> (p=0.002)*	Equal	> (p=0.003)*
Trans Ischiofemoral	---	---	Equal	> (p=0.005)*

Table 4.7 Paired t-test results for specimen 2 (Neutral Position).

FULL FLEXION	Trans Ischiofemoral		Trans Ischio and Lat Ilio	
	Adduction	Abduction	Adduction	Abduction
Intact Capsule	Smaller	Smaller	---	---
Trans Ischiofemoral	---	---	---	---

Table 4.8 Paired t-test results for specimen 2 (Full Flexion).

FULL FLEX AND INT ROT	Trans Ischiofemoral		Trans Ischio and Lat Ilio	
	Adduction	Abduction	Adduction	Abduction
Intact Capsule	> (p=0.008)*	> (p=0.004)*	> (p=0.003)*	> (p=0.003)*
Trans Ischiofemoral	---	---	> (p=0.003)*	> (p=0.001)*

Table 4.9 Paired t-test results for specimen 2 (Full Flexion and Internal Rotation).

FULL INTERNAL ROTATION	Trans Ischiofemoral		Trans Ischio and Lat Ilio	
	Adduction	Abduction	Adduction	Abduction
Intact Capsule	Smaller	> (p=0.03)*	> (p=0.062)	> (p=0.031)*
Trans Ischiofemoral	---	---	> (p=0.022)*	> (p=0.035)*

Table 4.10 Paired t-test results for specimen 2 (Full Internal Rotation).

Specimen 3

NEUTRAL POSITION	Trans Ischiofemoral		Trans Ischio and Lat Ilio	
	Adduction	Abduction	Adduction	Abduction
Intact Capsule	> (p=0.012)*	> (p=0.005)*	> (p=0.013)*	> (p=0.005)*
Trans Ischiofemoral	---	---	> (p=0.014)*	> (p=0.018)*

Table 4.11 Paired t-test results for specimen 3 (Neutral Position).

FULL FLEXION	Trans Ischiofemoral		Trans Ischio and Lat Ilio	
	Adduction	Abduction	Adduction	Abduction
Intact Capsule	Equal	> (p=0.004)*	---	---
Trans Ischiofemoral	---	---	---	---

Table 4.12 Paired t-test results for specimen 3 (Full Flexion).

FULL FLEX AND INT ROT	Trans Ischiofemoral		Trans Ischio and Lat Ilio	
	Adduction	Abduction	Adduction	Abduction
Intact Capsule	> (p=0.044)*	> (p=0.02)*	> (p=0.04)*	> (p=0.014)*
Trans Ischiofemoral	---	---	Equal	Equal

Table 4.13 Paired t-test results for specimen 3 (Full Flexion and Internal Rotation).

FULL INTERNAL ROTATION	Trans Ischiofemoral		Trans Ischio and Lat Ilio	
	Adduction	Abduction	Adduction	Abduction
Intact Capsule	> (p=0.044)*	> (p=0.053)	> (p=0.038)*	> (p=0.056)
Trans Ischiofemoral	---	---	> (p=0.007)*	> (p=0.062)

Table 4.14 Paired t-test results for specimen 3 (Full Internal Rotation).

Specimen (1), 2 and 3

NEUTRAL POSITION	Trans Ischiofemoral		Trans Ischio and Lat Ilio	
	Adduction	Abduction	Adduction	Abduction
Intact Capsule	Equal	> (p=0)*	> (p=0.029)*	> (p=0)*
Trans Ischiofemoral	---	---	> (p=0.015)*	> (p=0.024)*

Table 4.15 Paired t-test results for joint data of specimen 2 and 3 (Neutral Position).

FULL FLEXION	Trans Ischiofemoral		Trans Ischio and Lat Ilio	
	Adduction	Abduction	Adduction	Abduction
Intact Capsule	Equal	Equal	---	---
Trans Ischiofemoral	---	---	---	---

Table 4.16 Paired t-test results for joint data of specimen 2 and 3 (Full Flexion).

FULL FLEX AND INT ROT	Trans Ischiofemoral		Trans Ischio and Lat Ilio	
	Adduction	Abduction	Adduction	Abduction
Intact Capsule	> (p=0.046)*	> (p=0.002)*	> (p=0.002)*	> (p=0.014)*
Trans Ischiofemoral	---	---	> (p=0.047)*	Equal

Table 4.17 Paired t-test results for joint data of specimen 2 and 3 (Full Flexion and Internal Rotation).

(FULL INT ROTATION)	Trans Ischiofemoral		Trans Ischio and Lat Ilio	
	Adduction	Abduction	Adduction	Abduction
Intact Capsule	Equal	> (0.003)*	> (p=0.016)*	> (p=0.012)*
Trans Ischiofemoral	---	---	> (p=0.029)*	> (p=0.003)*

Table 4.18 Paired t-test results for joint data of specimen 1, 2 and 3 (Full Internal Rotation).

ALL JOINT POSITIONS	Trans Ischiofemoral		Trans Ischio and Lat Ilio	
	Adduction	Abduction	Adduction	Abduction
Intact Capsule	> (p=0.039)*	> (p=0.001)*	> (p=0)*	> (p=0)*
Trans Ischiofemoral	---	---	> (p=0.001)*	> (p=0.004)*

Table 4.19 Paired t-test results for joint data of all specimen (All Joint Positions).

4.4.2 Results for Anterior and Lateral Ligaments

The analysis on the statistical significance of stiffness reduction for specimens 4 and 5 was affected to a certain extent by the presence of the γ–nail type fracture fixator- as described in the methodology section. It can not be guaranteed that the presence of this fixator had no effect on the data acquisition. Based on x-ray observations, which showed that exostoses at the top of the greater trochanter were the only anomalies resulting from the presence of this nail, it was assumed that there would have only been an effect in the recorded data in case of femoral abduction. Therefore specimen 4 was analysed, additionally, with only considering its femoral adduction data, but the results of the paired t-tests did not reveal any differences. Therefore, all the test results are displayed in the following tables, including those for abduction of the femur in joint specimen 4..

Specimen 4

NEUTRAL POSITION	Trans Medial Ilio		Trans Med and Lat Ilio	
	Adduction	Abduction	Adduction	Abduction
Intact Capsule	Smaller	> (p=0.095)	> (p=0.035)*	> (p=0.11)
Trans Medial Ilio	---	---	> (p=0.026)*	Smaller

Table 4.20 Paired t-test results for specimen 4 (Neutral Position).

FULL EXTENSION	Trans Medial Ilio		Trans Med and Lat Ilio	
	Adduction	Abduction	Adduction	Abduction
Intact Capsule	Smaller	> (p=0.05)*	> (p=0.027)*	> (p=0.046)*
Trans Medial Ilio	---	---	> (p=0.014)*	Equal

Table 4.21 Paired t-test results for specimen 4 (Full Extension).

FULL EXT AND EXT ROT	Trans Medial Ilio		Trans Med and Lat Ilio	
	Adduction	Abduction	Adduction	Abduction
Intact Capsule	Smaller	> (p=0.093)	> (p=0.008)*	> (p=0.097)
Trans Medial Ilio	---	---	> (p=0.01)*	> (p=0.143)

Table 4.22 Paired t-test results for specimen 4 (Full Extension and External Rotation).

FULL EXT ROTATION	Trans Medial Ilio		Trans Med and Lat Ilio	
	Adduction	Abduction	Adduction	Abduction
Intact Capsule	> (p=0.009)*	Equal	> (p=0.01)*	> (p=0.087)
Trans Medial Ilio	---	---	> (p=0.011)*	> (p=0.097)

Table 4.23 Paired t-test results for specimen 4 (Full External Rotation).

Specimen 5

NEUTRAL POSITION	Trans Medial Ilio		Trans Med and Lat Ilio	
	Adduction	Abduction	Adduction	Abduction
Intact Capsule	> (p=0.023)*	Equal	> (p=0.025)*	> (p=0.067)
Trans Medial Ilio	---	---	> (p=0.104)	> (p=0.017)*

Table 4.24 Paired t-test results for specimen 5 (Neutral Position).

FULL EXTENSION	Trans Medial Ilio		Trans Med and Lat Ilio	
	Adduction	Abduction	Adduction	Abduction
Intact Capsule	> (p=0.018)*	> (p=0.005)*	> (p=0.016)*	> (p=0.006)*
Trans Medial Ilio	---	---	> (p=0.014)*	> (p=0.012)*

Table 4.25 Paired t-test results for specimen 5 (Full Extension).

FULL EXT AND EXT ROT	Trans Medial Ilio		Trans Med and Lat Ilio	
	Adduction	Abduction	Adduction	Abduction
Intact Capsule	> (p=0.009)*	> (p=0.006)*	> (p=0.013)*	> (p=0.007)*
Trans Medial Ilio	---	---	Equal	Equal

Table 4.26 Paired t-test results for specimen 5 (Full Extension and External Rotation).

FULL EXT ROTATION	Trans Medial Ilio		Trans Med and Lat Ilio	
	Adduction	Abduction	Adduction	Abduction
Intact Capsule	> (p=0.003)*	> (p=0.01)*	> (p=0)*	> (p=0.009)*
Trans Medial Ilio	---	---	> (p=0.014)*	Equal

Table 4.27 Paired t-test results for specimen 5 (Full External Rotation).

Specimen 4 and 5

NEUTRAL POSITION	Trans Medial Ilio		Trans Med and Lat Ilio	
	Adduction	Abduction	Adduction	Abduction
Intact Capsule	> (p=0.129)	> (p=0.104)	> (p=0.012)*	> (p=0.054)
Trans Medial Ilio	---	---	> (p=0.036)*	Equal

Table 4.28 Paired t-test results for specimen 4 and 5 (Neutral Position).

FULL EXTENSION	Trans Medial Ilio		Trans Med and Lat Ilio	
	Adduction	Abduction	Adduction	Abduction
Intact Capsule	Equal	> (p=0.001)*	> (p=0.001)*	> (p=0.001)*
Trans Medial Ilio	---	---	> (p=0.007)*	Equal

Table 4.29 Paired t-test results for specimen 4 and 5 (Full Extension).

FULL EXT AND EXT ROT	Trans Medial Ilio		Trans Med and Lat Ilio	
	Adduction	Abduction	Adduction	Abduction
Intact Capsule	Equal	> (p=0.003)*	> (p=0.001)*	> (p=0.003)*
Trans Medial Ilio	---	---	> (p=0.026)*	> (p=0.047)*

Table 4.30 Paired t-test results for specimen 4 and 5 (Full Ext and Ext Rotation).

FULL EXT ROTATION	Trans Medial Ilio		Trans Med and Lat Ilio	
	Adduction	Abduction	Adduction	Abduction
Intact Capsule	> (p=0.006)*	> (p=0.058)	> (p=0)*	> (p=0.003)*
Trans Medial Ilio	---	---	> (p=0.006)*	> (p=0.083)

Table 4.31 Paired t-test results for specimen 4 and 5 (Full External Rotation).

ALL JOINT POSITIONS	Trans Medial Ilio		Trans Med and Lat Ilio	
	Adduction	Abduction	Adduction	Abduction
Intact Capsule	> (p=0.124)	> (p=0)*	> (p=0)*	> (p=0)*
Trans Medial Ilio	---	---	> (p=0)*	> (p=0.041)*

Table 4.31 Paired t-test results for specimen 4 and 5 (All Joint Positions).

4.5 Comparison of Stiffness Rates

In the previous paragraph the effects of individual ligaments on the joint stiffness at various limb positions was highlighted. In this paragraph the attempt is to identify the consequences that dissection of different ligaments has on the joint stiffness rate. This rate represents how sudden the action of the ligaments start their restricting action when the limb is moved into extremes of abduction and adduction. For this purpose it was necessary to quantify the individual recorded stiffness curves, by means of a function. In order to allow a more precise comparison of the different

stiffness rates it was decided that the function would be the slope of the linear trend lines that would fit the individual stiffness curves. The function's general form is:

$$y = mx+b \qquad (4.1)$$

m is the slope and b the intercept of the trend line with the y-axis. For the comparison of the different stiffness rates for each stage of the sequential dissection it is the slope m that carries the greatest importance. Thereby the larger the trend line's slope (m) the more 'abrupt' or 'sudden' the tightening of the joint capsule in the particular case. Each trend line results from data points that lie in the sloped endings of each curve and not in the zero moments line in the middle region of the curve. Trend lines were drawn for each sloped region (abduction and adduction) individually as indicated by the yellow rings in Figure 4.31.

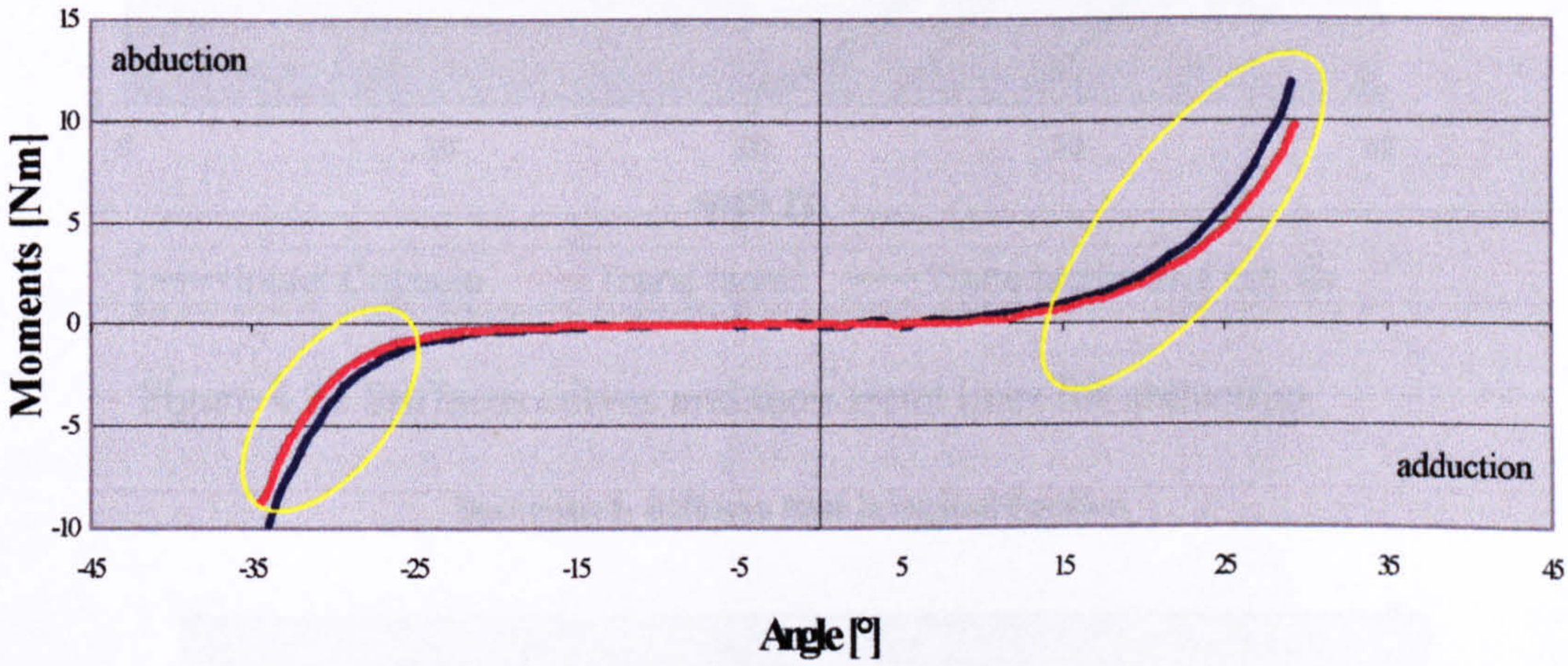

Figure 4.31 Areas of moment graphs that were considered for trend line comparison.

However, the trend lines were decided to be drawn only for those parts of the curve that were part of most of the recorded curves. This was done in order to assure that similar portions of the stiffness curves were compared with each other for their gradient. Therefore, an upper limit of ±3 Nm was applied to the stiffness curve for which the trend line fit was to be applied, as this value was included in most curves. Thereby, it was irrelevant how far up or down the resistance moment recordings reached. For example, in figure 4.31 the curves go to ±10 Nm, but for the slope fitting only the recordings up to ±3 Nm were considered. The lower limit of the curve to be

fitted by a trend line was set to be at 10% of the upper limit, namely at ±0.3 Nm. This coincided with the boundaries of the zero moment zone that was described in paragraph 4.2.5. Figure 4.32 and 4.33 show two graphs with the sloped areas of each curve for those portions of interest. In black are the linear fitted trend lines and their equivalent functions. The functions that provided the stiffness rates for the complete set of curves are shown in the appendix section IV.

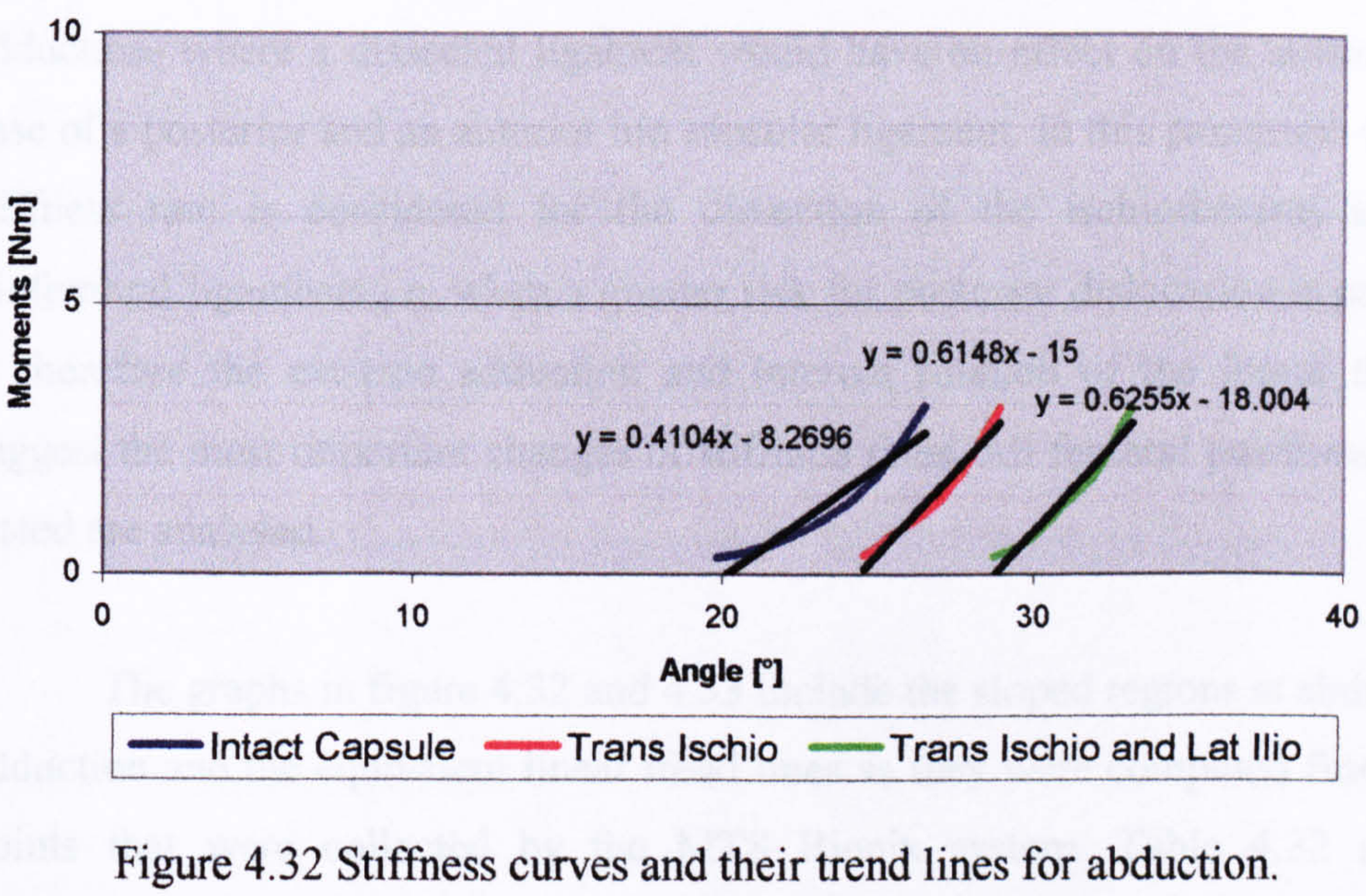

Figure 4.32 Stiffness curves and their trend lines for abduction.

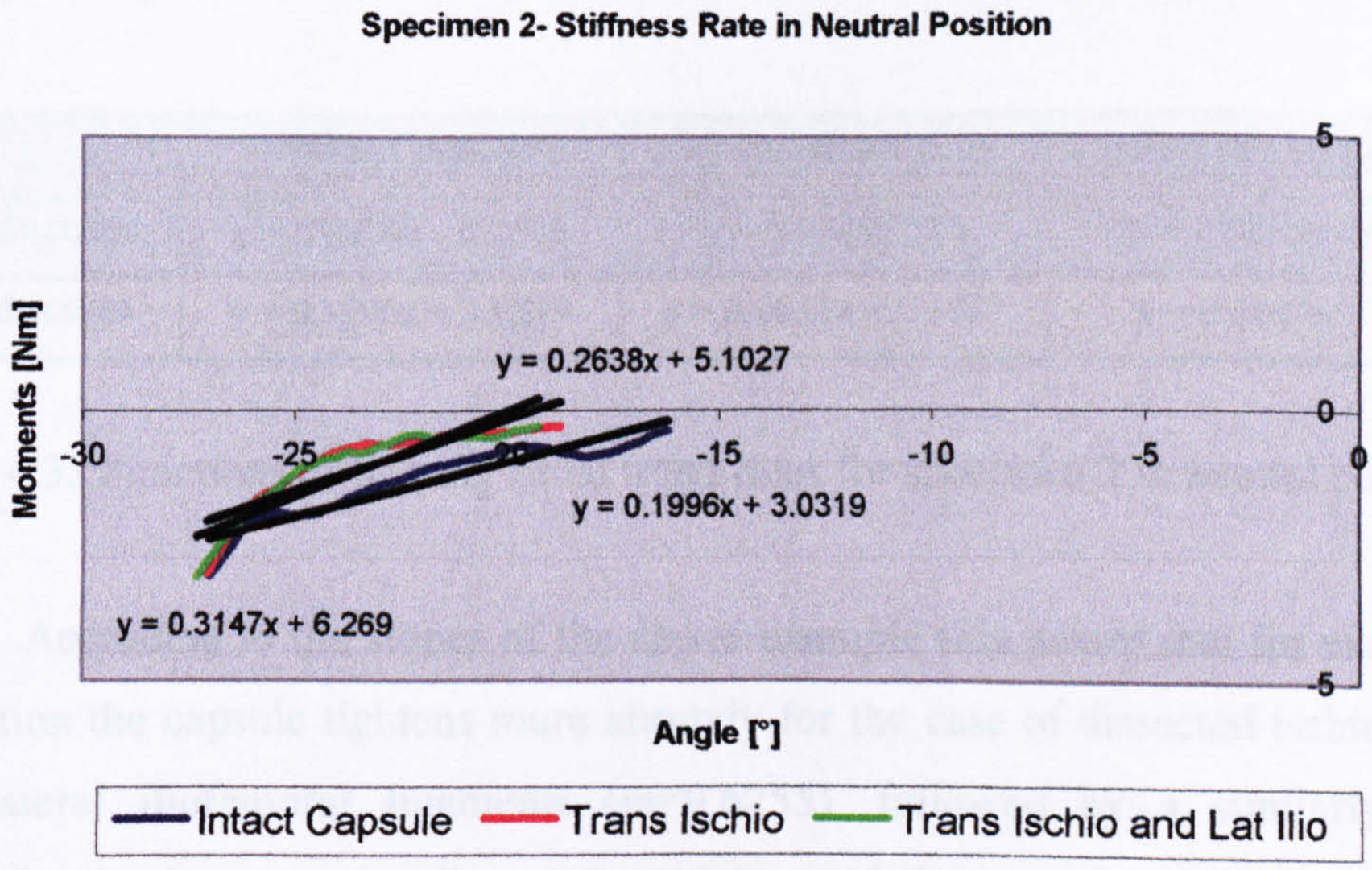

Figure 4.33 Stiffness curves and their trend lines for adduction.

The same procedure was followed for all hip joints that were tested and in all limb positions in which they were tested. The following pages are devoted to the representation of these curves and their trend lines, as well as the statistical analysis and comparison of their changes as they occurred with the sequential dissection of various capsular ligaments.

4.5.1 Stiffness Rates and Posterior and Lateral Ligaments

There are dissimilar positions of the femur- in terms of abduction and adduction- where a dissected ligament would have an effect on the stiffness rate in case of a posterior and an anterior hip capsular ligament. In this paragraph the shift in stiffness rate is considered for the dissection of the ischiofemoral and lateral iliofemoral ligaments i.e. when a greater risk for posterior dislocation is prevalent. It is therefore the extreme adduction and internal rotation of the femur that would suggest the most important changes of stiffness rates. All femoral positions that were tested are analysed.

The graphs in figure 4.32 and 4.33 include the sloped regions at abduction and adduction and the equivalent linear trend lines as they were computed from the data points that were collected by the MTS Bionix system. Table 4.32 shows the corresponding functions of each of these trend lines.

	Intact Capsule	**Trans Ischio Lig**	**Trans Ischio & Lat Ilio Lig**
Abduction	$y = 0.4104x - 8.2696$	$y = 0.6148x - 15$	$y = 0.6255x - 18.004$
Adduction	$y = 0.1996x + 3.0319$	$y = 0.2638x + 5.1027$	$y = 0.3147x + 6.269$

Table 4.32 Functions of linearly fitted trend lines for specimen 2 in neutral position.

According to the slopes of the above example this means that for example in abduction the capsule tightens more abruptly for the case of dissected ischiofemoral and lateral iliofemoral ligaments (m=0.6255), followed by a similarly abrupt tightening in the case of a dissected ischiofemoral ligament (m=0.6148). When the capsule was intact, the tightening was the least abrupt (m=0.410).

4.5.1.1 Joint in Neutral Position

In this paragraph all functions will be presented that relate to specimens that were tested for risk of posterior dislocation and in the neutral position, i.e. specimen 2 and 3.

SPECIMEN 2	Intact Capsule	Trans Ischio Lig	Trans Ischio & Lat Ilio Lig
Abduction	y = 0.4104x - 8.2696	y = 0.6148x - 15	y = 0.6255x - 18.004
Adduction	y = 0.1996x + 3.0319	y = 0.2638x + 5.1027	y = 0.3147x + 6.269

SPECIMEN 3	Intact Capsule	Trans Ischio Lig	Trans Ischio & Lat Ilio Lig
Abduction	y = 0.3341x + 7.406	y = 0.2258x + 4.863	y = 0.2595x + 5.824
Adduction	y = 0.6034x - 11.326	y = 0.4267x - 7.6953	y = 0.4118x - 8.0046

Table 4.33 a and b The slopes for specimen 2 and 3 in Neutral Position.

4.5.1.2 Joint in Full Flexion

SPECIMEN 2	Intact Capsule	Trans Ischio Lig	Trans Ischio & Lat Ilio Lig
Abduction	y = 0.2941x - 8.2108	y = 0.2076x - 3.5199	not tested
Adduction	y = 0.2058x + 4.4902	y = 0.1509x + 2.0593	not tested

SPECIMEN 3	Intact Capsule	Trans Ischio Lig	Trans Ischio & Lat Ilio Lig
Abduction	y = 0.2438x + 4.5725	y = 0.187x + 3.2845	not tested
Adduction	y = 0.2812x - 5.0535	y = 0.1442x - 1.7581	not tested

Table 4.34 a and b The slopes for specimen 2 and 3 in Full Flexion.

4.5.1.3 Joint in Full Flexion and Internal Rotation

SPECIMEN 2	Intact Capsule	Trans Ischio Lig	Trans Ischio & Lat Ilio Lig
Abduction	y = 0.2065x - 2.316	y = 0.2044x - 4.0885	y = 0.2433x - 6.7131
Adduction	y = 0.1497x + 1.9889	y = 0.0924x + 1.0328	remained zero

SPECIMEN 3	Intact Capsule	Trans Ischio Lig	Trans Ischio & Lat Ilio Lig
Abduction	y = 0.1791x + 3.2489	y = 0.185x + 3.6541	y = 0.2136x + 4.5085
Adduction	y = 0.4379x - 5.8832	y = 0.2949x - 4.6893	y = 0.3974x - 6.5607

Table 4.35 a and b The slopes for specimen 2 and 3 in Full Flexion and Int Rotation.

4.5.1.4 Joint in Full Internal Rotation

SPECIMEN 1	Intact Capsule	Trans Ischio Lig	Trans Ischio & Lat Ilio Lig
Abduction	y = 0.2221x + 4.1684	y = 0.246x + 5.0865	specimen failed
Adduction	y = 0.2399x - 2.5026	y = 0.2631x - 3.1771	specimen failed

SPECIMEN 2	Intact Capsule	Trans Ischio Lig	Trans Ischio & Lat Ilio Lig
Abduction	y = 0.3852x - 6.7427	y = 0.4262x - 9.8898	y = 0.3942x - 10.07
Adduction	y = 0.1666x + 2.3159	y = 0.2818x + 4.5103	y = 0.2212x + 3.9168

SPECIMEN 3	Intact Capsule	Trans Ischio Lig	Trans Ischio & Lat Ilio Lig
Abduction	y = 0.3952x + 12.442	y = 0.4404x + 14.491	y = 0.2415x + 7.9508
Adduction	y = 0.5542x - 13.706	y = 0.3326x - 8.611	y = 0.3351x - 9.0254

Table 4.36 a, b and c The slopes for specimen 1, 2 and 3 in Full Internal Rotation.

4.5.2 Stiffness Rates and Anterior and Lateral Ligaments

In this paragraph the shift in stiffness rate is considered for the dissection of the medial and lateral iliofemoral ligaments i.e. when a greater risk for posterior dislocation is prevalent.

4.5.2.1 Joint in Neutral Position

SPECIMEN 4	Intact Capsule	Trans Med Ilio Lig	Trans Med & Lat Ilio Lig
Abduction	y = 0.3706x + 7.8361	y = 0.5338x + 15.153	y = 0.4588x + 12.135
Adduction	y = 0.2932x - 5.0727	y = 0.284x - 4.3552	y = 0.194x - 3.7484

SPECIMEN 5	Intact Capsule	Trans Med Ilio Lig	Trans Med & Lat Ilio Lig
Abduction	y = 0.1699x + 2.6639	y = 0.1829x + 2.944	y = 0.1882x + 3.1842
Adduction	y = 0.1994x - 2.2708	y = 0.1467x - 1.6863	y = 0.1352x - 1.3843

Table 4.37 a and b The slopes for specimen 4 and 5 in Neutral Position.

4.5.2.2 Joint in Full Extension

SPECIMEN 4	Intact Capsule	Trans Med Ilio Lig	Trans Med & Lat Ilio Lig
Abduction	y = 0.254x + 5.2313	y = 0.4491x + 12.021	y = 0.3073x + 7.5528
Adduction	y = 0.3452x - 5.6249	y = 0.2523x - 2.5407	y = 0.2689x - 5.4798

SPECIMEN 5	Intact Capsule	Trans Med Ilio Lig	Trans Med & Lat Ilio Lig
Abduction	y = 0.1732x + 1.0013	y = 0.1529x + 1.4999	y = 0.1661x + 1.935
Adduction	y = 0.2753x - 1.1902	y = 0.3159x - 2.138	y = 0.2882x - 2.339

Table 4.38 a and b The slopes for specimen 4 and 5 in Full Extension.

4.5.2.3 Joint in Full Extension and External Rotation

SPECIMEN 4	Intact Capsule	Trans Med Ilio Lig	Trans Med & Lat Ilio Lig
Abduction	y = 0.4089x + 8.2066	y = 0.6748x + 16.909	y = 0.5917x + 15.382
Adduction	y = 0.2422x - 3.5495	y = 0.2178x - 2.5783	y = 0.2669x - 5.1742

SPECIMEN 5	Intact Capsule	Trans Med Ilio Lig	Trans Med & Lat Ilio Lig
Abduction	y = 0.2022x + 0.1024	y = 0.149x + 0.2499	y = 0.144x + 0.2241
Adduction	y = 0.3814x - 0.3557	y = 0.2602x - 0.4064	y = 0.2428x - 0.3298

Table 4.39 a and b The slopes for specimen 4 and 5 in Full Ext and Ext Rotation.

4.5.2.4 Joint in Full External Rotation

SPECIMEN 4	Intact Capsule	Trans Med Ilio Lig	Trans Med & Lat Ilio Lig
Abduction	y = 0.2732x + 4.0748	y = 0.3277x + 5.2491	y = 0.4356x + 11.274
Adduction	y = 0.1624x - 1.735	y = 0.1712x - 2.0923	remained zero

SPECIMEN 5	Intact Capsule	Trans Med Ilio Lig	Trans Med & Lat Ilio Lig
Abduction	y = 0.1987x + 0.1835	y = 0.1288x + 0.3879	y = 0.1212x + 0.3583
Adduction	y = 0.199x + 0.0547	y = 0.1823x - 0.4926	y = 0.1781x - 0.7869

Table 4.40 a and b The slopes for specimen 4 and 5 in Full External Rotation.

4.5.3 Overview of Stiffness Rates Changes

Tables 4.41 and 4.42 are an attempt to give an overview of the changes that occur with the sequential dissection of ligaments, based on the functions of the respective trend lines that are shown in tables 4.33 to 4.40 a and b. This is aimed at simplifying the content of the sheer volume of data. Therefore any changes of

stiffness rates are shown in the form of a numbering system that indicates whether stiffness rate was increased or decreased in the individual cases.

	Posterior and Lateral Ligaments					
	Intact Capsule		Trans Ischio		Trans Med Ilio	
	Femur 2	Femur 3	Femur 2	Femur 3	Femur 2	Femur 3
Neutral (Abduction)	3	1	1	3	2	2
Neutral (Adduction)	3	1	2	2	1	3
Full Flexion (Abd)	1	1	2	2	*	*
Full Flexion (Add)	1	1	2	2	*	*
Full Flex and Int Rot (Abd)	2	3	3	2	1	1
Full Flex and Int Rot (Add)	1	1	2	3	*	2
Full Int Rot (Abd)	3	2	1	1	2	3
Full Int Rot (Add)	3	1	1	3	2	2

Table 4.41 Numbers comparing the curve abruptness between the different cases.

The meaning of the numbers in table 4.41 is best explained as a type of scoring system that summarises the contents of tables 4.33 to 4.40. Thereby, 1 was given for the most abrupt stiffness rise i.e. for the largest slope (m) of the trend line equations. Scores 2 and 3 were given decreasingly.

	Anterior and Lateral Ligaments					
	Intact Capsule		Trans Med Ilio		Trans Lat Ilio	
	Femur 4	Femur 5	Femur 4	Femur 5	Femur 4	Femur 5
Neutral (Abduction)	3	3	1	2	2	1
Neutral (Adduction)	1	1	2	2	3	3
Full Extension (Abd)	3	1	1	3	2	2
Full Extension (Add)	1	3	3	1	2	2
Full Ext and Ext Rot (Abd)	3	1	1	2	2	3
Full Ext and Ext Rot (Add)	2	1	3	2	1	3
Full Ext Rot (Abd)	3	1	2	2	1	3
Full Ext Rot (Add)	2	1	1	2	3	3

Table 4.42 Same numbering system with previous table for anterolateral ligaments.

For the study on stiffness rates in relation with posterior and lateral ligaments the results on the abruptness of resistance rise of the capsular ligaments in its various conditions (i.e. intact, dissected ischiofemoral ligament and dissected ischiofemoral and medial iliofemoral ligament) were not as consistent as in the case of the anterior and lateral ligament dissections. Only for the case of full flexion the results showed similarly good consistency as for the anterolateral ligaments. In this situation the results showed that the stiffness rate curve is rising more abruptly in case of an intact capsule and reduces with the dissection of the ischiofemoral ligament. In what concerns the effect of anterior and lateral ligaments on the stiffness rate as shown in table 4.42, only specimen 5 showed meaningful results. Both in the cases of full extension with external rotation and in the case of external rotation alone a clear consistency was evident. Thereby, the most abrupt stiffness curve was observed to be for the intact capsule with decreasing abruptness as ligaments were dissected.

4.6 Summary of Stiffness Rates Changes

Posterior and Lateral Ligaments

The changes of stiffness rate showed good consistency (table 4.41) for the case of specimen 3, in particular for full flexion. Thereby, abruptness of joint stiffening was highest when the joint capsule was intact, suffering a loss in abruptness with the damage of its posterior and lateral ligaments.

Anterior and Lateral Ligaments

For specimen 5 it is noticeable (table 4.42) that stiffness rates were consistently highest when the capsule was intact and showed a reduction when one or two ligaments were damaged for all cases of limb positioning. This consistency was particularly good in full extension with external rotation as well as in full external rotation. This is in good agreement with the observations for specimen 3 and its posterolateral ligaments, enforcing the opinion that an intact capsule provides greater resistive hip joint moments.

4.7 Discussion

From the total of five complete and intact cadaveric human hip joint specimens, three yielded results that could be used for the evaluation of the mechanical properties of the ligamentous structures of the hip joint capsule. The first of the specimens could only be utilised for a single comparison- between the conditions of the intact capsule and with a divided ischiofemoral ligament- in full internal rotation of the femoral part. Thereafter the readings that were planned were not executed due to the unforeseeable early failure of the specimen, which was caused by an incorrect readjustment of the neutral specimen position, which resulted in the creation of a lever effect between the sidebars of the MTS system and the cementing pot support of the test rig when moved towards the extremes of the simulated joint movement. The result was that the capsular ligaments were loaded so excessively that they were torn and also after a continued external load application the acetabulum was levered out of its cementing pot. The damages were irrecoverable and the remaining tests were aborted. This was an important step in the learning process of setting up the test as it became apparent that the initial zero position of the rig had to be determined accurately. No compartments of the rig should be at risk of getting into contact with parts of the testing machine and building up external loads and create lever arms capable of destroying the cement bond.

In those cases where after the dissection of ligaments no resistance from the capsule was evident throughout the recorded spectrum of movement (like in Fig 4.25a or in Fig 4.26c for divided ischiofemoral and lateral iliofemoral ligaments) the curve was not as smooth as in the case of an intact capsule or for cases of one divided ligament. The significant reduction of resistance that results from the damage of capsular ligaments as was shown in the previous section leads to a reduced movement guidance. The presence of a frictional force, despite its marginal size, resulted in a jerky movement of the acetabular joint part, which could move freely for ±3.5cm in the x-y plane. However, it is noteworthy that the same effect was not observed during the tests for risk of anterior dislocation. None of the cases from the anterior dislocation tests presented flat lines for the moment curves and also they had a much smoother shape.

The test results for the stiffness rate development showed moderate consistency and only for certain limb positions for both the posterolateral and anterolateral approaches. However, those recordings from the tests for the developing peak stiffness showed a remarkable consistency, with the exception of specimen 2 in full flexion (figure 4.24a) and specimen 4 in nearly all joint positions (figures 4.27a-4.30). In the case of specimen 2 in full flexion the moment recordings of the intact capsule condition were lower than those for the case of divided ischiofemoral ligament. This would translate into greater stiffness after damaging the capsule. In the case of specimen 4 the same behaviour was noted for all positions, except for full external rotation, where the damaged capsule showed a drop in resistance to femoral movement.

For specimen 2 it should be noted that when the tests were executed, no Kirschner wires were used as an assistance in determining the ideal neutral position of the joint on the test rig. This additional navigational assistance was only used for specimens 3, 4 and 5. The determination of the ideal neutral position for the case of specimen 2 was done by the tester's visual judgement. This approach places restrictions to the accuracy of the test set-up and thoughts for improvement are given in the following sections of this paragraph.

In case of specimen 4 an inappropriately set up recording after the ligamentous dissections can be excluded. The effect of the γ-nail in the femoral shaft, however, which caused severe exostoses at the areas of the greater and lesser trochanter could have been the reason for disturbance throughout the data acquisition. In particular it was noticeable that after dividing the medial iliofemoral ligament first and when moving the femur into full abduction, a large bulk of the capsule was 'squeezed' between the acetabular rim and the greater trochanter, which was significantly enlarged by the new bone deposition, thereby raising the moments that were required to move the joint into the same positions.

For the above reasons the decision was taken not to consider these specimens in the evaluation of the test recordings and to base any conclusions from this study

on the effects of the remaining specimens. However, the data collected for specimens 2 and 4 could still be used for confirmation of any findings acquired from the other samples.

The age of the hip joint donors ranged from 54 years old (specimen 4, n=1) over 60 years old (specimens 1 and 5, n=2) to 73 years old (specimens 2 and 3, n=2). Even though age tends to be a factor affecting the mechanical properties of soft tissues as a result of altered collagen levels (Nigg et al, 1999), it is not considered to play a relevant role in this particular study, as information was only sought as to what degree individual capsule ligaments influence the hip joint stiffness. No inter-specimen comparison was made and therefore the age of the specimen as well as the donor's pre-mortal health need not be considered. However, in particular for specimen 4 the limitations to the range of movement that must have existed due to the fracture fixator, could have influenced the development of the ligamentous structures in such way that it may have played a role in the results that were recorded for this specimen.

One of the reasons that were in the author's mind when taking the decision to distinguish between risks for posterior and anterior dislocation, was to also show the effect of damaged ligaments in different limb positions which were considered to be critical for dislocation. For the tests of posterior dislocation risk the critical combinations are reported to be when adducting the limb under full flexion and internal rotation and secondly in full internal rotation. For the tests of anterior dislocation risk these combinations are for full extension and external rotation as well as for external rotation only, again mainly under adduction (Romanes, 1977). It was therefore in these positions where the intact capsular ligaments were expected to play a more significant role in providing stabilising resistance for the joints as they become more tightened then.

For those specimens that were tested for risk of posterior dislocation in neutral position, a noticeable fall in capsular resistance was observed after dividing the ischiofemoral ligament and an even further drop after the additional division of

the lateral iliofemoral ligament, both for adduction and abduction. However, when under full flexion the drop is not so intense, especially when the limb is moved into adduction, on average 3.6% (table 4.3) in the case of dissected ischiofemoral ligament. For those positions at which the joint is at highest risk for posterior dislocation (i.e. full flexion with internal rotation and full internal rotation) the resistance reduction after ligament dissections was more extreme, around 70% (table 4.3). This suggests that the loss of capsular ligaments at locations where their contribution to stability is highest has a more deleterious effect than in more neutral limb positions. In other words this means that in those positions, where their action is highest under normal conditions (i.e. intact capsule), their absence in very common post-operative conditions (i.e. with damaged capsular ligaments) gains importance.

For the specimens tested for risk of anterior dislocation- in particular for specimen 5- it was observed that the span between abduction and adduction, in which no moments were recorded is much narrower than was the case for the specimens tested for risk of posterior dislocation (specimens 1,2 and 3). Specifically for joint positions other than neutral, the zero moment range virtually vanished. This shows that the anterior ligaments have a much shorter travel during the movement of the limb than do the posterior ligaments and that is what limits the ability to hyperextend excessively and also acts as some kind of support to standing. It is during standing- or even more during walking and running- that larger forces are transmitted by joints (Paul, 1999) and where the limbs are moved into extreme positions (i.e. extension). By tightening within a much smaller range they guard the joint from anterior dislocation. Another important observation for the anterior dislocation study was that in none of the cases was there a complete extinction of abduction-adduction resistance after dividing any of the ligaments. This observation was in contrast to the observations made in the study for risk of posterior dislocation, where a severe drop in resistance was observed- especially after cutting through a second ligament (i.e. ischiofemoral) as can be seen clearly in figures 4.25a or 4.26c. This suggests that access to the hip joint surfaces using an anterolateral surgical approach causes less disturbance to the overall resistance that the joint produces to moving the limb into abduction and adduction in comparison to the effects that occur

when a posterolateral approach is selected, which involves the damage of posterior and lateral ligaments.

However, by looking at the curves in different joint positions for all capsular states it can be noticed that similar curve patterns remain even after dissecting one or two capsular ligaments. This means that despite the absence of the particular dissected ligaments a similar trend in capsular resistance is still present. That suggests that no individual ligament plays an exclusive role in stabilising a joint when the limb is moving in a certain direction, but that all ligaments have a secondary and tertiary support action. Thus, it is necessary to know which is the most important supporting action of each ligament and to see in which case a dissection has more detrimental effects in reducing hip stability thereby avoiding damage to these ligaments during THR. This is where the present study can support the computational model in drawing conclusions on the ideal location of the cut that should be placed on the capsule to allow access to the joint without reducing the resistance action of the capsule excessively.

In one case (full flexion and internal rotation with abduction for specimen 3, table 4.3) the recordings revealed an apparent contradiction, where the resistance from the capsule after cutting through two ligaments was higher than with one ligament cut. This occurrence was very unusual and could possibly be due to viscoelastic behaviour of the capsular ligaments. Thereby, during the testing procedure it is possible that between two separate test situations (i.e. full flexion with internal rotation and full internal rotation) the time that was used to reset the test rig was too much giving the tissues the chance to recover from the previous load cycles better than was the case between other two test cycles. An effort was made to adhere to the very strict protocol to determine the time lapse between two individual test cycles, to allow for stress relaxation to build up, but the difficulty of changing the angles on the test rig together with the extra care that was necessary to assure that the angles were chosen correctly, might have prolonged or exceeded this time gap in the particular case.

A test series of 30 cycles was also performed as an attempt to show the effect and extent of stress relaxation on the cadaveric specimens after repeated loading cycles. This test revealed that even after such a large number of cycle repetitions there was still some stress relaxation occurring, but at substantially lower levels than at earlier cycles. The actual recorded tests comprised five cycles, but it was only the last that was used for the data analysis. It needs to be stated that possibly a series of 30 cycles prior to each actual recording of the test would have given some extra confidence for the existence of similar degrees of stress relaxation. However, the time required for this would have been too much placing a risk on the specimens to possibly dry out too much. The compromise that was found in this dilemma was to run five cycles of abduction-adduction and to use the last of them for statistical and numerical evaluation.

The use of an abduction: adduction ratio of 56.25%: 43.75% as referred to in the literature (Gerhardt and Rippstein, 1990) seemed a necessary compromise, in order to make it possible to determine to what extent the limb was moving into abduction or adduction. Had it been agreed not to calculate this angle by using the above ratio, it would still have been possible to reproduce the same range of motion for all capsular states (i.e. intact or with divided ligaments). This would have still allowed a comparison of the effect of the various ligaments, but it would not have revealed the actual angles at certain moment recordings in the various capsule states. In this way the cadaveric study of the capsular ligaments would not have been of use for the validation of the computer model of the hip joint, because the absolute angles between femur and acetabulum as tested and recorded in the cadaveric model would not be known and could therefore not be reproduced in the computer model. A downside of the use of a predefined relation of abduction and adduction, however, is that it might lose its validity when the limb is in full flexion or extension, as the ratio has only been proposed for a neutral degree of flexion, which is the case when a subject lies in supine position (Gerhardt and Rippstein, 1990). When the limb is moved into full flexion or extension this ratio might be different and therefore there could have been a distortion in the way the curves are presented in the moment-angle graphs presented above.

The value of the present approach in determining the individual contribution of each capsular ligament may be criticised based upon the argument that a relatively crude method was used to establish the ideal neutral abduction-adduction position of the femur relative to the pelvis. However, in the absence of large and popular anatomical landmarks (e.g. knee joint and anterior superior iliac spine) in the utilised specimens, this method deserves some appreciation. In support of this study it needs to be mentioned that in no other previous work was it attempted to study the involvement of the various ligaments as they are in situ in the human anatomy. Hewitt et al (2001 and 2002) and Ahlers et al (1978) used excised ligamentous structures under tension bearing all the consequences that such an excision carries. The risk of removing excessive or insufficient parts of the capsule and label them as a certain capsular ligament is one obvious risk. Removing the contribution of the capsule's structural integrity by studying the individual ligaments in a linear tension is another risk. The power of the approach that was presented in this chapter lies in the fact that it considers the joint function that all ligaments have when the joint angle is modified- just like in a real situation. Also, the effects of any damage to the capsule approximate a situation as it could emerge after a surgical intervention- like a THR- where parts (either anterior or posterior) of the capsule are removed and the joint is expected to continue to perform in activities of daily living. However, the present study does under any circumstance sustain its validity for the purpose of comparing situations before and after the dissection of certain ligaments, whether the exact joint angle can be established to satisfaction or not.

Two different approaches to a similar problem, which is the identification of the mechanical properties of the capsular ligaments and the individual and overall contribution to joint stability, are currently available- namely the method that was presented in this chapter and the tensile testing of excised capsular ligaments. Even though it is extremely difficult to perform a comparison between them, it is attempted to evaluate their outcomes. Thereby, the use of the computational model as it will be presented in the following chapters shall be of use by utilising the data available on the mechanical properties of the individual ligaments and comparing the

output of moving the joint into a different position with the data that was produced with the work presented in this chapter.

In proposing a better way of determining the absolute position angles between the femoral and acetabular parts of the joint the use of a robotic arm comes into mind, much in the same way as Ishibashi et al (1997) used when studying the effect of ligament fixation site at the tibia on knee stability. A similar robotic system was also used by Rudy et al (1996) to determine *in situ* forces of knee ligaments. This method would not provide any improvement in terms of comparing the effect of the various ligaments in providing stabilising action to the joint. However, it would be possible to drive the limbs into predetermined positions based on co-ordinates. Markers inserted into the femur and parts of the acetabulum of complete cadaveric bodies aided by the use of visualisation utilities like x-rays or CT scans would make it possible to identify relative positions of these marker points on the bone at similar limb angles like those used in the present study (neutral position, full flexion etc.). These relative positions could then be reproduced for the excised cadaveric joints, like those used in this work, assuring that the cadaveric specimens simulate realistic positions that are also possible by the complete limb.

Another possible improvement of this study could have been to perform the sequential dissecting of ligaments in reverse order. This way it could have been possible to collect further information on the individual importance of the different ligaments. At the current state it is not possible to state whether the absence of any significant differences between the situations of one and two dissected ligaments- like in the case of adduction and full internal rotation for specimen 3 (table 4.3)- is due to the greater importance that the first dissected ligament carries in stabilising the hip joint or if there wouldn't be any difference. However, for this purpose it would have been required to have more specimens available, which is a difficult task given the current situation in the UK, which limits the use of human specimens for biomechanical studies.

4.8 Summary

It has been shown that it is possible to perform a comparative study of the individual and total contribution of various hip joint capsular ligaments, using complete human cadaveric specimens, comprising bones and ligaments. The validity of this comparison for the purpose of comparing the effects of the absence of individual ligaments could be shown regardless of the absolute angles of the joint positions. The advantages of using complete cadaveric specimens is apparent and was explained and also the conclusions that could be drawn from using a complete cadaveric specimen model were shown to be immediate and representative to those situations that arise after conventional THR surgery, where the capsular ligaments are commonly damaged.

Advice on choosing the most beneficial or least damaging site of access to the joint surfaces could initially be given, based on the analysis of the results yielded in this study. It was suggested that the use of an anterolateral approach would produce a less drastic drop of capsular resistance than a posterolateral approach. In the following chapters it will be attempted to confirm these conclusions by simulating the same joint positions in the computer model.

Finally, the use of the present results in combination to the data available from other studies makes it possible to generate a computer simulated model comprising, too, bones and ligaments exclusively. That model can be used to simulate even more situations, which are complicated to be simulated in the cadaveric model. A more detailed analysis on this follows in the next chapters.

Chapter 5- Creation of 3-D Model

5.1 Introduction

The accuracy of a numerical simulation of anatomical structures such as the hip joint and its ligaments depends largely on how accurately the method utilised is in producing the 3-D model. This in turn, depends primarily on the available imaging modalities and on the software that is employed for the detection of the structures of interest. The quality of the imaging modalities becomes even more crucial in the present application, considering that the structures of interest are the deep lying hip ligaments, which are embedded in the capsular matrix and are in immediate contact with the musculature that surrounds the hip joint. In many imaging systems the representation of soft tissues is particularly bad, whereas in others, where soft tissues can be reproduced, the image sharpness may be low. In the following paragraphs it is attempted to describe these restrictions in more detail and to explain the selection that was made both in terms of utilised technology for the imaging of the structures and also in terms of the selected software.

5.2 Selection of Imaging Modalities

Three-dimensional models of anatomical structures have been created extensively in the past, mainly for the purpose of studying the interface between the anatomical part and an implant (Kang et al, 1993). Also the femur and pelvis have been modelled frequently using two-dimensional CT (Computerised Tomography) scans (Keyak et al, 1993). The major advantage of using CT scans for the modelling of bone, is that there is little distortion on the image and a good contrast between bone tissue and other tissues can be achieved (figure 5.1). The good image contrast makes it possible for the software application to achieve good recognition of the tissue's boundaries and to automatically draw the boundary lines. Furthermore, a resolution of 512 pixels by 512 pixels can be achieved in CT scans, each one with 12bits of grey tone resolution. However, for the case of soft tissues it is not possible to distinguish easily between the various soft tissue types and therefore modelling ligaments can be problematic.

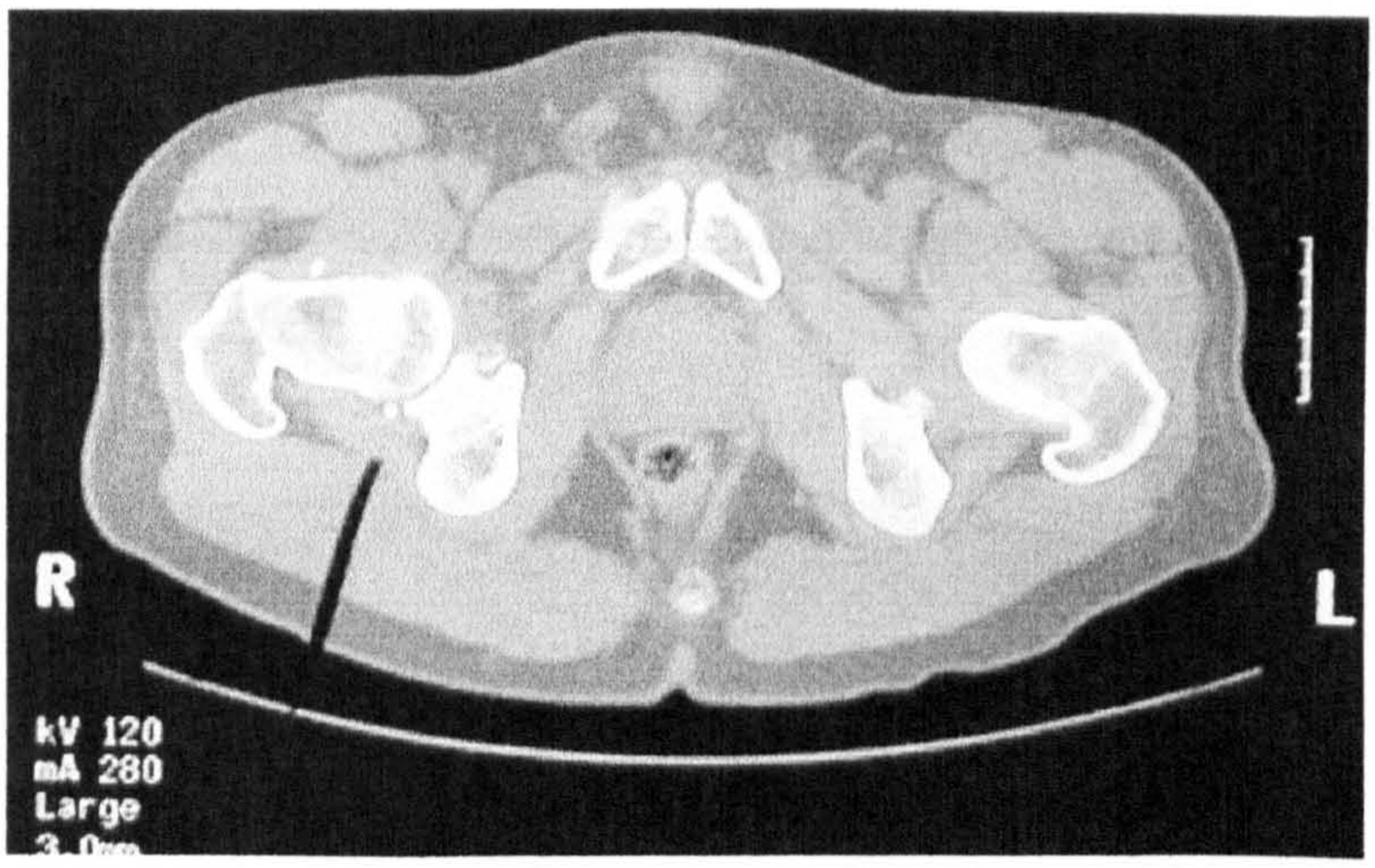

Fig 5.1 CT scan of a human cadaveric hip joint specimen.

In contrast to the CT scan's resolution, MRI scans usually result in 256 pixel by 256 pixel resolution with each pixel again having a 12 bit grey tone resolution (figure 5.2). Object boundaries end up being more diffuse than in case of CT scans and an automatic edge detection is almost impossible. Just like with CT scans, it is not possible to distinguish small soft tissues such as ligaments from other soft tissues.

Fig 5.2 MRI scan of hip joint area shows diffuse boundaries.

A third type of available image for three-dimensional model creation was the cryo-section image dataset of the 'Visible Human' that was created by the National Library of Medicine (Schubert et al, 1997). This dataset comprises among others

high resolution colour images of transverse cross-sections of a male and a female human cadaver (figure 5.3). The resolution of these images is 2048 pixels by 1216 pixels, which are defined by 24 bits of colour and have a size of 0.33 mm by 0.33 mm.

Fig 5.3 Cryo-section image from the 'Visible Human' dataset at the cross-sectional height of the hip joint.

The male dataset consists of 1871 cryo-section images in 1 mm increments from the top of the head to the bottom of the feet. These images were taken after the human cadaver of a male volunteer was set into resin (blue coloured matrix shown in figure 5.3). The complete cadaver within the resin matrix was subsequently frozen and 0.33 mm thick layers were sequentially abraded and pictures were taken of the remaining cross section.

Some years later, similar images were taken of a female cadaver in resin with smaller increments (0.33 mm) between two consecutive layers. This was done for the purpose of creating pixels with cubic dimensions of 0.33*0.33*0.33 mm^3, in order to enable investigators to work with cubic voxels. For the purpose of this study it was chosen to use the female dataset, as it was felt that a smaller increment would assist in minimising the error in the three-dimensional reconstruction. However, after creating the three-dimensional object, it became apparent that too high an image density is not beneficial either. This is discussed in further detail in paragraph 5.4.

Comparing the three different types of imaging modalities described above, it is apparent that MRI offers the least advantages for the particular use, since the overall resolution of the resulting images is smaller than that of the CT scans and the cryo-sections and at the same time does not allow a clear distinction of the different soft tissue structures. CT scans have a much better resolution, but also suffer from limited differentiation of the various soft tissues. The cryo-sections have the greatest resolution and also allow a good distinction of the various soft tissues (figure 5.4).

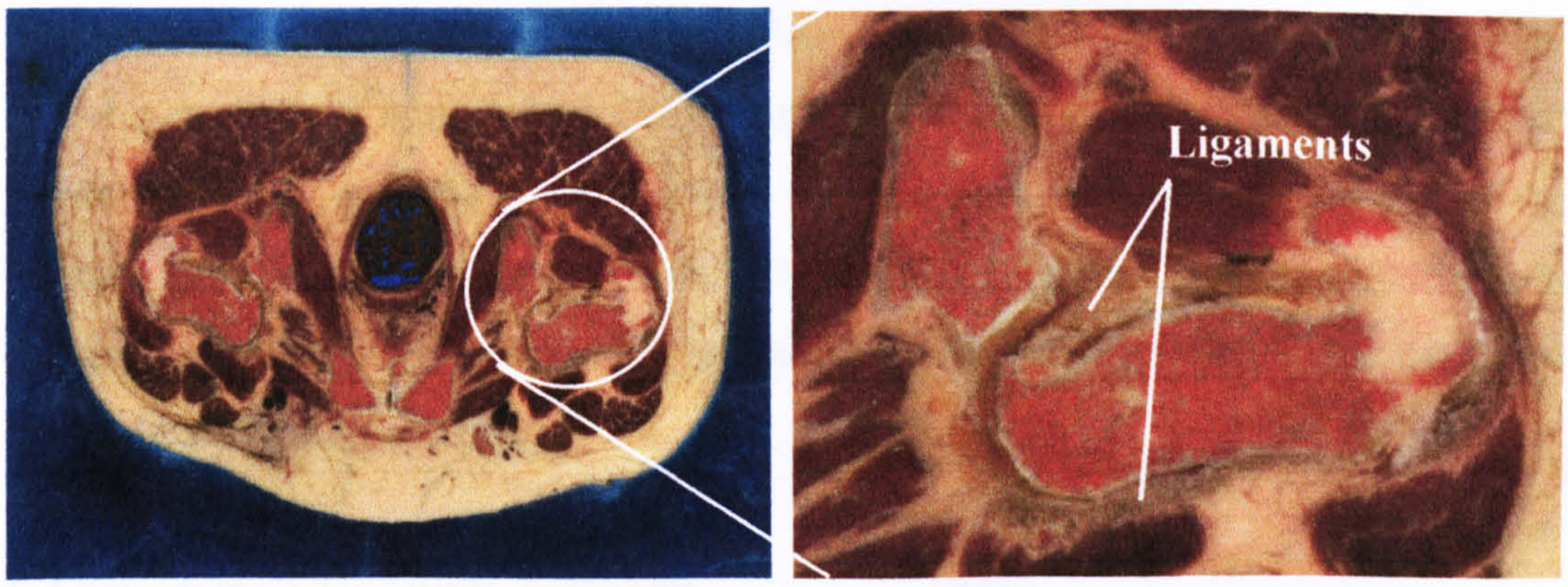

Fig 5.4 Difference in appearance of dissimilar soft tissues on a cryo-section image.

Despite the advantage of *in vivo* image acquisition with CT and MRI scans, it was decided to proceed with using the cryo-section images from the 'Visible Human' female dataset. However, an additional model based on CT images of a dissected cadaveric human hip joint (figure 5.5) was also created.

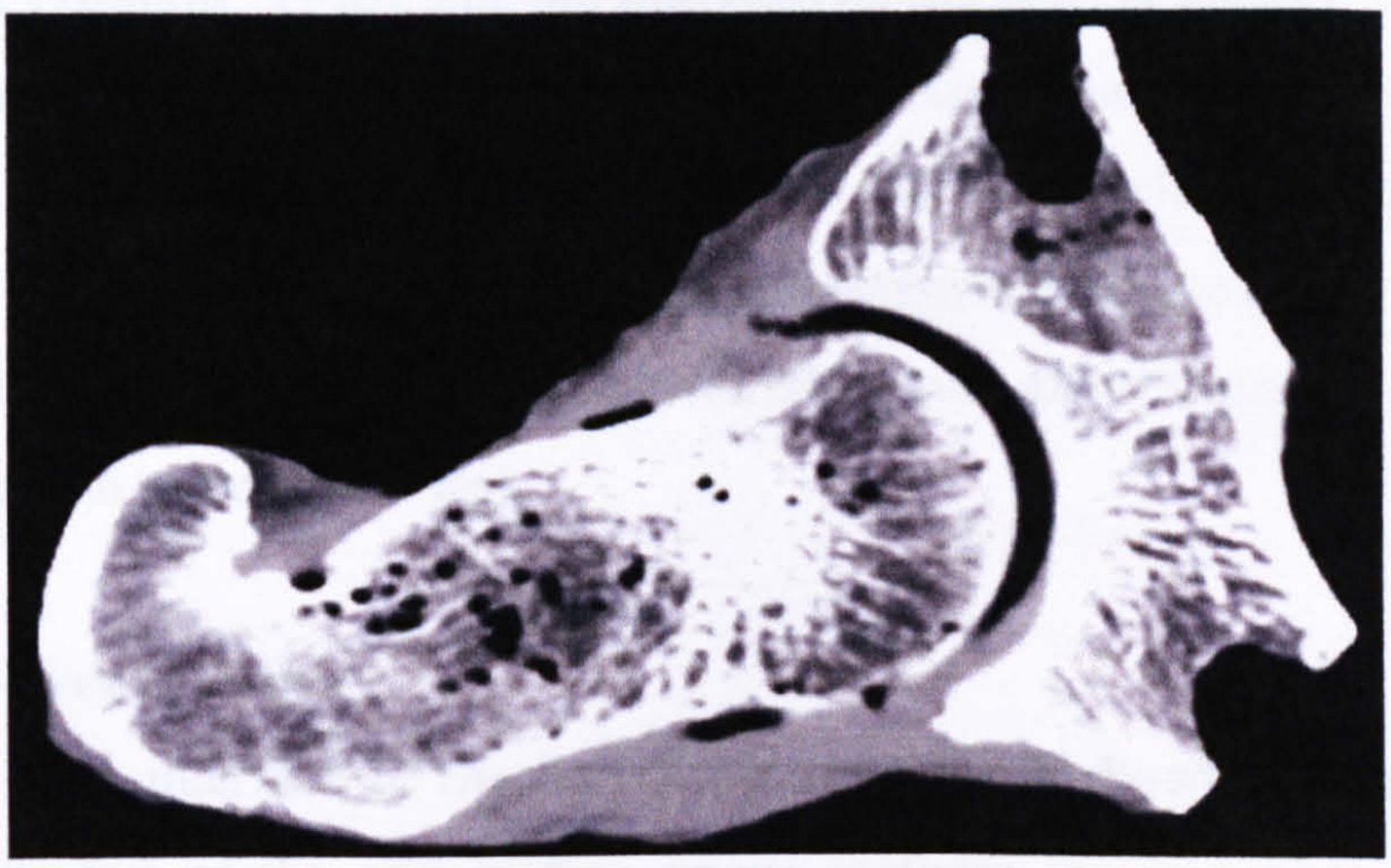

Fig 5.5 CT scan of hip joint comprising bones and ligaments.

The CT scans were taken on a cadaveric hip joint that had been previously prepared for tests on the mechanical test rig that was described in chapters 3 and 4. All the soft tissues apart from the capsular ligaments and the capsule itself were removed and only the parts that were eventually tested on the rig for their stiffness were introduced into the CT scanner. The device that was used for this purpose was the SIEMENS SOMATOM Plus 4 (SIEMENS AG, Erlangen, Germany) of the general hospital at Barmbek in Hamburg, Germany. The scans, which are stored in the usual DICOM file format, had to be converted into a more common and easy to read file format, such as bitmap (.bmp). For this purpose a DICOM viewer software called Accu View (Accu Image Corp, San Francisco, USA) was used. The interval between two sequential slices was 2 mm, which is substantially less than that of the 'Visible Human' dataset. However, the advantage of not having any other soft tissues causing confusion with the capsular ligaments, is of such importance that the larger intervals can be accepted.

5.3 Selection of Modelling Software

The most common technique for shape reconstruction is the use of sequential cross-section images of the anatomy. Thereby the boundaries of the anatomical part of interest can be traced in each of the cross-sectional images where it appears. The individual traces can then be stitched together forming a three-dimensional and shell-type object of the anatomical structure. There are several software packages that are capable of performing this task, like IMOD (Kremer et al, 1996) or SurfDriver (Moody and Lozanoff, 1998). For the purposes of the present project the latter was the software of choice for the reasons of simplicity of software layout, ease of familiarisation and large number of file formats that are available for export of the final model files- a feature that is of great importance, considering the intention to further work on the models. Finally, SurfDriver's cost-effectiveness is satisfactory, as the acquisition price is very low.

5.3.1 SurfDriver Interface

The main interface of the SurfDriver software is shown in figure 5.6. The toolbar to the left of the cryo-section image includes the important functions of

automatic or manual edge detection. In manual mode it is possible to set the density of boundary vertices, which affects the difficulty of stitching the individual layers together. In automatic mode the threshold can also be adjusted, which influences the sensitivity of the edge detection. The toolbar on the bottom of the image allows switching from one object to another, which is particularly useful in parallel editing of the femoral and acetabular boundaries, which can be individually altered having the boundaries of the other anatomical part in front.

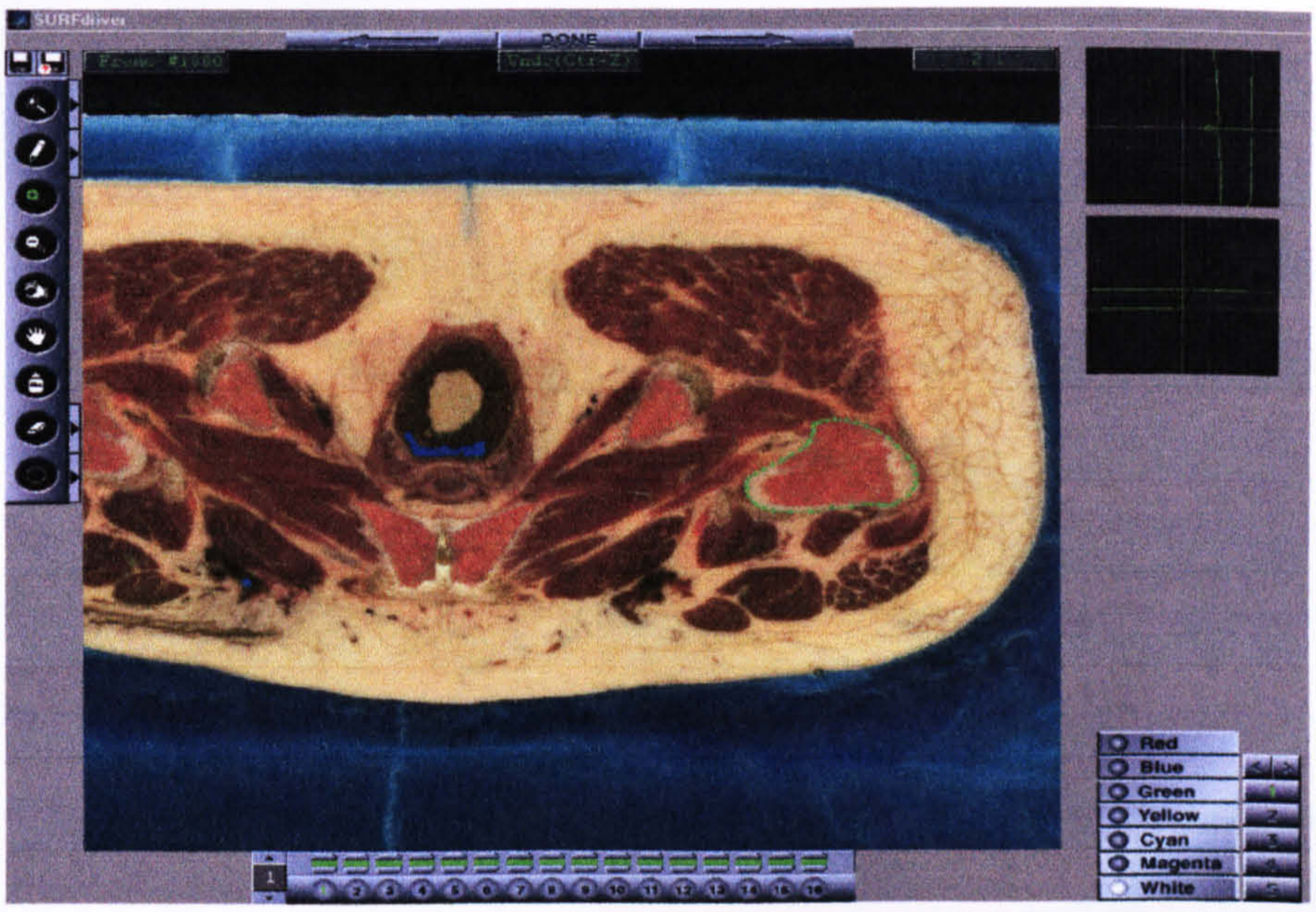

Fig 5.6 The SurfDriver interface here in use with a cryo-section image.

The alignment of the sequential image slices is done automatically, given that the images were taken with a perfect alignment initially. In the case of the cryo-sections from the 'Visible Human' dataset this was taken care of during the image acquisition. In the case of the CT images it was achieved by ensuring that no change of position was imposed on the cadaveric joint during the tomographic process. Further, at the beginning of editing an object, it was always specified what thickness each slice had, in order to enable the software's compiler to stitch the individual traces at a correct distance along the third (axial) dimension. Also the width of each slice was specified in a similar manner.

5.3.2 Basic Operation of SurfDriver

The main feature of SurfDriver is a function that enables the software to stitch together the traces that were selected for various anatomical objects on consecutive cross-section layers (figure 5.7).

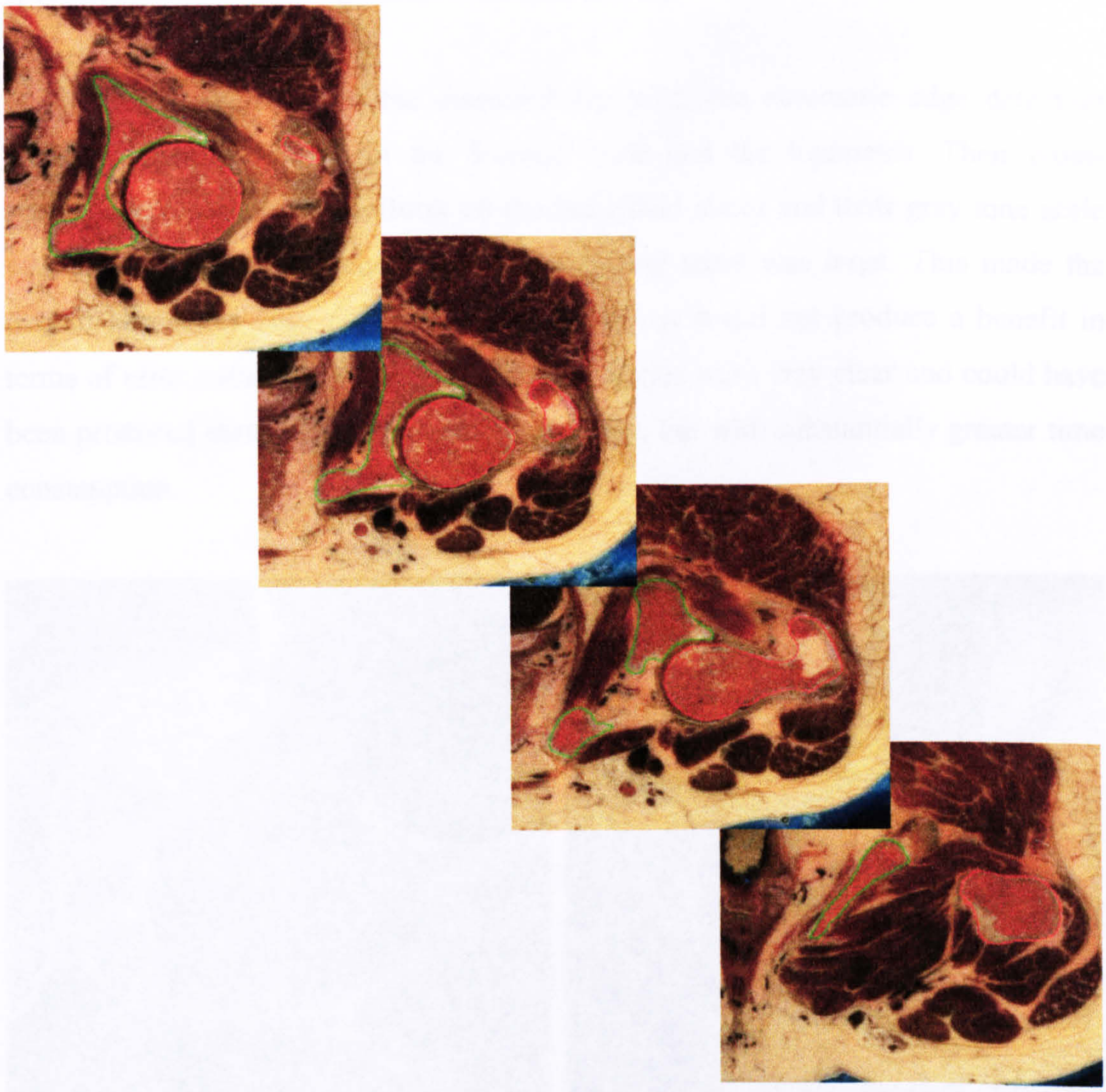

Fig 5.7 Sequential cryo-section images of the femur and acetabulum with their borders marked in red and green respectively.

The determination of object boundaries on the cryo-section images was done manually as the contrast to the neighbouring soft tissues was insufficient making an automatic edge detection impossible. For correct manual edge detection it was considered necessary to obtain a preserved human specimen for dissection that would

assist in identifying the insertion areas of the various ligaments into the femoral and acetabular bones. The help of Dr John Shaw-Dunn from the Department of Human Anatomy at Glasgow University, was thereby of immense importance. By comparing the structures on the cryo-section images and at the same time utilising the cadaveric specimen the individual ligaments were determined.

In the CT scans of the dissected hip joint, the automatic edge detection worked well particularly for the femoral bone and the ligaments. Their cross-sectional appearance was uniform on the individual slices and their grey tone scale was constant, whilst the contrast to neighbouring areas was large. This made the overall process of edge detection much easier, but it did not produce a benefit in terms of error reduction, since the tissue boundaries were very clear and could have been produced manually without any uncertainty, but with substantially greater time consumption.

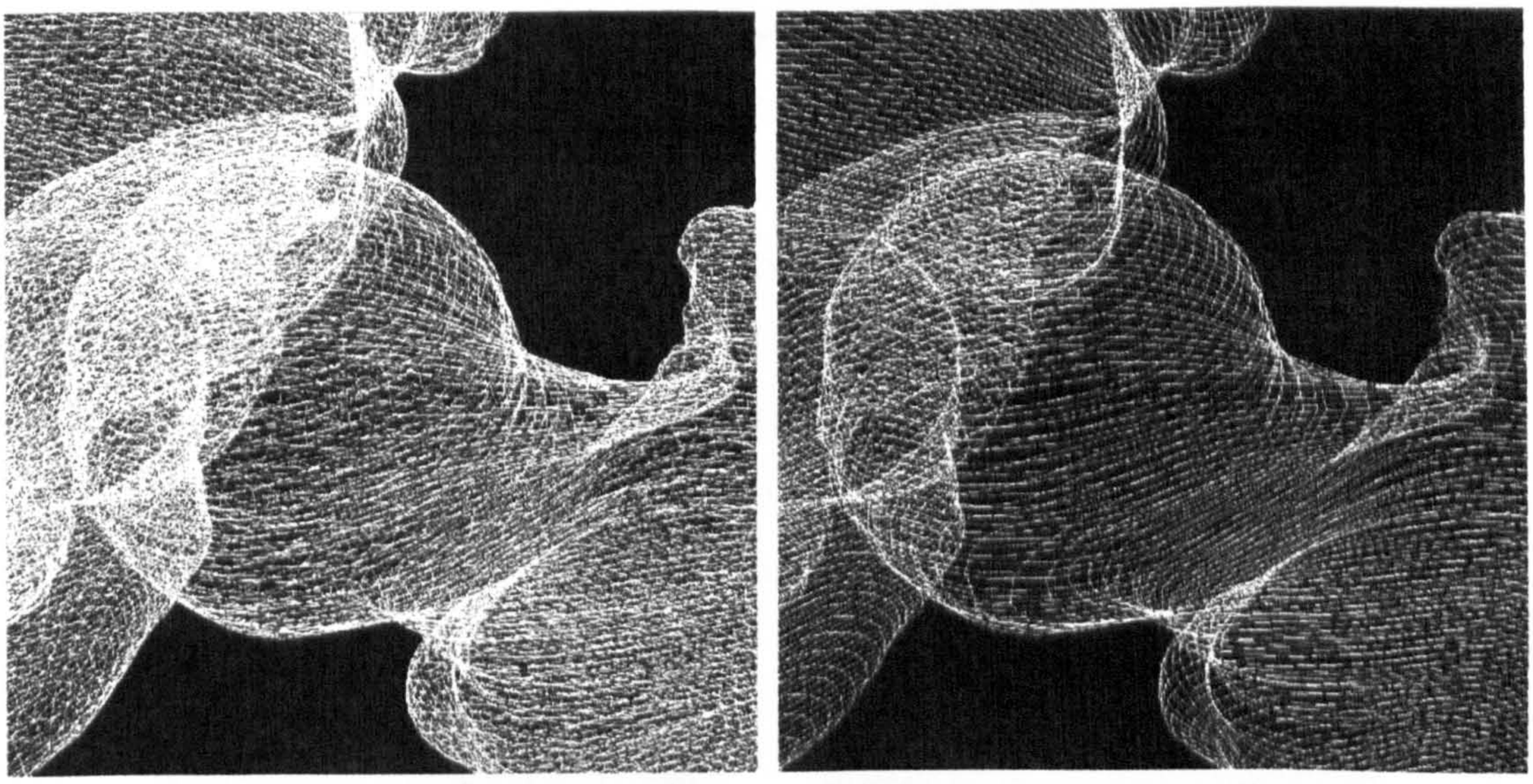

Fig 5.8 a and b Left is the hip joint as tiled geometry and right as wire frame model.

By stitching the individual boundaries together, the final three-dimensional object could be represented as a 'tiled surface' geometry (figure 5.8a). Alternatively the original wire frame model could be maintained (figure 5.8b). A third option of representing the object within the SurfDriver software would be to render the complete wire frame model (figure 5.9), much in the same way as placing a web over

the existing wire frames. In all three cases the model would have the characteristics of a shell and the difference would be in the ease to further process the model, i.e. in translating the three-dimensional shell object into a solid. This process is described in more detail in chapter 6.

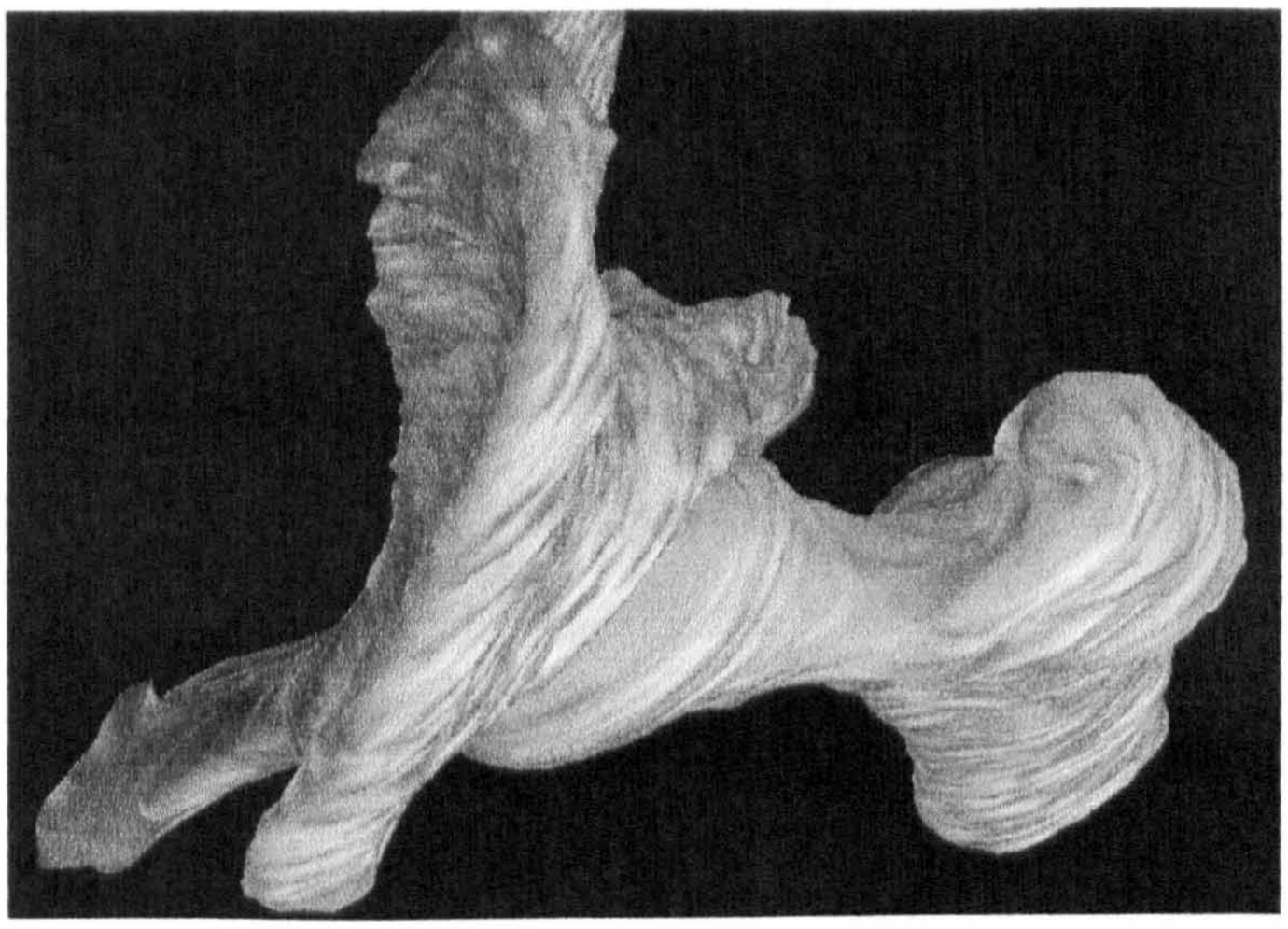

Fig 5.9 The hip joint of figure 5.8a and b in rendered mode.

Another important feature of SurfDriver is the smoothing function. The software simplifies the boundaries and cuts those vertices that stick out and thus produces a smoother surface (figures 5.10 a and b). This might result in less geometric accuracy of the joint, but produces a closer to natural anatomical shape. Smoothing can be done to a lesser, normal or greater extend, but the software does not specify a percentage of surface stripping for the individual cases.

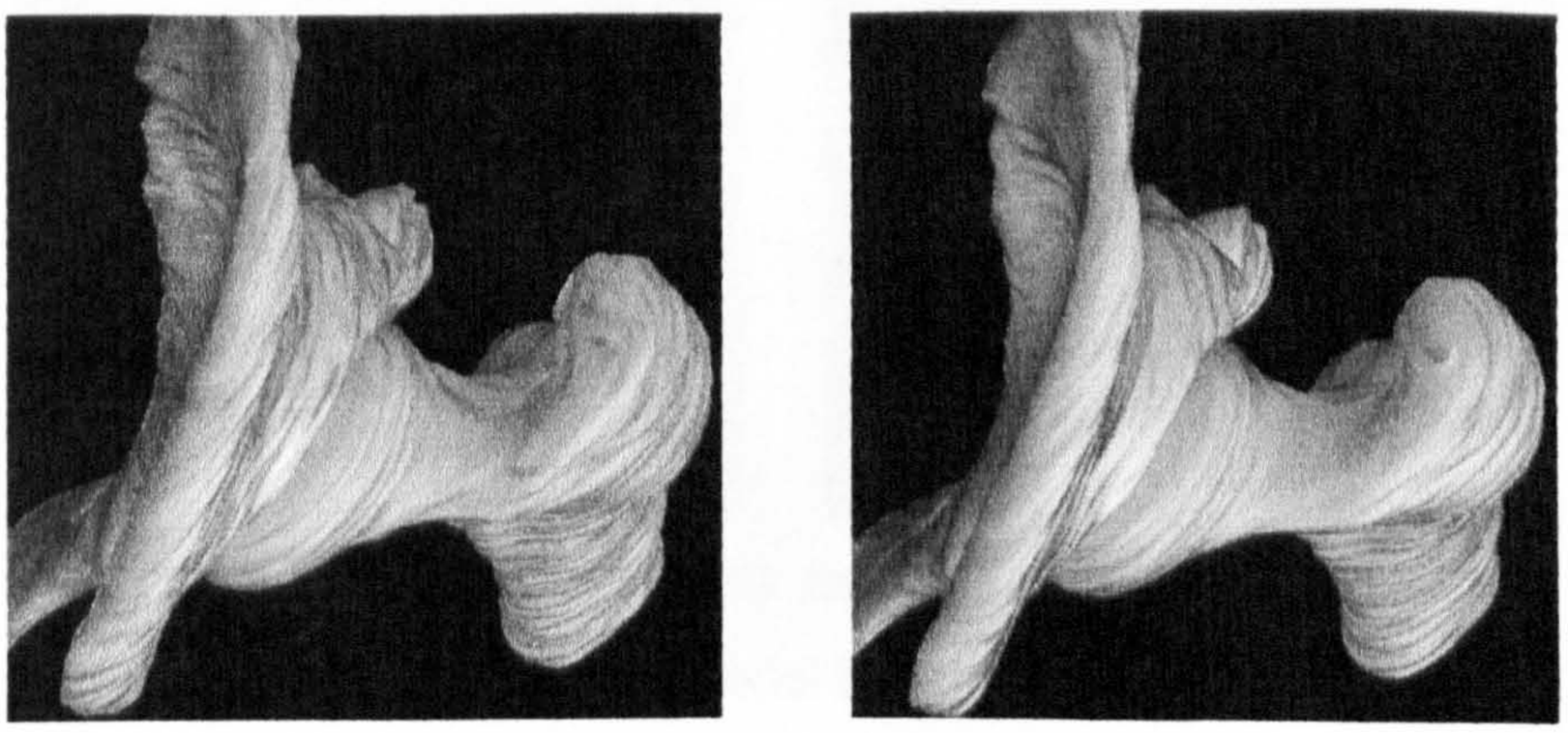

Fig 5.10 a and b Less (left) and more (right) smoothing of same joint.

5.4 Volumetric Comparison of Different Models

In order to compare the feasibility of different image types for the creation of three-dimensional anatomical objects, another function of SurfDriver was employed. The volumetric calculation can be used to determine the total volume of each object, but also of individual parts of the object. Therefore, the following volumes were determined as an approximate comparison between the two different imaging types.

Whole Femora

In the case of the femur that was modelled based on the cryo-section images, 150 slices were used, starting from the one that first includes the femoral head. Only every third slice of those available in the female 'Visible Human' was used for this model. In order to correctly compare the volume of this model to that produced using the CT images of the cadaveric joint (figure 5.11b), both must have the same length. The total length of the femur that was modelled with the cryo-sections is 150 mm (figure 5.11a). However, the cadaveric joint was cut in such a way as to fit the available cementing pot and had a total length of 136 mm. Therefore, prior to their comparison, the cryo-section based model was also cropped down to 136 mm length with SurfDriver's crop feature.

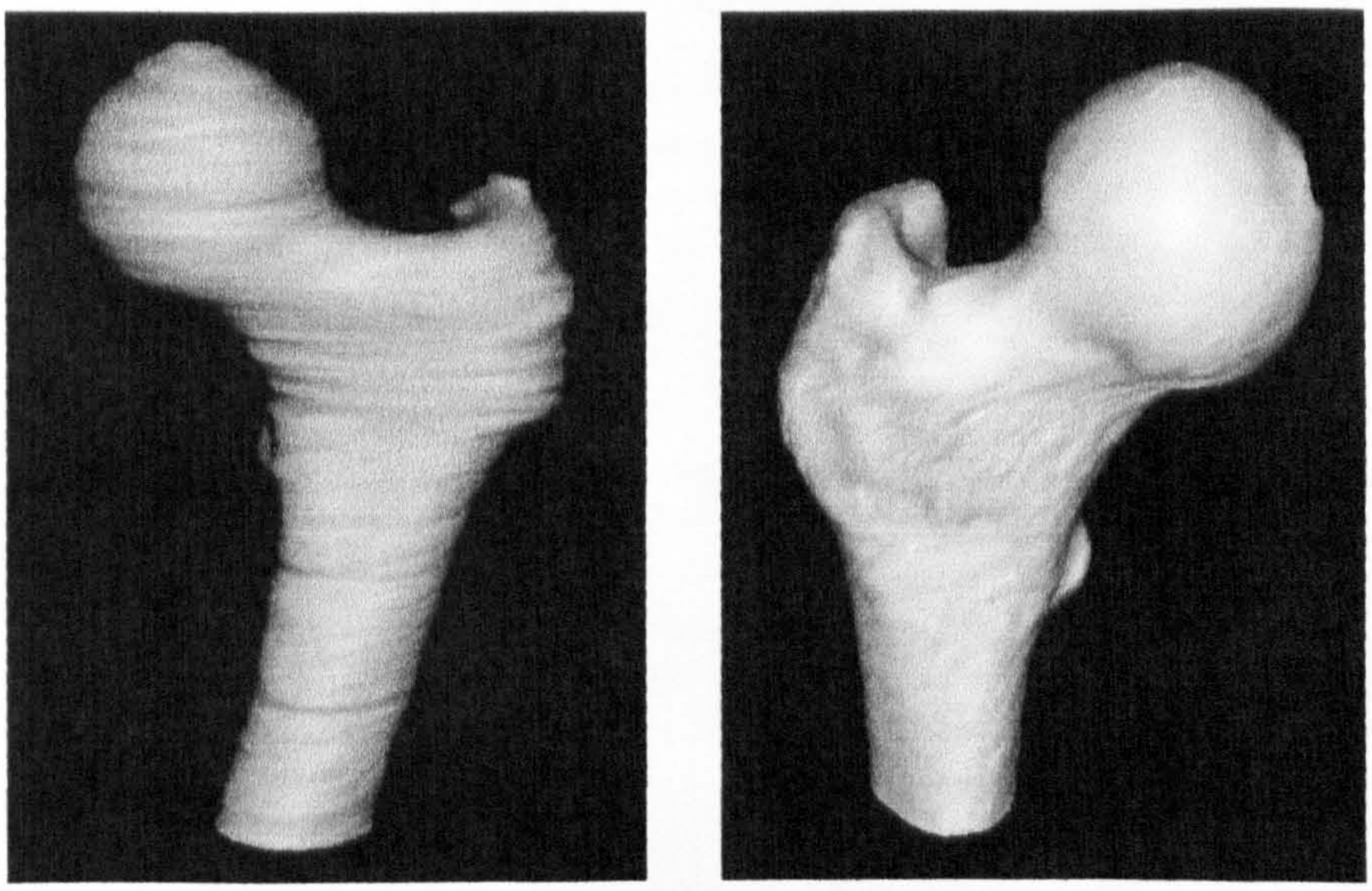

Fig 5.11 a and b Model of left female femur from cryo-section images and right male femur model based on cadaveric CT scans.

	Cryo-section Femur	CT Femur
Total Volume [mm^3]	170460	214335
Femoral Shaft Diameter at Tip [mm]	31	33

Table 5.1 Dimensions of the femoral objects based on the two different imaging types.

All calculations of the volumetric analysis are listed in table 5.1. One of the recordings for the two femoral models was the total volume, which was greater in the case of the CT based model by 25.75% in comparison to the cryo-section images based model. Another record was the diameter of the femoral shaft at the tip of the modelled femur, which was also greater for the CT based model by 6.5%. Differences between the two models are anticipated, because they are reconstructions of male (CT-based model) and female (cryo-section based model) joints. The usual differences between male and female femora are outlined in the table 5.2.

	Time of death			
Dimension	**1900-20**	**1980s**	**Increase (%)**	**P value**
Femoral length (mm):				
Men	457.3 (4.3)	464.9 (5.2)	1.7 (0.6)	0.05
Women	422.0 (3.1)	428.4 (4.1)	1.5 (0.5)	0.05
Neck length (mm):				
Men	34.9 (0.6)	38.3 (0.8)	9.7 (1.0)	<0.001
Women	32.5 (0.9)	35.0 (0.7)	8.7 (0.9)	<0.001
Neck width (mm):				
Men	34.1 (0.4)	35.8 (0.6)	5.0 (0.6)	<0.05
Women	30.6 (0.6)	32.1 (0.4)	4.9 (0.6)	<0.05
Head diameter (mm):				
Men	48.5 (0.4)	50.2 (0.6)	3.5 (0.4)	<0.05
Women	43.7 (0.5)	45.2 (0.6)	3.4 (0.5)	<0.05
Anteversion (degrees):				
Men	7.9 (0.8)	4.4 (1.3)		NS
Women	7.5 (1.2)	7.4 (1.0)		NS

Table 5.2 Osteometric gender differences for femoral bones (Duthie et al, 1998).

Duthie et al (1998) produced an osteometric study of gender differences on various dimensions of the femoral bone (table 5.2). These differences are in good agreement with the differences resulting from the volumetric comparisons carried out in the present work.

Femoral Heads

The diameter of both femoral heads was measured in the three major axes of both models. The readings revealed similar femoral head sizes as shown in table 5.3.

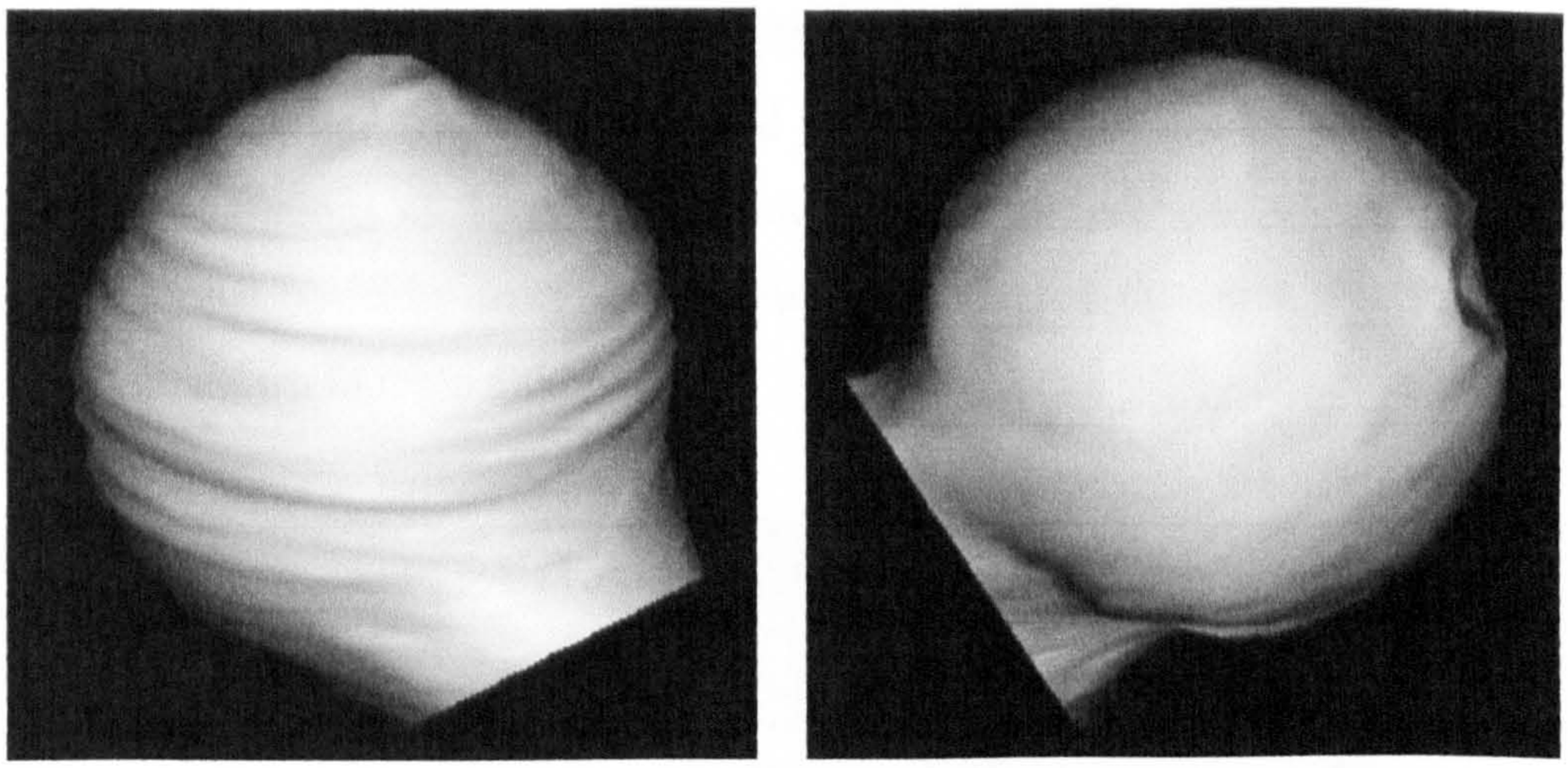

Fig 5.12 a and b Femoral heads of the two models for dimensional comparison.

As expected the femoral head dimensions were greater for the case of the male model that was created using CT images. The difference was on average at 13.5% for the head dimensions. This is in good correlation with the findings of Duthie et al (1998), which shows differences of 10% (table 5.2).

	Cryo-section Femur	**CT Femur**
Diameter in x-axis [mm]	43	49.5
Diameter in y-axis [mm]	43.5	48.5
Diameter in z-axis [mm]	44	50

Table 5.3 Dimensions of the femoral heads based on the two different image types.

The small differences between the three readings do not suggest errors or inaccuracies of the employed method or types of images used, but are merely variations that result from the not completely round shape of the femoral heads.

Acetabuli

The acetabular model that was created based on the cryo-section images is part of the complete hemi pelvic model and is not a separate structure as in the case of the CT based model. The latter had been modelled separately as the cadaveric joint that was used for the scans, had previously been dissected in a way similar to a triple pelvic osteotomy for ease of cementation. This means that the two models are different by definition (figures 5.13 a and b) and for the purpose of comparison the volumetric operations of SurfDriver would have to be restricted to both acetabuli. These comprise basically readings of diameters at three different locations of the acetabuli as shown in table 5.4.

	Cryo-section Acetabulum	**CT Acetabulum**
Diameter 1 [mm]	49.5	53
Diameter 2 [mm]	50	53
Diameter 3 [mm]	57	58

Table 5.4 Dimensions of the femoral heads based on the two different imaging types.

The differences between the two models was 5%, whereby again the male CT-based reconstruction was larger. Even though the osteometric study of Duthie et al (1998) did not include data on the acetabulum, it can be assumed that the differences between the male and female populations would have been of the same order of magnitude as those for the femoral head diameter, namely 10%. This means that the observed dimensions that are shown in table 5.4 can also be attributed to gender differences.

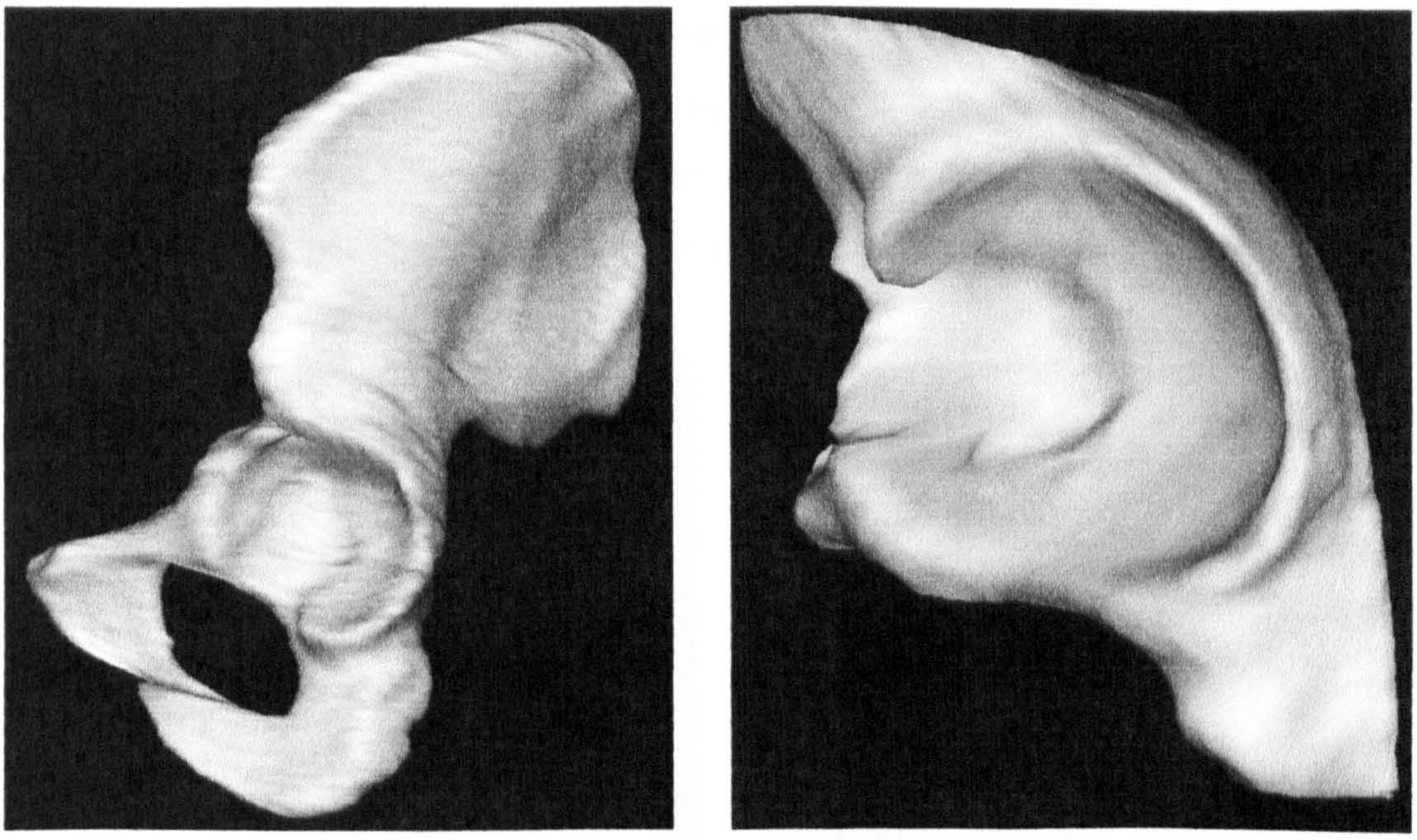

Fig 5.13 a and b The complete pelvis modelled with the cryo-section images and the cadaveric acetabulum that was created with the CT scan images.

Ligaments

The ligaments of the joint capsule are those structures that initiated the thought of attempting to reconstruct them into three-dimensional models by using CT images of dissected parts. The great advantage thereby was that no differentiation from surrounding structures was needed. However, another difficulty was to identify boundaries between individual ligaments within the hip joint capsule. Whatever the different threshold that was used, the ligamentous structures of the capsule still looked like one uniform and continuous structure. For this reason it was required to model the capsule as one single object for the CT based reconstruction and to not take into account the individual ligaments that are embedded within this tissue (figure 5.14a).

The difficulty in modelling soft tissues and ligaments in particular lies in the fact that they are easy to deform and therefore tend to change their shape depending on the way they are placed onto the surface. This is the major drawback in using cadaveric joints in CT scanners, where soft ligaments are immediately exposed to external surfaces without the presence of other overlying soft tissues.

As expected and due to all the aforementioned limitations and difficulties of creating three-dimensional models of ligaments based on the above described methods, the outcome from the SurfDriver software for the ligaments (figures 5.14 a and b) was not as satisfactory as it was for the bone elements of the hip joint.

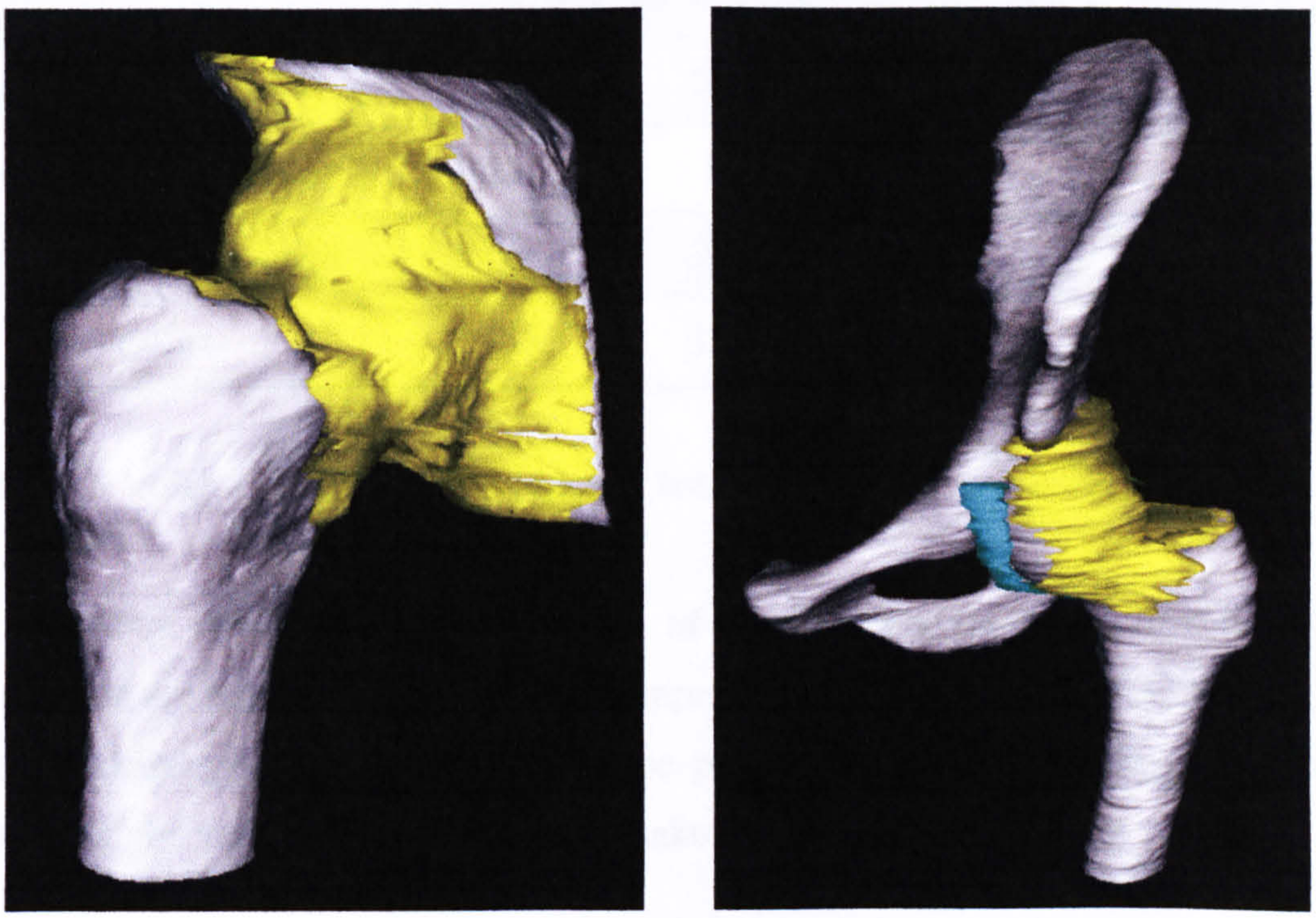

Figures 5.14 a and b CT (left) and cryo-section based (right) models of hip joint.

The following comparative data between the capsular tissues modelled with the CT and cryo-section based images was applied on the smoothed models shown in figures 5.15 a and b and the results are shown in table 5.5. It is noticeable that the volumetric differences of the capsule are large, but this is due to the different ways in which the soft tissues were modelled. In particular, for the case of the cryo-section based reconstruction, it was only the individual ligaments that were traced, whereas for the CT-based reconstruction all soft tissues that form the capsule were included. That means that the complete 'sleeve' that surrounds the joint was modelled as part of the capsule. This was done, because no contrast between actual ligamentous structures with higher collagen density and connecting parts of capsule tissue with lower collagen density is visible in CT scans. However, these differences are visible

in the cryo-section images and the actual ligament strands can be isolated and modelled separately.

	Cryo-section Model		CT Model	
	Volume [mm^3]	Surface [mm^2]	Volume [mm^3]	Surface [mm^2]
Iliofemoral Ligament	17131	10388	-	-
Ischiofemoral Ligament	3433	3265	-	-
Pubofemoral Ligament	1872	1920	-	-
TOTAL	22436	15573	77020	37926

Table 5.5 Volumetric data for the capsular tissues based on the two imaging types.

After applying a certain degree of SurfDriver's smoothing function the quality of the ligament reconstructions improved (figures 5.15 a and b). However, further shaping and adjustment had to be performed in the parametric modelling section of the FEA software, in order to make the model look smoother.

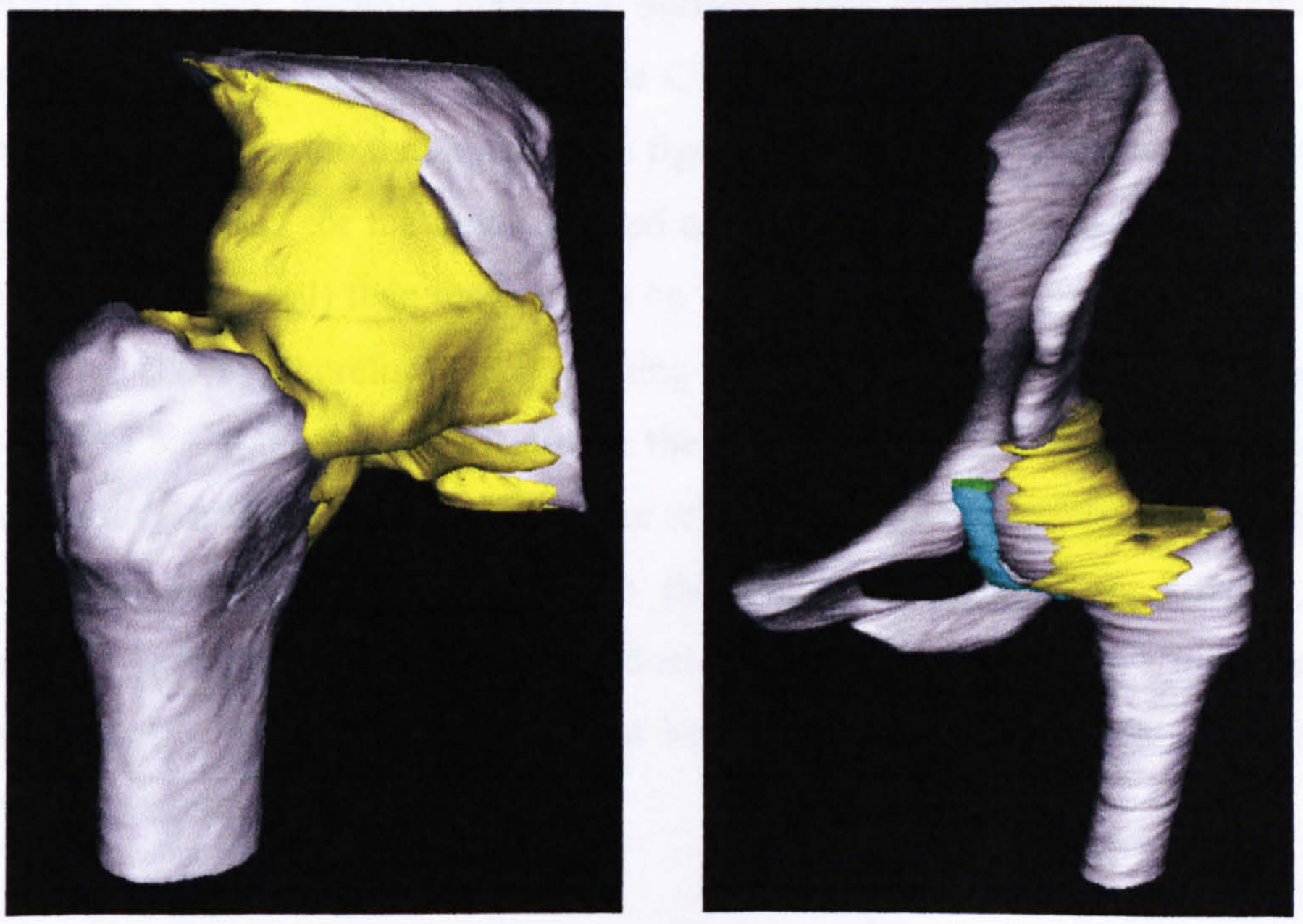

Figures 5.15 a and b Same models as in figures 5.14 a and b after smoothing.

5.5 Discussion

The models that were created based on the CT scan images were shown to be greater in size than those resulting from the cryo-section images due to the fact that the CT scans were taken on a male subject in the contrast to the cryo-based images from the 'Visible Human' female dataset. Therefore, the conclusion is that both imaging modalities are suitable for creating three-dimensional models of bone elements. However, for the purpose of creating reconstructed 3-D models of capsular ligaments, CT-based images have shown to place restrictions due to the absence of sufficient contrast. However, because it is very simple to create CT images of cadavers that only include those anatomical structures that are of interest, it is worthwhile to further investigate the possibility of developing a stain that will highlight the ligament bands within the capsular tissue in a CT scan. Thus it will be a very suitable image base for the 3-D volume segmentation and rendering of joint models. In the meantime it appears that the use of cryo-section based reconstructions is the only alternative for the case of models that include ligaments. For this reason it was decided to employ the cryo-section based models for the present work.

However, those bone models that were created using the CT images resulted generally in a more naturally appearing surface. Thus, the femoral bone shown in figure 5.11b that was created using these CT images has a more bone like surface appearance than does the femur shown in figure 5.11a. This is due to the fact that the slices that were used for the models based on the cryo-section images had a higher density (1 mm interval) than those based on the CT images (2 mm interval between consecutive slices). Therefore the smoothing function showed a smaller effect on the cryo-section based models than it did on the CT based models. In order to improve the appearance of the bone elements of the cryo-section based models, it was decided to also increase the distance between the utilised image slices. Thereby, an appropriate distance between the individual slices was found to be 3 mm for the reconstruction of the bone elements, but keeping the density at 1 mm for all the ligament structures (figure 5.16).

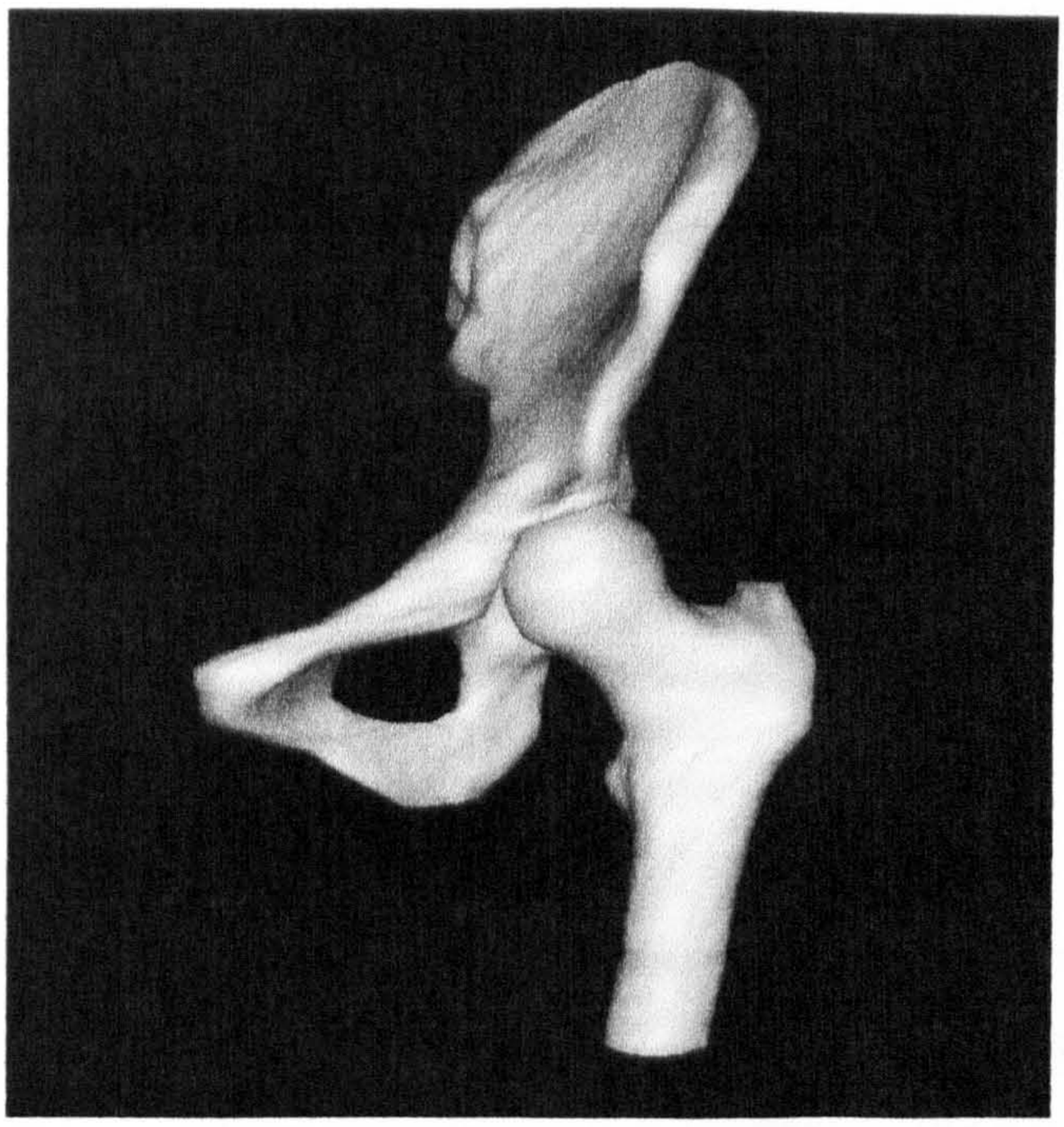

Figure 5.16 Reconstructed anatomy of hip joint at lower slice interval density.

Further shaping and geometrical improvement of the modelled joint ligaments was undertaken in a more suitable environment, like the I-DEAS 8 software that was used for the numerical analysis. That was, because I-DEAS 8 is not only an FE and mechanism analysis software, but also has a very advanced parametric modelling environment, in which three-dimensional parameter alterations can be achieved with much greater ease than could be done in SurfDriver. The following chapter describes these parametric improvements of the three-dimensional joint reconstruction in more detail.

5.6 Summary

The CT based model that has been presented in this work has two disadvantages compared to the cryo-section based model. First, the acetabular element is of too small a dimension and does not assist very well in determining the neutral joint position, because most anatomical landmarks have been previously dissected. Secondly, the contrast between the individual capsular ligaments is very low and distinguishing them is extremely difficult.

Further improvements are necessary to make CT based model reconstruction a good alternative for cryo-section images based models. Complete hemi pelvises should be used for the collection of the CT images and not only acetabuli as in the present case that limit correct joint positioning. For the improvement of distinction of individual ligaments, CT images could be taken after each sequential removal of the various ligaments. All ligaments could then be reproduced, whilst the position of the other joint components (i.e. femur and pelvis) would be kept stable relative to each other and in relation to the scanning area.

In conclusion, CT based images of the hip joint capsule has great potential, but certain further adjustments will have to be made. The cryo-section based images have proven to be a very good base for model reconstruction of both bony and ligamentous anatomical parts; at least for the hip joint area. The more comprehensive appearance of the hip joint qualified this model for further use in the numerical simulation that follows in the next chapter, more than the CT based models.

Chapter 6- Numerical Analysis of Hip Joint Moments

6.1 Introduction

Finite element analysis (FEA) has been proposed for solving engineering problems as early as 1943, when it was attempted to solve the torsion problem in elastic media by using finite elements, but never gained popularity due to the great amount of calculations that needed to be performed by hand. Later, digital computers made it possible in the 1950's to develop FEA into matrix calculations, suggesting the use of a stiffness matrix to describe the examined object's behaviour under certain types of stress. The progress since then has been continuous and the growth of acceptance in new products development immense.

FEA can be described as a process of converting a 2D or 3D model topology into a finite number of structural elements (finite element mesh), applying case loads and boundary conditions, and processing and displaying the results. Initially FEA programs could only be used with powerful high-end workstations, but in recent years economic desktop solutions have made them readily available. An FE model can be compared to a brick wall, where the individual bricks are the equivalent of the elements that form the model's mesh. The individual elements of this mesh are interconnected and it is possible to determine the response at any point on the wall for a load applied at any other point. The larger the number of finite elements, the more accurately the true shape of the block can be usually modelled. However, a convergence test can clarify whether this is the case or not, by running a series of tests with increasing element density. Furthermore, sensitivity tests provide information on how critical various model parameters are on the analysis results.

Whilst in engineering the use of computer models was driven by the need for reduction of time, effort and expenses involved in the development and testing of new products, their use in studies of anatomical parts and structures was the result of the limitations associated with testing actual cadaveric parts. These limitations can be ethical or practical. Cadaveric parts can only be used for a limited time, as

decomposition sets in and the material properties begin to change. Furthermore, any destructive intervention like a dissection is irreversible and requires- for repetitive purposes- the use of another specimen. However, not all specimens of the same anatomical structure have also the same composition and properties, which in certain tests might lead to inconclusive results. The use of a computer model in a constant and controlled environment like a software application is a powerful method that can help to overcome all the above limitations.

6.2 Finite Element Analysis in Biomechanics

One of the most common uses of the FE method in biomechanics has been for the study of implant performance in biological environments. These simulations are of great importance for design development and for pre-clinical analysis of implants (Huiskes and Vroemen, 1986) and other orthopaedic devices. Simulations include studies on the loosening behaviour of prosthetic hip (Weinans et al, 1993) and knee (Cheal et al, 1985) replacements. Further studies involved the determination of stress development for shape optimisation of intramedullary nails (Beaupre et al, 1984), bone plates, pins and screws as well as external fracture fixators (Prendergast et al, 1994).

Another use of the FE method in biomechanics has been in the study of tissue adaptation (Roesler, 1987) where it is employed in predicting how the mechanical environment affects the growth, development and remodelling of tissues that are subjected to certain loading. The FE method has been most commonly utilised to predict the adaptation of bone under loading. Huiskes et al (1987) present an FE analysis for the prediction of bone remodelling under the influence of loads resulting from the presence of an implant. In that application FEA was used to optimise the design of the prosthetic component under the scope of the host environment's reaction.

Finally, another application of the FE method in biomechanics is for the analysis of myoskeletal parts. Examples of such applications include the study of stress distribution in the individual osteons of small bone samples reconstructed

using micro-CT images (Hogan, 1992) and the development of micro cracks as a result of stresses. In soft tissues, FE models have been used for the simulation of force-displacement responses to compressive loading of the human cervical spine facet joint capsule ligaments (Kumaresan et al, 1998). Thereby it was attempted to identify different approaches that best simulate the actual response behaviour of the various tissues. These approximations included hyperelastic definitions for the simulation of the articulating cartilages, whereby the synovial fluid between these cartilages was approximated using incompressible solid elements.

6.3 Stages in Finite Element Analysis

There are a number of steps involved in carrying out an FE analysis. The initial step is solid modelling the correct geometry of the individual structures that are analysed. Solid modelling is carried out in the parametric modelling environment of the analysis software when the geometries of the solids are combinations of basic solid shapes, like spheres, cylinders and blocks. In the present case solid modelling follows another procedure, which involves importing the reconstructed geometry as it was created using the Surf Driver software. Thereby, the main difficulty is to achieve a structurally sound model, which does not alter the relative position of the individual joint components (femur, acetabulum and all the capsular ligaments) to each other.

Pre-processing involves definition of the element mesh, characterisation of material properties, establishing boundary conditions, constraints and loads. Automatic mesh generation is the function where the software creates the entire mesh on each of the structures individually, while the user simply needs to select the element type. The optimal element size is then determined by the software. Even small changes to the ideal element size that the software has determined, results in the software attempting to create a new mesh, but may not lead to a valid mesh in cases of complex model geometry. In these cases a labour-intensive manual mesh repair is necessary. Using automatic mesh generation reduces the effort and improves the quality and refinement of the final mesh compared to a manually created mesh.

Each mesh and load case is associated to the solid for which it is generated. Within minutes it is possible to define an analysis for a particular solid by selecting a mesh and load case, the element type and the sort of analysis. The load case becomes associated to the mesh once the analysis is executed. The loads specified on the solid are applied to the finite element mesh. Pressures on complex surfaces are converted without error to nodal or element forces, using very limited CPU time. Restraints on surfaces are converted to nodal restraints with correct surface orientation. However, applying the various constraints in a joint mechanism like the present one, requires a good understanding of the mechanism's function and a very accurate model geometry, which allows easy identification of the areas in which ligaments insert into the bone, because constraints are applied onto the nodes in these regions.

The next stage in the analysis, is where the software calculates the effects of the loading cases on the model geometry, considering any boundary condition and constraint that has been applied during the pre-processing. If the solver has achieved a solution, then the final stage of the analysis can be carried out, which is the post-processing where the results are presented in either tabular or graphical form. In the first case it is possible to see the results from the analysis for individual elements or particular nodes that connect them. This allows a statistical comparison for different loading situations at certain areas of interest. A graphical representation makes comparison at a single glance possible. The types of results that are displayed can be selected and usually include reaction forces at certain locations on the model and stress distributions within the model. Further, von Mises stress distribution can be shown, which is a good indication of how close the model under investigation is to its yield point under the applied loads. Strains are another commonly selected result for the post-processing.

The analysis software translates the engineering problem into a mathematical model, which contains as much information as possible on the properties as well as on the loading condition that is studied. It is the accuracy of this mathematical model that determines the quality of the solution. However, there are limits to how much information can be included into the mathematical model, without overloading the

calculation resources that are required for producing a solution. Finding the right compromise on the refinement of the model so that viable solutions can be produced without complicating it too much, is the greatest skill in numerical analysis. The individual stages of the numerical analysis are described in the following paragraphs as they were applied to the present problem.

6.4 Solid Modelling

The model data that was created in the Surf Driver software can be exported either as a tiled surfaces geometry that is created by the individual vertices that were placed on the outlined boundaries of the model geometry or as a wire frame geometry that is built by the traced contours. The choice between these two modes depends exclusively on the capabilities of the numerical analysis software. After an extensive review of the available software packages that could have been made available for this project it was found that only I-DEAS Master Series 8 (Electronic Data Systems, Plano, Texas, USA) was capable of reproducing an accurate model geometry, whilst producing solid objects from the imported model data. This capability was the main criterion in choosing a numerical analysis software.

6.4.1 Procedure of Model Import

In this paragraph it is attempted to explain the differences between the two individual methods that exist for importing the model geometry from the contour tracing software Surf Driver into the numerical analysis software I-DEAS 8. The objectives during the import were two-fold. First, it was aimed to achieve an error-free model geometry that would maintain the correct dimensions and analogies of the joint construct as they had been established in the Surf Driver software. The second aim was to turn the models into solid objects from shells within the Surf Driver software. This would allow further shape manipulations, for example the introduction of prosthetic joint components that may alter the geometry of the complete hip joint construct.

Initially it was attempted to import the geometry from the Surf Driver software as a wire frame geometry (figure 6.1), where each of the contours that were

traced in the Surf Driver software are exported separately, using the common IGES (Initial Graphics Exchange Specification) file format. The individual vertices that originally created these wire frames in the Surf Driver software are used in this method for indicating a starting and an ending point on the closed-loop of each wire frame. The starting points on each wire frame are an important navigational landmark for the software in the attempt to 'loft' one wire frame to the other creating in this way a 'virtual skin' that is drawn over all cross-sectional wire frames. If the complete cover of the model geometry with this 'virtual skin' is achieved, then the software creates a solid object of that geometry.

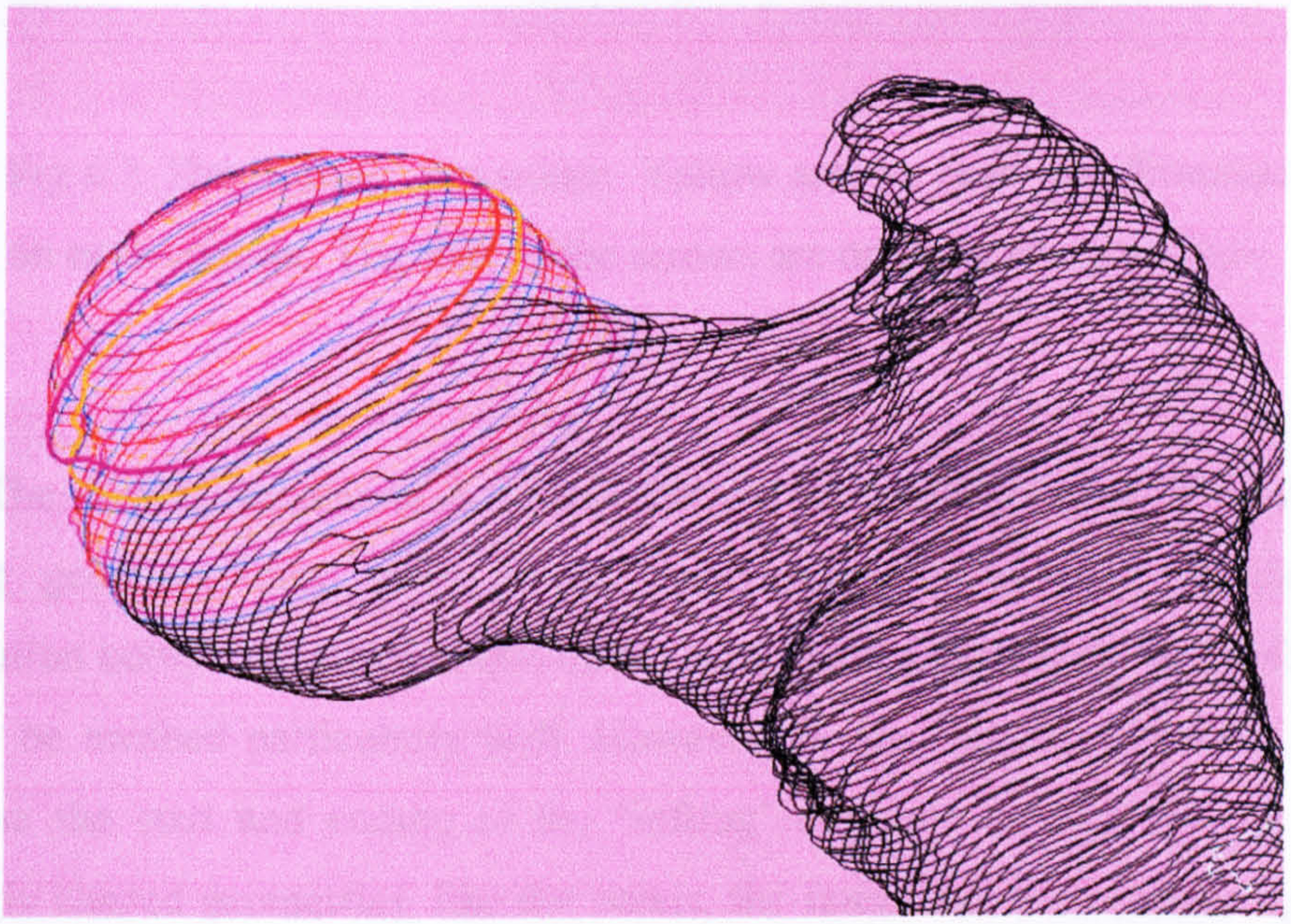

Fig 6.1 Imported wire frame geometry of the femur. Some have been highlighted as to be turned into individual surfaces.

The direction of the lofting has to be determined by the user and care must be taken that the same 'lofting' direction is applied for all wire frames (figure 6.2). In order to achieve the correct lofting direction it is required to have the starting points of each wire frame at adjacent locations, which is not always easy and sometimes even impossible, due to the irregular shape of the anatomy.

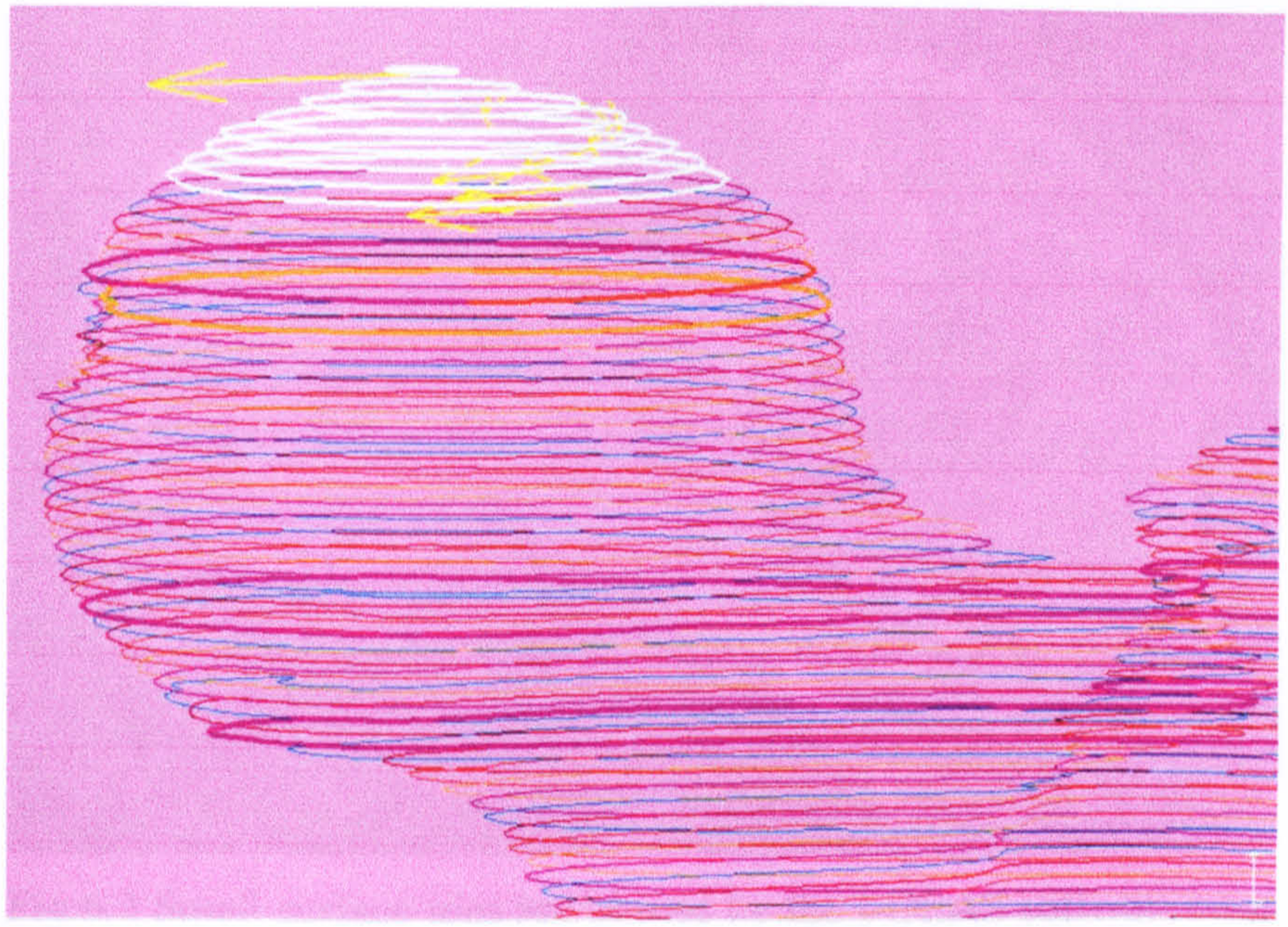

Fig 6.2 The 'lofting' procedure. Yellow arrows show the direction on each contour. The start of the arrows are on the starting vertices.

The 'lofting' technique is a quick method for creating 3-D solid models. The resulting geometry may suffer some inaccuracies as a result of the linear interpolation between any two neighbouring wire frames, but results in a solid object that can be meshed particularly well. However, it does require a certain effort to determine the start and ending of the 'lofting' direction at least for the case of irregularly shaped geometries, like the pelvis, the femur and the capsular ligaments. The generation of a solid based on the 'lofting' procedure becomes demanding in these cases, and, in the presence of an alternative method, is not the approach of choice.

The alternative method in the I-DEAS software is a function that imports the model geometry from the Surf Driver software, again in IGES file format, but as a tiled geometry(figures 6.3 and 6.4). If this tiled geometry was created without any intervals in Surf Driver and was also imported into I-DEAS without any errors, then the software can stitch the individual neighbouring surface tiles into one large solid volume that follows the object's geometry accurately.

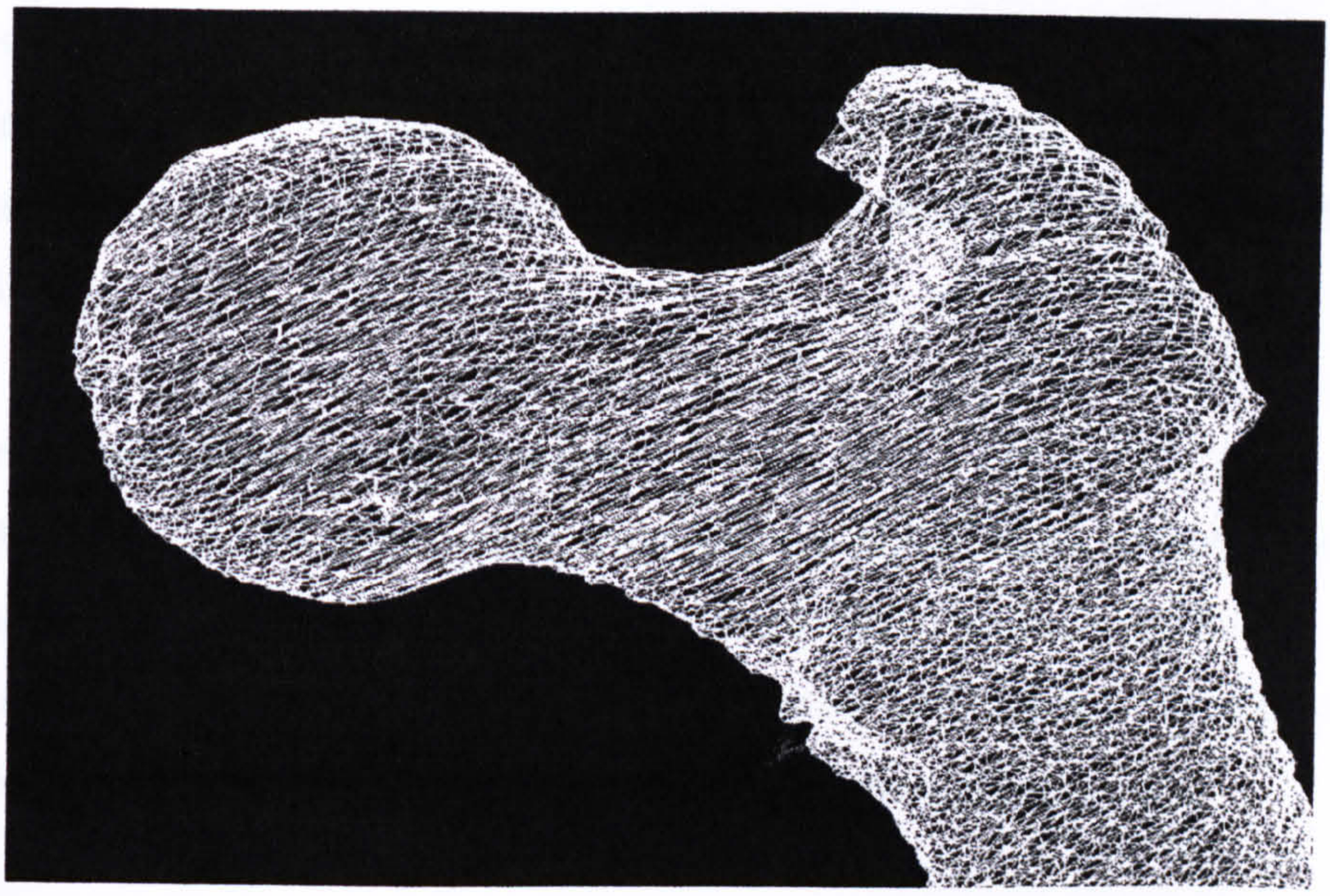

Fig 6.3 Small surface tiles are placed by the I-DEAS software over the contour geometry, created in the Surf Driver software.

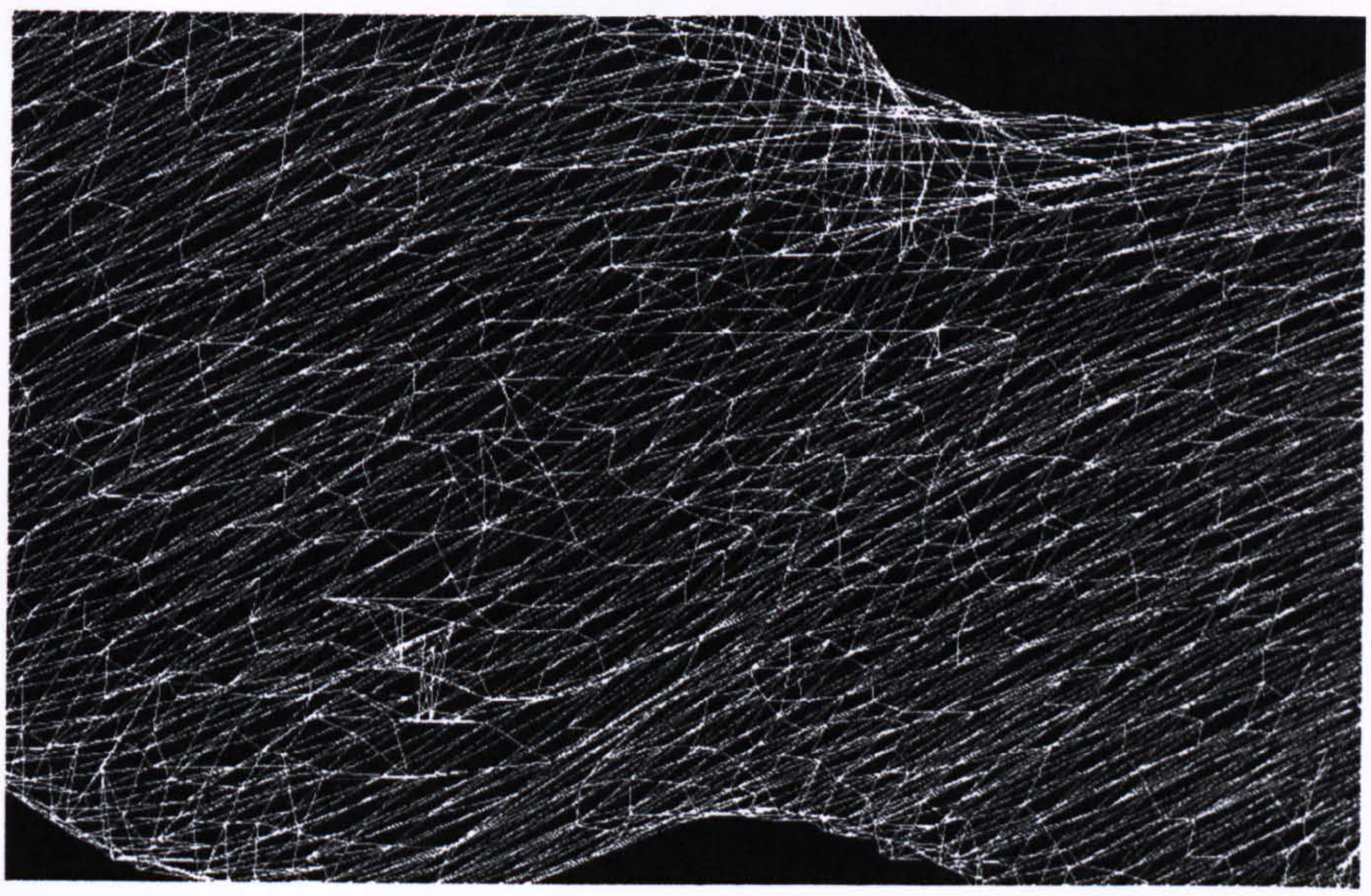

Fig 6.4 Details of surface tiles as they are imported into I-DEAS.

After the objects have been turned into solids, it is possible to perform various operations on them like alterations of the geometry and cutting or cropping functions. This is an operation of great relevance for this study, because of the intention to investigate the effects of changing the anatomy to a post-operative replaced anatomy of the joint surfaces. These anatomy modifications are presented in

greater detail in paragraph 6.4.3. Further, it is possible to establish their material properties and set up various relations that exist between the individual joint components, like the hinge mechanism that exists between the femoral head and the acetabulum.

6.4.2 Creation of Hip Joint Mechanism

An initial coordinate system is created by the I-DEAS software when the individual model components are imported from Surf Driver. Thereby the vertical axis is collinear with that of the complete female body of the 'Visible Human' (figure 6.5), which goes from the head to the toes of the cadaveric body.

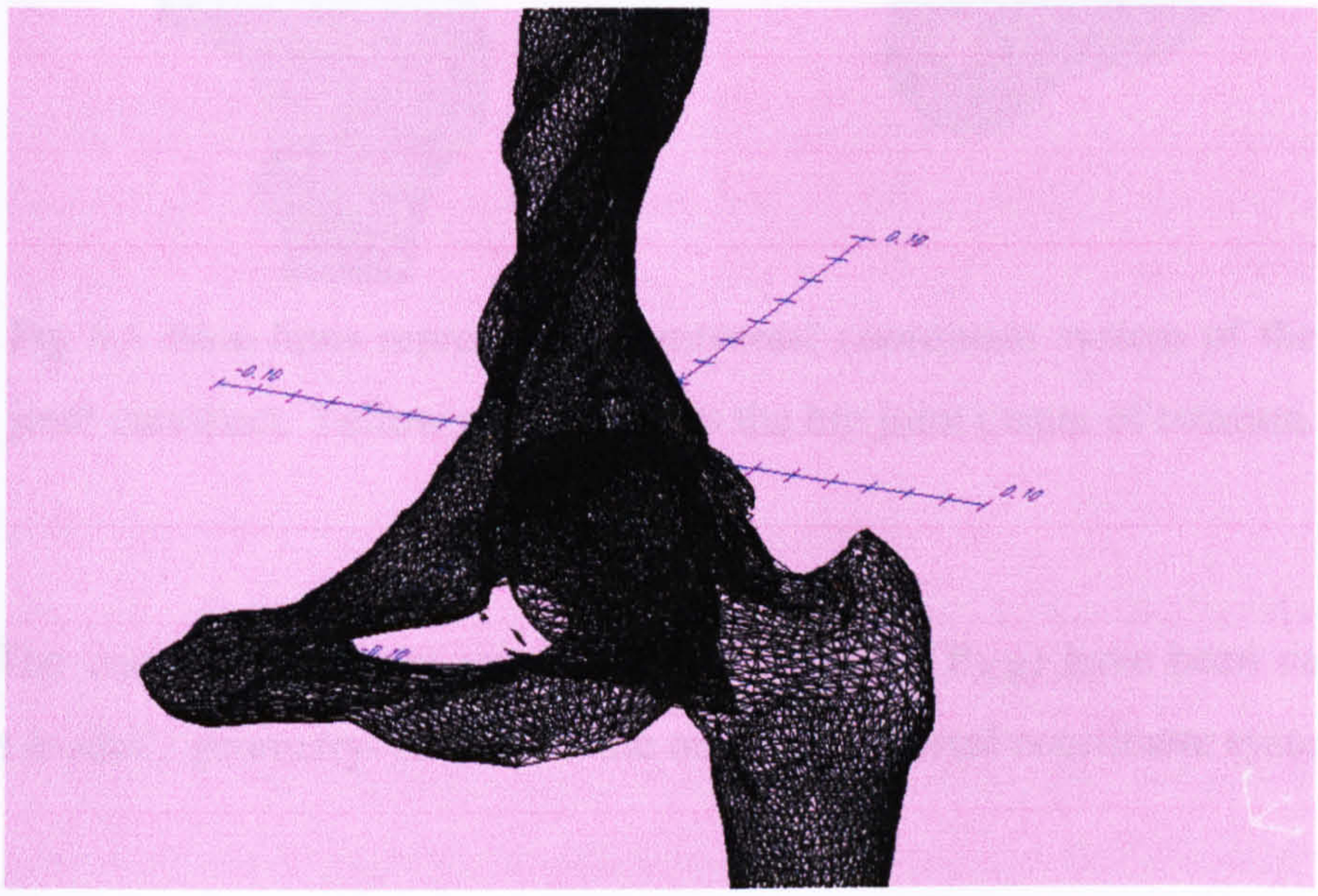

Fig 6.5 Universal coordinate system adopted for the joint in I-DEAS.

However, when looking at the femoral part of the joint (figure 6.6) it is noticeable that the origin of the universal coordinate system does not coincide with the joint centre of rotation, which is highlighted by the yellow marker in the centre of the femoral head. Thereby, any rotational movement that is to be simulated by the femur has to be applied around this hip joint centre of rotation. It has to be mentioned that for reasons of simplicity it is assumed that the hip joint is a symmetric spherical joint and that during limb movement all rotations occur around the joint centre of

rotation, which coincides with the centre of the femoral head. In terms of contact between the acetabulum and the femoral head, it results from the created models, that there is no contact in the initial neutral position. The initial neutral position is the one that was created in the Surf Driver software. The gap that exists between these two surfaces is in reality taken up by the cartilage, which intentionally was left out of the modelling process. This means that, if the assumption of complete sphericity of the hip joint is valid, no contact should occur in any limb position.

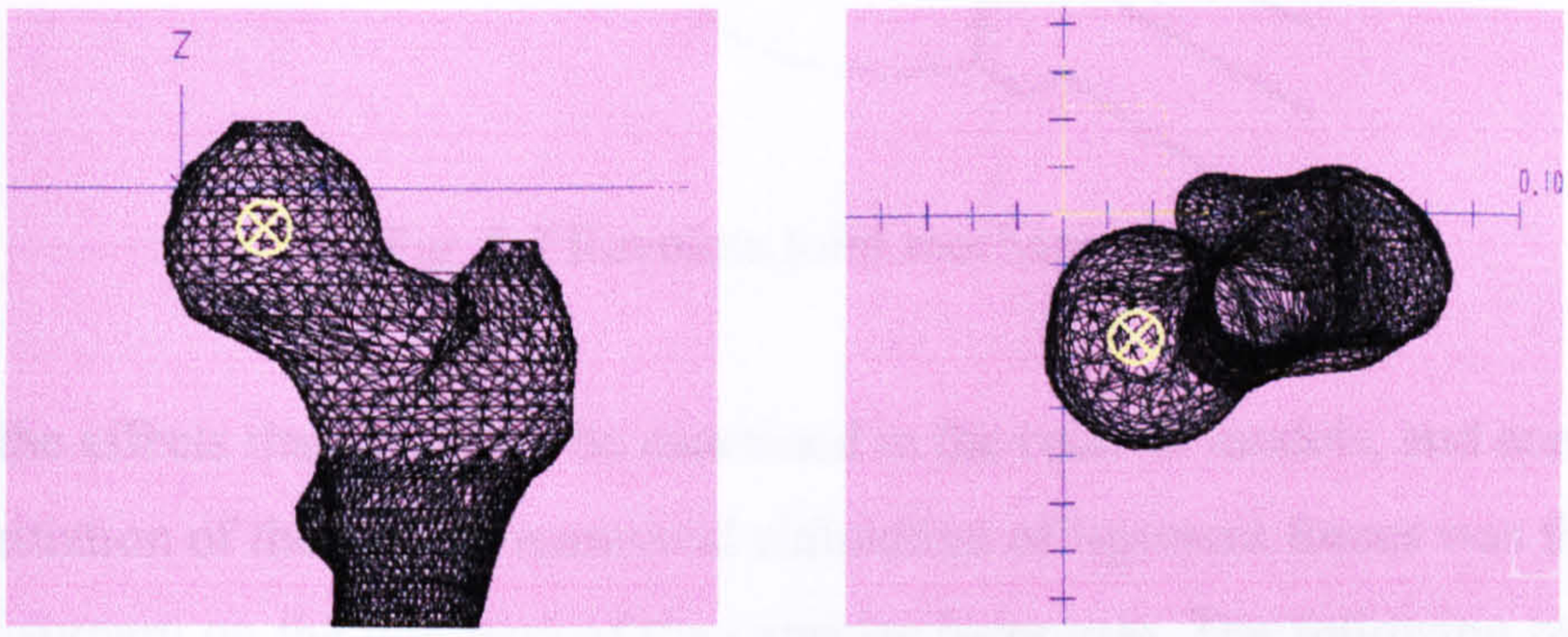

Fig 6.6 Blue lines represent the universal coordinate system of the joint construct. Yellow marker shows the hip joint centre of rotation.

The coordinates of the joint centre of rotation ($\mathbf{P}_{JCR}$) have been calculated from the model's geometry- relative to the original universal coordinate system (6.1).

$$\mathbf{P}_{JCR}(X,Y,Z) = (19.77,-25.41,-9.33)\ [mm] \qquad (6.1)$$

Therefore, any movements of the femur that are executed for the purpose of simulating abduction/adduction, flexion/extension and internal/external rotation have to be around the joint centre of rotation, which is located in the centre of the femoral head. For this purpose a frictionless joint mechanism was selected to be placed at the location of the joint centre. The I-DEAS software includes a great choice of different types of joint mechanisms, including a spherical joint, which can best simulate the actual hip joint. However, one of the aims of the present numerical analysis was to be able to compare the results to those produced with the cadaver specimens. This

meant that the set-up had to be as close as possible to that in the cadaver tests. For this reason the joint mechanism of choice would only allow rotation in around one axis. For this reason a revolute joint was selected that allows rotation only in abduction/adduction (figure 6.7).

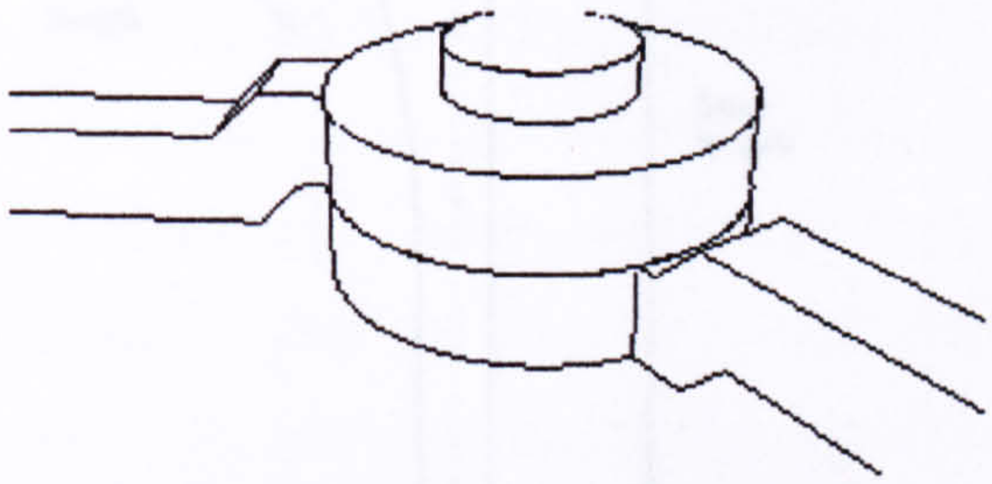

Fig. 6.7 Revolute joint mechanism for hip.

One of the effects that could not be examined in the cadaver models, and contributed to the initiation of the present numerical simulation of ligament forces was the effect of THR surgery on the tightness of the capsular ligaments. The following paragraph explains the approach that was taken to simulate and analyse these effects.

6.4.3 Model Geometries of Post-Operative Hip Joints

For the purpose of creating models of post-operative hip joints it was assumed that the joint centre of rotation remains at the same location, coinciding with the prosthetic femoral head centre. For a small femoral head component size of 22.225 mm this means, that the distance to the long axis of the prosthesis- called medial offset (figure 6.8)- is compensated by the femoral neck length. Two scenarios that could take place in THR surgery were considered, a shortening (figure 6.9b) and a lengthening (figure 6.9c) of the femoral neck in relation to the anatomical hip joint (figure 6.9a) after the insertion of a prosthesis. In the first scenario the effect is that the capsular ligaments are in a more relaxed state compared to the original anatomy and whilst the limb is in the neutral position (figure 6.10). In the second scenario the capsular ligaments are pre-tensioned again compared to the original anatomy and whilst the limb is kept in neutral position. The neck lengths in the models were altered by ±4 mm, meaning a shortening and lengthening by 4 mm respectively.

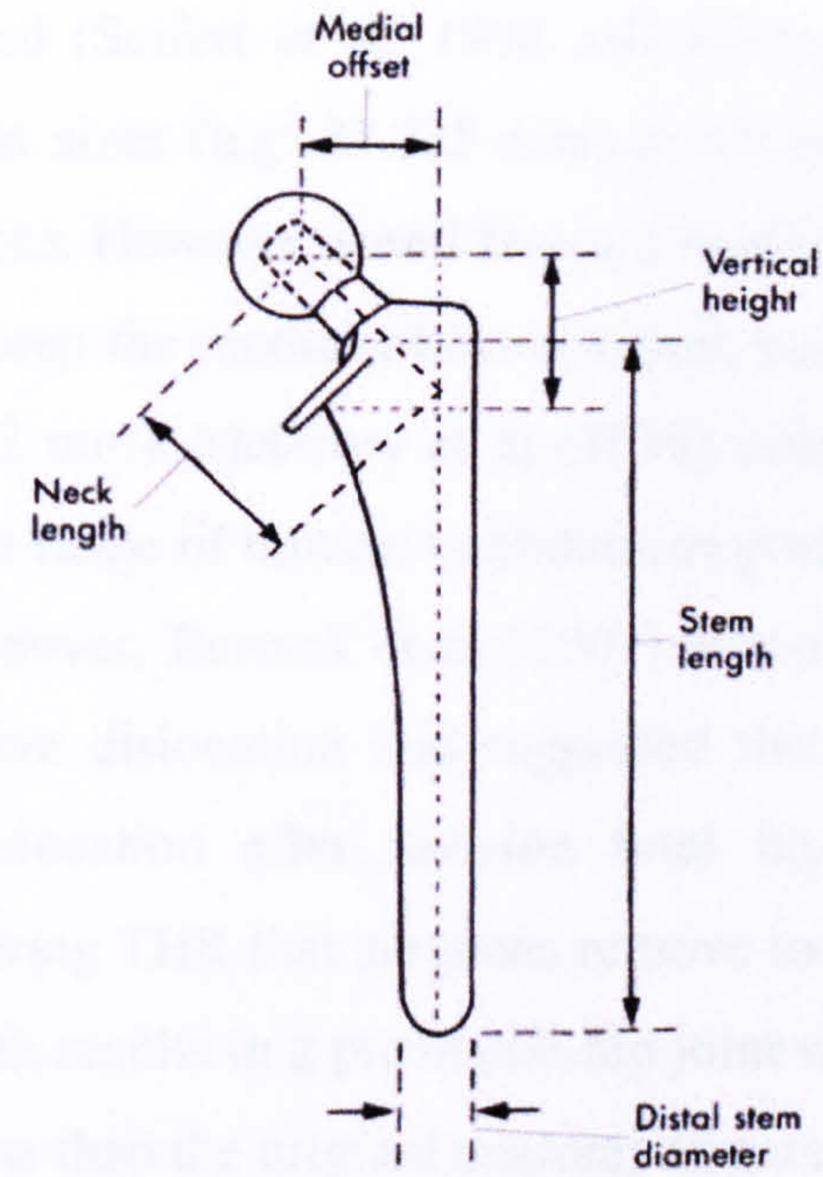

Fig 6.8 Medial offset and neck length in a hip stem (ISO7206/1).

In the post-operative models it was assumed that the insertion locations of the ligaments into the femoral and pelvic bones did not change and that, further, no changes to the original length of the individual ligaments occurred, despite the incision through the capsular structures.

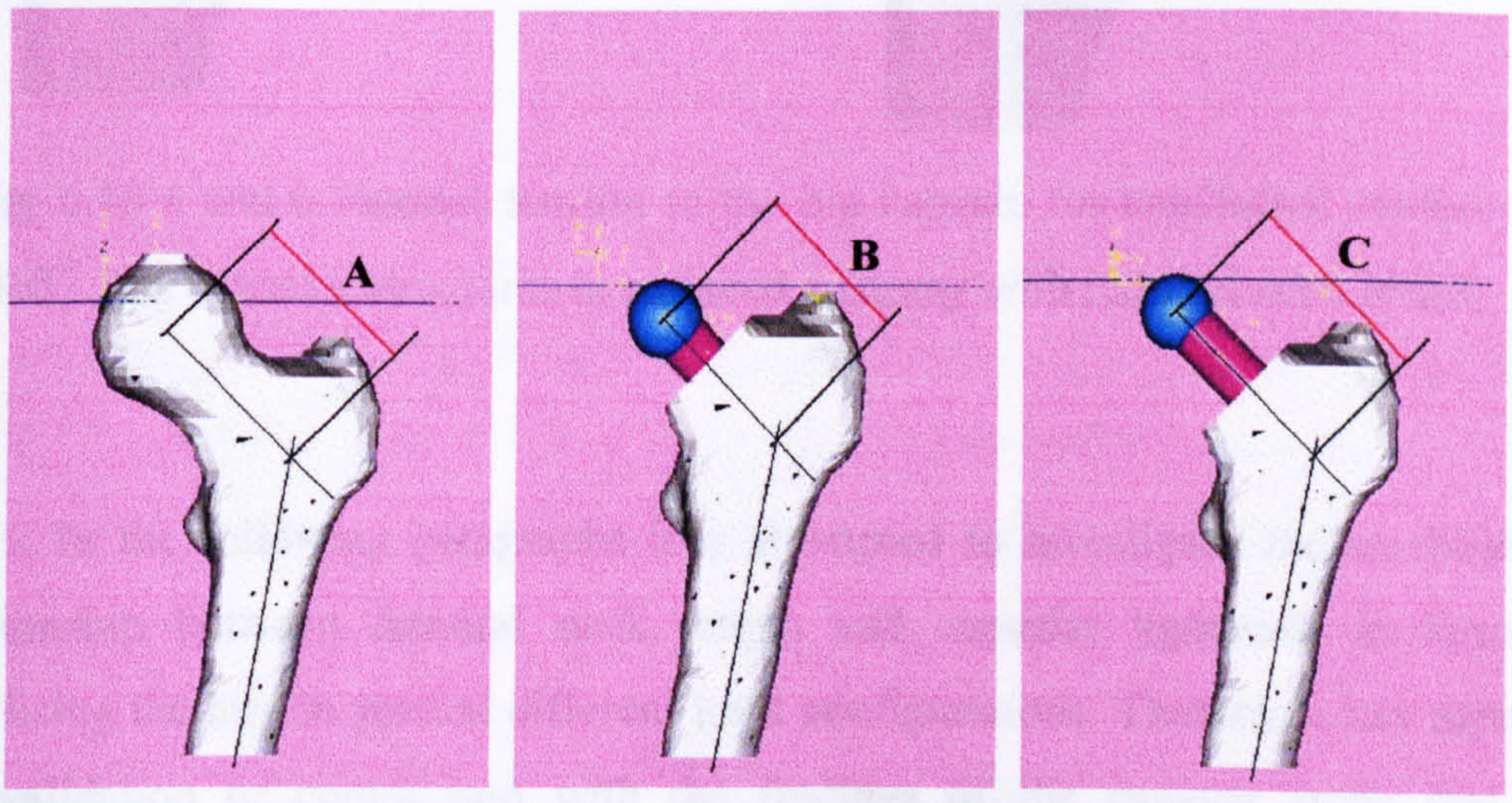

Fig 6.9 a, b and c Femoral neck lengths of normal hip anatomy (left) and of replaced anatomy (centre and right). Neck length dimensions C>A>B.

It has been stated (Scifert et al, 1998 and Kelley et al, 1998) that small femoral head component sizes (e.g. 22.225 mm) result in increased rates of post-operative joint dislocations. However, small femoral head components require longer neck sizes, in order to keep the medial offset constant, compared to bigger femoral head sizes (e.g. 28 or 32 mm). McGrory et al (1995) concluded in their study that large offsets improve the range of motion in abduction post-operatively and increase abduction strength. Moreover, Barrack et al (2001) found that large offsets reduce the risk for post-operative dislocation and suggested that neck design may be an important factor in dislocation after revision total hip arthroplasty. However, sometimes it happens during THR that surgeons remove too much or too little of the femoral neck bone, which results in a prosthetic hip joint with shorter (figure 6.10b) or longer neck dimensions than the original anatomy (figure 6.10a), respectively.

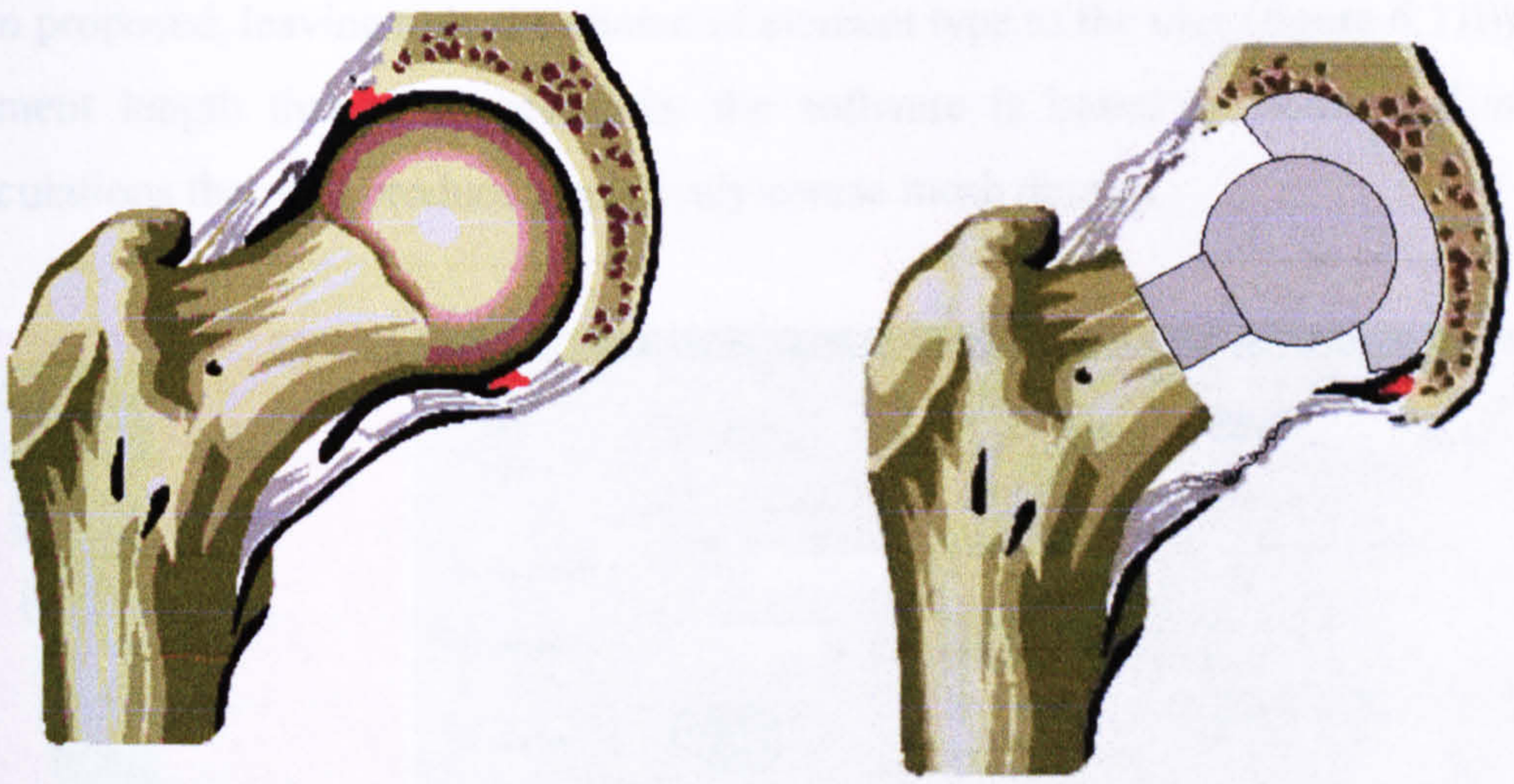

Fig 6.10 a and b Normal tension in the hip capsule for unaffected anatomy (left). Lax capsular structures in replaced anatomy with reduced neck length.

In the following paragraphs it is attempted to investigate and establish the relationship between femoral neck length and capsular ligaments in terms of stabilising the hip, in several different joint configurations. Thereby, a key aspect is the validation or comparison with the findings of the cadaver study that was performed on anatomical hip joints with intact and impaired capsular structures.

6.5 Pre-Processing

The pre-processing task in an FEA software involves all functions that will determine a load system for the models that were created or imported into the software. These functions cover the range from creating a mesh for each of the model parts, selecting and defining materials and their behaviour for all parts and also placement of constraints on certain areas of the model where this is relevant. The pre-processing procedure that was followed in the present case is presented in this paragraph.

6.5.1 Mesh Generation

During this process the individual model geometries are divided into finite elements and nodes that connect these elements (figure 6.11a). Automatic mesh generation of the I-DEAS software is able to calculate an ideal element length that is then proposed, leaving only the choice of element type to the user (figure 6.11b). The element length that is suggested by the software is based on some preliminary calculations that will produce a relatively coarse mesh density.

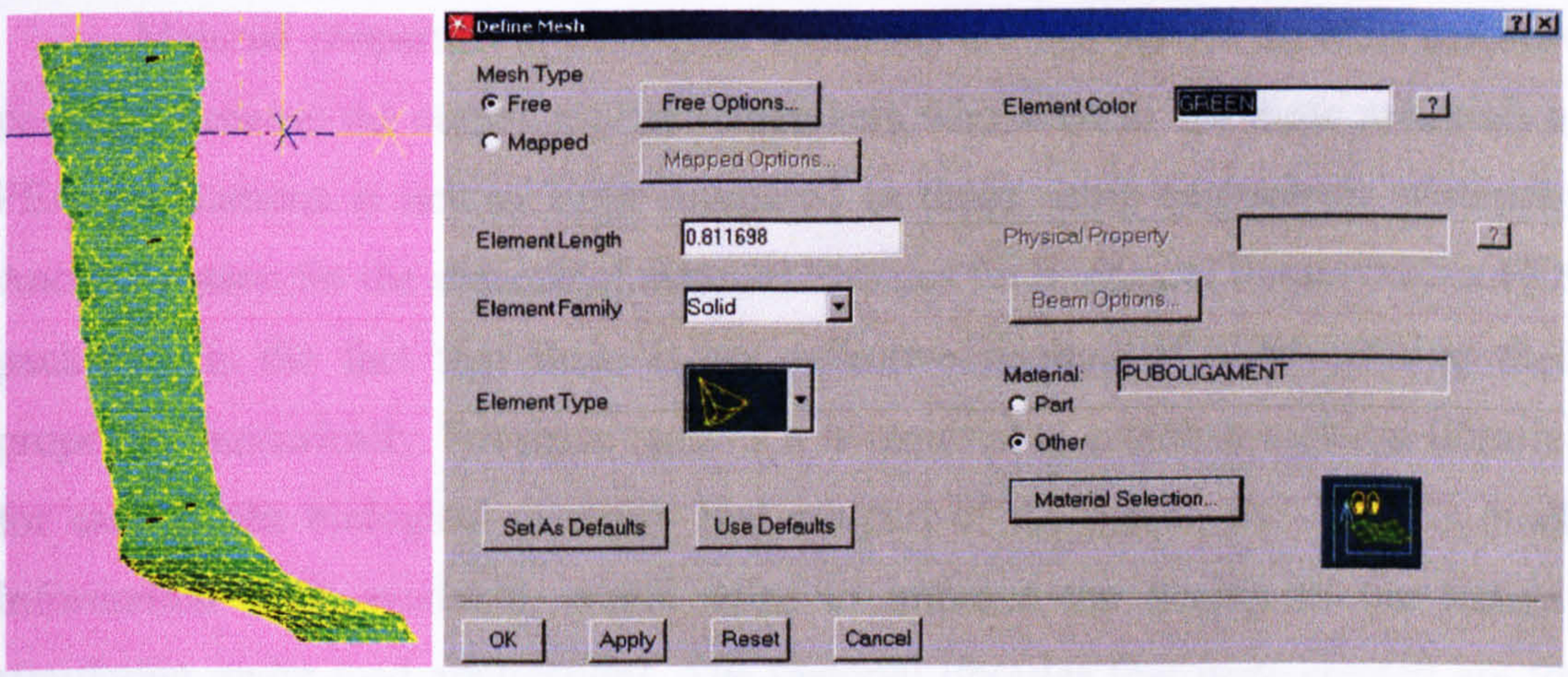

Fig 6.11 a and b On the left is a mesh for the pubofemoral ligament as it was suggested by I-DEAS. The mesh definition frame is shown on the right.

The usual procedure that is followed in mesh generation is that a low density mesh is produced initially and a second or even third round of mesh refinement follows, until no large differences in the resulting model solution occur between two

sequential iterations. A good mesh density for a model of volume equal to that of a ligament, would include about 8000 to 10000 elements. In total this results in about 50000 elements among all the ligaments that are considered in this study. Given the complicated nature of the material properties the mesh size has to be kept within reasonable limits. However, these estimations can only be based on the individual's experience and can only be based on other FEA studies performed on similar tissues under consideration of the total volume of the models studied in those cases.

It should be mentioned at this point, that no mesh was attempted for the bone elements of the hip joint construct. This was due to the fact that it was not the intention to produce data on the response of the femur or pelvis under load application. For this reason the bones were simply considered as beam elements that form part of a mechanism that produces loads on the ligaments as a result of their rotational movement. The ligaments are constrained to the bone parts at their insertion areas.

6.5.2 Material Properties

Material properties of biological materials are not part of an FEA software package, because the community of researchers who need to use these materials in FEA applications is not so large compared to those using engineering materials. Another reason for the absence of material libraries for biological tissues within FEA packages, is the fact that there is no definitive method of characterising their properties numerically. For these reasons it is required to establish material libraries for each of the biological materials that are part of the model, including as much information as is available, which helps to improve the quality of the tissues' simulation under load applications. The material libraries that were created are for three types of ligaments, namely the lateral and medial iliofemoral ligaments and the ischiofemoral ligament. There are no data available for the pubofemoral ligament and therefore the same properties as those defined for the ischiofemoral ligament were accepted. The properties of bone are relatively well established- at least for the purpose of the present work. The properties that were defined for the individual materials are:

Bone (Nigg and Herzog, 1999)

It was already mentioned in paragraph 3.2 that the accuracy of material properties for the bone tissues is not of great importance, because bone could be considered a rigid body compared to the ligaments. However, it was decided to make use of the great amount of data that is available on the material properties of bone and to set up a bone material library. The main data that was included were based on cortical bone:

Elastic modulus	20 GPa
Mass density	1850 kg/m^3
Tensile strength	120 MPa
Poisson's ratio	0.29

Ligaments (Hewitt et al, 2001)

The published data of Hewitt et al (2001) was the basis for the creation of the material library for the ligaments:

	Medial Ilio	Lateral Ilio	Ischiofem
Elastic modulus	242.2 MPa	113.3 MPa	99.5 MPa
Mass density	850 kg/m^3	850 kg/m^3	850 kg/m^3
Tensile strength	6.2 MPa	2.7 MPa	2.0 MPa
Poisson's ratio	1.4	1.3	1.4

The above data are recordings at 80% of the failure strain. No data was published for the material properties of the pubofemoral ligament, thus, they were assumed to be similar to those for the ischiofemoral ligament.

6.5.3 Model Constraints

For the model simulation in a numerical analysis environment it is necessary to provide some information on the constraints that apply to the model. Applying constraints means that definitions need to be applied as to the way the model is able to move and deform. The constraints for the present model were that at their insertion points into the pelvic bone, all ligaments must remain stationary in all six degrees of freedom (three translations along XYZ axes and three rotations around them). Further they were required to be constrained to the femoral bone and therefore no rotation or translation was permitted relative to the femoral rigid body.

6.6 Model Solution Failure

After setting all the parameters and trying to run the simulation of the above described model, it was found impossible to solve the problem. There are two reasons for this, namely the fact that in the FE model solution of the I-DEAS software there is no possibility to use the joint mechanism that was outlined in paragraph 6.4.2 and also the fact that the complex material behaviour of the soft tissue models made the model solution difficult.

Modelling the hip joint as a mechanism in I-DEAS does not allow the creation of FE models on the individual components, which are the bones and ligaments. Therefore, it is necessary to substitute the kinematic simulation with forces applied at the correct ligament locations in a similar way to those that would result from the limb movement. Incorporating these forces into the model is a difficult undertaking that is probably not justified in view of what it aims to achieve.

The FE package of I-DEAS does not include a facility for defining biphasic material properties like those of soft tissues. An additional plug-in software called FEMAP, which was not available for the present project, has this function and enables the user to employ biphasic theories, as they were already described in paragraph 3.3.3. The only possibility to include time dependency to the material behaviour within the I-DEAS environment is to use a standard creep function, but that never produced a solution when tried to be applied to a single ligament model.

6.7 Alternative Solution Methods

I-DEAS was found to be a very good and robust application for creating solid model geometries, especially when it was attempted to import models that were created in other modelling environments, which is often necessary for the creation of biomechanics models. However, generating an FE model is not the most direct approach, when trying to calculate moments around the joint centre of rotation under kinematic simulation of limb movement where large displacements are present. These models can be attempted for the purpose of calculating internal loads and their effects on the soft tissues, to which the stress is applied. Efforts towards such models are still made at present by many centres around the world, and many problems still exist, mainly due to the large amount of information that needs to be processed by the software due to the complex response of soft tissues. Trying to develop such a method, in order to provide solutions to the questions raised by the present work, would be too ambitious and possibly even unjustified.

The next step in the process of finding an appropriate method for calculating the hip joint moments, was to identify alternative ways of applying resistance forces to the moving part of the hip joint mechanism, namely the femoral bone. The main intention in this part of the work was to compare the moments at the hip joint centre when all ligaments were present to a case where some of them had been removed, considering also femoral neck length changes after THR. For this reason it was chosen to replace the ligaments as main resistance providers to hip movement, with linear spring elements. Using linear elements, which do not include any time dependency might be a great simplification, although it seems a valid tool for comparisons of situations of different femoral neck length, as long as the test parameters are kept the same for all test cycles.

6.7.1 Use of Linear Spring Element Models

Using an FE model of the hip joint mechanism is a difficult undertaking at the present stage, because of too many parameters. Before being able to use such a model for calculating moments around the hip joint centre of rotation it is necessary to understand how loads develop within the ligaments as a result of limb movement.

As the limb moves into different positions, the total lengths of various ligaments change. These length changes in turn determine whether or not the individual ligaments generate a resistance force, which in turn contributes to hip joint moments around the hip joint centre. The most simple elements that are capable of producing such resistance forces replacing the non-linear ligaments, are linear spring elements (figure 6.12) that are acting along the line that connects their insertion points on the pelvic and femoral bones.

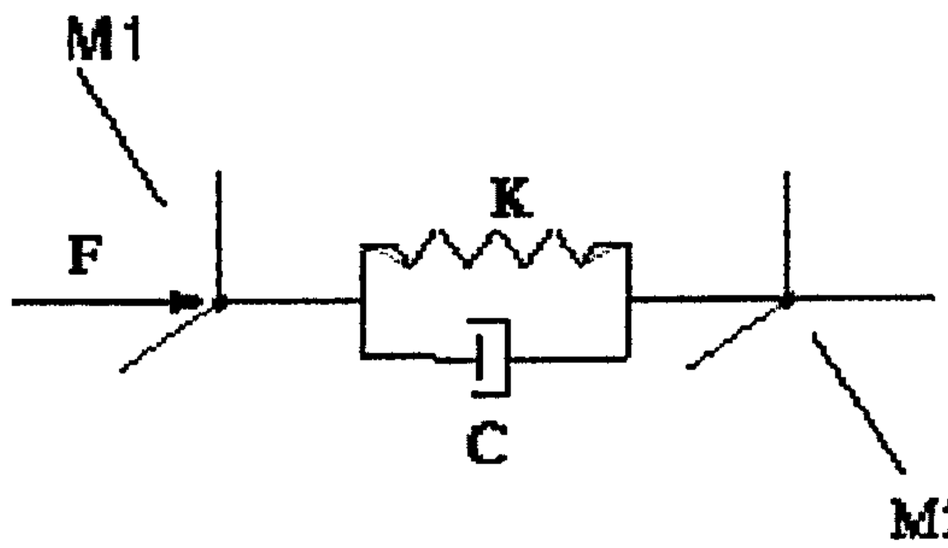

Fig 6.12 Spring and dashpot model as they can be set up with an I-DEAS mechanism.

The type of spring elements that are available in I-DEAS is based on the Voigt model, which means that there is no delay in responding to a load application. However, it is possible to characterise the spring elements that play the role of the ligament resistance, as extension springs only. This means that whenever the initial distance between the two insertion points of a spring element reduces during a limb movement, the spring does not generate a resistance force, which is the same effect that a similar shortening would have on a ligament as it would become more lax. However, the spring elements in the model could not simulate the behaviour of the real ligaments at the early part of the limb rotation where they are not yet pre-tensed. This meant that a response to limb rotation from the springs would be produced immediately, which is not what happens with the actual ligaments that do not tighten up right away. This could be done by requesting from the software not to consider any negative forces i.e. compressive forces generated by compressing the spring. The use of a dashpot was omitted completely, after trying a few different values for it on the present hip joint model, without any noticeable effects on the resulting moments.

6.7.2 Bone Insertion Locations

The insertion points of the linear spring elements were identified, based on the 3-D models of the femoral and pelvic bones, together with the models of the ligaments. Thereby, it was accepted that the point located at the centre of the common contact line between the bone and any ligament, would be considered the insertion point for the individual spring elements (figure 6.13).

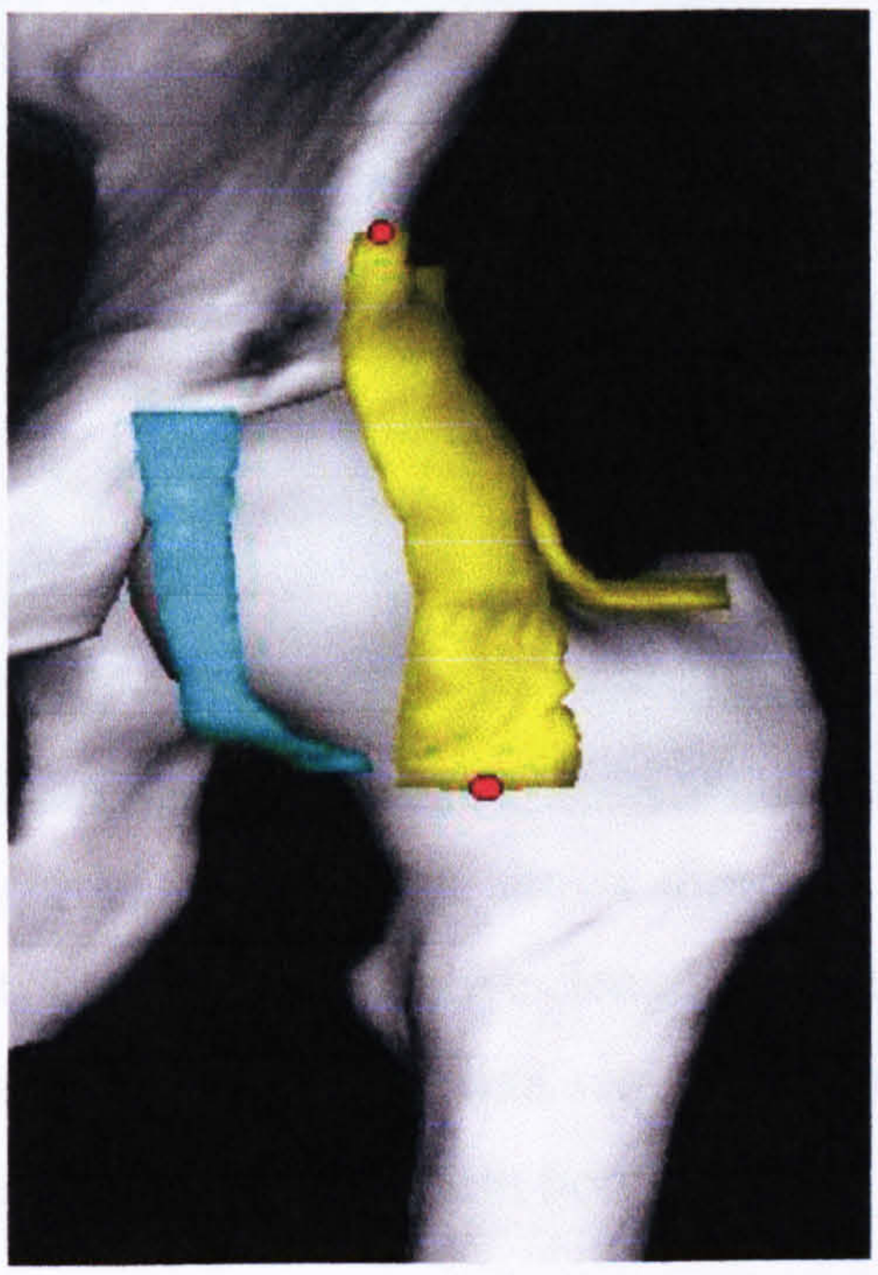

Fig 6.13 Red markers show insertion point locations for spring element.

The direct line that connects the insertion points of the spring element that plays the role of the pubofemoral ligament, passes through the actual body of the femoral bone. However, this has no consequences for the behaviour of the spring elements, as the software only takes into account that the springs are mounted rigidly at their insertion points and that the movement is taking place around the known centre of rotation. The actual body mass of the two rigid bodies- femur and pelvis- is left without any effects on the total moments that are generated.

6.7.3 Calculation of Effective Length Changes

As the limb is moved into various positions, the linear or effective distance between the pelvic and femoral insertion locations of the different ligament bands either reduces or increases.

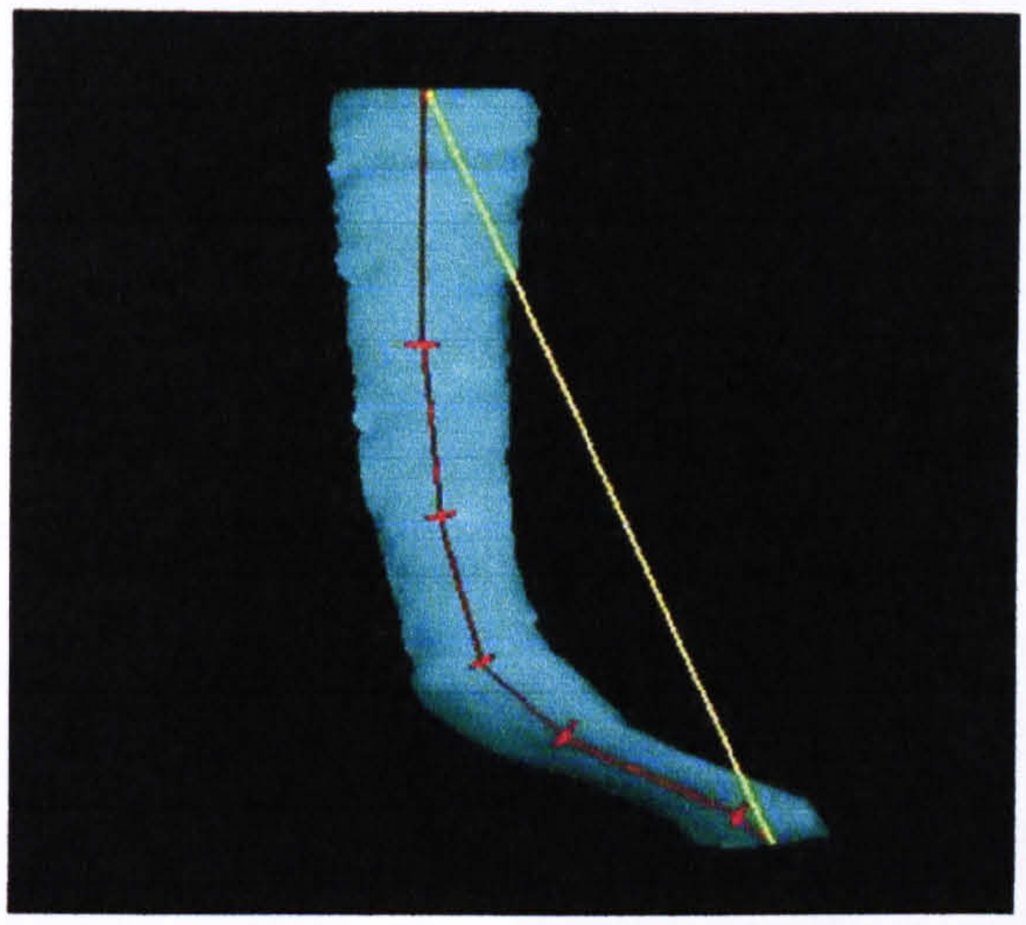

Fig 6.14 Yellow line shows direction of the calculated effective length between insertion points. Red line sequence shows actual length of ligament body.

Even though this particular distance does not follow a straight line in the case of ligaments, it is argued here that, if the linear or effective distance between its insertion points increases, also the distance along the ligament body will be increasing (figure 6.14). In the opposite case, a drop in effective distance means that the ligament is basically not stretched and does therefore not generate any resistance force. Occasionally, no change of effective distance occurs, in which case the ligaments maintain their initial shape and dimension. It is understood that the total extension that the various ligaments experience is greater than that calculated by the straight line stretch, because of the ligaments' wrapping around the femoral bone. Nevertheless, for the purpose of the present analysis this has no big effect. The following table shows the effective distances (in millimetres) for various limb positions.

	Zero			45° Abduction			35° Adduction		
Neutral									
Medial Iliofemoral	73.30	69.93	76.75	57.16	54.95	59.59	79.53	75.66	83.45
Lateral Iliofemoral	57.78	53.74	61.86	33.22	29.65	36.93	73.57	69.51	77.67
Ischiofemoral	41.91	38.68	45.30	41.34	38.05	44.80	41.03	37.94	44.33
Pubofemoral	56.30	52.66	60.01	57.76	54.82	60.87	50.81	46.44	54.06
90° Flexion									
Medial Iliofemoral	35.17	34.09	36.71	52.06	49.62	54.72	31.60	31.07	32.66
Lateral Iliofemoral	56.84	54.92	59.00	62.61	60.79	64.66	56.55	54.27	58.94
Ischiofemoral	61.30	57.31	65.31	45.74	42.79	48.89	67.64	63.52	71.77
Pubofemoral	27.73	24.78	30.98	44.56	40.66	48.51	16.81	15.93	18.64
90° Flexion and 20° Internal Rotation									
Medial Iliofemoral	26.46	26.40	27.19	44.78	42.87	47.00	24.03	24.69	24.10
Lateral Iliofemoral	45.56	43.87	47.57	52.65	51.12	54.46	45.18	43.03	47.51
Ischiofemoral	61.25	57.31	65.24	43.97	40.82	47.29	68.45	64.47	72.45
Pubofemoral	25.96	23.67	28.69	43.24	39.78	46.83	14.69	14.91	15.67
25° Internal Rotation									
Medial Iliofemoral	69.33	66.34	72.45	54.04	52.30	56.04	74.53	71.01	78.12
Lateral Iliofemoral	55.36	51.22	59.52	29.08	24.90	33.28	71.57	67.54	75.63
Ischiofemoral	51.89	48.39	55.50	51.31	47.73	54.98	51.2	47.81	54.71
Pubofemoral	54.97	51.89	58.19	56.83	54.37	59.50	48.55	45.42	51.83
	Zero			**25° Abduction**			**20° Adduction**		
12° Extension									
Medial Iliofemoral	76.26	72.79	79.81	68.54	65.62	71.60	80.44	76.64	84.28
Lateral Iliofemoral	56.66	52.49	60.84	43.12	39.10	47.19	66.40	62.21	70.60
Ischiofemoral	39.36	36.54	42.42	39.15	36.27	42.27	39.09	36.35	42.07
Pubofemoral	58.72	55.00	62.50	60.36	56.95	63.87	55.88	52.05	59.78
12° Extension and 25° External Rotation									
Medial Iliofemoral	80.74	76.91	84.61	74.01	70.60	77.51	84.29	80.23	88.37
Lateral Iliofemoral	60.73	56.61	64.87	50.78	46.96	54.67	68.28	64.08	72.48
Ischiofemoral	27.54	25.26	30.25	27.50	25.21	30.06	27.07	24.90	29.69
Pubofemoral	58.84	54.78	62.92	60.86	57.06	64.71	55.79	51.63	59.97
35° External Rotation									
Medial Iliofemoral	79.77	75.91	83.67	72.72	69.27	76.26	83.57	79.49	87.67
Lateral Iliofemoral	63.45	59.49	67.44	54.88	51.35	58.51	69.89	65.78	74.01
Ischiofemoral	26.65	24.11	29.58	26.98	24.38	29.96	25.95	23.51	28.82
Pubofemoral	57.75	53.62	61.87	59.47	55.60	63.40	54.81	50.60	59.02

Table 6.1 Effective ligament lengths in millimetres for anatomical (columns 1, 4 and 7), short (columns 2, 5 and 8) and long neck lengths (columns 3, 6 and 9).

Based on the data shown in table 6.1 it is possible to calculate the overall elongation and thus the total strain that the individual ligaments experience when the limb is moved into the various positions. The majority of those strains are in the range of 8% to 12%. However, in certain limb positions there are strains of up to 68% (pubofemoral ligament at 90° flexion with 20° internal rotation and in 45° abduction for the case of a shortened neck length). The occurrence of such exceptional strains means, that by moving the limb into those positions, the ligaments would be stretched far beyond its failure strain, which is at 10% to 15% (Fung, 1993). The conclusion from this has to be that those joint configurations, where strains greater than 15% result, are only possible in theory and could not be achieved in reality, without permanently damaging the ligaments. This is in agreement with the findings of the cadaver study that have been presented in chapter 4, where the moment recordings were also noticed to rapidly increase once the joint was driven to a 35° abduction (figures 4.25a and b), which could only mean that the pubofemoral ligament's elongation reaches the upper limit at 35° of abduction. Therefore, it needs to be stated that calculating hip joint moments beyond this particular limb position is unrealistic and only produces useful information for use in the comparison of the effect of different neck lengths on total hip joint moments. Reducing the angles of abduction and adduction at which hip joint moments are calculated, will ensure that no strain exceeds 15%. Nevertheless, the comparative study on the effect of different neck lengths remains unaffected by the total elongation of the individual spring elements. The total resulting strain rate also affects the final joint moments that are calculated (figures 6.9 to 6.15), in addition to the effects that the springs' stiffness has.

Table 6.2 shows whether or not a certain ligament has any action when the limb is moved into different locations. These conclusions are based on the measurements of the effective distances between ligament insertion points given in the previous tables. Thereby a drop in effective distance means that the ligament becomes more lax and has no active role in the joint resistance. In contrast, an increase indicates that the ligament is stretched and therefore provides resistance to that limb movement.

6.7.4 Effect of Limb Position on Ligament Actions

As was briefly mentioned earlier, the spring elements only contribute to the total moments around the joint centre of rotation when they are forced into extension, which is whenever the effective distance between their insertion points increases. In the case of their compression or when their total length remains the same as their initial length, they do not contribute towards the total hip joint moment. This paragraph identifies which spring has an active role in the different simulated limb positions. In particular, tables 6.2 through to 6.8 show which ligaments were found to be playing a role in the various joint configurations. Thereby, it has to be mentioned that each joint position was treated individually and used only for moment comparisons between the cases of normal, long and short neck length sizes. The same comparison was repeated for all seven joint positions that were used in the model. The following sign convention is used: "⊕" for any spring that experiences an increase to its total length and "⊖" for any spring element that remains the same length or undergoes compression, in which case it does not produce a force.

NEUTRAL	45° Abduction			35° Adduction		
	Normal Neck	Short Neck	Long Neck	Normal Neck	Short Neck	Long Neck
Medial Iliofemoral	⊖	⊖	⊖	⊕	⊕	⊕
Lateral Iliofemoral	⊖	⊖	⊖	⊕	⊕	⊕
Ischiofemoral	⊖	⊖	⊖	⊖	⊖	⊖
Pubofemoral	⊕	⊕	⊕	⊖	⊖	⊖

Table 6.2 Action of spring elements for initial neutral hip joint position.

90° FLEXION	45° Abduction			35° Adduction		
	Normal Neck	Short Neck	Long Neck	Normal Neck	Short Neck	Long Neck
Medial Iliofemoral	⊕	⊕	⊕	⊖	⊖	⊖
Lateral Iliofemoral	⊕	⊕	⊕	⊖	⊖	⊖
Ischiofemoral	⊖	⊖	⊖	⊕	⊕	⊕
Pubofemoral	⊕	⊕	⊕	⊖	⊖	⊖

Table 6.3 Action of spring elements for hip joint position at 90° flexion.

90° FLEXION 20° INTERN ROT	45° Abduction			35° Adduction		
	Normal Neck	Short Neck	Long Neck	Normal Neck	Short Neck	Long Neck
Medial Iliofemoral	⊕	⊕	⊕	⊖	⊖	⊖
Lateral Iliofemoral	⊕	⊕	⊕	⊖	⊖	⊖
Ischiofemoral	⊖	⊖	⊖	⊕	⊕	⊕
Pubofemoral	⊕	⊕	⊕	⊖	⊖	⊖

Table 6.4 Action of springs for hip joint at 90° flexion and 20° internal rotation.

25° INTERN ROT	45° Abduction			35° Adduction		
	Normal Neck	Short Neck	Long Neck	Normal Neck	Short Neck	Long Neck
Medial Iliofemoral	⊖	⊖	⊖	⊕	⊕	⊕
Lateral Iliofemoral	⊖	⊖	⊖	⊕	⊕	⊕
Ischiofemoral	⊖	⊖	⊖	⊖	⊖	⊖
Pubofemoral	⊕	⊕	⊕	⊖	⊖	⊖

Table 6.5 Action of spring elements for hip joint position at 25° internal rotation.

12° EXTENSION	25° Abduction			20° Adduction		
	Normal Neck	Short Neck	Long Neck	Normal Neck	Short Neck	Long Neck
Medial Iliofemoral	⊖	⊖	⊖	⊕	⊕	⊕
Lateral Iliofemoral	⊖	⊖	⊖	⊕	⊕	⊕
Ischiofemoral	⊖	⊖	⊖	⊖	⊖	⊖
Pubofemoral	⊕	⊕	⊕	⊖	⊖	⊖

Table 6.6 Action of spring elements for hip joint position at 12° extension.

12° EXTENSION 25° EXTERN ROT	25° Abduction			20° Adduction		
	Normal Neck	Short Neck	Long Neck	Normal Neck	Short Neck	Long Neck
Medial Iliofemoral	⊖	⊖	⊖	⊕	⊕	⊕
Lateral Iliofemoral	⊖	⊖	⊖	⊕	⊕	⊕
Ischiofemoral	⊖	⊖	⊖	⊖	⊖	⊖
Pubofemoral	⊕	⊕	⊕	⊖	⊖	⊖

Table 6.7 Action of springs for hip joint at 12° extension and 25° external rotation.

35° EXTERNAL ROTATION	25° Abduction			20° Adduction		
	Normal Neck	Short Neck	Long Neck	Normal Neck	Short Neck	Long Neck
Medial Iliofemoral	⊖	⊖	⊖	⊕	⊕	⊕
Lateral Iliofemoral	⊖	⊖	⊖	⊕	⊕	⊕
Ischiofemoral	⊕	⊕	⊕	⊖	⊖	⊖
Pubofemoral	⊕	⊕	⊕	⊖	⊖	⊖

Table 6.8 Action of spring elements for hip joint position at 35° external rotation.

In most of the above cases any spring element that experiences an increase in its effective length during limb movement, will also be producing a contribution to the total hip joint moment. However, in some cases it might be that no force is generated, because the spring element does not reach the initial resting length for the particular hip joint configuration. For example, in the case of 25° internal rotation of the hip joint, the initial resting length of the pubofemoral spring is based on the neutral abduction/adduction position with a normal offset and is equal to 54.97 mm (table 6.1). However, when referring to a shortened femoral neck length and still for 25° internal rotation, the spring's resting length at zero abduction/adduction reduces to 51.89 mm. When the joint is brought into 45° abduction, the final spring length is 54.37 mm, which represents an increase relative to the 51.89 mm, but not relative to the initial resting length of the normal offset, which represents the unaffected resting length of the pubofemoral ligament at 25° internal rotation. Similar effects are also noticed for the neutral position, for 12° extension, for 12° extension with 25° external rotation and for 35° of external rotation for the cases of shortened femoral necks.

6.8 Validation of Spring Element Model

One of the major improvements to the credibility of computer models for the simulation of joint biomechanics would be the possibility to validate the numerical calculations against any findings from cadaver experiments or with other physical models. This is the case for both the FE analysis as well as other numerical methods (Prendergast 1997). For this reason it was attempted to compare the findings from

the numerical analysis that follow against those that were collected on the cadaver models and were presented in chapter 4.

Mabuchi et al (1991) found from animal experiments that joint ligament stiffness is insensitive to the applied strain rate, as long as this is within a range of 100 to 1000 mm/s, but this behaviour changes for strain rates below 100 mm/s, as Noyes et al (1974) reported, where increasing strain rates result in increased stiffness recordings. The strain rate of 25 deg/s (≡10 mm/s) that was used in the cadaver tests of the present study were different to those applied by Hewitt et al (2001 and 2002), which are near static (0.04 mm/s) and both were below 100 mm/s, which would suggest that a certain effect could be attributed to the different strain rates. However, since the numerical analysis that was used in the present study is based on linear elastic spring elements, strain rate would have no effect on the results and can be neglected as a criterion.

The first aim of the model validation was to confirm the use of the elastic stiffness data produced by Hewitt et al (2002). A number of calculations were performed based on the model in initial neutral joint configuration, but with the femur moved into 30° of adduction. A few combinations were tried out for the lateral and medial iliofemoral ligament spring elements, which were all in the region of the elastic stiffness values as they were published by Hewitt et al (2002):

Lateral Iliofemoral Ligament	97.8±67.5 N/mm
Medial Iliofemoral Ligament	100.7±54.0 N/mm
Ischiofemoral Ligament	36.9±24.4 N/mm

The following combinations of stiffness values (k) were used for the calculations:

k_{med} = 100.7 N/mm	k_{lat} = 97.8 N/mm	M_{JCR} = 21.7 Nm
k_{med} = 65 N/mm	k_{lat} = 55 N/mm	M_{JCR} = 12.5 Nm
k_{med} = 50 N/mm	k_{lat} = 48 N/mm	M_{JCR} = 10.7 Nm
k_{med} = 46.7 N/mm	k_{lat} = 30.3 N/mm	M_{JCR} = 9.4 Nm

The final combination, which was based on the lowest recordings of Hewitt et al (2002), for medial and lateral iliofemoral ligament stiffness (k_{med} = 46.7 N/mm and k_{lat} = 30.3 N/mm) resulted in a total hip joint moment of 9.4 Nm, which is a good match with those readings collected during the cadaver tests. As a result of this, the above stiffness values were accepted for these two spring elements. Furthermore, it was decided to select the lowest recording for the ischiofemoral ligament stiffness from the same study k_{ischio} = 12.5 N/mm.

The second aim of the present validation was to establish the elastic stiffness properties for the spring that was used in place of the pubofemoral ligament. The study that provided the same type of information for all the other ligaments (Hewitt et al, 2002) did not include any data on the pubofemoral ligament. It was decided to use a similar stiffness for the pubofemoral spring element (k_{pubo} = 35 N/mm) as was selected for all other elements in the initial neutral joint position, and when moving the limb into abduction (30°). The reason for choosing abduction in neutral joint position was because the pubofemoral ligament is the only one undergoing effective length increase in this limb movement, and therefore, contributes exclusively to the hip joint moments. The resulting moment value for this stiffness was 0.33 Nm, which is substantially less than what was recorded during the cadaver tests (figures 4.23b and 4.27b). A series of higher values was tried for the pubofemoral ligament stiffness in order to find out whether that would bring the total moment closer to those recorded in the cadaver tests without any success.

k_{pubo} = 35 N/mm	M_{JCR} = 0.33 Nm
k_{pubo} = 60 N/mm	M_{JCR} = 0.56 Nm
k_{pubo} = 100 N/mm	M_{JCR} = 0.93 Nm

The failure to create a match between the hip joint moments that were calculated with the present computer model and those recorded in the cadaver study is believed to be due to the different strain rates, under which the two different hip joint moment data sets were recorded. In particular, the study from which the spring stiffness data has been taken from (Hewitt et al, 2002) used very low strain rates in

order to produce information on the stiffness properties of the various hip joint ligaments. The hip joint moments that were calculated with the present computer model were based on these stiffness values, yet it was tried to match them with hip joint moment data from the cadaver tests presented in chapter 4, which were based on a strain rate of 25 deg/s (≡10 mm/s). According to Noyes et al (1974) increasing the strain rate would result in increased recorded stiffness of ligaments, which explains the failure to match the hip joint moment recordings from the computer model with those from the cadaver tests. Nevertheless, using the data of Hewitt et al (2002) at present represents the only possibility to produce information based on a computer model of the hip joint.

Thus, for the validity of the utilised model it can be said that it does not reproduce the recordings of the cadaver tests, at least not for the case where there is more than one spring element contributing to the total hip joint moments. The reasons for these differences are clear and it is understood that any conclusions that are drawn from an analysis that uses the present model, must be under consideration of this fact. For the further analysis within the present work this means that the model can only be used, under consideration of the following conditions:

- Comparisons that involve abduction/adduction angle changes can only be made when they refer to the same single joint configuration (i.e. neutral or 90° flexion etc).
- No comparisons should be made between different joint configurations, as the changes of effective distances that occur as a result of the configuration change can have an effect on the calculated total moments.
- All comparisons within the same joint configurations should be based on the same angles of abduction and adduction.

If all the above conditions are fulfilled, then the comparison of the effect of different femoral neck lengths will remain valid. Suggestions for the model's improvement are outlined in the final sections of this chapter.

6.9 Joint Resistance Moments

The following seven bar charts show how the individual spring ligament elements contribute to the total moments around the hip joint centre of rotation by being extended to their effective lengths that are shown in table 6.1. The layout is the same for all the graphs and includes readings for normal (first and second bars), long (third and fourth bars) and short femoral neck lengths (fifth and sixth bars).

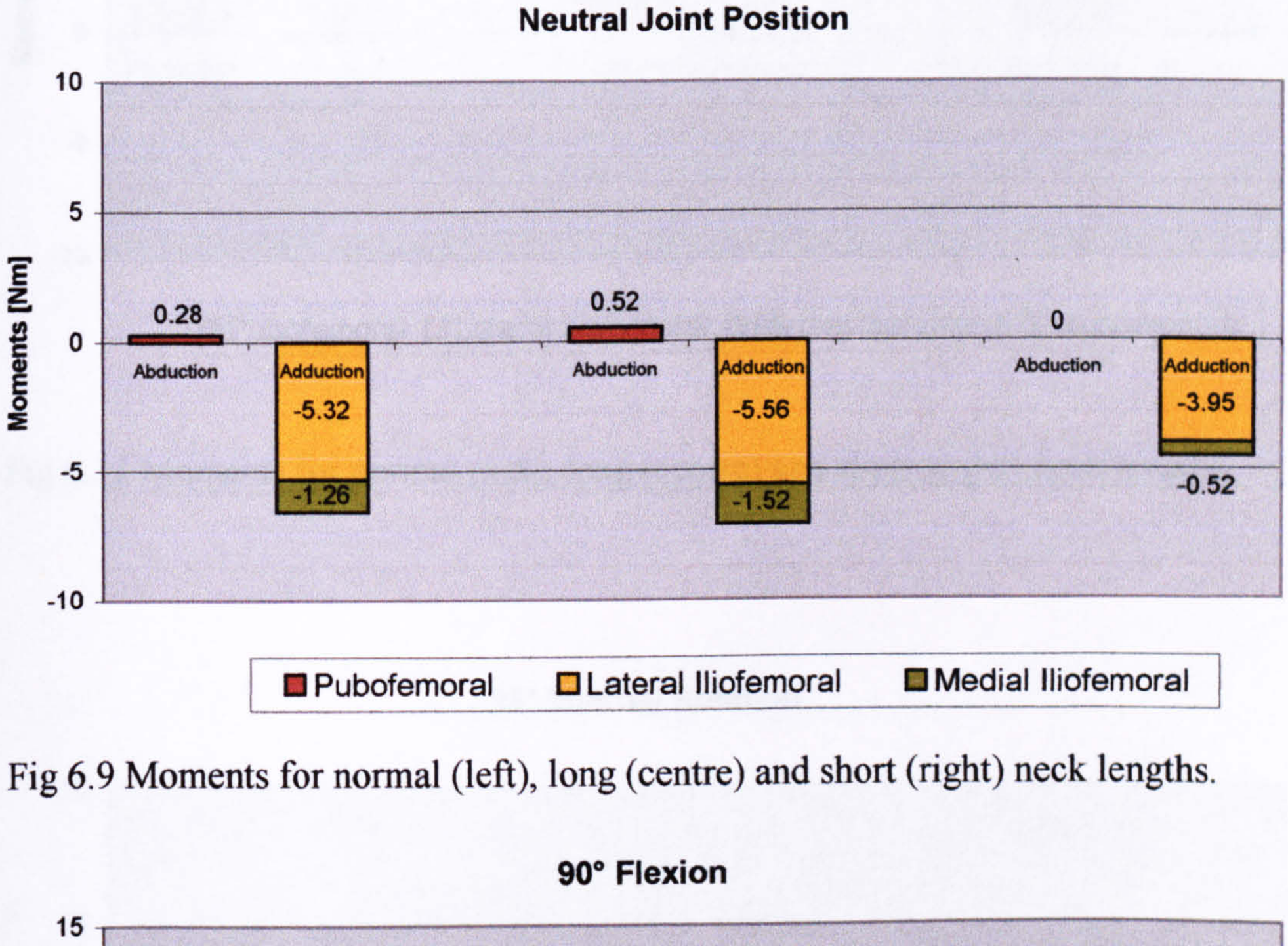

Fig 6.9 Moments for normal (left), long (centre) and short (right) neck lengths.

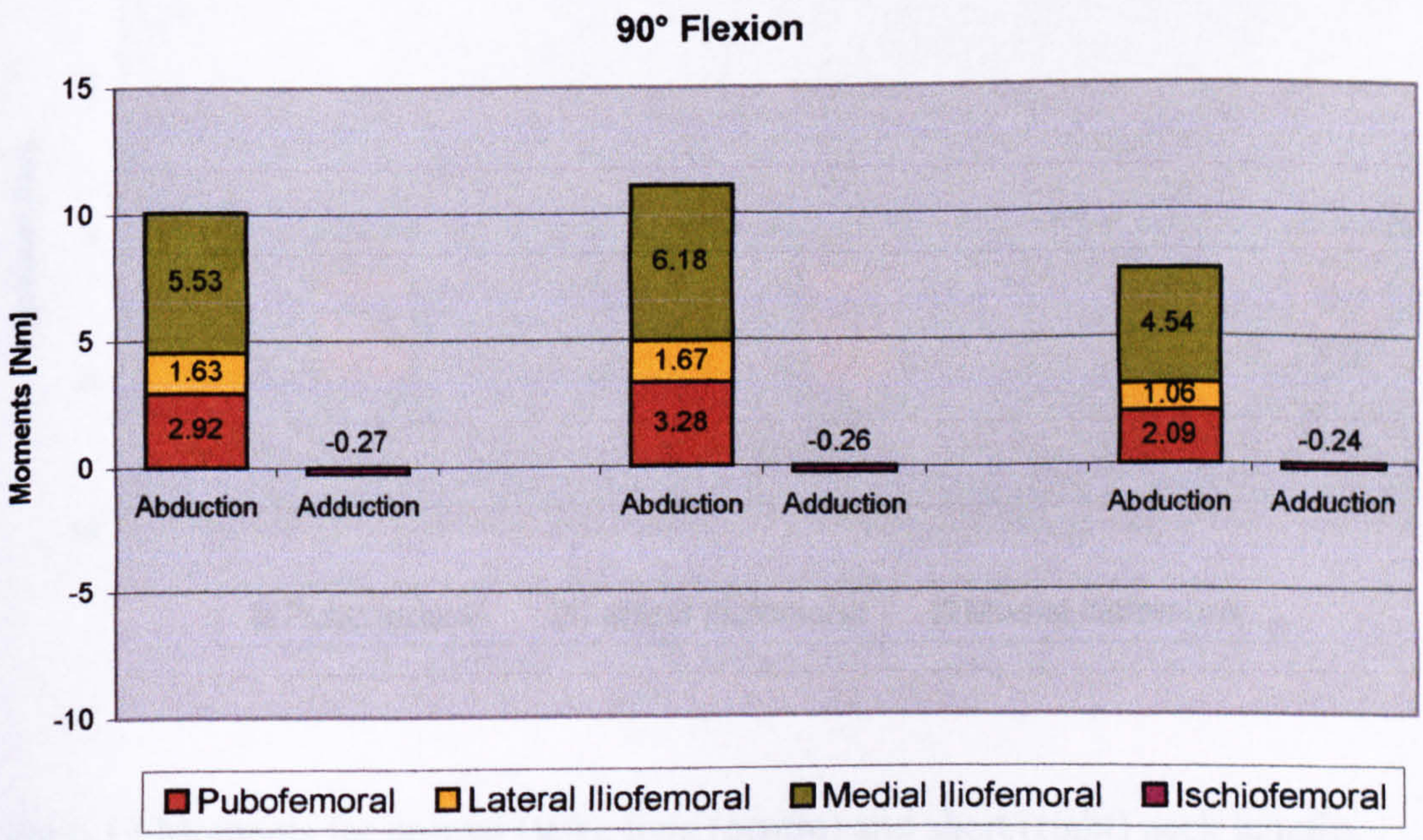

Fig 6.10 Moments for normal (left), long (centre) and short (right) neck lengths.

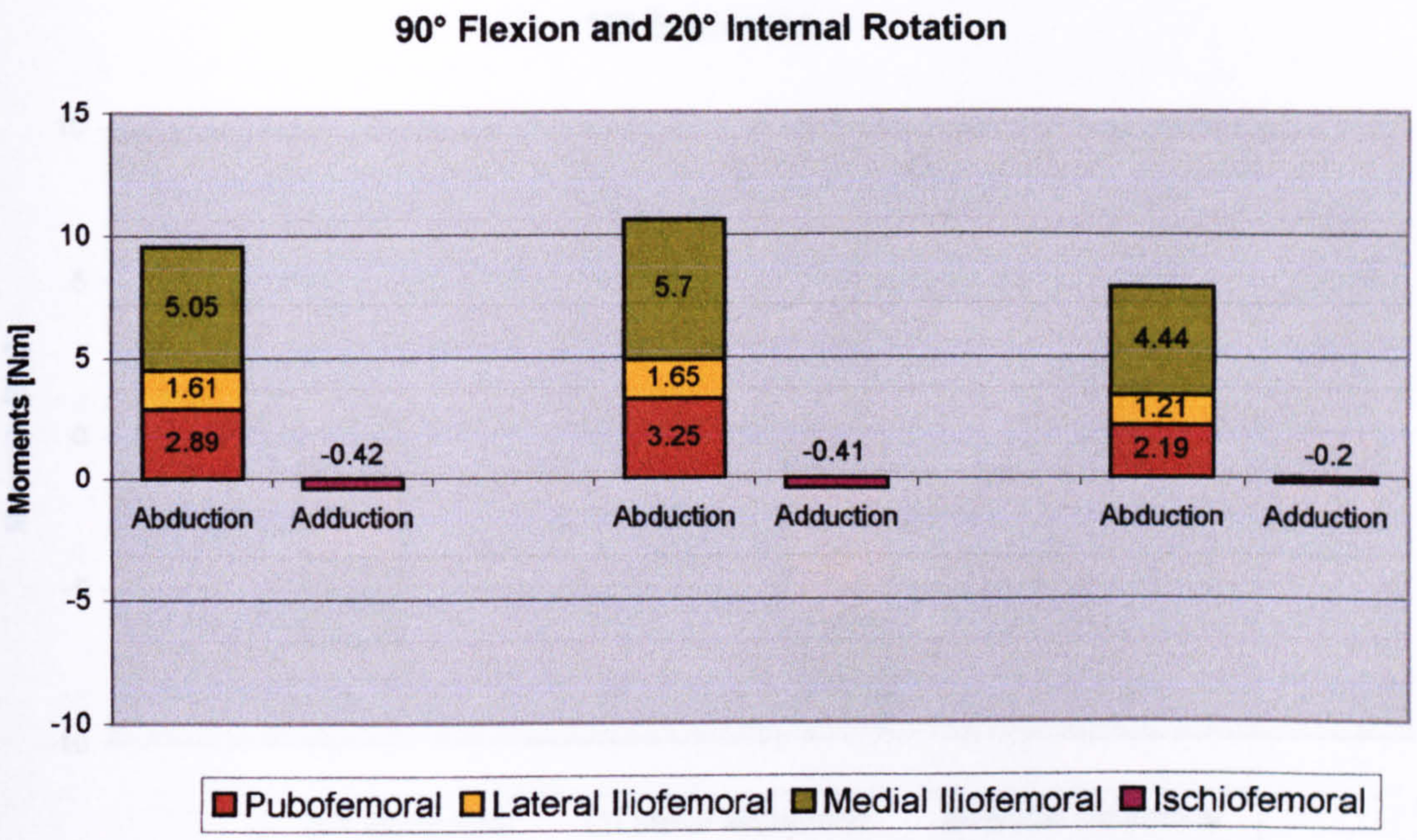

Fig 6.11 Moments for normal (left), long (centre) and short (right) neck lengths.

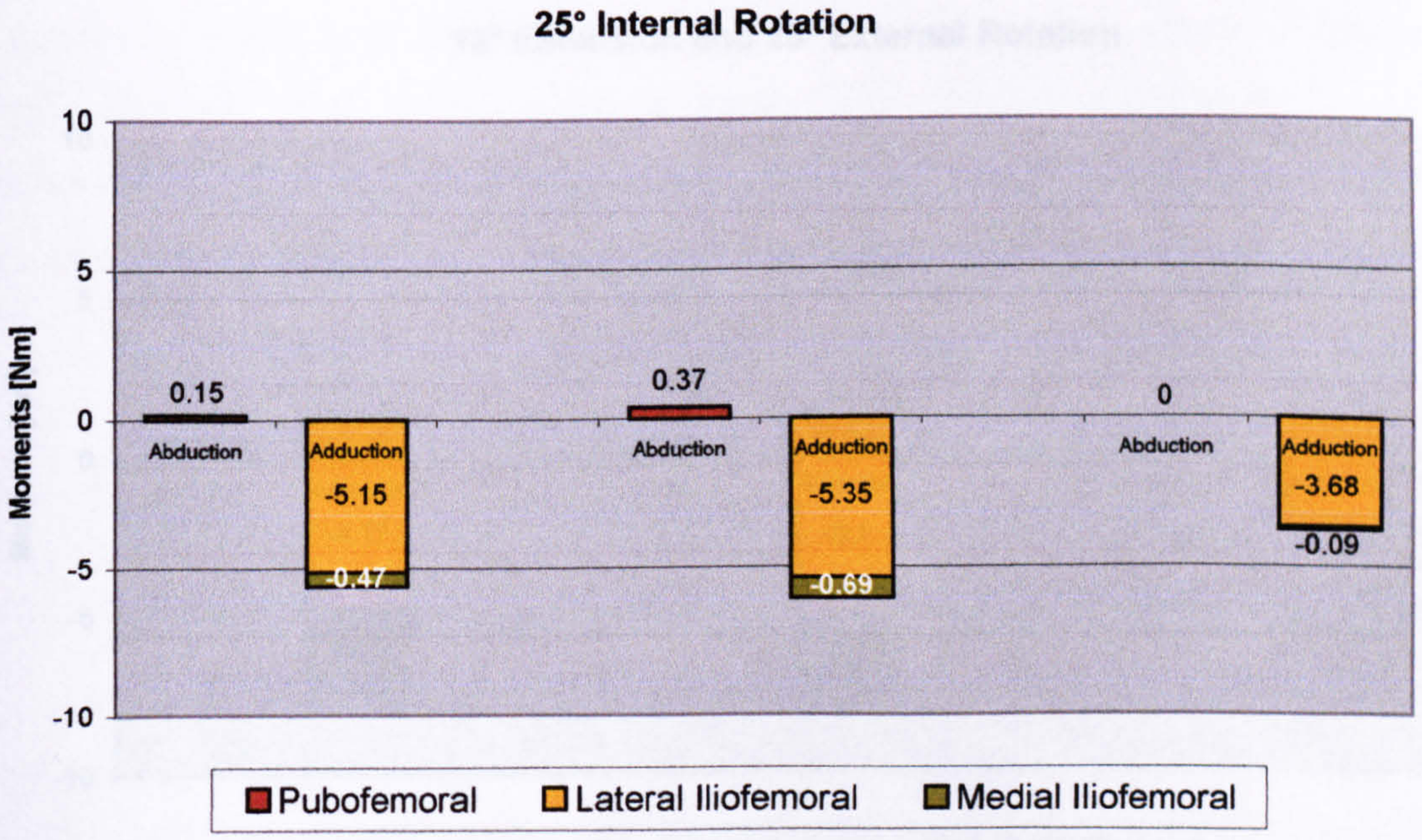

Fig 6.12 Moments for normal (left), long (centre) and short (right) neck lengths.

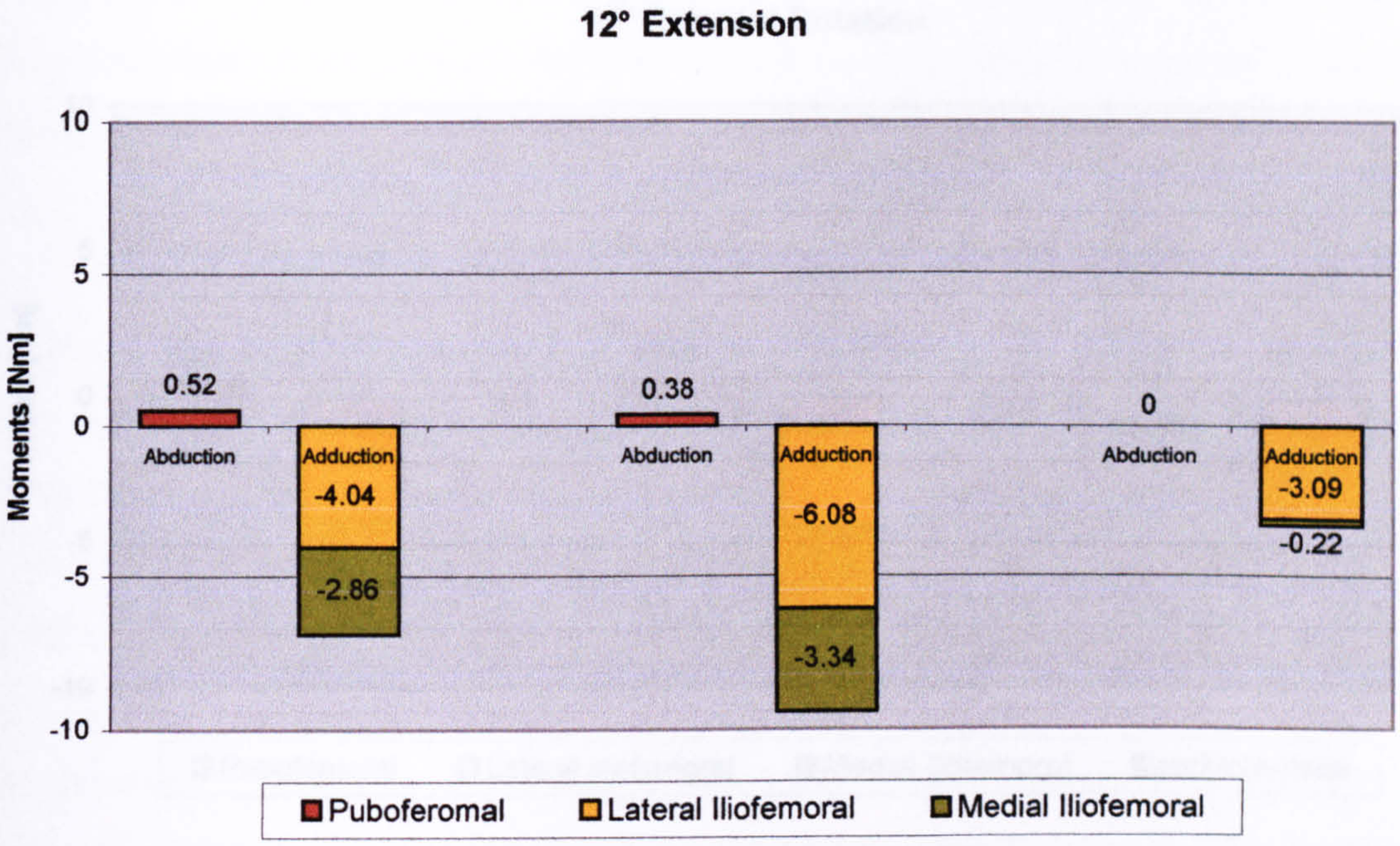

Fig 6.13 Moments for normal (left), long (centre) and short (right) neck lengths.

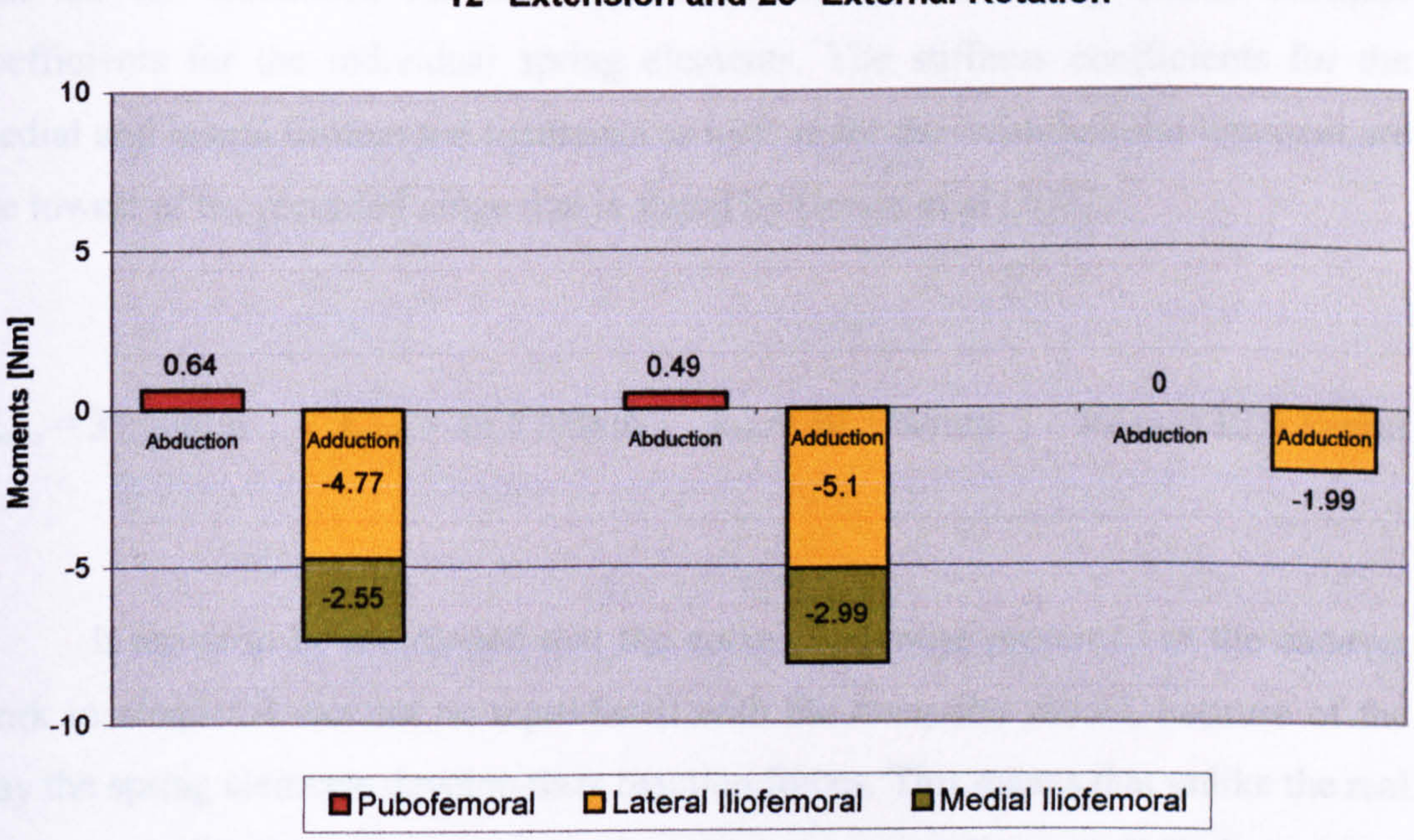

Fig 6.14 Moments for normal (left), long (centre) and short (right) neck lengths.

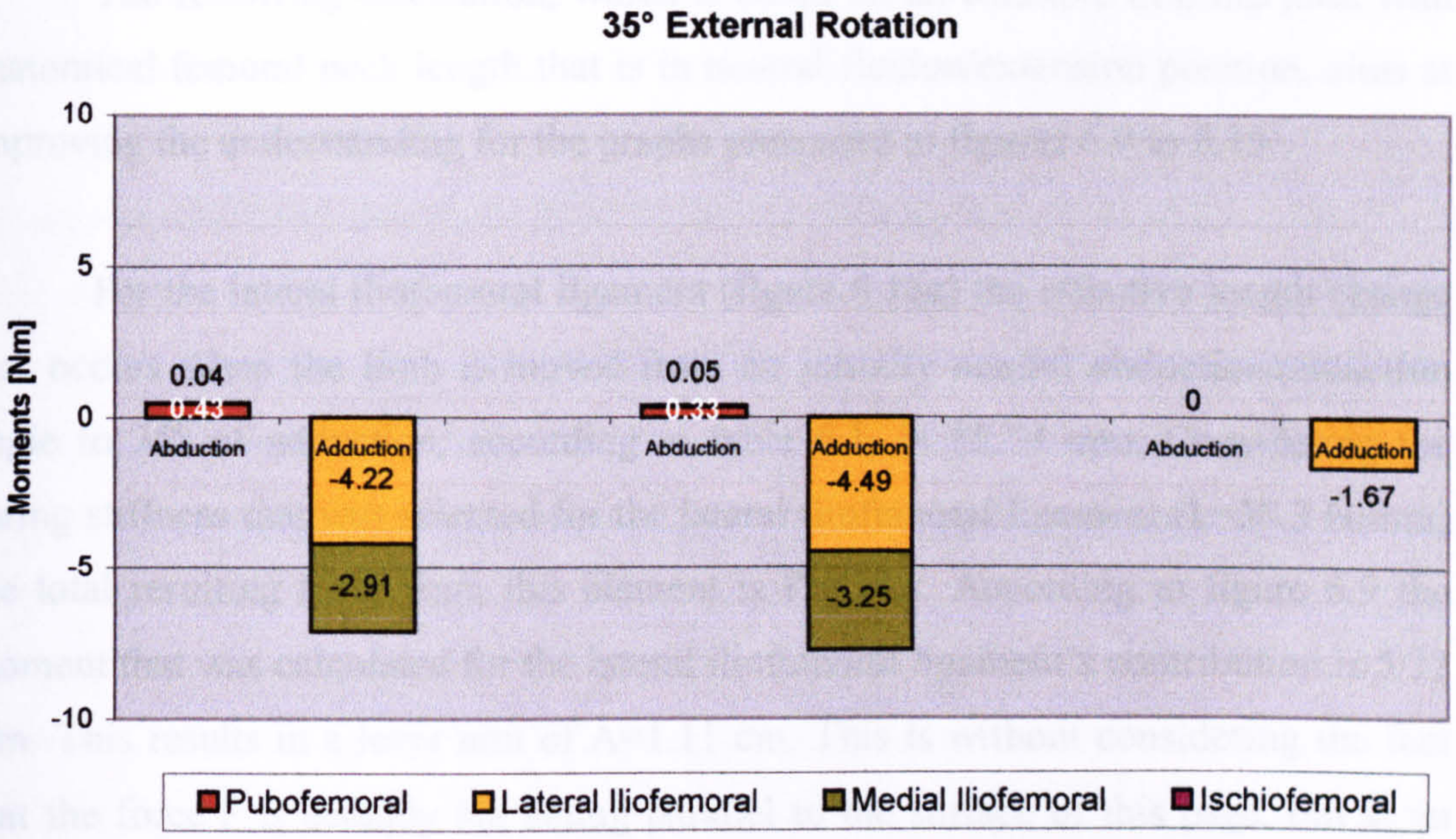

Fig 6.15 Moments for normal (left), long (centre) and short (right) neck lengths.

Before analysing the above graphs in greater detail, it should be mentioned that all the calculated moments are based on the following elastic stiffness coefficients for the individual spring elements. The stiffness coefficients for the medial and lateral iliofemoral ligaments as well as for the ischiofemoral ligament are the lowest of the recorded range that is stated by Hewitt et al (2002):

$k_{pubo} = 35$ N/mm $\quad k_{med} = 46.7$ N/mm $\quad k_{lat} = 30.3$ N/mm $\quad k_{ischio} = 12.5$ N/mm

It needs to be mentioned that the curves that were presented in the cadaver work in chapter 4 can not be reproduced with the computer model, because of the way the spring elements develop their reaction forces. This means that unlike the real cadaver model, the spring model produces moment recordings at all limb positions other than neutral. In other words there is no flat part in the moment curve as it appeared in the cadaver tests, and this is a major drawback of the present model.

The following calculation, which is based on an example of a hip joint with anatomical femoral neck length that is in neutral flexion/extension position, aims at improving the understanding for the graphs presented in figures 6.9 to 6.15:

For the lateral iliofemoral ligament (figure 6.16a) the effective length change that occurs when the limb is moved from an initially neutral abduction/adduction angle to 35° of adduction, according to table 6.1, is 15.79 mm. Considering the spring stiffness that was selected for the lateral iliofemoral ligament (k=30.3 N/mm) the total resulting force from this element is F=478N. According to figure 6.9 the moment that was calculated for the lateral iliofemoral ligament's contribution is 5.32 Nm. This results in a lever arm of A=1.11 cm. This is without considering the fact that the force F is actually not acting parallel to the surface of this page, but at an angle, which means that the effective force that produces the moment is, indeed, less than 478N and, therefore, the lever arm must be somehow greater than 1.11 cm. This lever arm is confirmed by the dimensions of the femoral head (diameter: 4.5 cm) as they are shown in table 5.3 and in figure 6.16a.

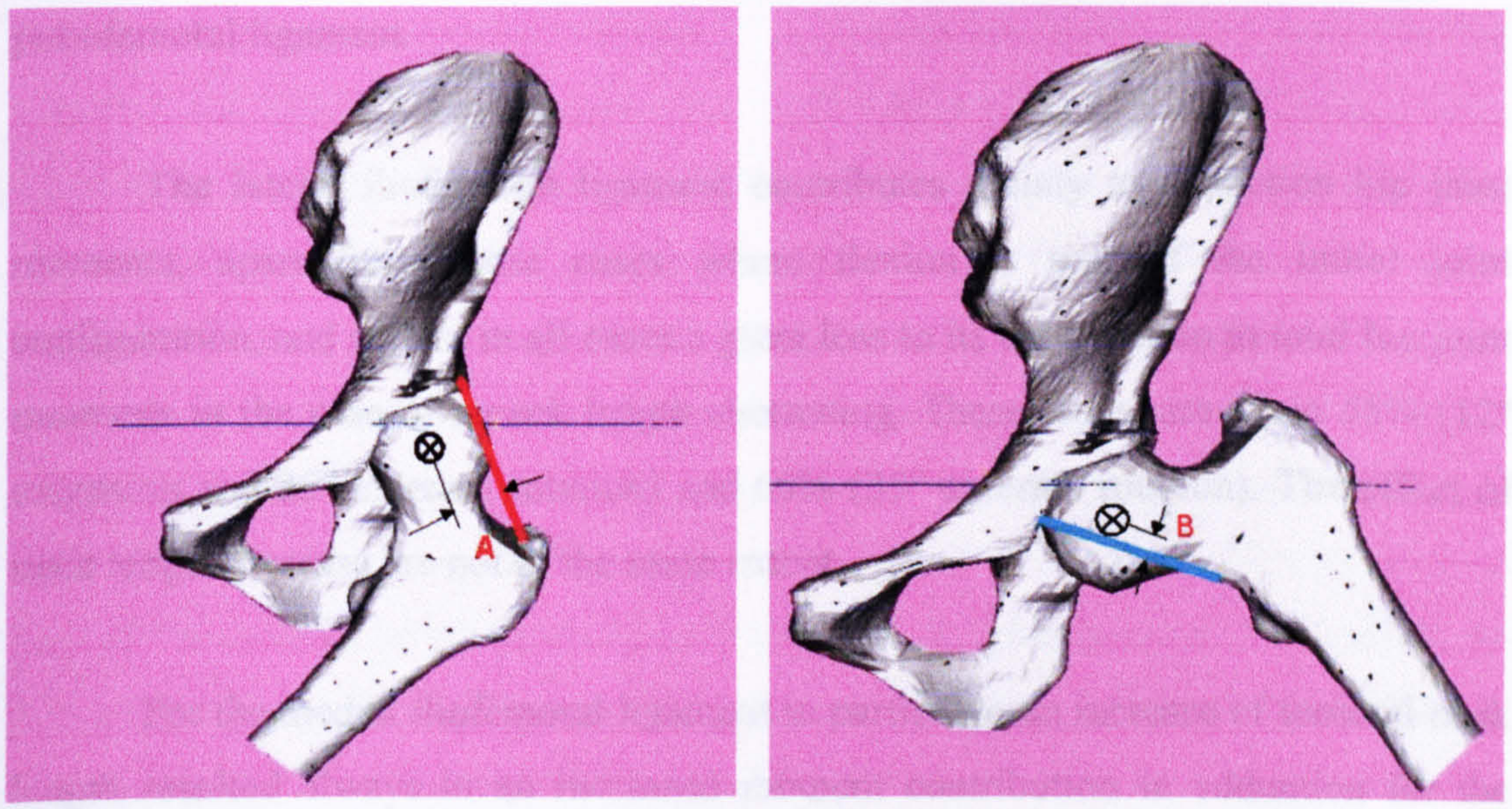

Fig 6.16 a and b The lever arm of the lateral iliofemoral spring increases in abduction (left), whereas that of the pubofemoral ligament nearly becomes zero (right).

For the pubofemoral ligament (figure 6.16b) the effective length change that occurs when the limb is moved to 45° abduction, is 1.46 mm. With a stiffness of k=35 N/mm, this produces a total force of F=51.1 N. However, the calculated moment produced by this force is 0.28 Nm (figure 6.9), which results in a lever arm of B=0.5 cm.

The first observation that stands out from the above numerical analysis is that if the initial joint configuration involves flexion of the femur, the greatest hip joint moments are produced in abduction (figures 6.10 and 6.11). In contrast, when the femur is moved into adduction, the largest moments occur in all positions that involve extension and also in the initial neutral position (figures 6.9, 6.13 and 6.14). Moreover, it is the ligament structures that contribute to these moments that create the interest in this observation. In the cases where there is flexion in the initial neutral position of the joint, it is the medial iliofemoral together with the pubofemoral ligament that contribute mainly to the hip joint abduction moments and the lateral iliofemoral ligament secondarily. However, even when extension is part of the initial neutral joint position, the hip joint adduction moments are largely made up by the contributions of the medial and lateral iliofemoral ligaments, but not of the pubofemoral ligament.

The lateral iliofemoral ligament contributes mainly to adduction hip joint moments, apart from those cases where flexion is part of the initial joint configuration, and suffers in all cases a great loss to its contribution to total hip joint moments in the case of a neck length shortening. These losses are about 58% (12° extension and 25° external rotation) and 60% (35° external rotation). The effect of neck length increase are not of the same extent.

For the medial iliofemoral ligament in particular, an increase of femoral neck length resulted always in an increased moment contribution in adduction for the configurations that involve extension and external rotation (figures 6.13, 6.14 and 6.15). A femoral neck length shortening had the adverse effect for the same joint configurations. In those joint positions that include flexion an increase of femoral neck length resulted in an increase of abduction moment by 11.75% (90° flexion)

and 12.85% (90° flexion with 20° internal rotation). A drop to zero contribution to adduction moments in case of a 12° extension with 25° external rotation (figure 6.14) and for the case of 35° of external rotation were the main effects of femoral neck length changes that were observed.

In what concerns the role of the ischiofemoral ligament in the present computer model, it might not be too obvious at first sight, but there are some changes in the total hip joint moments that involve the ischiofemoral ligament. In particular it appears that there is almost no change in the total moment that is provided by the ischiofemoral ligament when the femoral neck length is increased, but in case of a femoral neck length shortening the drop of adduction moment that this element produces is by 52.77% in case of a 90° of flexion and 20° of internal rotation. In no other position did the femoral neck length changes have an effect on the ischiofemoral ligament's moment contribution, despite the fact that the ischiofemoral ligament is the main stabilising structure on the posterior aspect of the hip joint.

Action of the pubofemoral ligament was only observed for the abduction movement, as was expected. However, an interesting observation was that the pubofemoral ligament contributed more to the total abduction hip joint moments when an initial flexion configuration of the joint was present (figures 6.10 and 6.11) rather than when the joint had an initial extension or was in neutral flexion/extension angle. Furthermore, an increase in the femoral neck length resulted in an increased contribution to abduction joint moments by 12.2% in the case of initial 90° flexion (figure 6.10) and an increase by 12.35% for the case of 90° flexion with 20° of internal rotation (figure 6.11). In contrast, a shortening of the femoral length resulted in a 28.5% drop for 90° flexion (figure 6.10) and a 24.35% drop for 90° flexion with 20° of internal rotation (figure 6.11). No great changes were observed for the pubofemoral ligament in the other joint configurations.

6.10 Discussion

A linear spring element model was employed for the evaluation of the effects of a shortening or lengthening of the neck length on the total hip joint moments,

which are indicators for the total hip joint stability and resistance to painful dislocation. This model does not reproduce faithfully the behaviour of the human hip joint with all its ligaments, mainly because the stiffness of the various spring elements does not match with the stiffness that the hip joint ligaments have during different activities of gait. Furthermore, because the various spring elements were considered to be acting along the linear connection of the ligament insertion points into pelvis and femur rather than following their wrapping direction around the femoral bone (figure 6.14), the calculated moments can never match those recorded in the cadaver tests. Nevertheless this model is still useful for comparative work on the effect of different femoral component neck lengths on the resistive moments produced by the spring elements. It was shown that by standardising the test procedure, it is possible to draw useful conclusions on how altered femoral neck lengths in post-THR joints can affect the stability and what further effects could result from partial or complete damage of the capsule. The comparative nature of the present analysis gives confidence that the conclusions drawn from it are valid.

Regardless of the extreme position of the femoral bone (extension or flexion), it was mainly the medial and subsequently the lateral iliofemoral ligaments that showed to be playing the main role in stabilising the joint. This observation differs partly from what was observed in the cadaver tests, where the most important role of the medial iliofemoral ligament became apparent when the joint was in partial extension, but not so much when there was flexion in the initial joint position. Thereby, it must be mentioned that no tests were carried out on the cadavers with the removal of the medial iliofemoral ligament whilst the joint was in partial flexion and therefore it is not clear if similar responses would have been observed. The role that the ischiofemoral ligament showed to be playing in the cadaver tests was of much greater importance than at the present numerical analysis. However, it can be concluded for the ischiofemoral ligament that its contribution to adduction hip joint moments is affected negatively with the shortening of the femoral neck length.

Reviewing the observations on the hip joint moments, it can be stated that the effect of a femoral neck length shortening on the resulting hip joint moments, and

therefore on the joint stability, were more substantial than those from a lengthening of the femoral neck length. Furthermore, the changes resulting from a femoral neck lengthening would not have a negative consequence on the hip joint stability, because they are towards increased total hip joint moments. Unless an over-tightening of the capsular structures resulted from this lengthening, in which case a reduced range of motion of the affected hip joint would be the case, no other problems would be anticipated.

Also it is apparent that, depending on the approach that was taken to access the hip joint surfaces during THR surgery, permanent damage to the capsule could have dramatic outcomes on the post-operative joint stability. In particular, in case of a posterior approach that would result in permanently damaging the ischiofemoral ligament, the post-operative resistance of the joint capsule to adduction movements of the limb would be reduced to zero for the cases of the joint being in 90° flexion or in 90° flexion together with a 20° of internal rotation. The effect of an absent ischiofemoral ligament would not be as great in the case of abduction movements whilst the joint is in 35° of external rotation, because of the presence of the pubofemoral ligament, which is not usually damaged during THR, regardless of the approach taken by the surgeon.

However, the use of an anterior approach for THR surgery that would cause damage to the medial iliofemoral ligament without a subsequent anterior capsular closure, could result in dramatic loss of hip joint resistance moments. For example, in case of a joint position of 12° extension (figure 6.13) or 12° extension with 25° external rotation (figure 6.14) or even just 35° external rotation (figure 6.15) a drop by up to 72% when a neck shortening is the case, would occur at 35° external rotation alignment of the hip. However, with an additionally damaged medial iliofemoral ligament, even in case of an increased femoral neck length there would still be a loss of up to 27% in total hip joint resistance for a 35° external rotation joint position. Major drops in joint resistive moments can also be seen during abduction of the limb, whilst the joint is in 90° flexion (figure 6.1) or 90° flexion together with 20° of internal rotation. However, the continuing presence of the pubofemoral

ligament would still allow a certain joint resistance to be present. Finally, synchronous damage of two anterior-lateral ligaments, namely the medial and lateral iliofemoral ligaments, which is a scenario that can occur during THR using an anterior-lateral approach without capsular repair would result in almost all cases (figure 6.12 to 6.15) in a complete loss of hip joint moments, regardless of the femoral neck length.

Summarising the effects of capsular damage in association with altered femoral neck lengths it can be stated that the worst consequences result from damage without repair of the ischiofemoral ligament, which in certain cases results in a complete loss of hip joint resistive moments. Detrimental consequences also result from a non-repaired destruction of the medial iliofemoral ligament. However, in most cases of THR surgery, where no capsular repair is attempted, more than one ligament can be damaged, which again may result in a complete loss of hip joint resistance, depending on the joint configuration. Therefore, a suggestion that can result from this analysis is that capsular repair should always be attempted, after THR to restore the initial function of the capsule as much as possible, whilst shortening of the femoral neck length should also be avoided. Post-operative neck lengthening will not have any negative consequences to the joint's stability, unless it is accompanied by an over-tightening or with an omitted repair of any damaged capsular ligaments.

Reviewing the methodology that was followed it can be said that the use of finite element models for the ligament structures together with the modelling of the bone elements as rigid bodies did not result in a solution as part of a joint mechanism simulation. The large volume of information that was supplied to the solver on material properties of the soft tissues, but also the presence of a mechanism as part of the loading case made this a very ambitious undertaking. However, the alternative solution method that was presented here and involved the modelling of the ligaments as spring elements that resisted the motion of the two rigid bodies as part of a mechanism and relative to each other, worked particularly well and formed a good foundation for comparative purposes. Thus, it has been possible to identify the role

that a pre-tension or loosening of the ligament bands can have on the total resistance that is provided to limb abduction and adduction. However, the first major improvement that needs to be made to the existing model has to be the way the forces generated by the ligaments are applied onto the joint mechanism. The use of spring elements instead of the ligaments should be avoided, because both the vector direction of the produced force as well as the size of the force that is generated by the spring elements is not accurate and allows only comparisons that need to be carried out under controlled conditions.

In order to overcome this problem, it is suggested that in the future the use of linear spring elements is replaced by 'cable elements' that can act along the boundaries of the actual ligaments, rather than on the line that connects their insertion points into pelvis and femur. In this way the actual lever arms under which also the ligaments contribute to joint moments could be reproduced correctly. Furthermore, in order to overcome the linear dependency of the ligament forces on the stiffness of the spring elements, a force vector function F(t) needs to be used to substitute for each spring element. This force vector has to be expressed as a function of time and would result from previous tensile tests on excised individual ligaments. Thereby, the force deformation curve would be recorded for an elongation similar to the one that actually occurs in the individual ligaments and is somehow different to those calculated in table 6.1. This actual elongation would have to be determined using an alternative method.

The strain rate that is to be applied for such tensile tests, would have to be calculated from the elongation that is applied to the ligaments during normal human gait. In chapter 4 it was already stated that in normal gait conditions a limb movement at angular velocities of 25 deg/s (≡10 mm/s) can be recorded, and this was also applied to the abduction/adduction movements during the cadaver tests. This angular velocity of 25 deg/s means that a 30° abduction or adduction movement is achieved in 1.2 seconds. Therefore, the equivalent linear deformation of the excised ligament, which is the same as the previously calculated ligament elongation, should also be carried out within 1.2 [s], which is the required strain rate for the linear

tensile tests. By developing similar F(t) functions for all hip joint ligaments, the computer model that was used in this study could be employed again, using force vectors that incorporate non-linear material behaviour instead of linear spring elements, as well as including restraints for the line of action of the force F(t), along the actual boundary lines of the individual ligaments.

Another intended improvement of the current model in future work would include the possibility for changes in the ligaments' response to load, as a result of post-operative capsular repair. Finding the optimised location for placing the incision into the capsule will be based on the effects that any incision would have on the resulting total hip joint moments. Further, in the future model it would be possible to include effects of surgical shortening or lengthening of the capsular structures as a result of capsular repair of these tissues after THR.

In agreement with what Eftekhar (1978) states, the main structure that contributes to the stability of the hip joint after THR, apart from the tensor fascia femoris and the glutei, is the hip joint capsule with its strengthening ligaments, which tend to become lax when an excessive shortening of the femoral neck results post-operatively. The suggestion that shortening of the femoral neck length has to be avoided, because of the severe reduction of hip joint moments that result from this, is in good agreement with the statements of Eftekhar. Also the necessity to repair the anterior structures of the capsule after THR as is proposed by Eftekhar is confirmed in this study, since absence of any of the anterior structures would result in great losses in the total hip joint moments, regardless of the femoral neck length.

6.11 Summary

Time restrictions in the present work demanded a simplification of the computer model that was to be developed for the numerical analysis of the role of the hip joint capsule and its ligaments after THR and with the consideration of parameters like post-operative femoral neck length. Nevertheless, it is felt that a valid model was created that allowed some useful conclusions and simple comparisons with the cadaver experiments that preceded the development of the

computer model. Important matters for consideration in THR were raised. Also knowledge was generated on the restrictions and requirements set to a computer model, for the simulation of soft tissues' effects on joint stability. Ideas were developed for the further improvement of the model that will allow additional investigations of subjects that could not be studied with the present model. A large number of further questions have been generated in the attempt to produce answers to previous problems that were set out to be solved with the present work.

Chapter 7- Conclusions

7.1 General

The hip joint capsule has always been considered by surgeons to be a tissue that is commonly removed during THR, driven by standardised surgical approaches. Its removal has usually been advocated by 'the need to gain clear access' to the joint surface. Also, it has been assumed that in a diseased hip joint that has been by affected by rheumatoid arthritis, inflammatory episodes would have damaged the capsular tissues irrecoverably. This scenario can be true quite often, however, whenever no inflammation is present, it is worth attempting to maintain the capsular structures and even spend some extra surgery time to repair the capsule after completion of the THR procedure. This project set out to provide the necessary data and numerical information that would show the capsule's contribution to joint stability, by means of numerical values highlighting the necessity to preserve the capsule.

It was discovered that only a very small amount of work had been done, regarding the role and properties of the hip capsule The anatomical and structural complexity of this dense tissue network that lacks visible boundaries between its individual components may be an explanation for the lack of studies. This complexity became apparent during the attempt within this study to develop a useful method for testing the capsule's strength as a whole and continuous structure, which would also allow the characterisation of the individual ligaments' strength and role. Another difficulty was to find an imaging modality that would be capable of depicting each of the capsular ligaments and its boundaries, as to be able to reconstruct its 3-D geometry. Finally, the greatest of all difficulties was to develop a valid computer model of the hip joint, on which it would be possible to alter the parameters that characterise the capsular ligaments and also to create different situations as they could, indeed, occur after THR.

With the completion of this study, a beginning has been made for further work on the hip joint capsule. Even though many questions remain unanswered, it is felt that some insight has been gained into the function and role of the hip joint capsule. Hopefully, as work continues, the computer model will acquire more capabilities that will allow a more realistic simulation of the capsule's behaviour under consideration of more parameters that influence the tissue's behaviour.

7.2 Project Contributions

In this paragraph it is stated what contributions have been made with this work towards the advancement of understanding of the hip joint capsule. The specific aims that were set to this work included the characterisation of the hip joint ligaments' mechanical properties and the study of their role in stabilising the hip joint as part of an unaffected anatomy, but also as part of an artificial hip joint after THR surgery. It has been achieved with this work to produce information on the extent of resistance moments that the intact hip joint capsule is capable of producing in response to a movement of the femoral bone relative to the pelvis with three degrees of freedom (rotations around the three principal axes). The consequences from excising the hip joint capsule partially or completely during THR have also been identified in the cadaver models. The worst limb positions for a hip joint with a partially or completely removed capsule have been revealed and compared with each other, allowing in this way the detection of the least desirable combinations of joint position and capsule state, in terms of the resulting risk for joint dislocation.

Another specific aim that had been set for the present study was to develop an accurate and valid 3-D model of the hip joint with its capsular ligaments. In fact, two models of the hip joint with its capsule were created, one based on cryo-section images taken from the female 'Visible Human' project (National Library of Medicine, United States) and another based on CT scans that were taken using the cadaver specimen number five of those shown in chapter 4. The CT scans were particularly easy to use for boundary detection, because all the unwanted tissues like muscles and other connective tissues had previously been removed, and only the remaining parts of the femoral and pelvic bones as well as the capsule tissues were

put through the CT scanner. In spite of all structures being visible in the CT images it was not possible to identify any boundaries between the individual ligament strands. In contrast, in the images from the 'Visible Human Project' the individual ligaments were able to be distinguished, which made the creation of their respective solid objects possible. A comparison of the basic dimensions of the two models (i.e. the CT based and the cryo-section based) showed good agreement, which was considered to be a validation of the model dimensions.

The final goal that had been set to be achieved in this work was to form a comparison of different post-operative situations in a hip joint using the 3-D model reconstruction. The post-operative situations that were studied in the 3-D model-based analysis were different femoral neck lengths of the reconstructed hip geometry and the effect of partial removal of capsular ligaments on the hip joint moments, which is a factor predicting the risk for joint dislocation. A worst case scenario has been identified from this simulation and recommendations were made as to how to reduce the risk for dislocation as a result of femoral neck length changes.

Finally, suggestions have been made regarding the surgical approach to THR that minimises disturbance to the capsular function. In particular, the study revealed that the effect on the capsule's performance is least when it is ensured that no femoral neck shortening results from the THR, when capsular ligament bands are repaired whenever they are not diseased and when the incision through the capsule is attempted between the ligaments rather than across their long axis.

Reviewing the outcomes of both the cadaver tests and the computer simulation, it is apparent that during a posterior approach to the hip joint, which requires an incision through the ischiofemoral ligament, the drop of resistive hip moments is most drastic, if no capsular repair is attempted after THR. This is because in certain positions there is no contribution from any other capsular ligament that could compensate for the lost function of the ischiofemoral ligament. In contrast, whenever an anterior-lateral approach was used, the resistance drop that resulted from a transsected lateral iliofemoral ligament, was partly compensated by the

function of the medial iliofemoral ligament. Especially when it was possible to avoid introducing a femoral neck shortening, the capsular resistance to limb motion was maintained at a substantial level.

Therefore, it is suggested as an outcome from this work, that the preferred choice for access to the hip joint surfaces, if joint stability and risk for dislocation are an issue of concern for the surgeon, should be the following. Use of anterior-lateral approach accompanied with the initial cut through the lateral iliofemoral ligament, followed by capsular reconstruction. Thereby, it is felt that if a transverse cut through the ligament's body can be avoided and a cut parallel to the collagen fibres i.e. along the long axis can be placed instead, a faster and more effective repair will be achieved, because a smaller number of collagen fibres is divided.

It should be mentioned at this stage, that a personal oral communication with Dr MS Bhamra, a consultant orthopaedic surgeon at Rotherham General Hospital in Trent, UK, resulted in an attempt to reproduce the above suggestion of parallel-fibred capsular incision in theatre. The general observation of this attempt on a small number of patients was quicker post-operative recovery and an accelerated weight-bearing on the affected side. However, these observations are very subjective and a much more detailed study needs to be undertaken for more appropriate documentation of this method.

7.3 Critical Review of Present Work

Even though using the cryo-section based images was better in terms of differentiating between them compared to the CT based images, the distinction between the lateral and medial aspect of the iliofemoral ligament was still a difficult objective and was only achieved with the support of an experienced anatomist. It was only when the complete 3-D geometry was reconstructed that a certainty was acquired as for the accuracy and correctness of the boundary selection within the boundary reconstruction software. This method of reconstruction proved very labour intensive and involved a human factor in the achievement of correct geometry.

Therefore, it resembles a potential source of error, which has to be accepted in the absence of a more accurate technique, but needs to be acknowledged.

Furthermore, in what regards the way that the spring elements were applied to the model geometry as substitutes to the actual ligament geometry, it is possible that there has been an effect to the lever arms for the calculated moments. This is, because the ligament action is represented by a single line that connects the insertion points to the femoral and pelvic bones, rather than using the complete solid body of the ligament. Even though this assumption may introduce errors in the calculations for the total joint moments, it is believed that for the purpose of comparing the individual ligaments in relation to the femoral neck length it is still valid.

It is acceptable and fair to state, under consideration of the fact that at the beginning of the present work very little was known on the behaviour and role of the joint capsule in the biomechanics of the hip, that a great amount of knowledge and understanding has been gathered through the present work. Also, having developed a computer model that can compare two different approaches of testing the biomechanics of the hip joint capsule, namely tensile tension experiments of excised capsular ligaments and moment recording experiments of complete and intact capsules *in situ*, is another achievement.

7.4 Future Work

The main considerations that involve future work are the further development and improvement of the computer model and its capabilities. The spring elements that act as ligament substitutes will have to be replaced with something closer to the real ligament function, which would also account for the time dependency of the ligaments' response to loads. Also the vector directions of the ligament forces will have to be included in the improved model, which will allow an accurate validation of the model's response against the actual response as it was recorded on the cadaver models. Furthermore, some tensile tests on all capsular ligaments have to be carried out, in order to record the force changes that occur in each ligament under deformations that match their actual deformations *in situ* when the femur moves

relative to the pelvis. Thereby, the strain rate will be the same as the real strain rate that is applied to the ligaments during human gait.

Secondary future considerations involve a post-mortem clinical study for the development of an optimised incision through the capsule during THR. Thereby it will be attempted to find an anterior-lateral location on the capsule that allows access of a small sized prosthesis and the equivalent tools to the joint surface while damaging the ligaments as little as possible. This study should also address the problem of over-stretching the capsular structures with the retractors that would hold the capsule open. After the identification of the most suitable location for capsular incision, a study should be conducted to reveal whether or not there are any benefits resulting from an altered incision method i.e. parallel rather than perpendicular to the collagen fibres.

Finally, it would be beneficial for the better understanding of the hip joint capsule's function to investigate the proprioceptive role of the capsule and whether or not there are any proprioceptive nerves in the capsule tissues, that provide signals which induce the tightening of the musculature that surrounds the hip joint and supports the joint stability. Possibly, an EMG study could help to determine this role of the capsule, which would mean that in case of its excision not only its passive function would become redundant, but also an active role, namely the muscle activation signal function. Eventually, EMG studies could be expanded to investigate the delay of muscle activation that is involved in fast unexpected manoeuvres that involve the hip joint. This study would produce knowledge on the extent of limb motion that occurs in sudden and unexpected manoeuvres, before the muscles are set into function as stabilisers of the hip joint. This could reveal another function of the capsule as an immediate passive stabilising structure playing the role of a 'safety-belt'.

References

Ahlers J, Walde H-J, Lörincz G, Hücker H (1978), Untersuchungen über die physikalischen Eigenschaften des menschlichen Hüftkapselgewebes, Verhandlungen der Deutschen Gesellschaft für Rheumatologie, Vol 5, pp. 224-226.

Akeson WH (1961), An experimental study of joint stiffness, Journal of Bone and Joint Surgery (Am), Vol 43, pp. 1022-1034.

Almeida ES, Spilker RL (1998), Finite element formulations for hyperelastic transversely isotropic biphasic soft tissues, Computer Methods in Applied Mechanics and Engineering, Vol 151, pp. 513-538.

Amstutz HC, Markolf KL (1974), Design features in total hip replacements. In: The hip. Proceedings of the second open scientific meeting of the hip society. CV Mosby, Louis.

Barrack RL, Butler RA, Laster DR, Andrews P (2001), Stem design and dislocation after revision total hip arthroplasty: clinical results and computer modelling, Journal of Arthroplasty, Vol 16, No 8 (Supplement 1), pp. 8-12.

Beaupre GS, Schneider E, Perren SM (1984), Stress analysis of a partially slotted intramedullary nail, Journal of Orthopaedic Research, Vol 2, pp. 369-376.

Bellabarba C, Sheinkop MB, Kuo KN (1998), Idiopathic hip instability- an unrecognized cause of coxa saltans in the adult, Clinical Orthopaedics and Related Research, Vol 355, pp. 261-271.

Bickels J, Meller I, Henshaw RM, Malawer MM (2000), Reconstruction of hip stability after proximal and total femur resections, Clinical Orthopaedics and Related Research, Vol 375, pp. 218-230.

Bilgen M, Insana MF (1996), Deformation models and correlation analysis in elastography, Journal of the Acoustical Society of America, Vol 99, No 5, pp. 3212-3224.

Binkley J (1989), Overview of ligament and tendon structure and mechanics: implications for clinical practice, Physiotherapy Canada, Vol 41, No 1, pp. 24-30.

Cheal EJ, Hayes WC, Lee CH, Snyder BD, Miller J (1985), Stress analysis of a condylar knee tibial component: influence of metaphyseal shell properties and cement injection depth, Journal of Orthopaedic Research, Vol 3, pp. 424-434.

Chiu FY, Chen CM, Chung TY, Lo WH, Chen TH (2000), The effect of posterior capsulorrhaphy in primary Total Hip Arthroplasty- a prospective randomised study, Journal of Arthroplasty, Vol 15, No 2, pp. 194-199.

Claes L, Biomechanical properties of human ligaments (1983), Aktuelle Probleme Chirurgischer Orthopaedie, Vol 26, pp. 10-17.

Crisp JDC (1972), Properties of tendon and skin, In: Biomechanics- Its foundations and objectives, Edited by: Fung YC, Perrone N, Anliker M, Prentice-Hall, NY.

DeButtet M, Pasquier G (1999), Capsular closure to prevent posterior dislocation after primary Total Hip Arthroplasty through the posterior approach, Hip International, Vol 9, No 4, pp. 186-193.

Dorr LD, Wolf AW, Chandler R, Conaty JP (1983), Classification and treatment of dislocations of Total Hip Arthroplasty, Clinical Orthopaedics and Related Research, Vol 173, pp. 151-158.

Duthie RA, Bruce MF, Hutchison JD (1998), Changing proximal femoral geometry in northeast Scotland: an osteometric study, British Medical Journal, Vol 316, pp. 1498-1500.

Eftekhar NS (1978), Principles of Total Hip Arthroplasty, The CV Mosby Company, St. Louis, Missouri 63141.

Eklund A, Bergh A, Lindahl OA (1999), A catheter tactile sensor for measuring hardness of soft tissue: measurement in a silicone model and in an *in vitro* human prostate model, Medical & Biological Engineering & Computing, Vol 37, pp. 618-624.

Eldred E, Yung L, Eldred D, Roy RR (1998), Distribution of muscle spindles in a simply structured muscle: integrated total sensory representation, Anatomical Record, Vol 251, No 2, pp. 161-172.

Elliott DM, Kydd SR, Perry CH, Setton LA (1999), Direct measurement of the Poisson's ratio of human articular cartilage in tension, Transactions of the Orthopaedic Research Society, Vol 24, p. 649.

Fung YC (1993), Biomechanics- Mechanical Properties of Living Tissues, Second Edition, Springer-Verlag, New York.

Fuss FK, Bacher A (1991), New aspects of the morphology and function of the human hip joint ligaments, The American Journal of Anatomy, Vol 192, pp. 1-13.

Gerhardt JJ, Rippstein J (1990), Measuring and recording of joint motion: instrumentation and techniques, Hogrefe and Huber Publishers, Lewiston, NY.

Goldsmith AA, Dowson D, Wroblewski BM, Siney PD, Fleming PA, Lane JM (2001), The effect of activity levels of total hip arthroplasty patients on socket penetration, Journal of Arthroplasty, Vol 16, No 5, pp. 620-627.

Graham B, Lapp RA (1990), Recurrent posttraumatic dislocation of the hip, Clinical Orthopaedics and Related Research, Vol 256, pp. 115-119.

Gray H, (1918). Anatomy of the human body, Philadelphia: Lea & Febiger, 1918. Bartleby.com 2000, www.bartleby.com/107/, 2002.

Grönblad M, Korkala O, Liesi P, Karaharju E (1985), Innervation of synovial membrane and meniscus, Acta Orthopaedica Scandinavica, Vol 56, No 6, pp. 484-486.

Hamilton PR, Broughton NS (1998), Traumatic hip dislocation in childhood, Journal of Pediatric Orthopaedics, Vol 18, pp. 691-694.

Hearmon RFS (1961), An introduction to applied anisotropic elasticity, Oxford University Press, London.

Hedlundh U, Ahnfelt L, Hybbinette CH, Wallinder L, Weckstrom J, Fredin H (1996), Dislocation and the femoral head size in primary Total Hip Arthroplasty, Clinical Orthopaedics and Related Research, Vol 333, pp. 226-233.

Hewitt J, Guilak F, Glisson R, Parker Vail T (2001), Regional material properties of the human hip joint capsule ligaments, Journal of Orthopaedic Research, Vol 19, pp. 359-364.

Hewitt JD, Glisson RR, Guilak F, Parker Vail T (2002), The Mechanical Properties of the Human Hip Capsule Ligaments, The Journal of Arthroplasty, Vol 17, No 1, pp. 82-89.

Hogan HA (1992), Micromechanics modelling of Haversian cortical bone properties, Journal of Biomechanics, Vol 25, pp. 549-556.

Huiskes R, Vroemen W (1986), A standardised finite element model for routine comparative evaluations of femoral hip prostheses, Acta Orthopaedica Belgica, Vol 52, pp. 258-261.

Huiskes R, Weinans H, Grootenboer HJ, Dalstra M, Fudala B, Slooff TJ (1987), Adaptive bone remodelling theory applied to prosthetic design analysis, Journal of Biomechanics, Vol 20, pp. 1135-1150.

Ingard KU (1988), Fundamentals of waves and oscillations, Cambridge University Press, Cambridge.

Ishibashi Y, Rudy TW, Livesay GA, Stone JD, Fu FH, Woo SLY (1997), The effect of anterior cruciate ligament graft fixation site at the tibia on knee stability: evaluation of using a robotic testing system, Arthroscopy: The Journal of Arthroscopic and Related Surgery, Vol 13, No 2, pp. 177-182.

Kang YK, Park HC, Youm Y, Lee IK, Ahn MH, Ihn JC (1993), Three dimensional shape reconstruction and finite element analysis of femur before and after the cementless type of total hip replacement, Journal of Biomedical Engineering, Vol 15, pp. 497-504.

Kastelic J, Galeski A, Baer E (1978), The multicomposite structure of tendon, Connective Tissue Research, Vol 6, pp. 11-23.

Kelley SS, Lachiewicz PF, Hickman JM, Paterno SM (1998), Relationship of femoral head and acetabular size to the prevalence of dislocation, Clinical Orthopaedics and Related Research, Vol 355, pp. 163-170.

Kennedy JC, Hawkins RJ, Willis RB, Danylchuk KD (1976), Tension studies of human knee ligaments, Journal of Bone and Joint Surgery (Am), Vol 58, No 3, pp. 350- 355.

Kennedy JC, Alexander IJ, Hayes KC (1982), Nerve supply of the human knee and its functional importance, American Journal of Sports Medicine, Vol 10, No 6, pp. 329-335.

Keyak JH, Fourkas MG, Meagher JM, Skinner HB (1993), Validation of an automated method of three-dimensional finite element modelling of bone, Journal of Biomedical Engineering, Vol 15, pp. 505-509.

Kleesattel C, Gladwell GML (1968), The contact-impedance meter- 1, Ultrasonics, pp. 175-180.

Kremer JR, Mastronarde DN, McIntosh JR (1996), Computer visualisation of three-dimensional image data using IMOD, Journal of Structural Biology, Vol 116, No 1, pp. 71-76.

Krouskop TA, Doughtery DR, Vinson MD (1987), A pulsed Doppler ultrasonic system for making non-invasive measurements of the mechanical properties of soft tissue, Journal of Rehabilitation Research and Development, Vol 24, No 2, pp 31-38.

Kumaresan S, Yoganandan N, Pintar FA (1998), Finite element modeling approaches of human cervical spine facet joint capsule, Journal of Biomechanics, Vol 31, pp. 371-376.

Lardner TJ, Archer RR (1994), Mechanics of solids: an introduction, McGraw-Hill, New York.

Lejman T, Strong M, Michno P (1995), Capsulorrhaphy versus capsulectomy in open reduction of the hip for developmental dysplasia, Journal of Paediatric Orthopaedics, Vol 15, pp. 98-100.

Lindahl OA, Omata S (1995), Impression technique for the assessment of oedema: comparison with a new tactile sensor that measures physical properties of tissue, Medical & Biological Engineering & Computing, Vol 33, pp. 27-32.

Lindahl OA, Omata S, Änquist K-A (1998), A tactile sensor for detection of physical properties of human skin *in vivo*, J of Med Eng and Technol, Vol 22, No 4, pp. 147-153.

McCollum DE, Gray WJ (1990), Dislocation after Total Hip Arthroplasty- causes and prevention, Clinical Orthopaedics and Related Research, Vol 261, pp. 159-170.

McGrory BJ, Morrey BF, Cahalan TD, An KN, Cabanela ME (1995), Effect of femoral offset on range of motion and abductor muscle strength after total hip arthroplasty, Journal of Bone and Joint Surgery (Br), Vol 77, No 6, pp.865-869.

McKee GM (1970), Development of total prosthetic replacement of the hip, Clinical Orthopaedics, Vol 72, pp. 85-103.

Maaß H, Kühnapfel U (1999), Noninvasive measurement of elastic properties of living tissues, Proceedings of the 13th International Congress on Computer Assisted Radiology and Surgery, Paris, pp. 865-870.

Mabuchi K, Hayatsu K, Fujie H, Yamamoto M (1991), Stiffness of canine stifle joint ligaments at relatively high rates of elongation, Journal of Biomechanical Engineering, Vol 113, No 4, pp. 404-409.

Massie WK, Howorth MB (1954), Congenital dislocation of the hip, Part III, Pathogenesis, Journal of Bone and Joint Surgery (Am), Vol. 33, pp. 190-198.

Moore AT (1957), The self-locking metal hip prosthesis, Journal of Bone and Joint Surgery (Am), Vol 39, pp. 811-827.

Moody D, Lozanoff S (1998), SURFdriver, http://surfdriver.edu.eu.org.

Morrey BF (1992), Instability after Total Hip Arthroplasty, Orthopaedic Clinics of North America, Vol 23, pp. 237-248.

Mow VC, Kuei SC, Lai WM, Armstrong CG (1980). Biphasic creep and stress relaxation of articular cartilage in compression: theory and experiments. Journal of Biomechanical Engineering, Vol 102, pp.73-84.

Müller ME (1970), Total hip prostheses, Clinical Orthopaedics, Vol 72, pp. 46-68.

Nigg BM, Herzog W (1999), Biomechanics of the Musculo-Skeletal System, John Wiley & Sons Ltd, 2nd Edition, New York.

Noyes FR, DeLucas JL, Torvik PJ (1974), Biomechanics of anterior cruciate ligament failure: an analysis of strain-rate sensitivity and mechanisms of failure in primates, Journal of Bone and Joint Surgery (Am), Vol 56, No 2, pp. 236-253.

Noyes FR, Grood ES (1976), The strength of the anterior cruciate ligament in humans and rhesus monkeys, Journal of Bone and Joint Surgery (Am), Vol 58, No 8, pp. 1074-1082.

Omata S, Terunuma Y (1992), New tactile sensor like the human hand and its applications, Sensors and Actuators, Vol 35, pp.9-15.

Ophir J, Cespedes I, Ponnekanti H, Yazdi Y, Li X (1991), Elastography: a quantitative method for imaging the elasticity of biological tissues, Ultrasonic Imaging, Vol 13, pp. 111-134.

Ophir J, Cespedes I, Garra B, Ponnekanti H, Huang Y, Maklad N (1996), Elastography: ultrasonic imaging of tissue strain and elastic modulus in vivo, European Journal of Ultrasound, Vol 3, pp. 49-70.

Ophir J, Alam SK, Garra B, Kallel F, Konofagou E, Krouskop T, Varghese T (1999), Elastography: ultrasonic estimation and imaging of the elastic properties of tissues, Proc Instn of Mechanical Engineers, Vol 213, Part H, pp. 203-233.

Paul JP (1999), Strength requirements for internal and external prostheses, Journal of Biomechanics, Vol 32, pp. 381-393.

Ponnekanti H, Ophir J, Cespedes I (1992), Axial stress distributions between coaxial compressors in elastography: an analytical model, Ultrasound in Medicine and Biology, Vol 18, No 8, pp. 667-673.

Prendergast PJ (1997), Finite element models in tissue mechanics and orthopaedic implant design, Clinical Biomechanics, Vol 12, No 6, pp.343-366.

Prendergast PJ, Toland SJ, Corrigan JP (1994), Finite element analysis and mechanical testing of external fixator designs, Proceedings of The Institution of Mechanical Engineers, Vol 208, Part H, pp.103-110.

Ralphs JR, Benjamin M (1994), The joint capsule: structure, composition, ageing and disease- a review, Journal of Anatomy, Vol 184, pp. 503-509.

Roesler H (1987), The history of some fundamental concepts in bone biomechanics, Journal of Biomechanics, Vol 20, pp. 1025-1034.

Romanes GJ (1977), Cunningham's manual of practical anatomy, 14th Edition, Vol 1, Oxford University Press, New York.

Rudy TW, Livesay GA, Woo SLY, Fu FH (1996), A combined robotic/universal force sensor approach to determine *in situ* forces of knee ligaments, Journal of Biomechanics, Vol 29, No 10, pp. 1357,-1360.

Saada AS (1974), Elasticity- theory and applications, Pergamon Press, Oxford.

Schubert R, Schiemann T, Tiede U, Hoehne KH (1997), Applications and Perspectives in Anatomical 3-Dimensional Modelling of the Visible Human with VOXEL-MAN, Acta Anatomica, Vol 160, No 2, pp. 123-131.

Scifert CF, Brown TD, Pedersen DR, Callaghan JJ (1998), A Finite Element Analysis of factors influencing Total Hip Dislocation, Clinical Orthopaedics and Related Research, Vol 355, pp. 152-162.

Setton LA, Perry CH, Elliott DM, Wyland DJ, LeRoux MA, Guilak F (1999), The anisotropic properties of the healing meniscus in tension. In: Summer Bioengineering Conference, American Society of Mechanical Engineers, Vol 42, pp. 73-74.

Shikata J, Sanada H, Yamamuro T, Takeda T (1979), Experimental studies of the elastic fiber of the capsular ligament: Influence of ageing and sex hormones on the hip joint capsule of rats, Connective Tissue Research, Vol 7, pp. 21-27.

Spilker RL, Maxian TA (1990), A mixed-penalty finite element formulation of the linear biphasic theory for soft tissues, International Journal for Numerical Methods in Engineering, Vol 30, pp. 1063-1082.

Torres-Moreno R (1991), Biomechanical analysis of the interaction between the above-knee residual limb and the prosthetic socket, PhD Thesis, University of Strathclyde.

Trent PS, Walker PS, Wolf B (1976), Ligament length patterns, strength and rotational axes of the knee joint, Clinical Orthopaedics and Related Research, Vol 117, pp.263-270.

Viidik A (1966), Biomechanics and functional adaptation of tendons and joint ligaments. In: Studies on the anatomy and function of bone and joints, edited by FG Evans, Springer-Verlag, New York, pp. 17-39.

von Langenbeck B, Vorstellung eines Falles von geheilter Enterotomie (1878), Verhandlungen der Deutschen Gesellschaft für Chirurgie, Vol 7, pp. 40-46.

Watson-Jones R (1936), Fractures of the neck of the femur, British Journal of Surgery, Vol 23, pp. 787-808.

Weber M, Ganz R (1997), Recurrent traumatic dislocation of the hip: report of a case and review of the literature, Journal of Orthopaedic Trauma, Vol 11, No 5, pp. 382-385.

Weinans H, Huiskes R, Grootenboer HJ (1993), Quantitative analysis of bone reactions to relative motions at implant-bone interfaces, Journal of Biomechanics, Vol 26, pp. 1271-1281.

White RE, Forness TJ, Allman JK, Junick DW (2001), Effect of posterior capsular repair on early dislocation in primary Total Hip Replacement, Clinical Orthopaedics and Related Research, Vol 393, pp. 163-167.

Williams JF, Gottesmann MJ (1982), Dislocation after Total Hip Arthroplasty-treatment with an above-knee hip spica cast, Clinical Orthopaedics and Related Research, Vol 171, pp. 53-58.

Wingstrand H, Wingstrand A, Krantz P (1990), Intracapsular and atmospheric pressure in the dynamics and stability of the hip- a biomechanical study, Acta Orthopaedica Scandinavica, Vol 61, No 3, pp. 231-235.

Woo SLY, Peterson RH, Ohland KJ, Sites TJ, Danto MI (1990), The effects of strain rate on the properties of medial collateral ligament in skeletally immature and mature rabbits: a biomechanical and histological study, Journal of Orthopaedic Research, Vol 8, pp. 712-721.

Wroblewski BM, Fleming PA, Siney PD (1999), Charnley low-frictional arthroplasty of the hip. 20 to 30 years results, Journal of Bone and Joint Surgery (Br), Vol 81, No 3, pp. 427-430.

Yamakoshi Y, Sato J, Sato T (1990), Ultrasonic imaging of internal vibration of soft tissue under forced vibration, IEEE Trans Ultrason Ferroelec Freq Control, Vol 37, pp. 45-53.

Yuan LJ, Shih CH (1999), Dislocation after Total Hip Arthroplasty, Archives of Orthopaedic Trauma Surgery, Vol 119, pp. 263-266.

Zuckermann S (1963), A new system of anatomy- A dissector's guide and atlas, Oxford University Press, Oxford.

APPENDIX

I. Tactile Sensor Theories

In this section of the appendix it is presented on which main functions and vibration properties the tactile biosensor's operation is based. The following equations are based on the analysis that has been reported by Kleesattel and Gladwell (1968) and involves the contact impedance meter theory.

Thereby the outline is based on a simple test arrangement of a plain rod on which an indenter is attached. This set-up is brought into contact with the surface of a large test-piece. Onto this set-up an alternating force with a given frequency is applied. Function (3.6) that has been presented in chapter 3 has resulted from a number of adjustments that have been applied on an ideal loss-less situation. This situation has been adjusted with the following features in order to make the stiffness measurement more realistic. These adjustment features include:

1. Adjustment for non-rigidity of indenter tip

This adjustment is expressed by the surface compliance of the indenter:

$$q_t = C \frac{1-\nu_t}{E_t \sqrt{S_c}} \qquad (1)$$

This part is incorporated into the final impedance function to make up for the initial assumption that the indenter tip is rigid, which is not the case

2. Adjustment for Finite Size of Test Piece

This adjustment is applied in order to compensate for the fact that the test-piece is not semi-infinite in size, but in fact has a finite size. This correction term that is applied has a value that is chosen empirically for the various contact materials, because of the fact that its calculation is a complex process that is depending on the vibration frequency of the rod.

II. Normality Tests for Populations in Study of Risk of Posterior Dislocation

The following graphs resulted from the normality tests that were performed for the data. These normality tests were necessary, because the employed statistical method for the comparison of the data (paired t-test) assumes normal distribution of the population. This test performs a null hypothesis test with H_0= the data follows a normal distribution versus H_1= the data does not follow a normal distribution. The y-axis shows the probability of certain values to actually occur. These values are on the x-axis. The red line indicates where these values would fall in a normal distribution.

Neutral

Specimen 2 (Abduction)

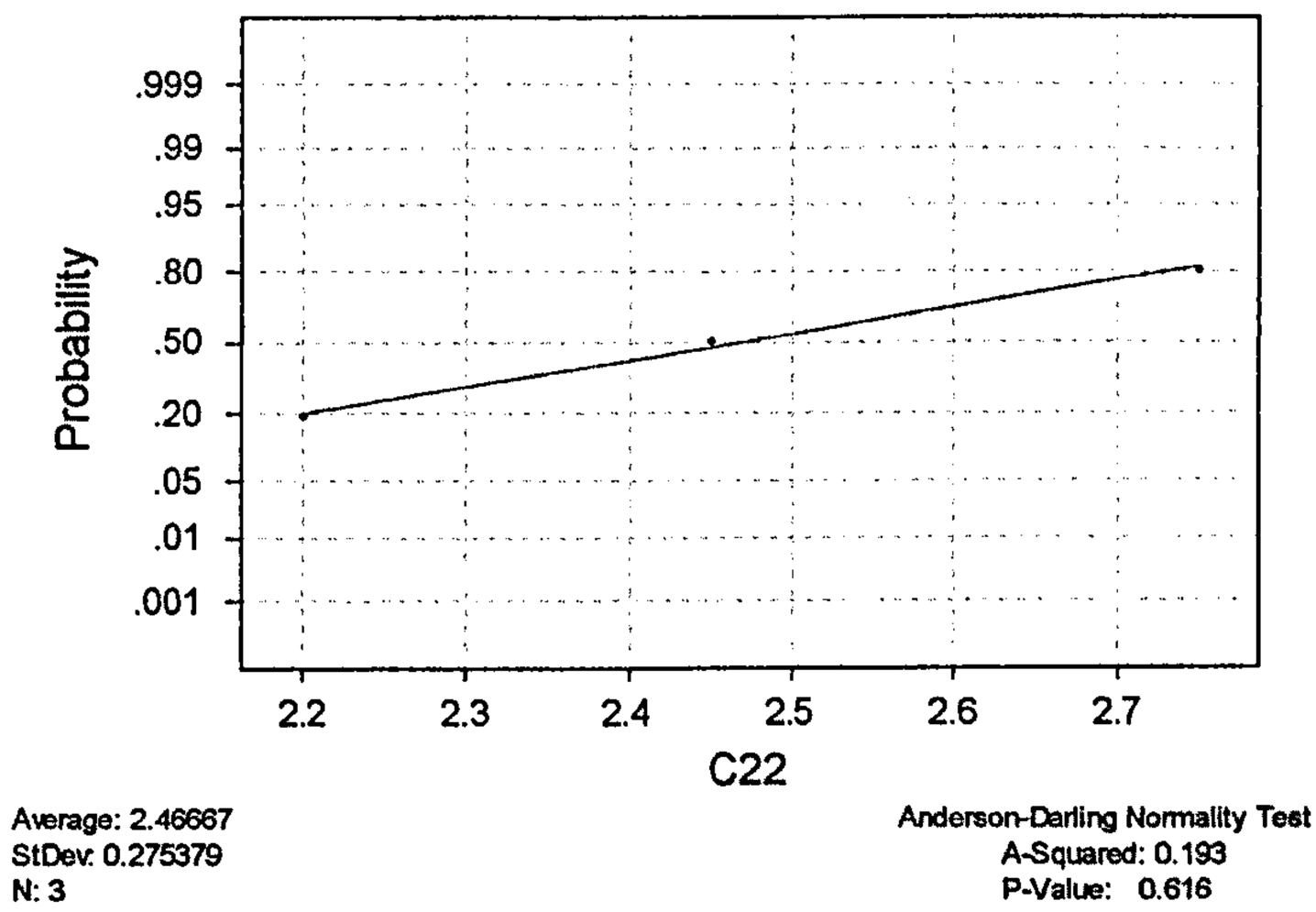

Fig. 3.1 Normality Test for the population (paired difference between data for **intact capsule** and **transsected ischiofemoral ligament**) used in the paired t-test

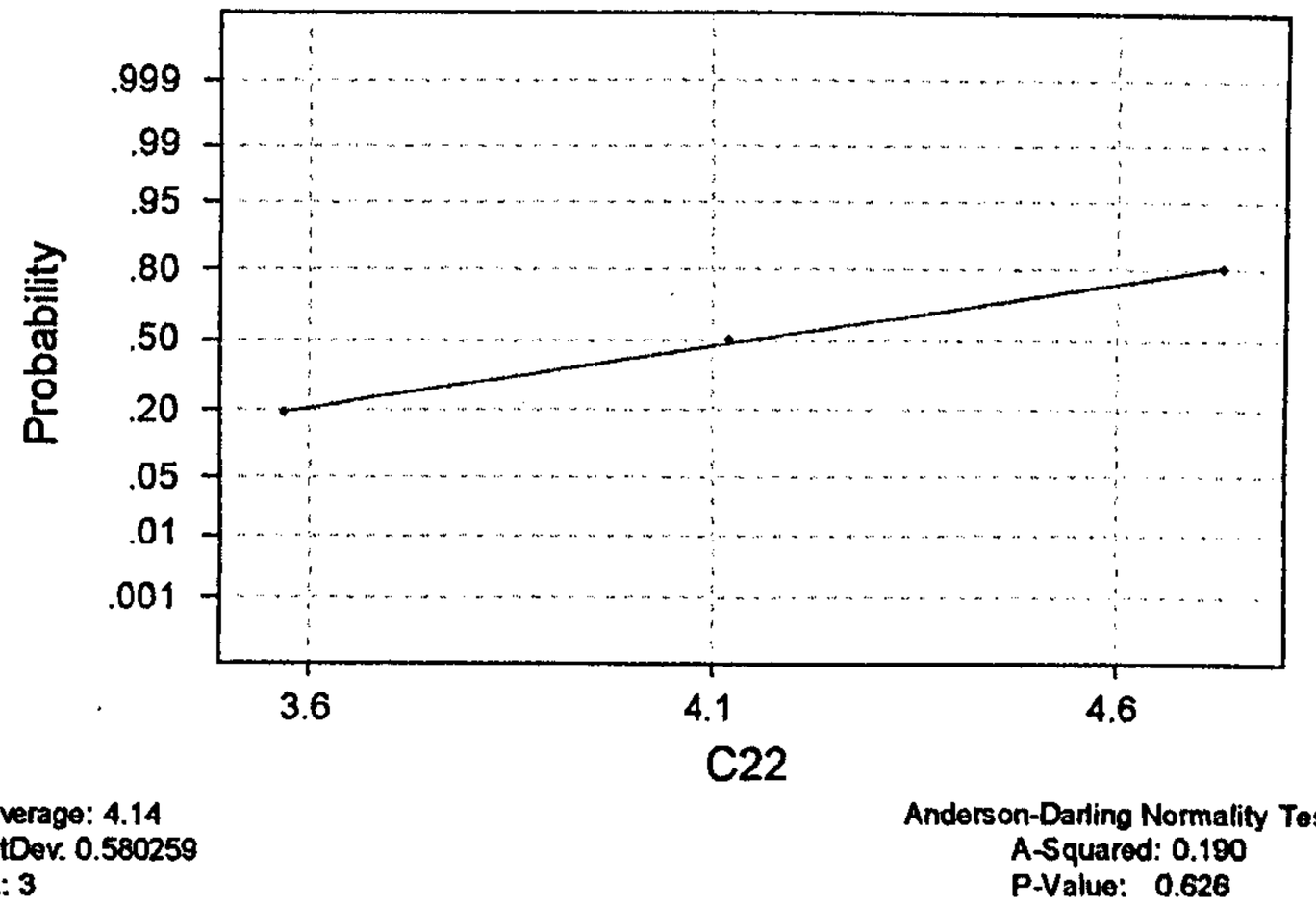

Fig. 3.2 Normality Test for the population (paired difference between data for **intact capsule** and **transsected ischiofemoral and lateral iliofemoral ligaments**) used in the paired t-test

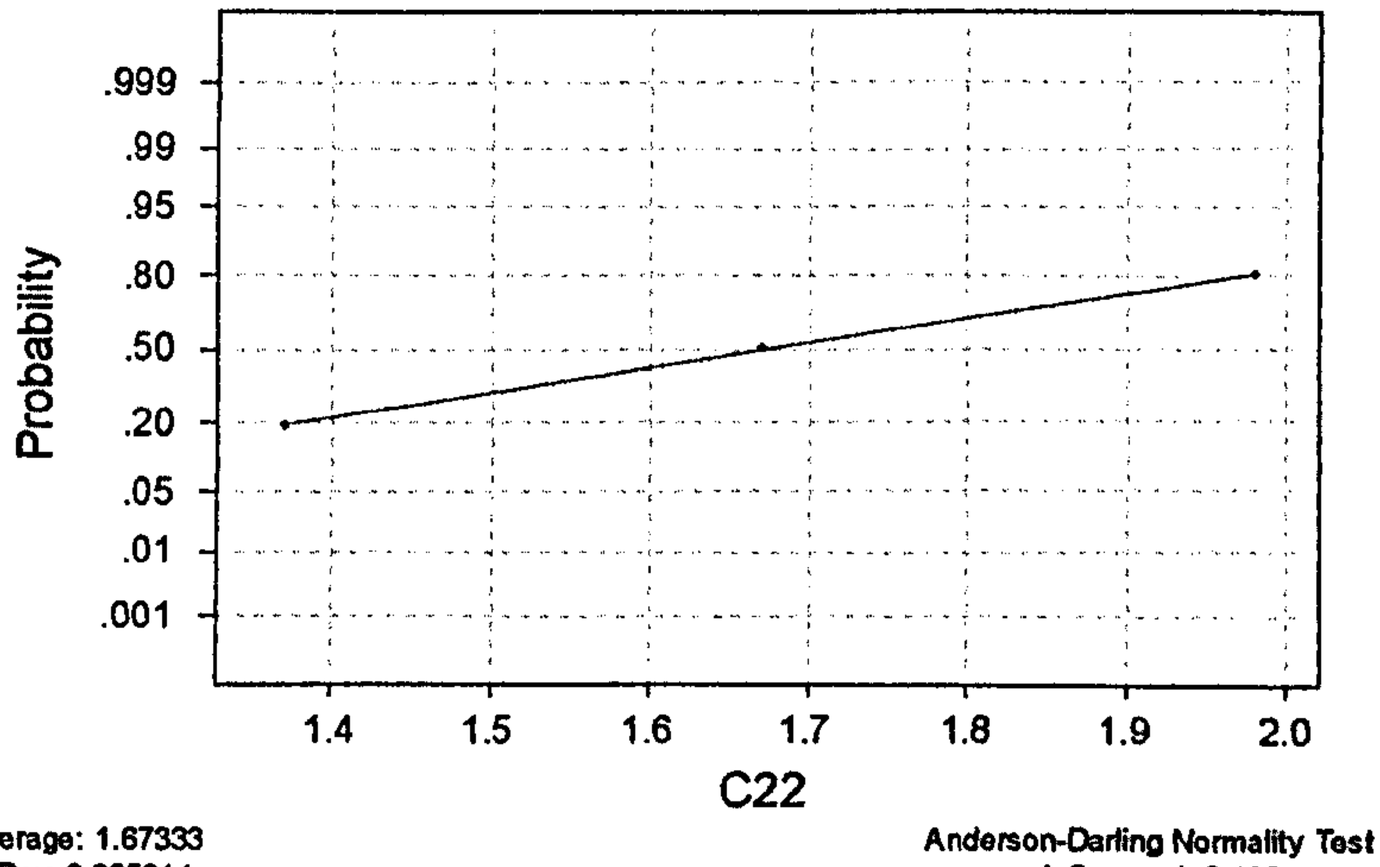

Fig. 3.3 Normality Test for the population (paired difference between data for **transsected ischiofemoral** and **transsected ischiofemoral and lateral iliofemoral ligaments**) used in the paired t-test

Specimen 2 (Adduction)

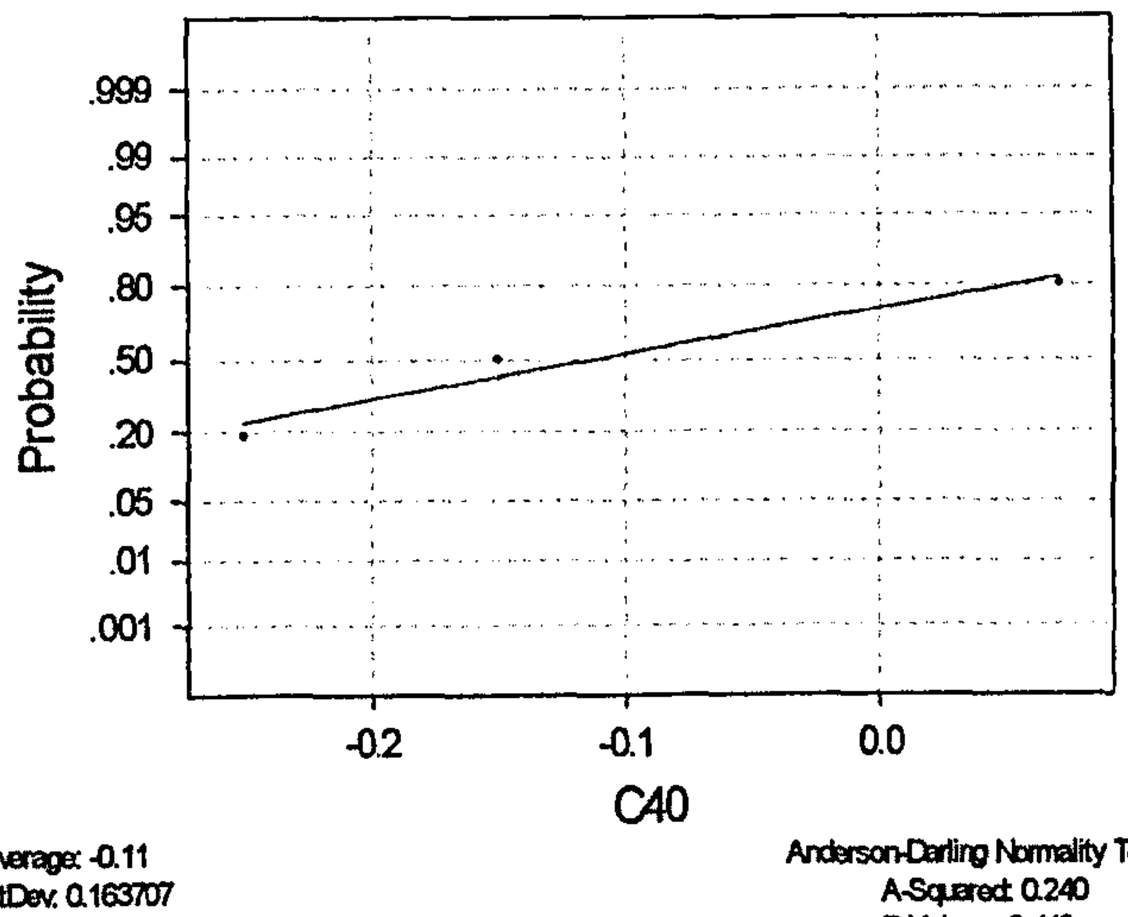

Fig 3.4 Normality Test for the population (paired difference between data for **intact capsule** and **transsected ischiofemoral ligament**) used in the paired t-test

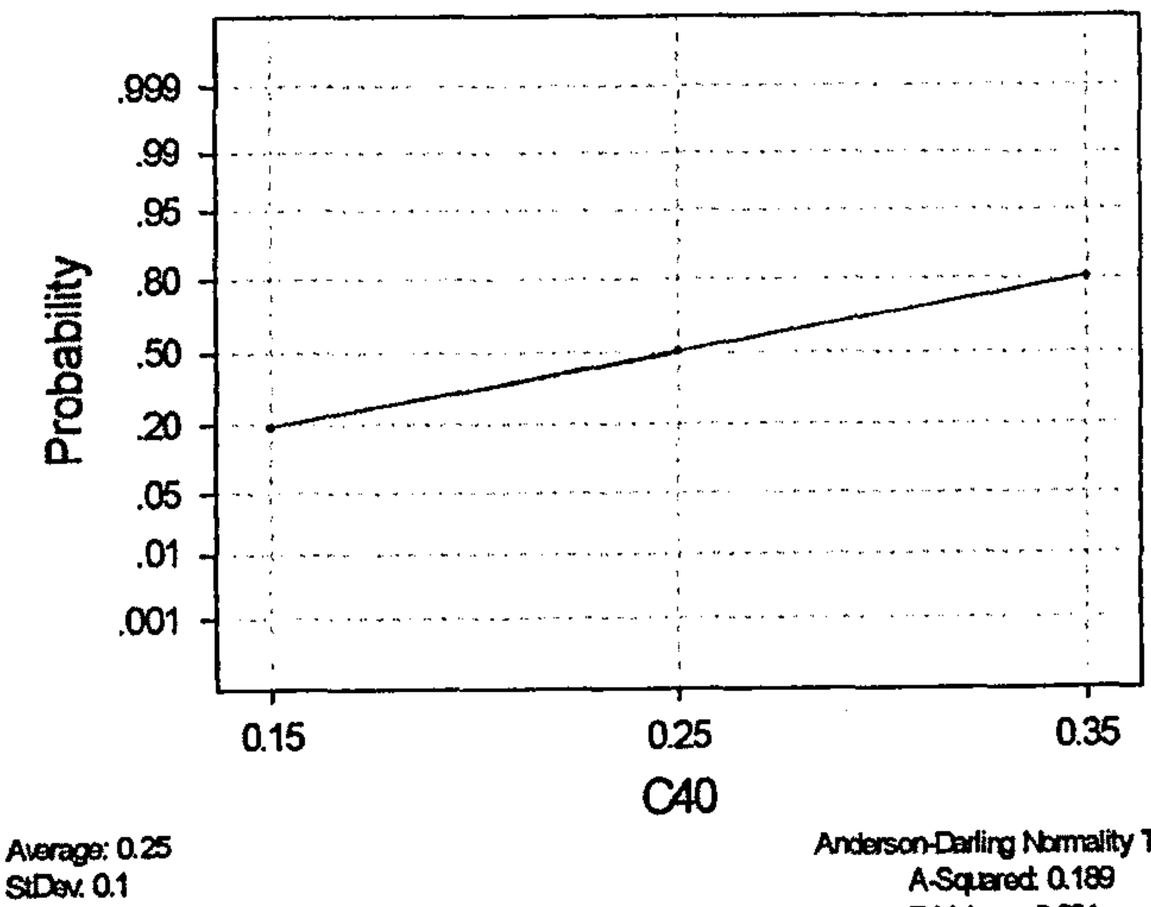

Fig 3.5 Normality Test for the population (paired difference between data for **intact capsule** and **transsected ischiofemoral and lateral iliofemoral ligaments**) used in the paired t-test

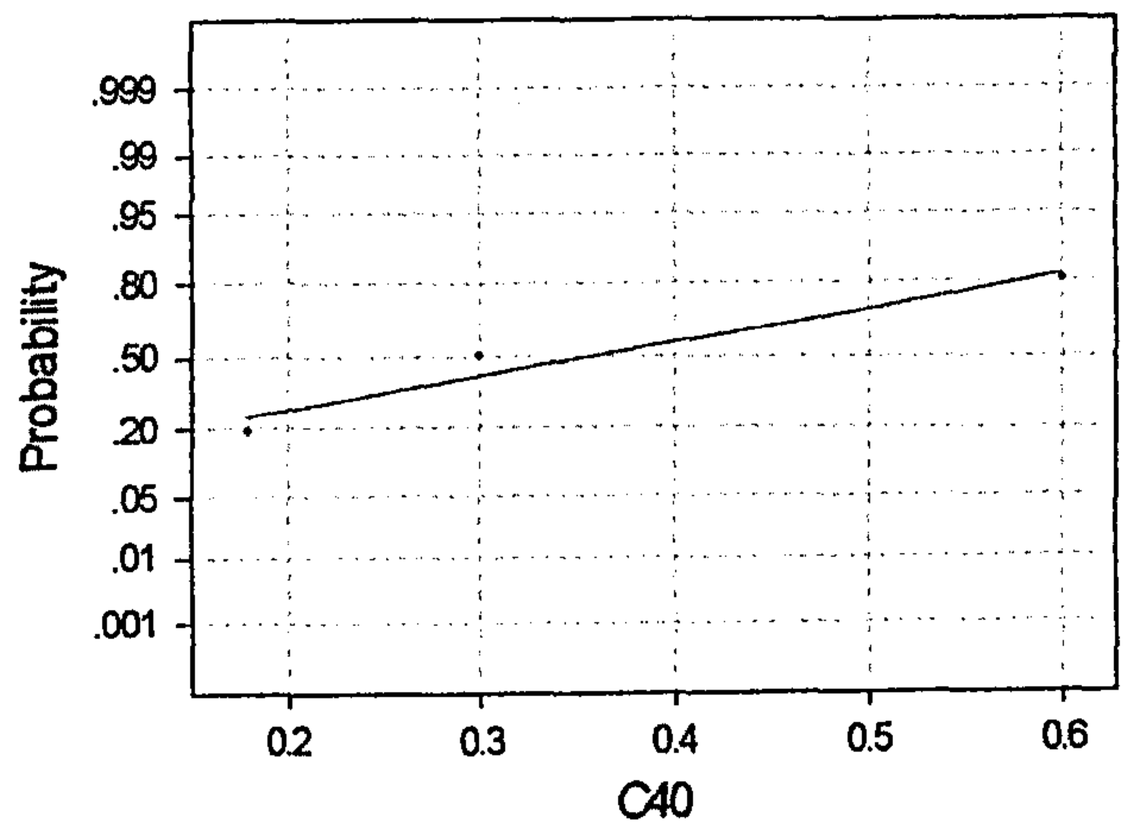

Fig 3.6 Normality Test for the population (paired difference between data for **transsected ischiofemoral &transsected ischiofemoral and lateral iliofemoral ligaments**) used in the paired t-test

Specimen 3 (Abduction)

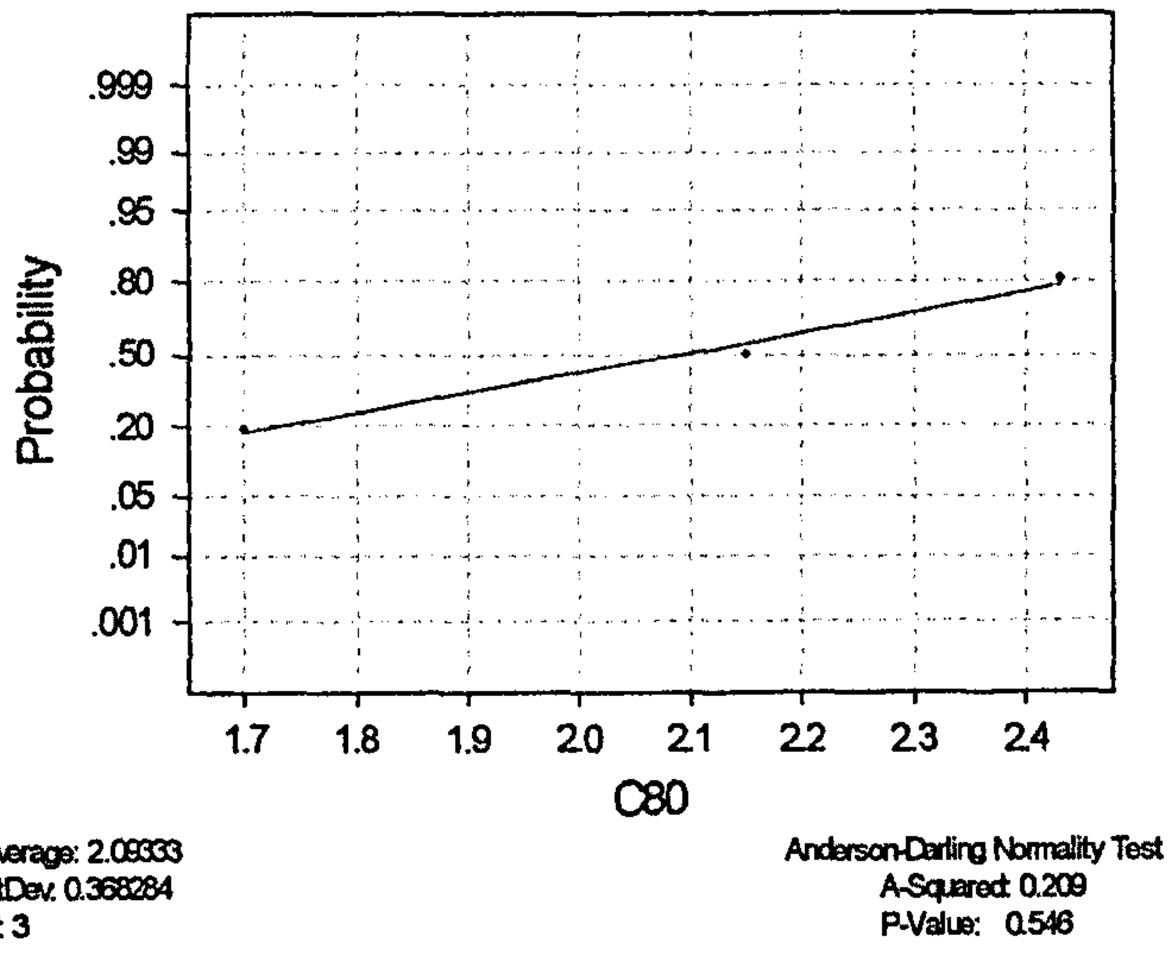

Fig 3.7 Normality Test for the population (paired difference between data for **intact capsule** and **transsected ischiofemoral ligament**) used in the paired t-test

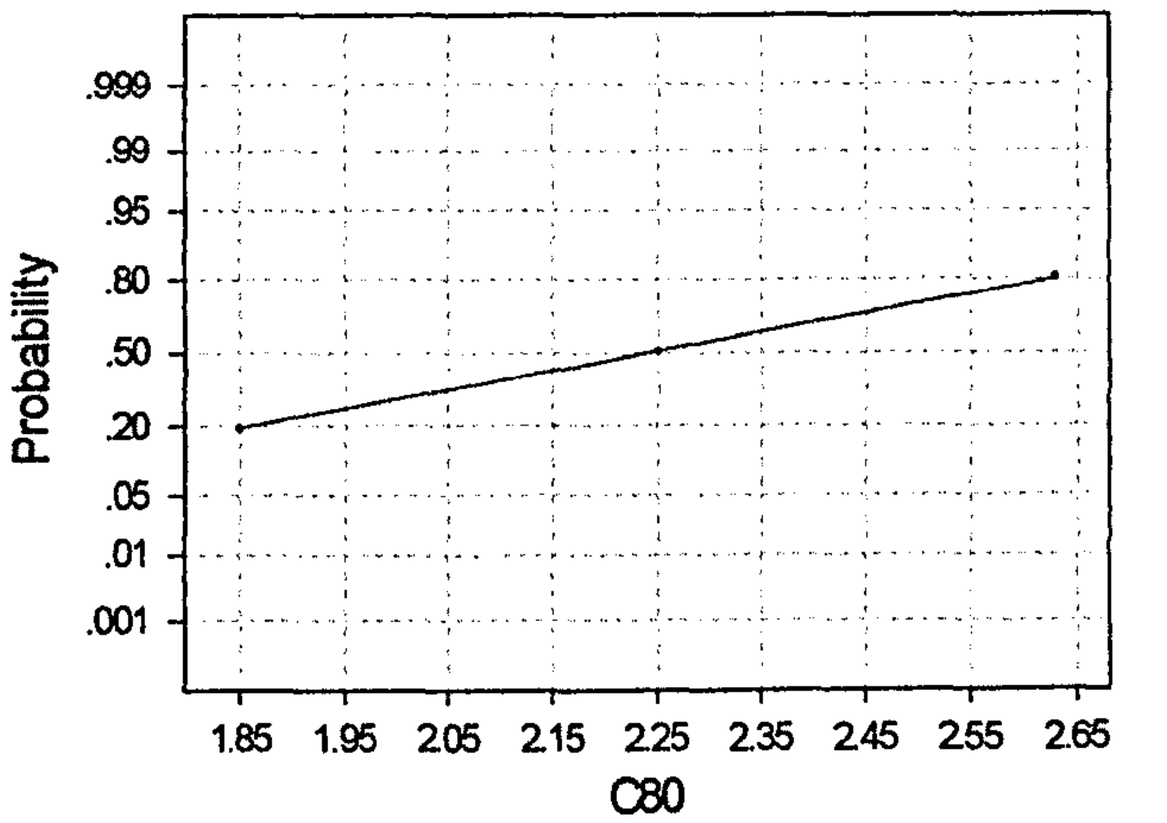

Fig 3.8 Normality Test for the population (paired difference between data for **intact capsule** and **transsected ischiofemoral and lateral iliofemoral ligaments**) used in the paired t-test

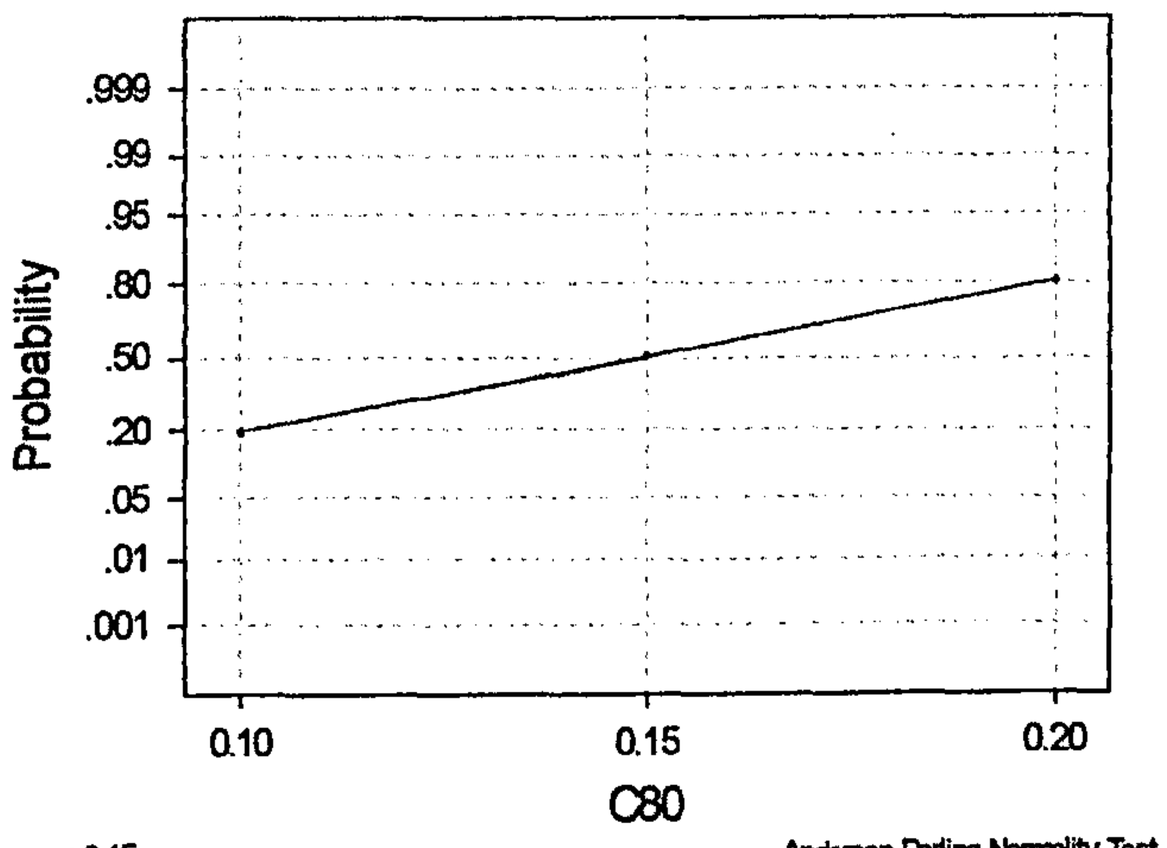

Fig 3.9 Normality Test for the population (paired difference between data for **transsected ischiofemoral &transsected ischiofemoral and lateral iliofemoral ligaments**) used in the paired t-test

Specimen 3 (Adduction)

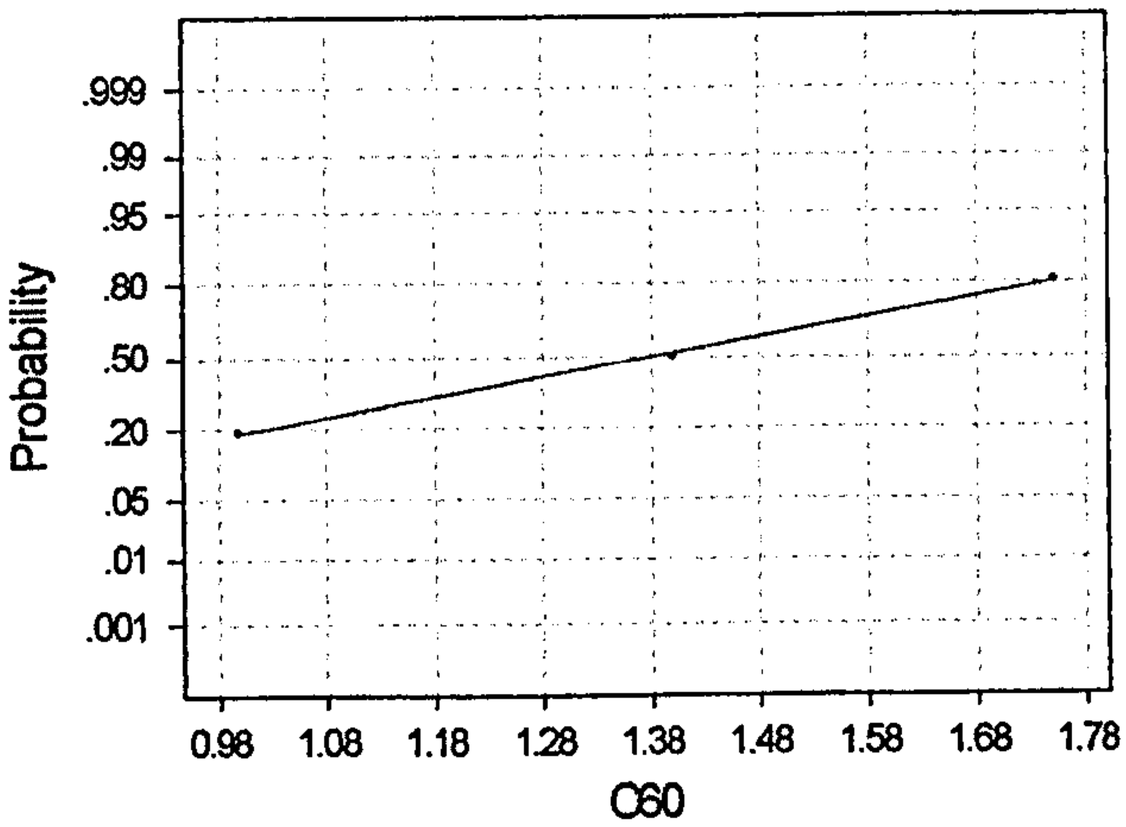

Fig 3.10 Normality Test for the population (paired difference between data for **intact capsule** and **transsected ischiofemoral ligament**) used in the paired t-test

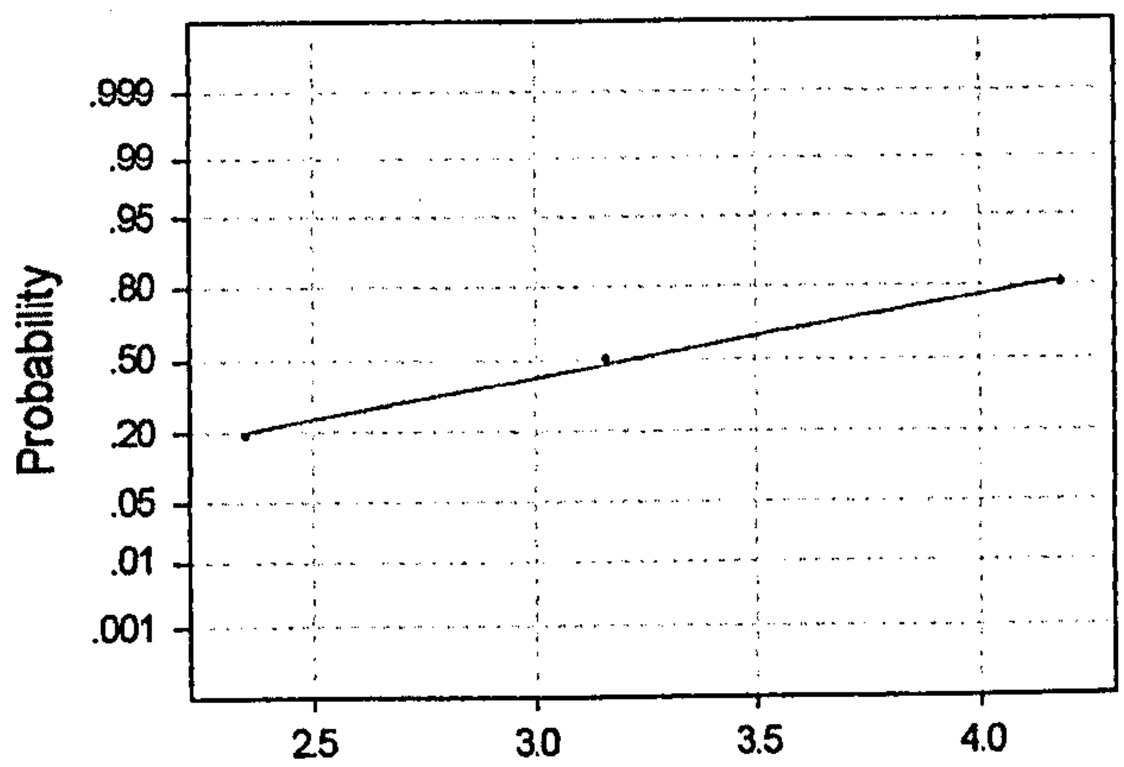

Fig 3.11 Normality Test for the population (paired difference between data for **intact capsule** and **transsected ischiofemoral and lateral iliofemoral ligaments**) used in the paired t-test

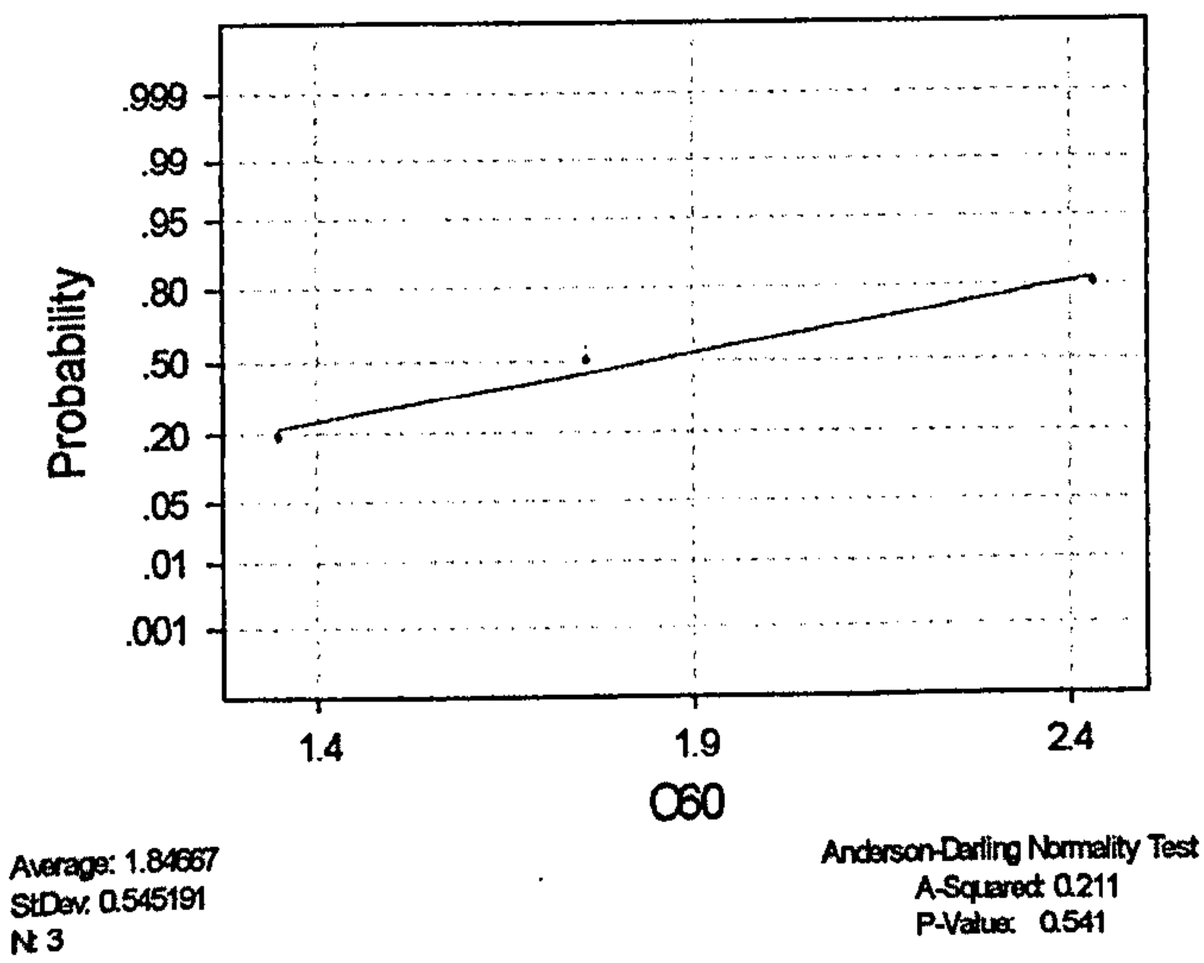

Fig 3.12 Normality Test for the population (paired difference between data for **transsected ischiofemoral &transsected ischiofemoral and lateral iliofemoral ligaments**) used in the paired t-test

Specimen 2 and 3 (Abduction)

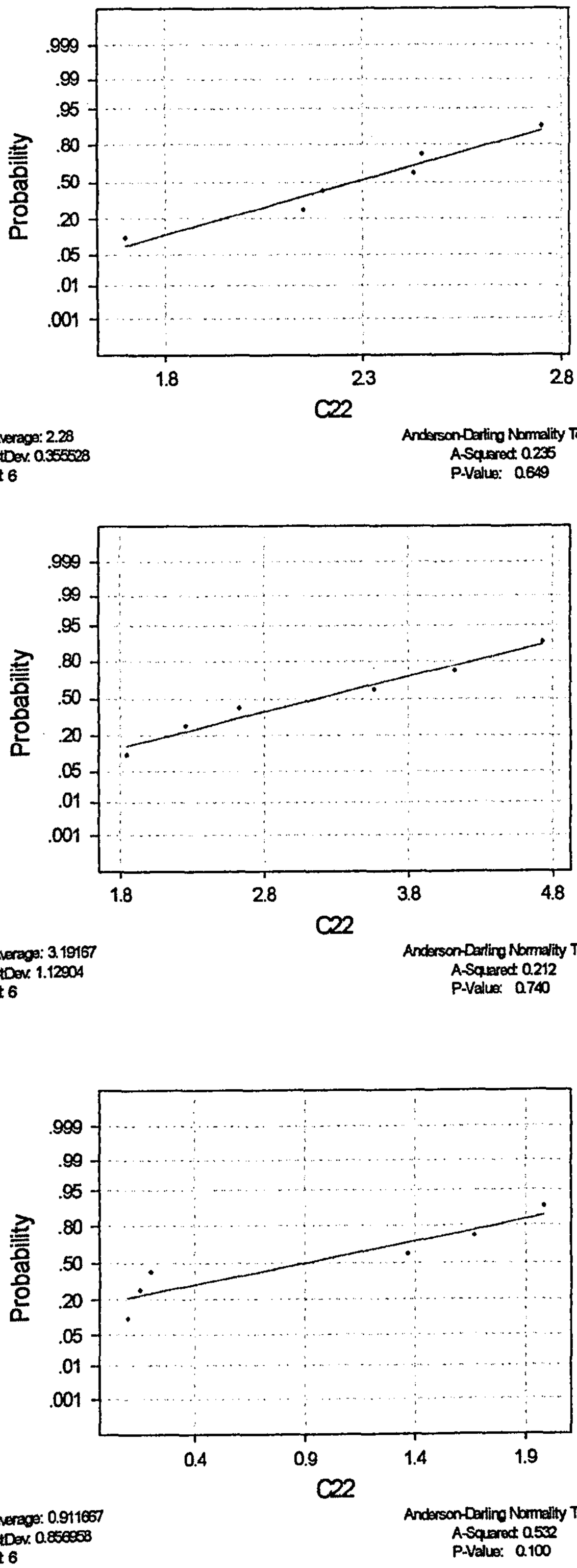

Fig 3.13 Normality Test for the population (paired difference between data for **intact capsule** and **transsected ischiofemoral ligament**) used in the paired t-test

Fig 3.14 Normality Test for the population (paired difference between data for **intact capsule** and **transsected ischiofemoral and lateral iliofemoral ligaments**) used in the paired t-test

Fig 3.15 Normality Test for the population (paired difference between data for **transsected ischiofemoral &transsected ischiofemoral and lateral iliofemoral ligaments**) used in the paired t-test

Specimen 2 and 3 (Adduction)

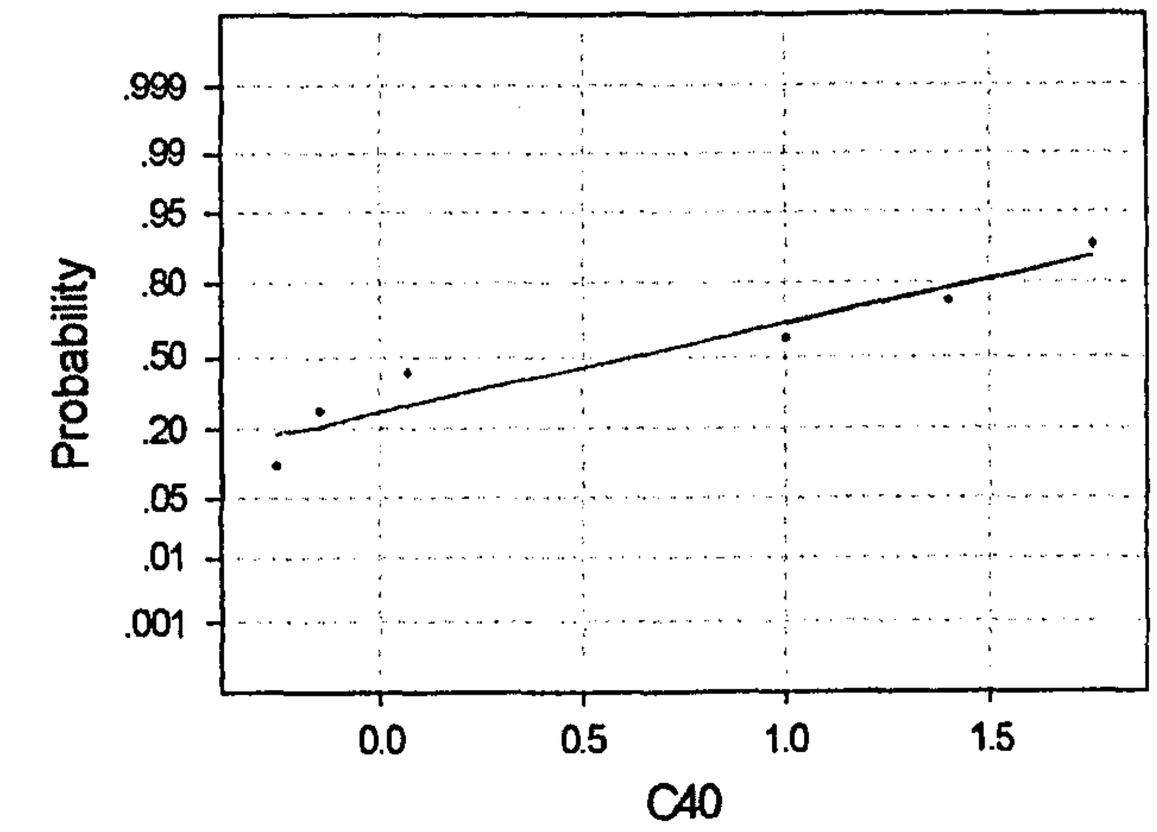

Fig 3.16 Normality Test for the population (paired difference between data for **intact capsule** and **transsected ischiofemoral ligament**) used in the paired t-test

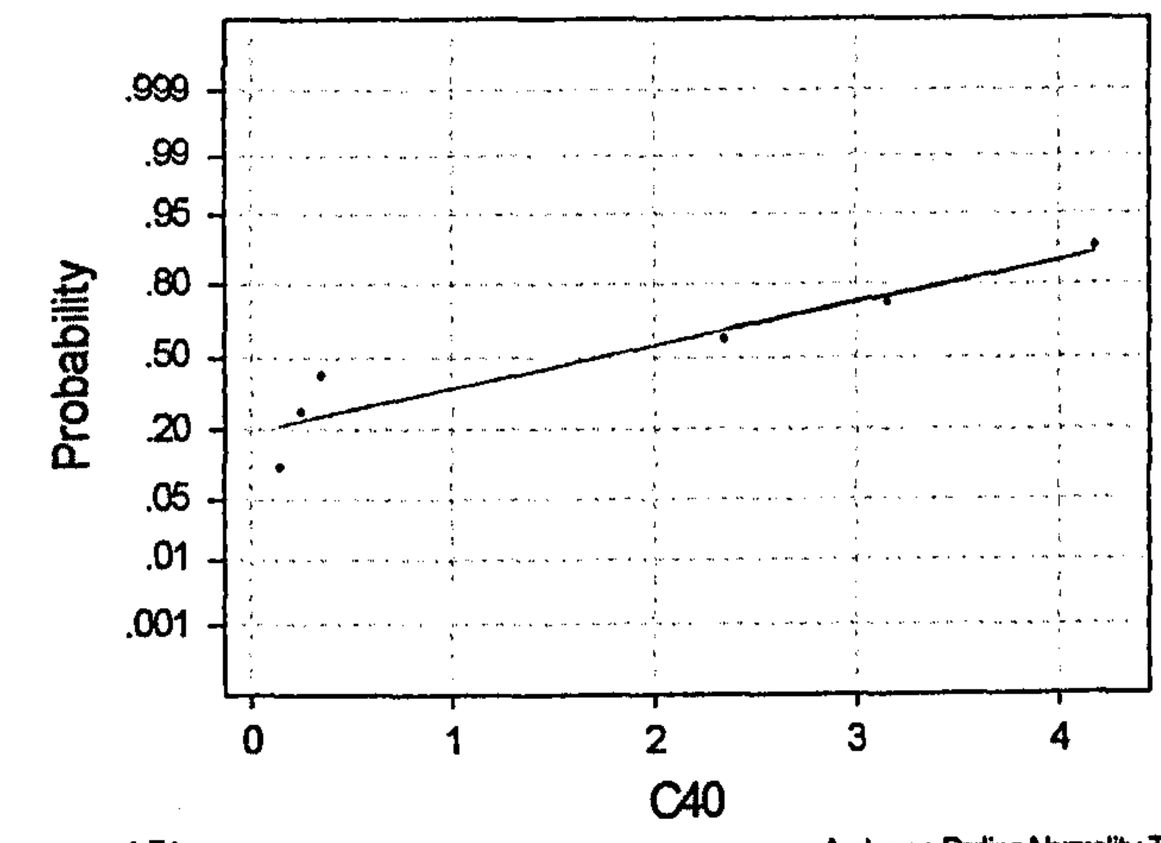

Fig 3.17 Normality Test for the population (paired difference between data for **intact capsule and transsected ischiofemoral and lateral iliofemoral ligaments**) used in the paired t-test

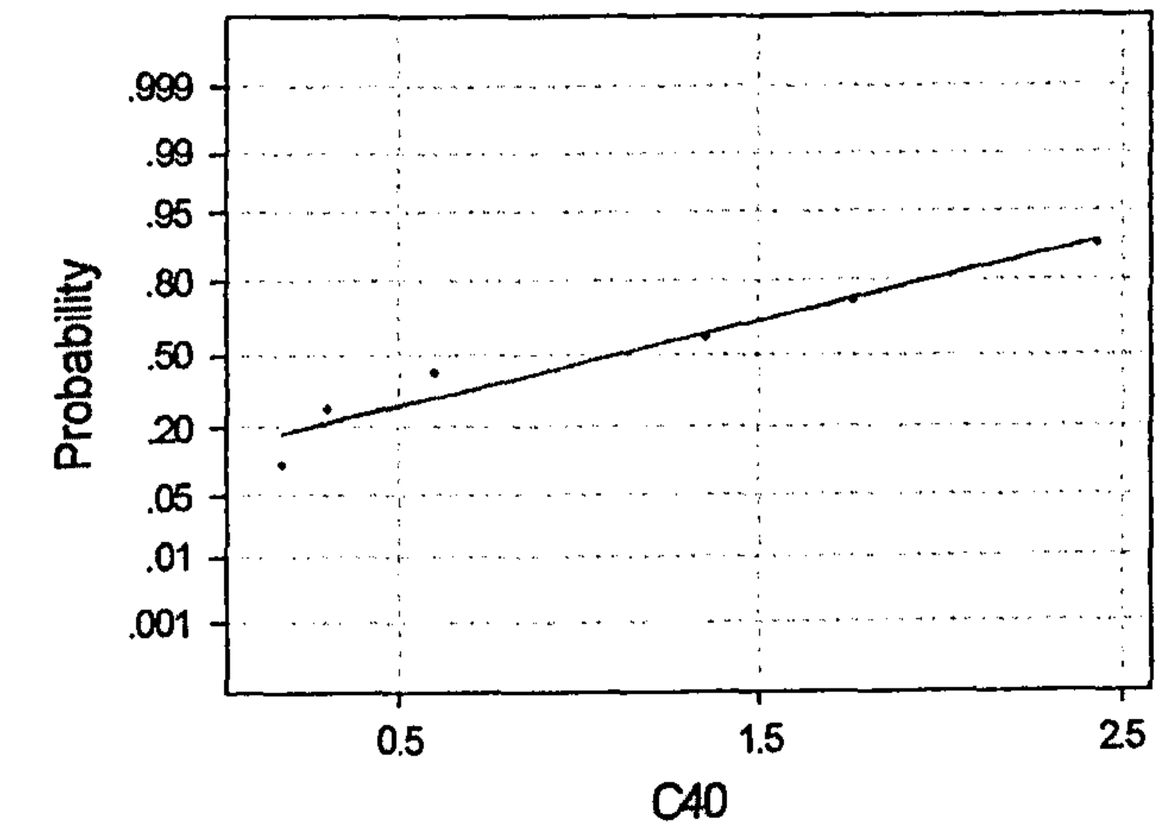

Fig 3.18 Normality Test for the population (paired difference between data for **transsected ischiofemoral &transsected ischiofemoral and lateral iliofemoral ligaments**) used in the paired t-test

Full Flexion

Specimen 2 (Abduction)

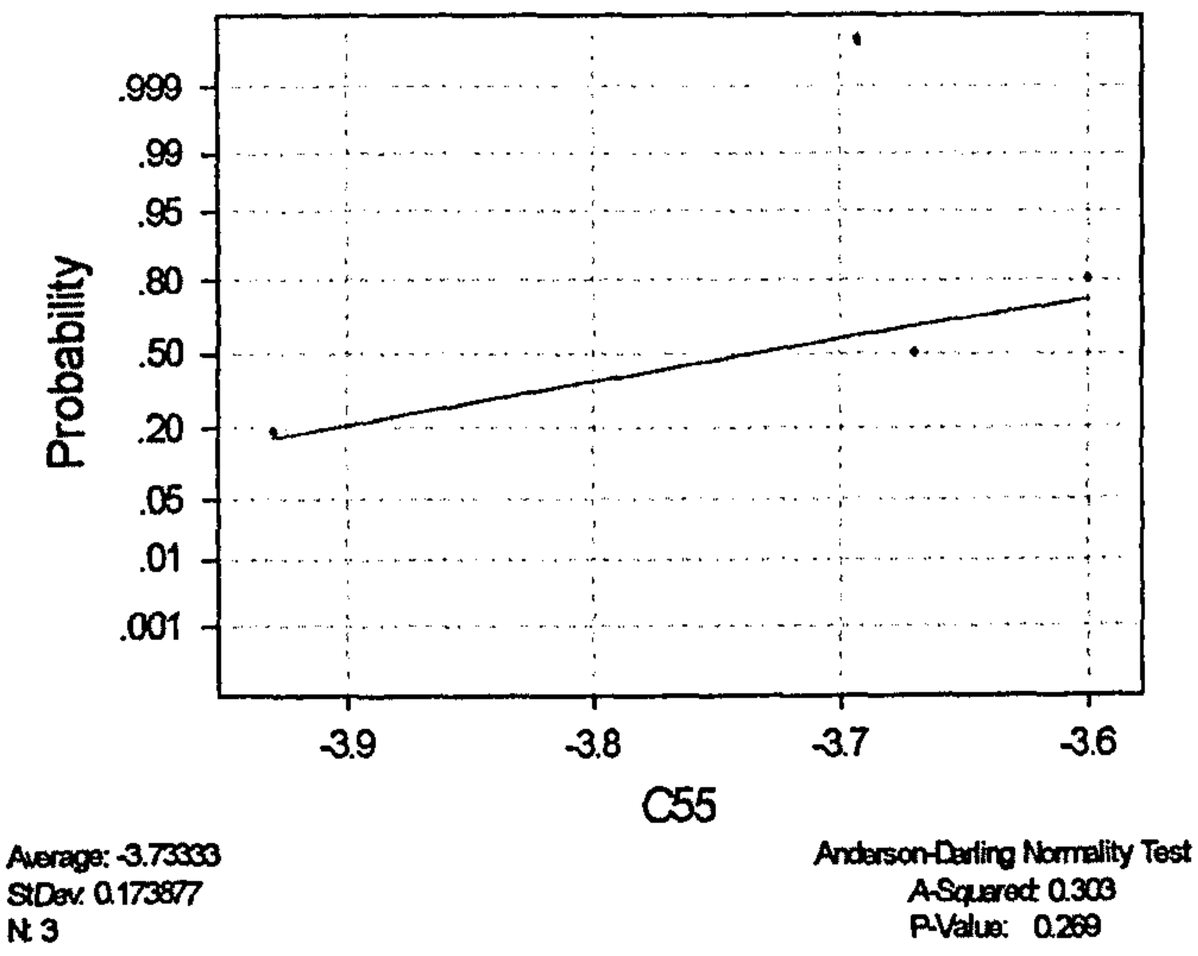

Fig 3.19 Normality Test for the population (paired difference between data for **intact capsule** and **transsected ischiofemoral ligament**) used in the paired t-test

Specimen 2 (Adduction)

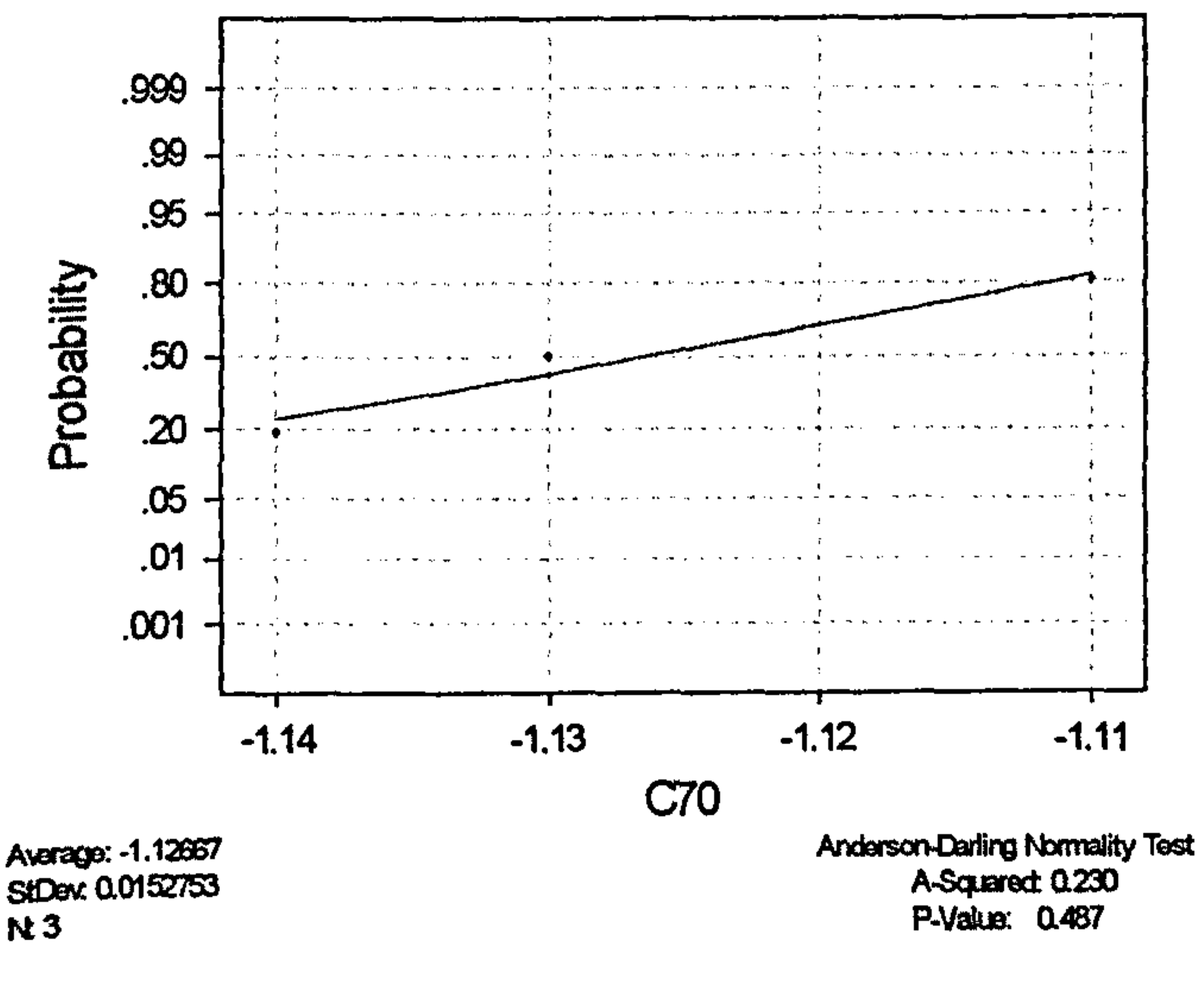

Fig 3.20 Normality Test for the population (paired difference between data for **intact capsule** and **transsected ischiofemoral ligament**) used in the paired t-test

Specimen 3 (Abduction)

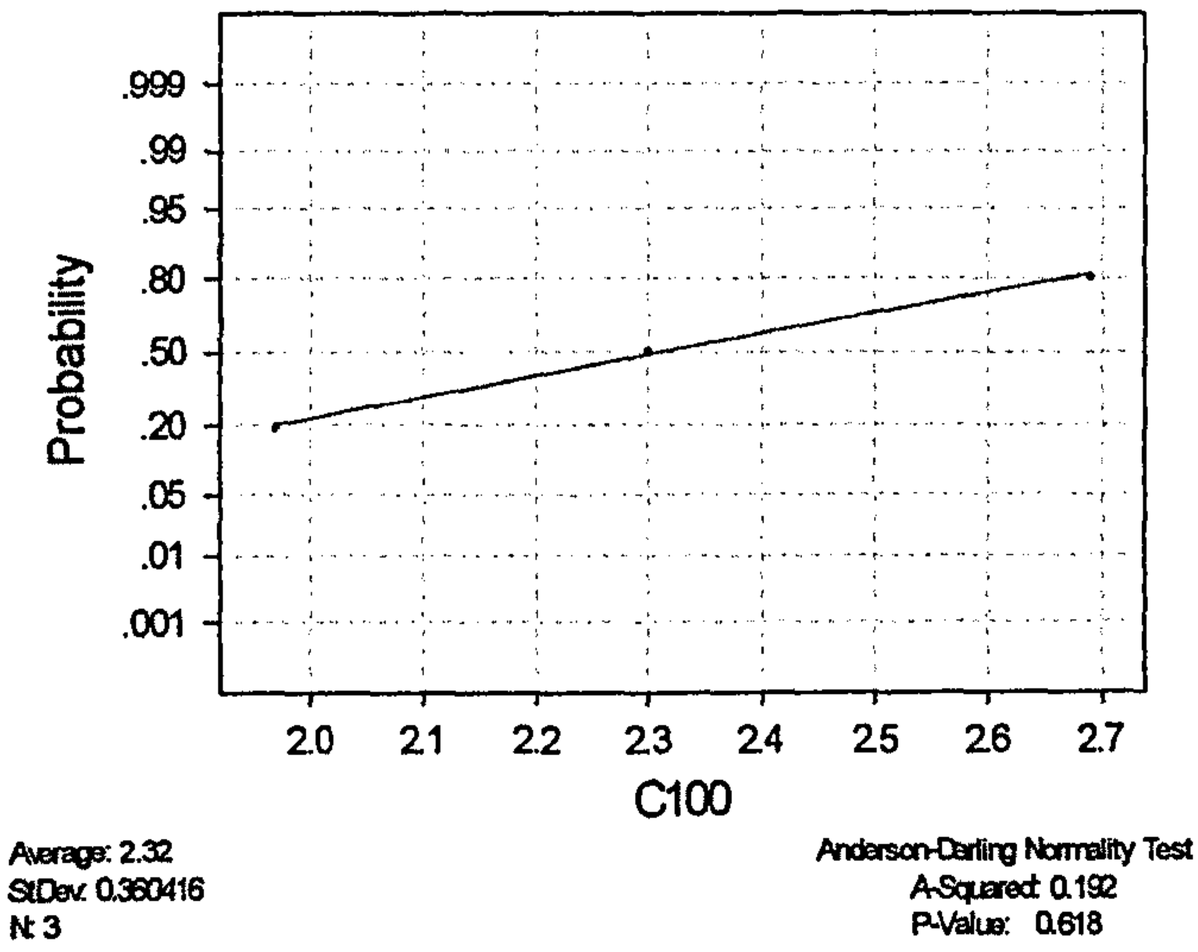

Fig 3.21 Normality Test for the population (paired difference between data for **intact capsule** and **transsected ischiofemoral ligament**) used in the paired t-test

Specimen 3 (Adduction)

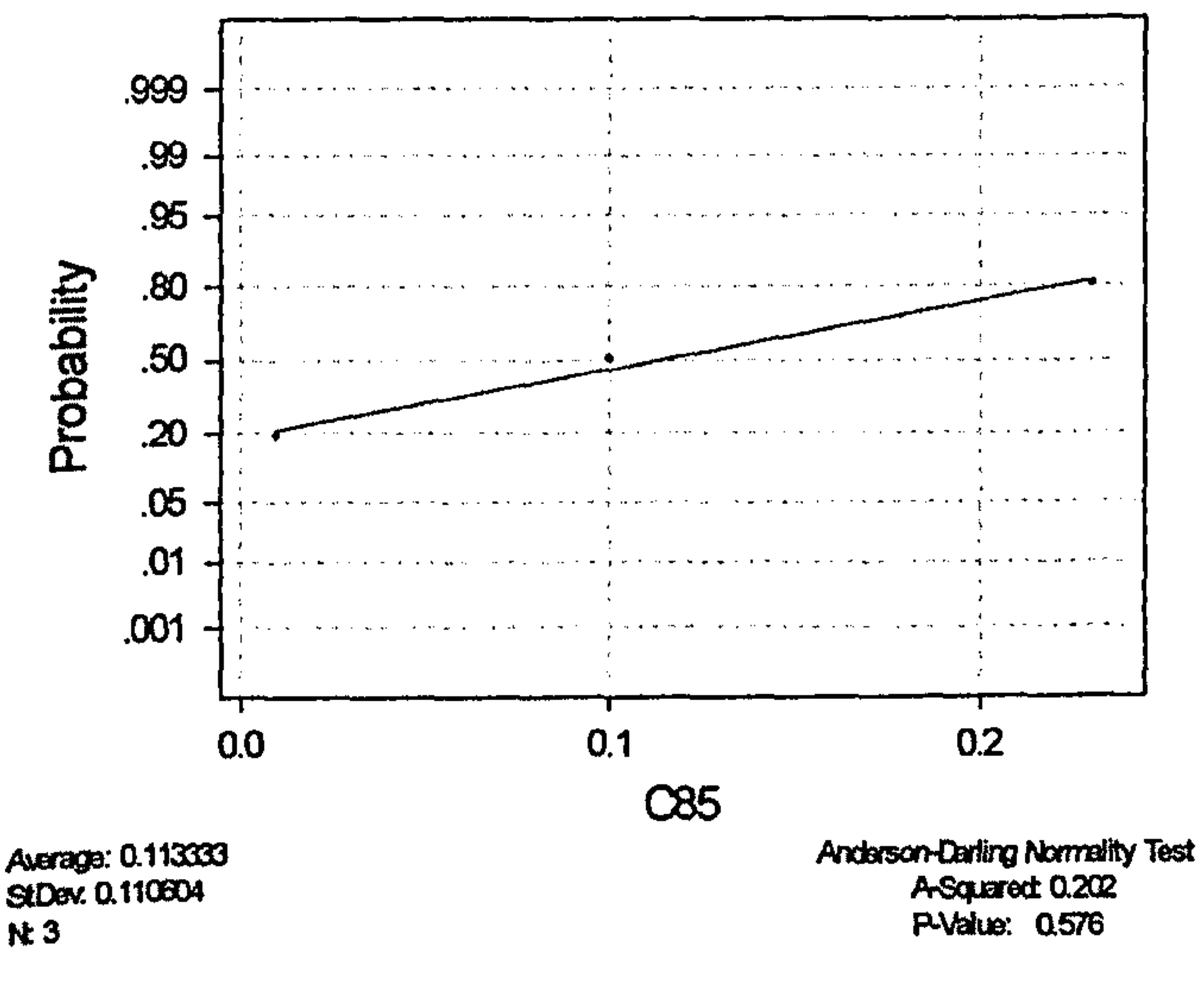

Fig 3.22 Normality Test for the population (paired difference between data for **intact capsule** and **transsected ischiofemoral ligament**) used in the paired t-test

Specimen 2 and 3 (Abduction)

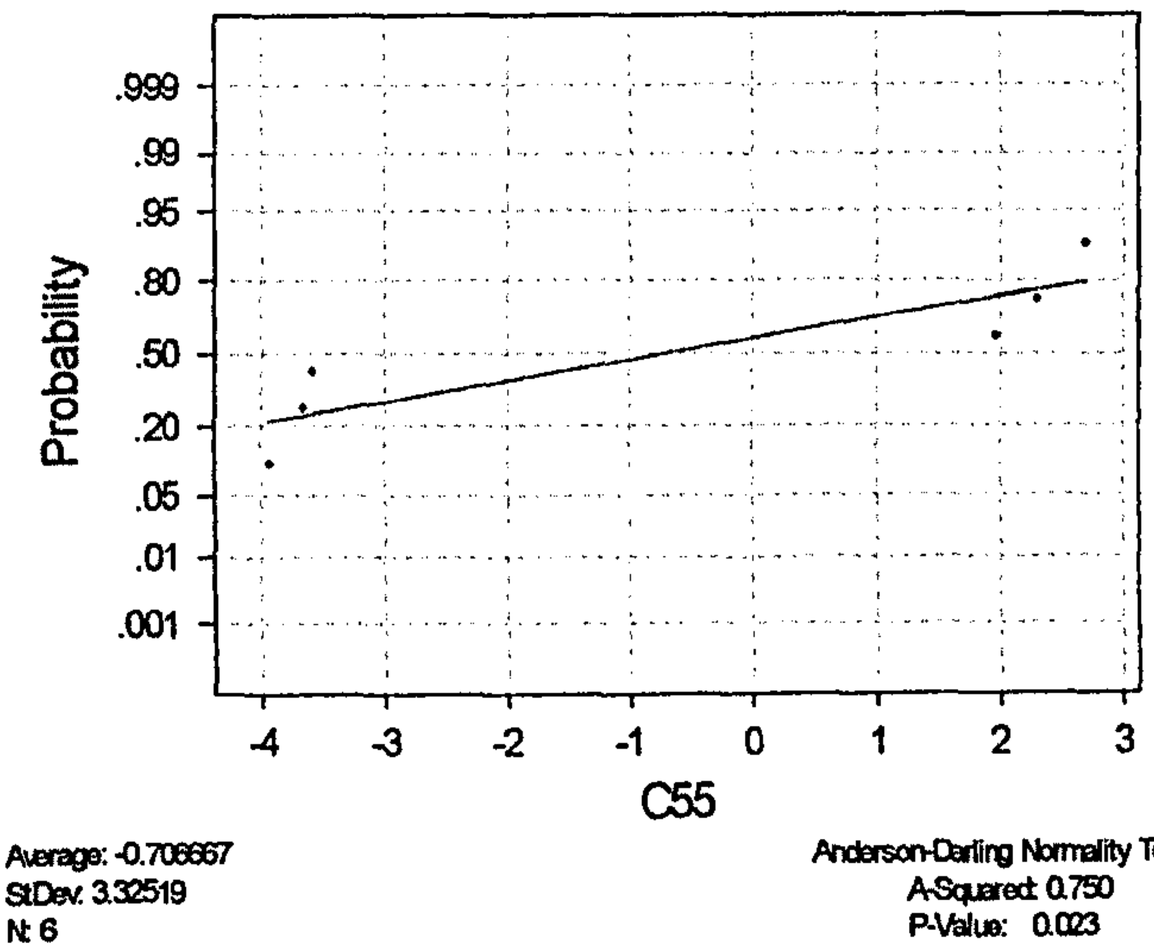

Fig 3.23 Normality Test for the population (paired difference between data for **intact capsule and transsected ischiofemoral ligament**) used in the paired t-test

Specimen 2 and 3 (Adduction)

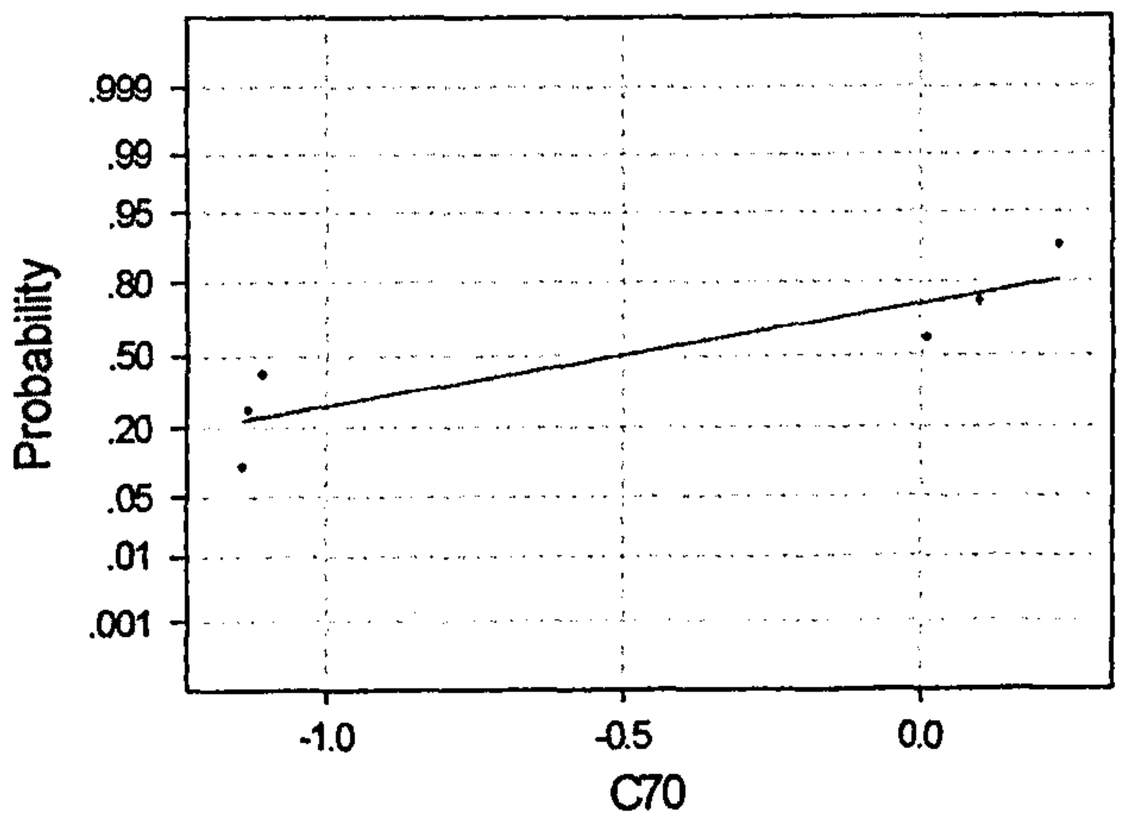

Fig 3.24 Normality Test for the population (paired difference between data for **intact capsule and transsected ischiofemoral ligament**) used in the paired t-test

Full Flexion and Internal Rotation

Specimen 2 (Abduction)

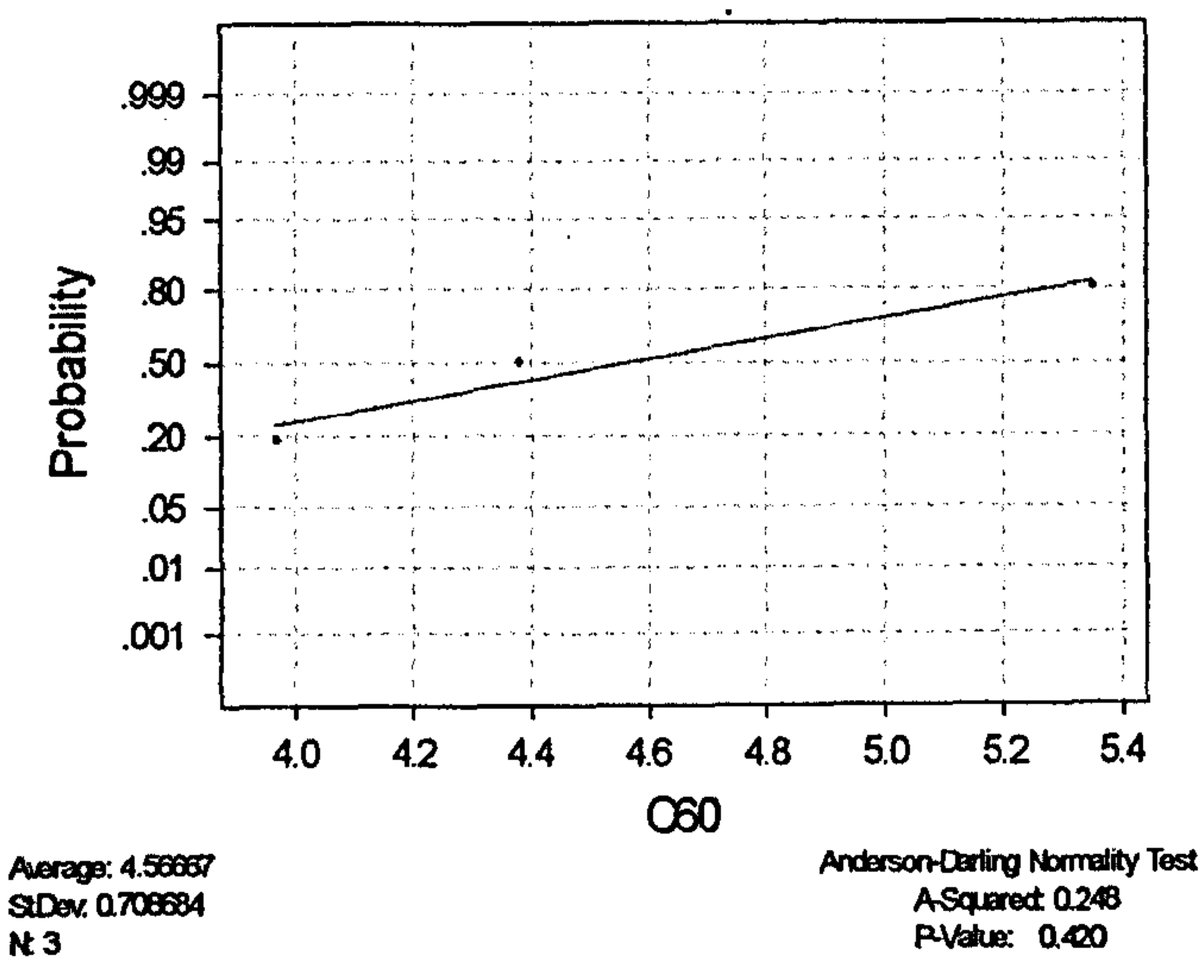

Fig 3.25 Normality Test for the population (paired difference between data for **intact capsule** and **transsected ischiofemoral ligament**) used in the paired t-test

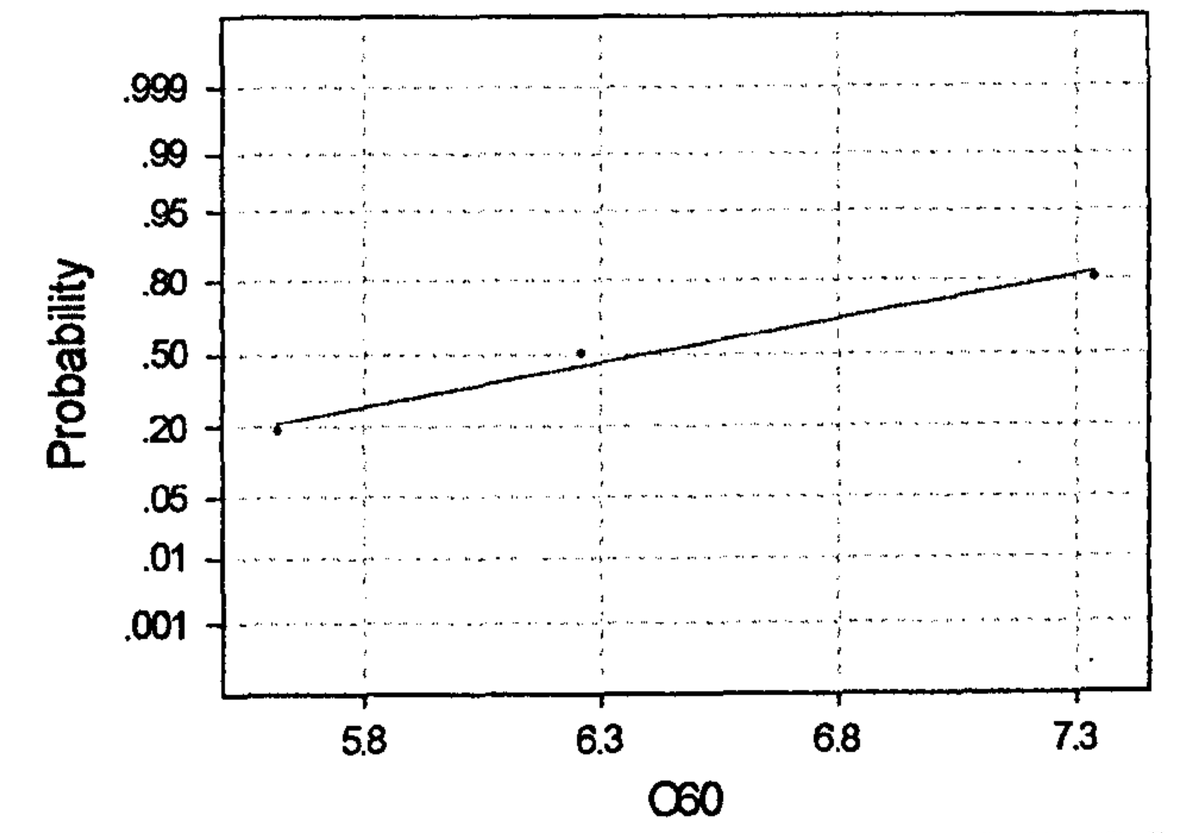

Fig 3.26 Normality Test for the population (paired difference between data for **intact capsule** and **transsected ischiofemoral and lateral iliofemoral ligaments**) used in the paired t-test

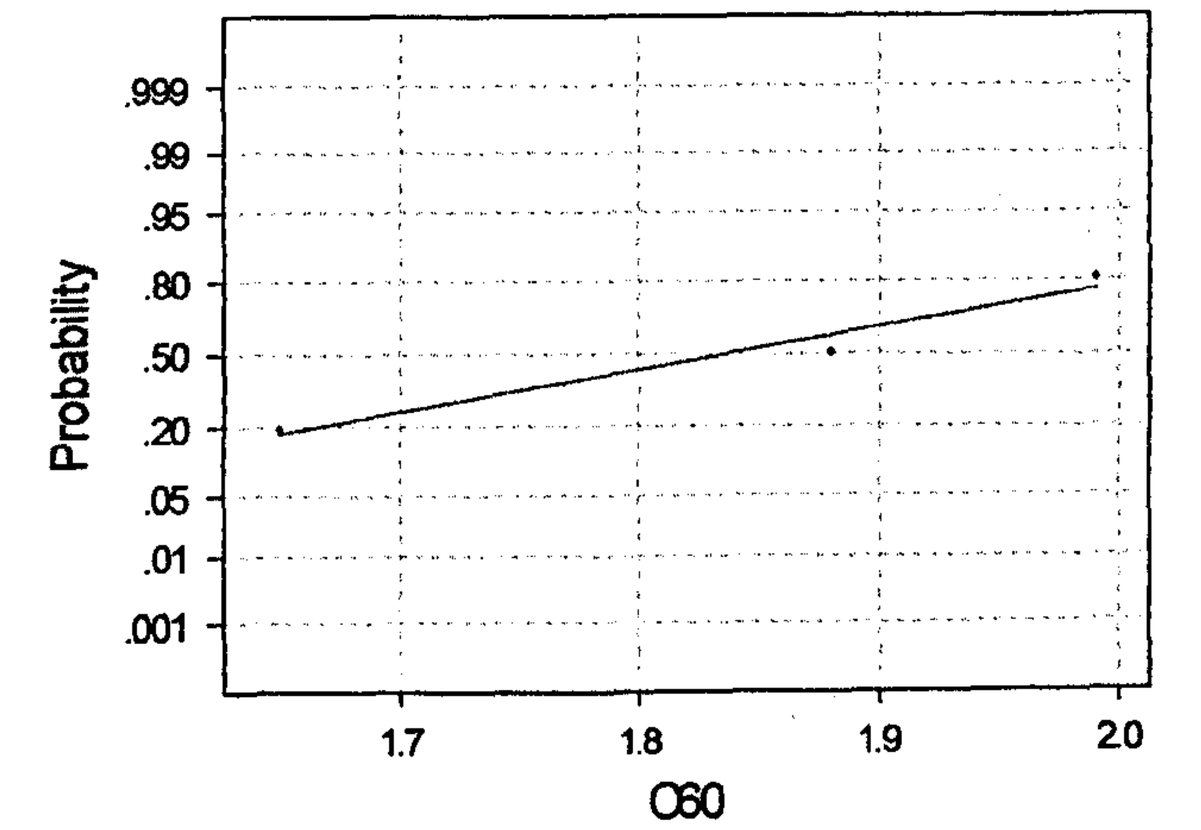

Fig 3.27 Normality Test for the population (paired difference between data for **transsected ischiofemoral &transsected ischiofemoral and lateral iliofemoral ligaments**) used in the paired t-test

Specimen 2 (Adduction)

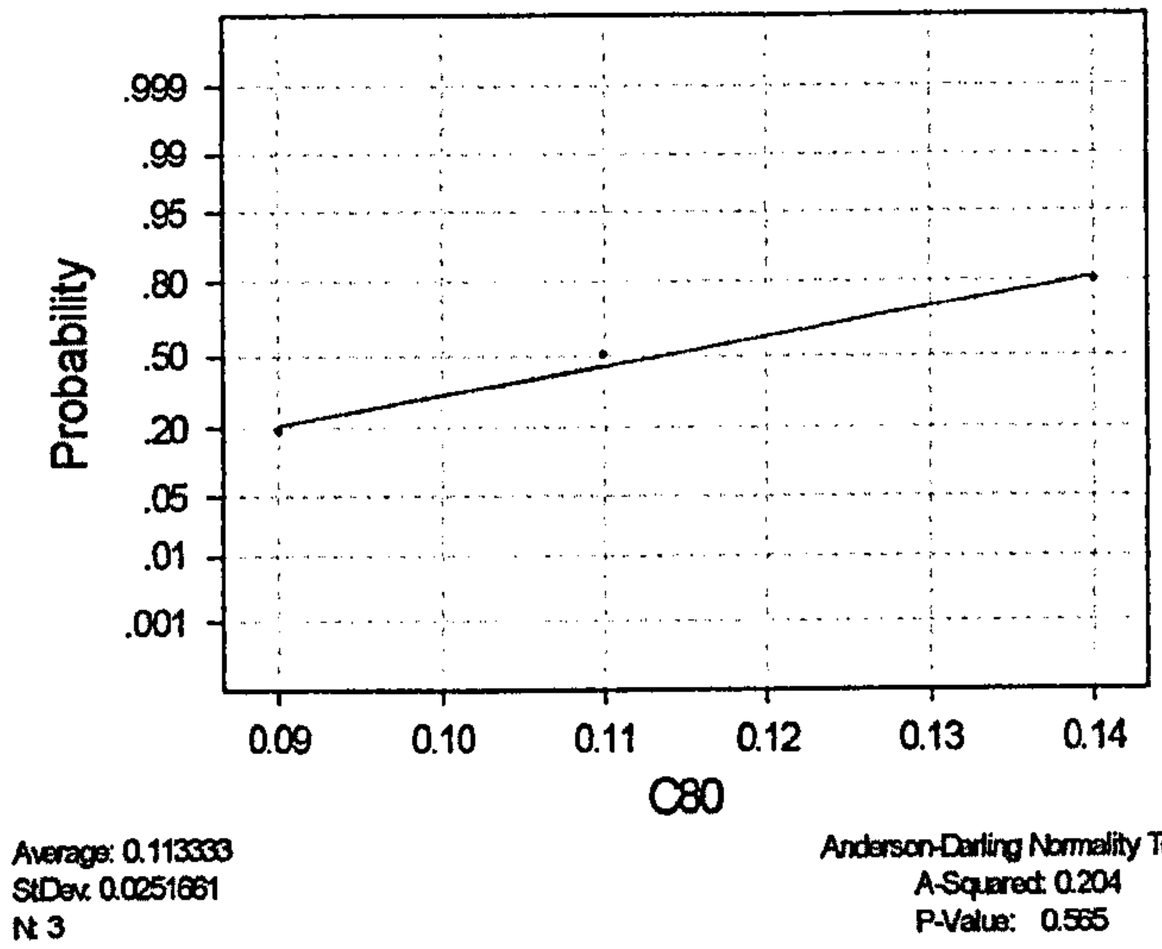

Fig 3.28 Normality Test for the population (paired difference between data for **intact capsule** and **transsected ischiofemoral ligament**) used in the paired t-test

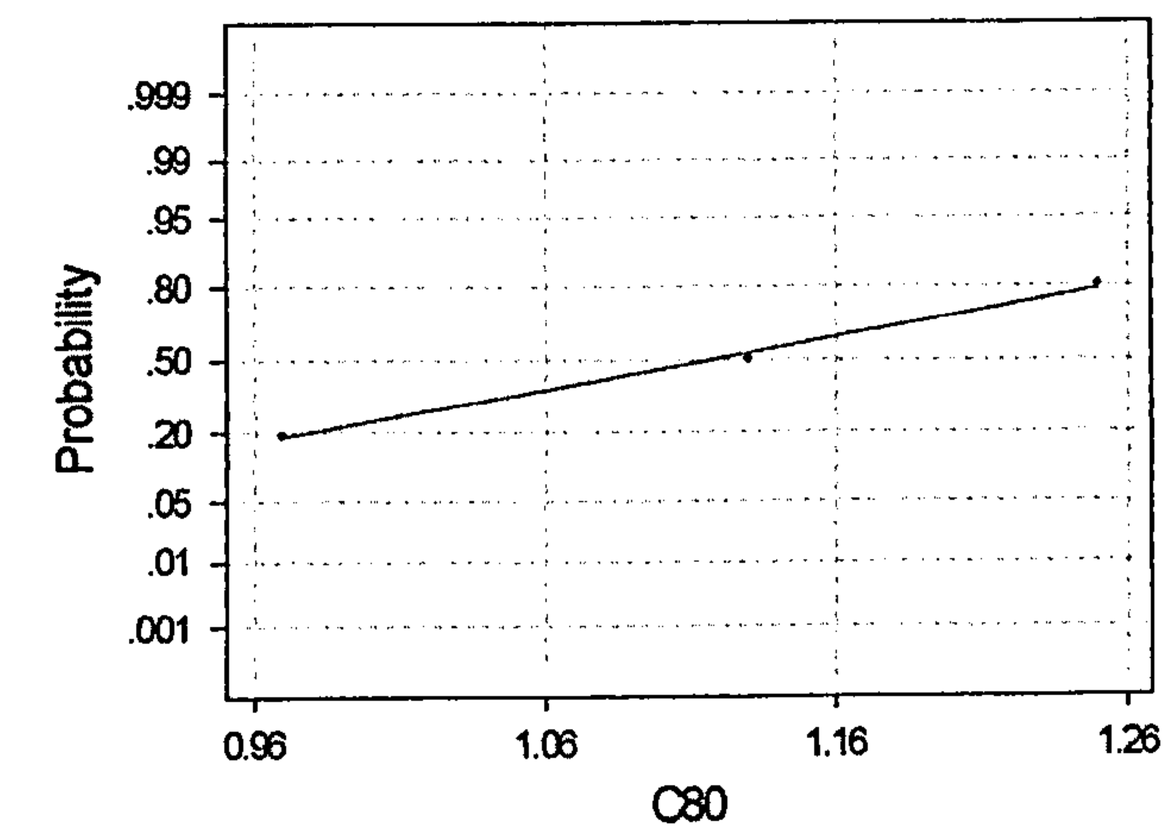

Fig 3.29 Normality Test for the population (paired difference between data for **intact capsule** and **transsected ischiofemoral and lateral iliofemoral ligaments**) used in the paired t-test

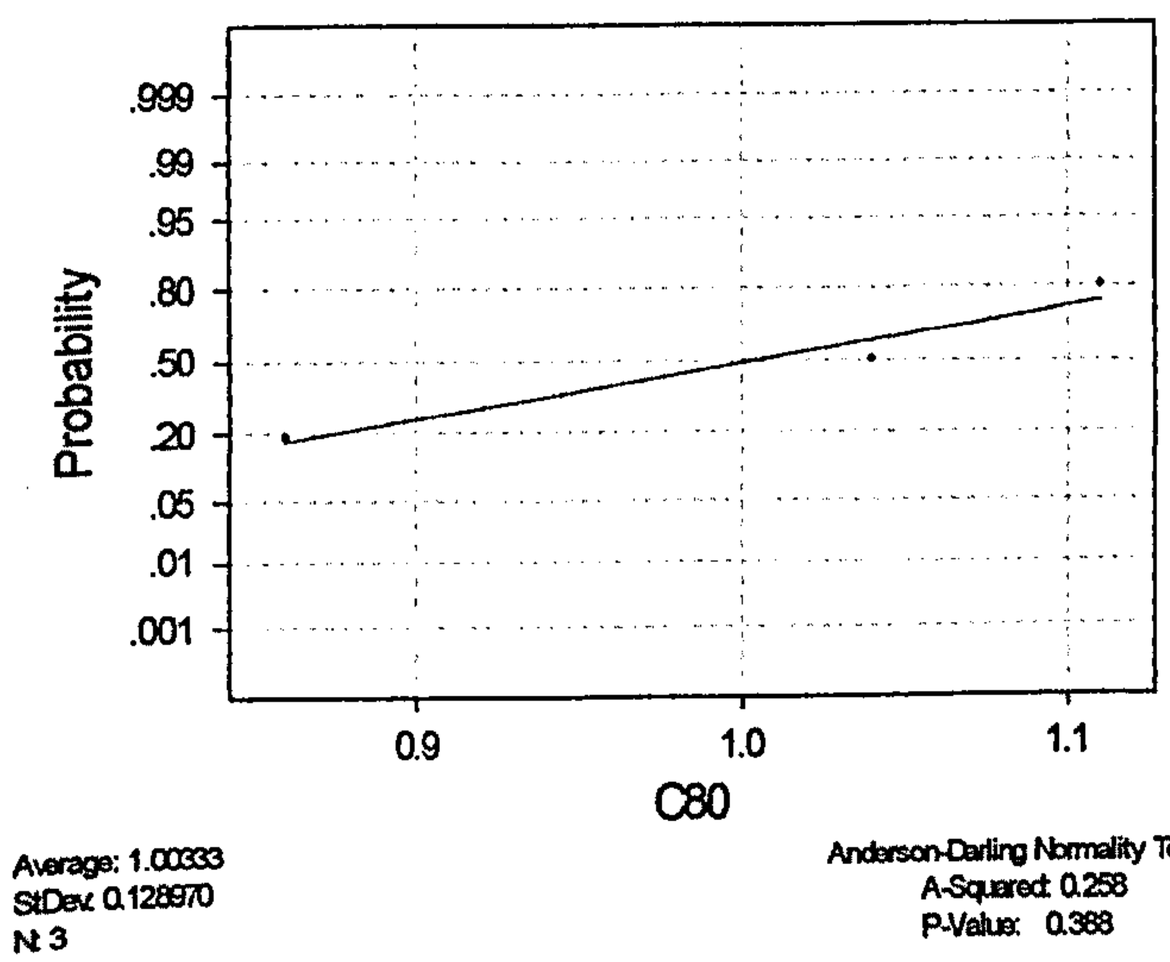

Fig 3.30 Normality Test for the population (paired difference between data for **transsected ischiofemoral &transsected ischiofemoral and lateral iliofemoral ligaments**) used in the paired t-test

Specimen 3 (Abduction)

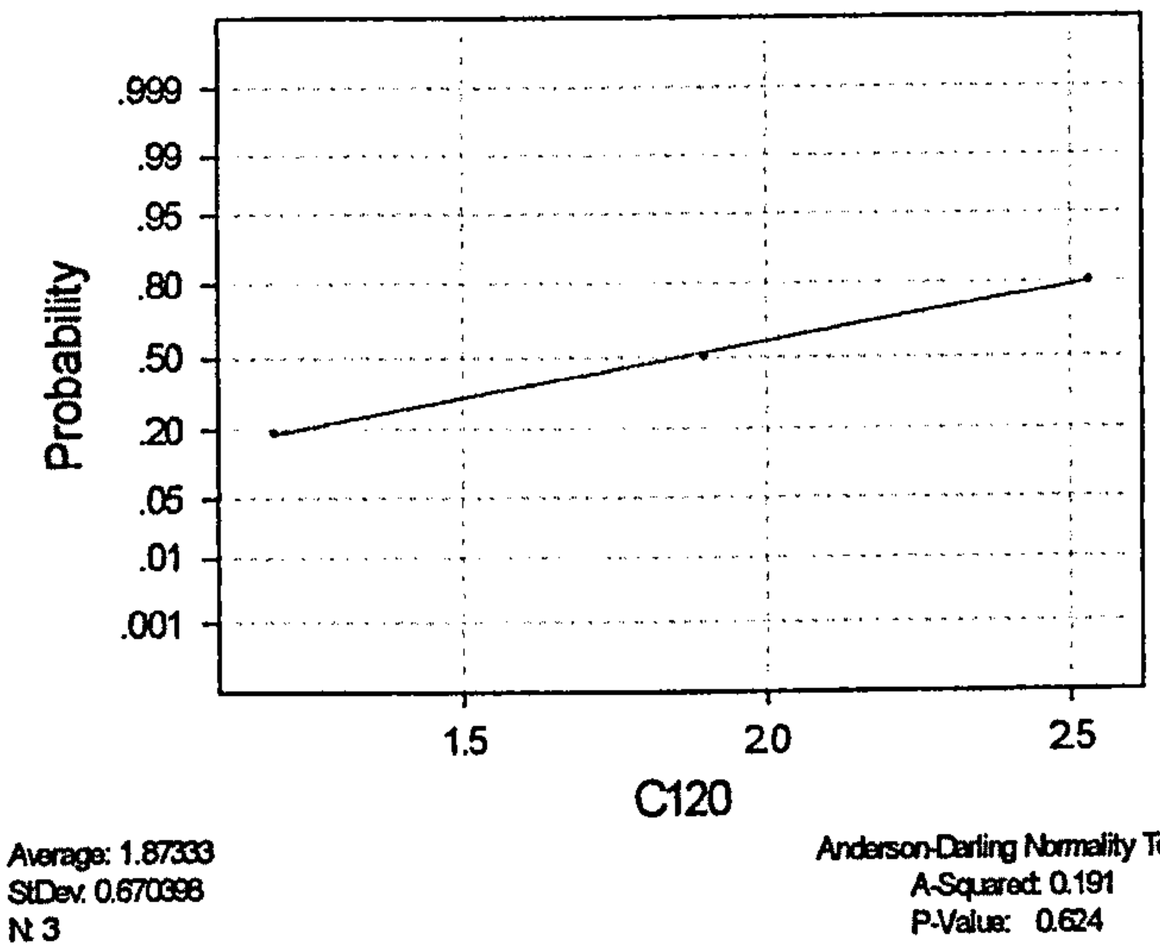

Fig 3.31 Normality Test for the population (paired difference between data for **intact capsule** and **transsected ischiofemoral ligament**) used in the paired t-test

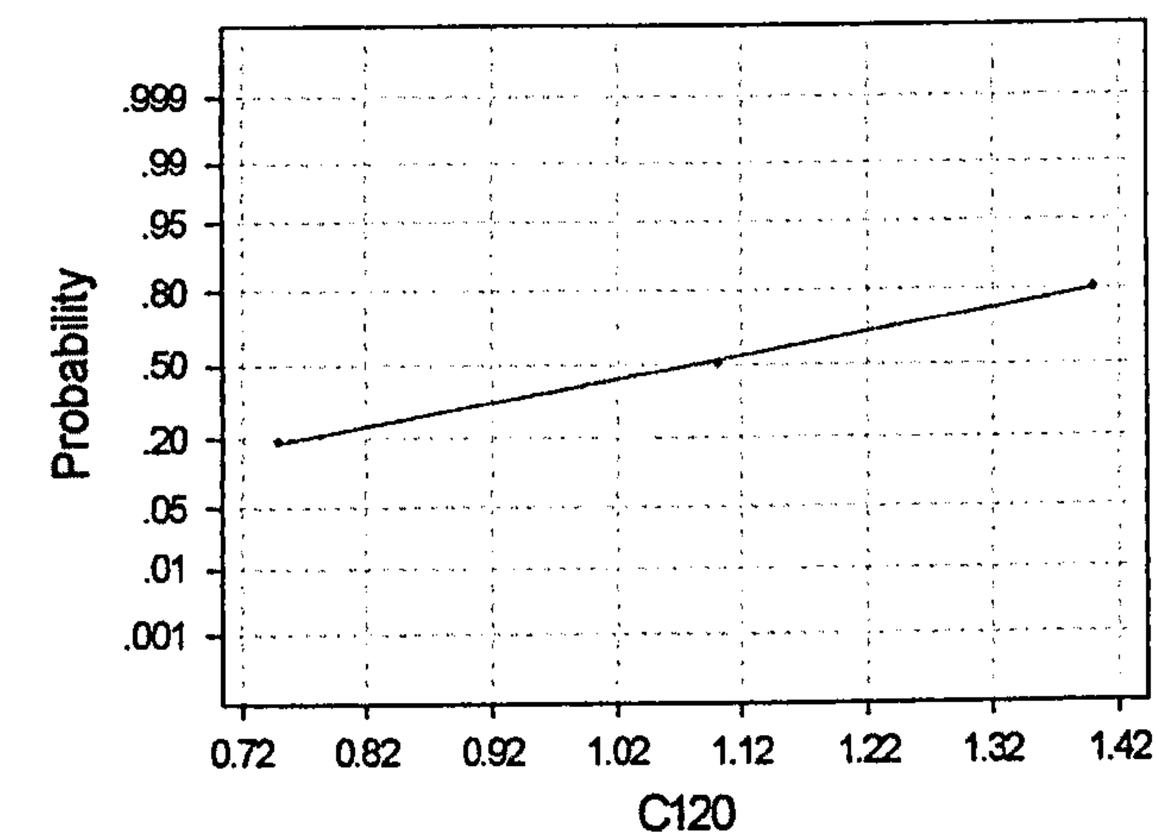

Fig 3.32 Normality Test for the population (paired difference between data for **intact capsule** and **transsected ischiofemoral and lateral iliofemoral ligaments**) used in the paired t-test

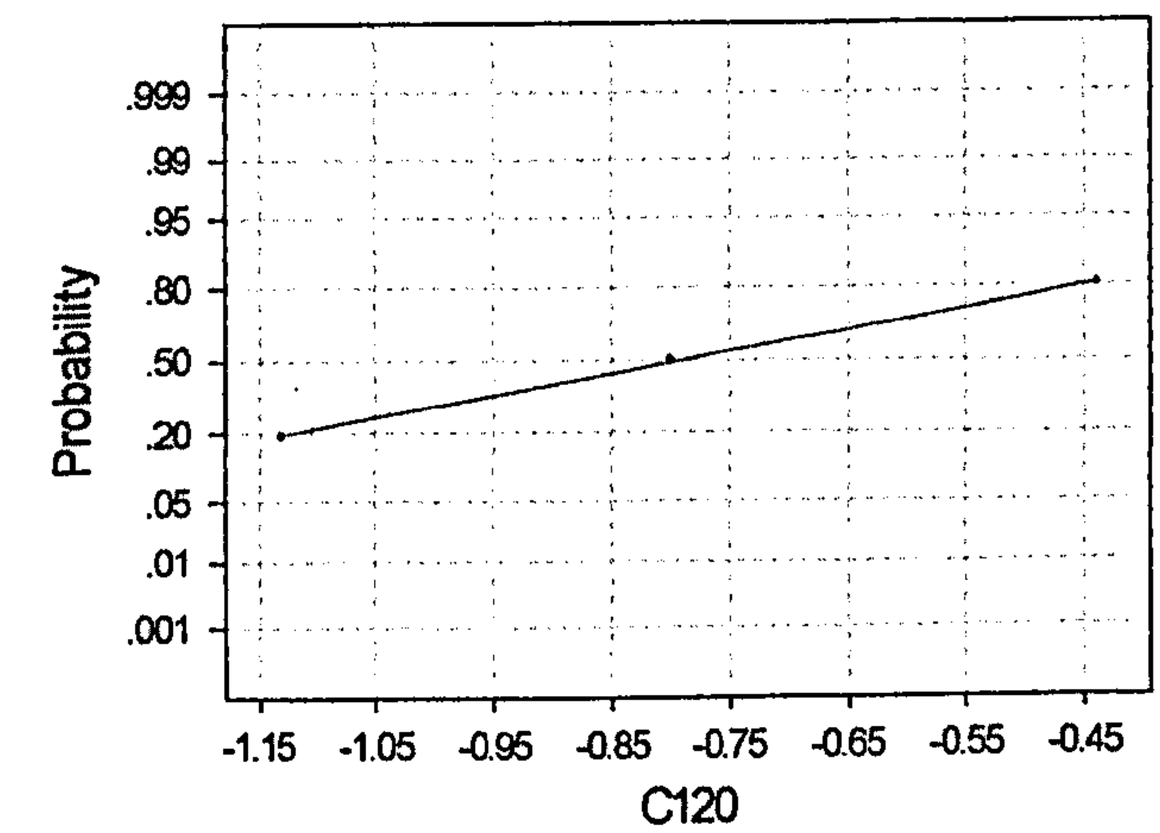

Fig 3.33 Normality Test for the population (paired difference between data for **transsected ischiofemoral &transsected ischiofemoral and lateral iliofemoral ligaments**) used in the paired t-test

Specimen 3 (Adduction)

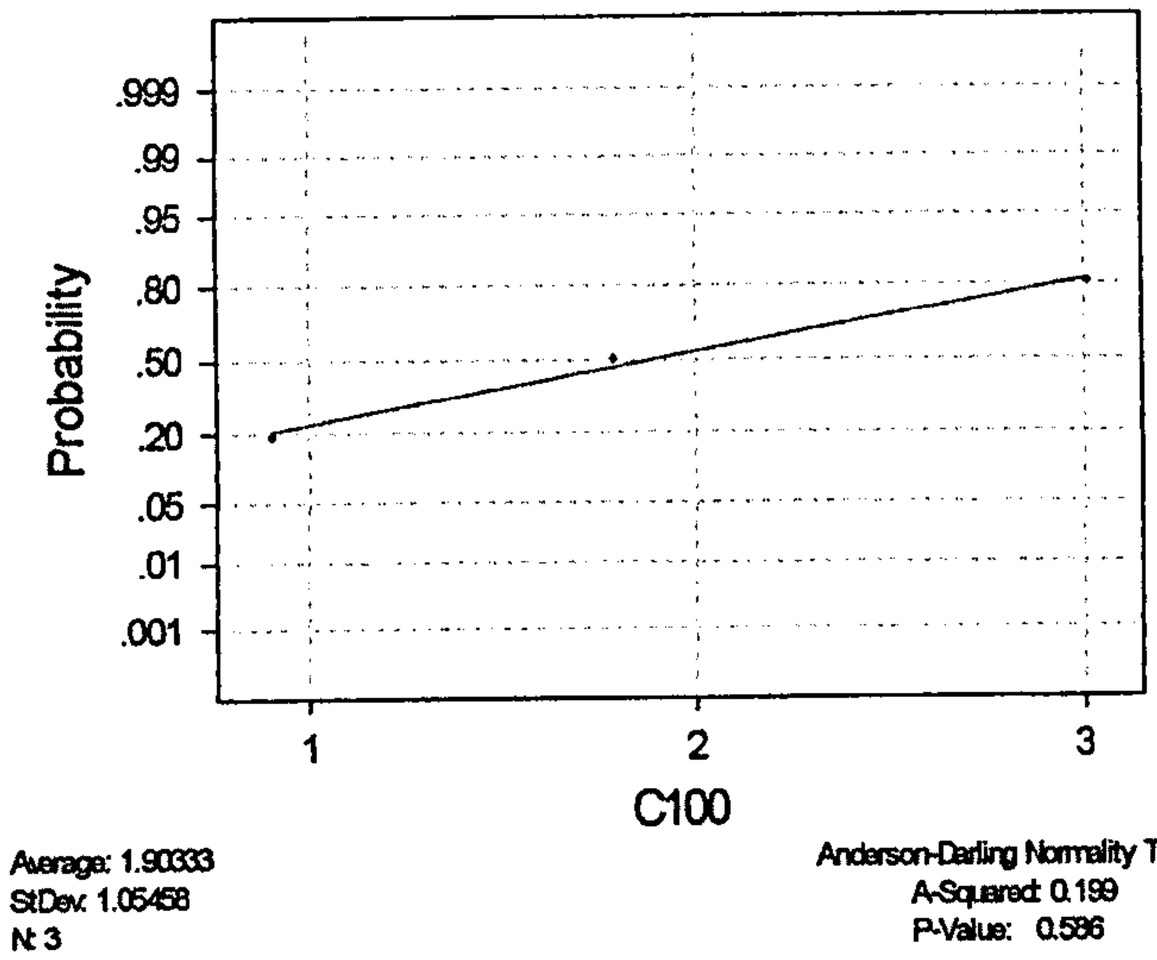

Fig 3.34 Normality Test for the population (paired difference between data for **intact capsule** and **transsected ischiofemoral ligament**) used in the paired t-test

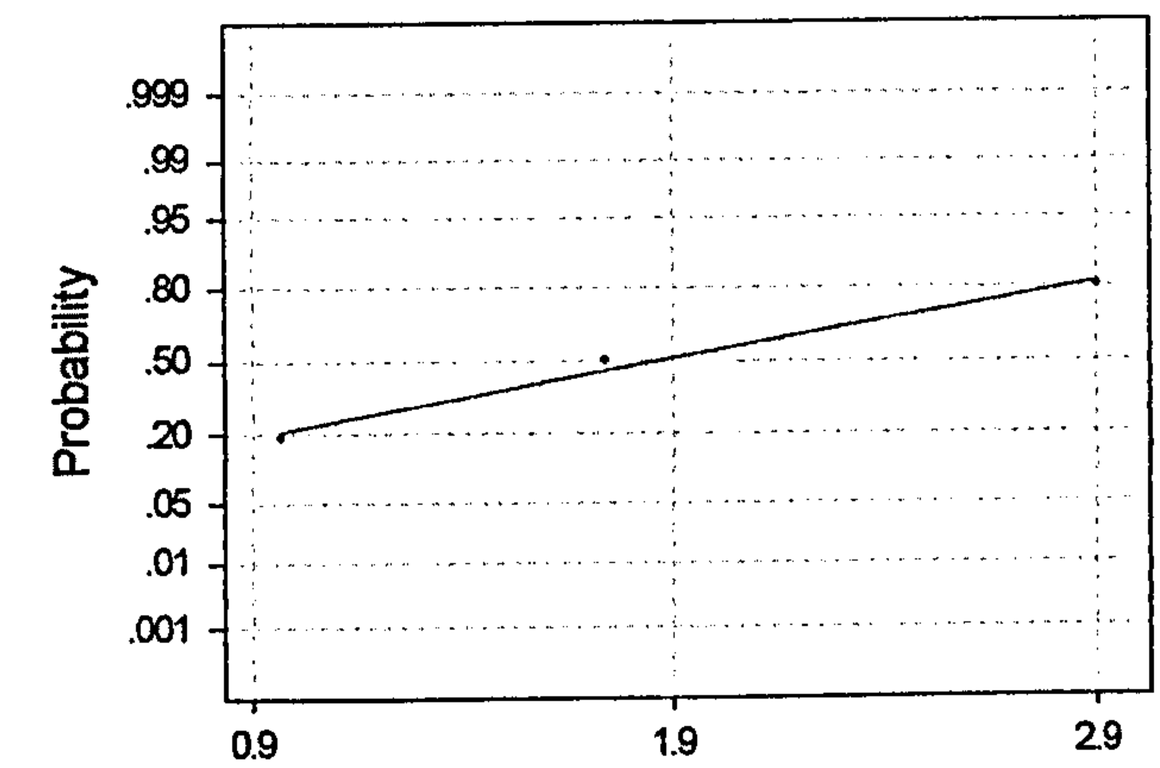

Fig 3.35 Normality Test for the population (paired difference between data for **intact capsule** and **transsected ischiofemoral and lateral iliofemoral ligaments**) used in the paired t-test

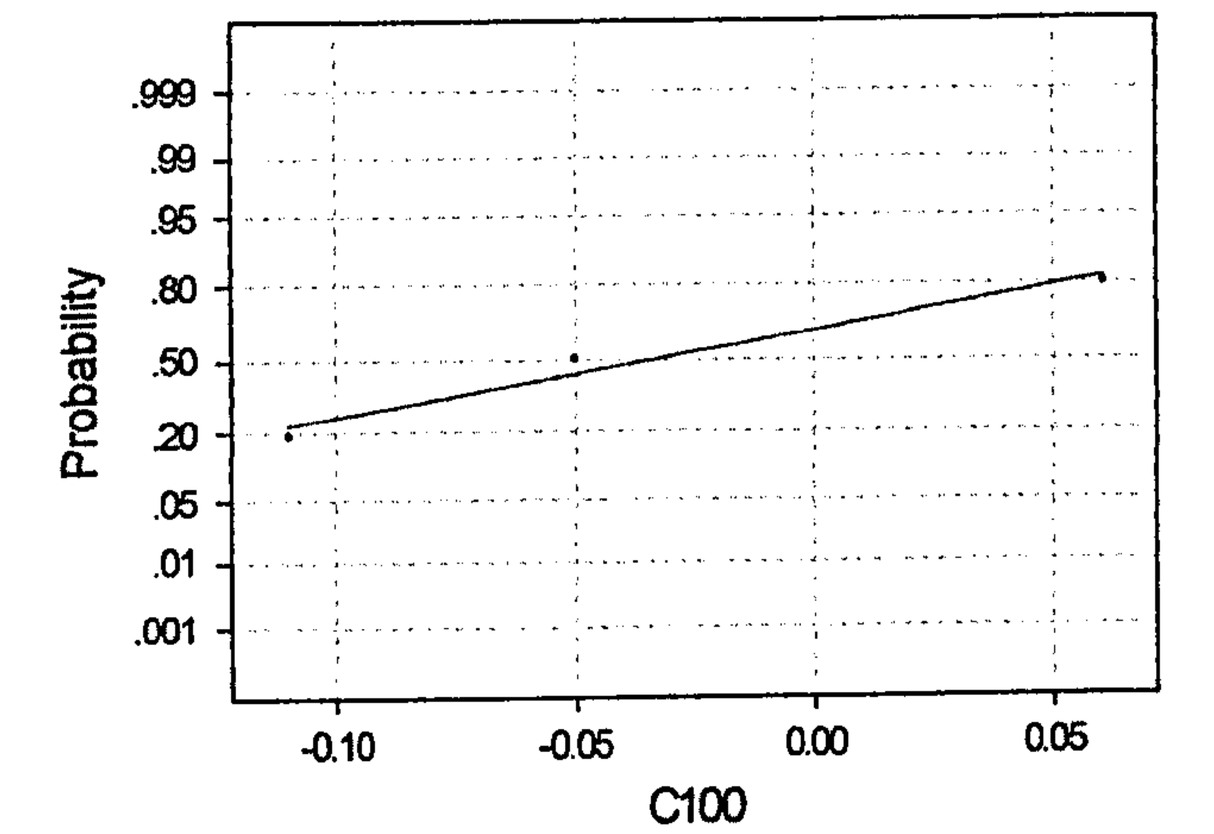

Fig 3.36 Normality Test for the population (paired difference between data for **transsected ischiofemoral &transsected ischiofemoral and lateral iliofemoral ligaments**) used in the paired t-test

Specimen 2 and 3 (Abduction)

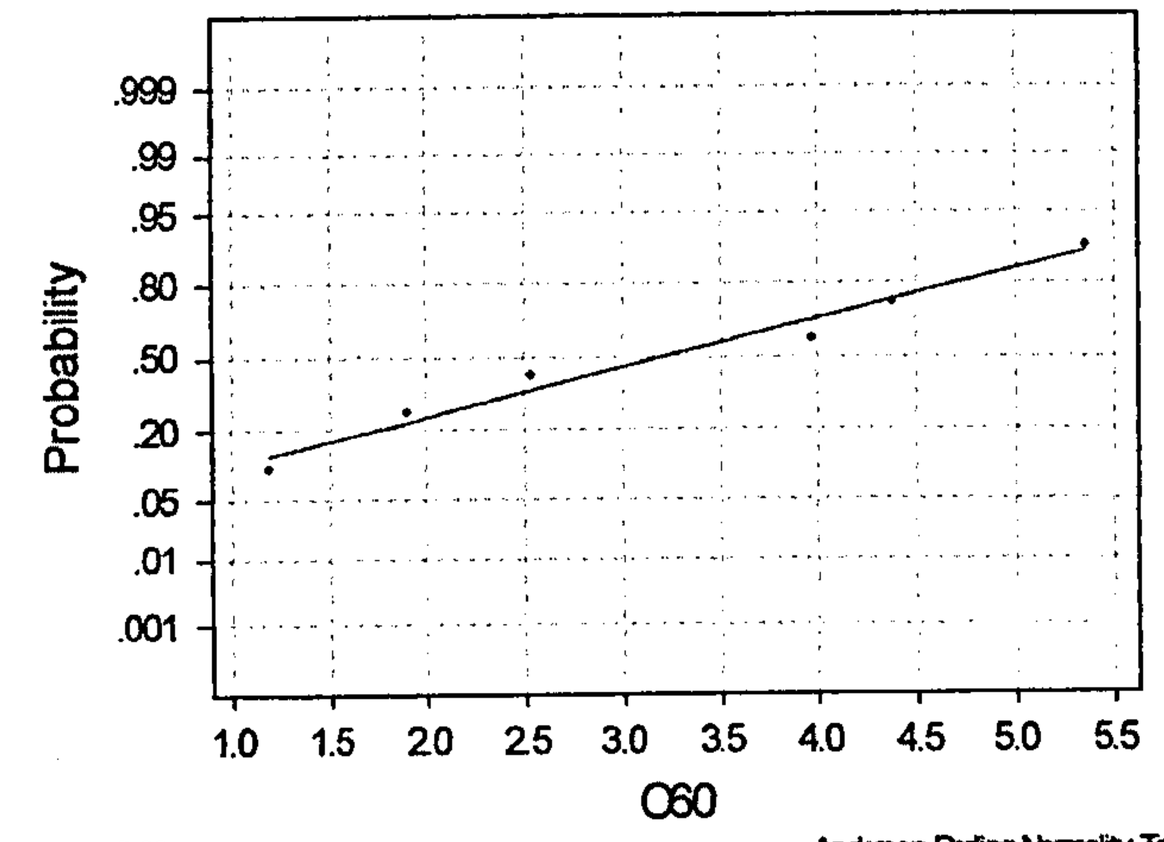

Fig 3.37 Normality Test for the population (paired difference between data for **intact capsule** and **transsected ischiofemoral ligament**) used in the paired t-test

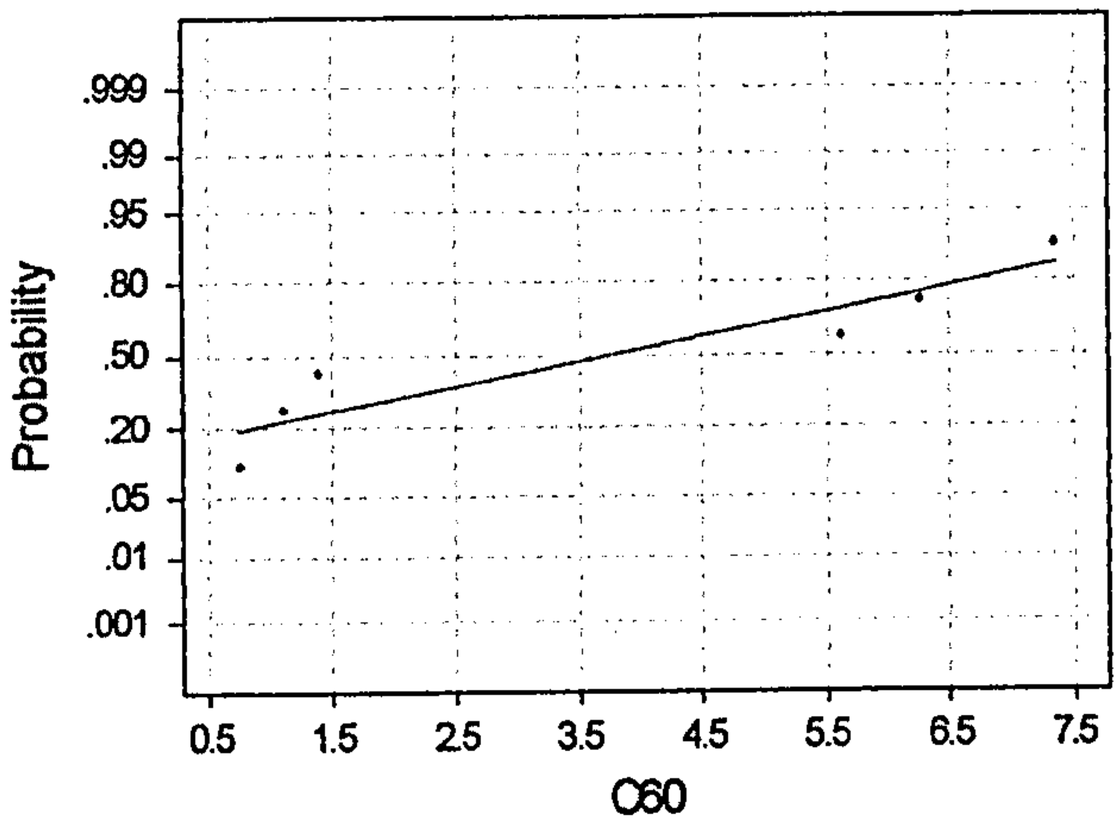

Fig 3.38 Normality Test for the population (paired difference between data for **intact capsule** and **transsected ischiofemoral and lateral iliofemoral ligaments**) used in the paired t-test

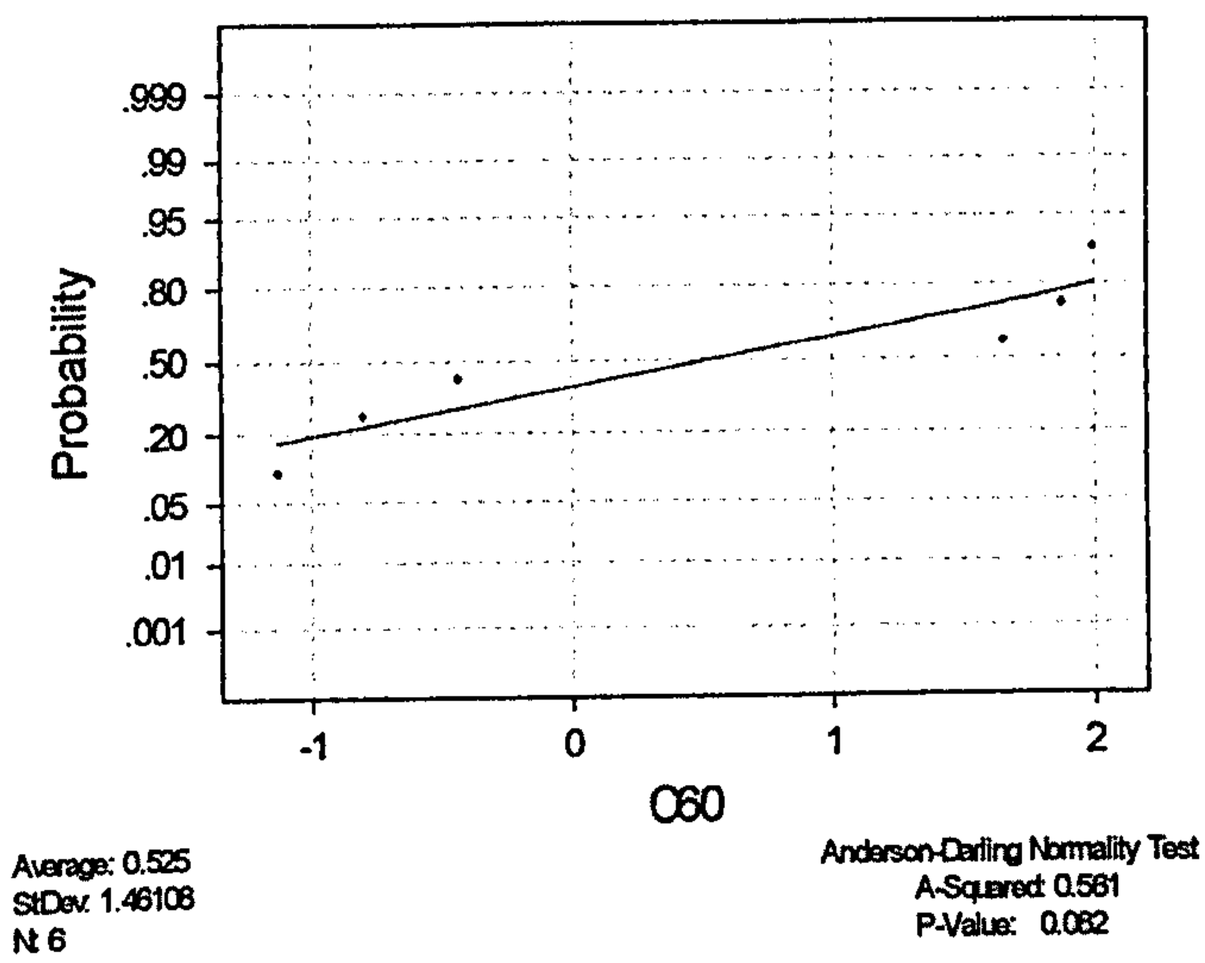

Fig 3.39 Normality Test for the population (paired difference between data for **transsected ischiofemoral &transsected ischiofemoral and lateral iliofemoral ligaments**) used in the paired t-test

Specimen 2 and 3 (Adduction)

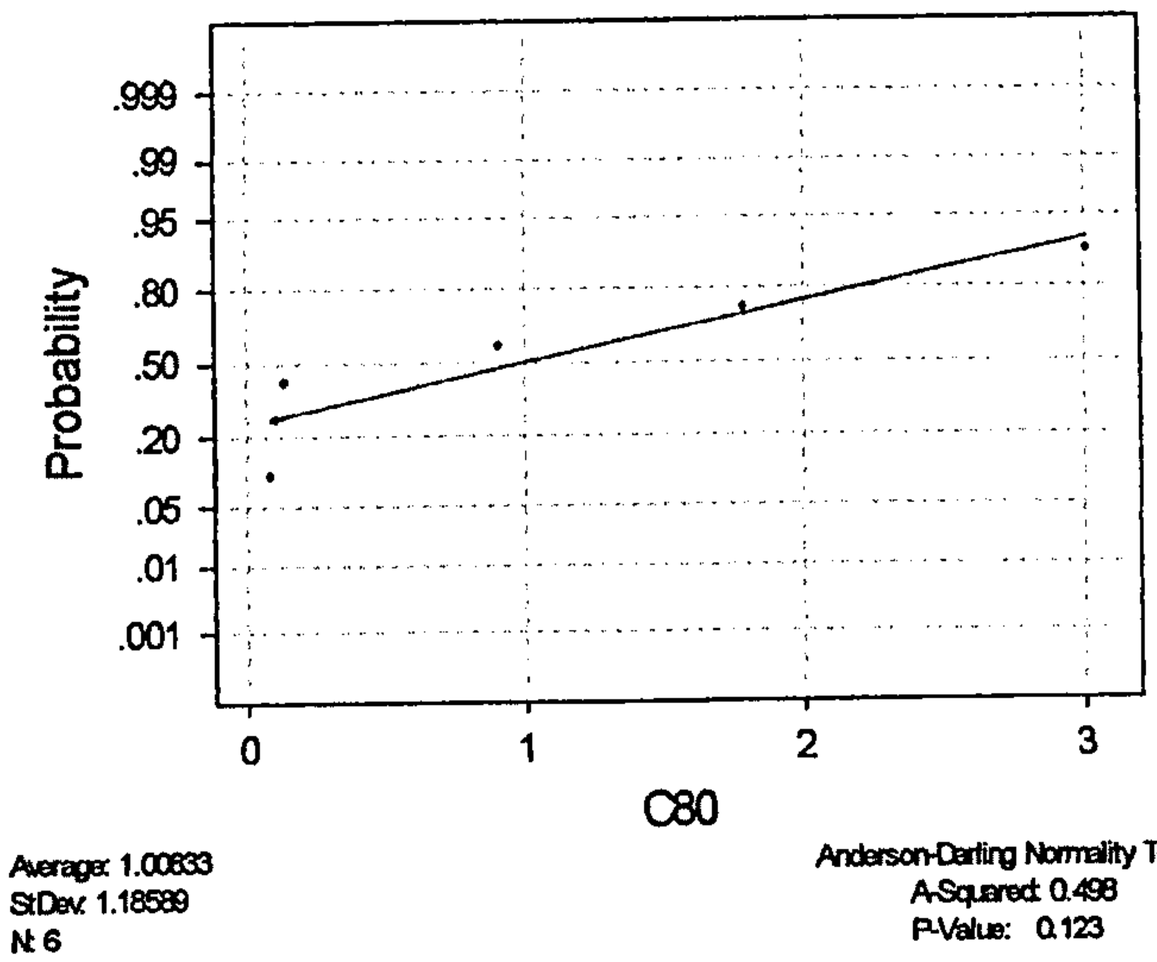

Fig 3.40 Normality Test for the population (paired difference between data for **intact capsule** and **transsected ischiofemoral ligament**) used in the paired t-test

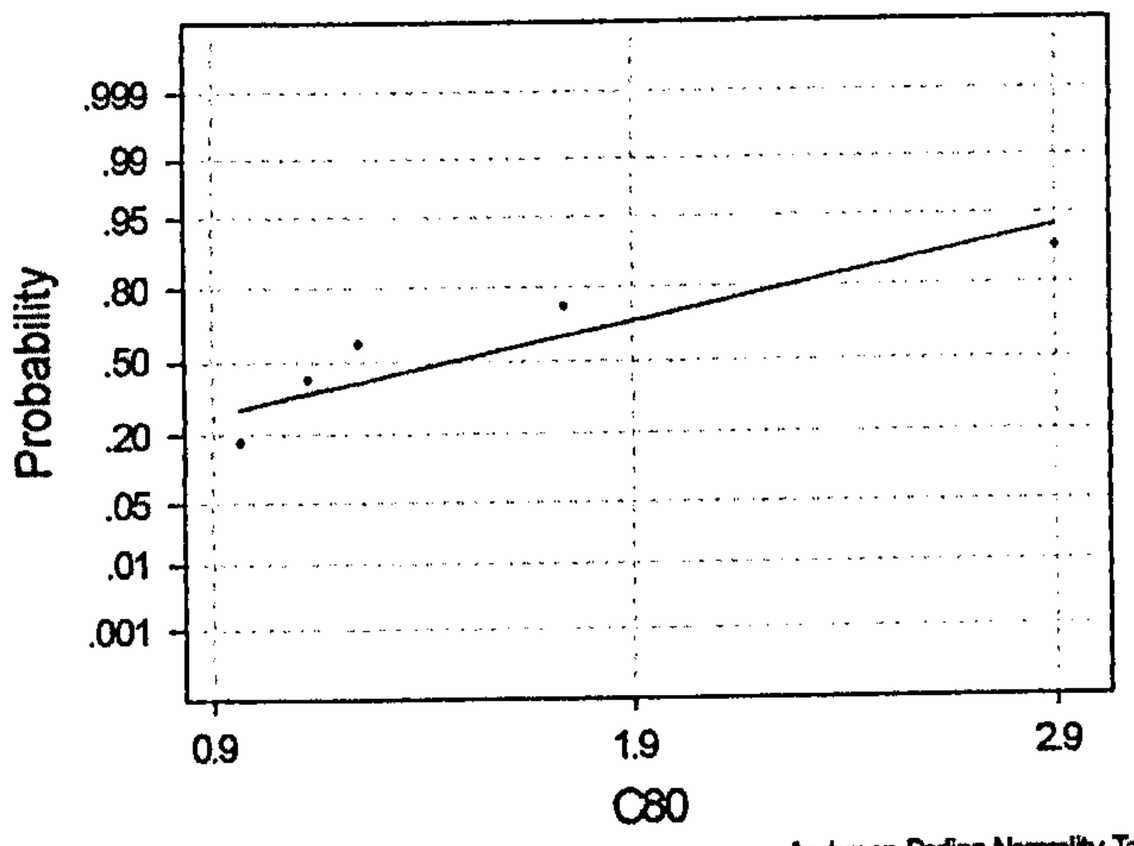

Fig 3.41 Normality Test for the population (paired difference between data for **intact capsule** and **transsected ischiofemoral and lateral iliofemoral ligaments**) used in the paired t-test

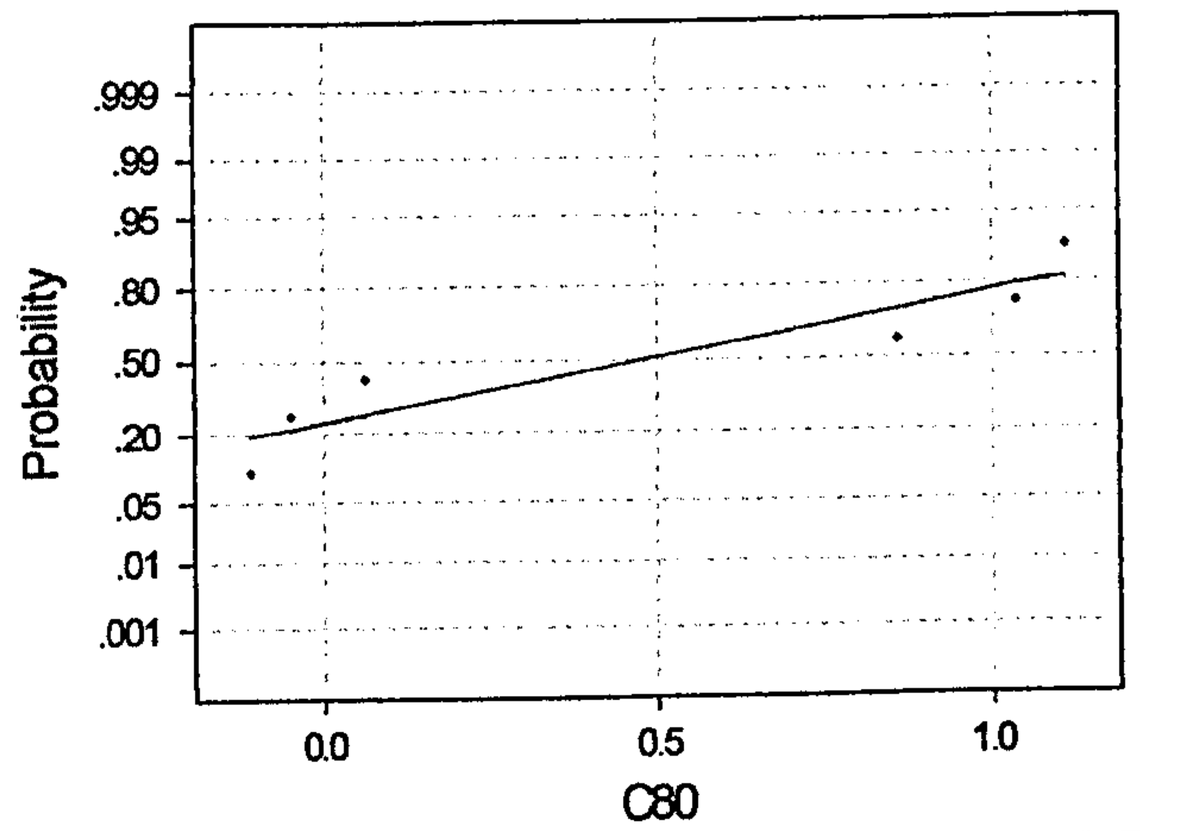

Fig 3.42 Normality Test for the population (paired difference between data for **transsected ischiofemoral &transsected ischiofemoral and lateral iliofemoral ligaments**) used in the paired t-test

Full Internal Rotation

Specimen 1 (Abduction)

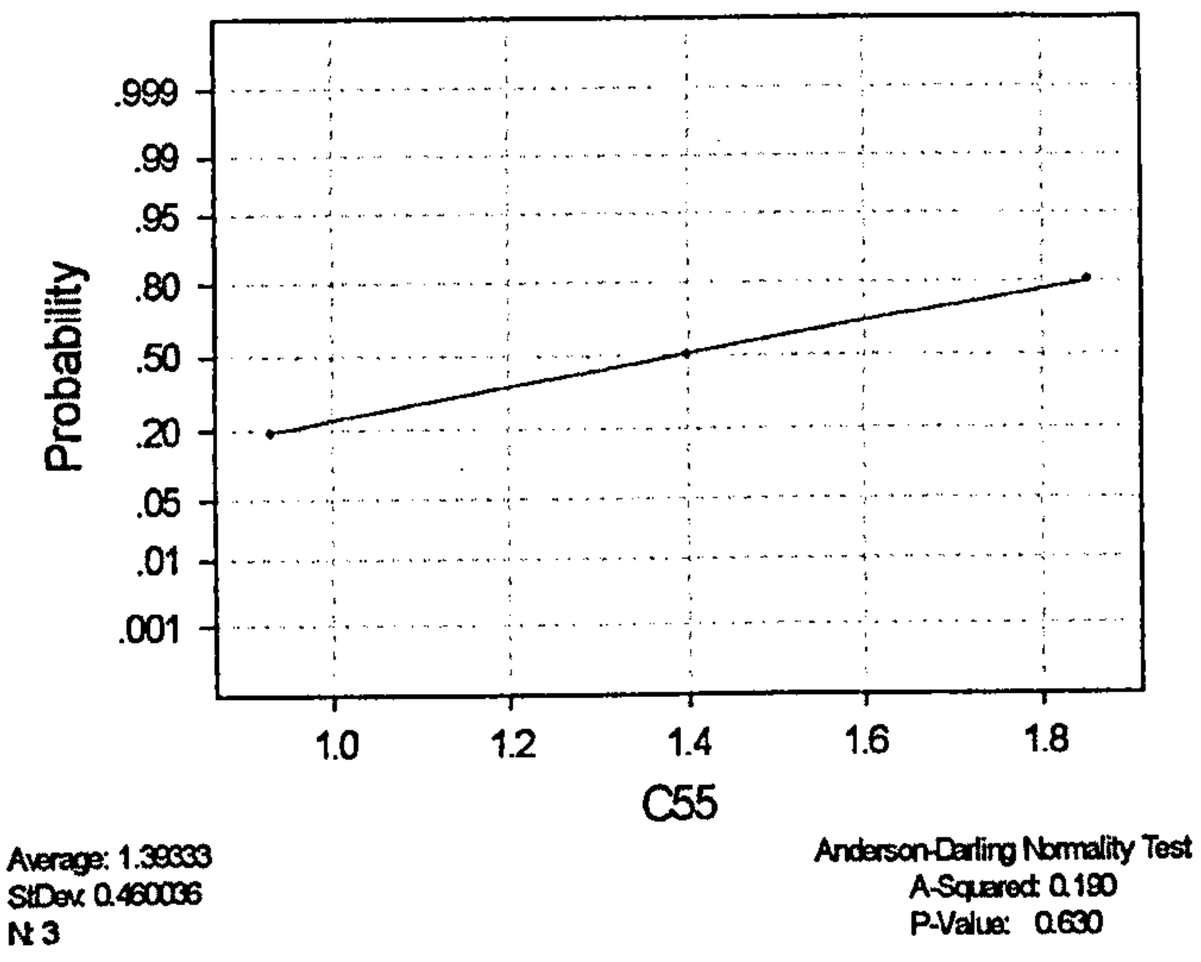

Fig 3.43 Normality Test for the population (paired difference between data for **intact capsule and transsected ischiofemoral ligament**) used in the paired t-test

Specimen 1 (Adduction)

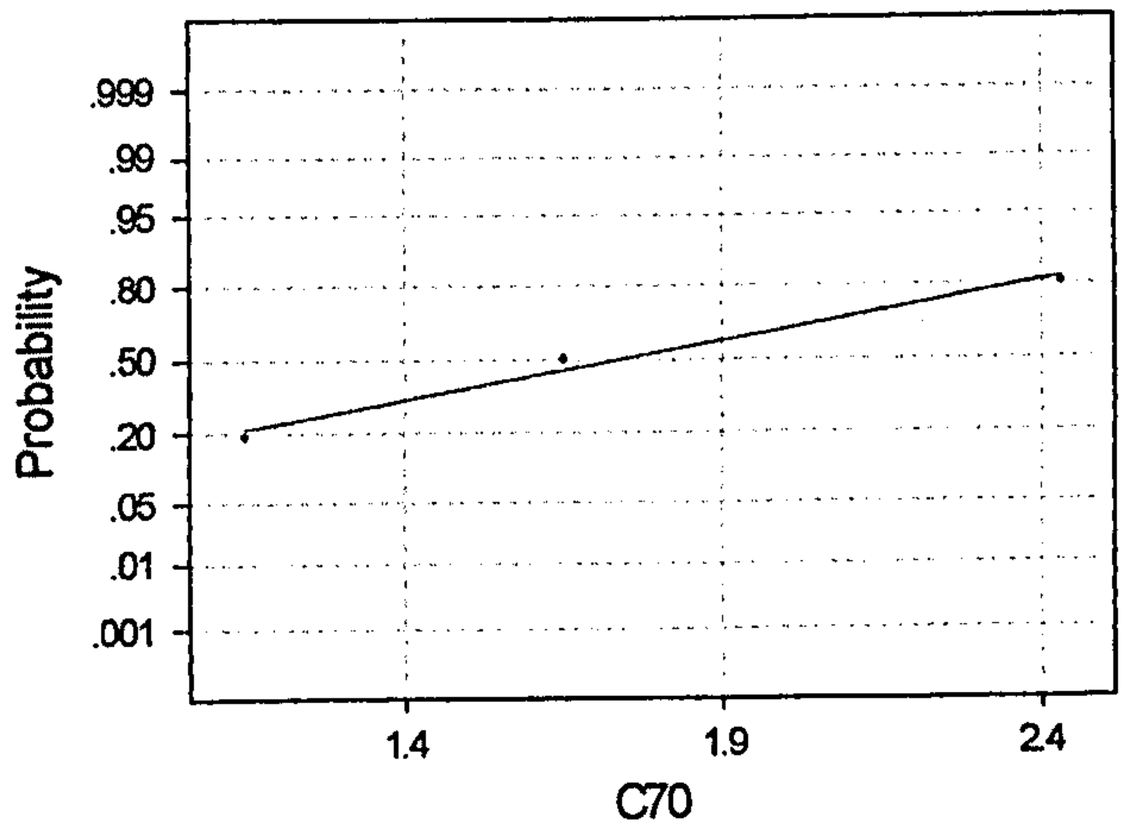

Fig 3.44 Normality Test for the population (paired difference between data for **intact capsule and transsected ischiofemoral ligament**) used in the paired t-test

Specimen 2 (Abduction)

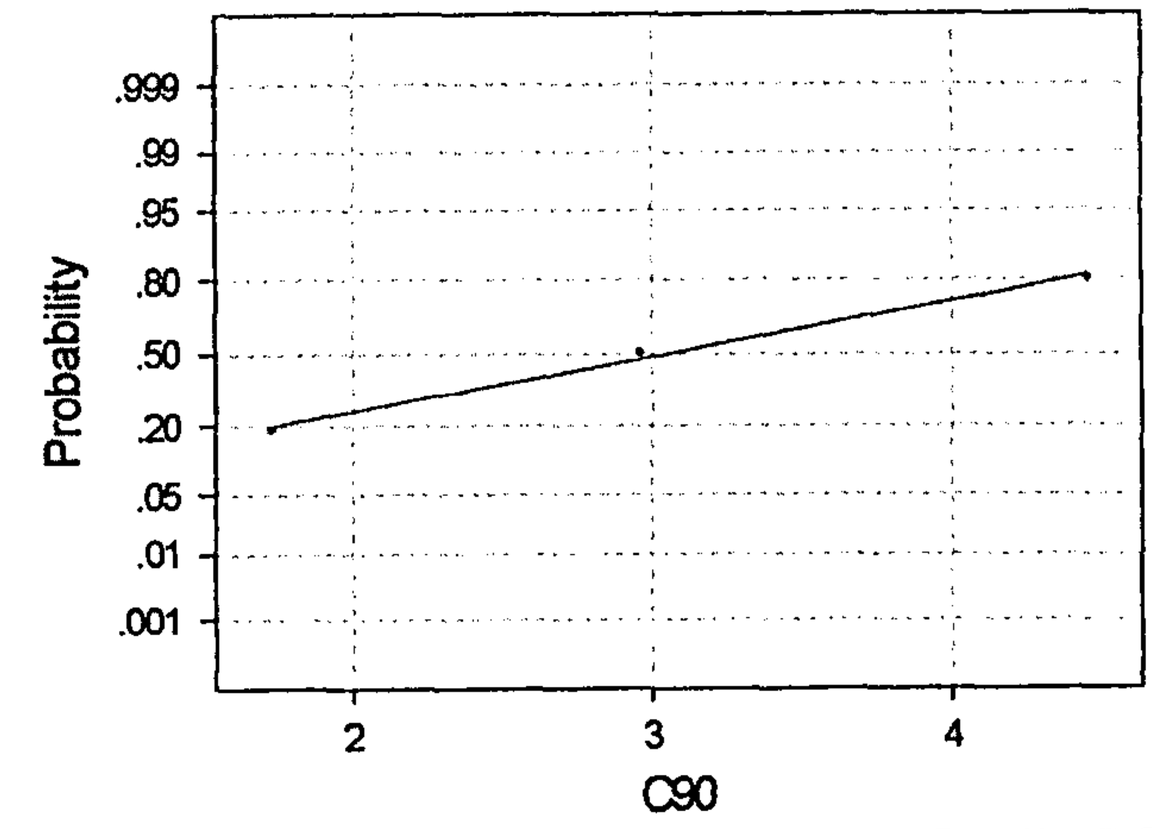

Fig 3.45 Normality Test for the population (paired difference between data for **intact capsule and transsected ischiofemoral ligament**) used in the paired t-test

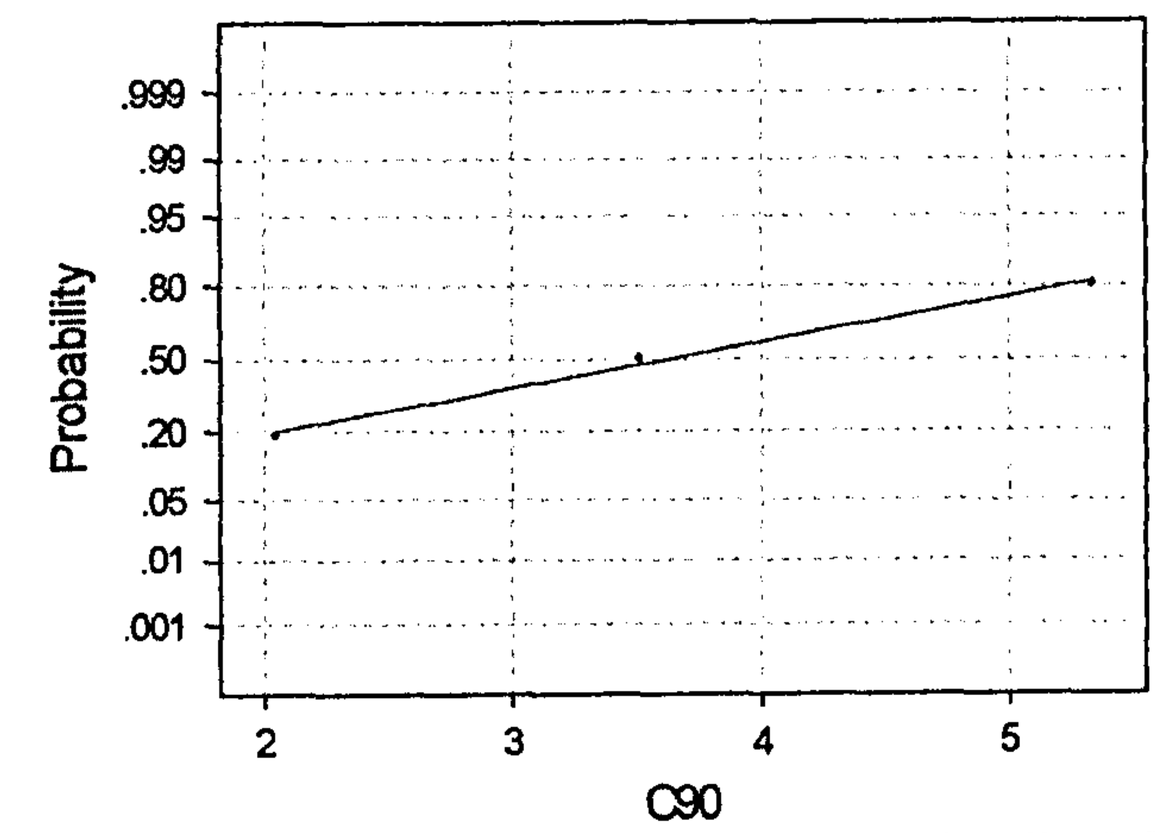

Fig 3.46 Normality Test for the population (paired difference between data for **intact capsule and transsected ischiofemoral and lateral iliofemoral ligaments**) used in the paired t-test

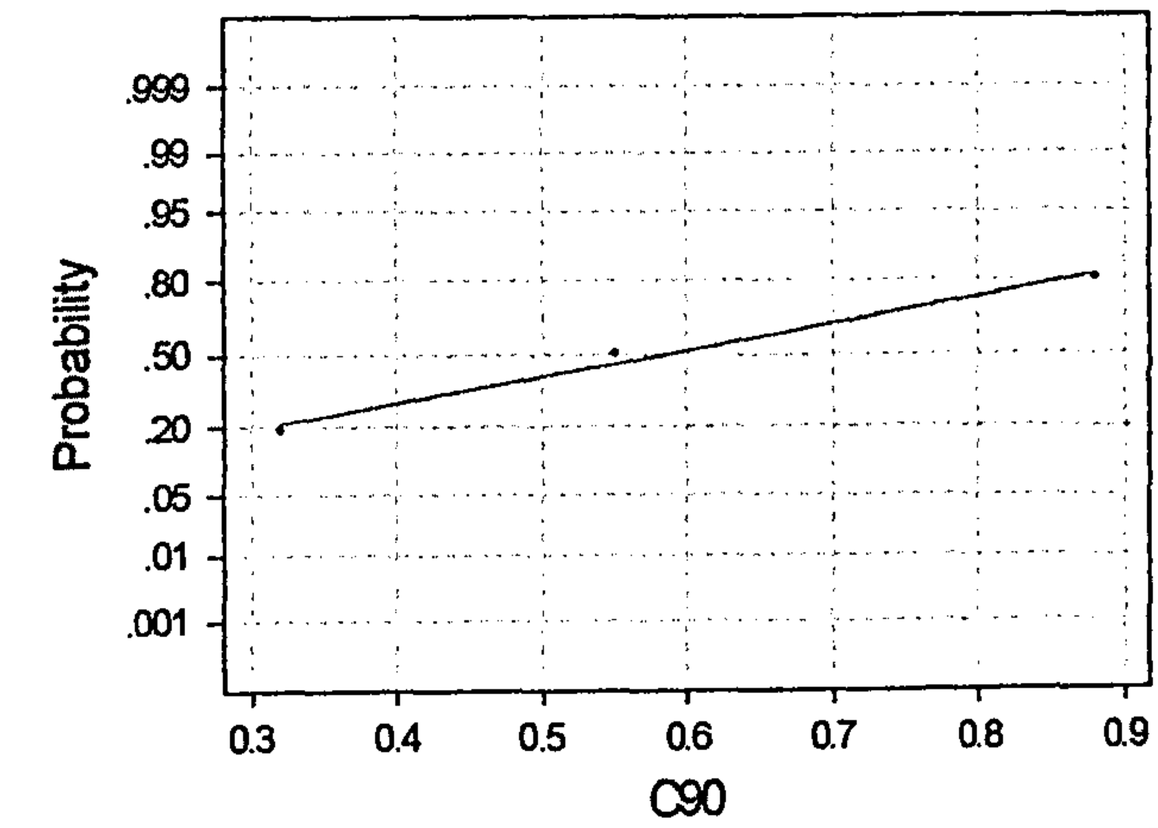

Fig 3.47 Normality Test for the population (paired difference between data for **transsected ischiofemoral &transsected ischiofemoral and lateral iliofemoral ligaments**) used in the paired t-test

Specimen 2 (Adduction)

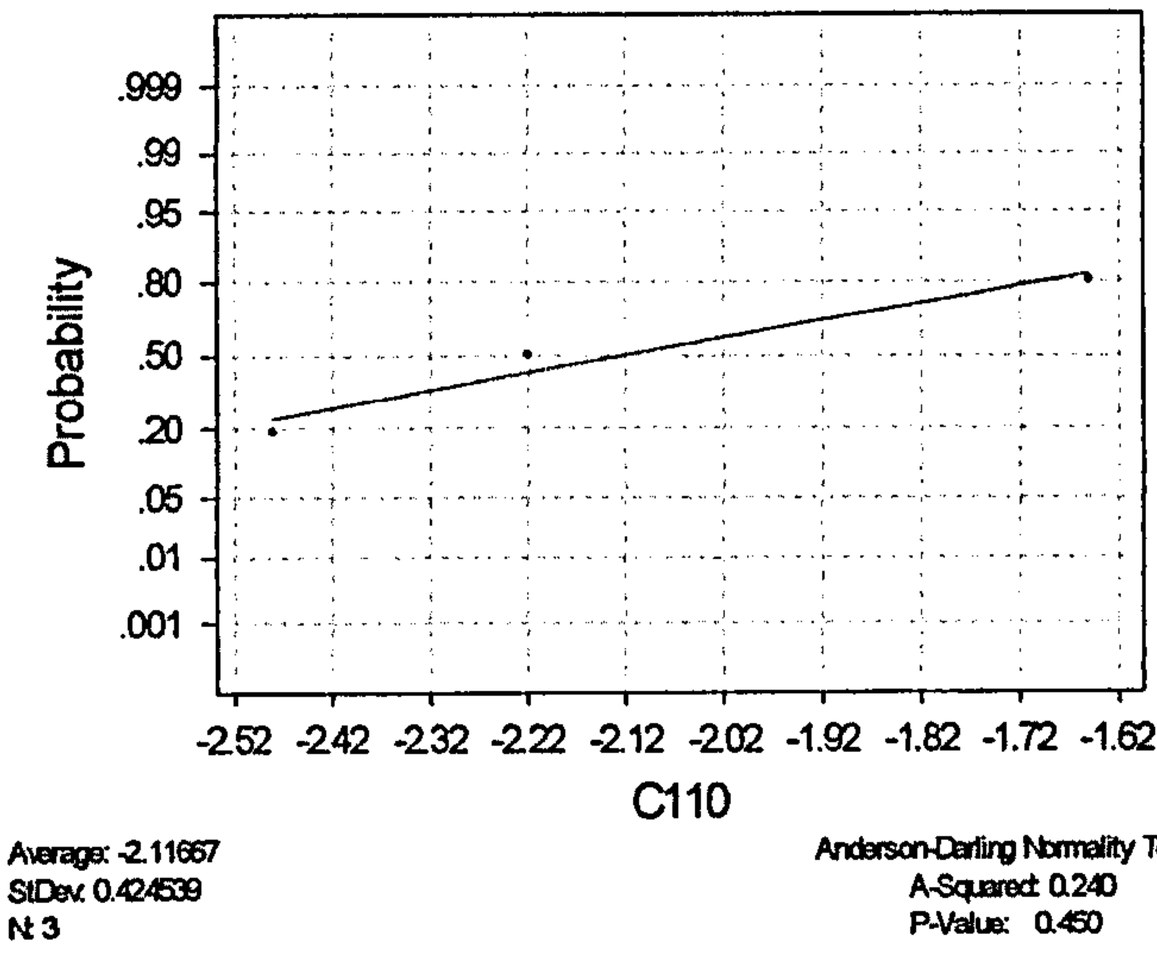

Fig 3.48 Normality Test for the population (paired difference between data for **intact capsule** and **transsected ischiofemoral ligament**) used in the paired t-test

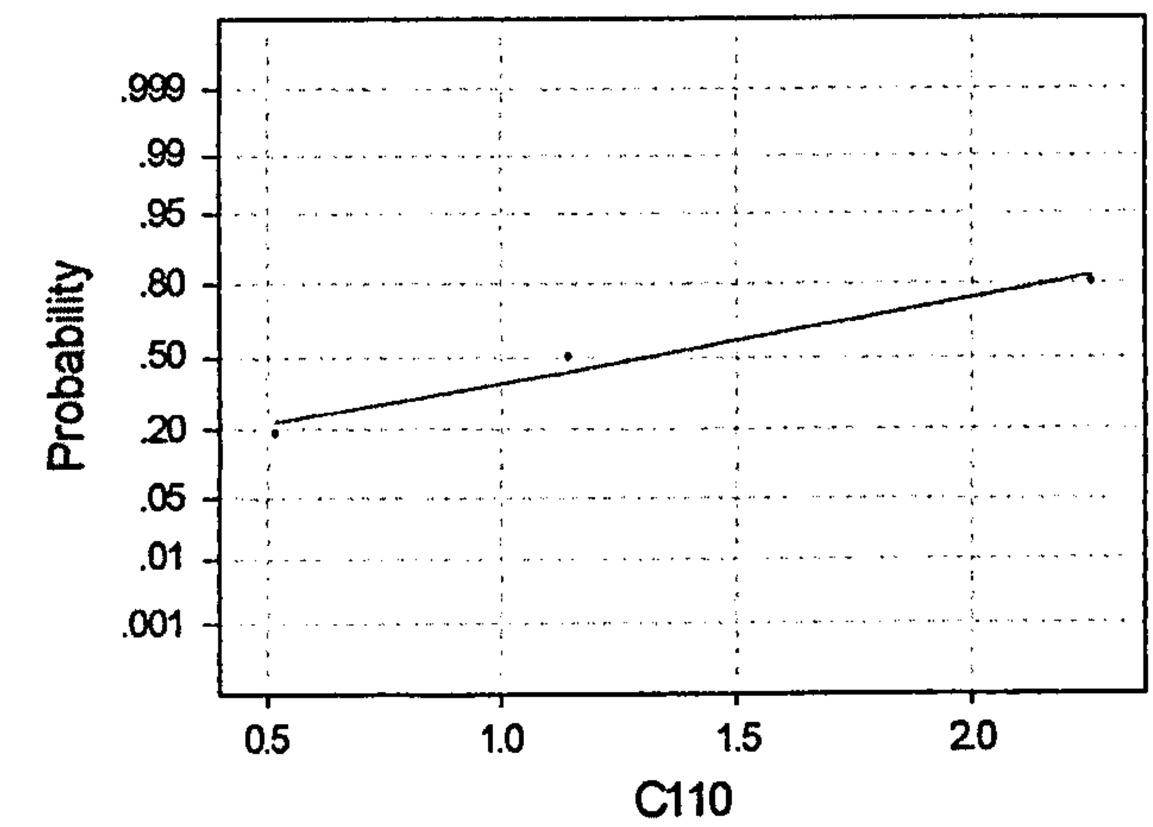

Fig 3.49 Normality Test for the population (paired difference between data for **intact capsule** and **transsected ischiofemoral and lateral iliofemoral ligaments**) used in the paired t-test

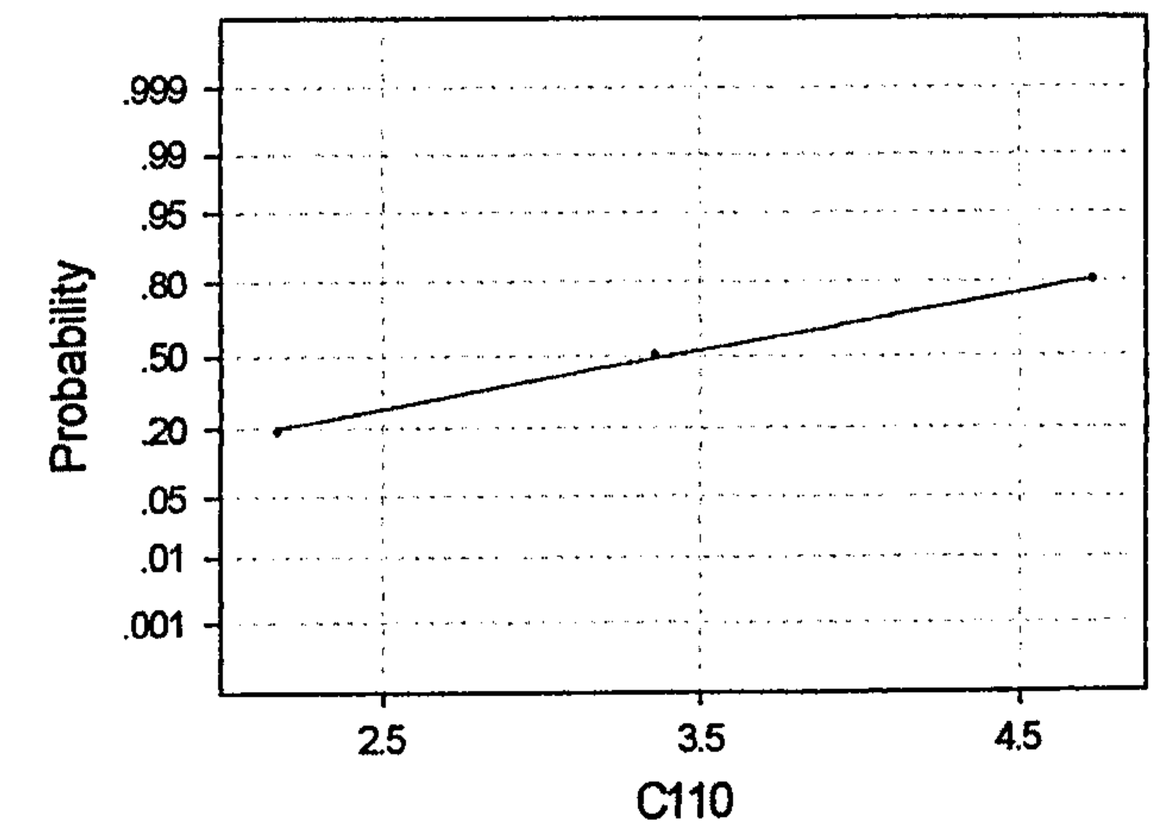

Fig 3.50 Normality Test for the population (paired difference between data for **transsected ischiofemoral &transsected ischiofemoral and lateral iliofemoral ligaments**) used in the paired t-test

Specimen 3 (Abduction)

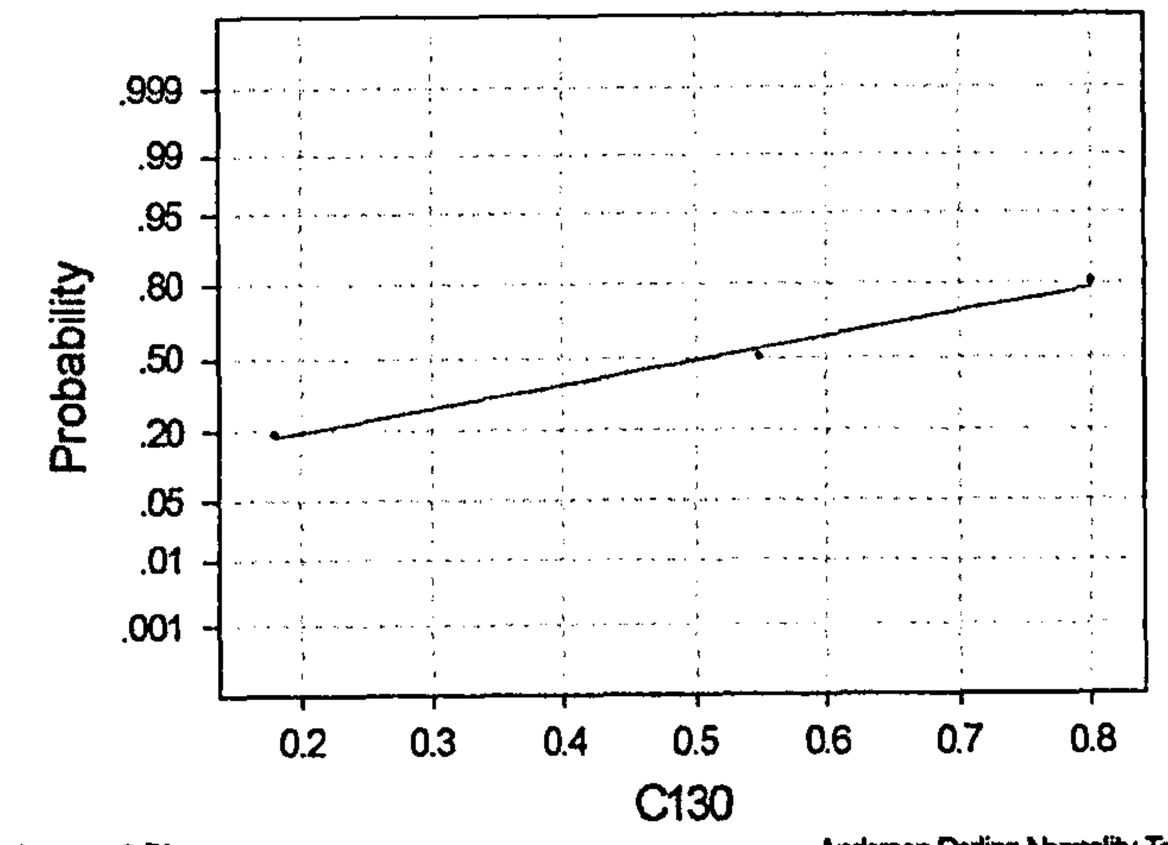

Fig 3.51 Normality Test for the population (paired difference between data for **intact capsule** and **transsected ischiofemoral ligament**) used in the paired t-test

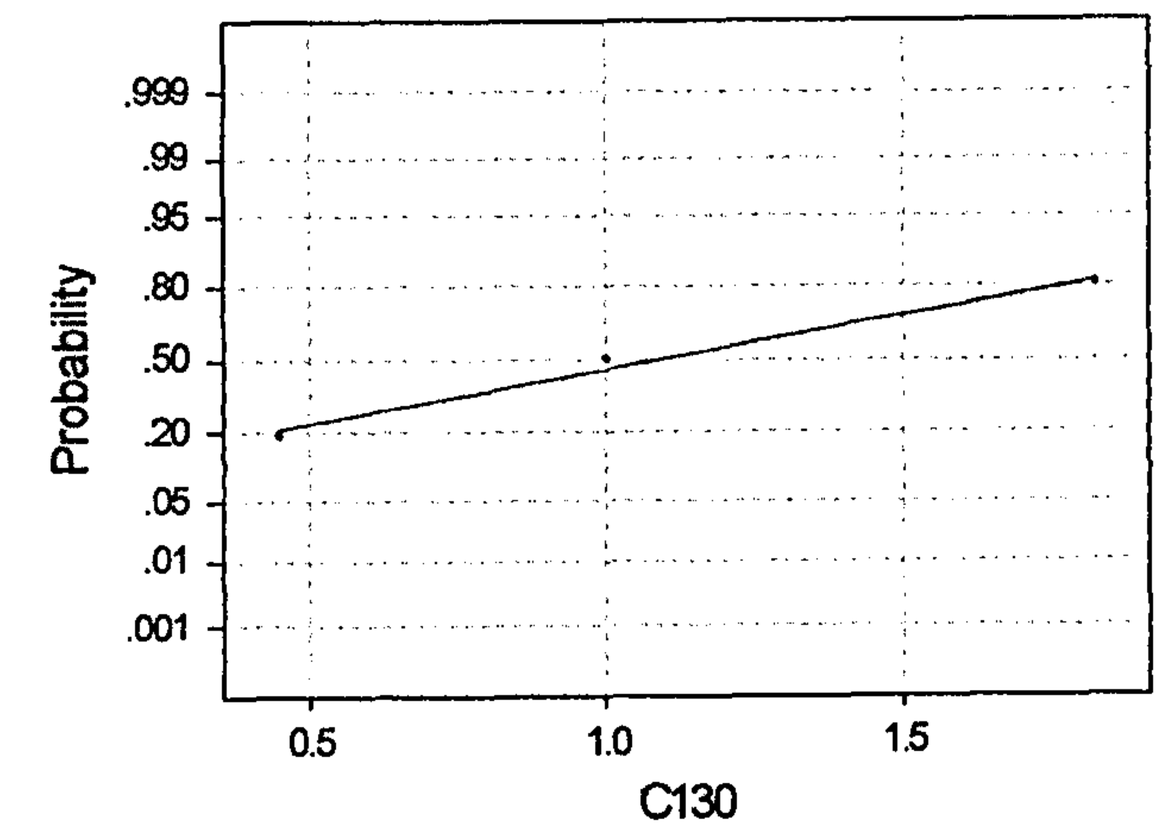

Fig 3.52 Normality Test for the population (paired difference between data for **intact capsule** and **transsected ischiofemoral and lateral iliofemoral ligaments**) used in the paired t-test

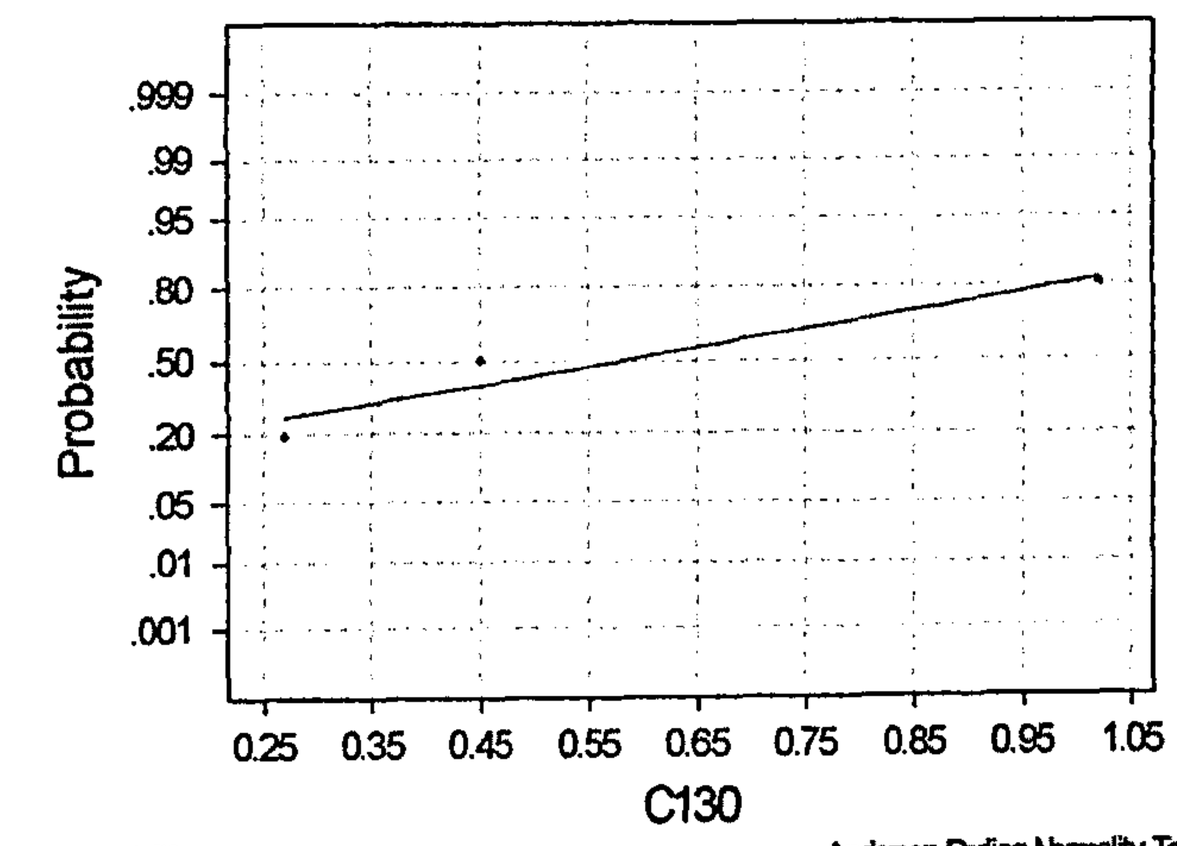

Fig 3.53 Normality Test for the population (paired difference between data for **transsected ischiofemoral &transsected ischiofemoral and lateral iliofemoral ligaments**) used in the paired t-test

Specimen 3 (Adduction)

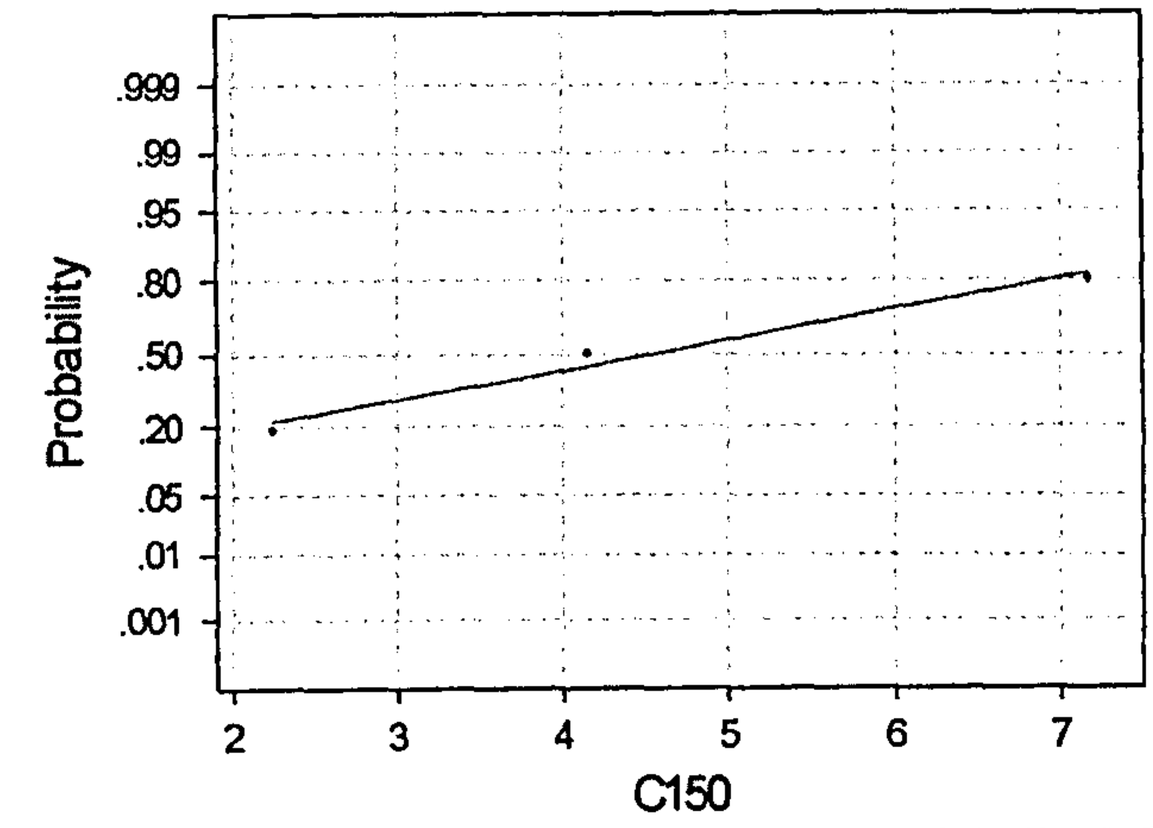

Fig 3.54 Normality Test for the population (paired difference between data for **intact capsule** and **transsected ischiofemoral ligament**) used in the paired t-test

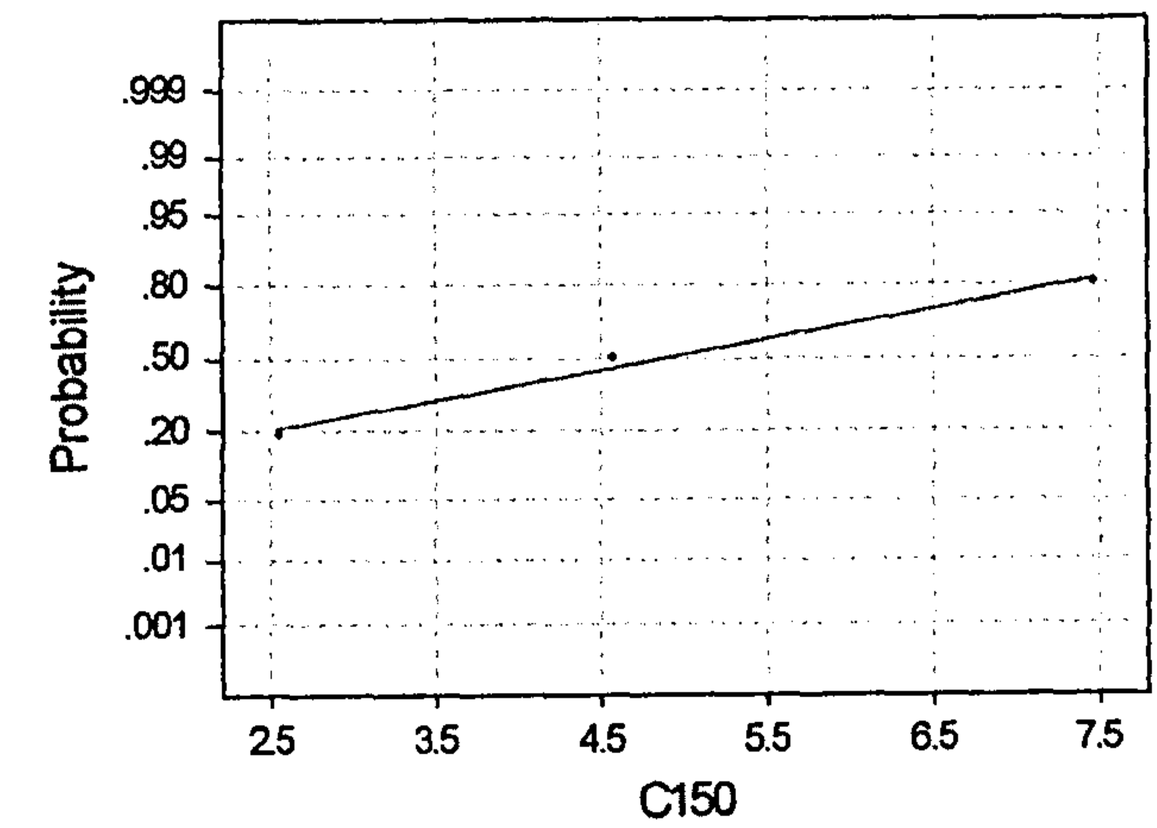

Fig 3.55 Normality Test for the population (paired difference between data for **intact capsule** and **transsected ischiofemoral and lateral iliofemoral ligaments**) used in the paired t-test

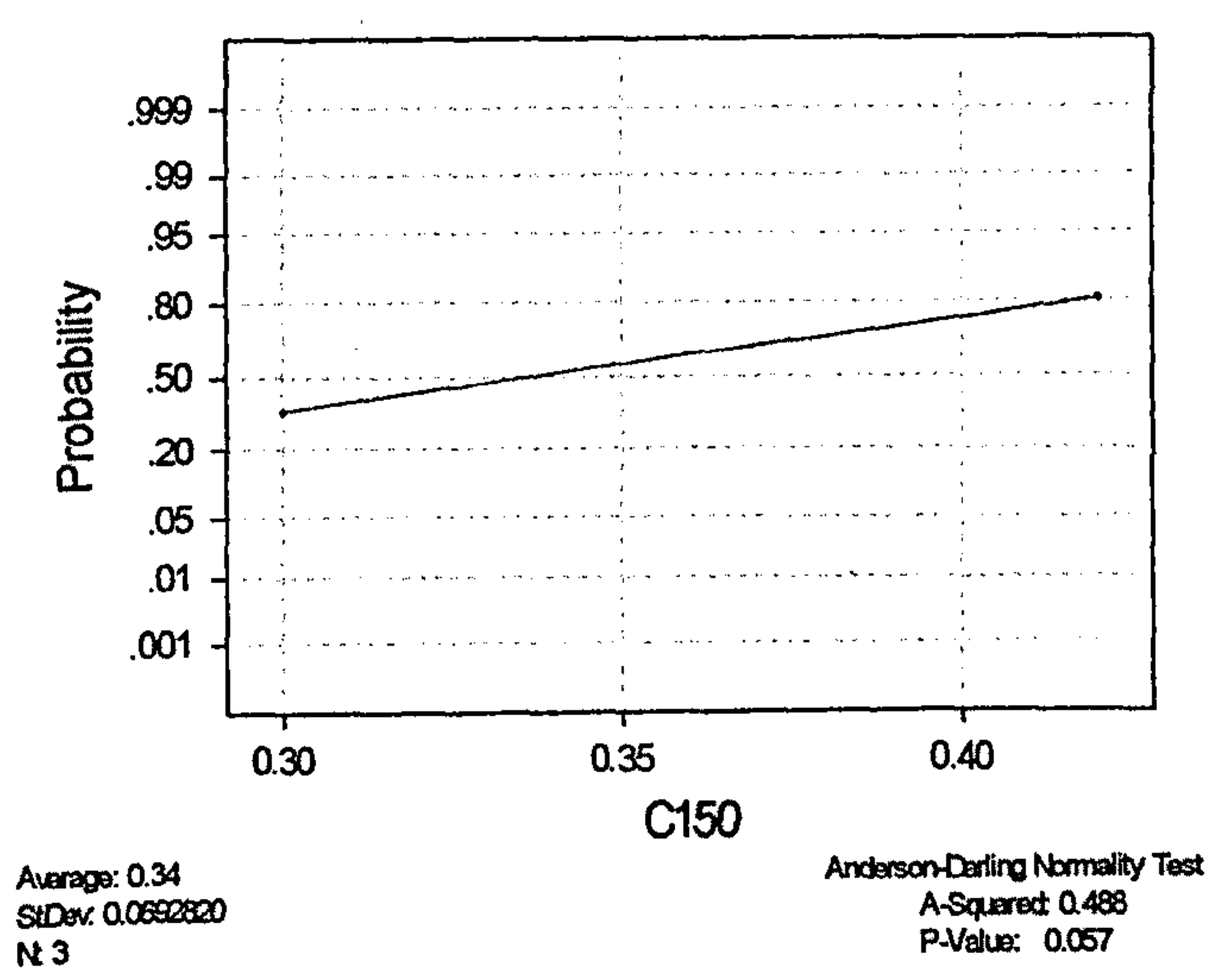

Fig 3.56 Normality Test for the population (paired difference between data for **transsected ischiofemoral &transsected ischiofemoral and lateral iliofemoral ligaments**) used in the paired t-test

Specimen (1), 2 and 3 (Abduction)

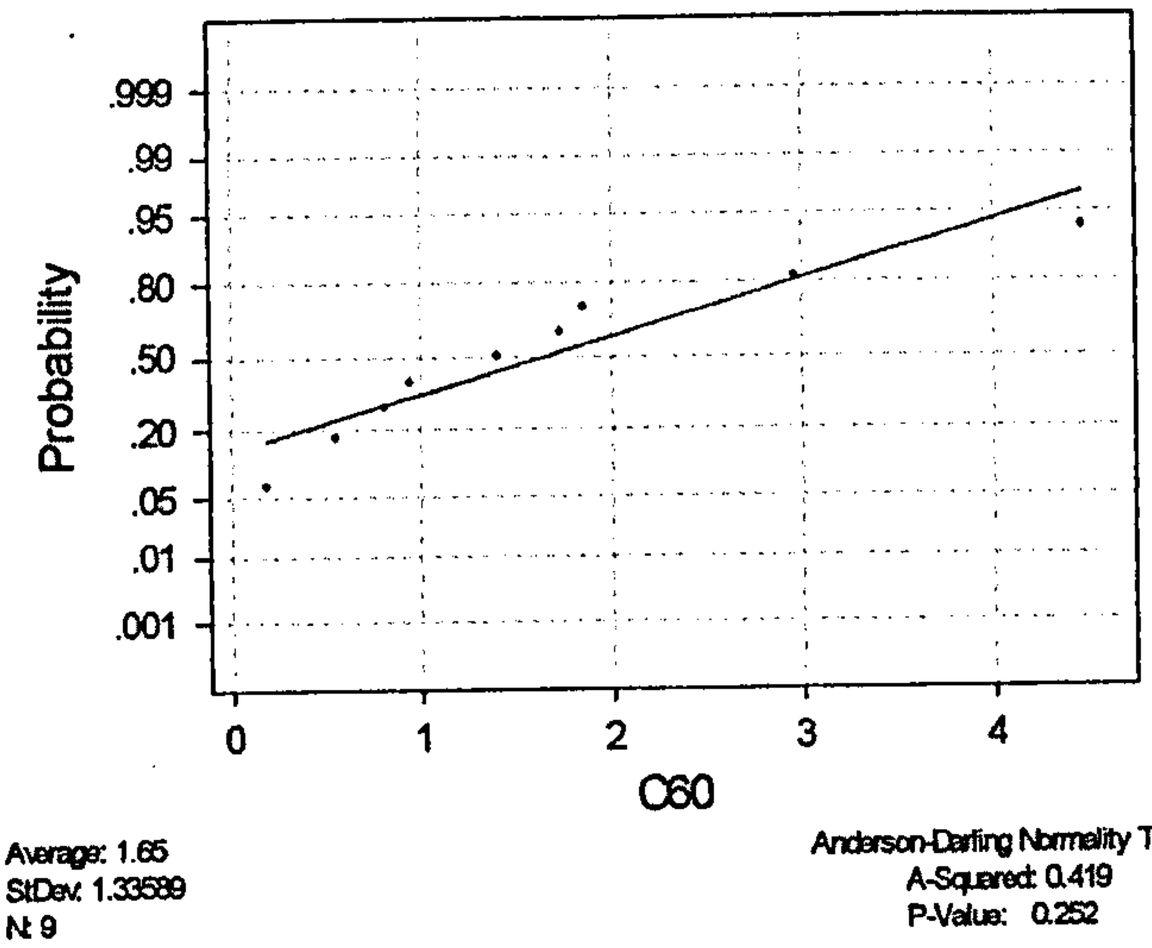

Fig 3.57 Normality Test for the population (paired difference between data for **intact capsule** and **transsected ischiofemoral ligament**) used in the paired t-test (including specimen 1)

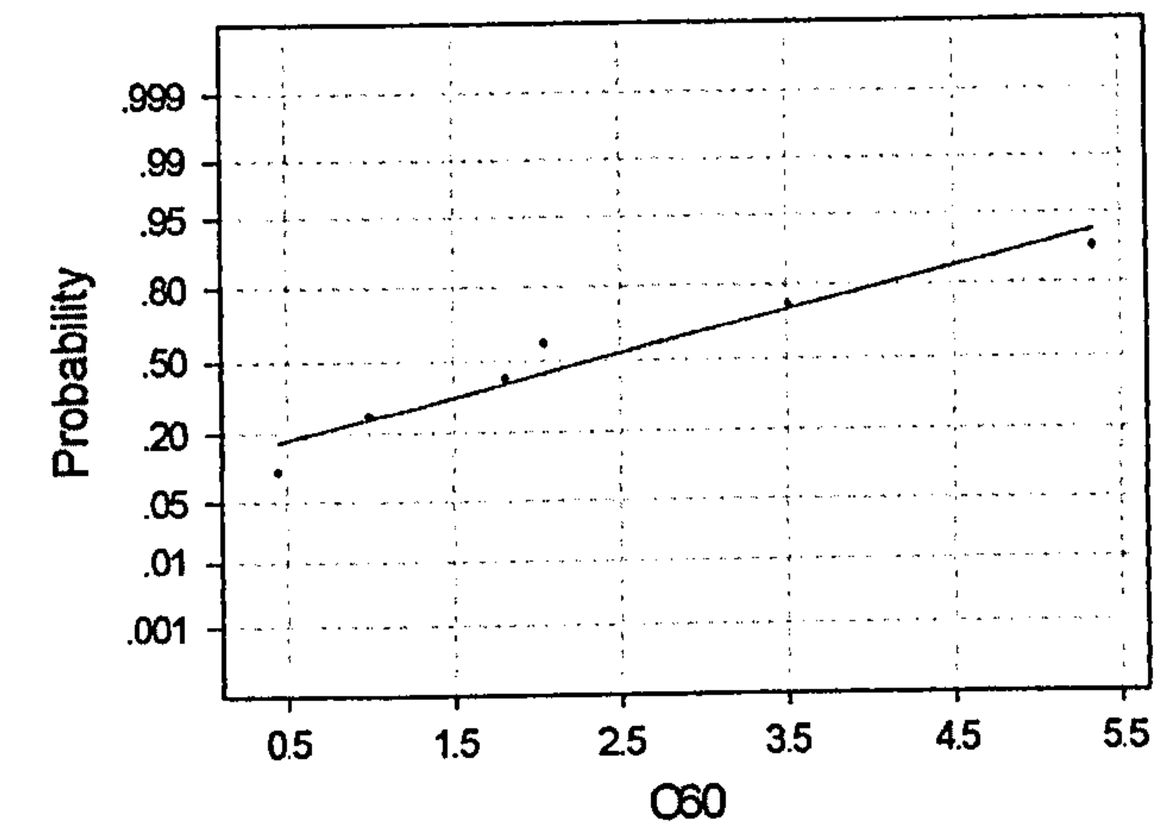

Fig 3.58 Normality Test for the population (paired difference between data for **intact capsule** and **transsected ischiofemoral and lateral iliofemoral ligaments**) used in the paired t-test

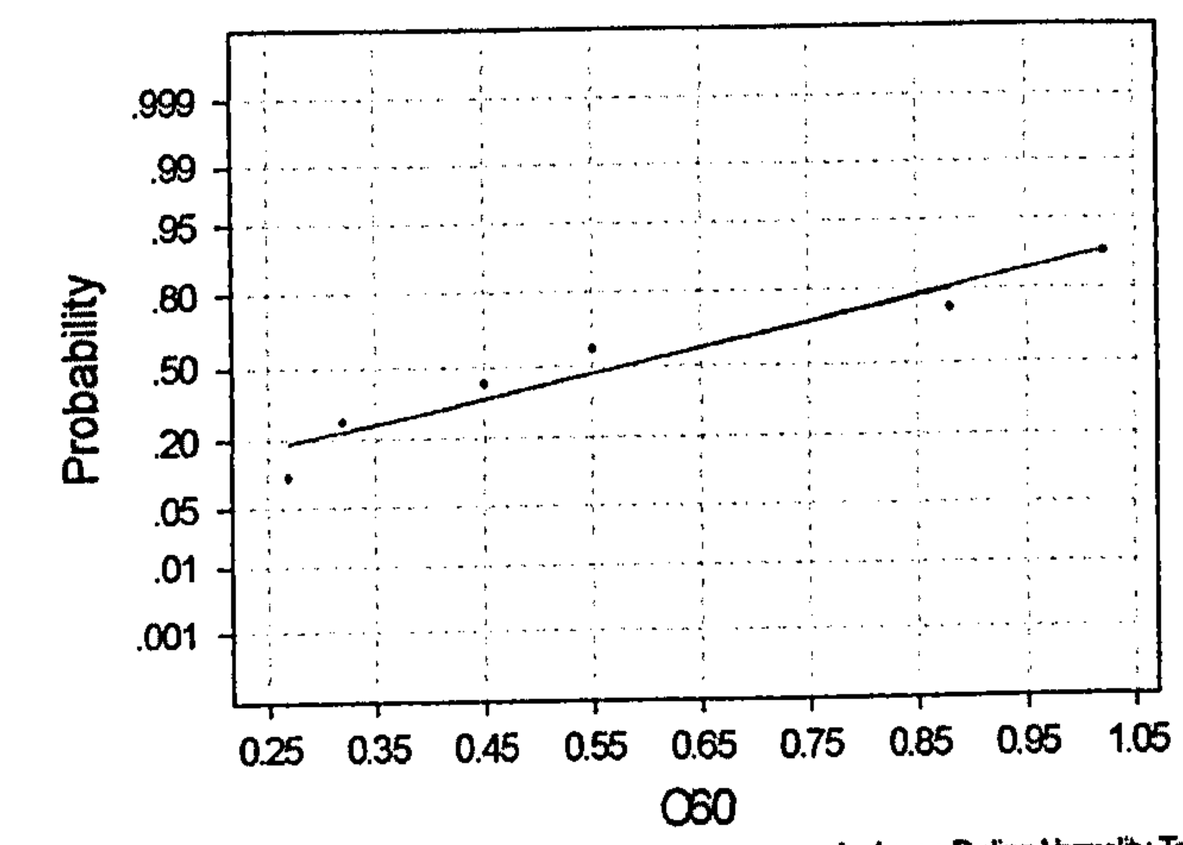

Fig 3.59 Normality Test for the population (paired difference between data for **transsected ischiofemoral &transsected ischiofemoral and lateral iliofemoral ligaments**) used in the paired t-test

Specimen (1), 2 and 3 (Adduction)

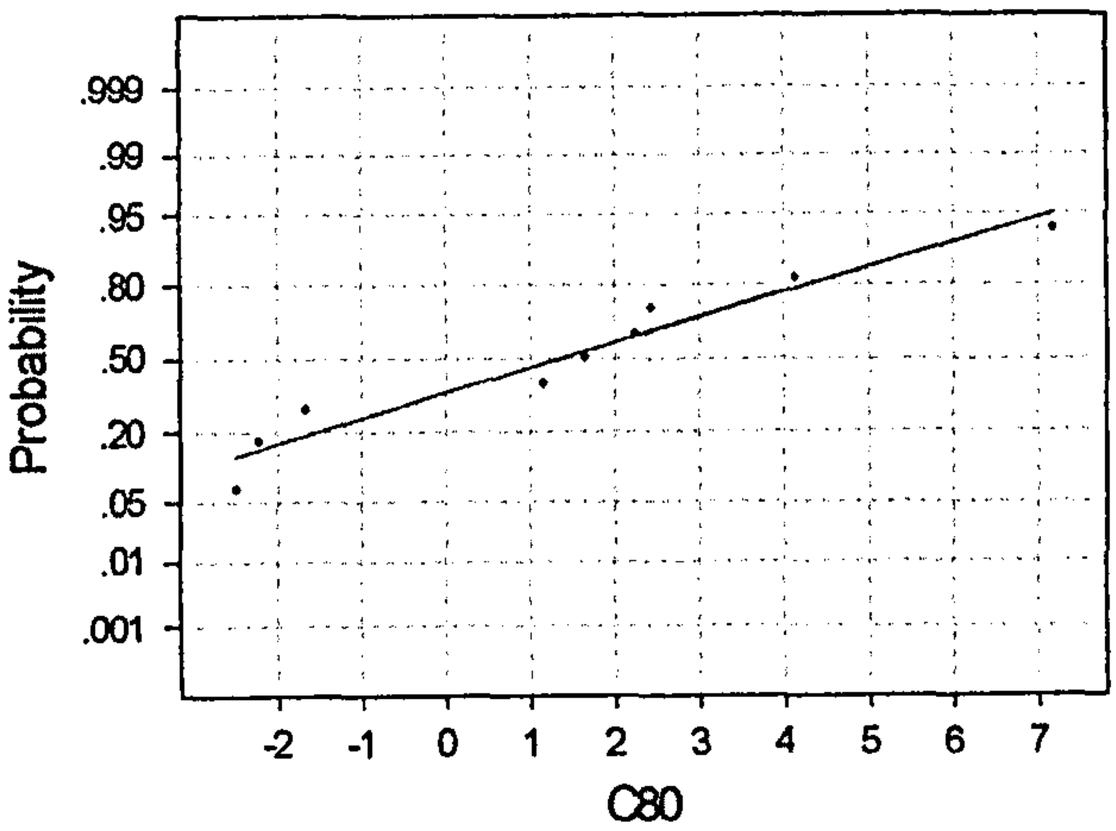

Fig 3.60 Normality Test for the population (paired difference between data for **intact capsule** and **transsected ischiofemoral ligament**) used in the paired t-test (including specimen 1)

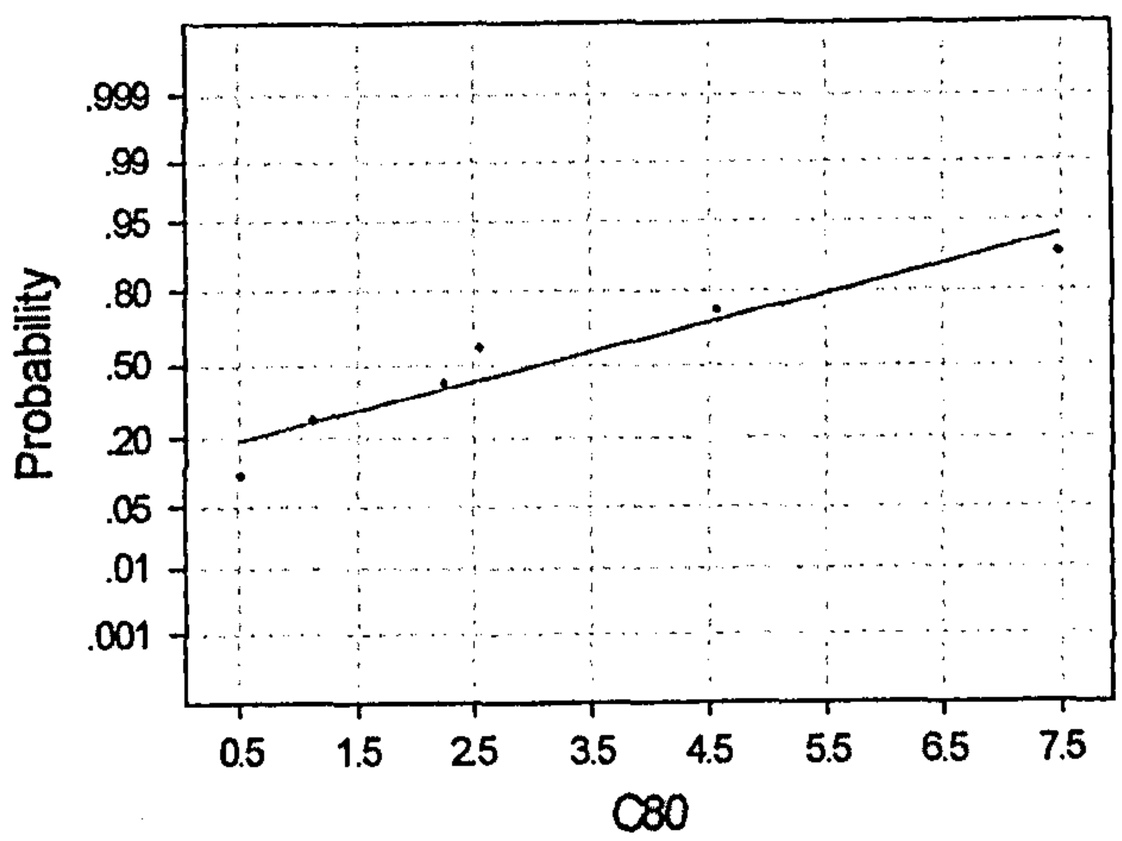

Fig 3.61 Normality Test for the population (paired difference between data for **intact capsule** and **transsected ischiofemoral and lateral iliofemoral ligaments**) used in the paired t-test

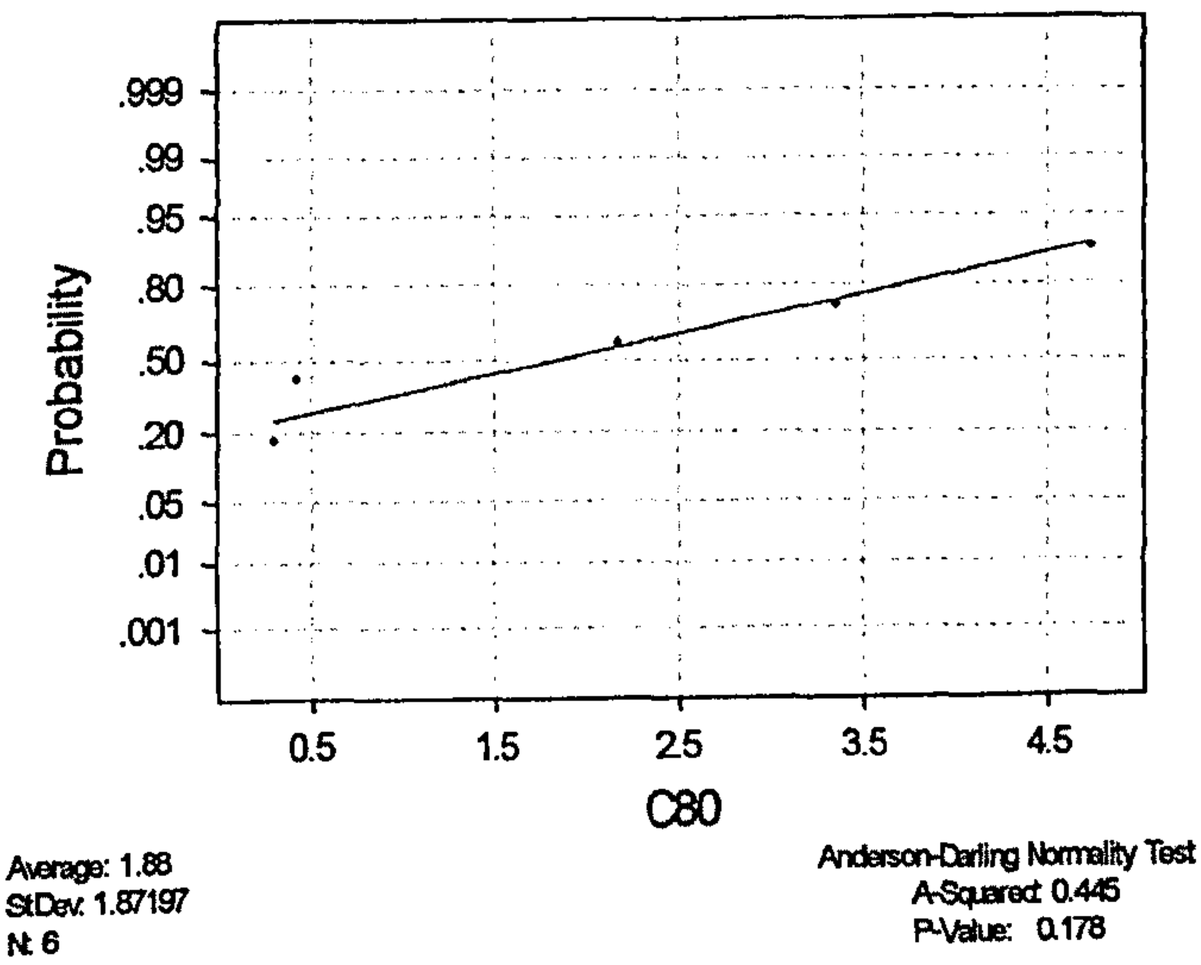

Fig 3.62 Normality Test for the population (paired difference between data for **transsected ischiofemoral &transsected ischiofemoral and lateral iliofemoral ligaments**) used in the paired t-test

All Positions

Specimen 1, 2 and 3 (Abduction)

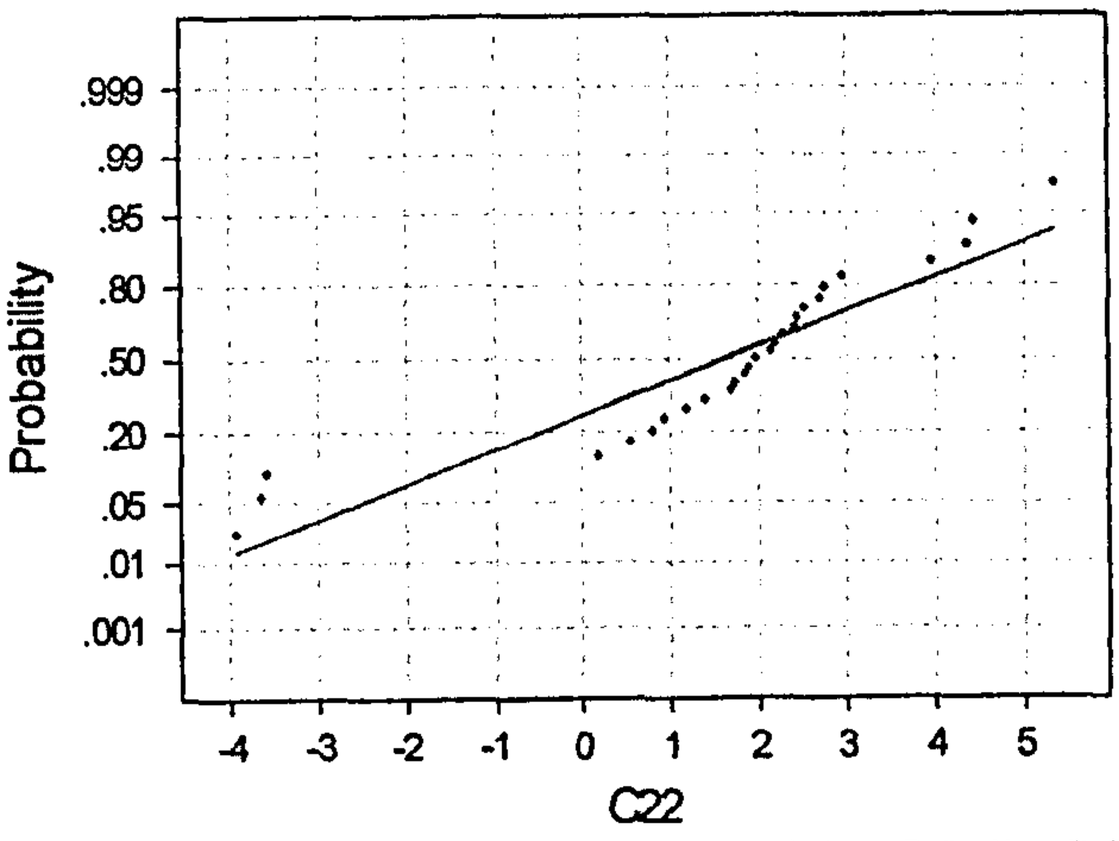

Fig 3.63 Normality Test for the population (paired difference between data for **intact capsule** and **transsected ischiofemoral ligament**) used in the paired t-test (including specimen 1)

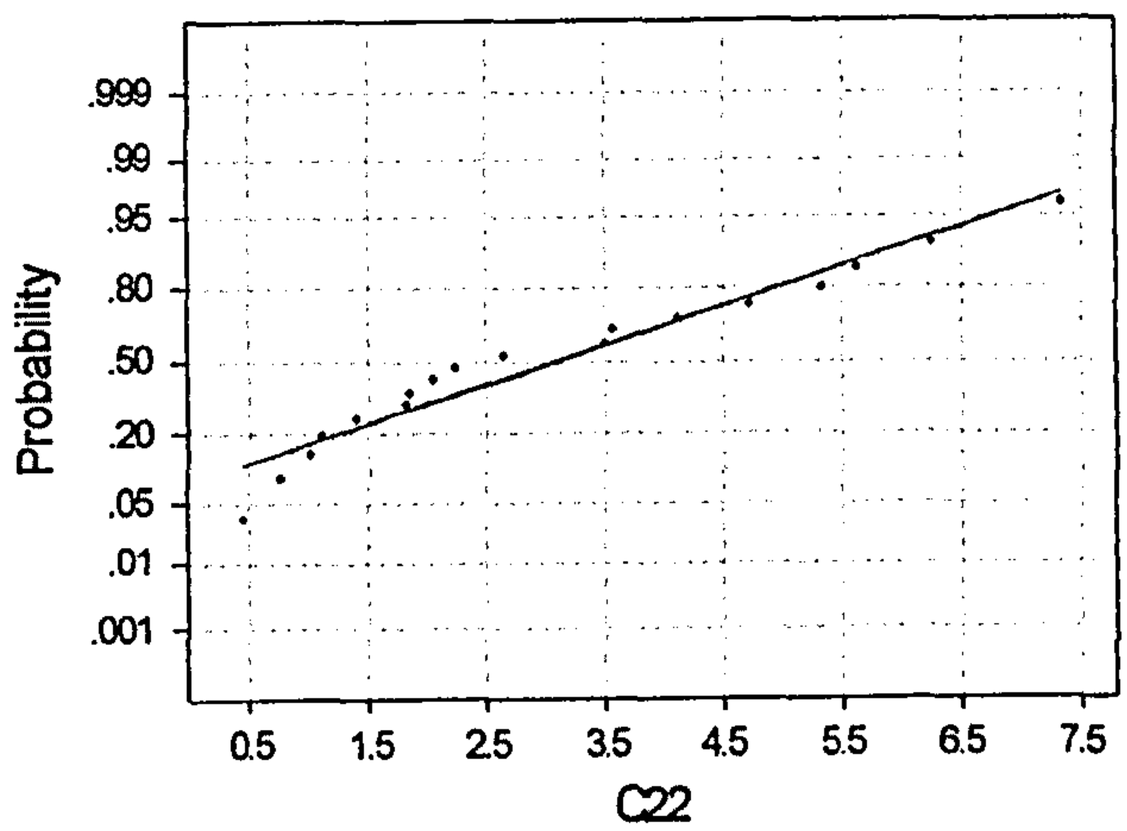

Fig 3.64 Normality Test for the population (paired difference between data for **intact capsule** and **transsected ischiofemoral and lateral iliofemoral ligaments**) used in the paired t-test

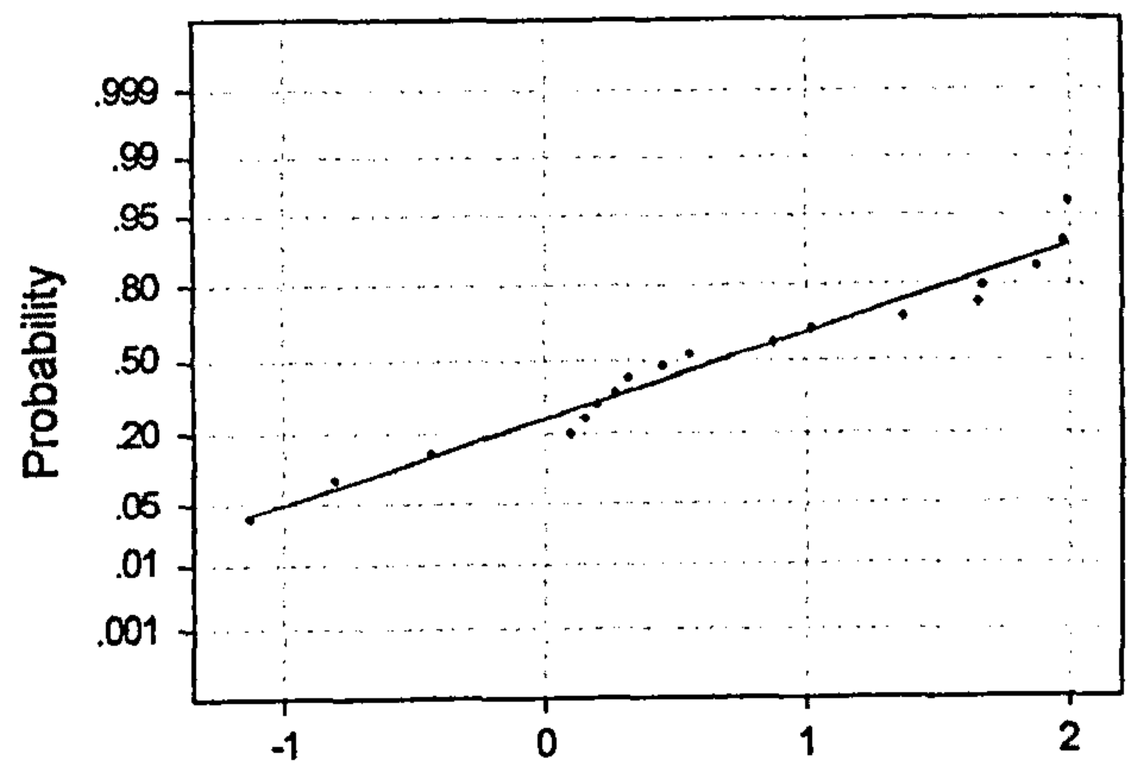

Fig 3.65 Normality Test for the population (paired difference between data for **transsected ischiofemoral &transsected ischiofemoral and lateral iliofemoral ligaments**) used in the paired t-test

Specimen 1, 2 and 3 (Adduction)

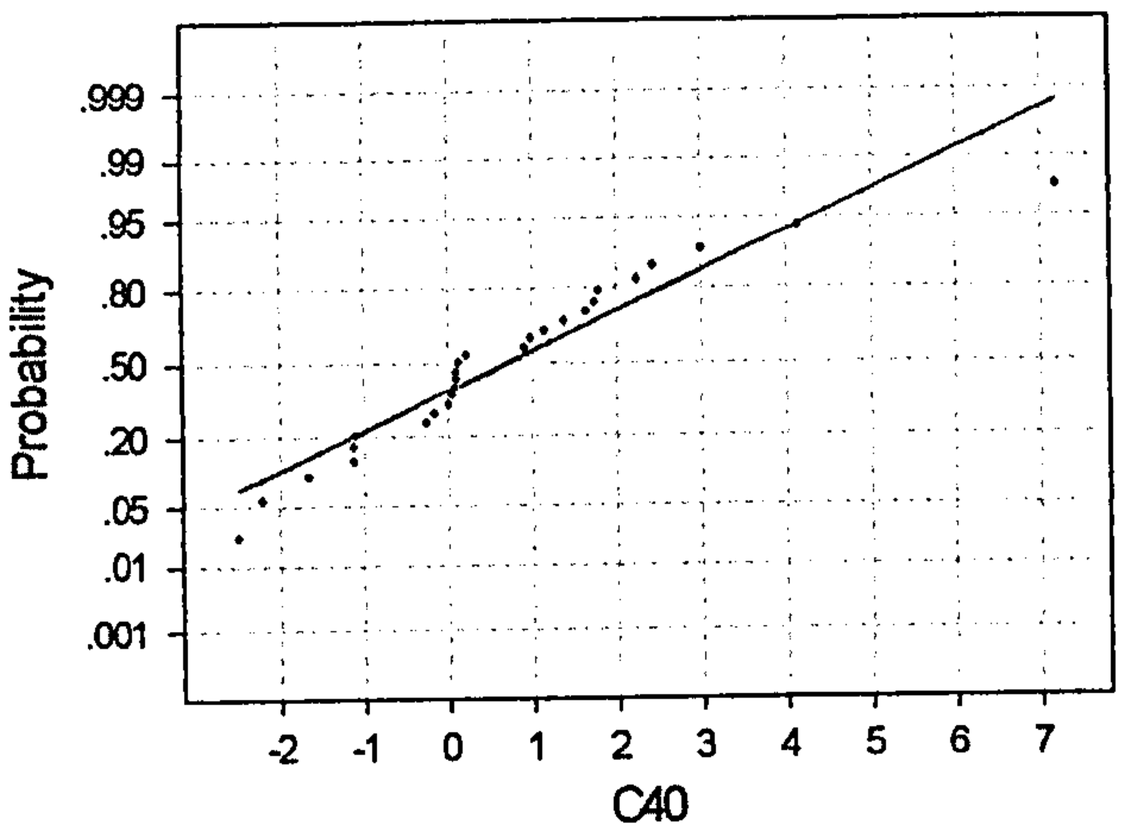

Fig 3.66 Normality Test for the population (paired difference between data for **intact capsule** and **transsected ischiofemoral ligament**) used in the paired t-test (including specimen 1)

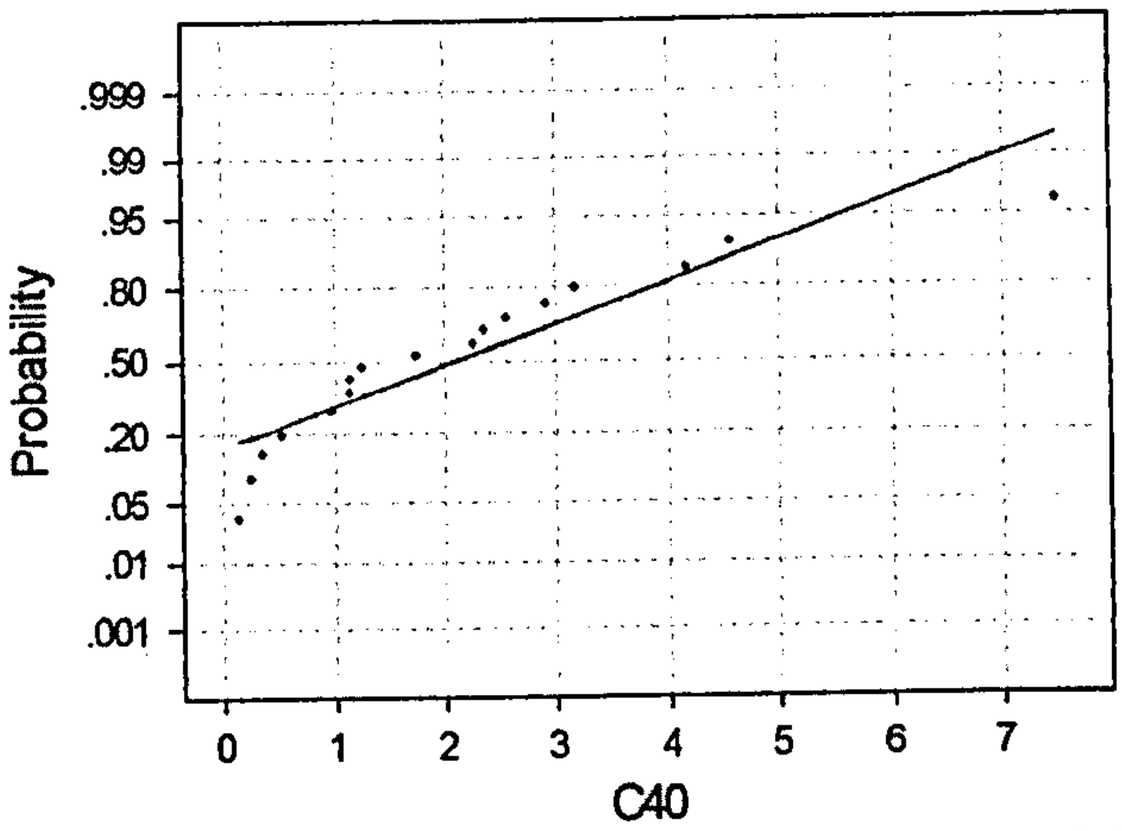

Fig 3.67 Normality Test for the population (paired difference between data for **intact capsule** and **transsected ischiofemoral and lateral iliofemoral ligaments**) used in the paired t-test

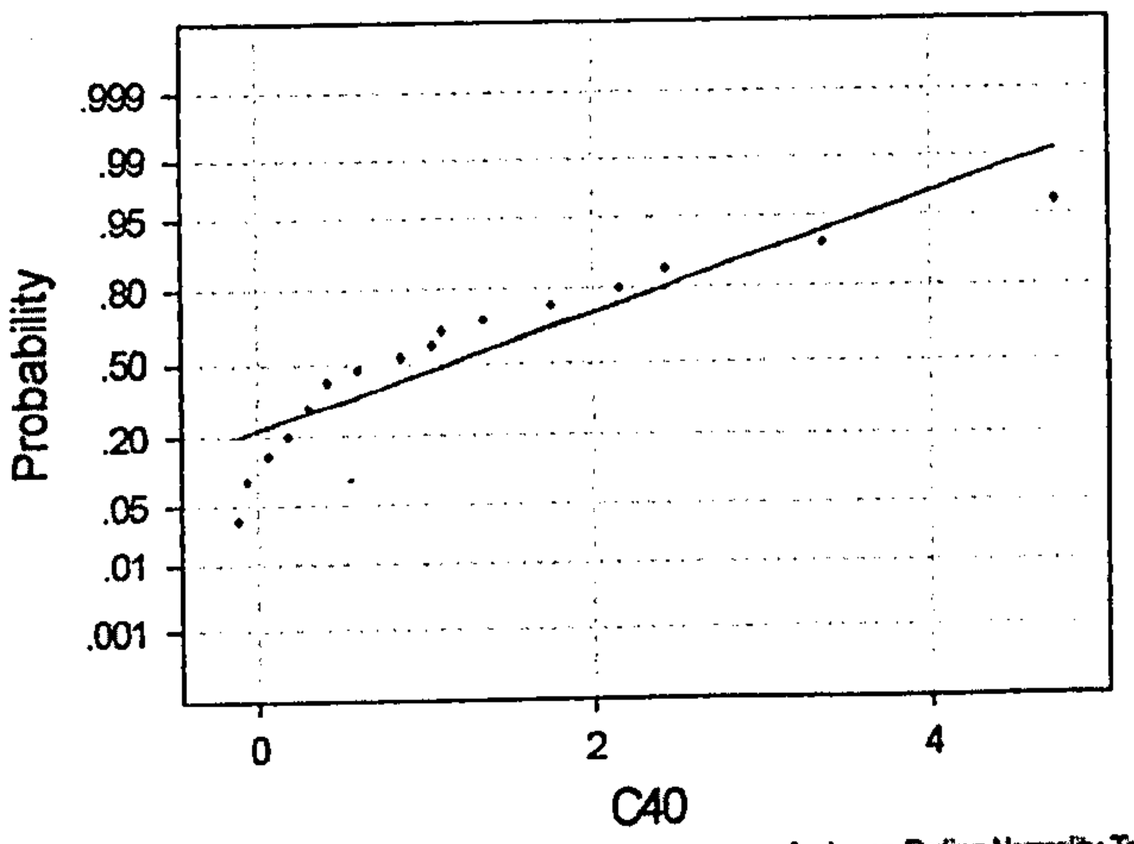

Fig 3.68 Normality Test for the population (paired difference between data for **transsected ischiofemoral &transsected ischiofemoral and lateral iliofemoral ligaments**) used in the paired t-test

III. Normality Tests for Populations in Study of Risk for Anterior Dislocation

The graphs that follow were generated from the normality tests that were performed for the data from the study for risk of anterior dislocation. Similar to the graphs in paragraph III of the Appendix the following were performed for the different limb positions and for the three capsule conditions (i.e. intact and dissected). The red line in the graphs is an estimate of the distribution function for the population from which data are drawn. The y-axis shows the probability of actual occurrence of certain values, which are shown in the x-axis, whereas the red line indicates where these values would fall in a normal distribution.

Neutral

Specimen 4 (Adduction)

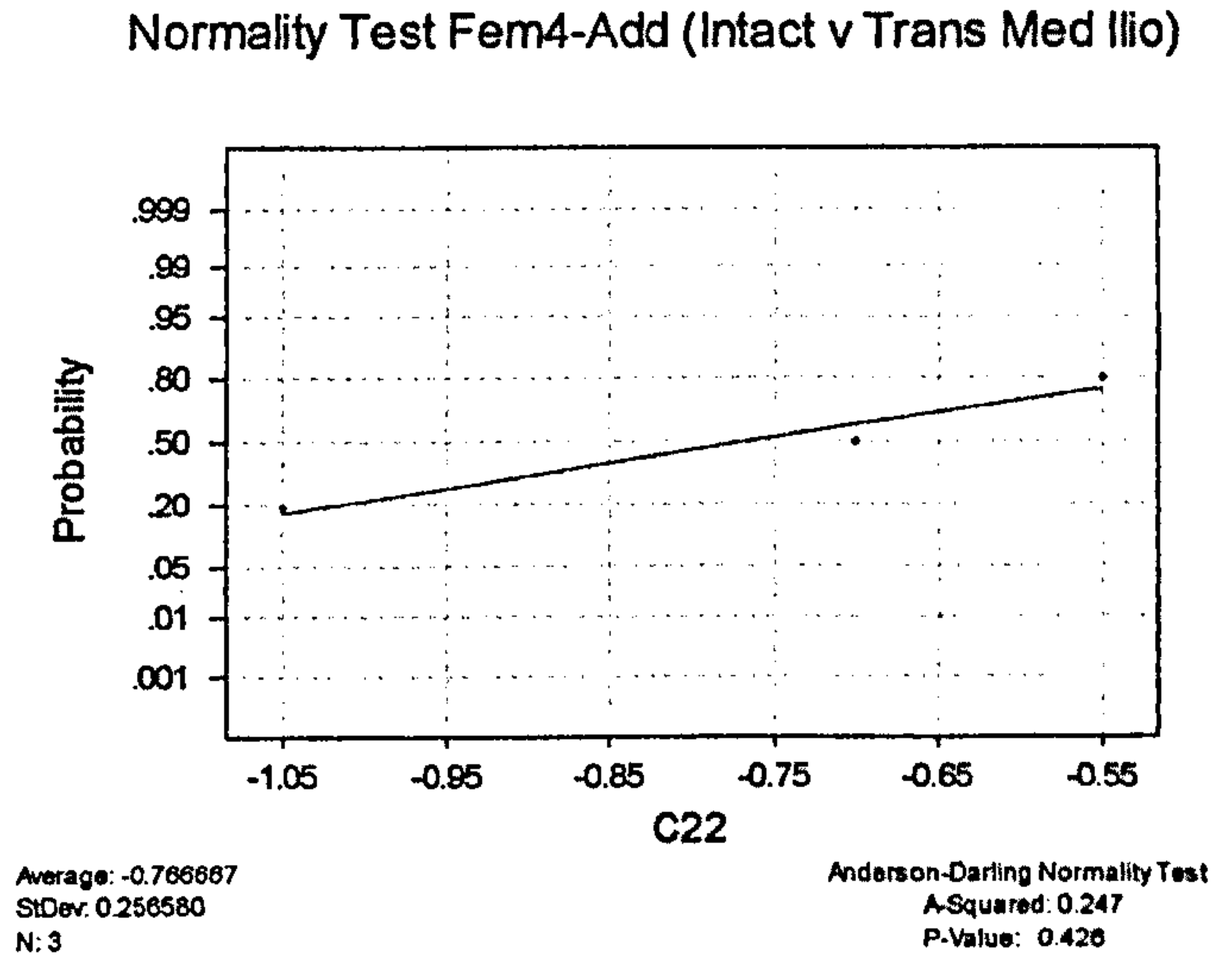

Fig. 4.1 Normality Test for the population (paired difference between data for **intact capsule** and **transsected medial iliofemoral ligament**) used in the paired t-test

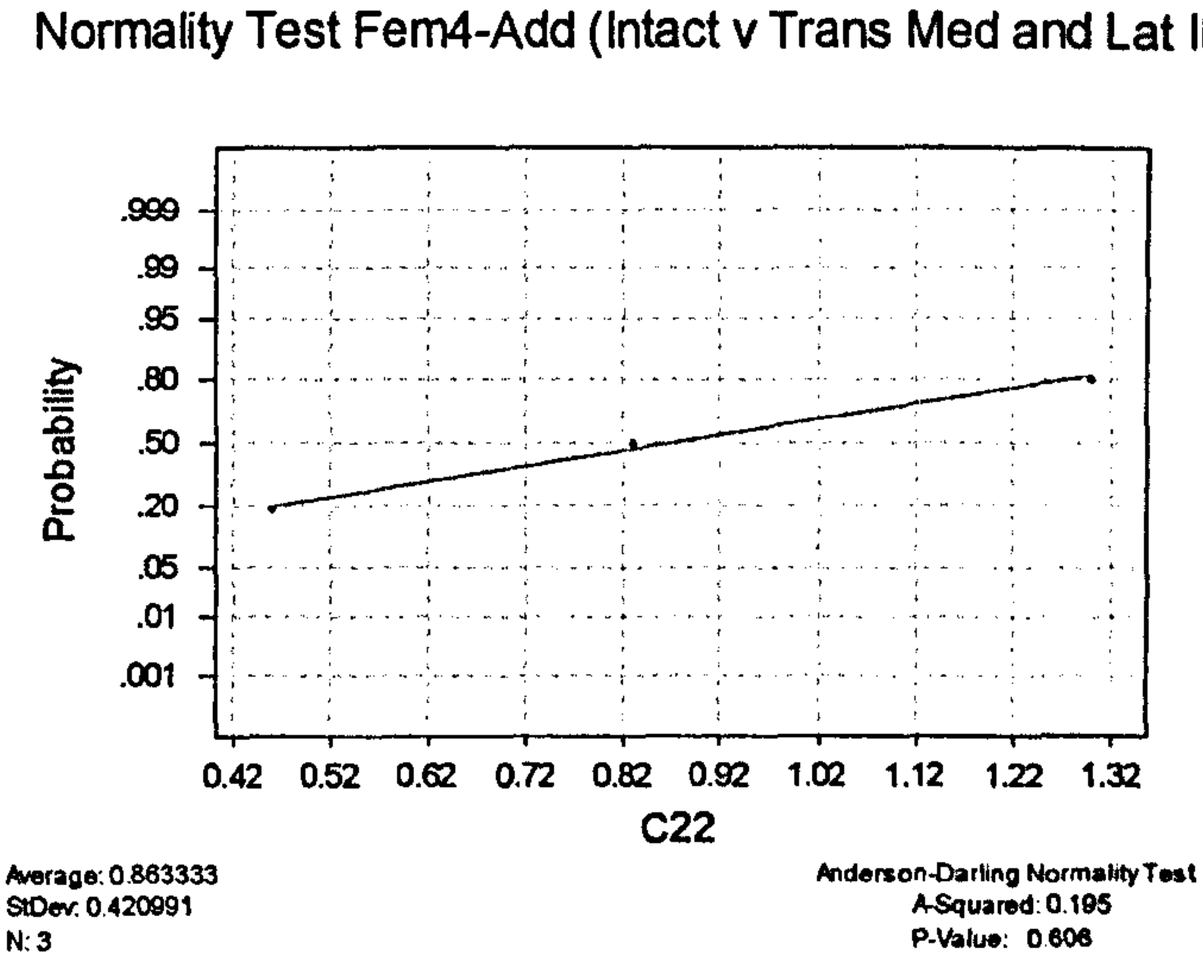

Fig. 4.2 Normality Test for the population (paired difference between data for **intact capsule** and **transsected medial and lateral iliofemoral ligaments**) used in the paired t-test

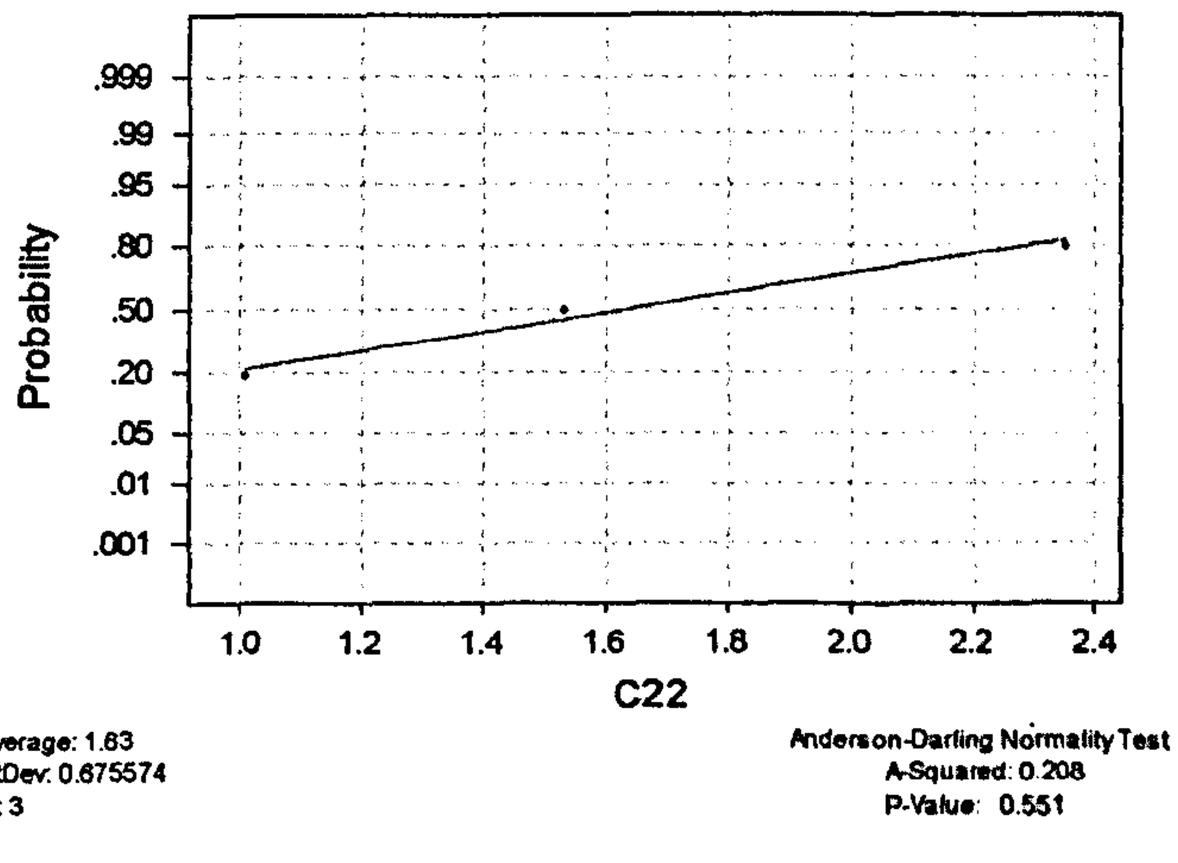

Fig. 4.3 Normality Test for the population (paired difference between data for **transsected medial iliofemoral ligament** and **transsected medial and lateral iliofemoral ligaments**) used in the paired t-test

Specimen 4 (Abduction)

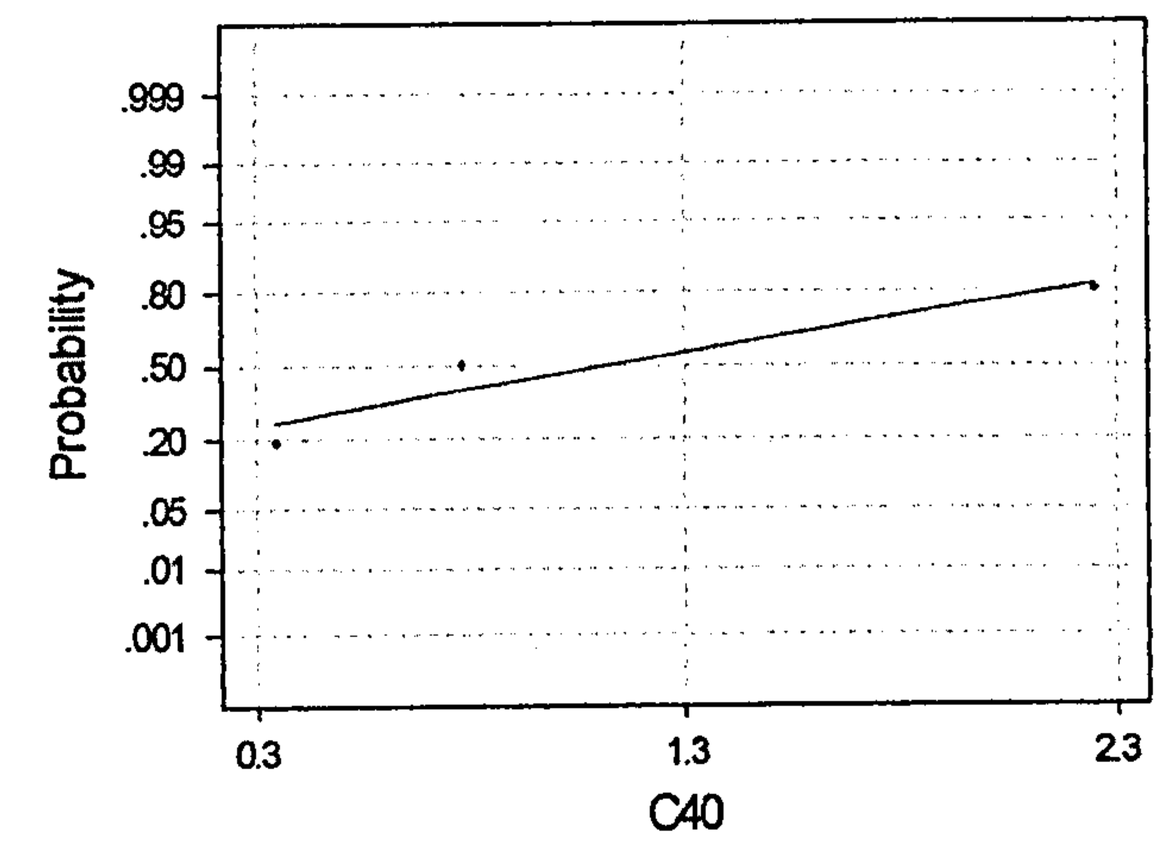

Fig 4.4 Normality Test for the population (paired difference between data for **intact capsule** and **transsected medial iliofemoral ligament**) used in the paired t-test

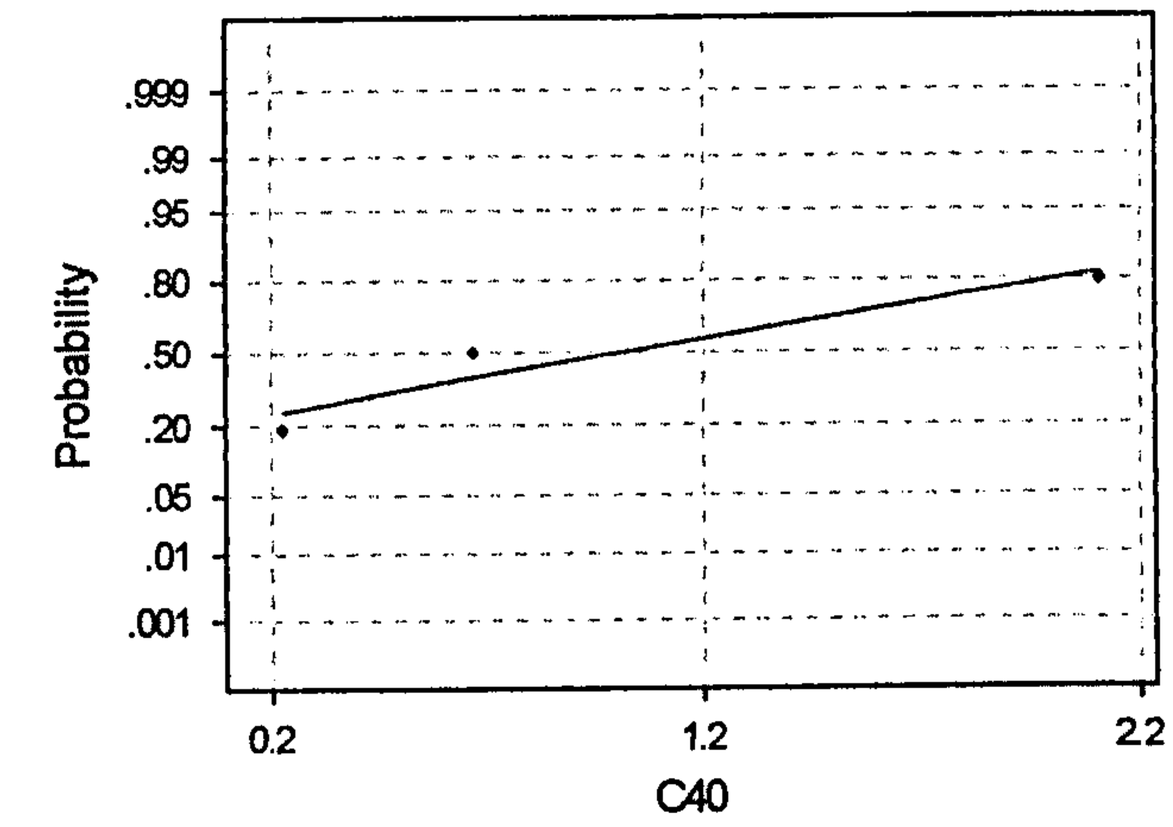

Fig 4.5 Normality Test for the population (paired difference between data for **intact capsule** and **transsected medial and lateral iliofemoral ligaments**) used in the paired t-test

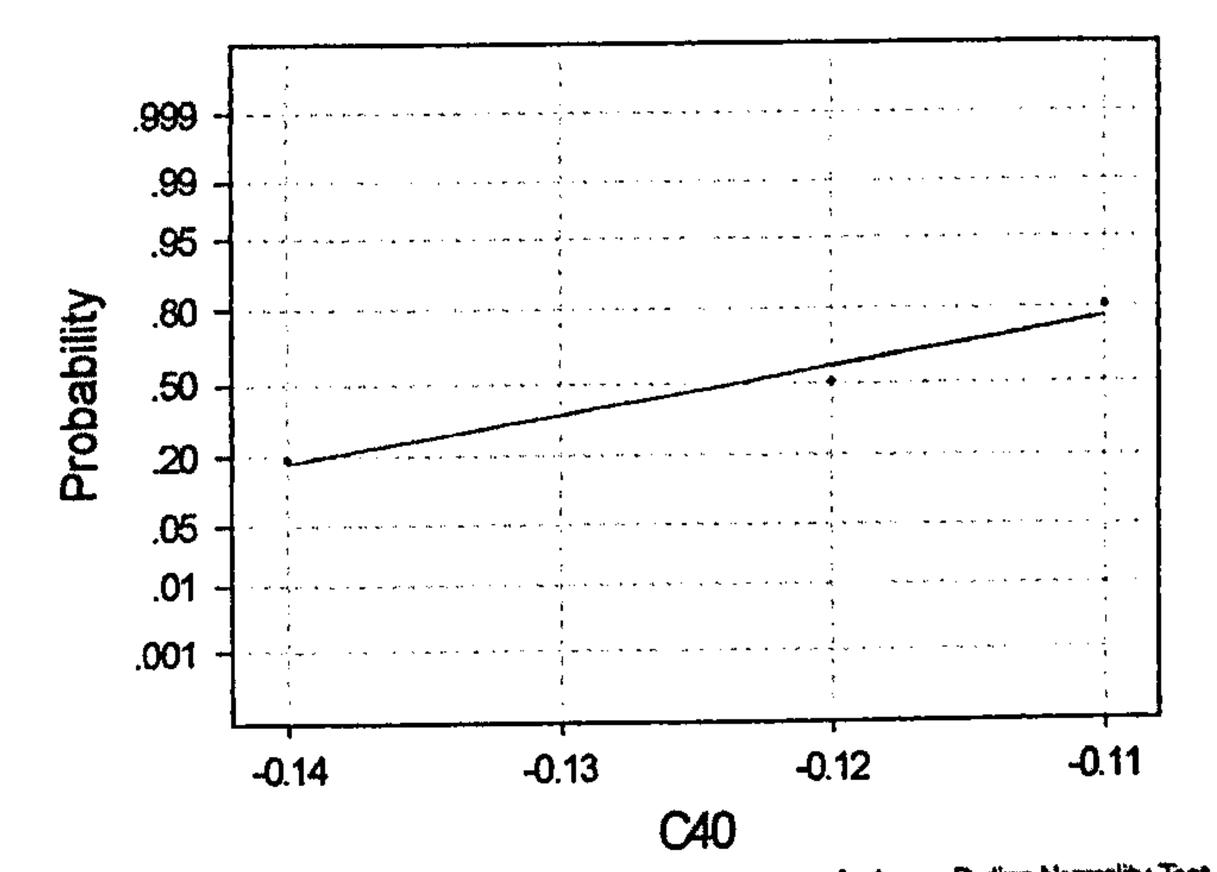

Fig 4.6 Normality Test for the population (paired difference between data for **transsected medial iliofemoral** and **transsected medial and lateral iliofemoral ligaments**) used in the paired t-test

Specimen 5 (Adduction)

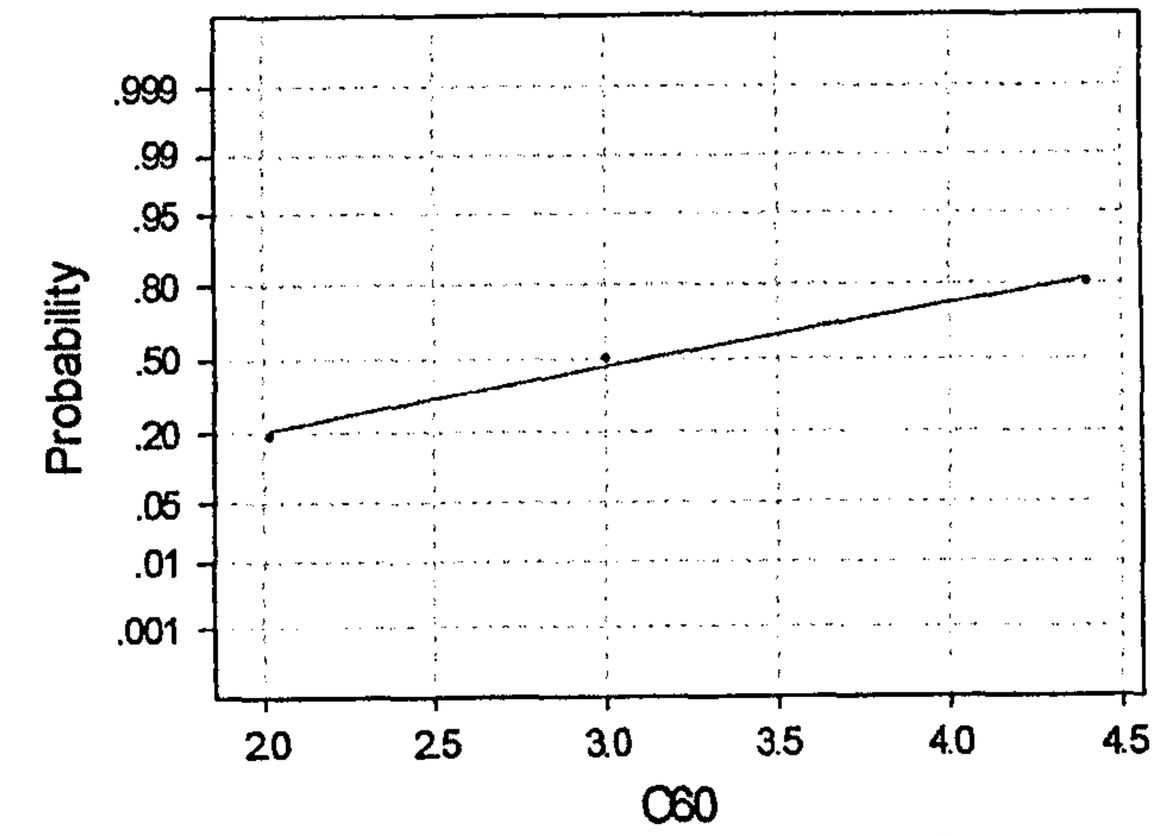

Fig 4.7 Normality Test for the population (paired difference between data for **intact capsule** and **transsected medial iliofemoral ligament**) used in the paired t-test

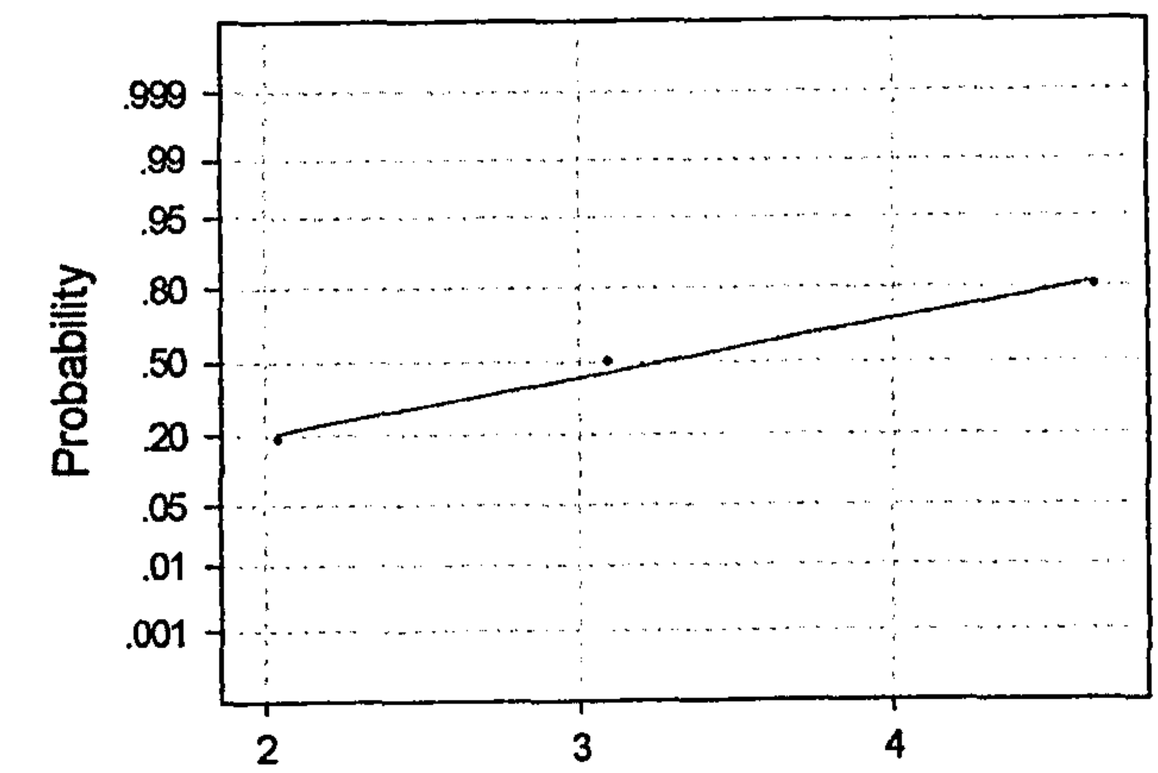

Fig 4.8 Normality Test for the population (paired difference between data for **intact capsule** and **transsected medial and lateral iliofemoral ligaments**) used in the paired t-test

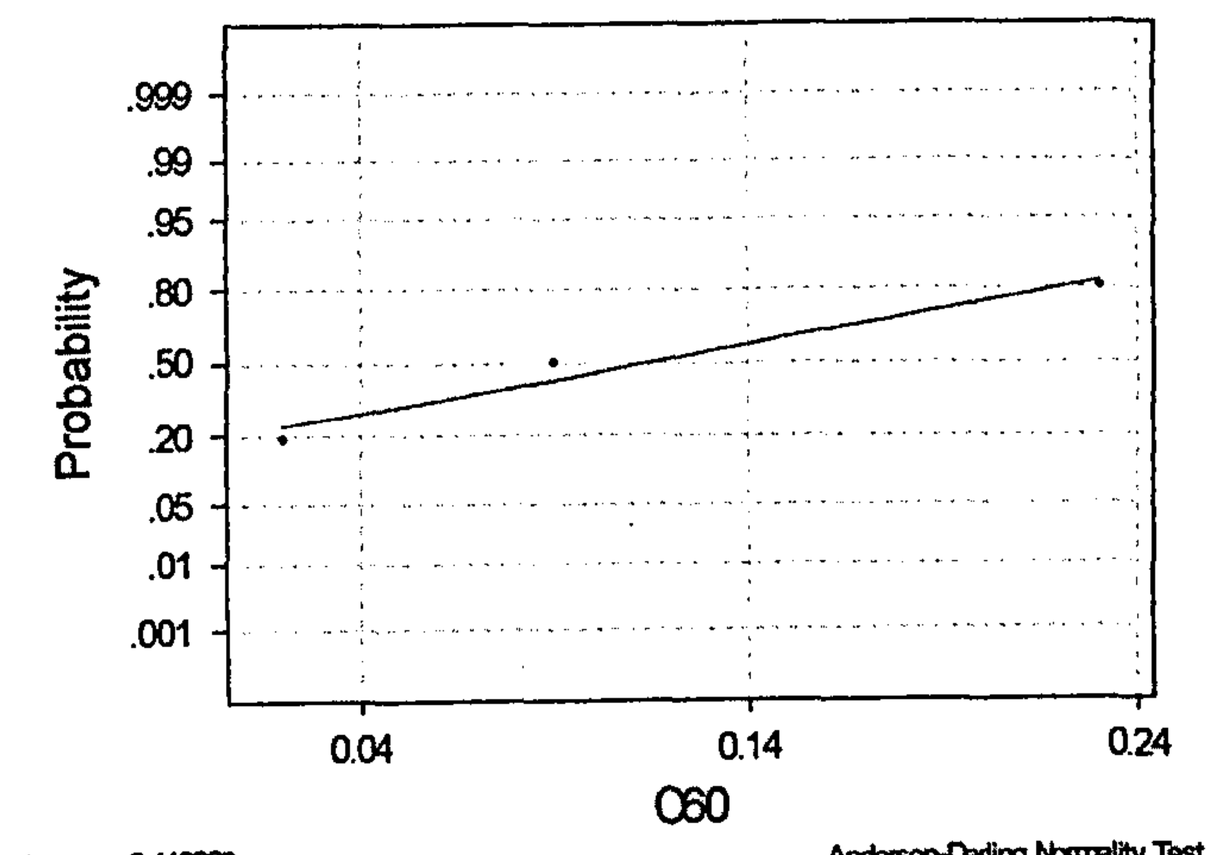

Fig 4.9 Normality Test for the population (paired difference between data for **transsected medial iliofemoral** and **transsected medial and lateral iliofemoral ligaments**) used in the paired t-test

Specimen 5 (Abduction)

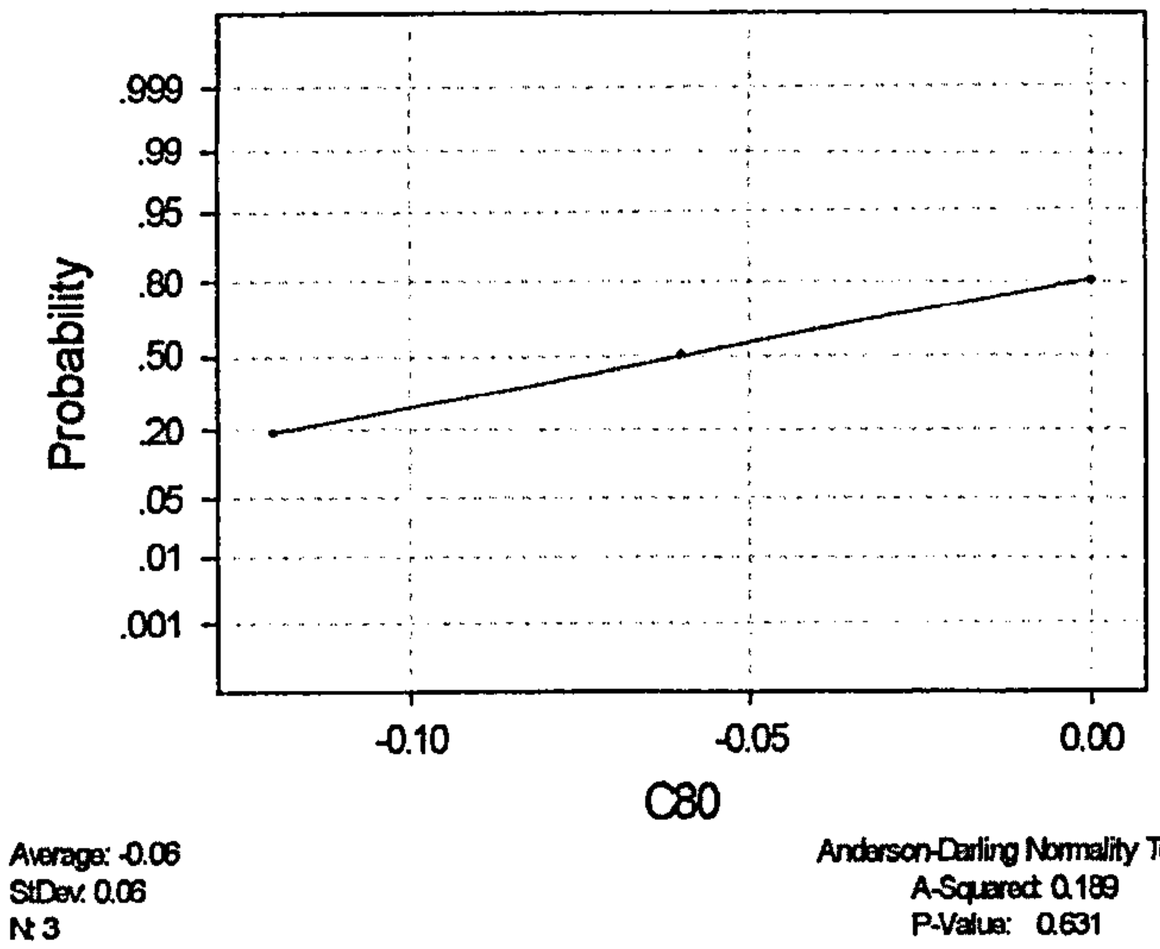

Fig 4.10 Normality Test for the population (paired difference between data for **intact capsule** and **transsected medial iliofemoral ligament**) used in the paired t-test

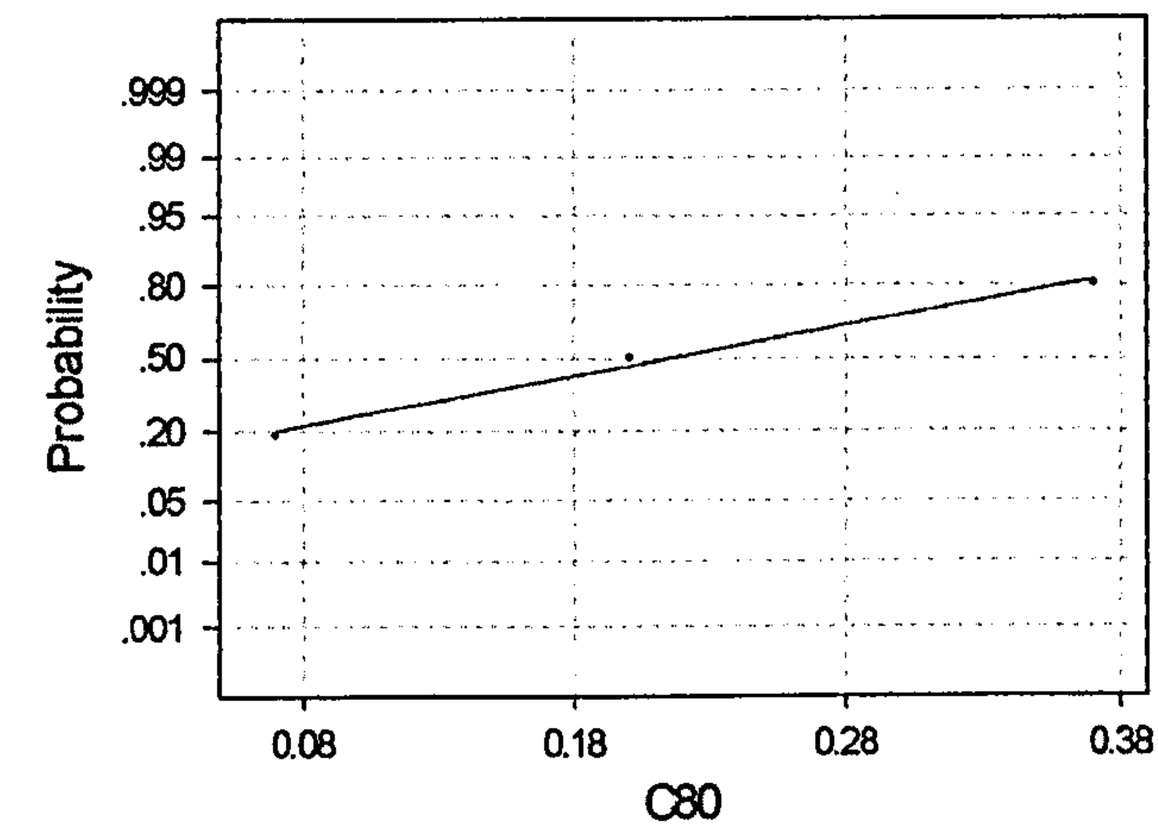

Fig 4.11 Normality Test for the population (paired difference between data for **intact capsule** and **transsected medial and lateral iliofemoral ligaments**) used in the paired t-test

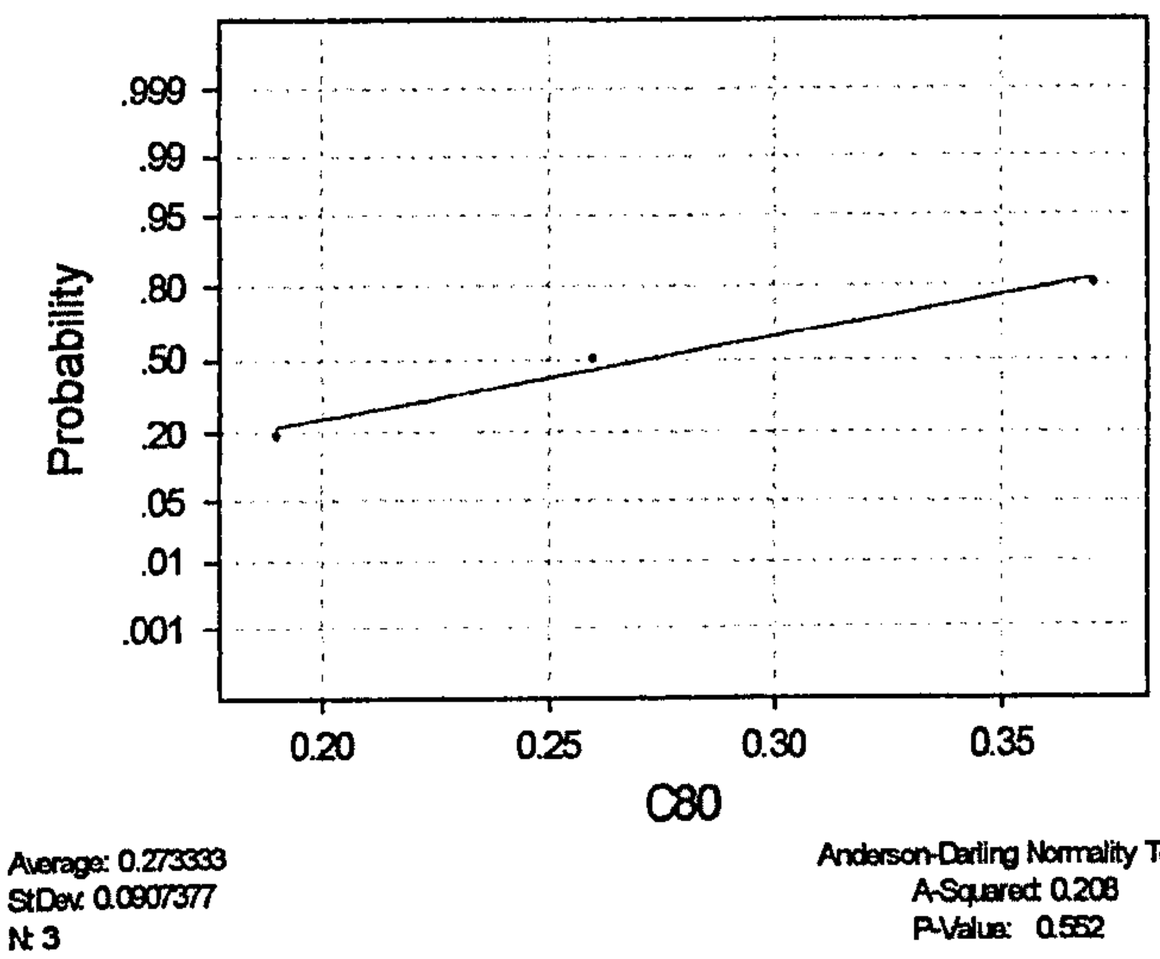

Fig 4.12 Normality Test for the population (paired difference between data for **transsected medial iliofemoral** and **transsected medial and lateral iliofemoral ligaments**) used in the paired t-test

Specimen 4 and 5 (Adduction)

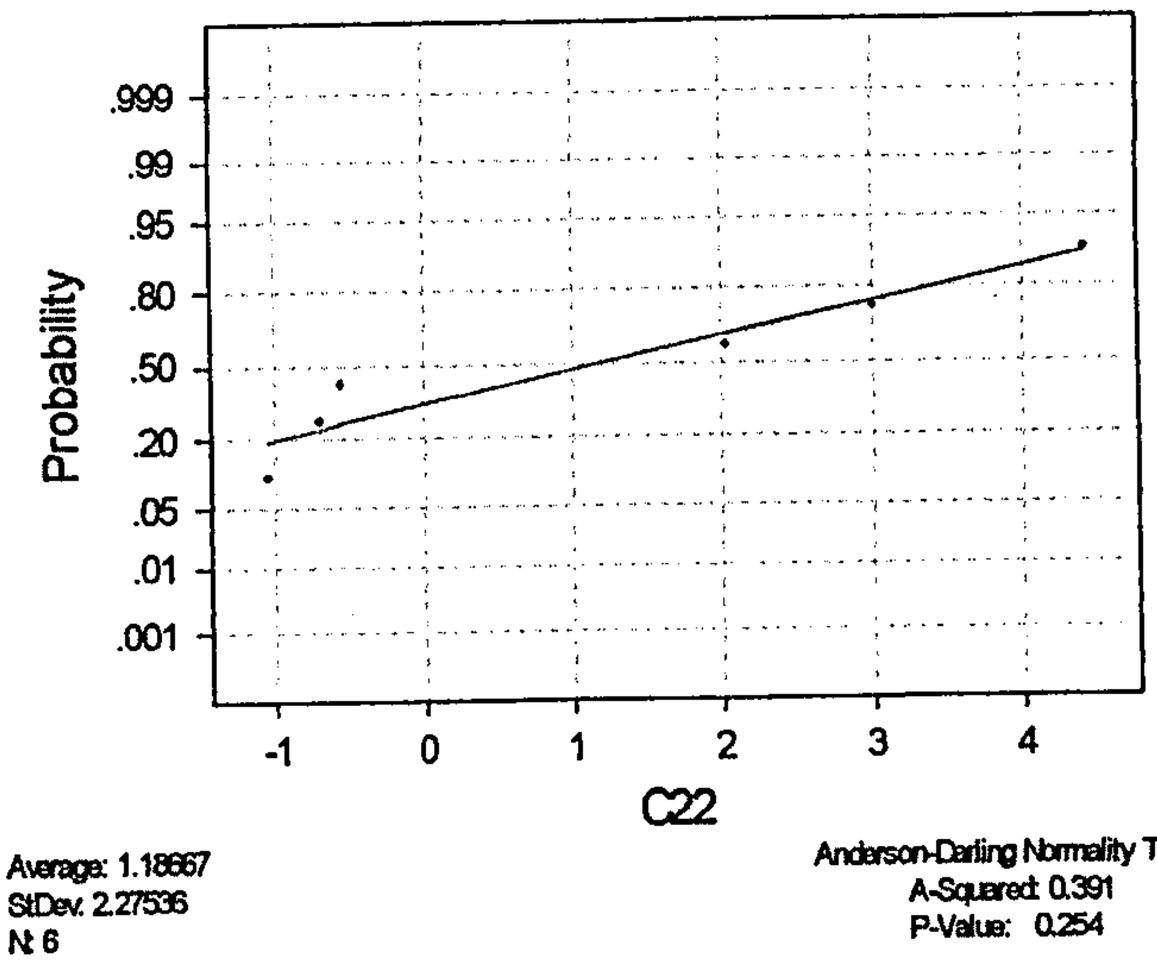

Fig 4.13 Normality Test for the population (paired difference between data for **intact capsule** and **transsected medial iliofemoral ligament**) used in the paired t-test

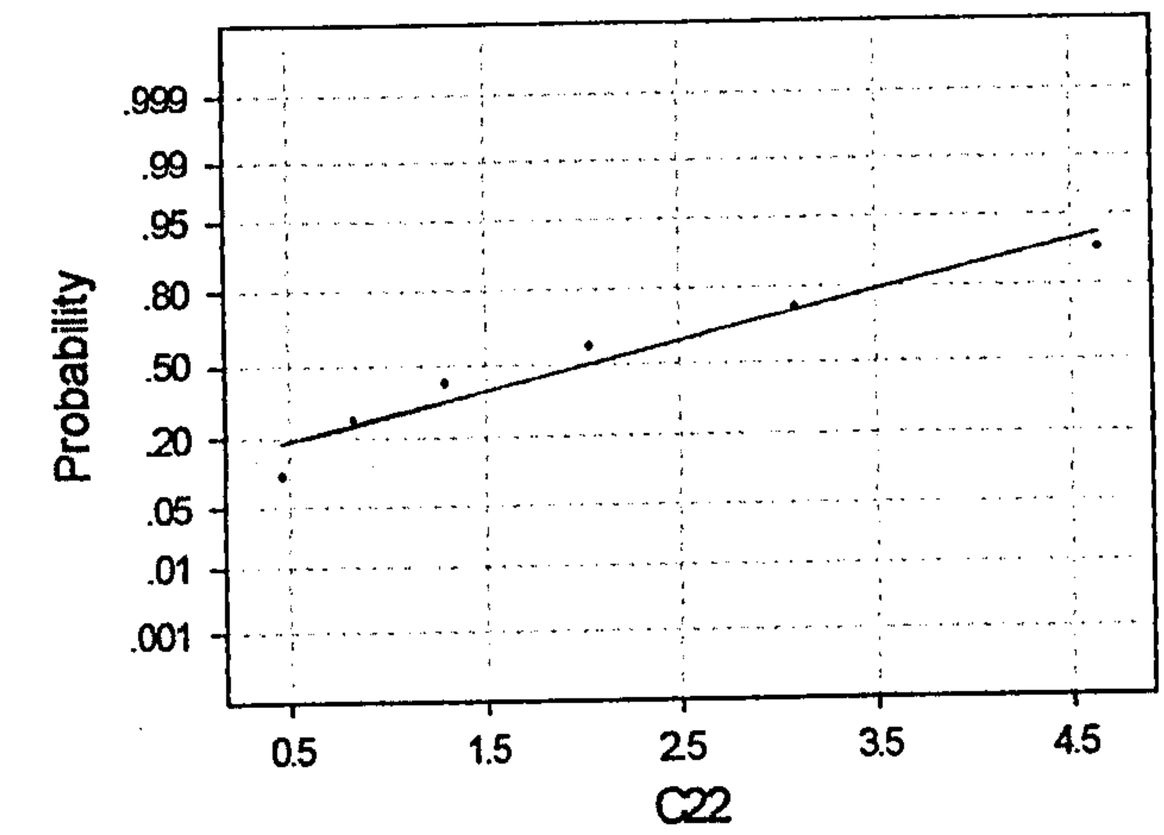

Fig 4.14 Normality Test for the population (paired difference between data for **intact capsule** and **transsected medial and lateral iliofemoral ligaments**) used in the paired t-test

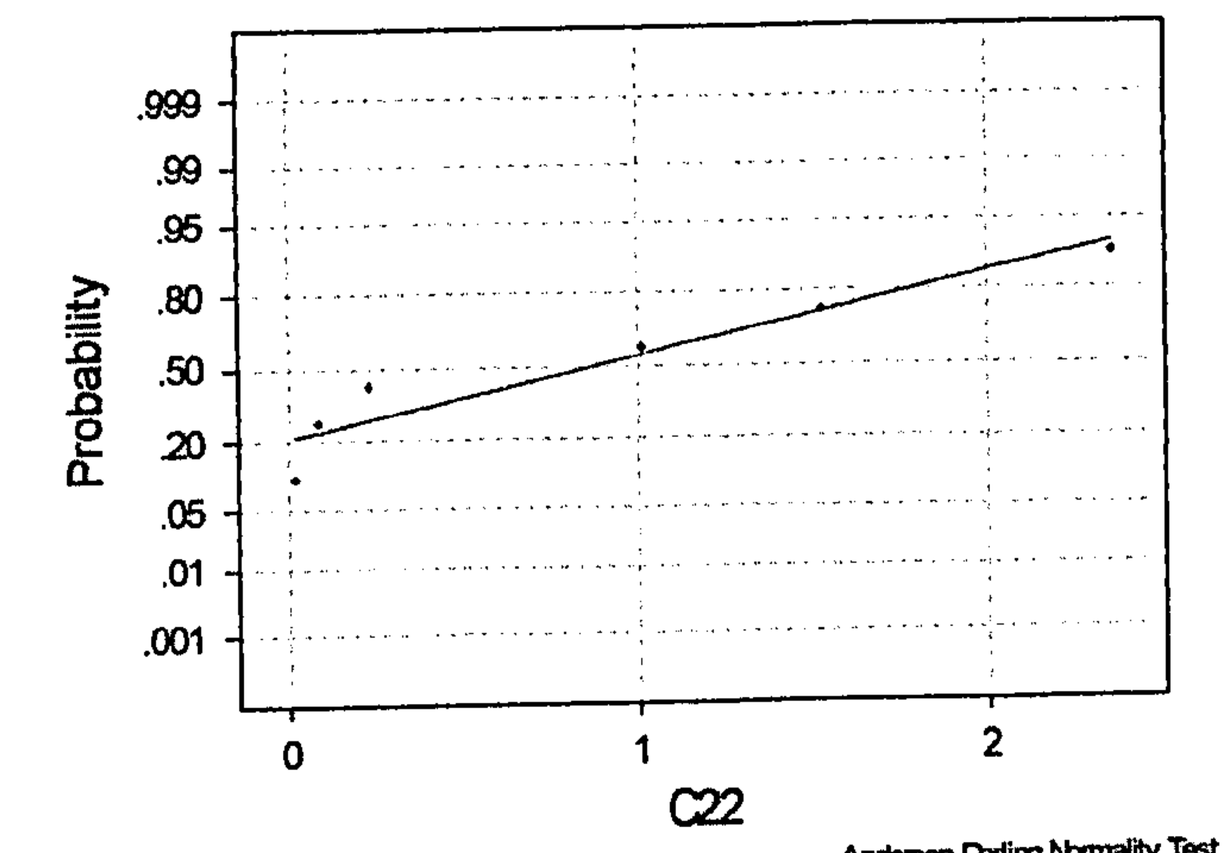

Fig 4.15 Normality Test for the population (paired difference between data for **transsected medial iliofemoral** and **transsected medial and lateral iliofemoral ligaments**) used in the paired t-test

Specimen 4 and 5 (Abduction)

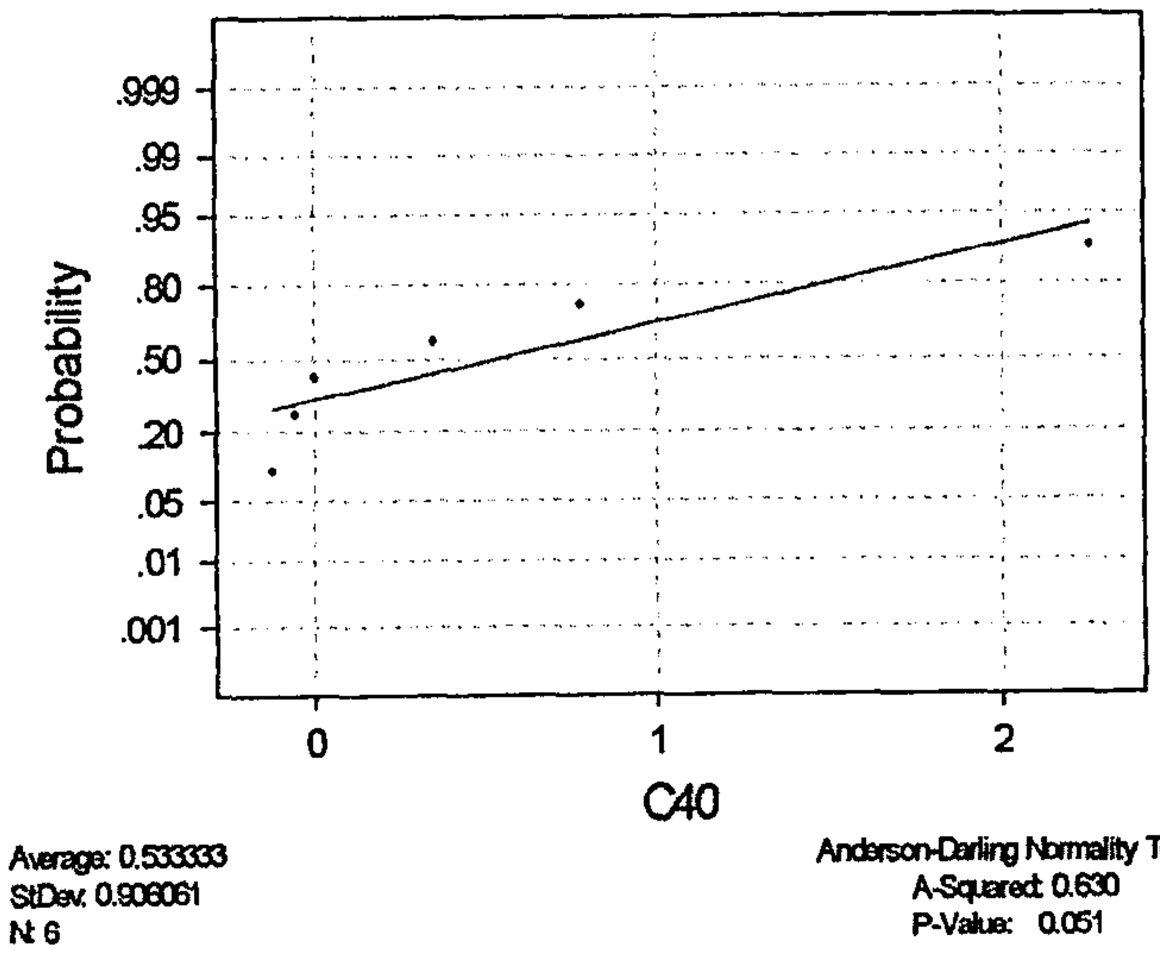

Fig 4.16 Normality Test for the population (paired difference between data for **intact capsule** and **transsected medial iliofemoral ligament**) used in the paired t-test

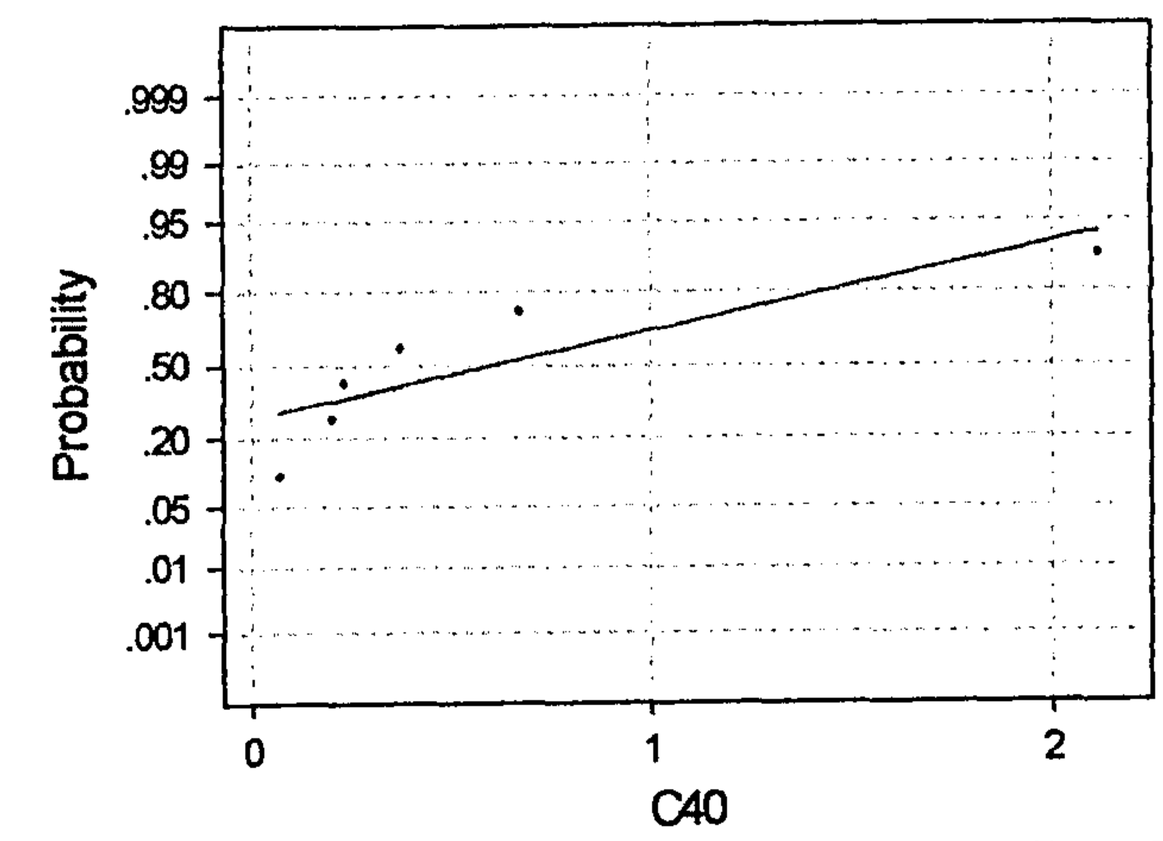

Fig 4.17 Normality Test for the population (paired difference between data for **intact capsule** and **transsected medial and lateral iliofemoral ligaments**) used in the paired t-test

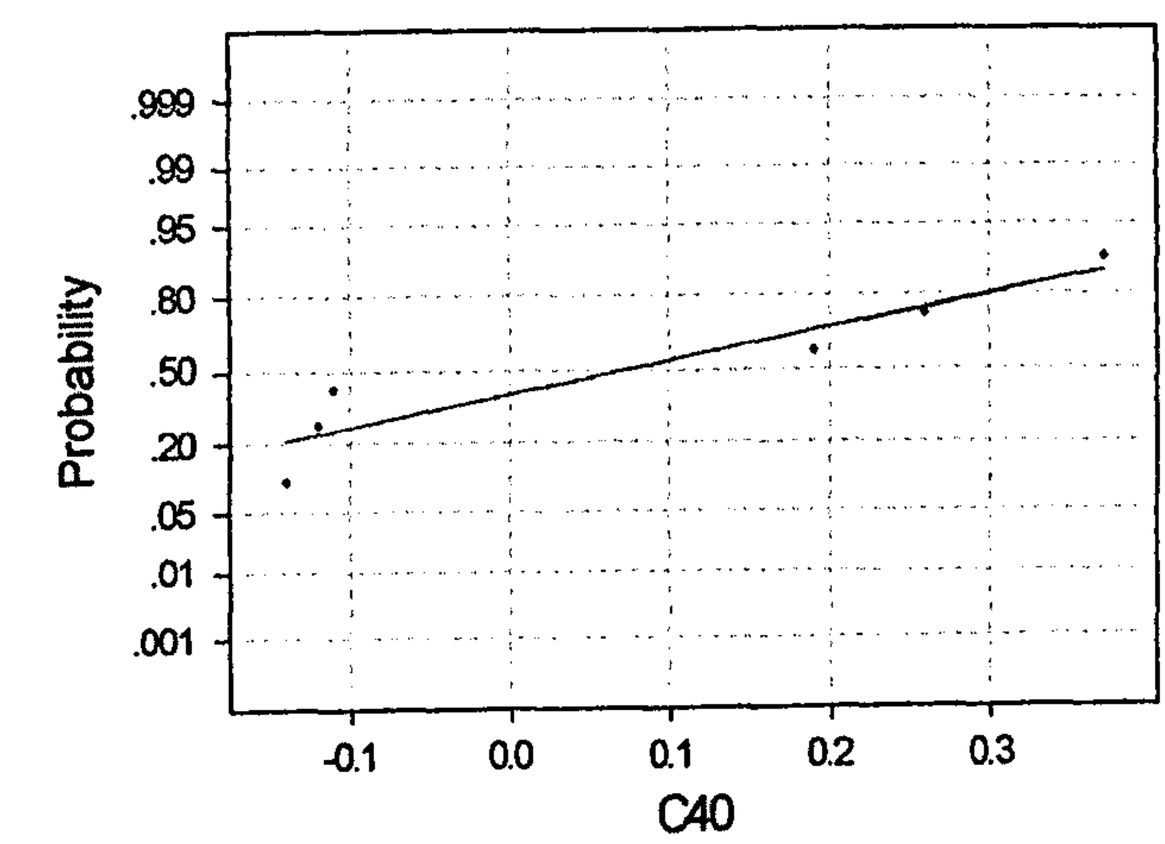

Fig 4.18 Normality Test for the population (paired difference between data for **transsected medial iliofemoral** and **transsected medial and lateral iliofemoral ligaments**) used in the paired t-test

Full Extension

Specimen 4 (Adduction)

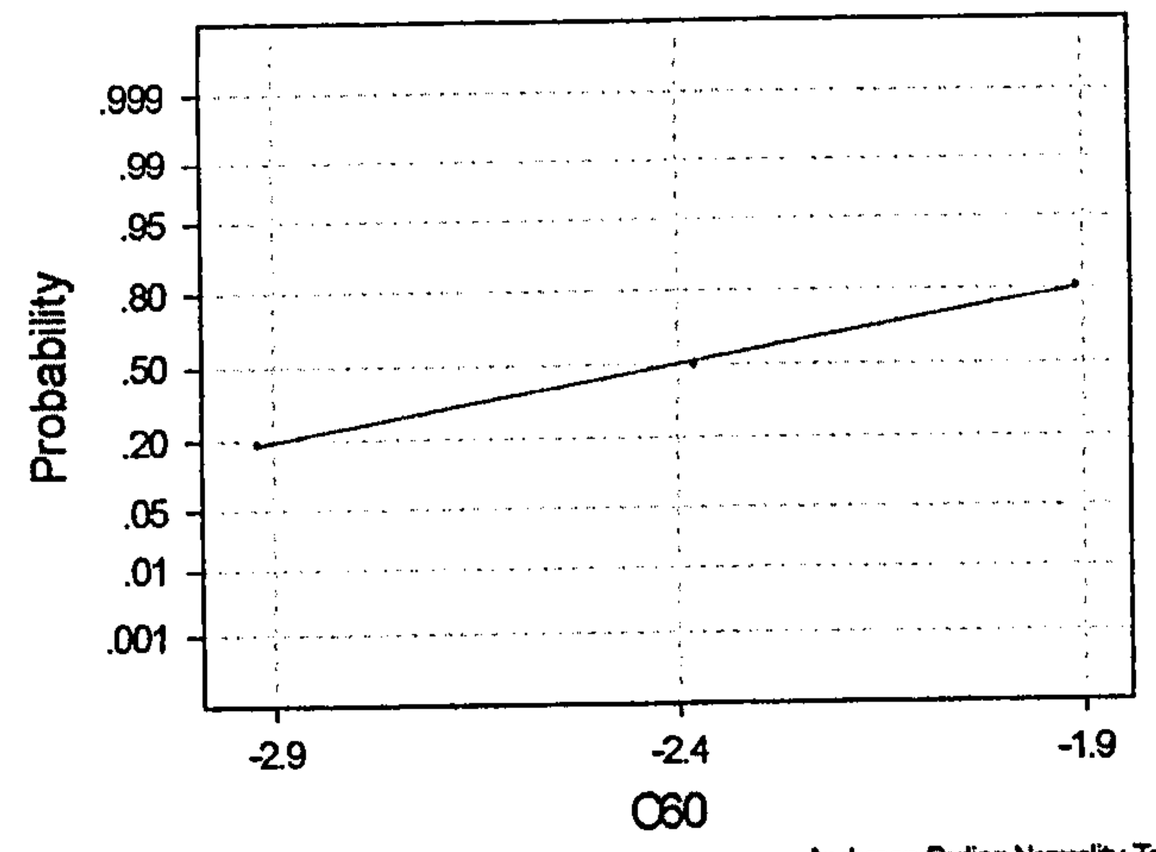

Fig 4.19 Normality Test for the population (paired difference between data for **intact capsule** and **transsected medial iliofemoral ligament**) used in the paired t-test

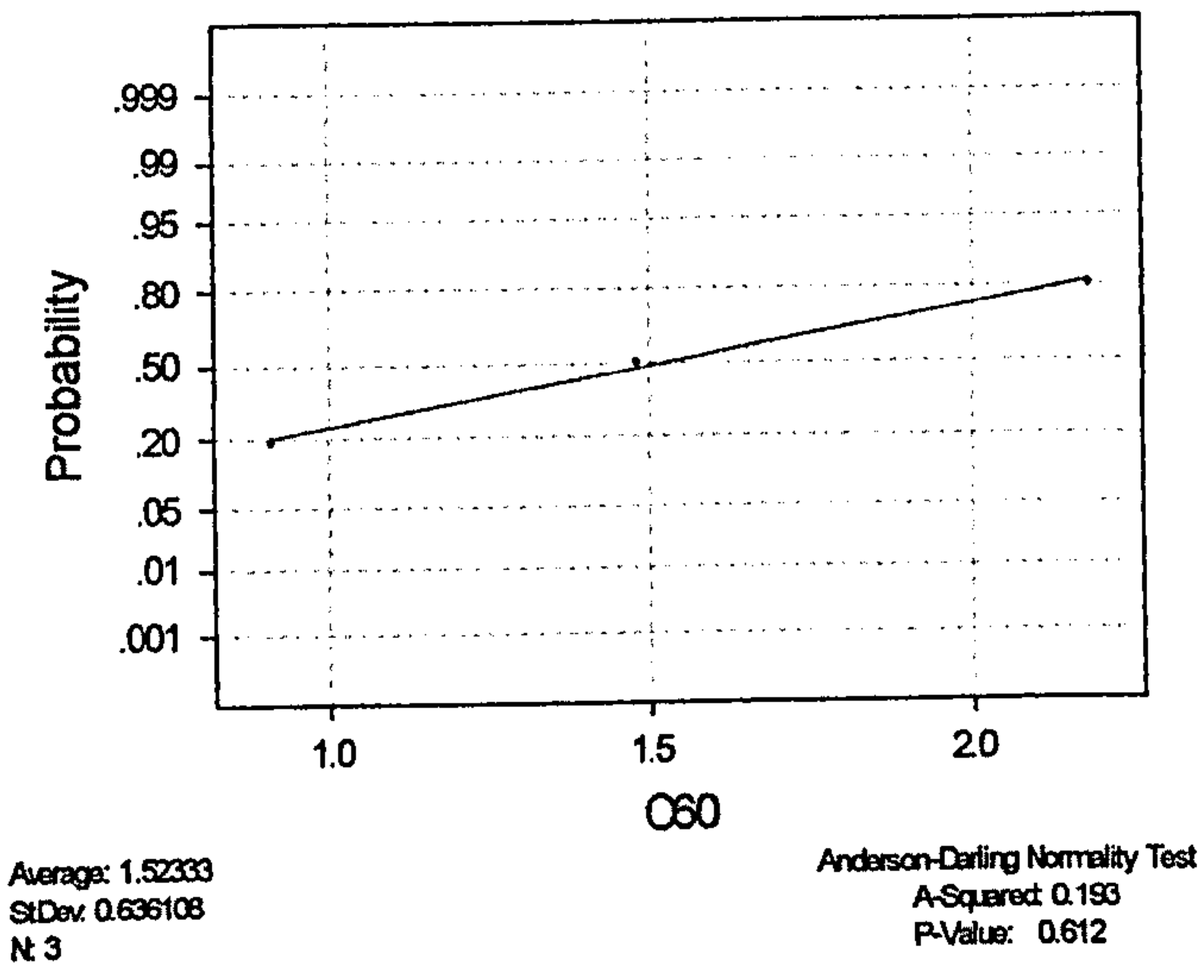

Fig 4.20 Normality Test for the population (paired difference between data for **intact capsule and transsected medial and lateral iliofemoral ligaments**) used in the paired t-test

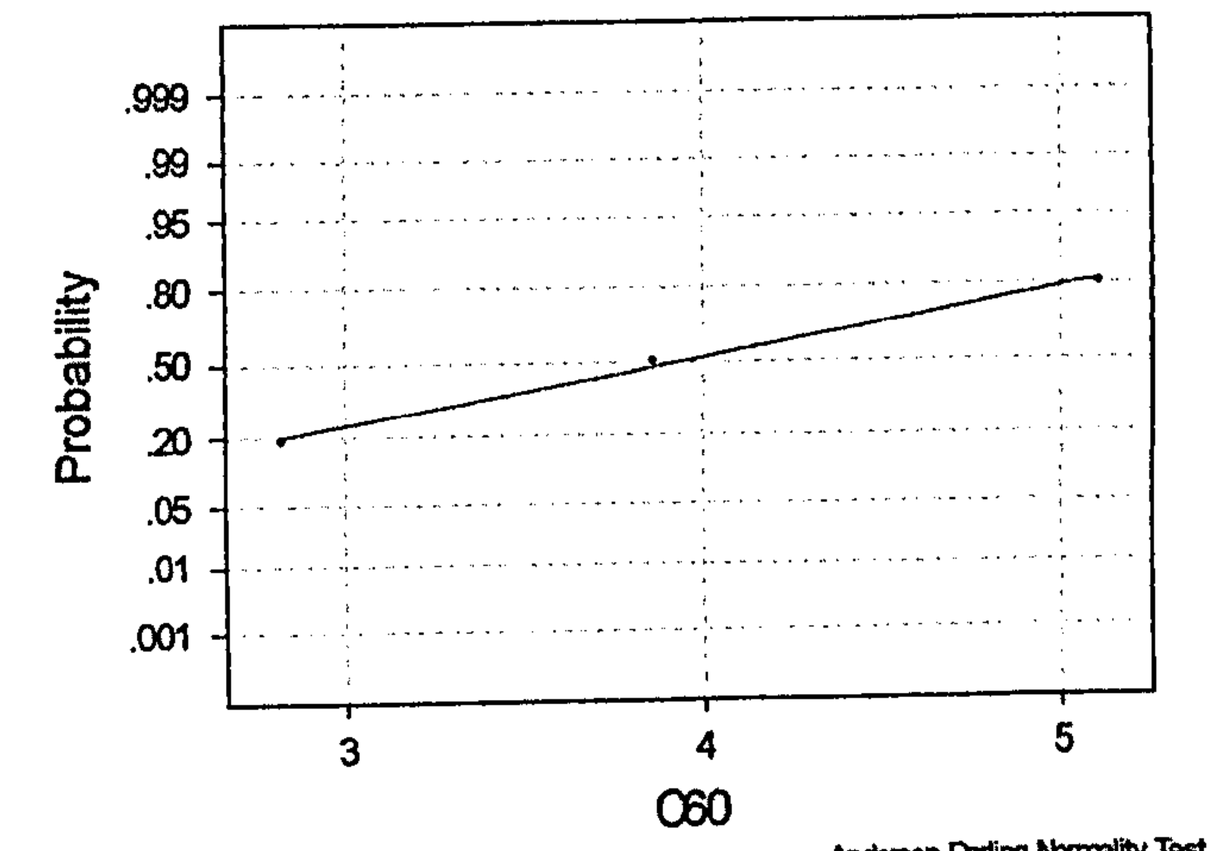

Fig 4.21 Normality Test for the population (paired difference between data for **transsected medial iliofemoral** and **transsected medial and lateral iliofemoral ligaments**) used in the paired t-test

Specimen 4 (Abduction)

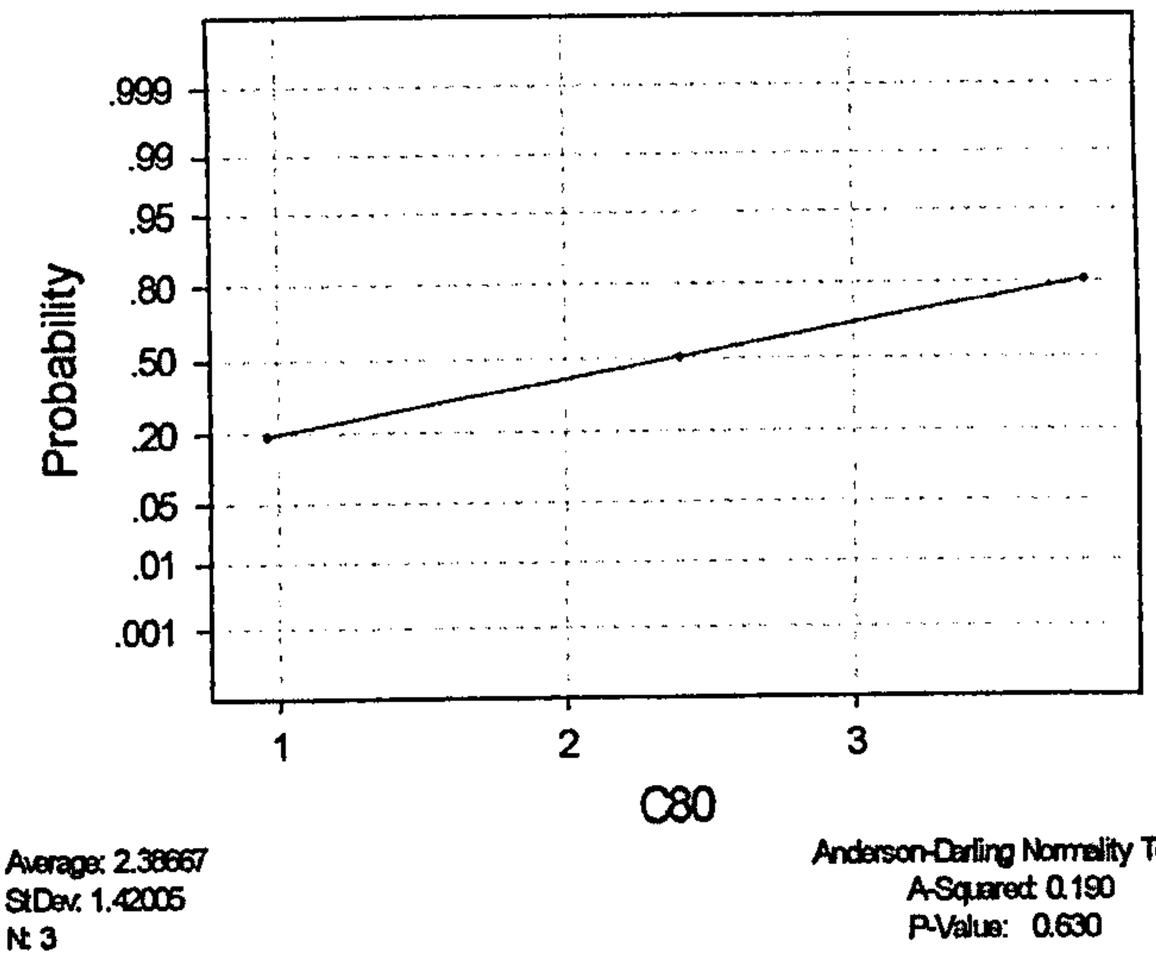

Fig 4.22 Normality Test for the population (paired difference between data for **intact capsule** and **transsected medial iliofemoral ligament**) used in the paired t-test

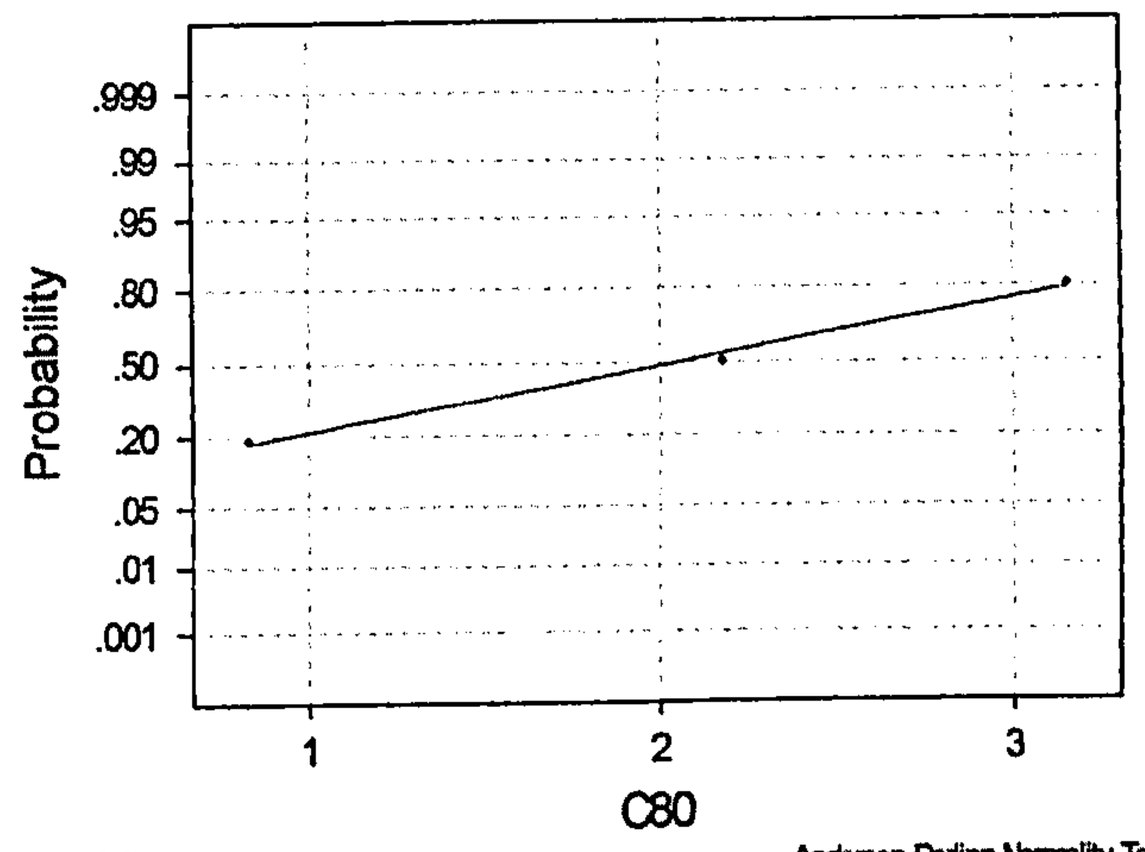

Fig 4.23 Normality Test for the population (paired difference between data for **intact capsule** and **transsected medial and lateral iliofemoral ligaments**) used in the paired t-test

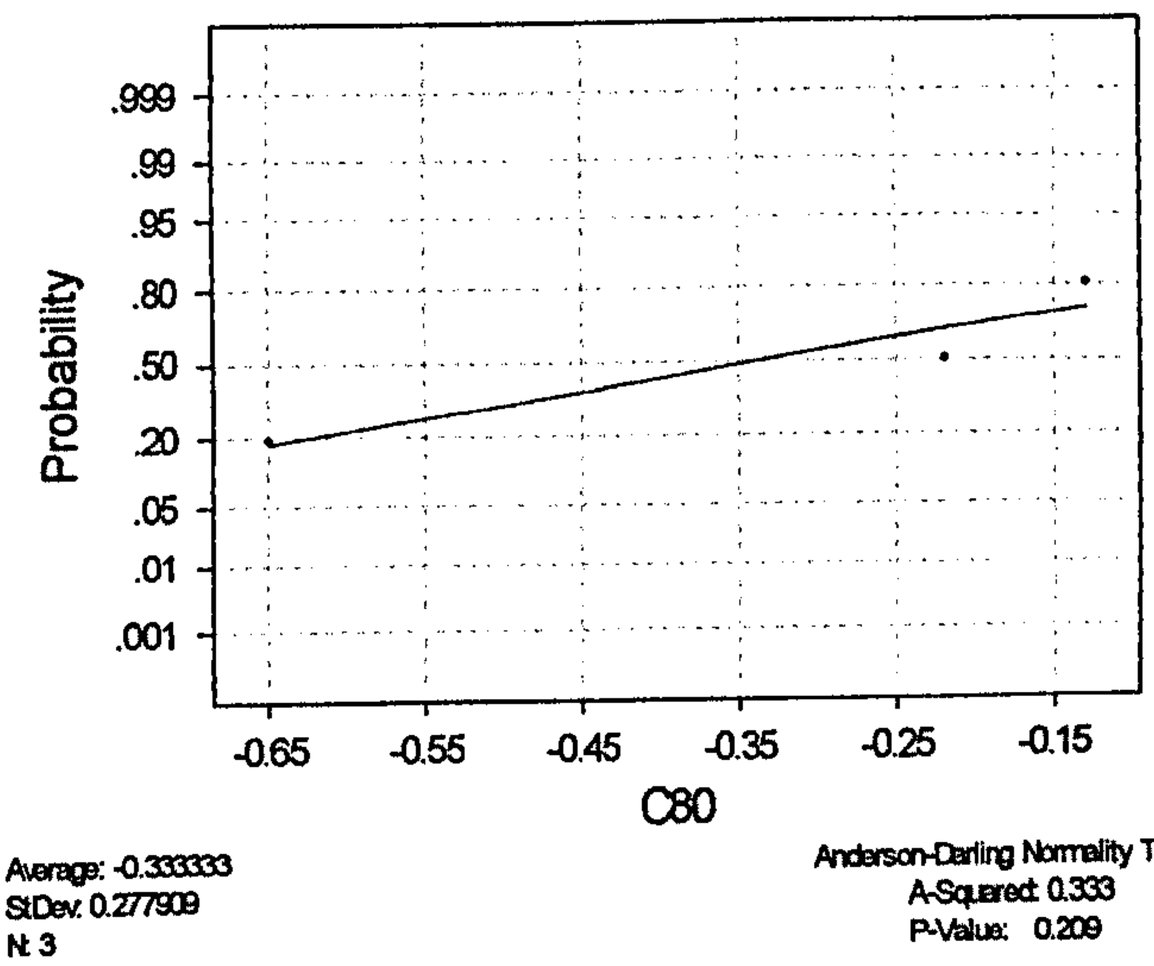

Fig 4.24 Normality Test for the population (paired difference between data for **transsected medial iliofemoral** and **transsected medial and lateral iliofemoral ligaments**) used in the paired t-test

Specimen 5 (Adduction)

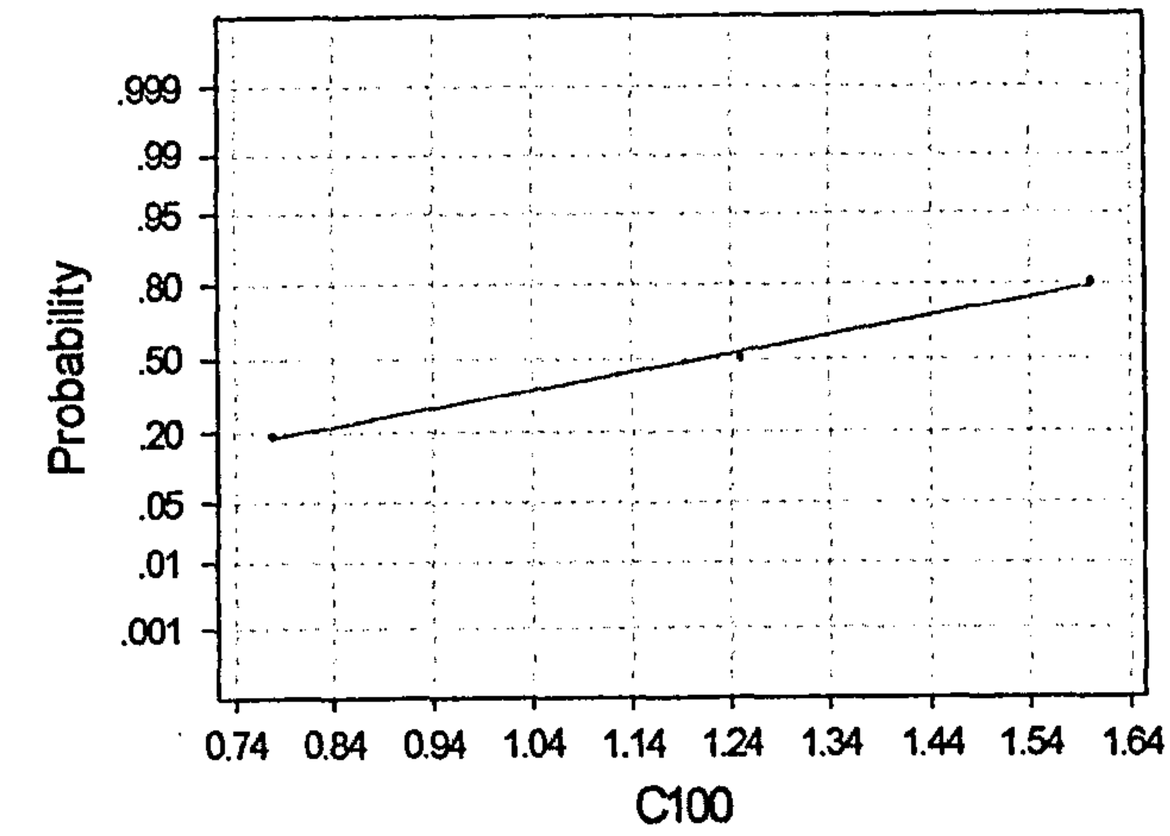

Fig 4.25 Normality Test for the population (paired difference between data for **intact capsule** and **transsected medial iliofemoral ligament**) used in the paired t-test

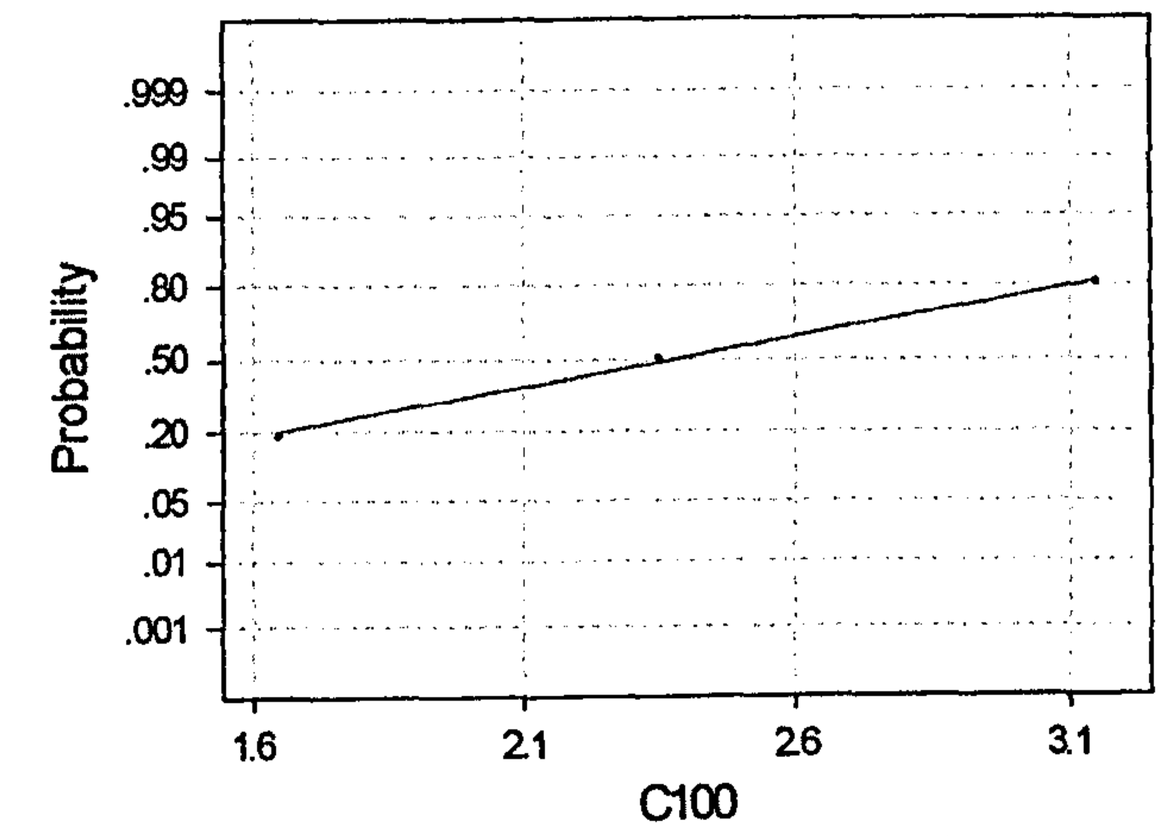

Fig 4.26 Normality Test for the population (paired difference between data for **intact capsule** and **transsected medial and lateral iliofemoral ligaments**) used in the paired t-test

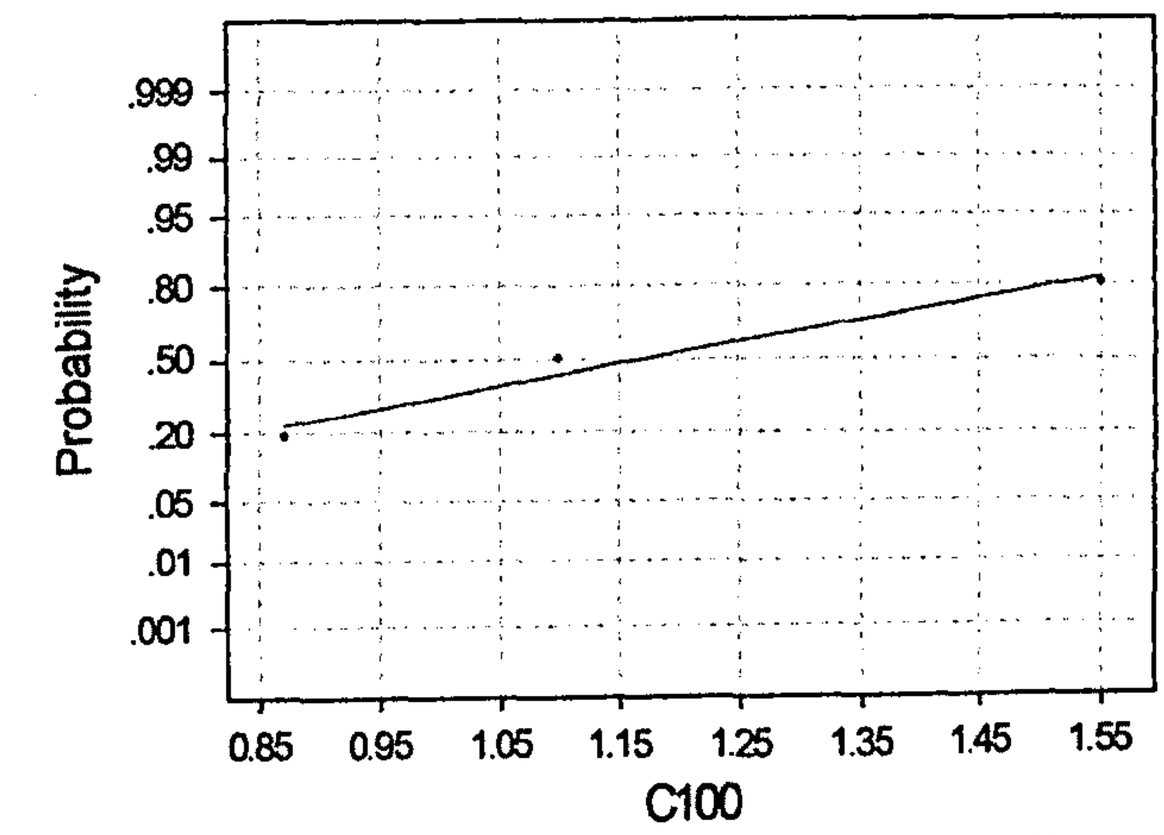

Fig 4.27 Normality Test for the population (paired difference between data for **transsected medial iliofemoral** and **transsected medial and lateral iliofemoral ligaments**) used in the paired t-test

Specimen 5 (Abduction)

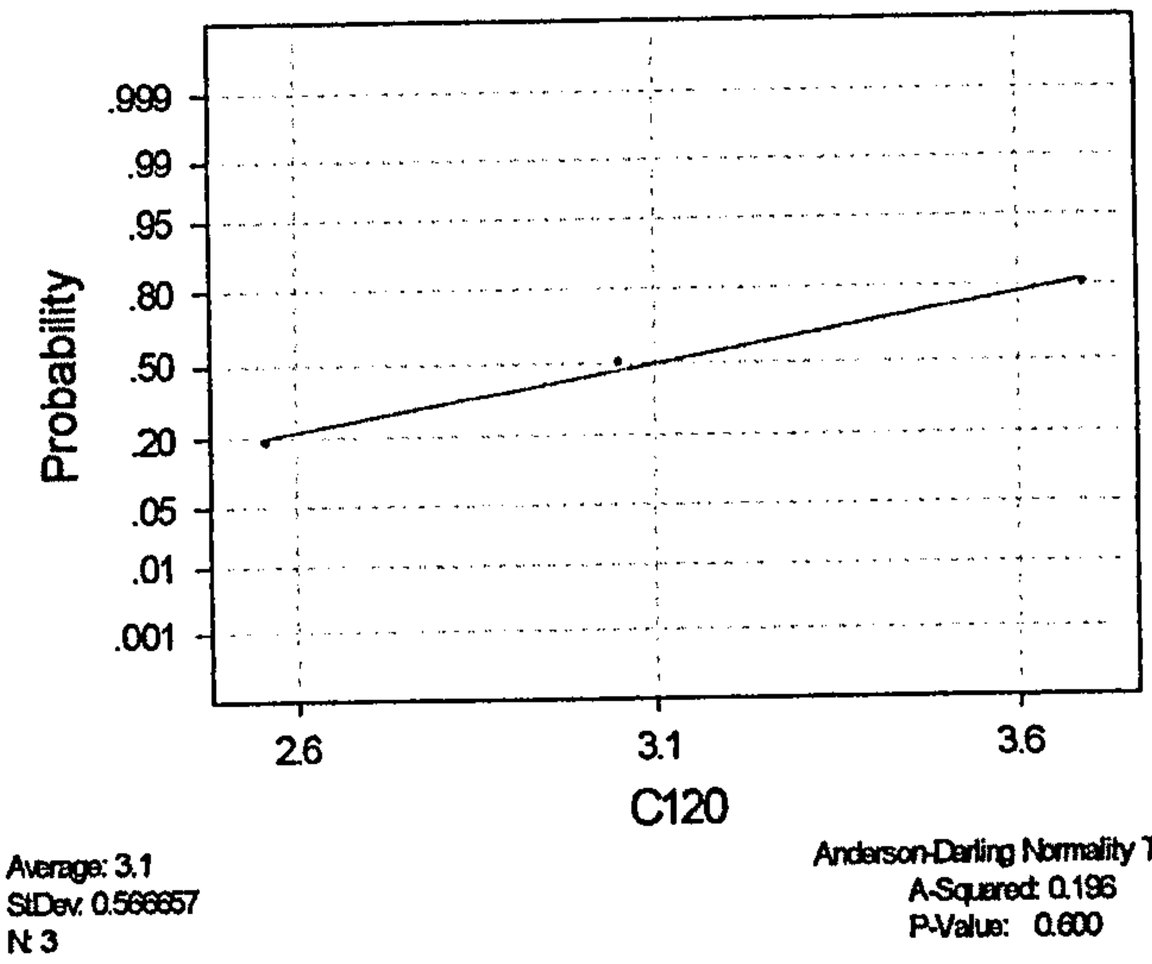

Fig 4.28 Normality Test for the population (paired difference between data for **intact capsule** and **transsected medial iliofemoral ligament**) used in the paired t-test

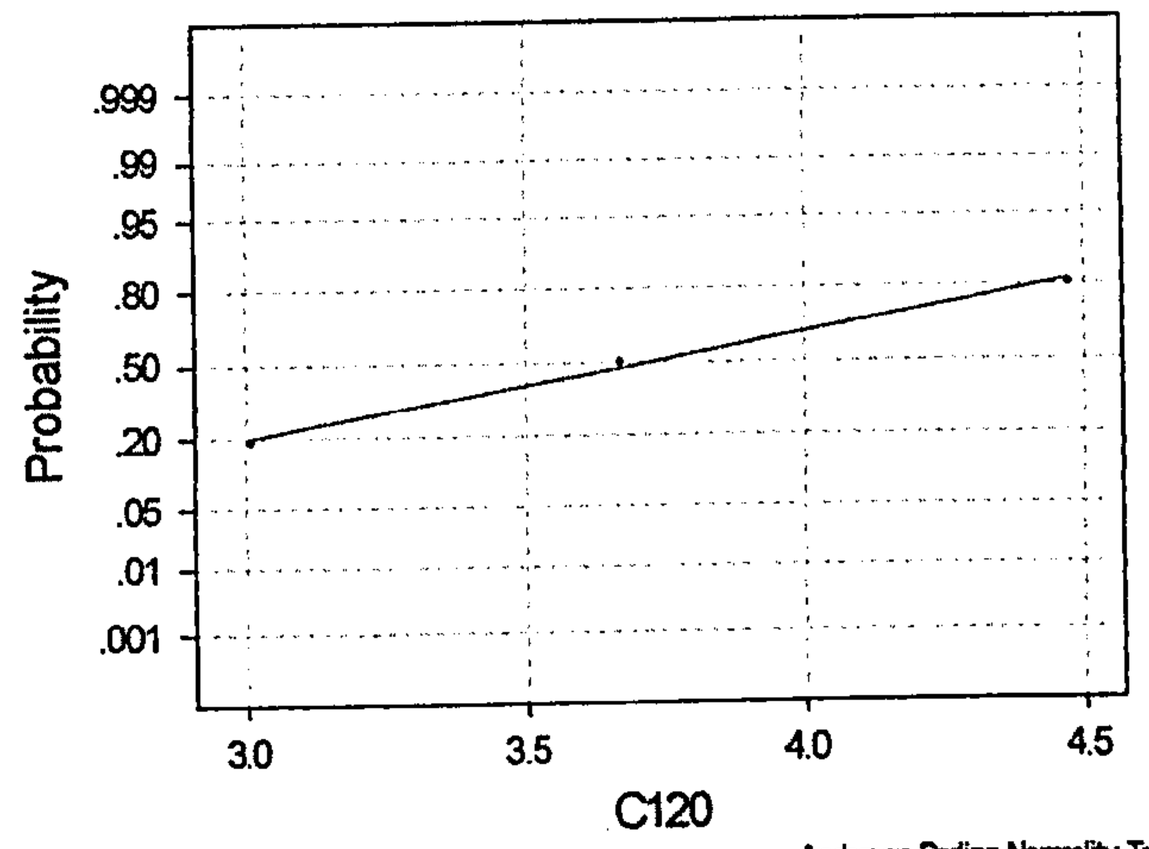

Fig 4.29 Normality Test for the population (paired difference between data for **intact capsule** and **transsected medial and lateral iliofemoral ligaments**) used in the paired t-test

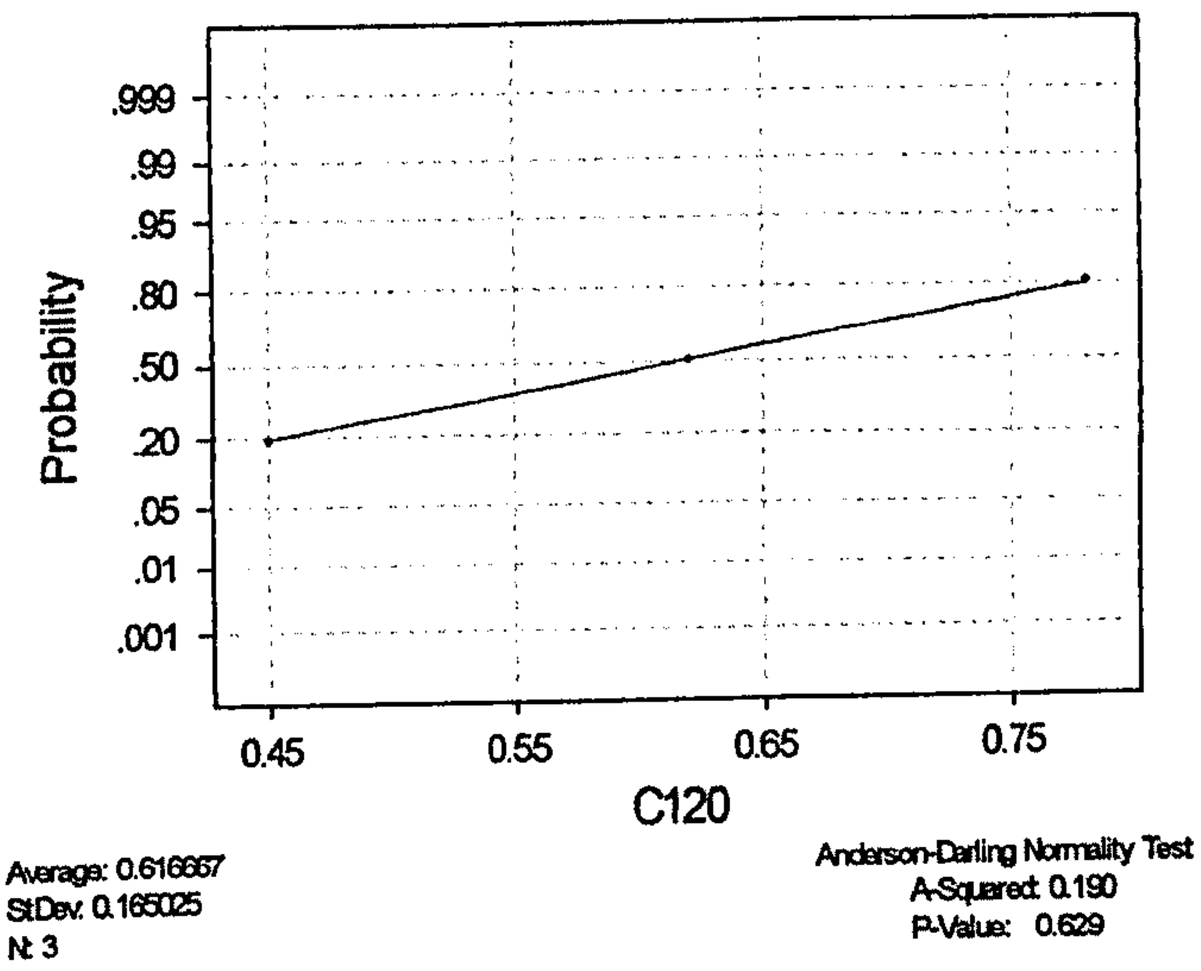

Fig 4.30 Normality Test for the population (paired difference between data for **transsected medial iliofemoral** and **transsected medial and lateral iliofemoral ligaments**) used in the paired t-test

Specimen 4 and 5 (Adduction)

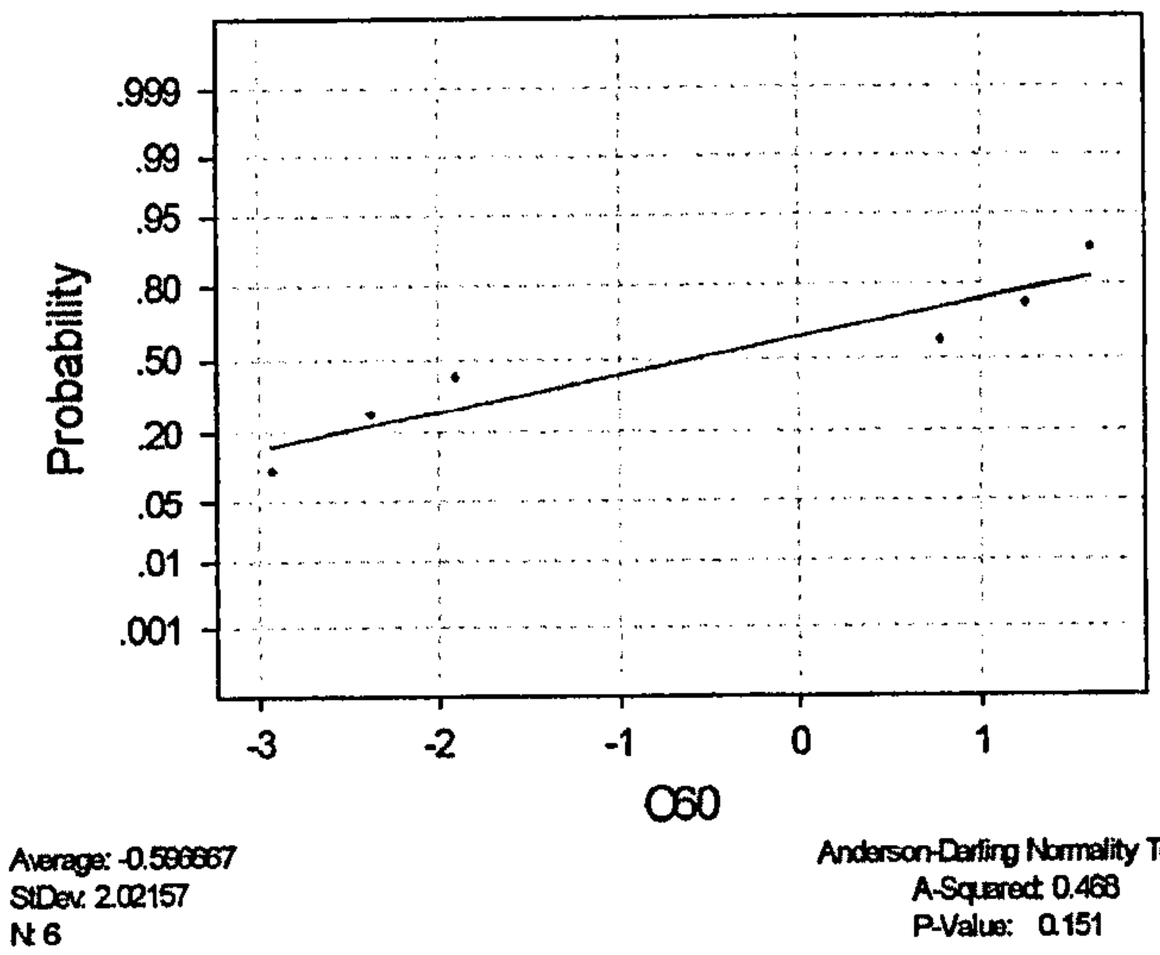

Fig 4.31 Normality Test for the population (paired difference between data for **intact capsule** and **transsected medial iliofemoral ligament**) used in the paired t-test

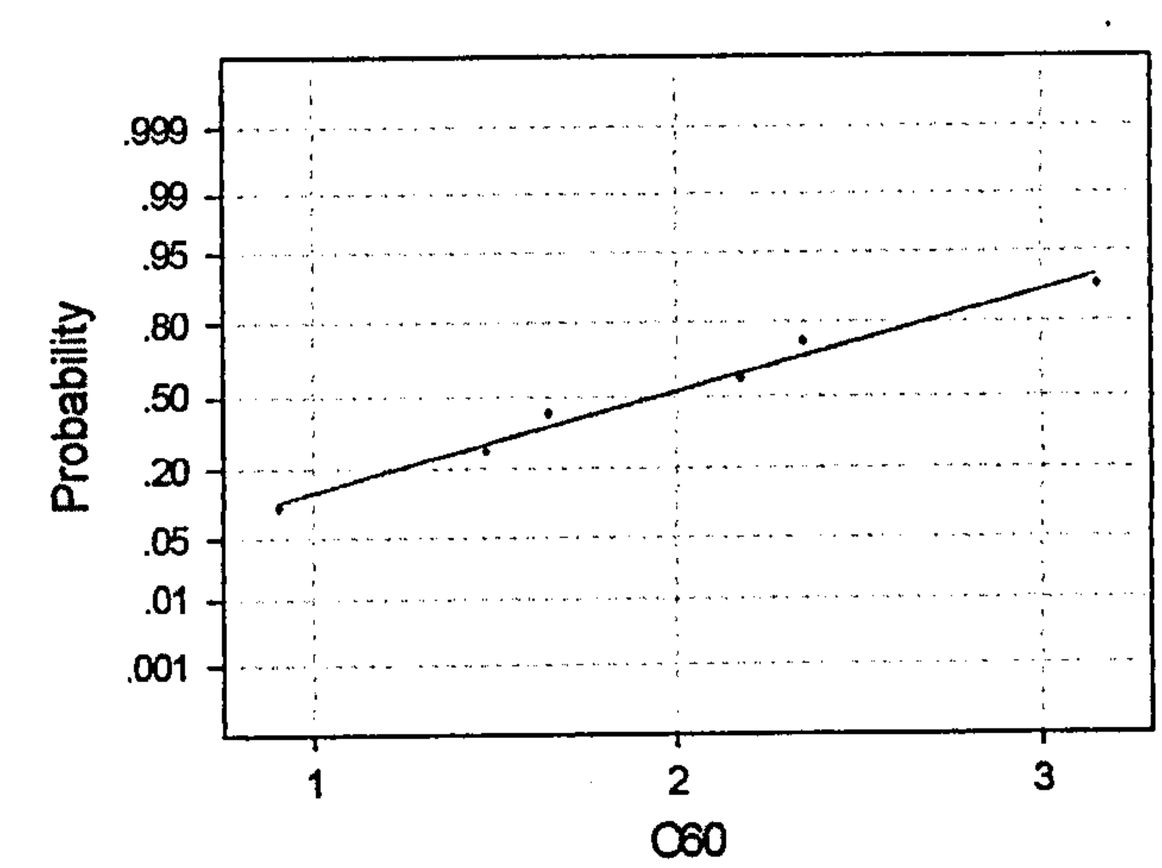

Fig 4.32 Normality Test for the population (paired difference between data for **intact capsule** and **transsected medial and lateral iliofemoral ligaments**) used in the paired t-test

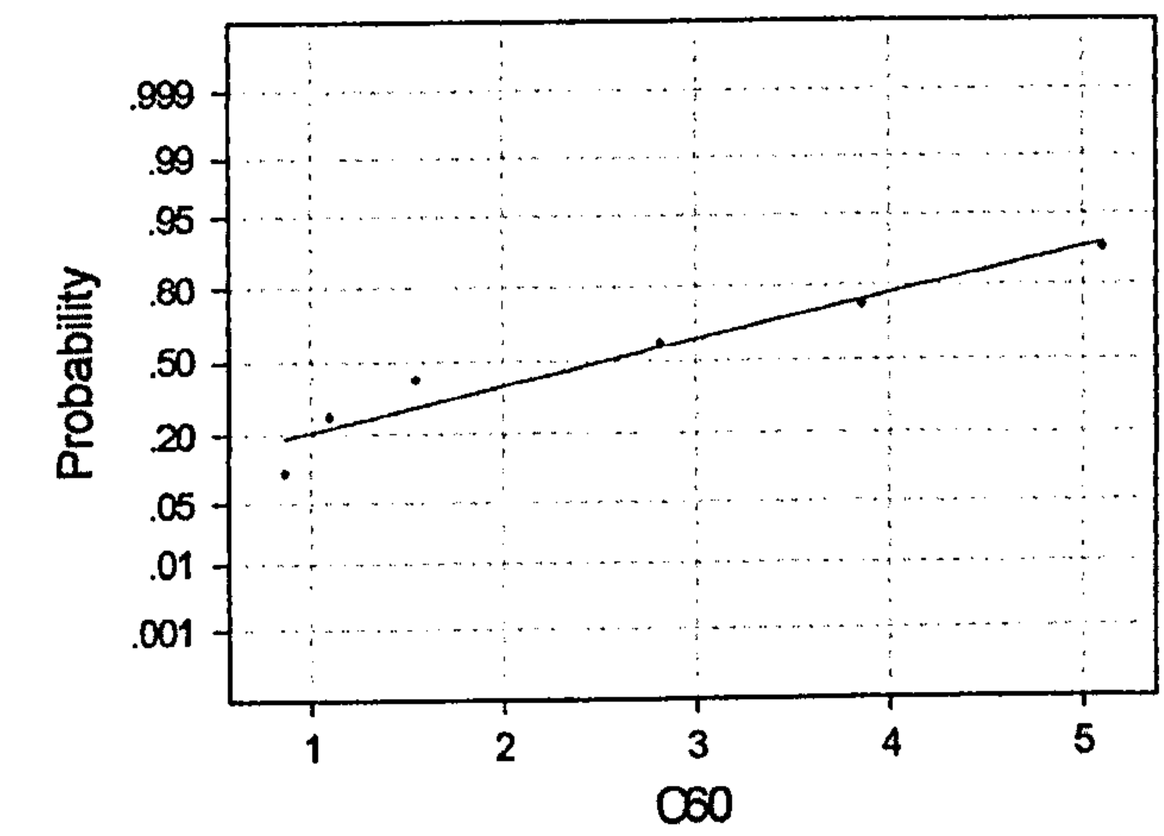

Fig 4.33 Normality Test for the population (paired difference between data for **transsected medial iliofemoral** and **transsected medial and lateral iliofemoral ligaments**) used in the paired t-test

Specimen 4 and 5 (Abduction)

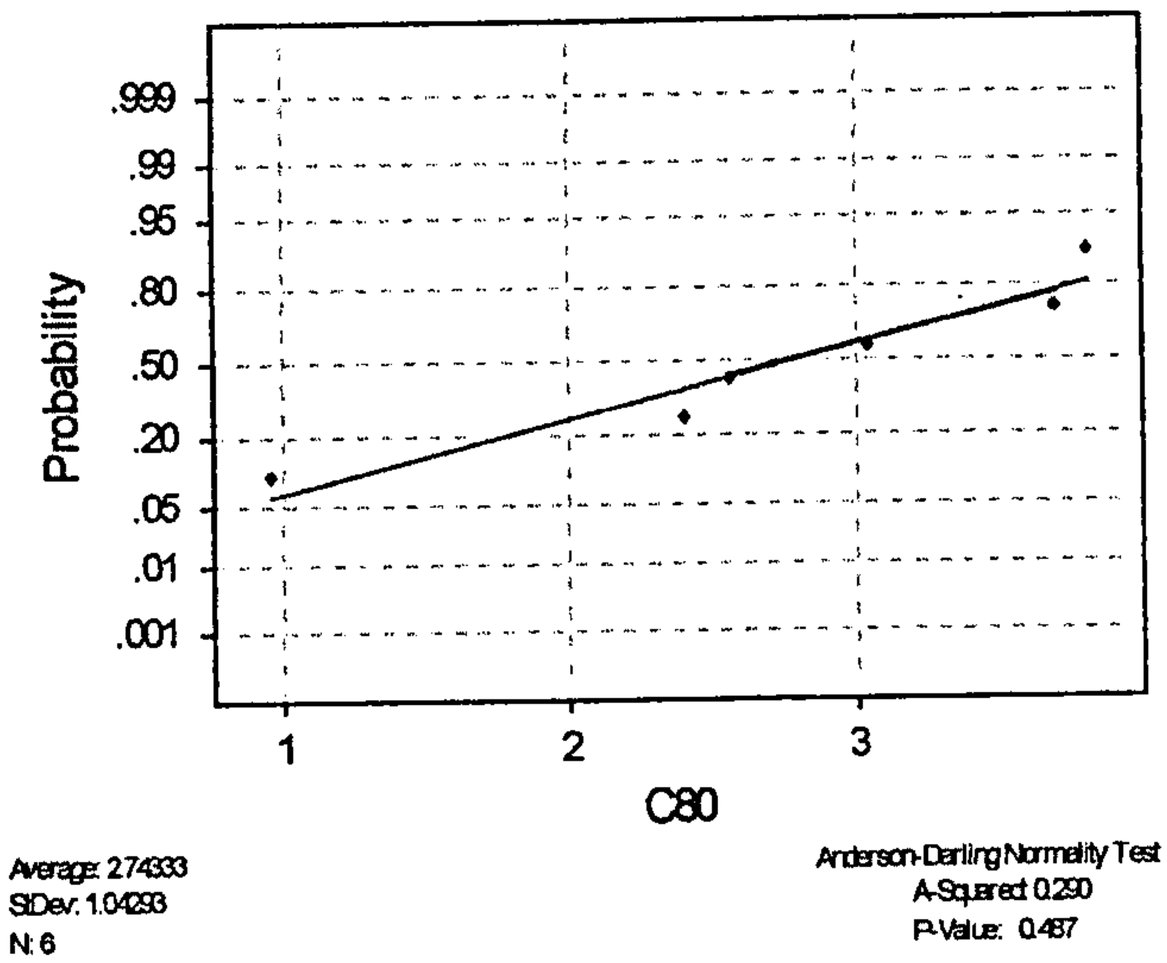

Fig 4.34 Normality Test for the population (paired difference between data for **intact capsule** and **transsected medial iliofemoral ligament**) used in the paired t-test

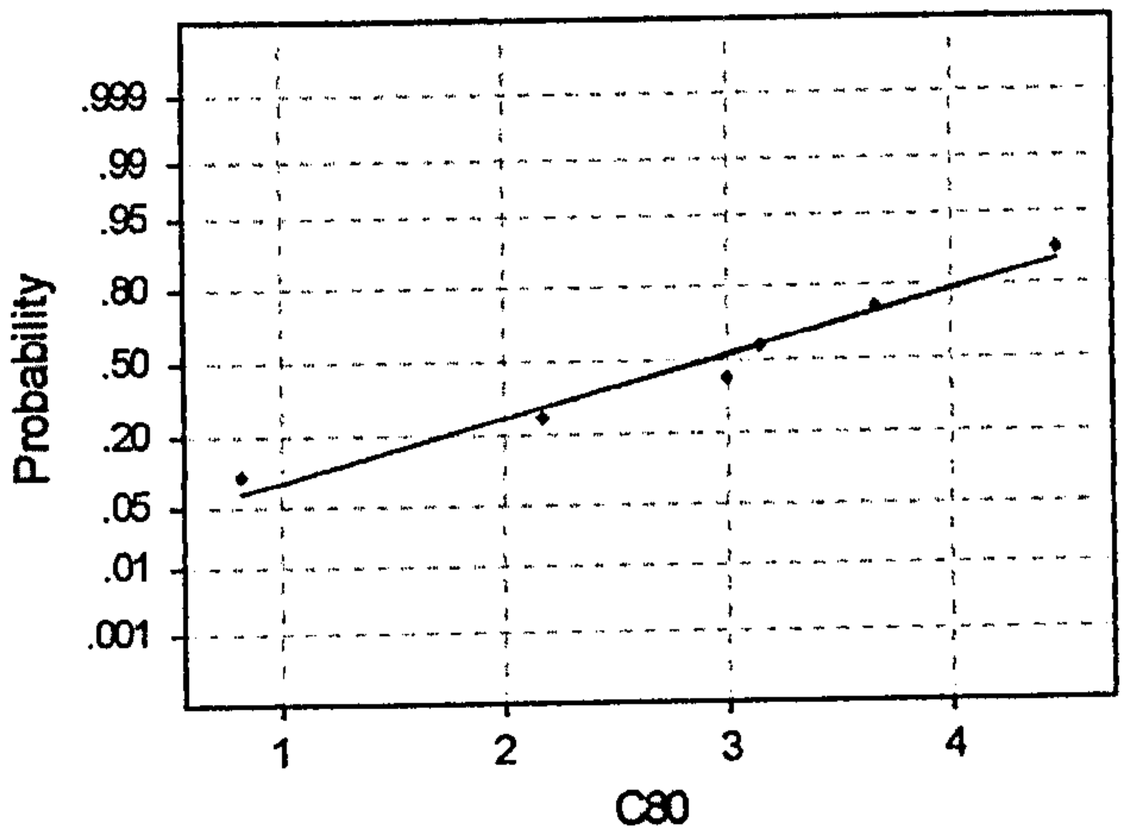

Fig 4.35 Normality Test for the population (paired difference between data for **intact capsule** and **transsected medial and lateral iliofemoral ligaments**) used in the paired t-test

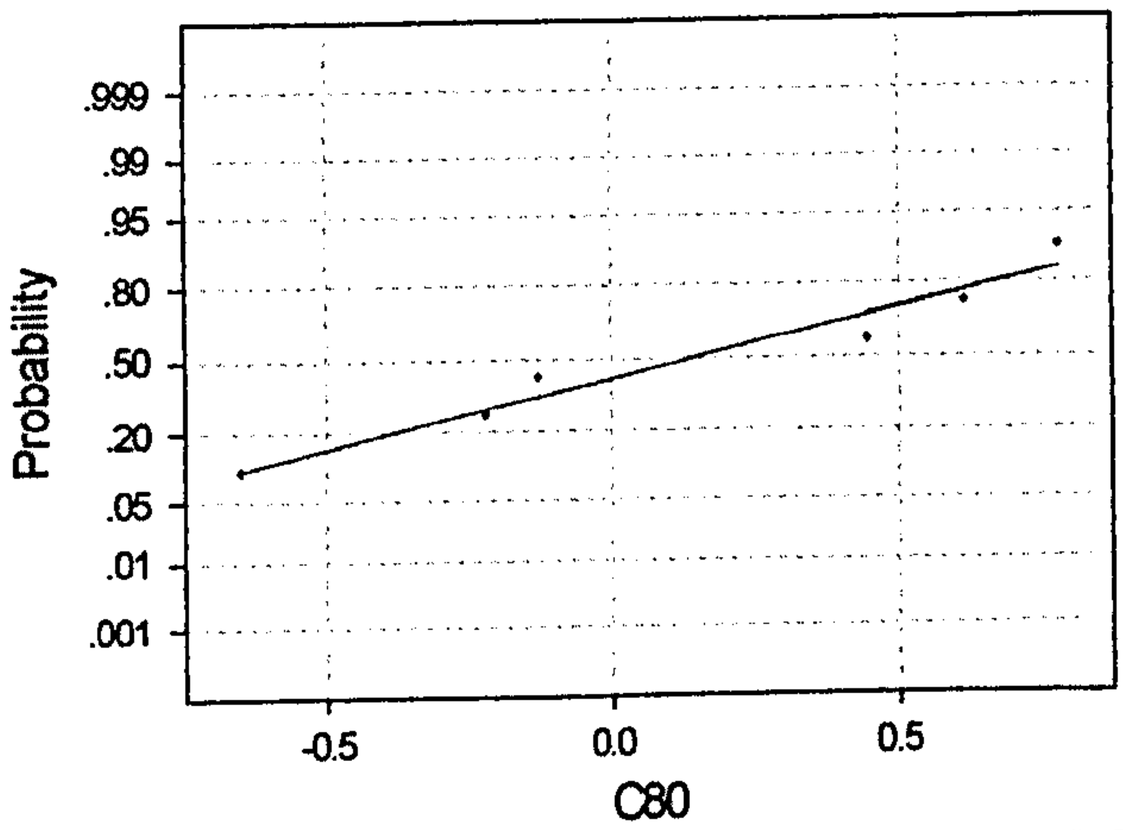

Fig 4.36 Normality Test for the population (paired difference between data for **transsected medial iliofemoral** and **transsected medial and lateral iliofemoral ligaments**) used in the paired t-test

Full Extension and External Rotation

Specimen 4 (Adduction)

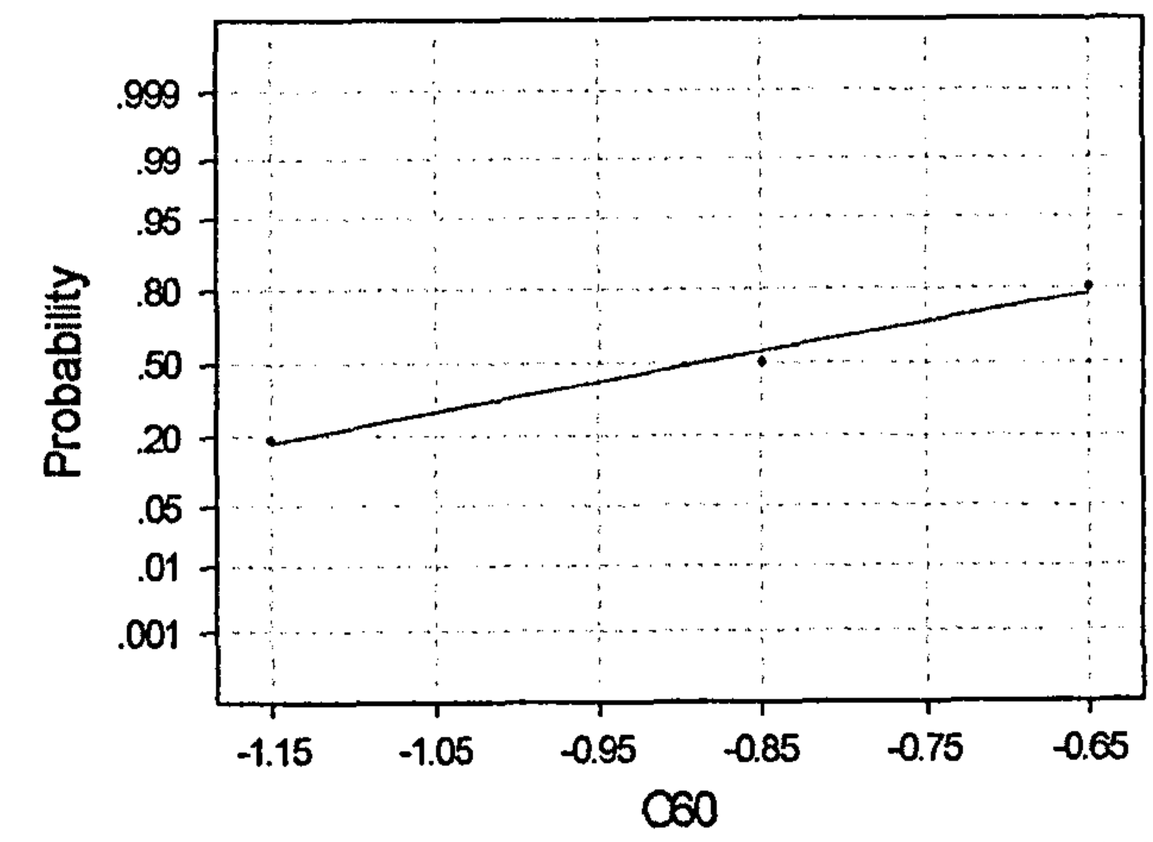

Fig 4.37 Normality Test for the population (paired difference between data for **intact capsule** and **transsected medial iliofemoral ligament**) used in the paired t-test

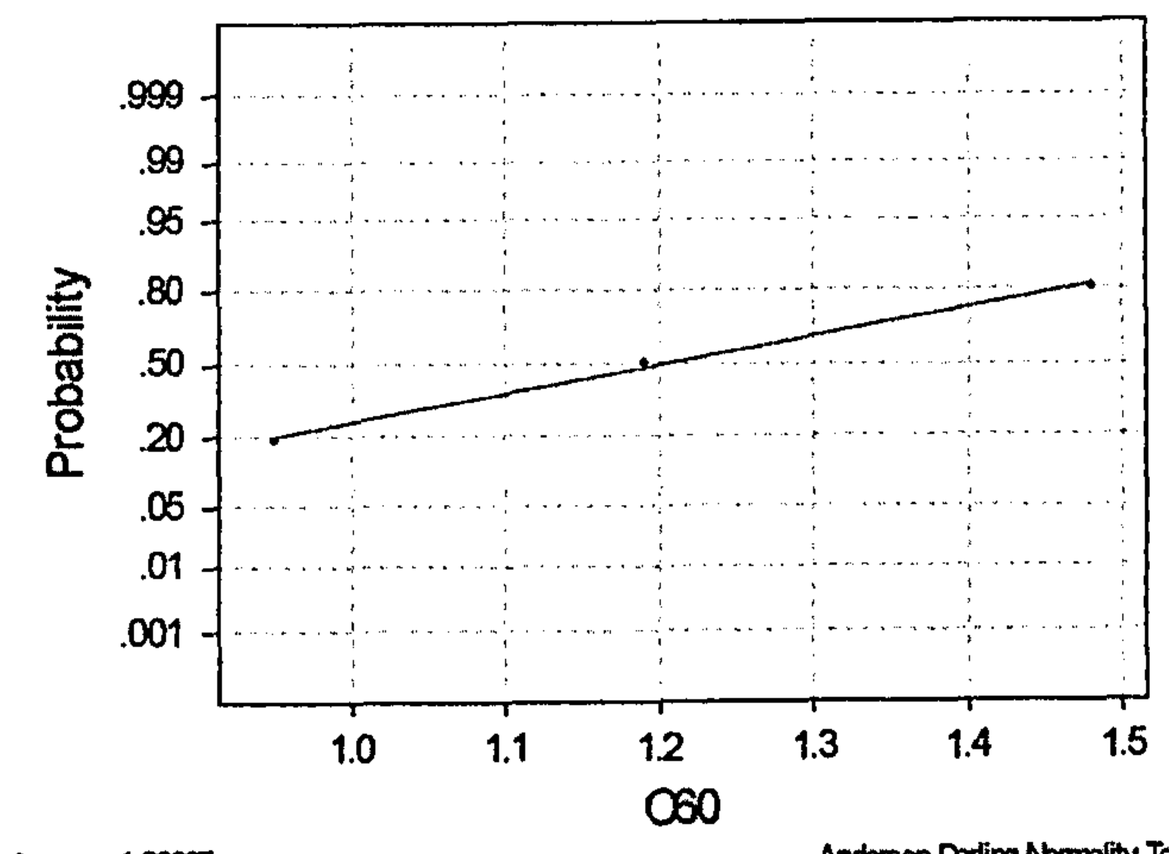

Fig 4.38 Normality Test for the population (paired difference between data for **intact capsule** and **transsected medial and lateral iliofemoral ligaments**) used in the paired t-test

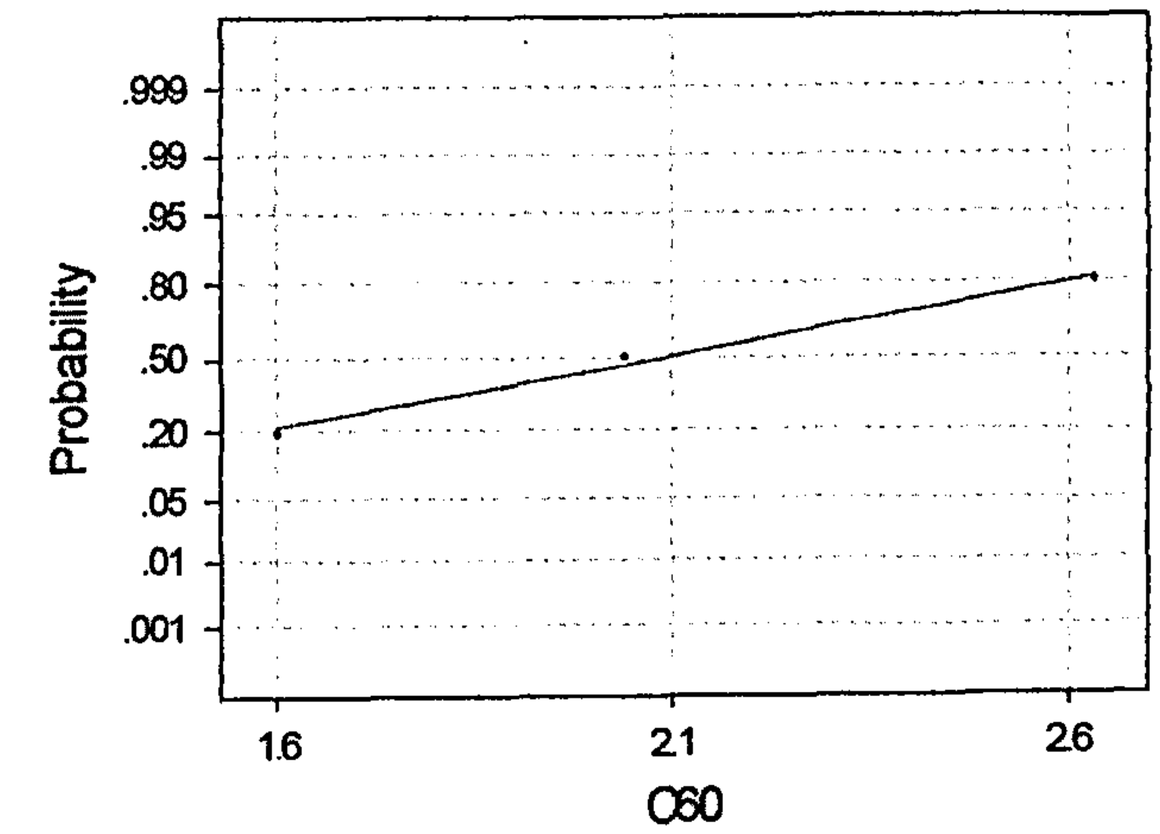

Fig 4.39 Normality Test for the population (paired difference between data for **transsected medial iliofemoral** and **transsected medial and lateral iliofemoral ligaments**) used in the paired t-test

Specimen 4 (Abduction)

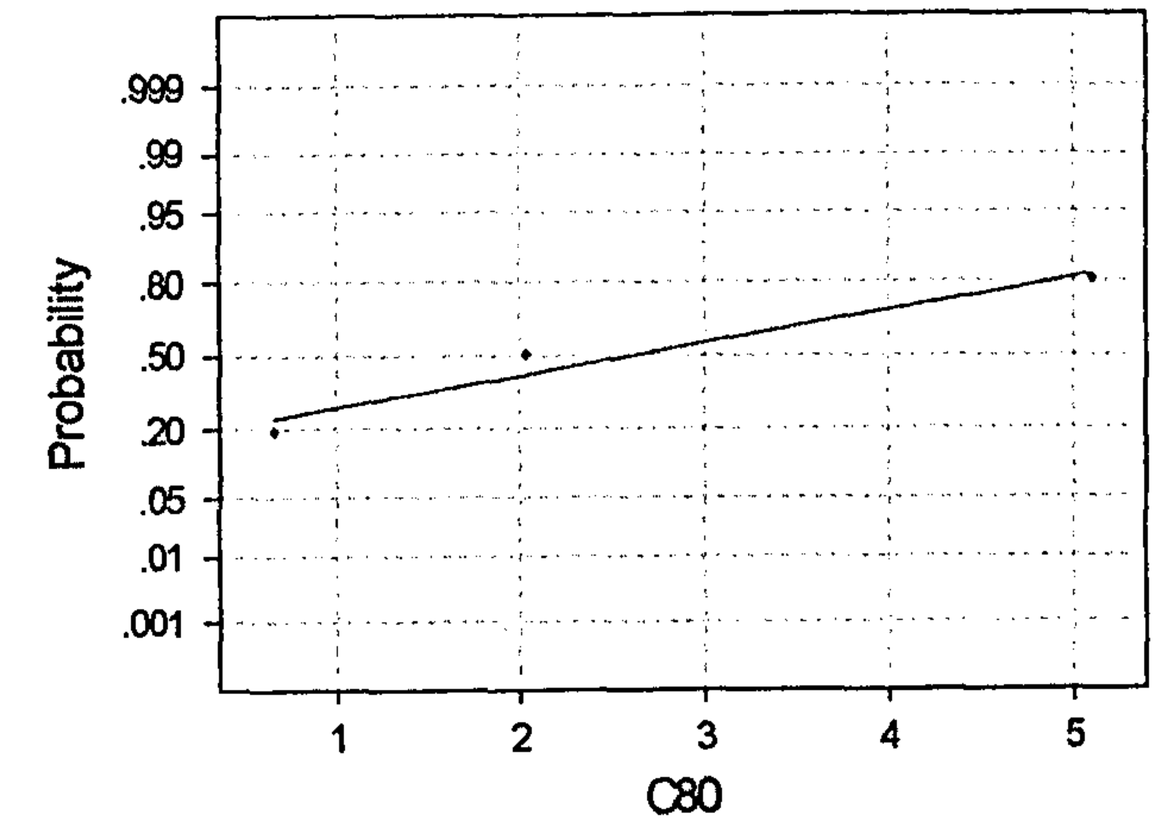

Fig 4.40 Normality Test for the population (paired difference between data for **intact capsule** and **transsected medial iliofemoral ligament**) used in the paired t-test

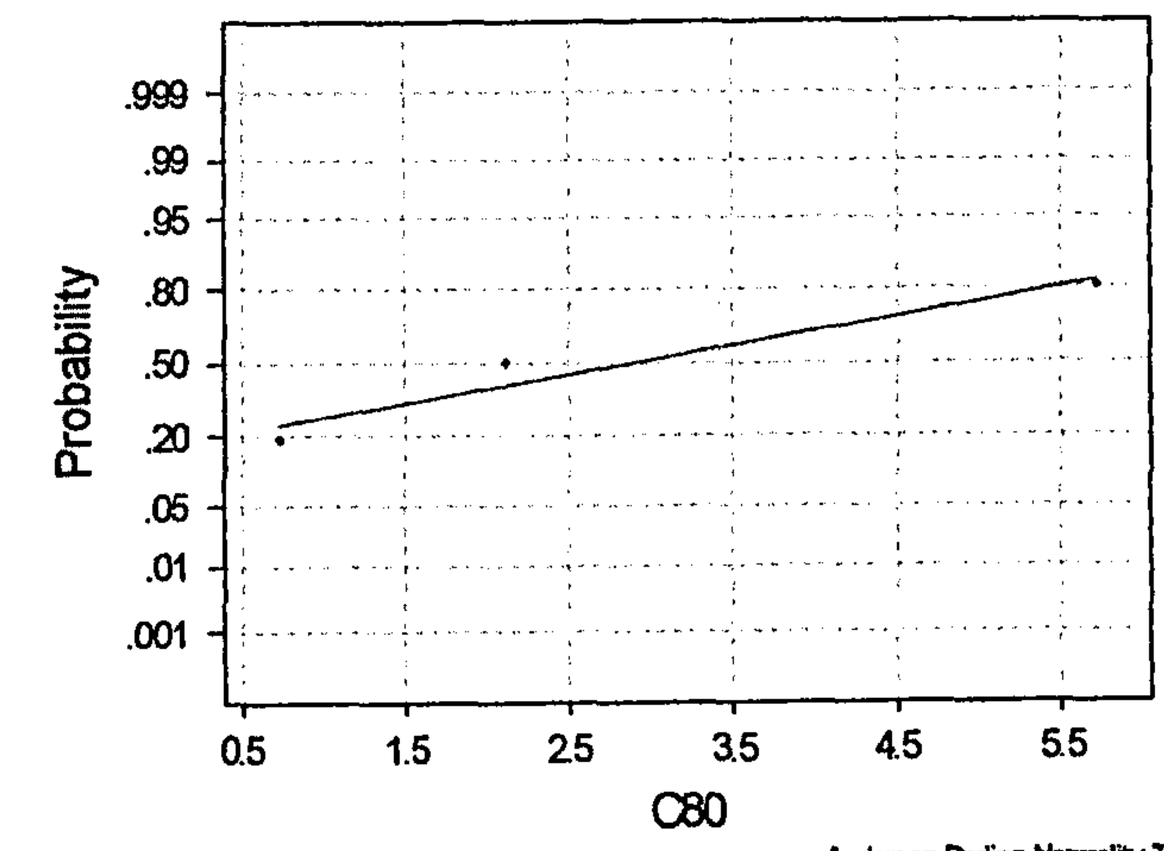

Fig 4.41 Normality Test for the population (paired difference between data for **intact capsule** and **transsected medial and lateral iliofemoral ligaments**) used in the paired t-test

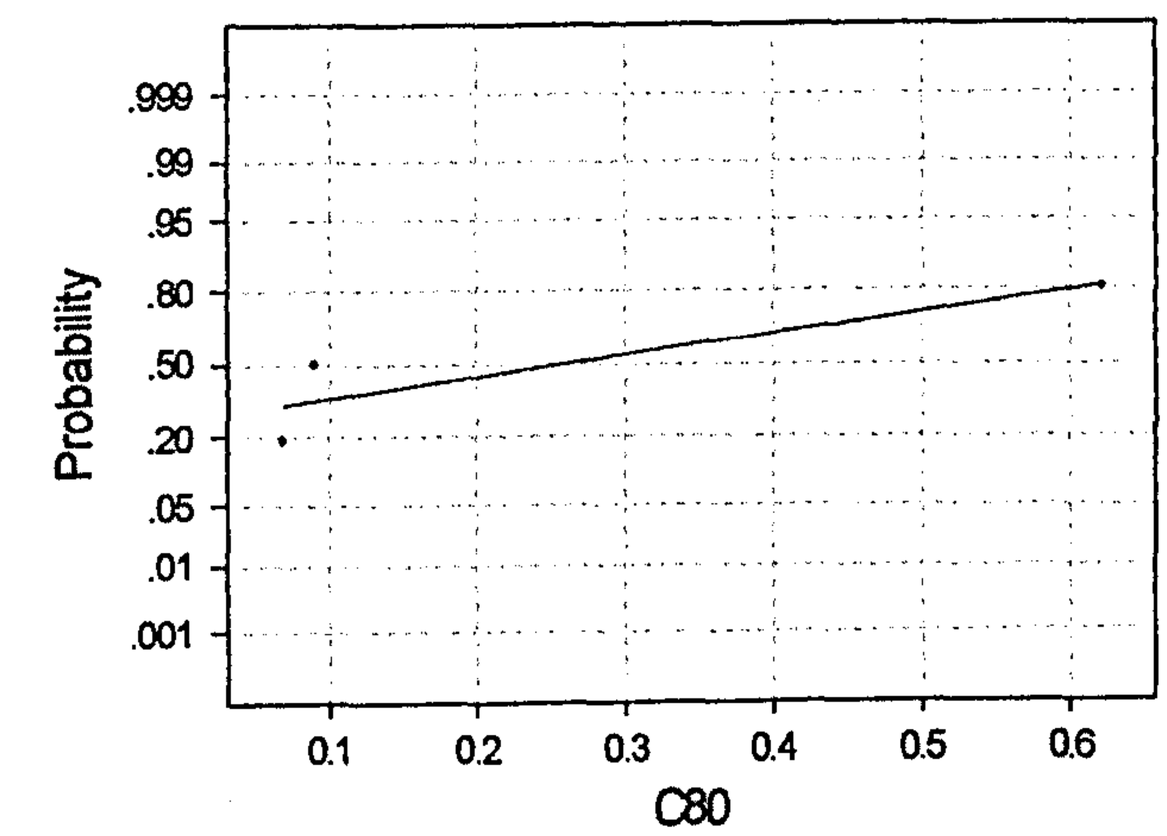

Fig 4.42 Normality Test for the population (paired difference between data for **transsected medial iliofemoral** and **transsected medial and lateral iliofemoral ligaments**) used in the paired t-test

Specimen 5 (Adduction)

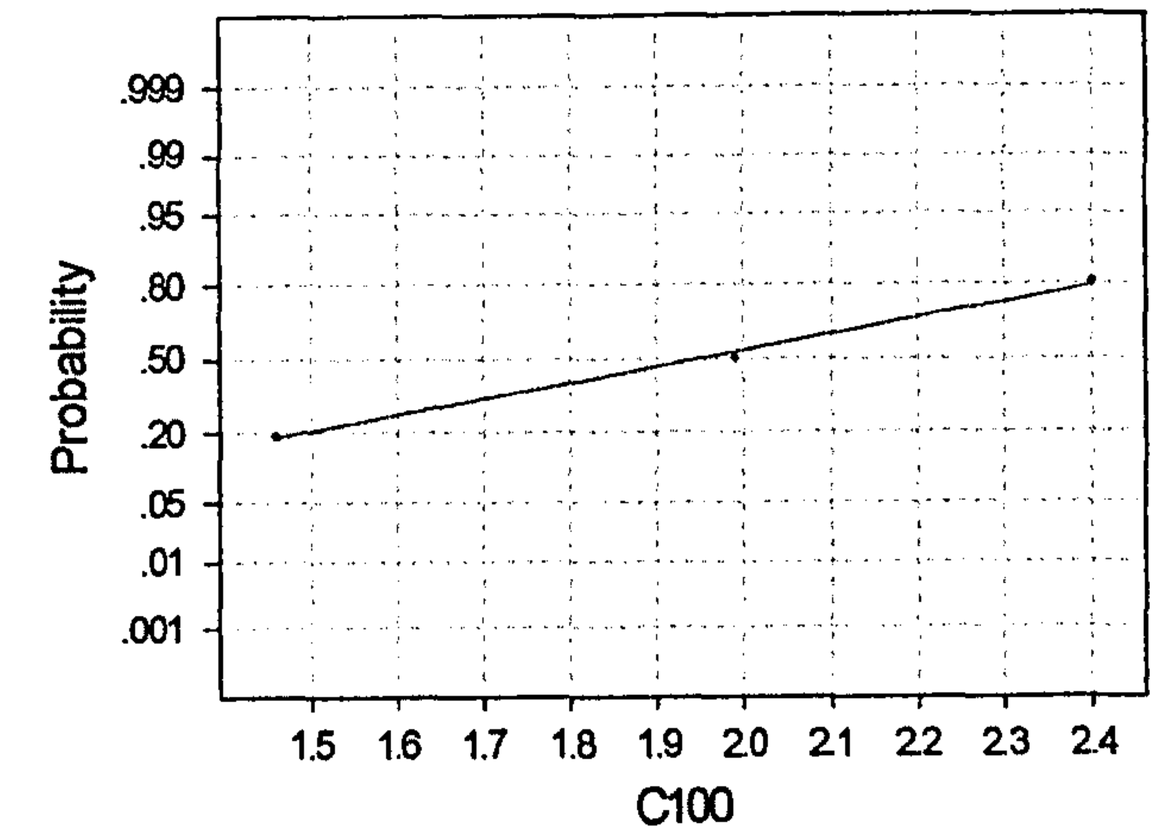

Fig 4.43 Normality Test for the population (paired difference between data for **intact capsule** and **transsected medial iliofemoral ligament**) used in the paired t-test

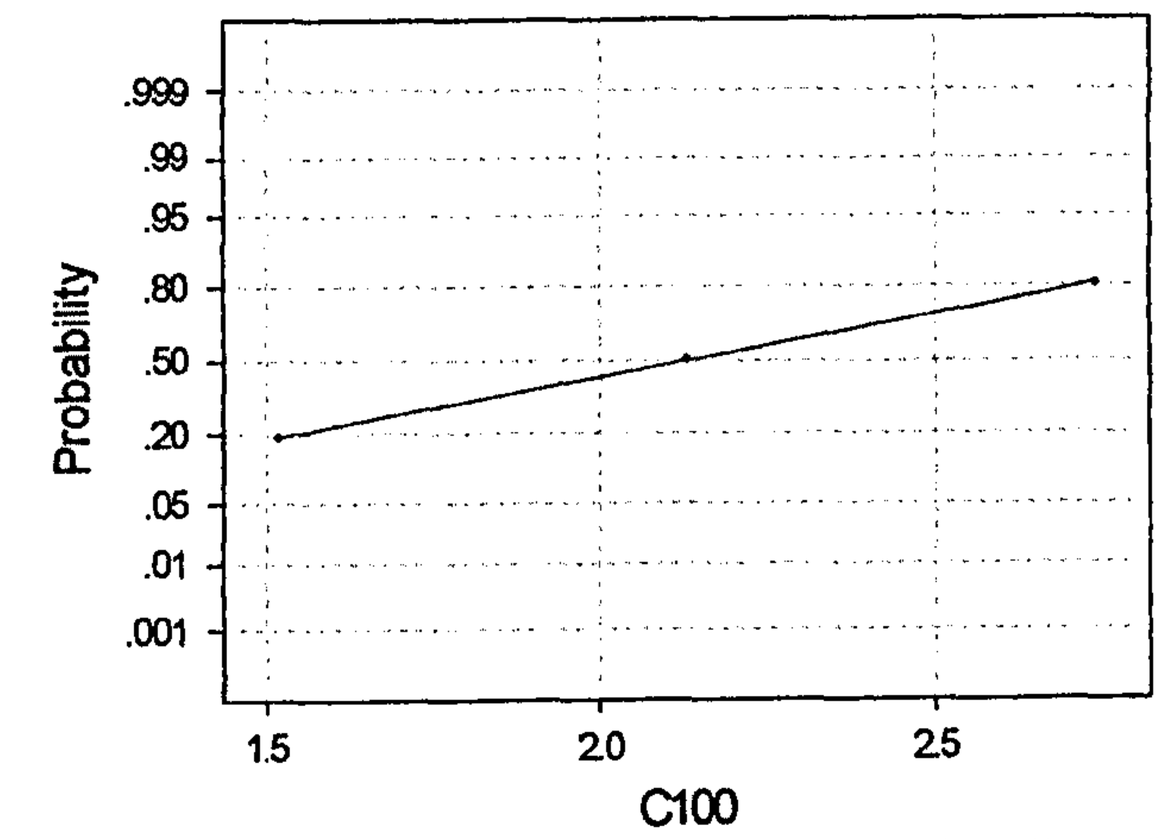

Fig 4.44 Normality Test for the population (paired difference between data for **intact capsule** and **transsected medial and lateral iliofemoral ligaments**) used in the paired t-test

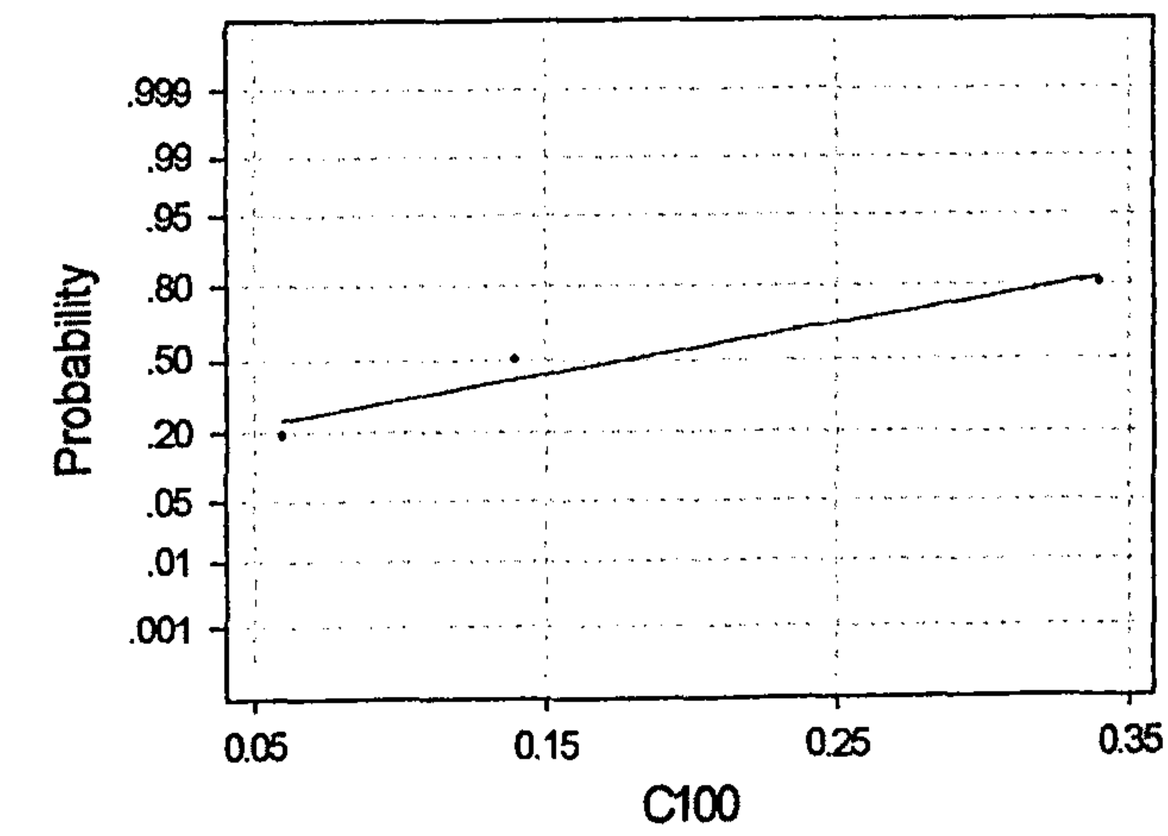

Fig 4.45 Normality Test for the population (paired difference between data for **transsected medial iliofemoral** and **transsected medial and lateral iliofemoral ligaments**) used in the paired t-test

Specimen 5 (Abduction)

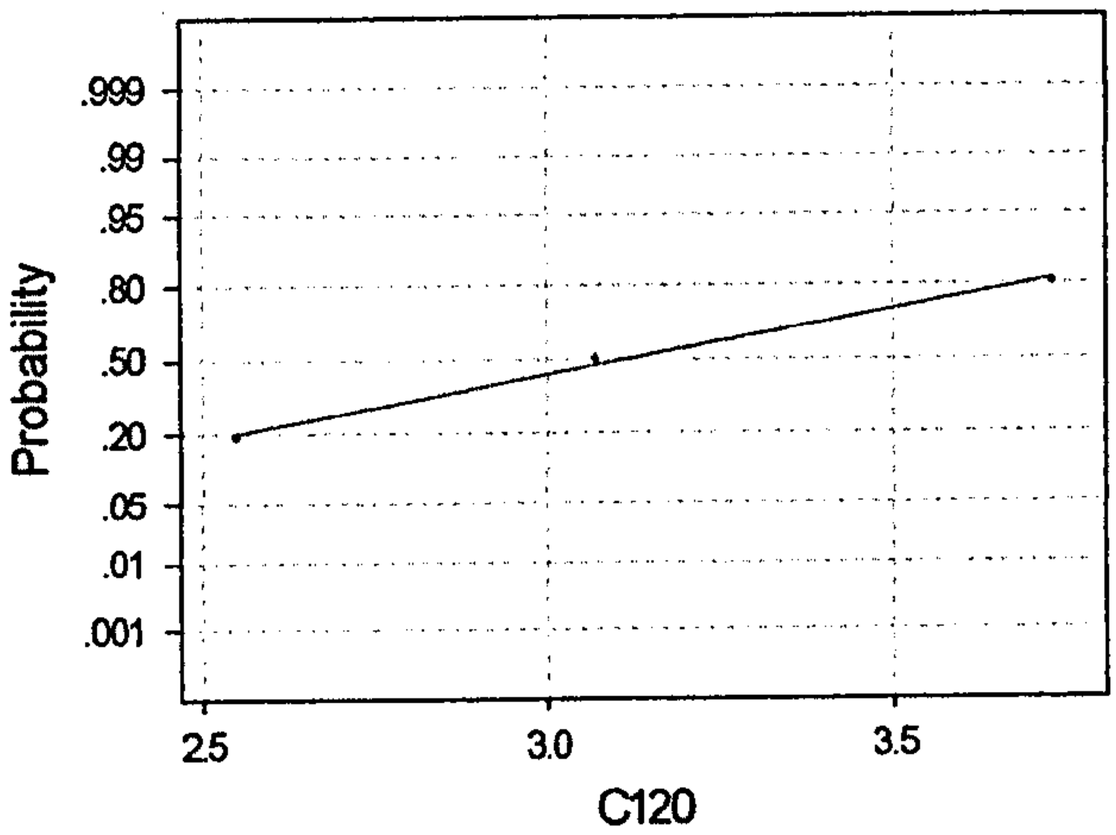

Fig 4.46 Normality Test for the population (paired difference between data for **intact capsule** and **transsected medial iliofemoral ligament**) used in the paired t-test

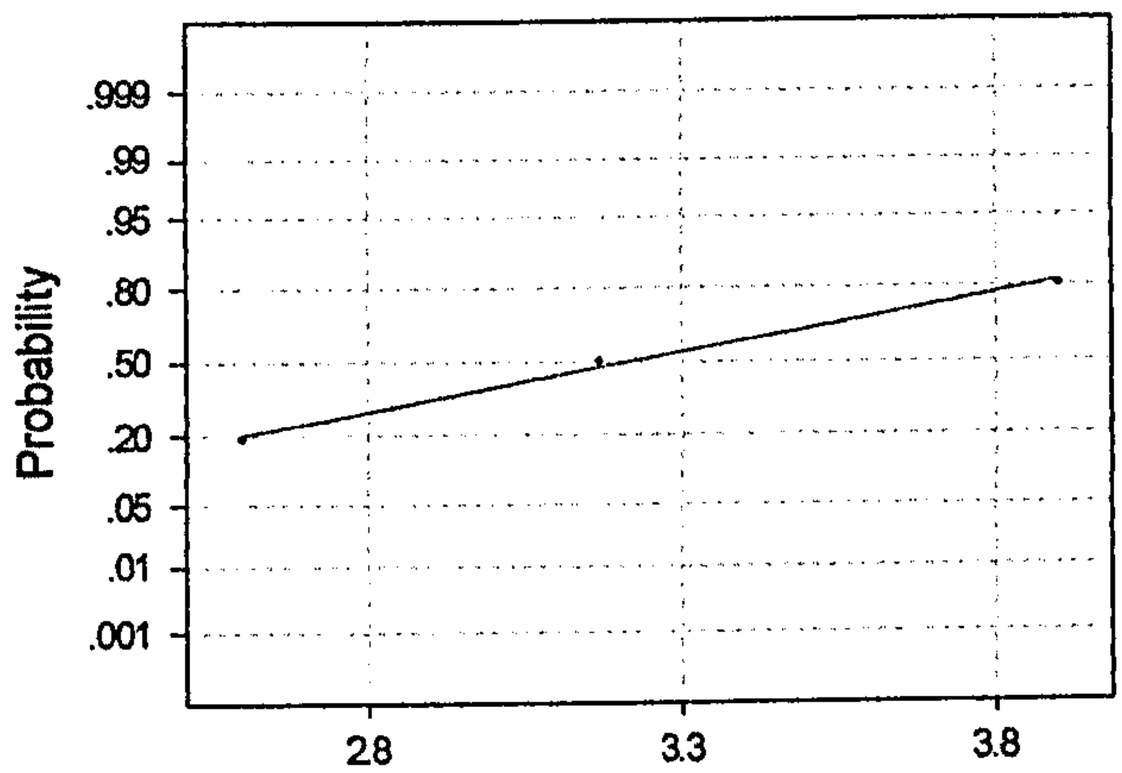

Fig 4.47 Normality Test for the population (paired difference between data for **intact capsule** and **transsected medial and lateral iliofemoral ligaments**) used in the paired t-test

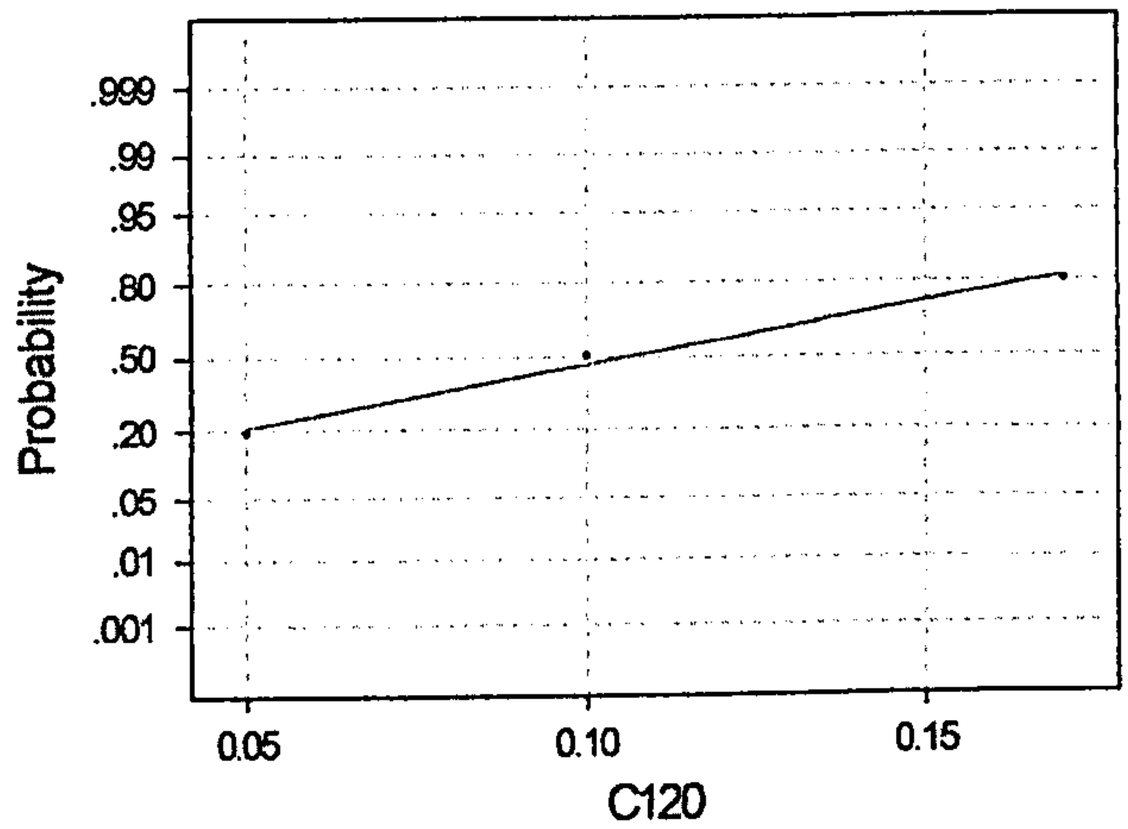

Fig 4.48 Normality Test for the population (paired difference between data for **transsected medial iliofemoral** and **transsected medial and lateral iliofemoral ligaments**) used in the paired t-test

Specimen 4 and 5 (Adduction)

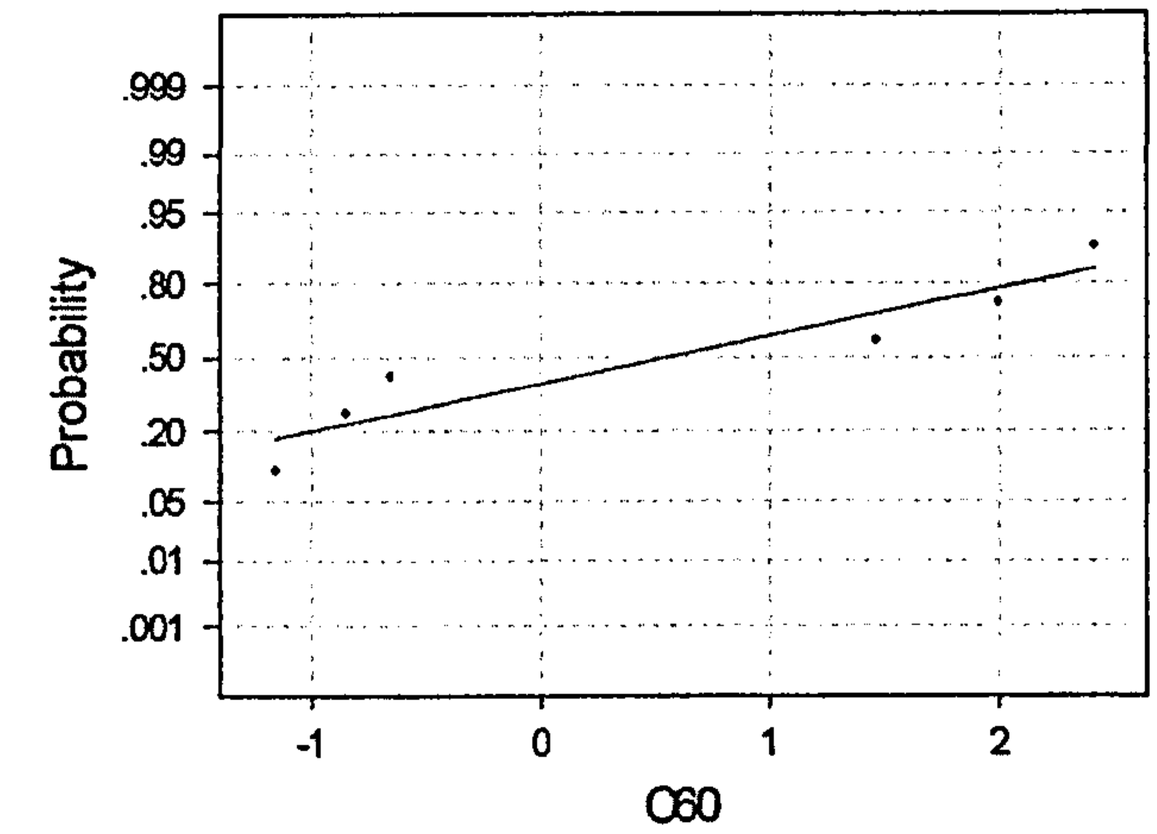

Fig 4.49 Normality Test for the population (paired difference between data for **intact capsule** and **transsected medial iliofemoral ligament**) used in the paired t-test

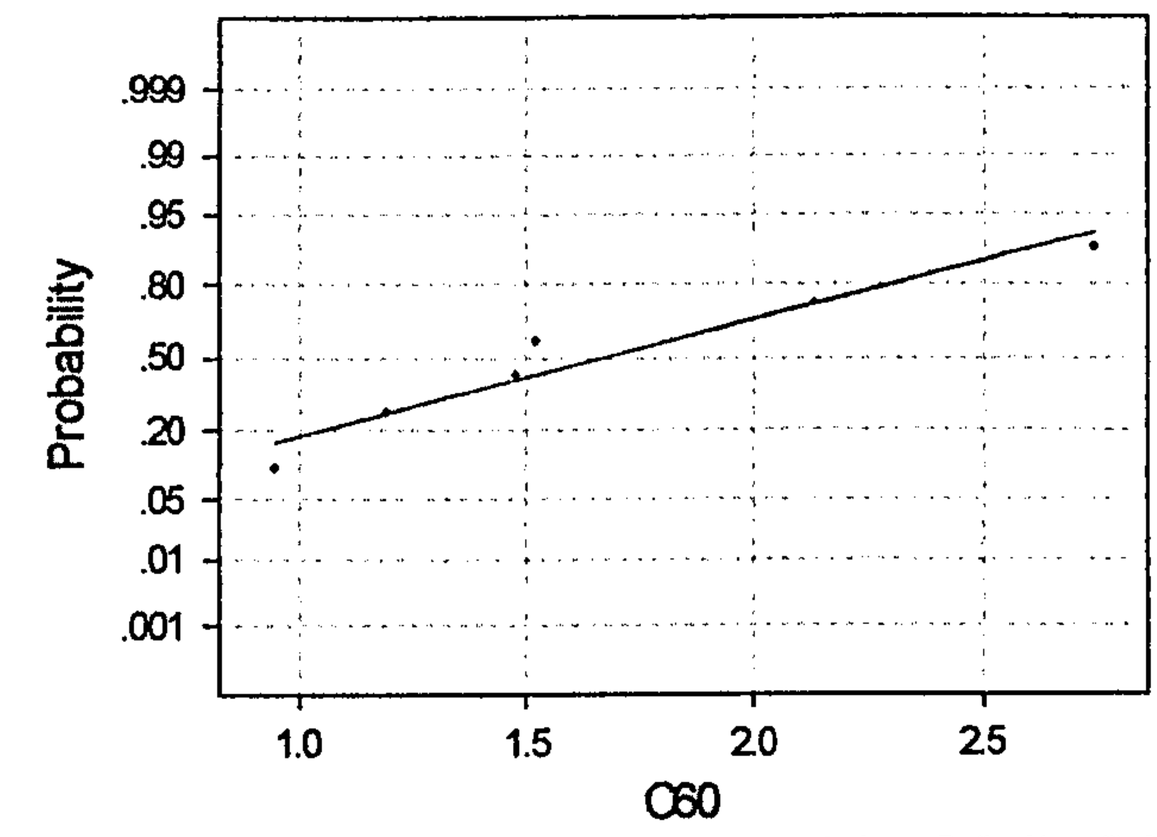

Fig 4.50 Normality Test for the population (paired difference between data for **intact capsule** and **transsected medial and lateral iliofemoral ligaments**) used in the paired t-test

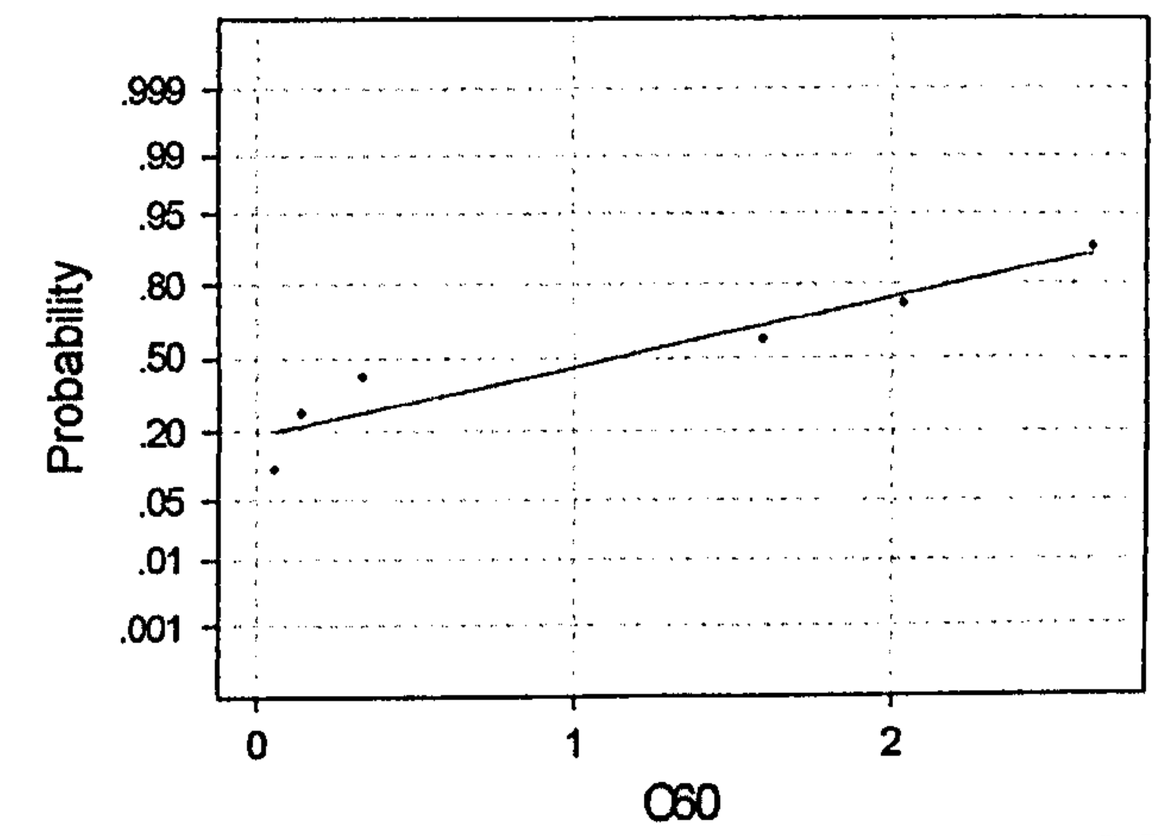

Fig 4.51 Normality Test for the population (paired difference between data for **transsected medial iliofemoral** and **transsected medial and lateral iliofemoral ligaments**) used in the paired t-test

Specimen 4 and 5 (Abduction)

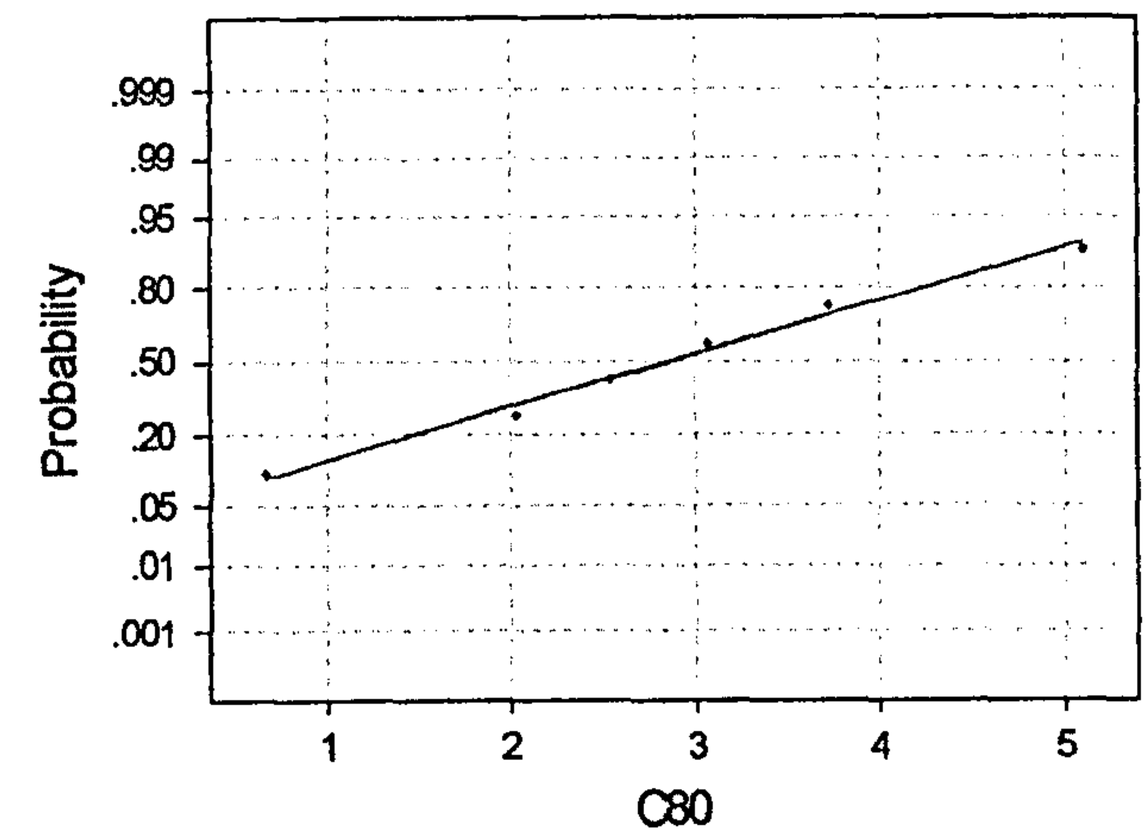

Fig 4.52 Normality Test for the population (paired difference between data for **intact capsule** and **transsected medial iliofemoral ligament**) used in the paired t-test

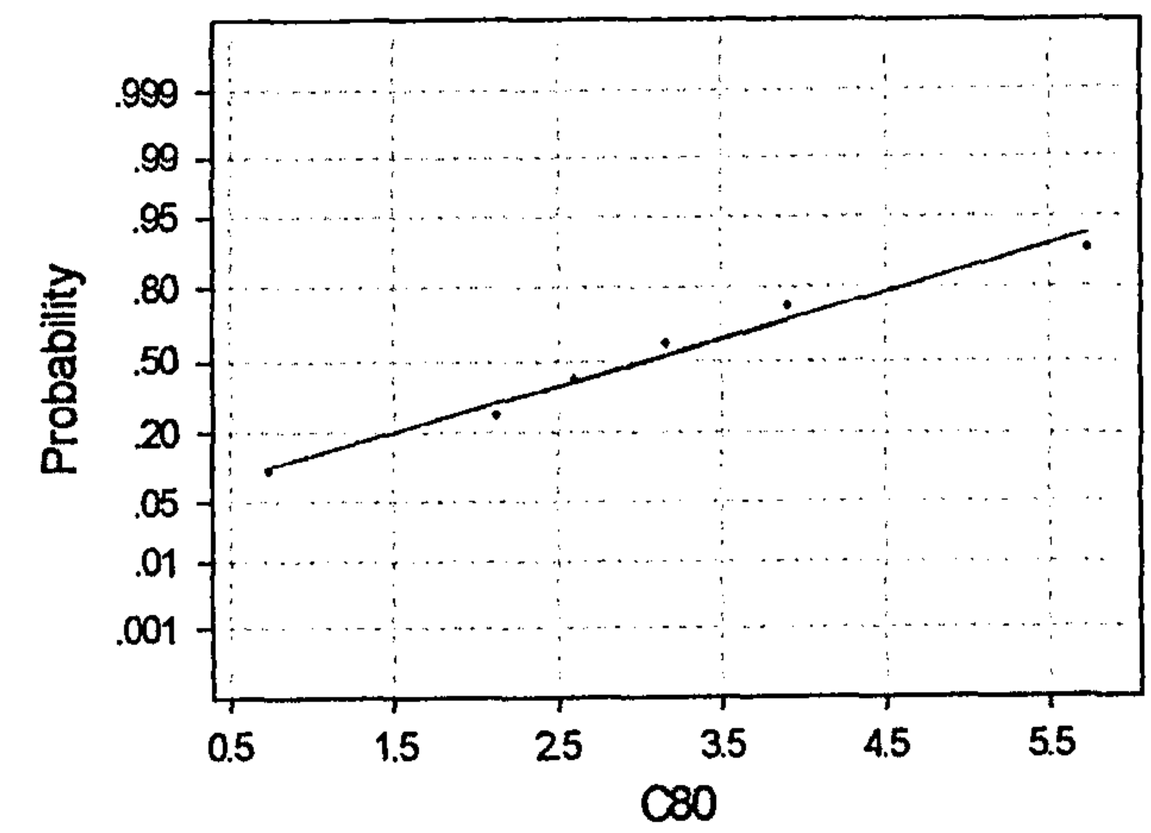

Fig 4.53 Normality Test for the population (paired difference between data for **intact capsule** and **transsected medial and lateral iliofemoral ligaments**) used in the paired t-test

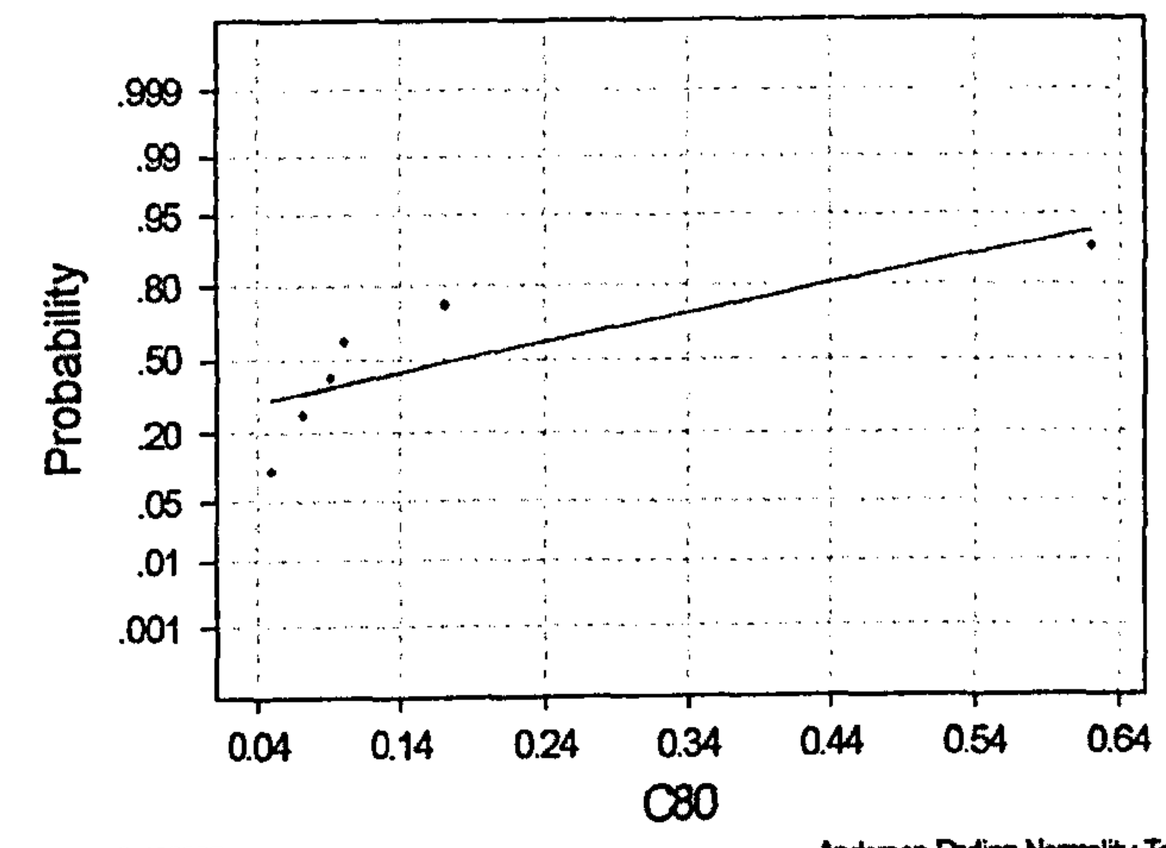

Fig 4.54 Normality Test for the population (paired difference between data for **transsected medial iliofemoral** and **transsected medial and lateral iliofemoral ligaments**) used in the paired t-test

Full External Rotation

Specimen 4 (Adduction)

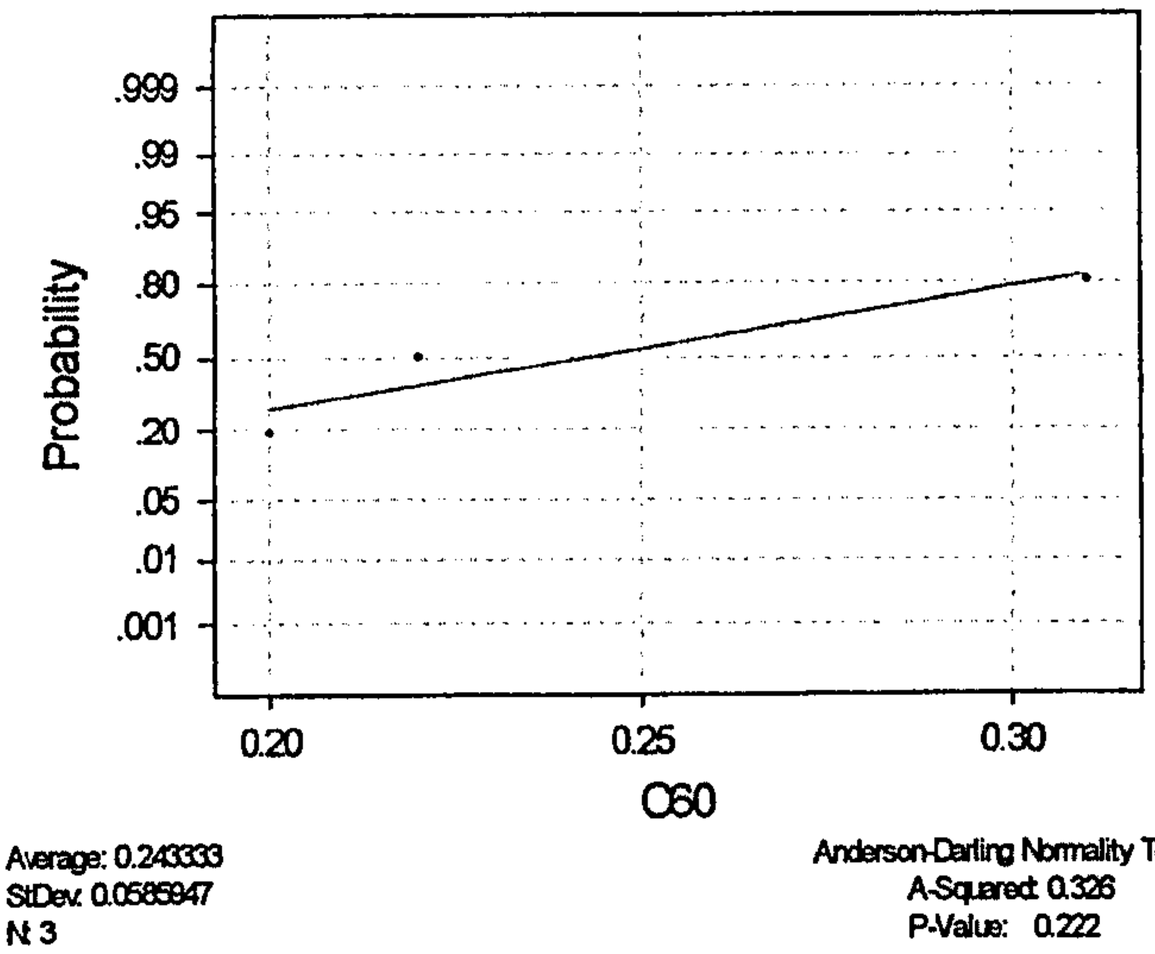

Fig 4.55 Normality Test for the population (paired difference between data for **intact capsule** and **transsected medial iliofemoral ligament**) used in the paired t-test

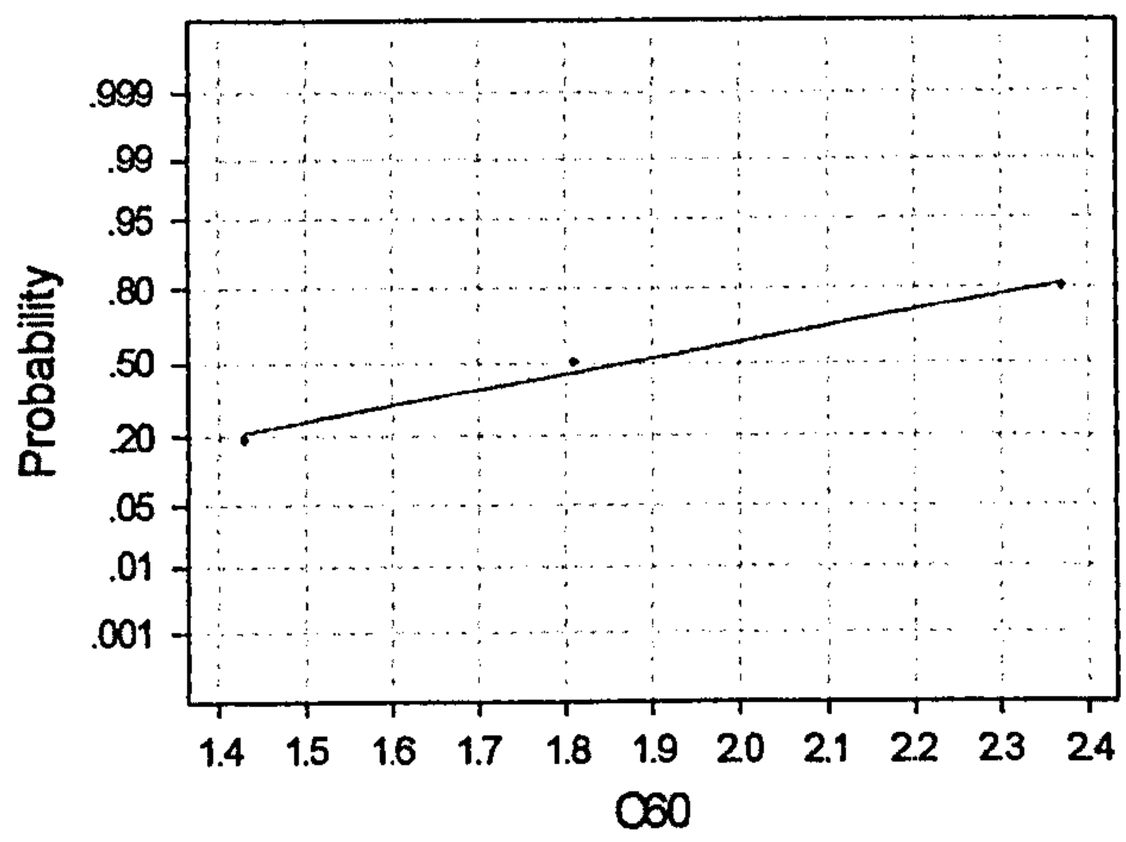

Fig 4.56 Normality Test for the population (paired difference between data for **intact capsule** and **transsected medial and lateral iliofemoral ligaments**) used in the paired t-test

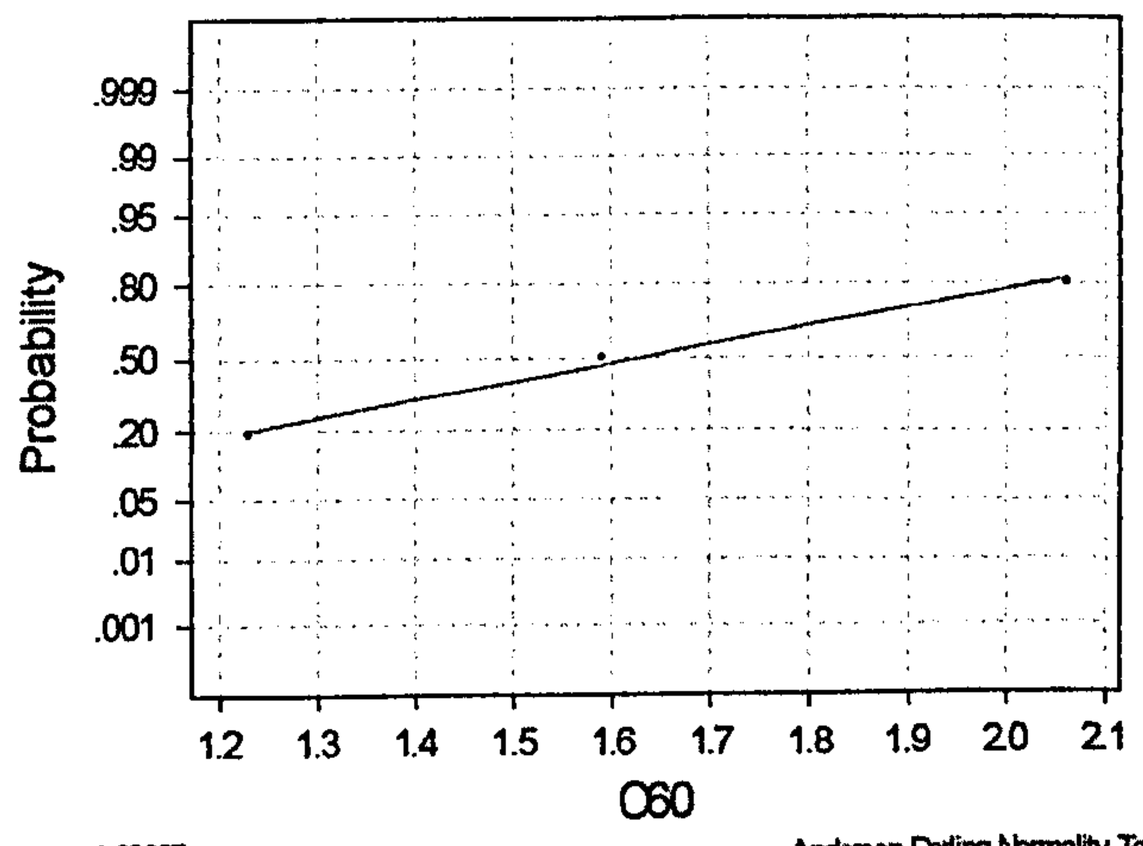

Fig 4.57 Normality Test for the population (paired difference between data for **transsected medial iliofemoral** and **transsected medial and lateral iliofemoral ligaments**) used in the paired t-test

Specimen 4 (Abduction)

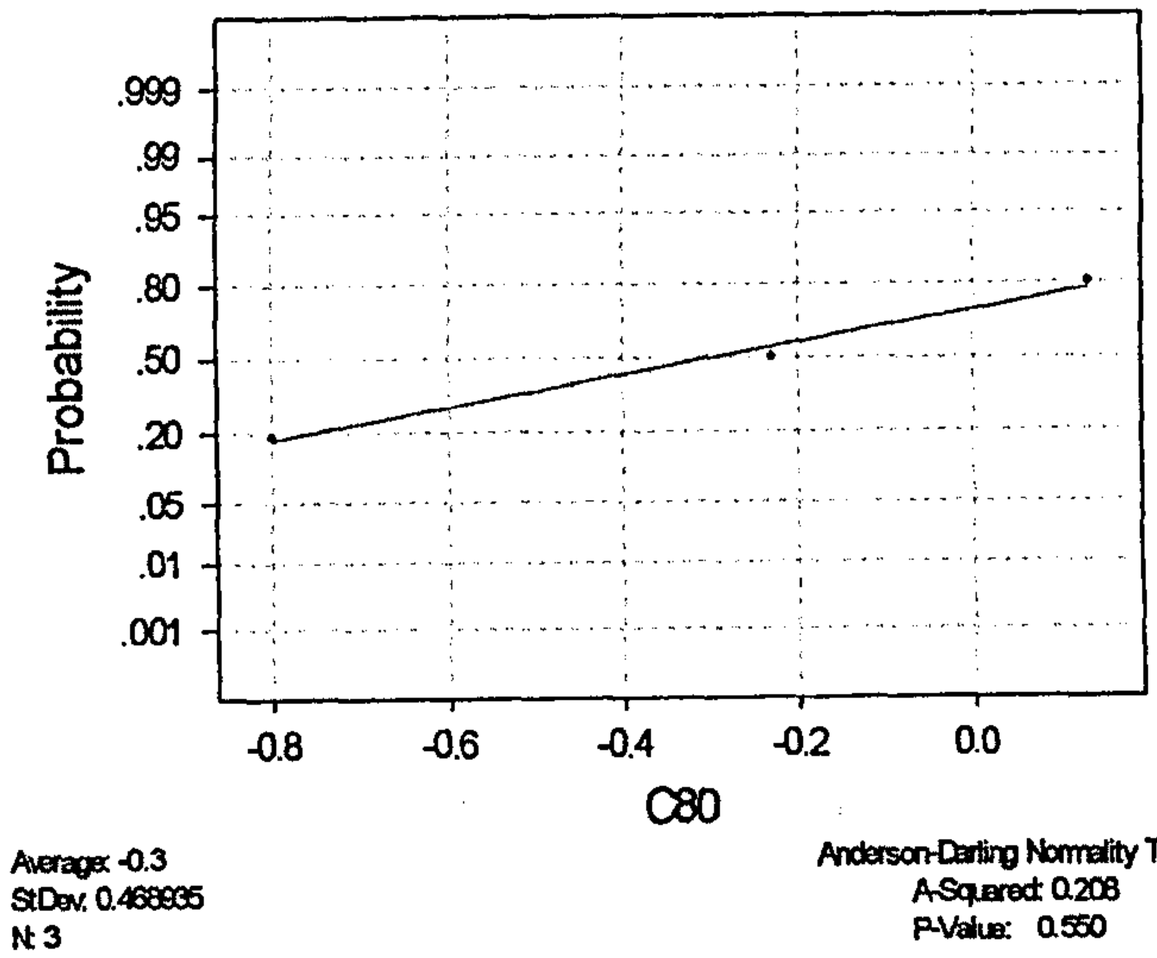

Fig 4.58 Normality Test for the population (paired difference between data for **intact capsule** and **transsected medial iliofemoral ligament**) used in the paired t-test

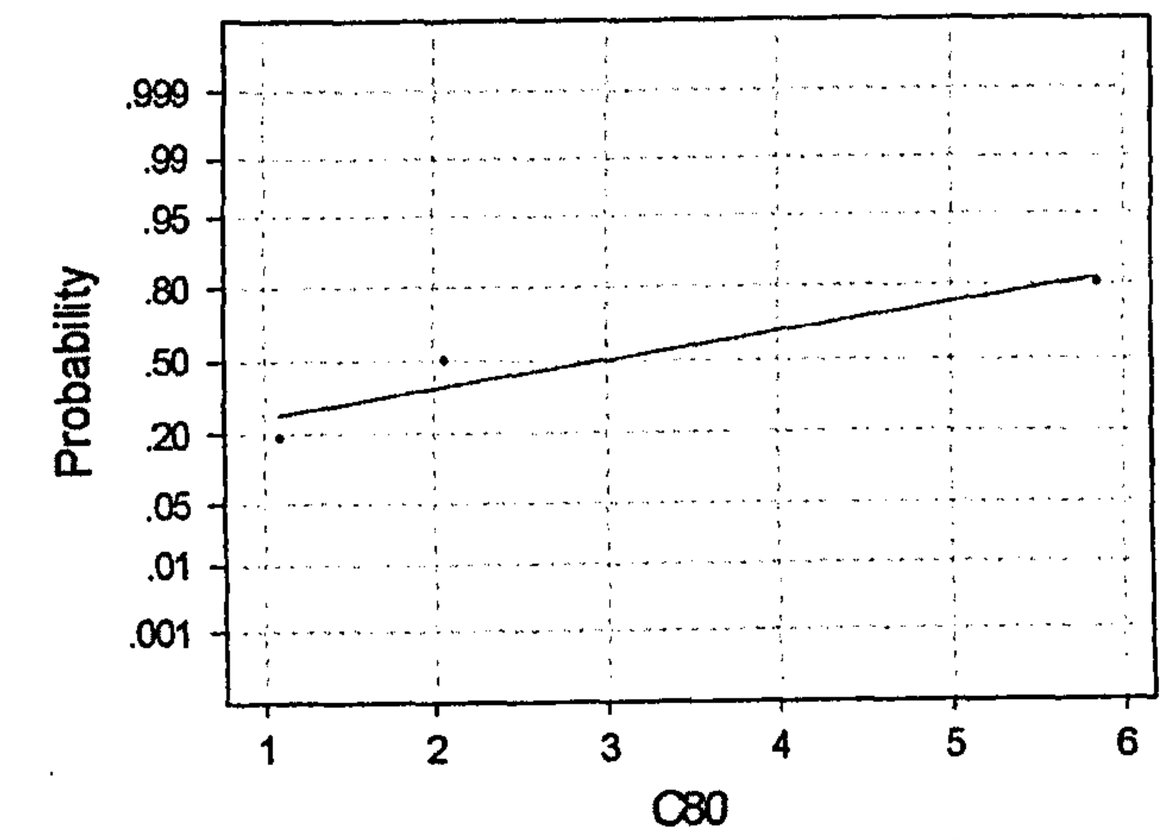

Fig 4.59 Normality Test for the population (paired difference between data for **intact capsule** and **transsected medial and lateral iliofemoral ligaments**) used in the paired t-test

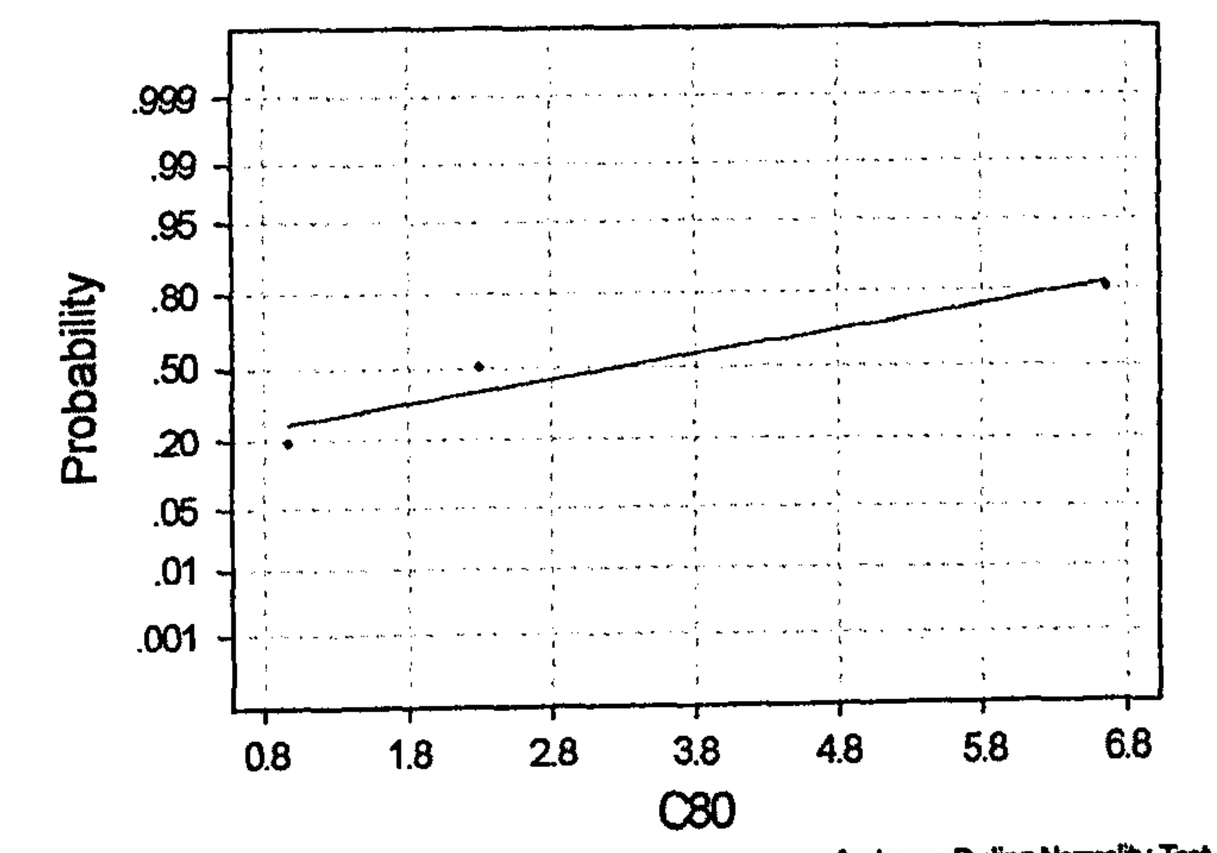

Fig 4.60 Normality Test for the population (paired difference between data for **transsected medial iliofemoral** and **transsected medial and lateral iliofemoral ligaments**) used in the paired t-test

Specimen 5 (Adduction)

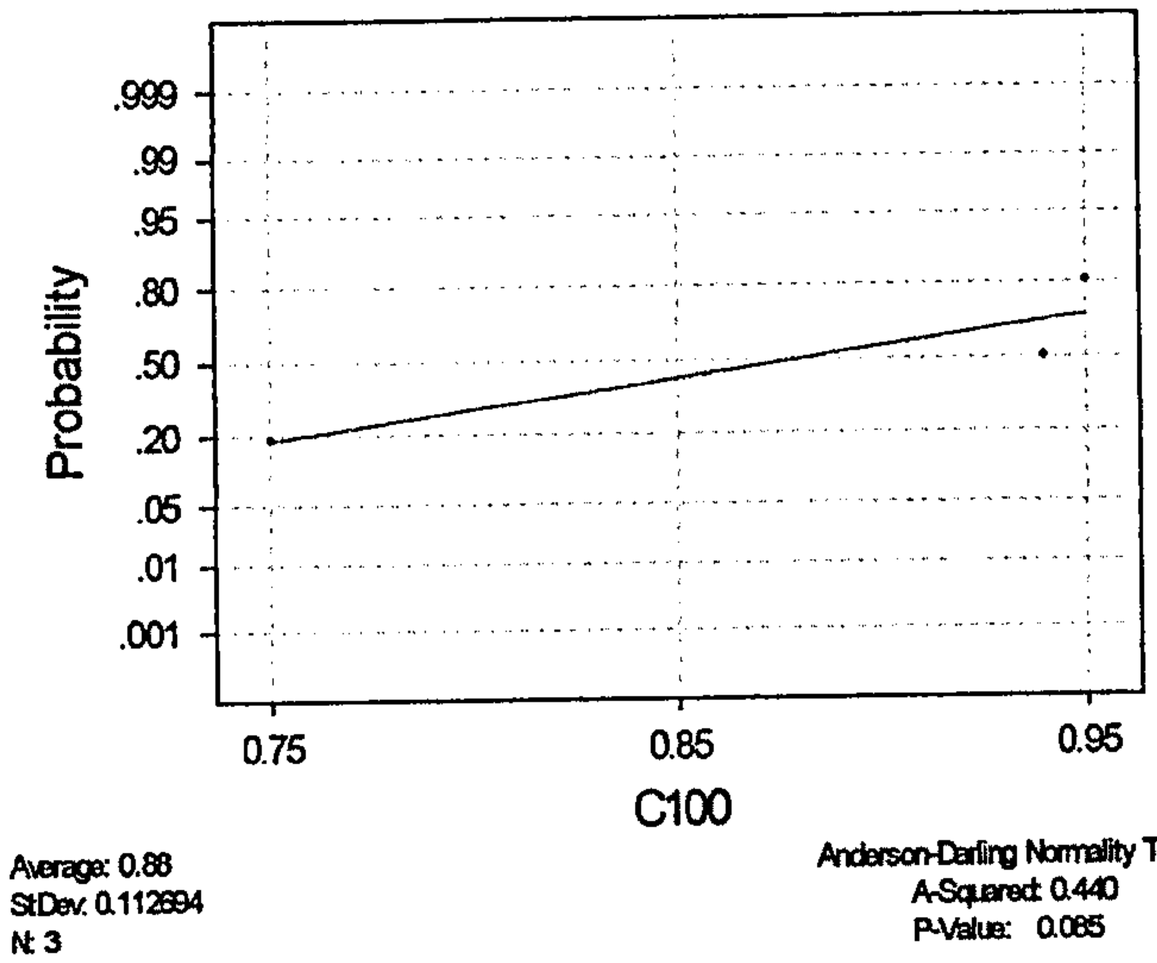

Fig 4.61 Normality Test for the population (paired difference between data for **intact capsule** and **transsected medial iliofemoral ligament**) used in the paired t-test

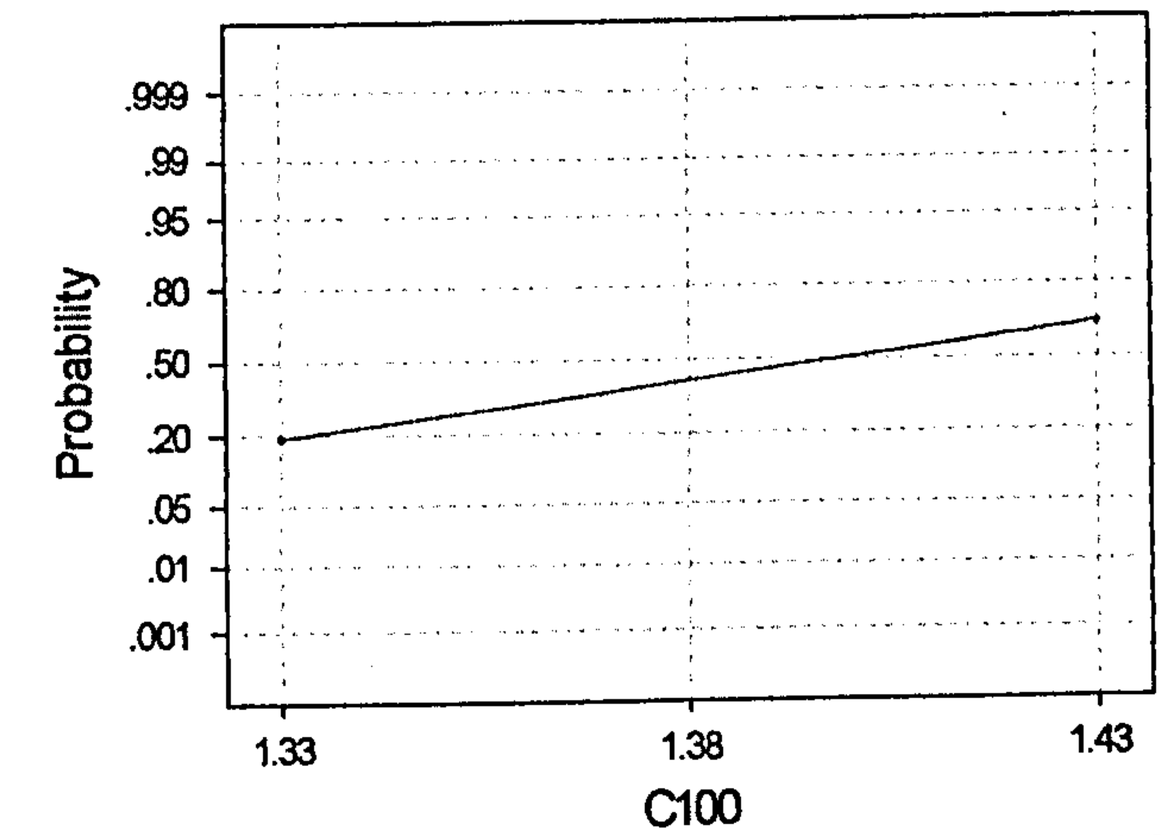

Fig 4.62 Normality Test for the population (paired difference between data for **intact capsule** and **transsected medial and lateral iliofemoral ligaments**) used in the paired t-test

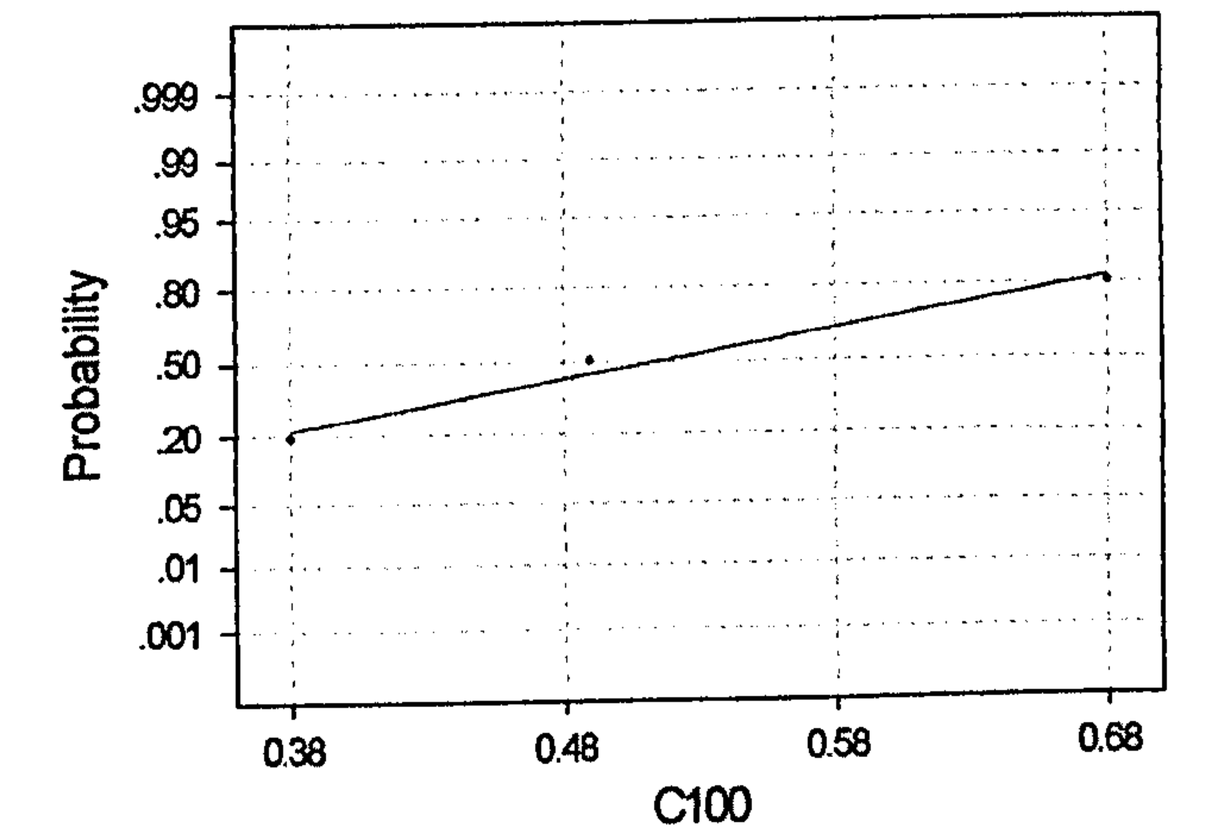

Fig 4.63 Normality Test for the population (paired difference between data for **transsected medial iliofemoral** and **transsected medial and lateral iliofemoral ligaments**) used in the paired t-test

Specimen 5 (Abduction)

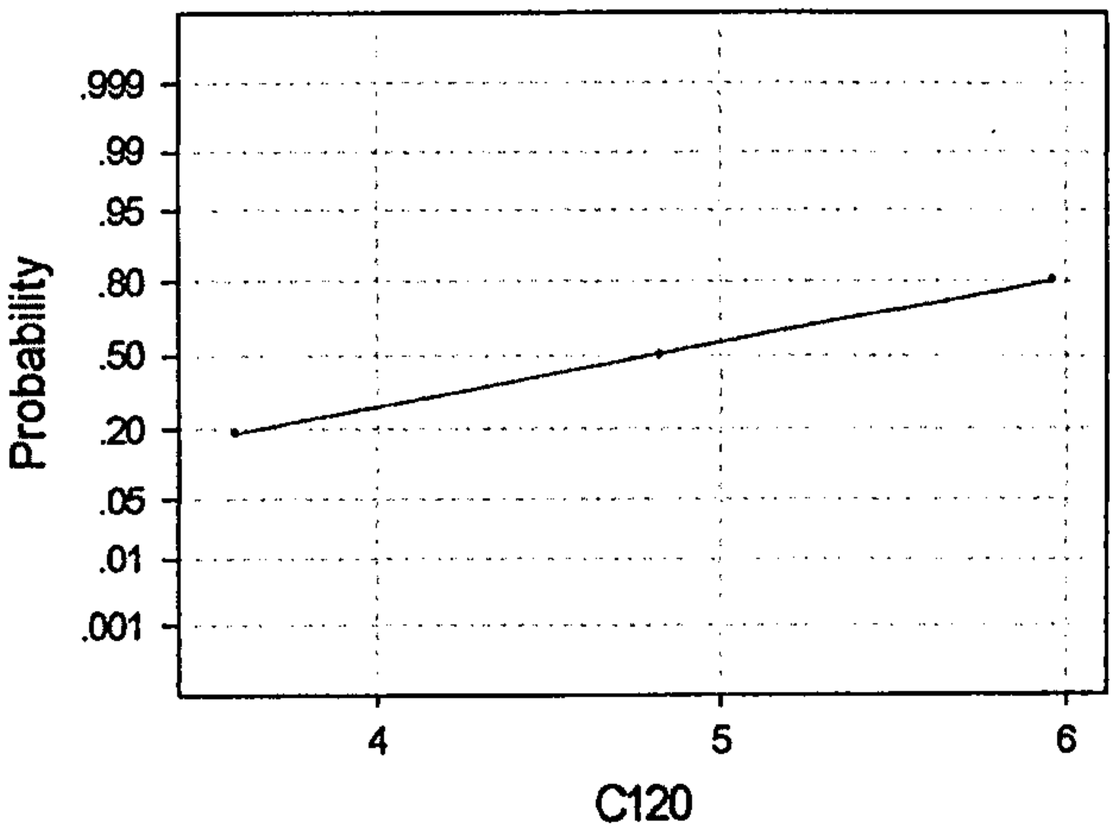

Fig 4.64 Normality Test for the population (paired difference between data for **intact capsule** and **transsected medial iliofemoral ligament**) used in the paired t-test

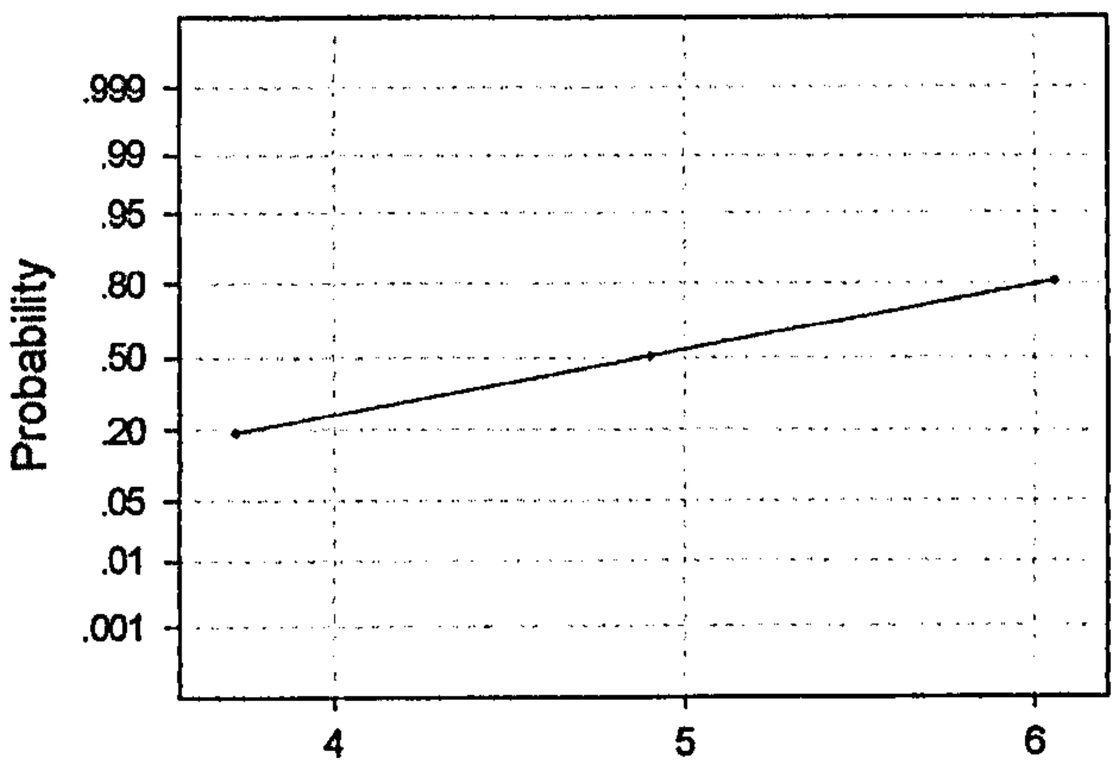

Fig 4.65 Normality Test for the population (paired difference between data for **intact capsule** and **transsected medial and lateral iliofemoral ligaments**) used in the paired t-test

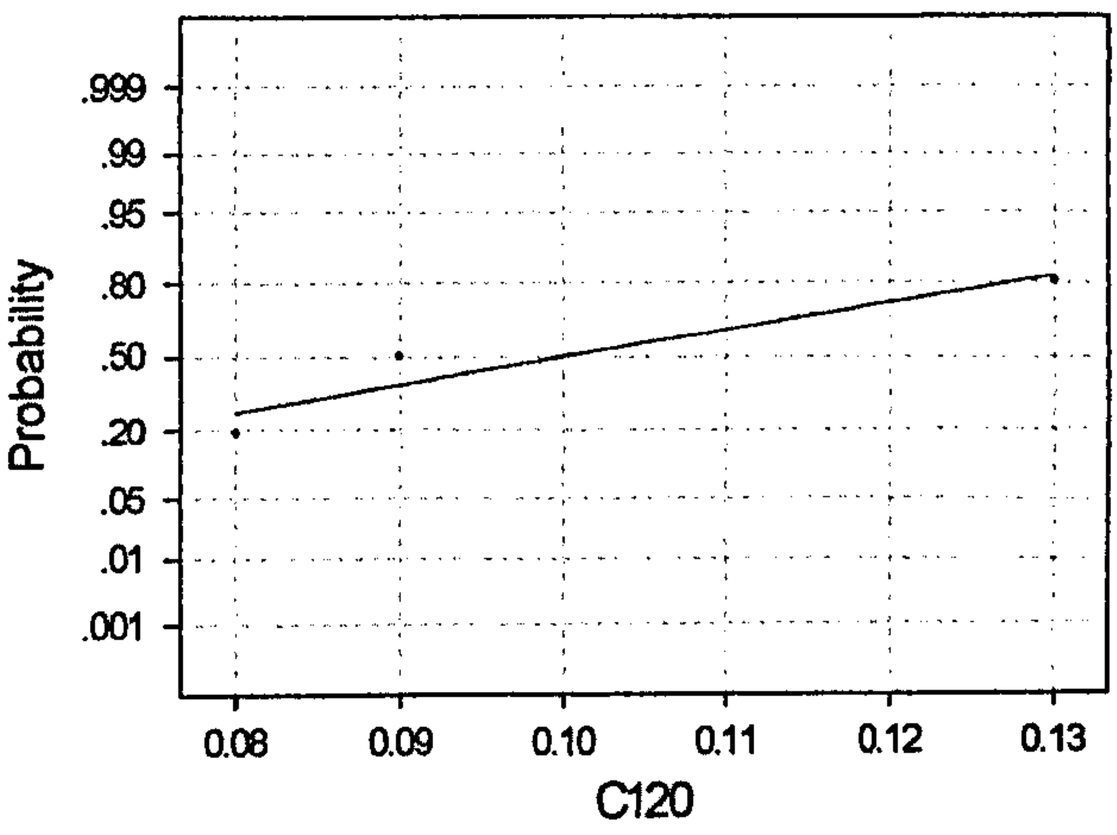

Fig 4.66 Normality Test for the population (paired difference between data for **transsected medial iliofemoral** and **transsected medial and lateral iliofemoral ligaments**) used in the paired t-test

Specimen 4 and 5 (Adduction)

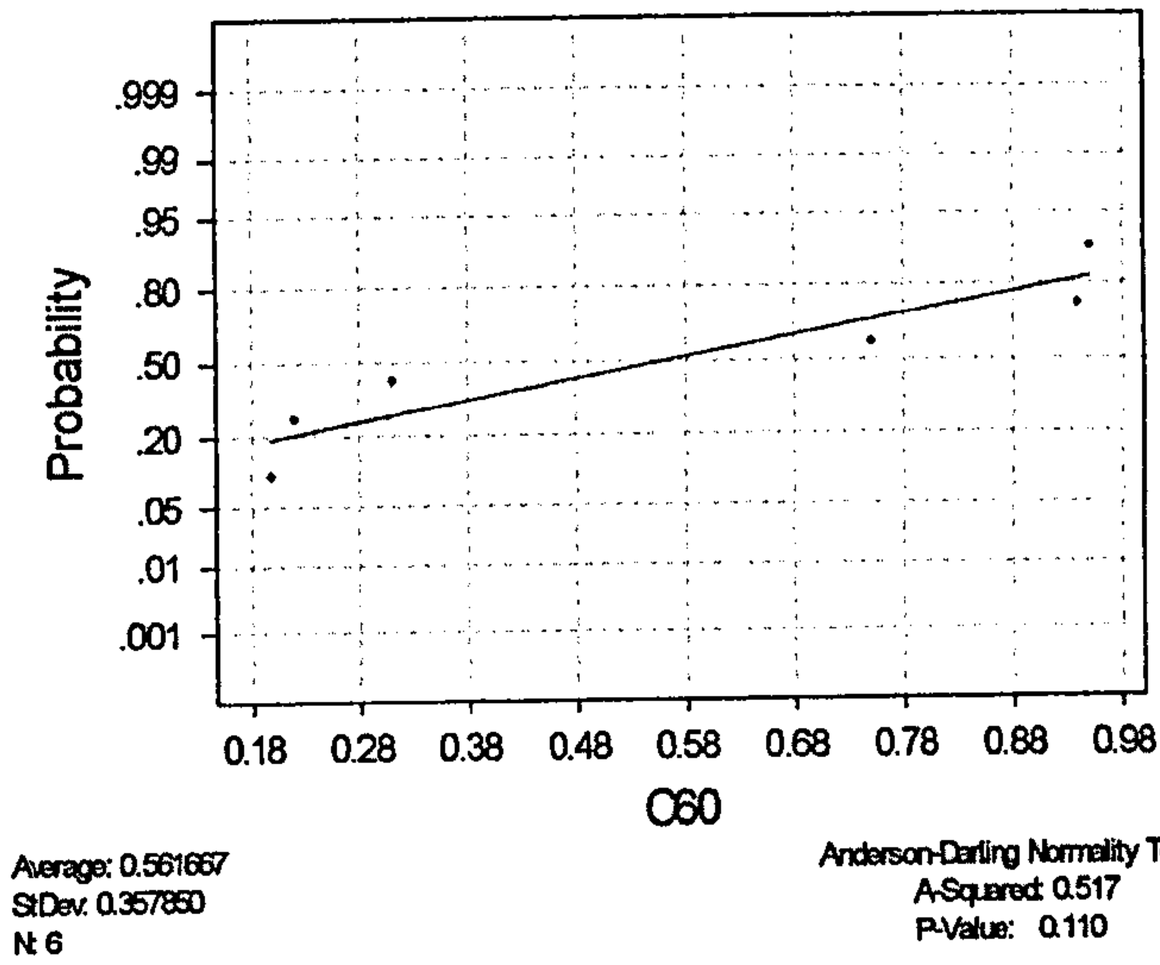

Fig 4.67 Normality Test for the population (paired difference between data for **intact capsule** and **transsected medial iliofemoral ligament**) used in the paired t-test

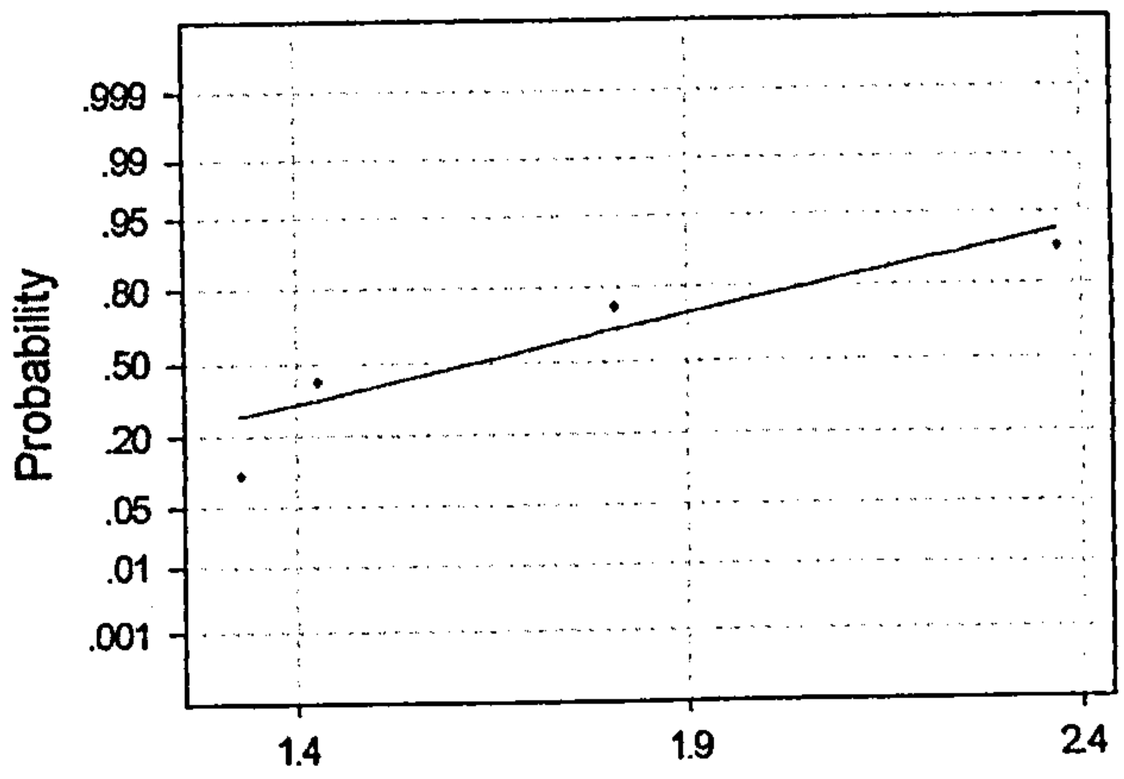

Fig 4.68 Normality Test for the population (paired difference between data for **intact capsule** and **transsected medial and lateral iliofemoral ligaments**) used in the paired t-test

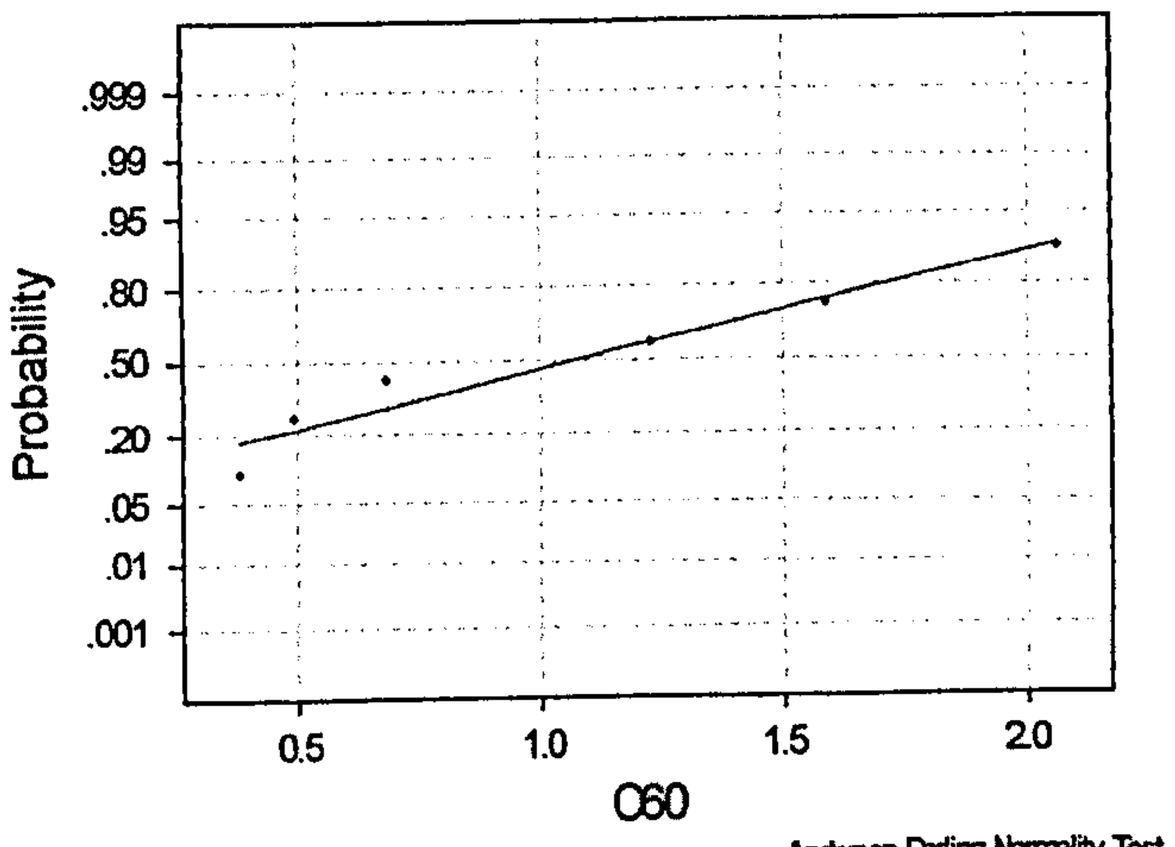

Fig 4.69 Normality Test for the population (paired difference between data for **transsected medial iliofemoral** and **transsected medial and lateral iliofemoral ligaments**) used in the paired t-test

Specimen 4 and 5 (Abduction)

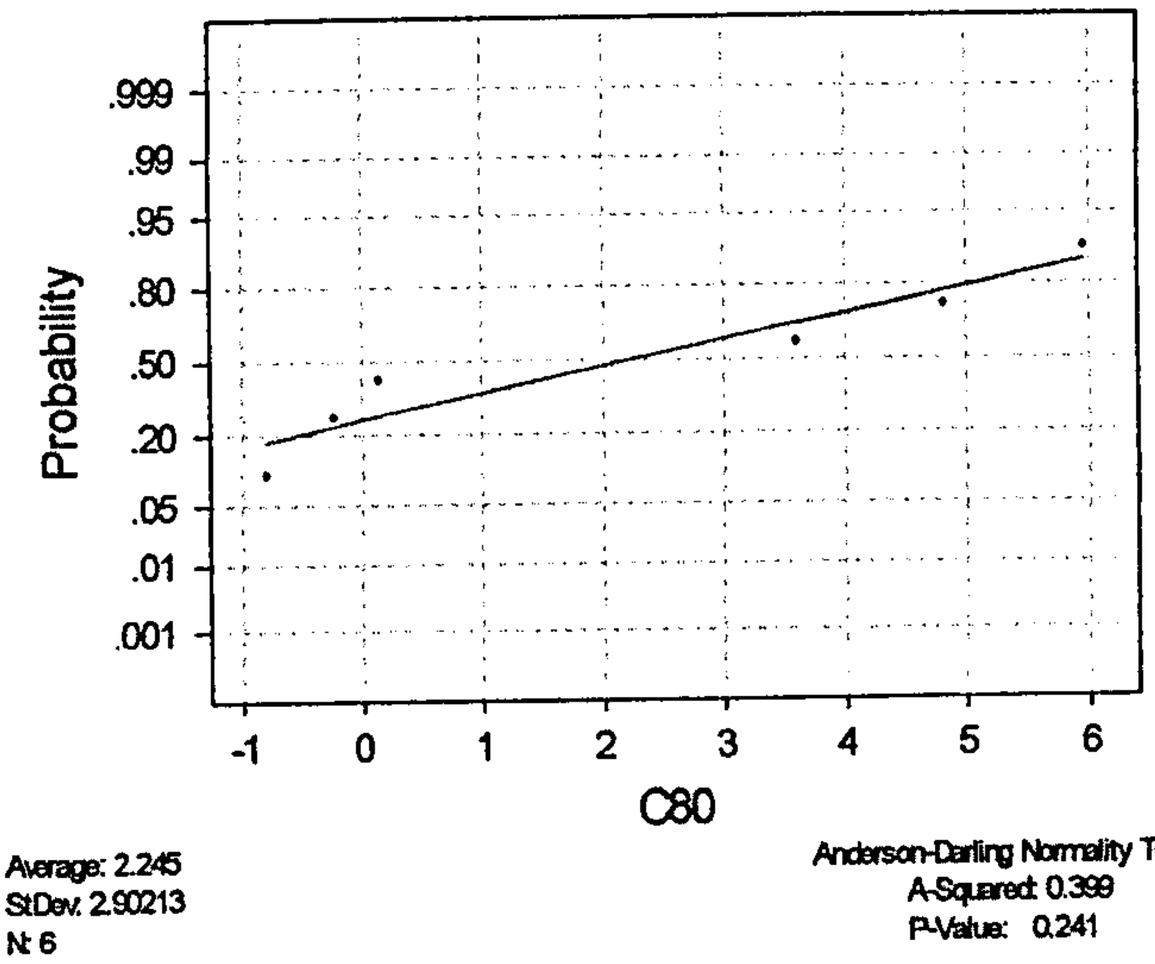

Fig 4.70 Normality Test for the population (paired difference between data for **intact capsule** and **transsected medial iliofemoral ligament**) used in the paired t-test

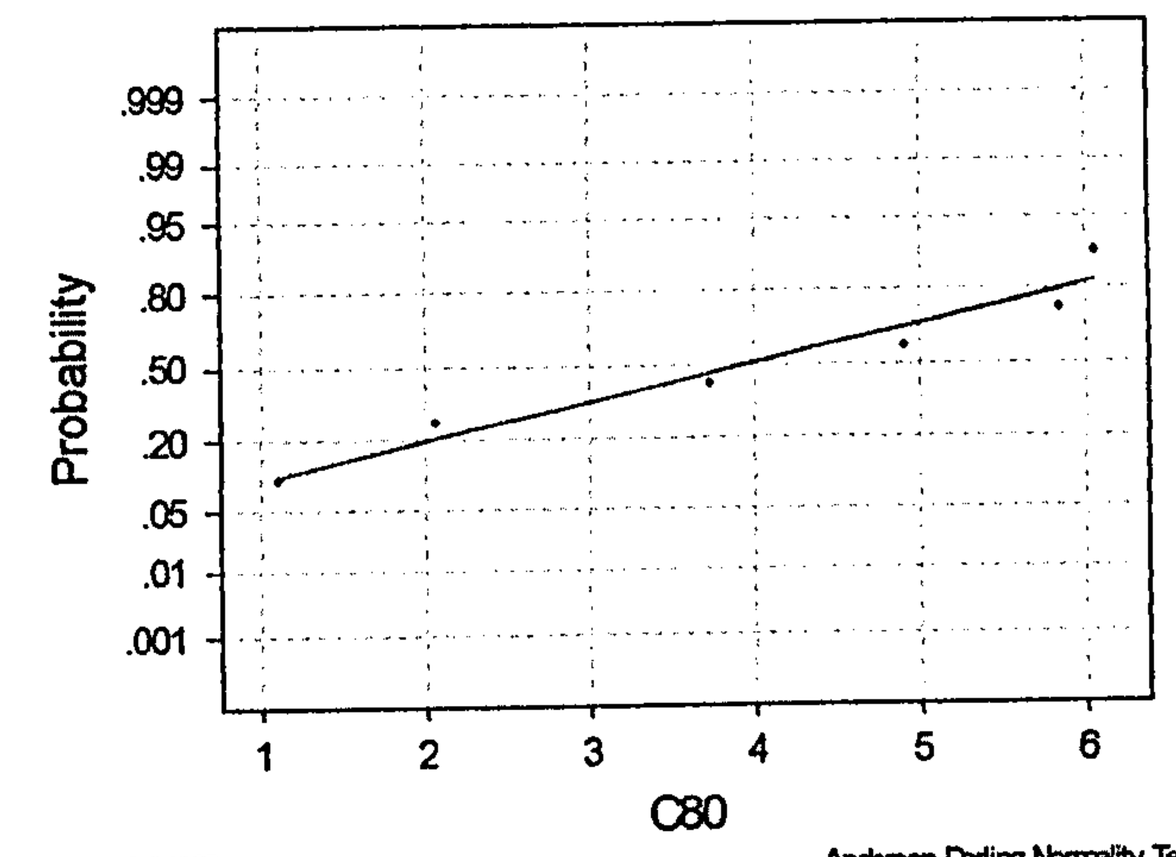

Fig 4.71 Normality Test for the population (paired difference between data for **intact capsule** and **transsected medial and lateral iliofemoral ligaments**) used in the paired t-test

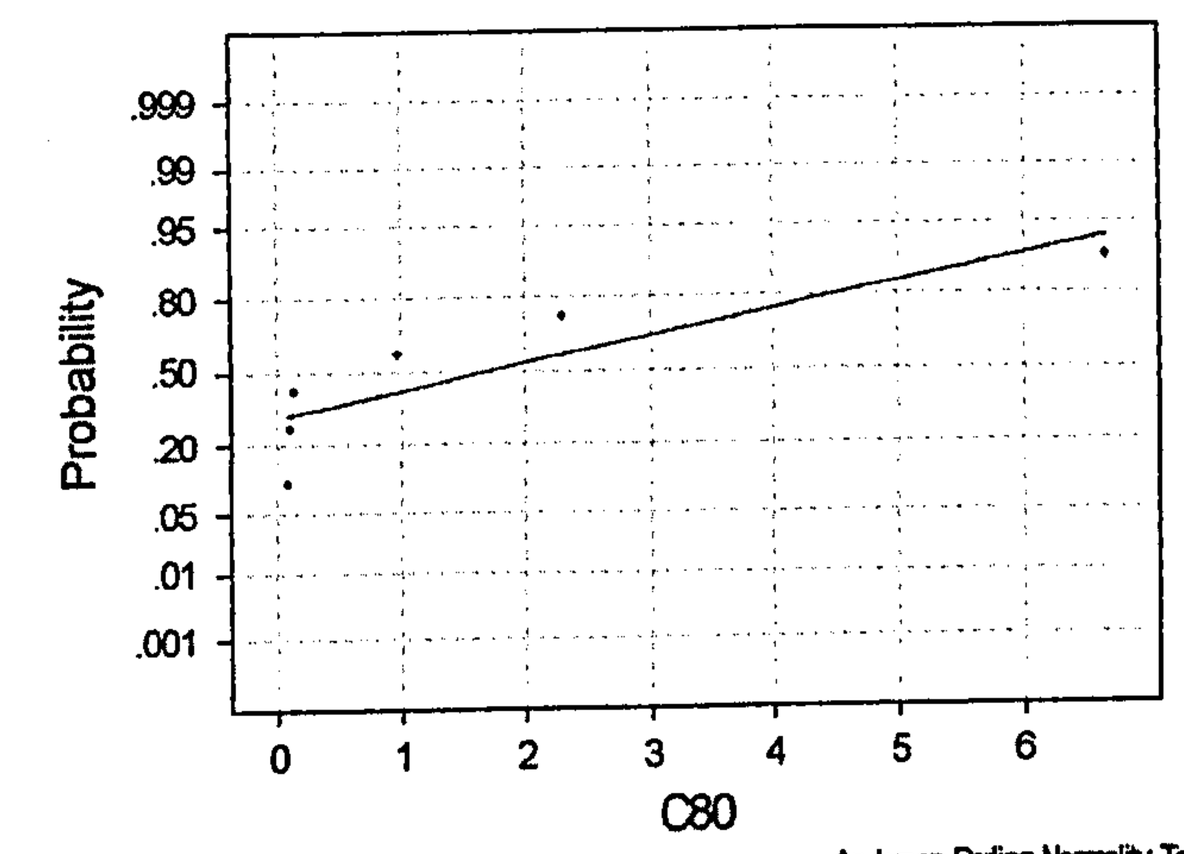

Fig 4.72 Normality Test for the population (paired difference between data for **transsected medial iliofemoral** and **transsected medial and lateral iliofemoral ligaments**) used in the paired t-test

All Joint Positions

Specimen 4 and 5 (Adduction)

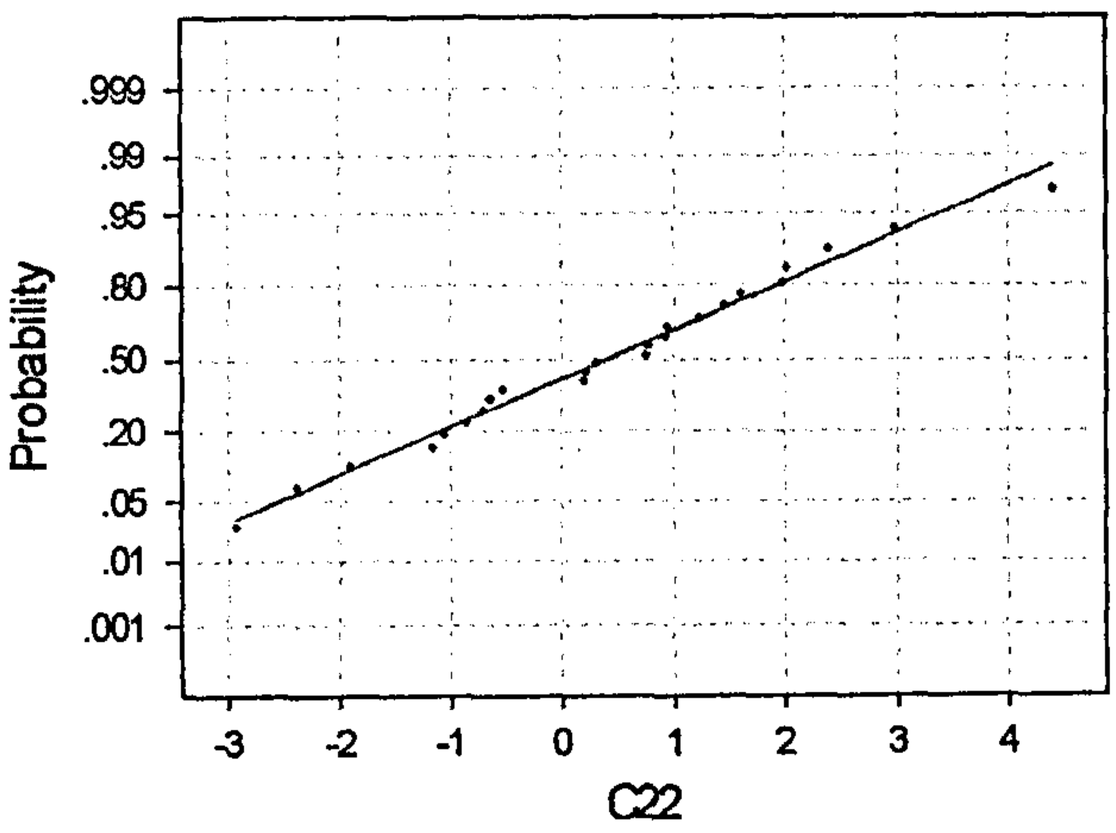

Fig 4.73 Normality Test for the population (paired difference between data for **intact capsule** and **transsected medial iliofemoral ligament**) used in the paired t-test

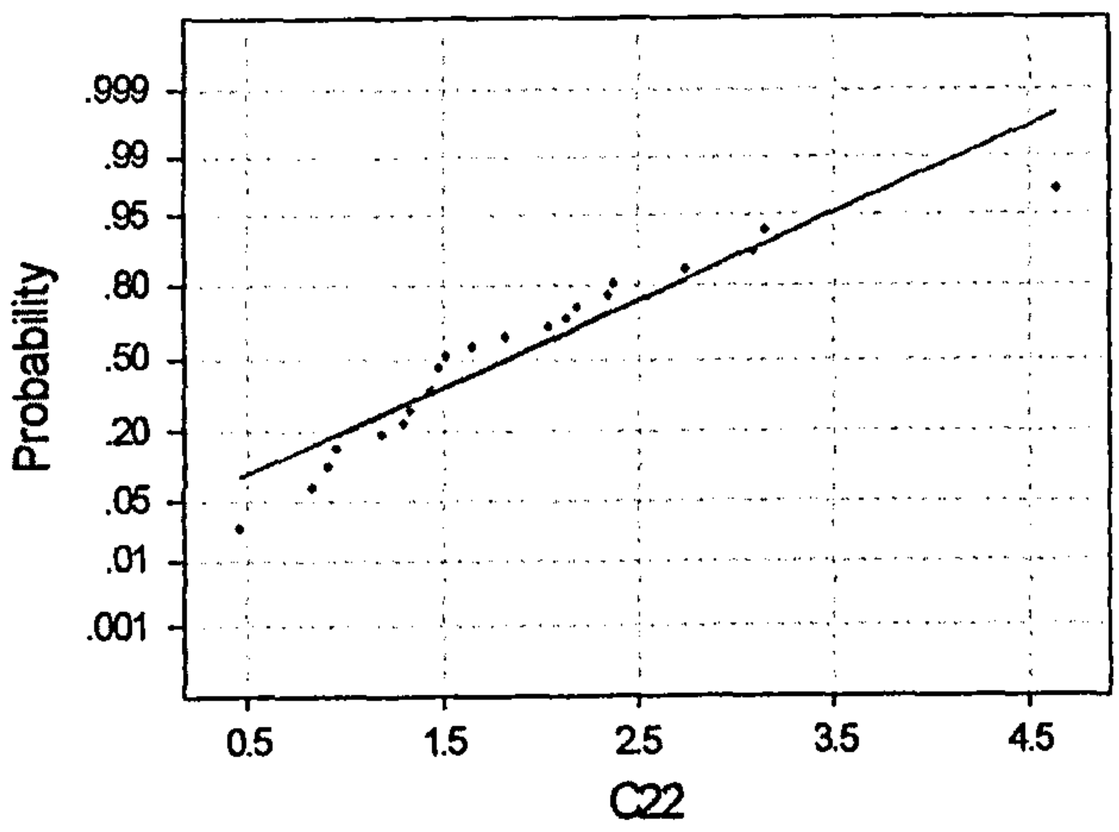

Fig 4.74 Normality Test for the population (paired difference between data for **intact capsule** and **transsected medial and lateral iliofemoral ligaments**) used in the paired t-test

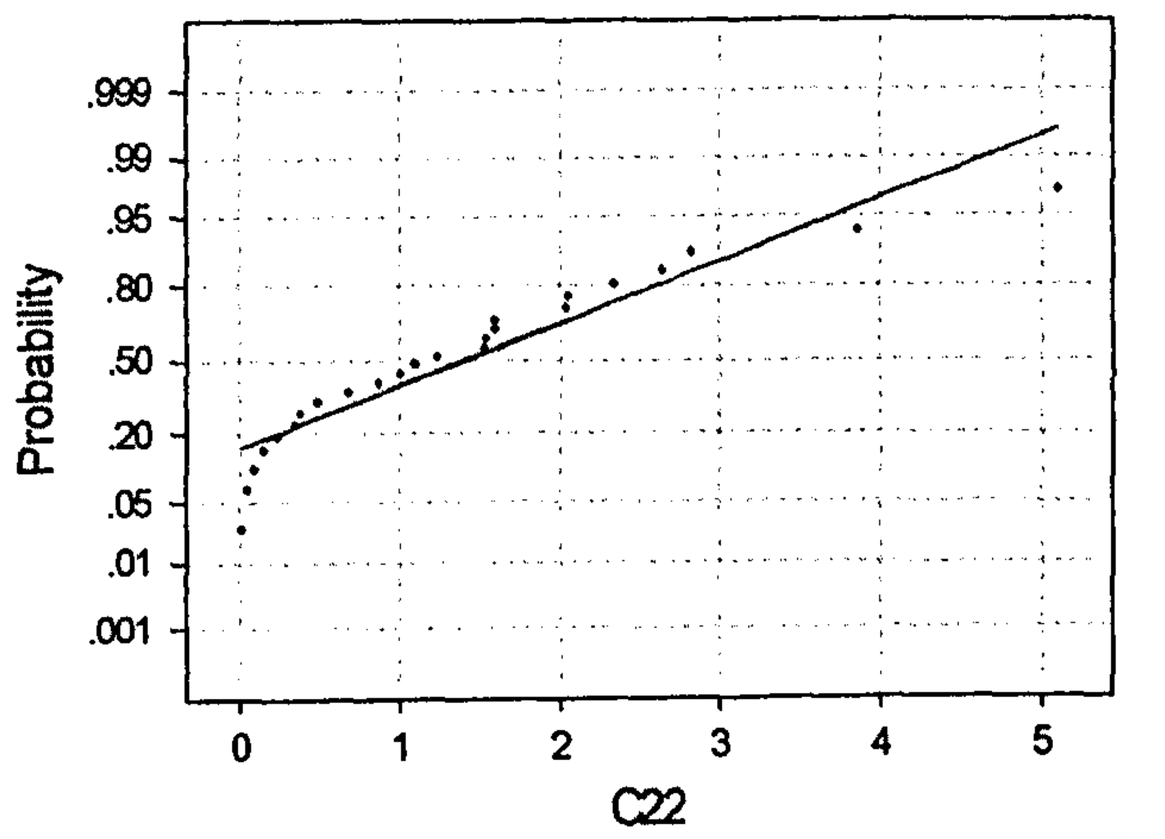

Fig 4.75 Normality Test for the population (paired difference between data for **transsected medial iliofemoral** and **transsected medial and lateral iliofemoral ligaments**) used in the paired t-test

Specimen 4 and 5 (Abduction)

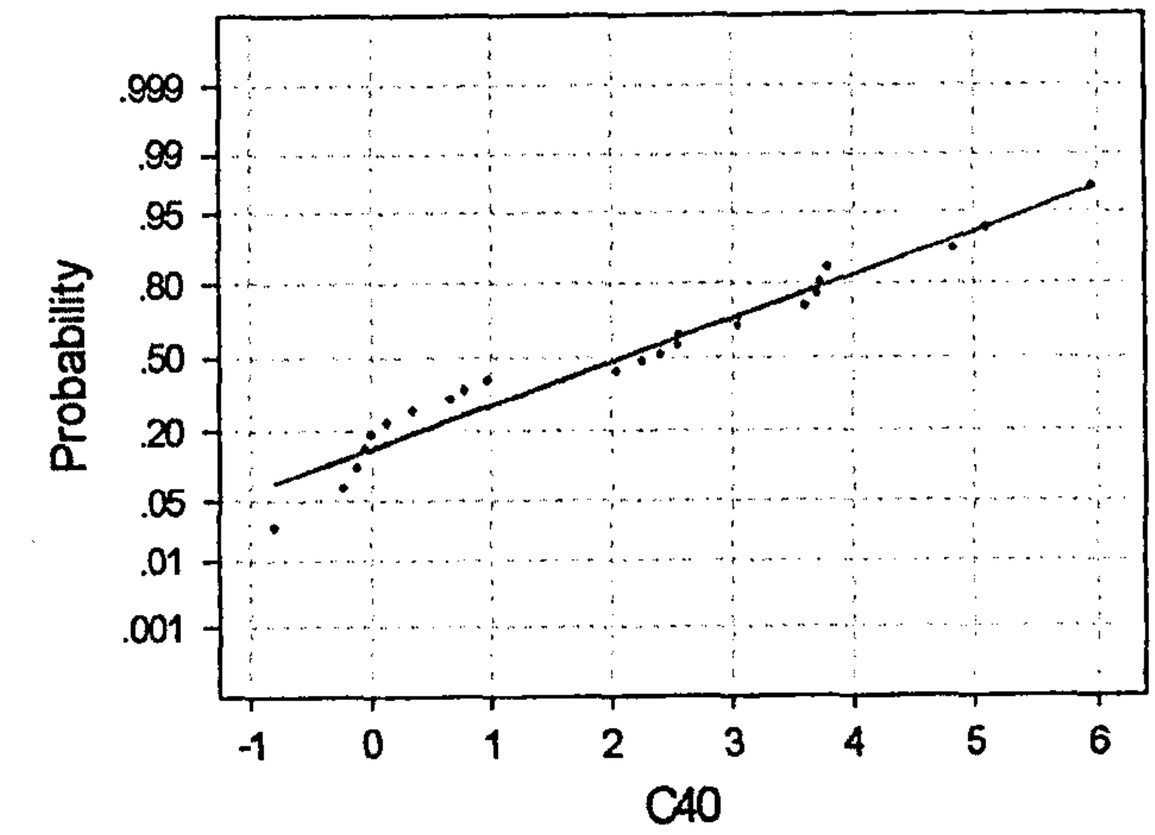

Fig 4.76 Normality Test for the population (paired difference between data for **intact capsule** and **transsected medial iliofemoral ligament**) used in the paired t-test

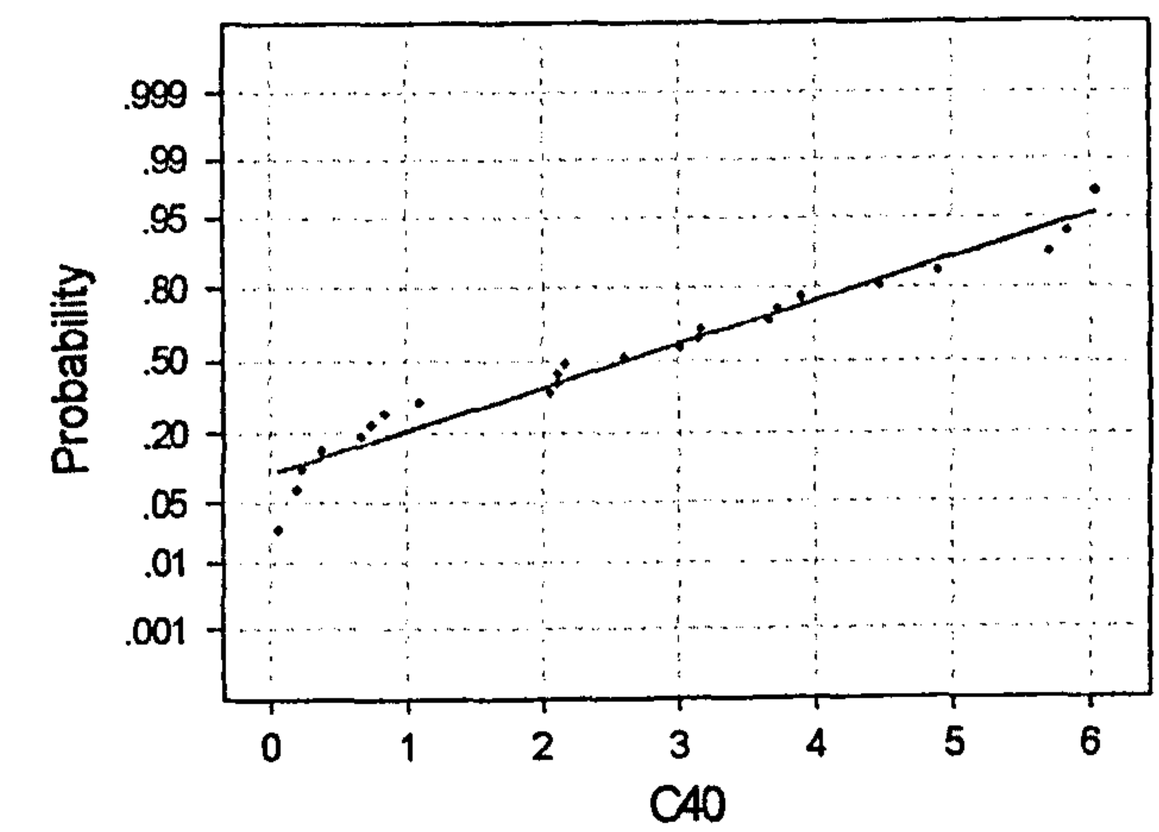

Fig 4.77 Normality Test for the population (paired difference between data for **intact capsule** and **transsected medial and lateral iliofemoral ligaments**) used in the paired t-test

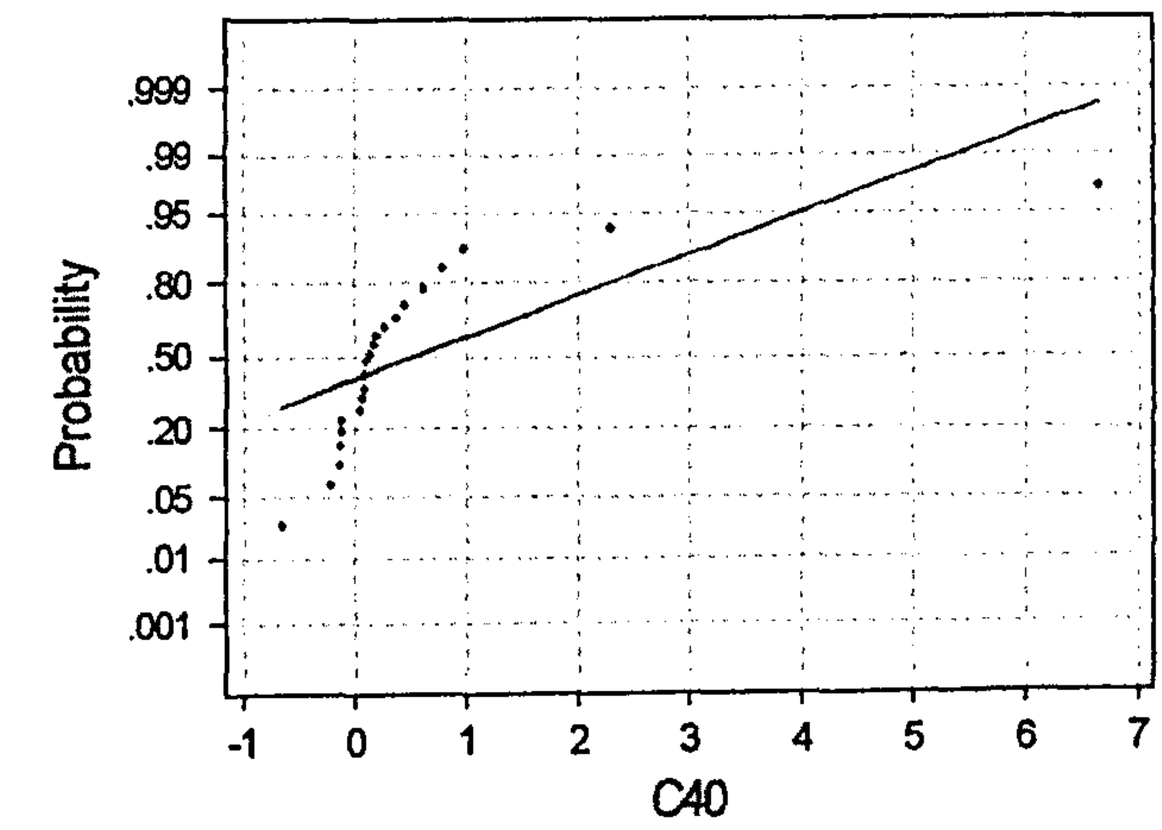

Fig 4.78 Normality Test for the population (paired difference between data for **transsected medial iliofemoral** and **transsected medial and lateral iliofemoral ligaments**) used in the paired t-test

IVa Stiffness Rates and Specimen at Risk for Posterior Dislocation

The following graphs show the moments and the stiffness rates as discussed in chapter 4 of the text. The stiffness rate functions have been calculated for values on the curve that were between ±0.3Nm and ±3Nm.

Neutral Position

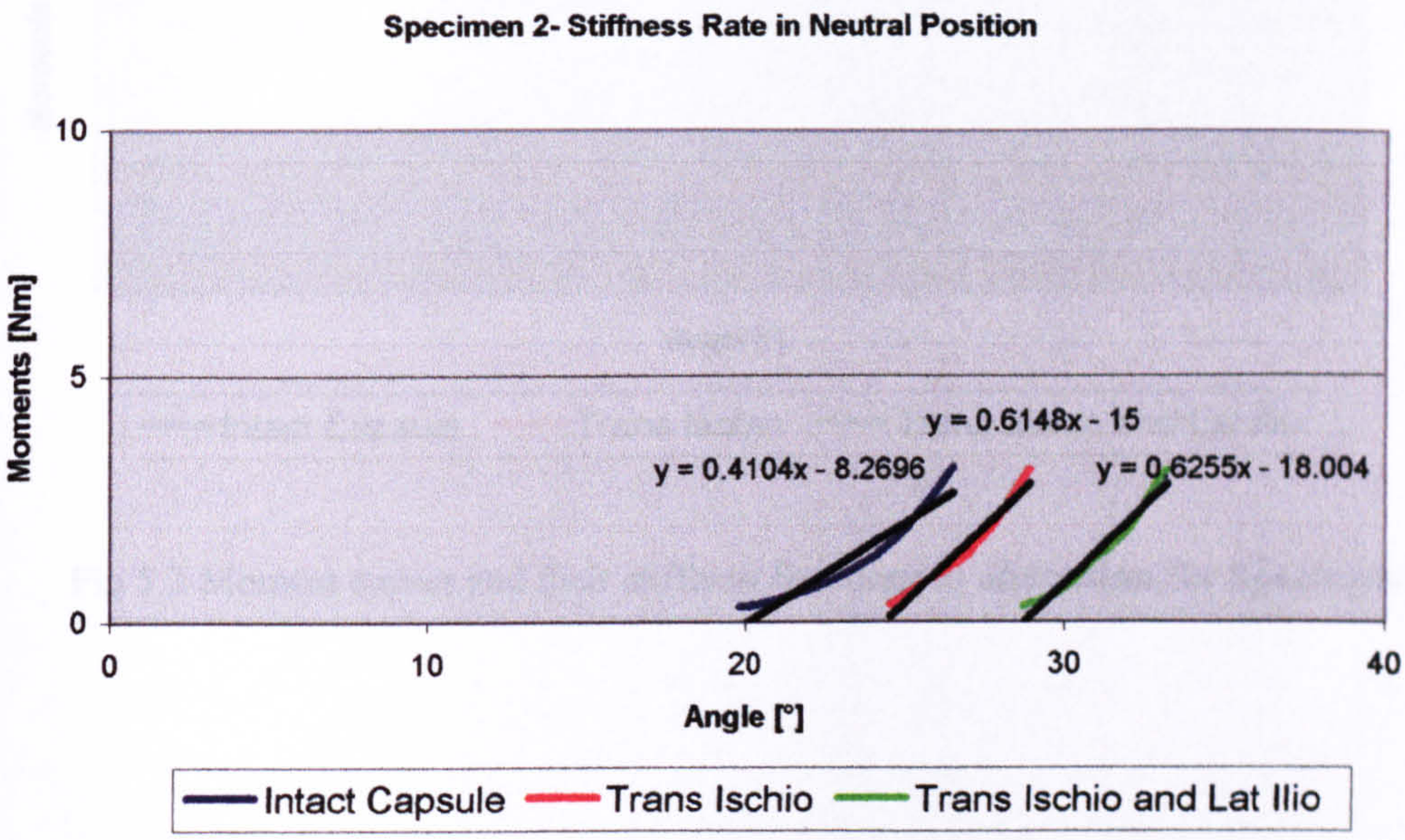

Fig 5.1 Moment curves and their stiffness functions in **abduction** for **Specimen 2**.

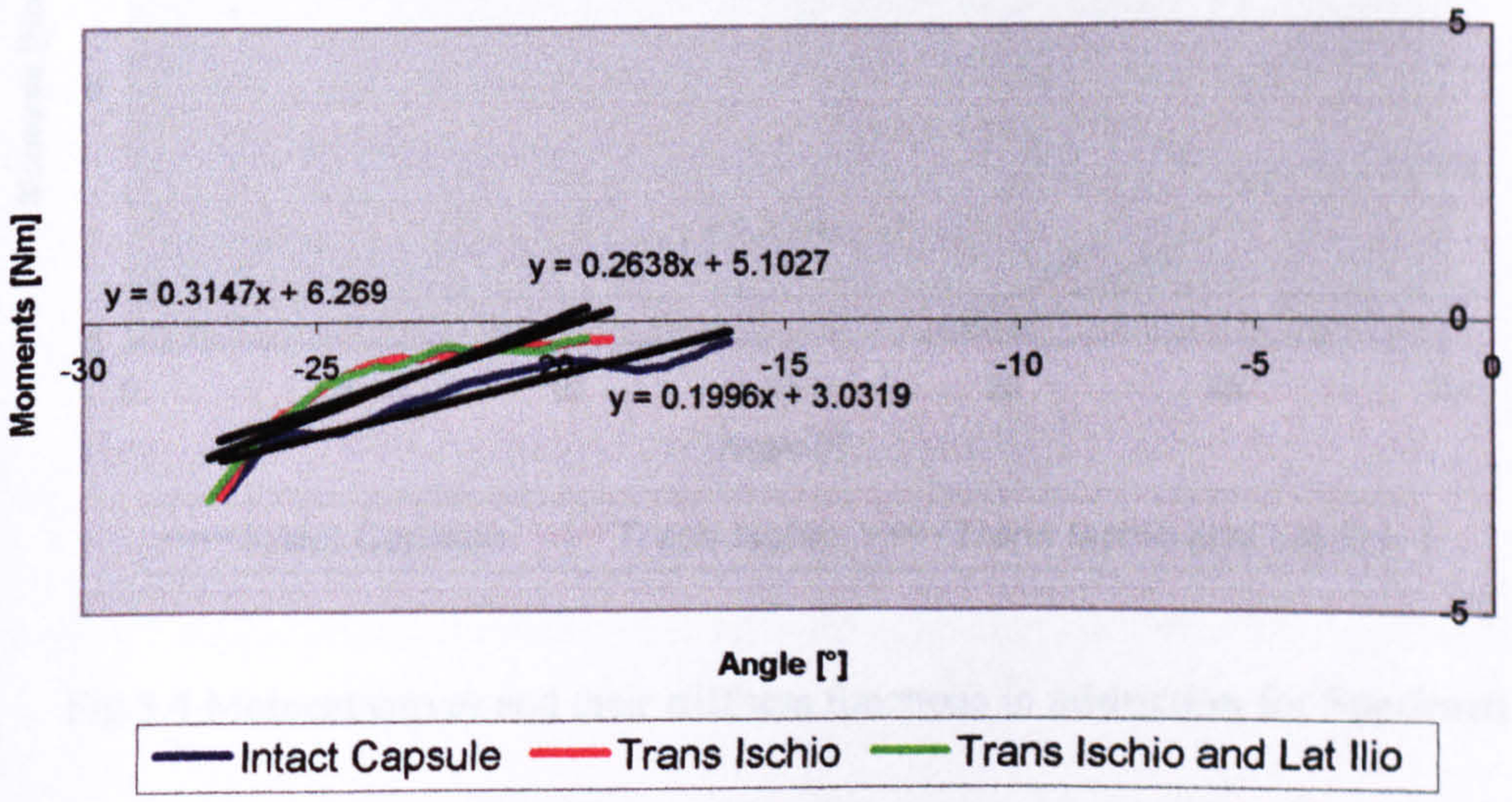

Fig 5.2 Moment curves and their stiffness functions in **adduction** for **Specimen 2**.

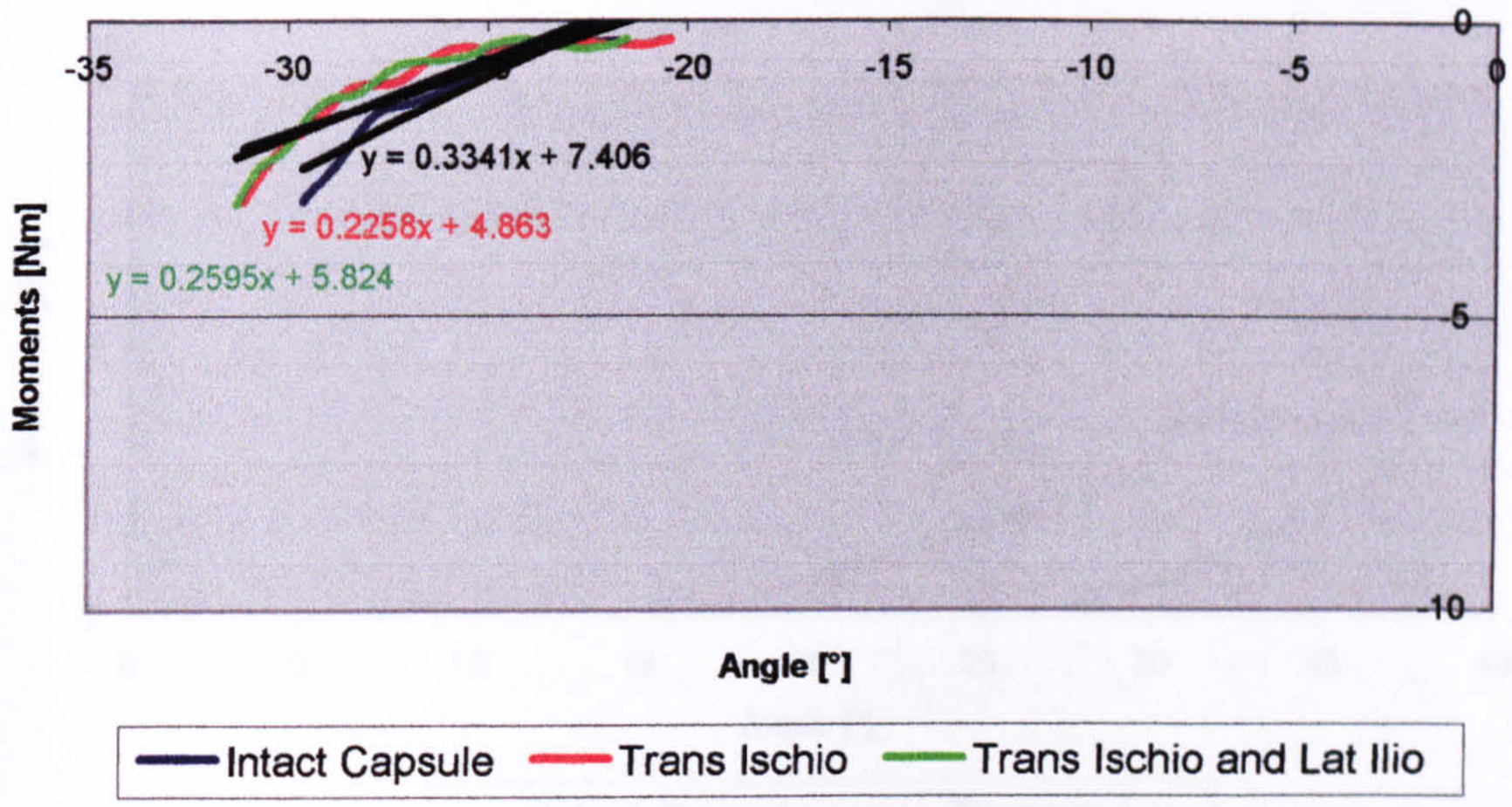

Fig 5.3 Moment curves and their stiffness functions in **abduction** for **Specimen 3**.

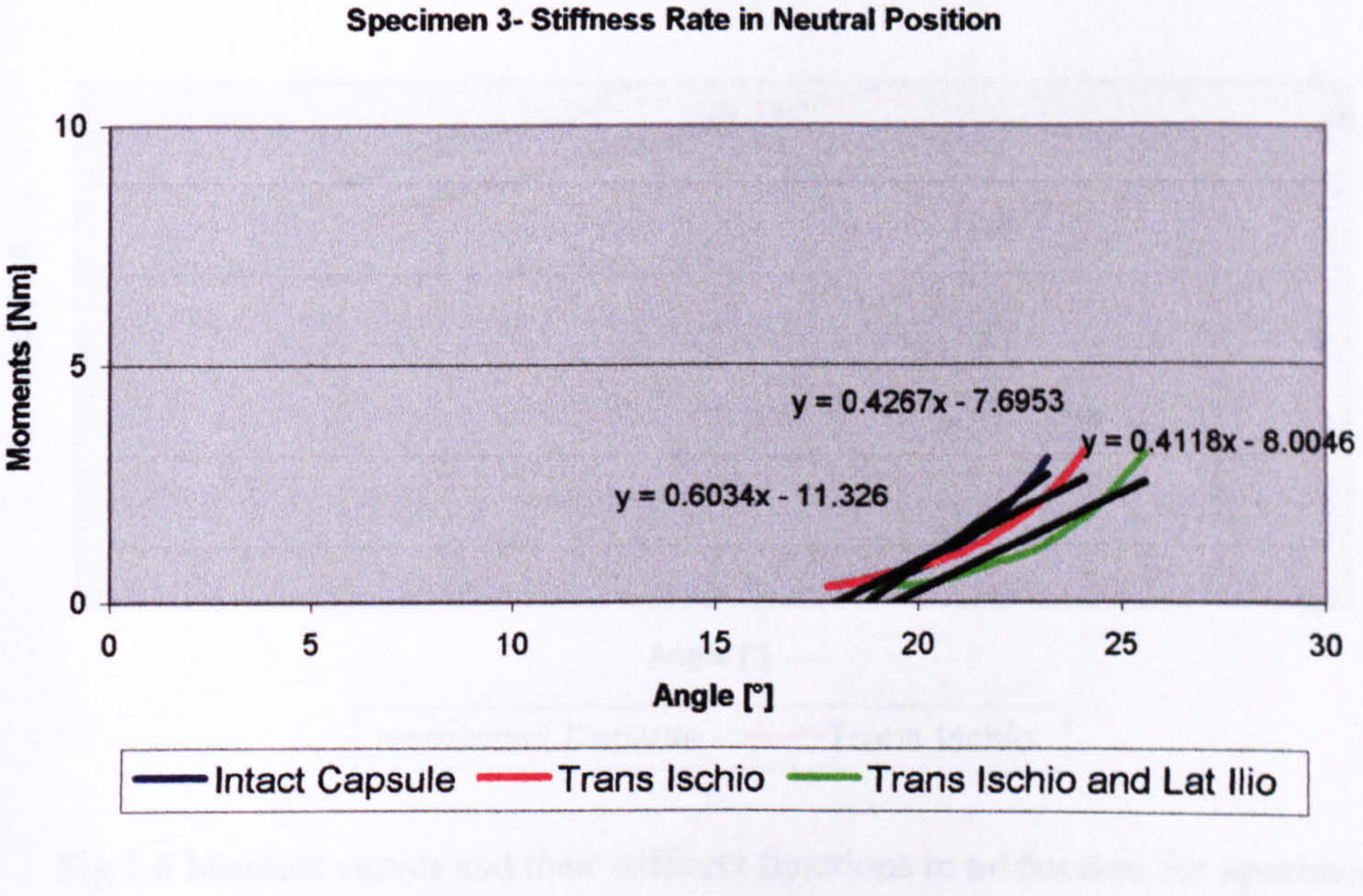

Fig 5.4 Moment curves and their stiffness functions in **adduction** for **Specimen 3**.

Full Flexion

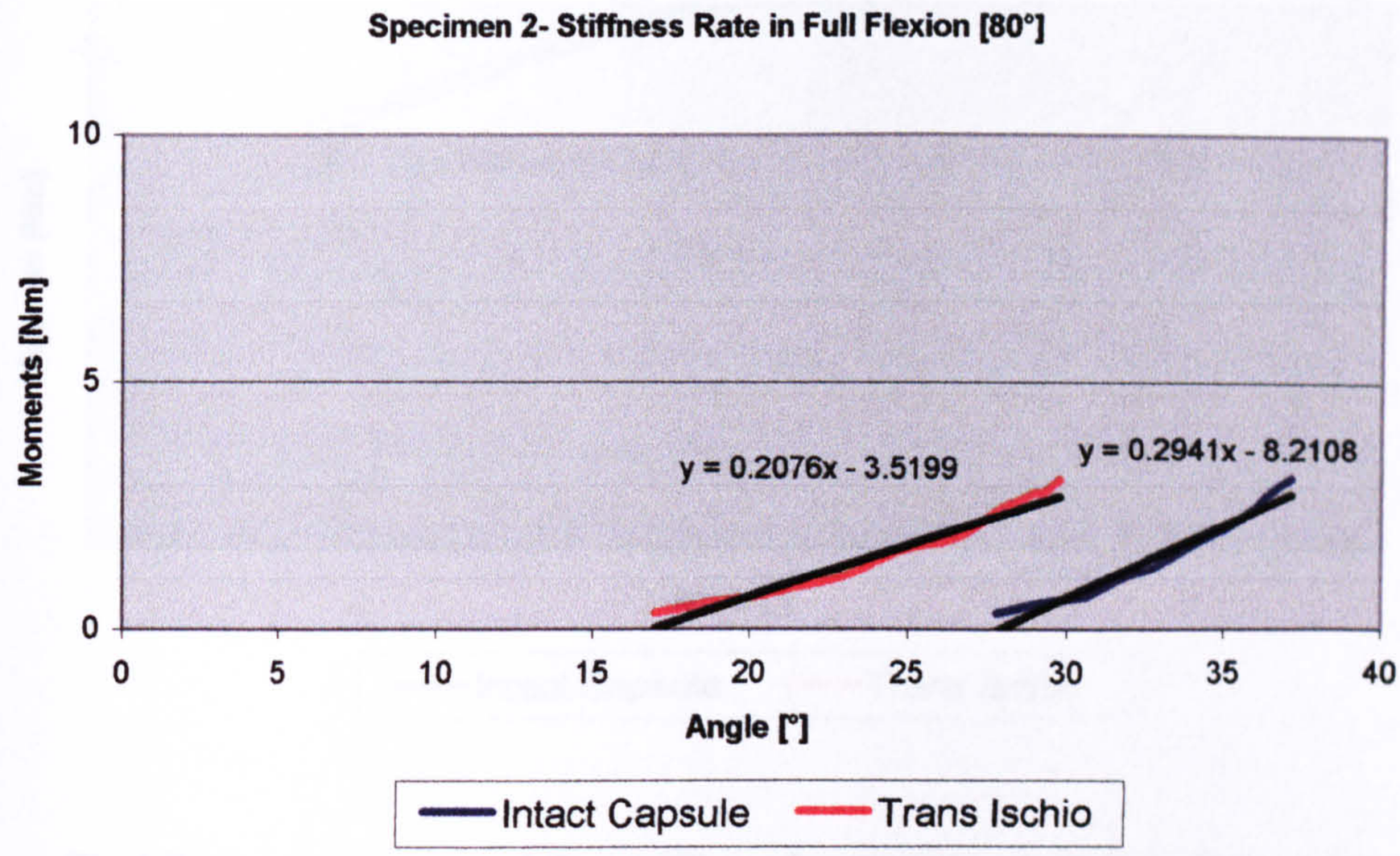

Fig 5.5 Moment curves and their stiffness functions in **abduction** for **specimen 2**.

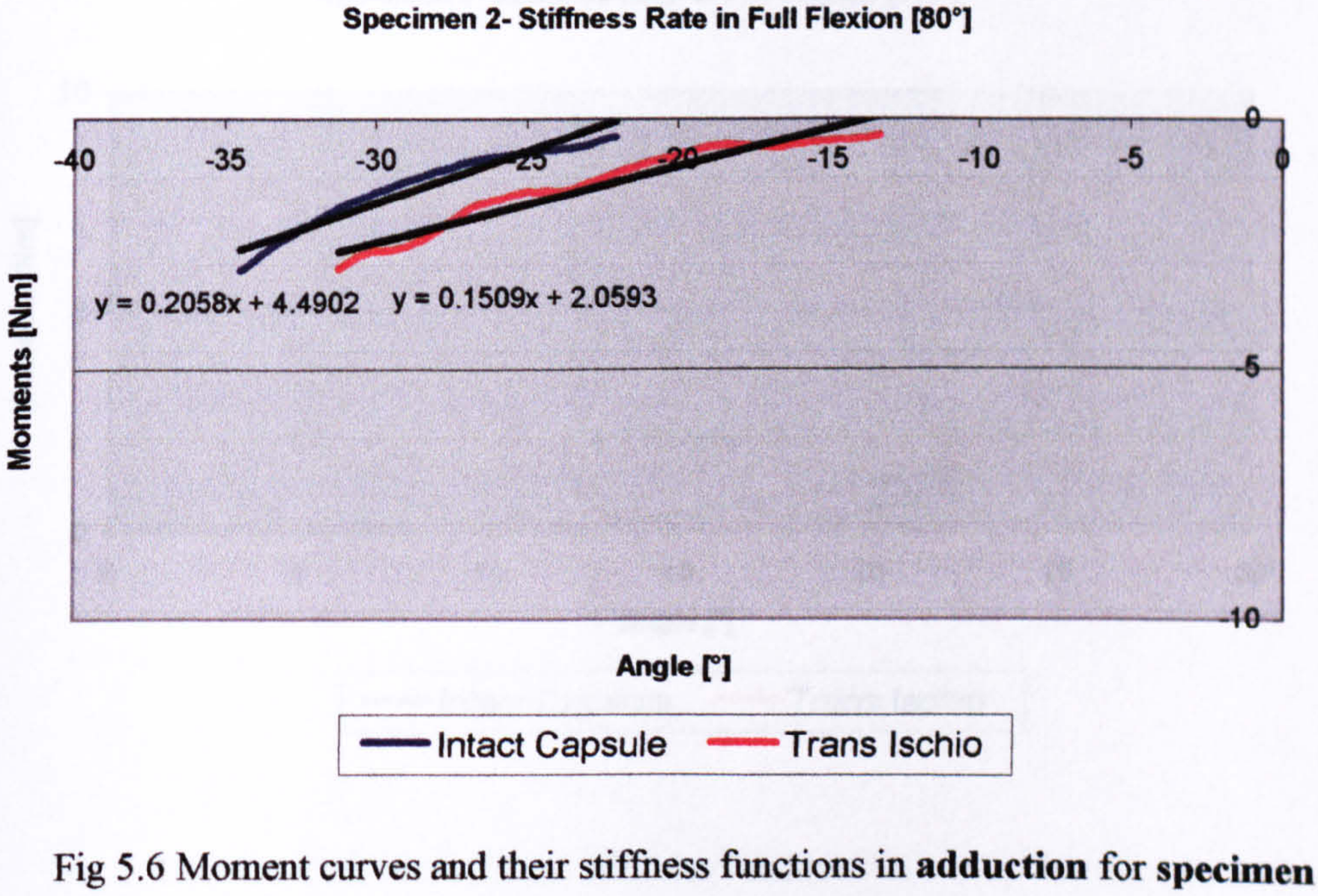

Fig 5.6 Moment curves and their stiffness functions in **adduction** for **specimen 2**.

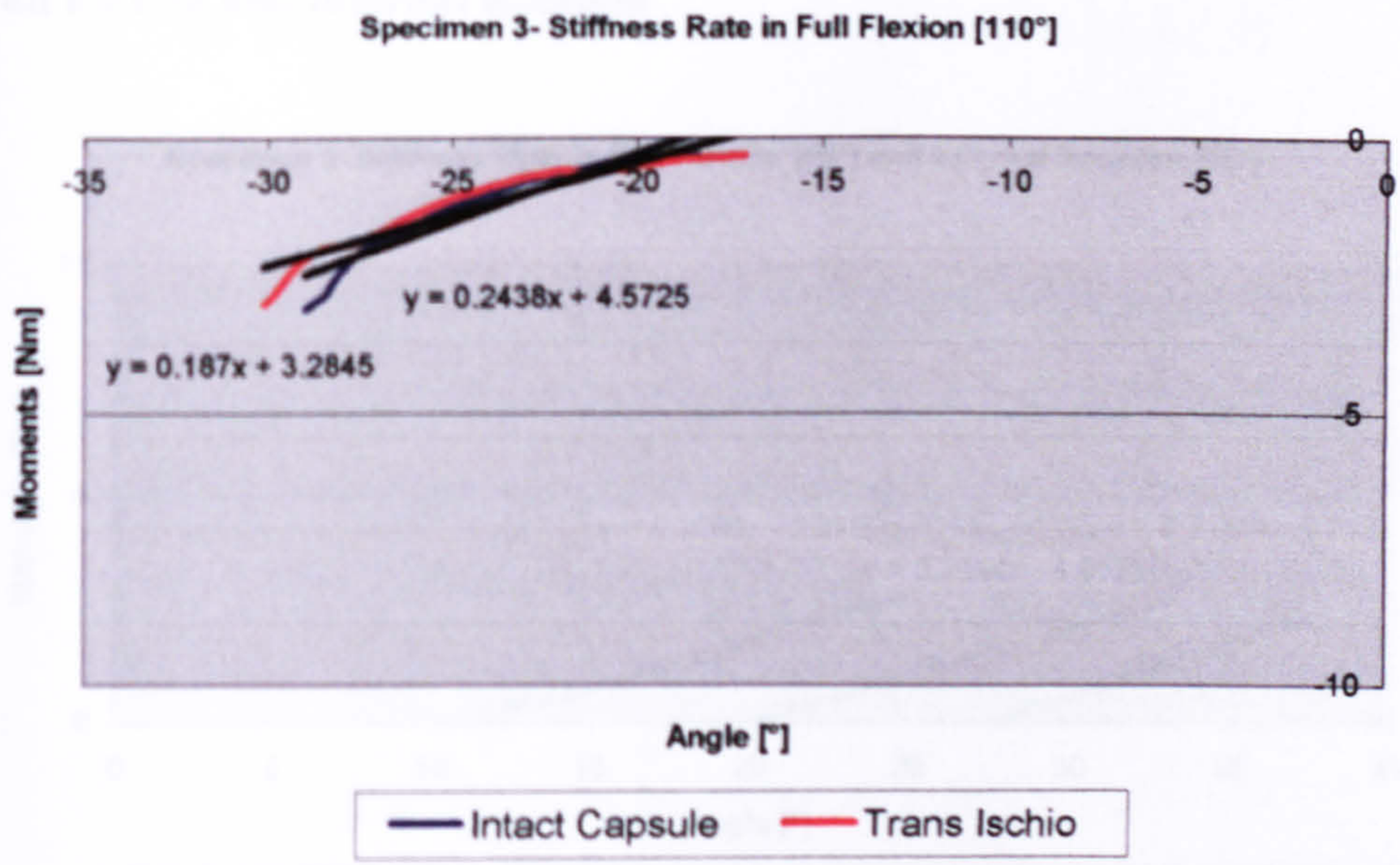

Fig 5.7 Moment curves and their stiffness functions in **abduction** for **specimen 3**.

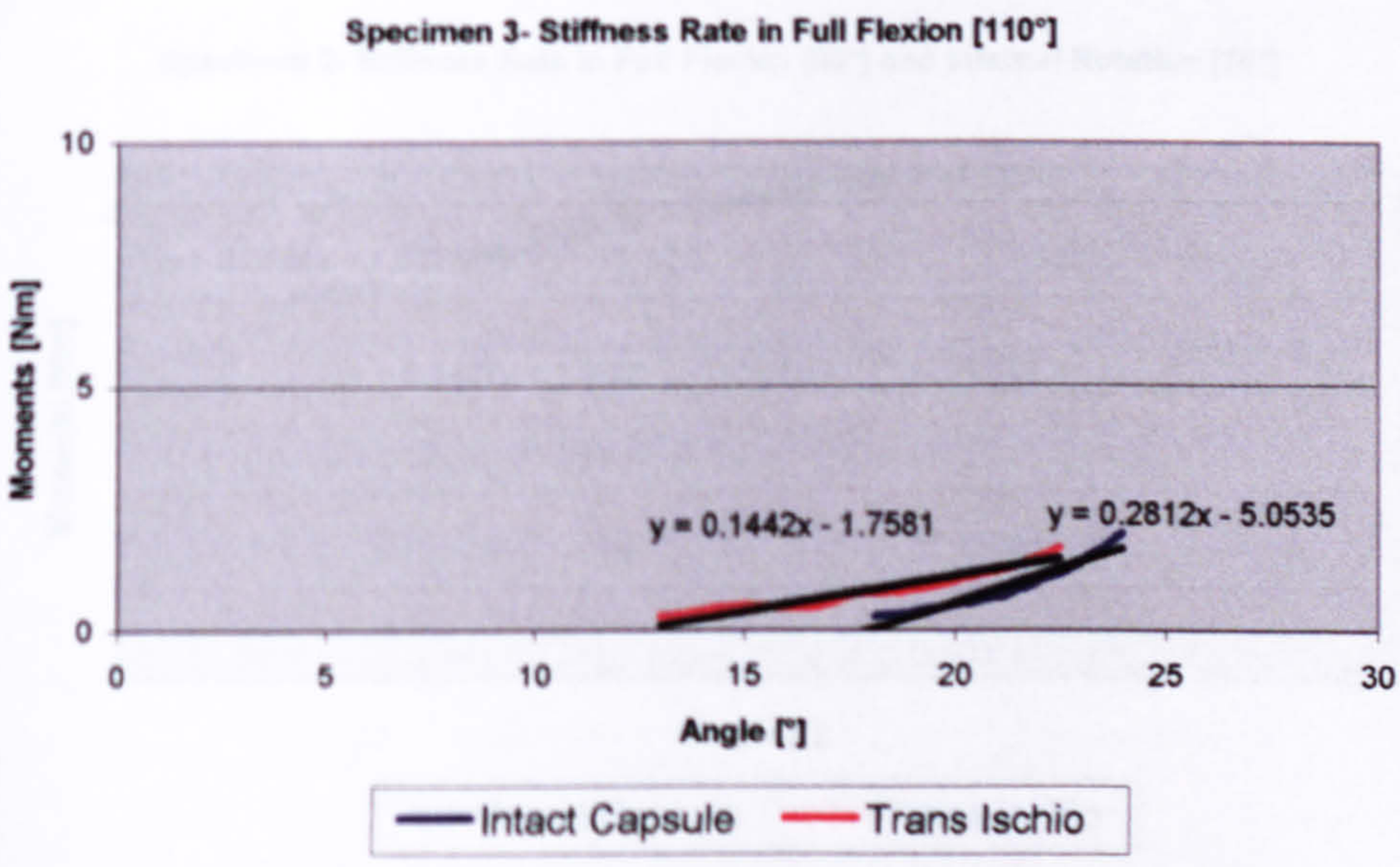

Fig 5.8 Moment curves and their stiffness functions in **adduction** for **specimen 3**.

Full Flexion and Internal Rotation

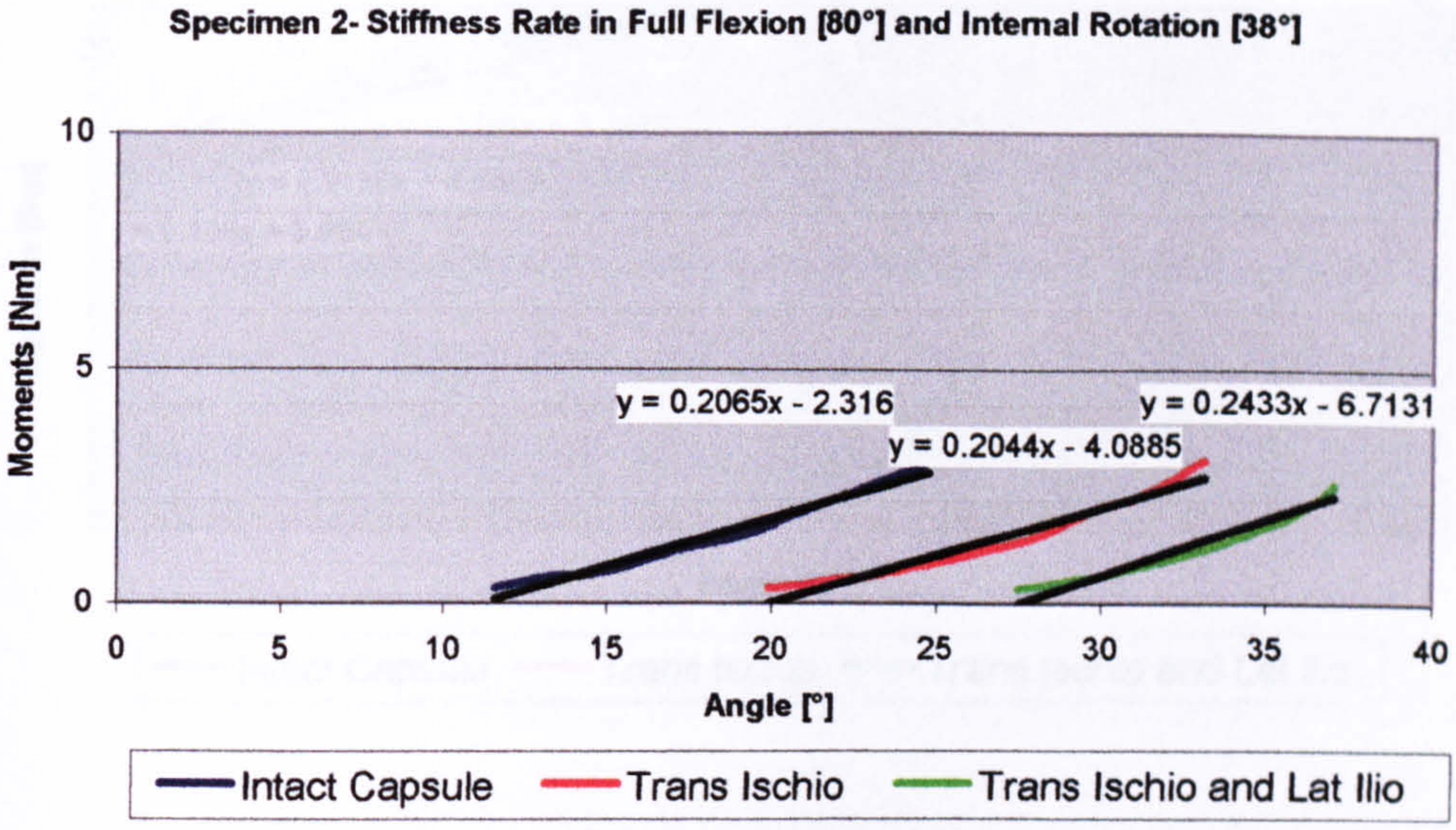

Fig 5.9 Moment curves and their stiffness functions in **abduction** for **specimen 2**.

Specimen 2- Stiffness Rate in Full Flexion [80°] and Internal Rotation [38°]

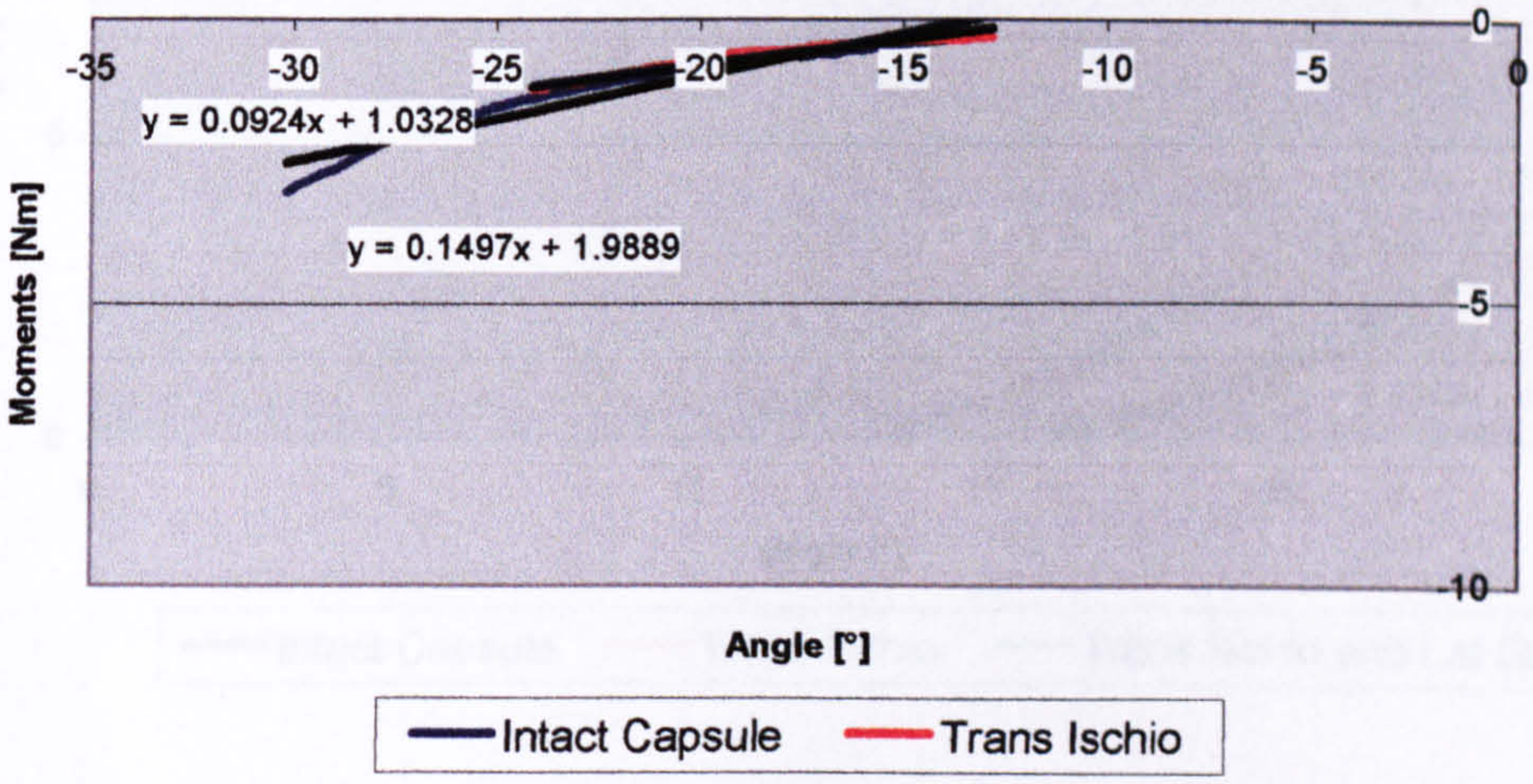

Fig 5.10 Moment curves and their stiffness functions in **adduction** for **specimen 2**.

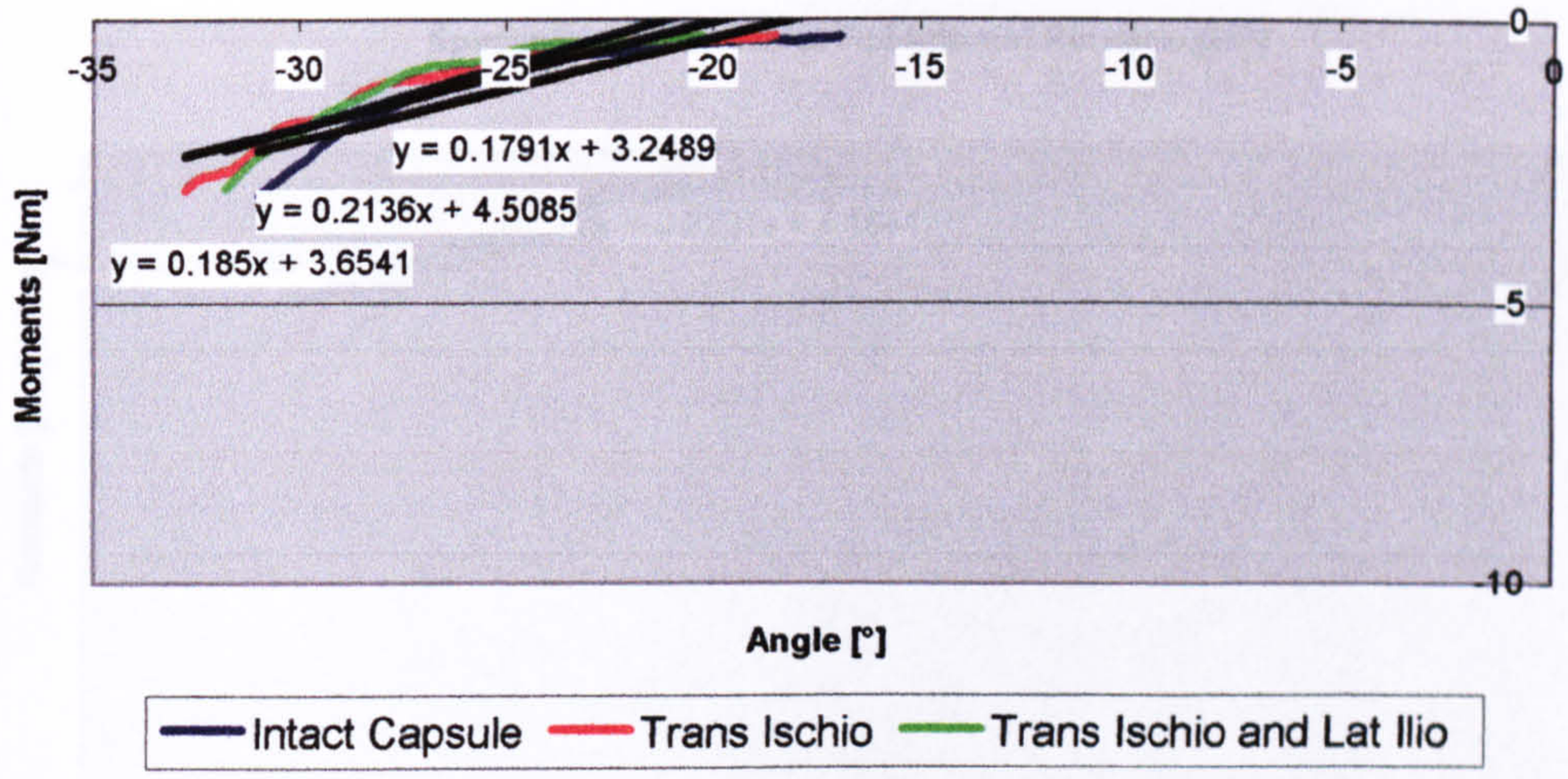

Fig 5.11 Moment curves and their stiffness functions in **abduction** for **specimen 3**.

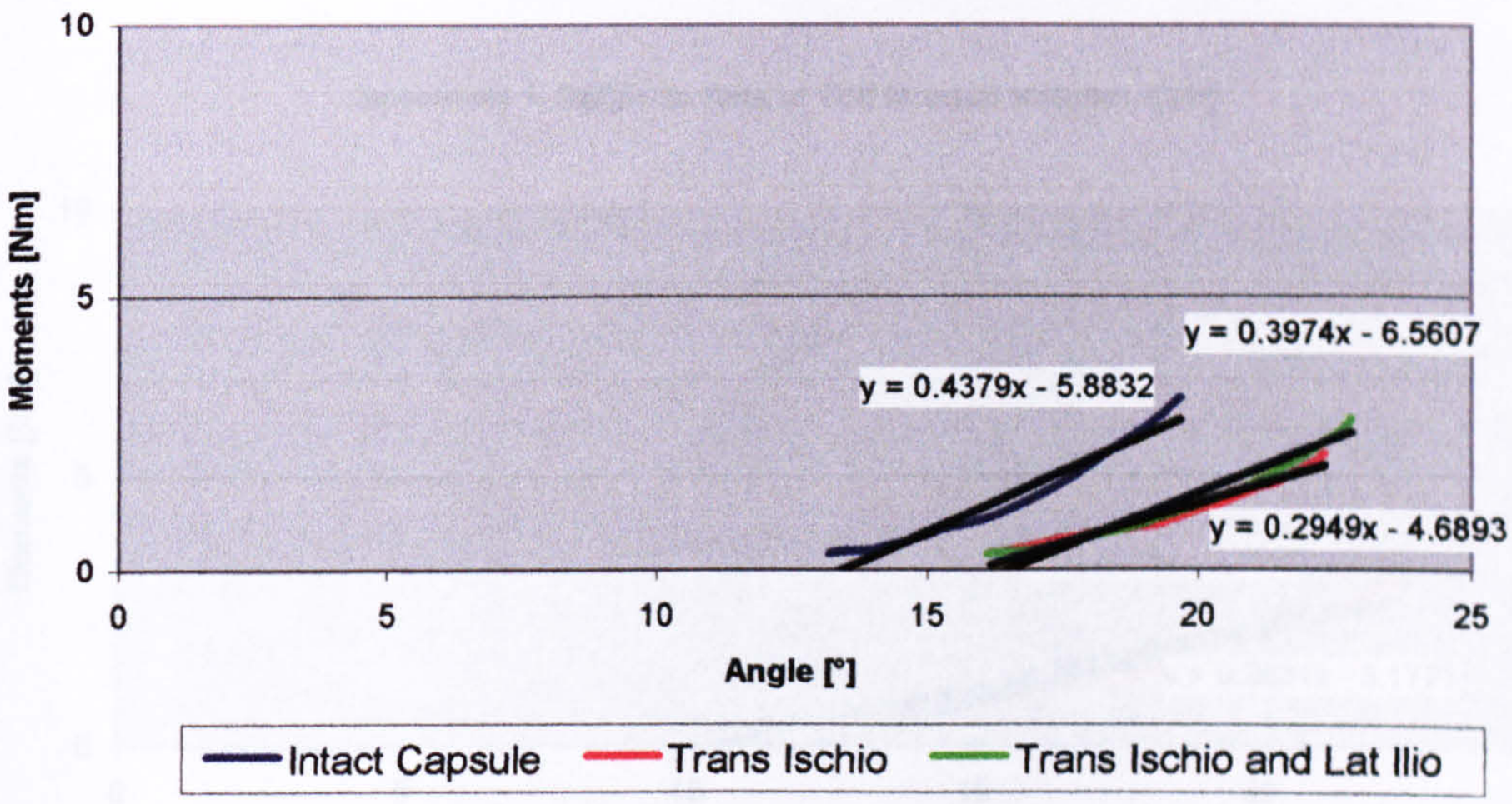

Fig 5.12 Moment curves and their stiffness functions in **adduction** for **specimen 3**.

Full Internal Rotation

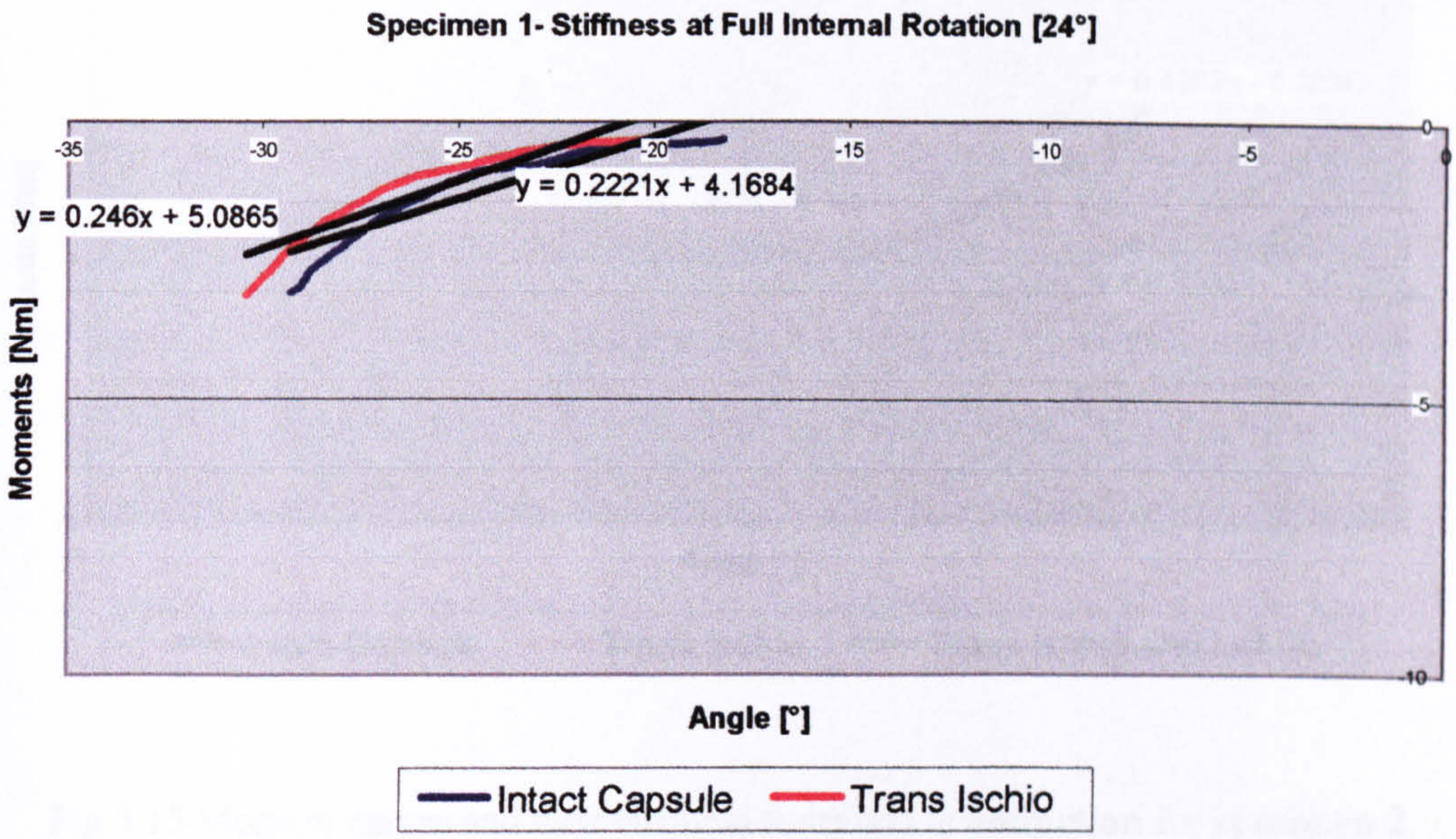

Fig 5.13 Moment curves and their stiffness functions in **abduction** for **specimen 1**.

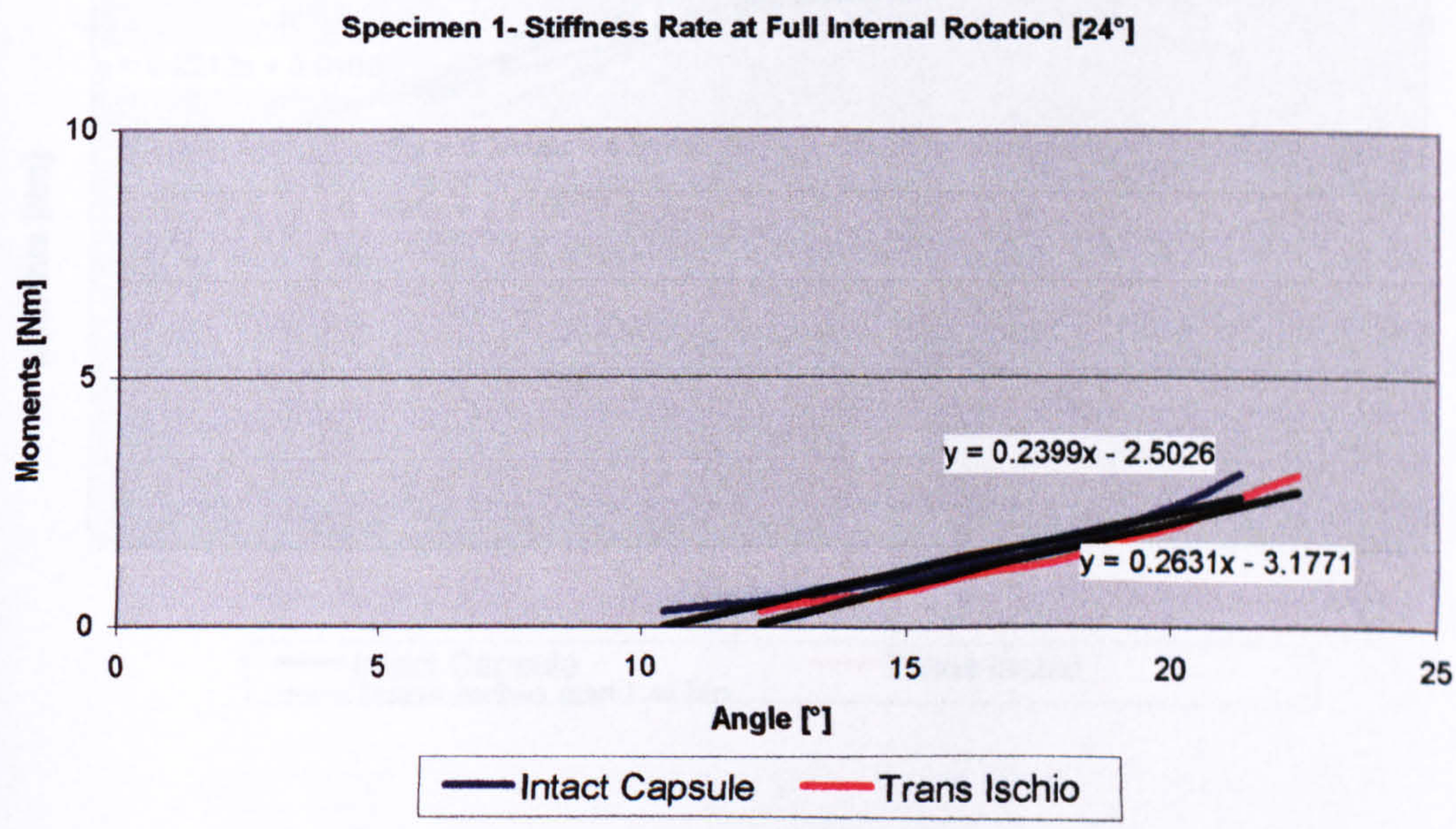

Fig 5.14 Moment curves and their stiffness functions in **adduction** for **specimen 1**.

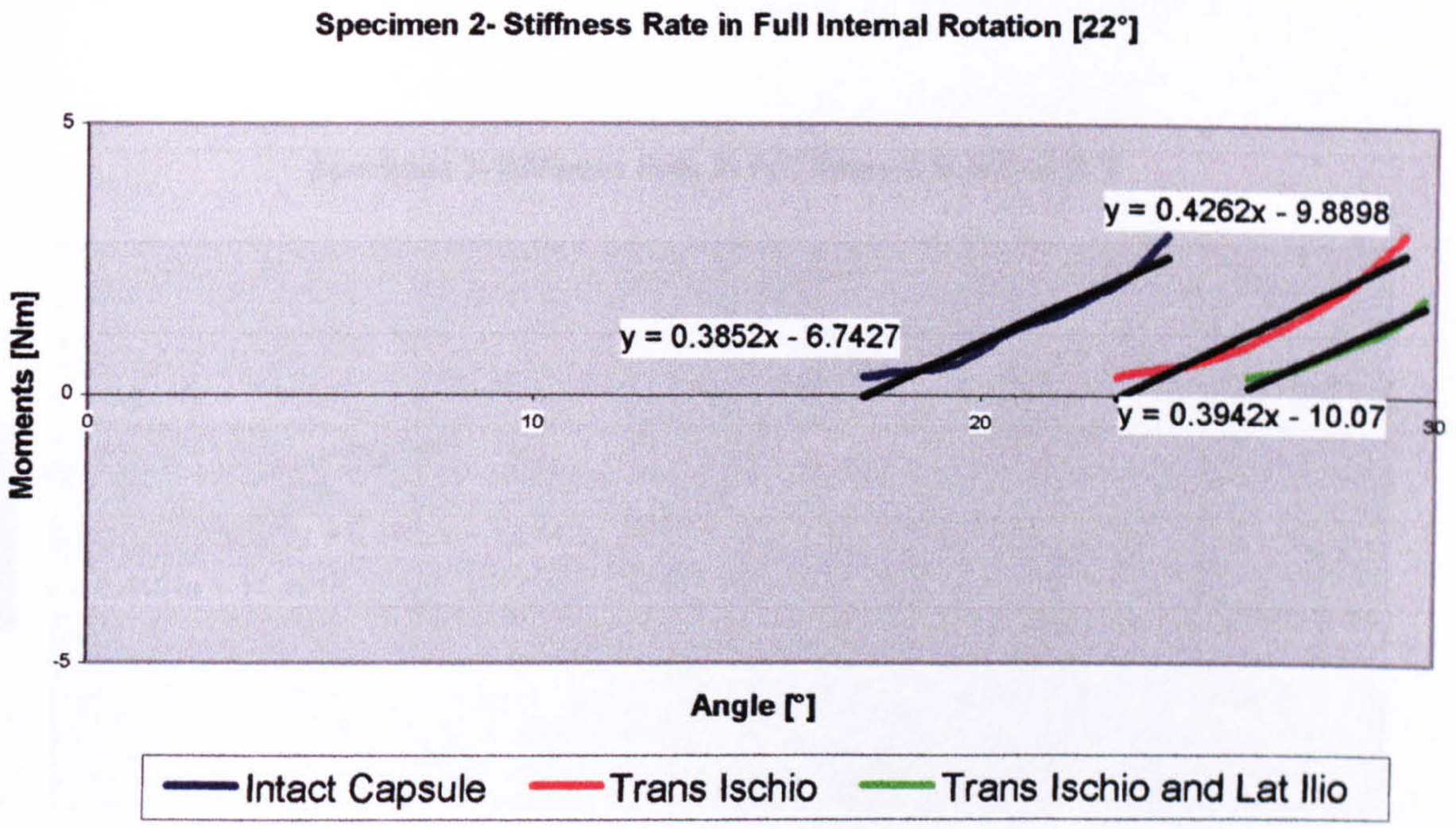

Fig 5.15 Moment curves and their stiffness functions in **abduction** for **specimen 2**.

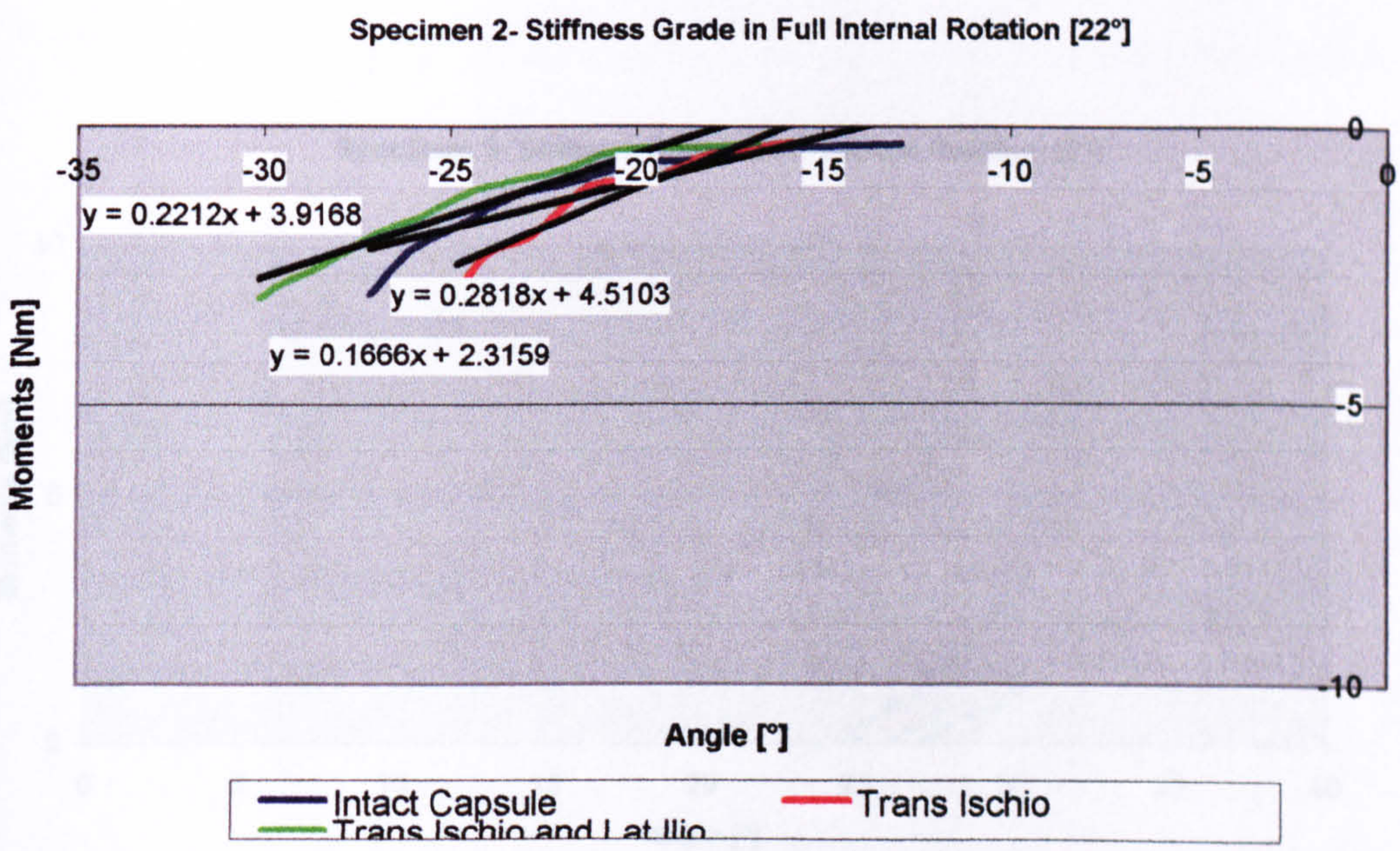

Fig 5.16 Moment curves and their stiffness functions in **adduction** for **specimen 2**.

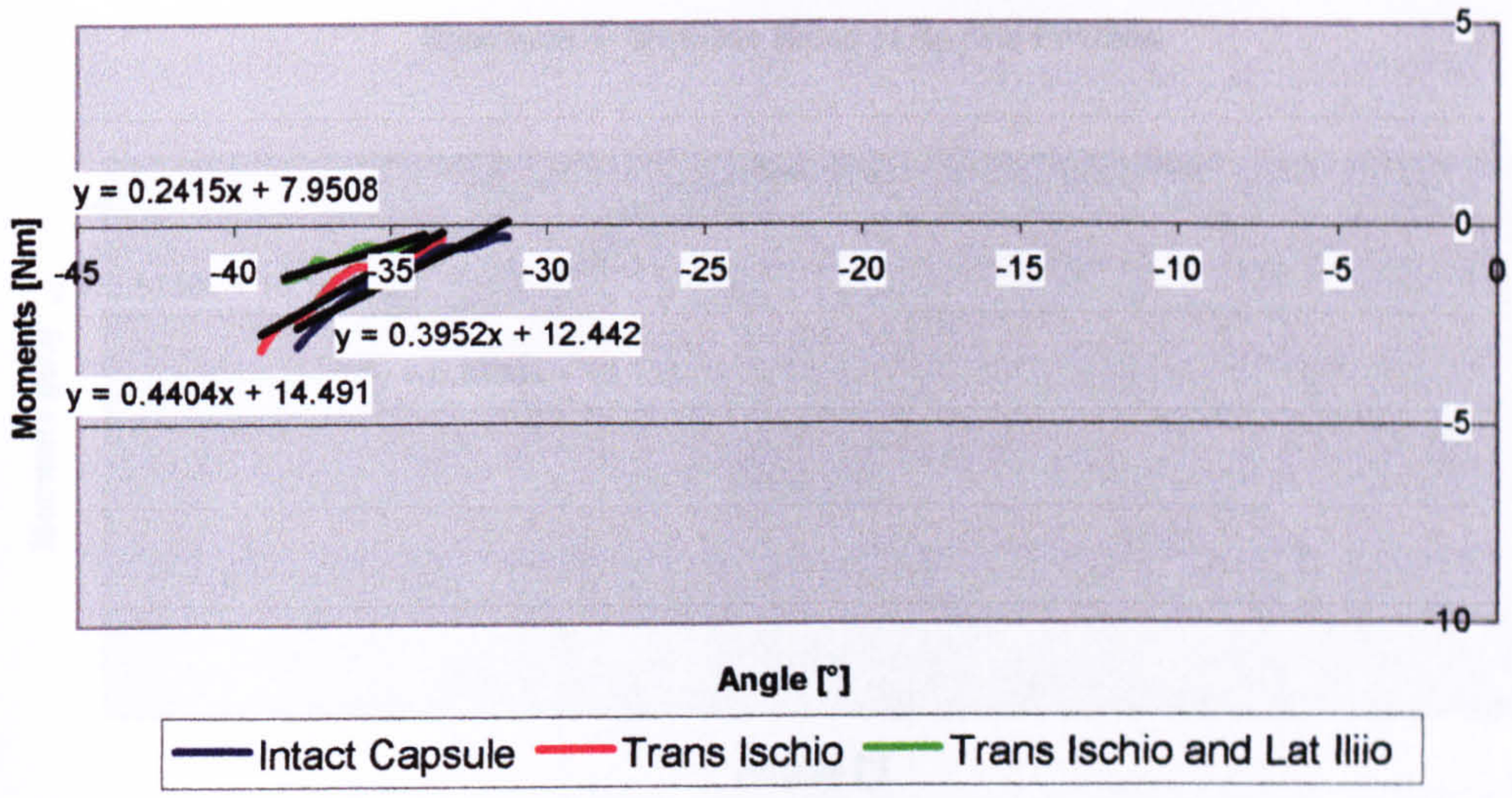

Fig 5.17 Moment curves and their stiffness functions in **abduction** for **specimen 3**.

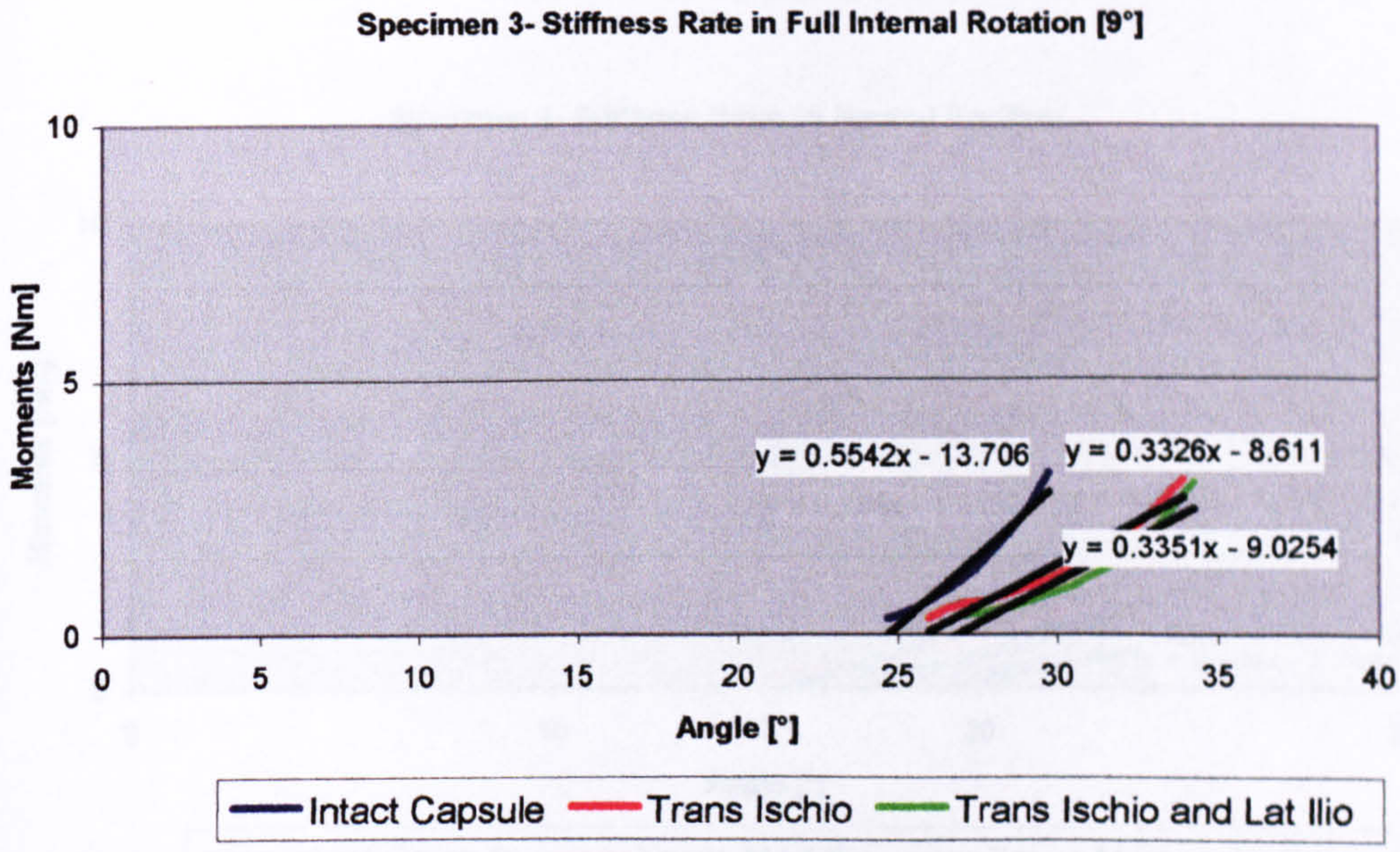

Fig 5.18 Moment curves and their stiffness functions in **adduction** for **specimen 3**.

IVb Stiffness Rates and Specimen at Risk for Anterior Dislocation

Neutral Position

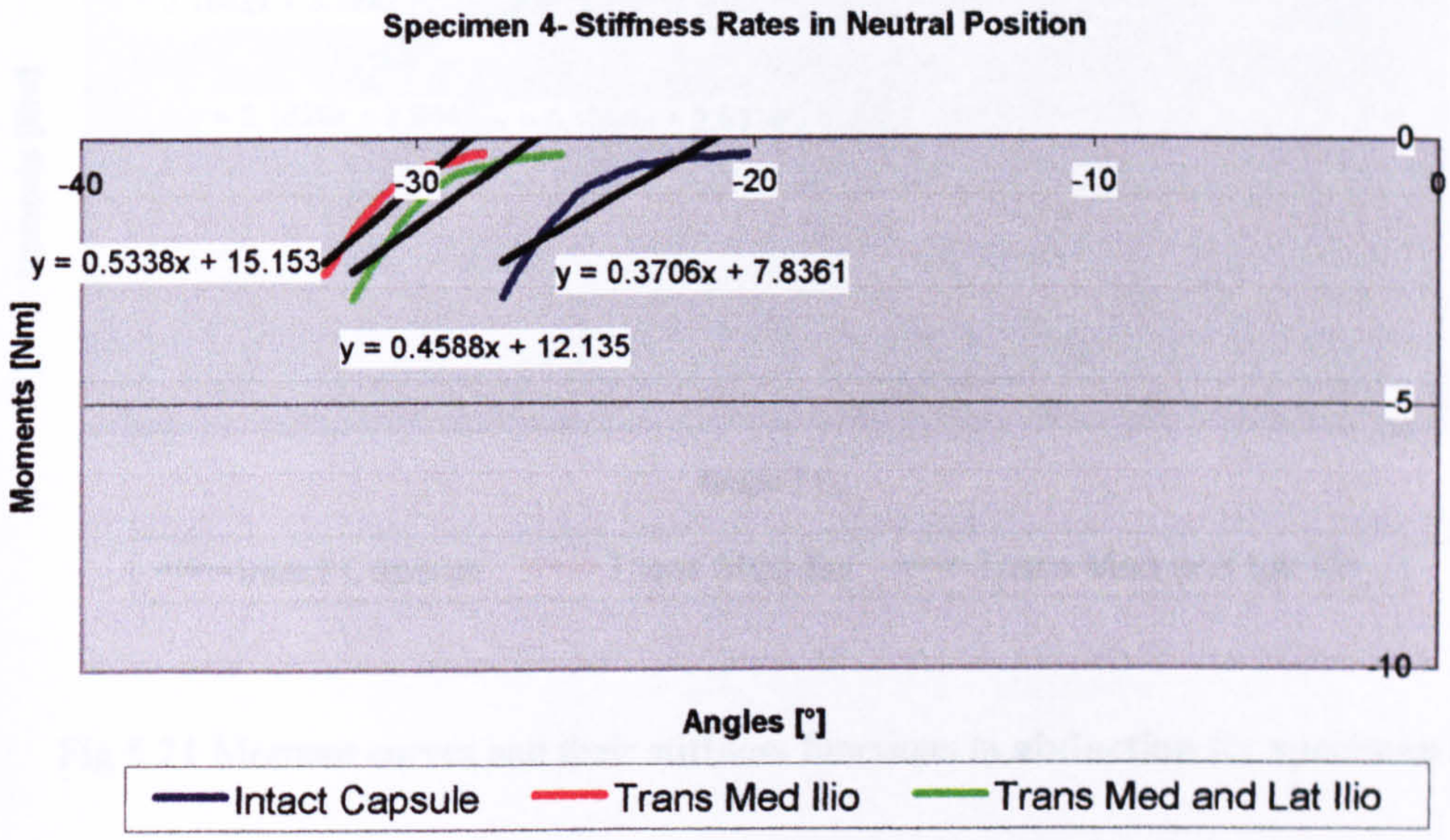

Fig 5.19 Moment curves and their stiffness functions in **abduction** for **specimen 4**.

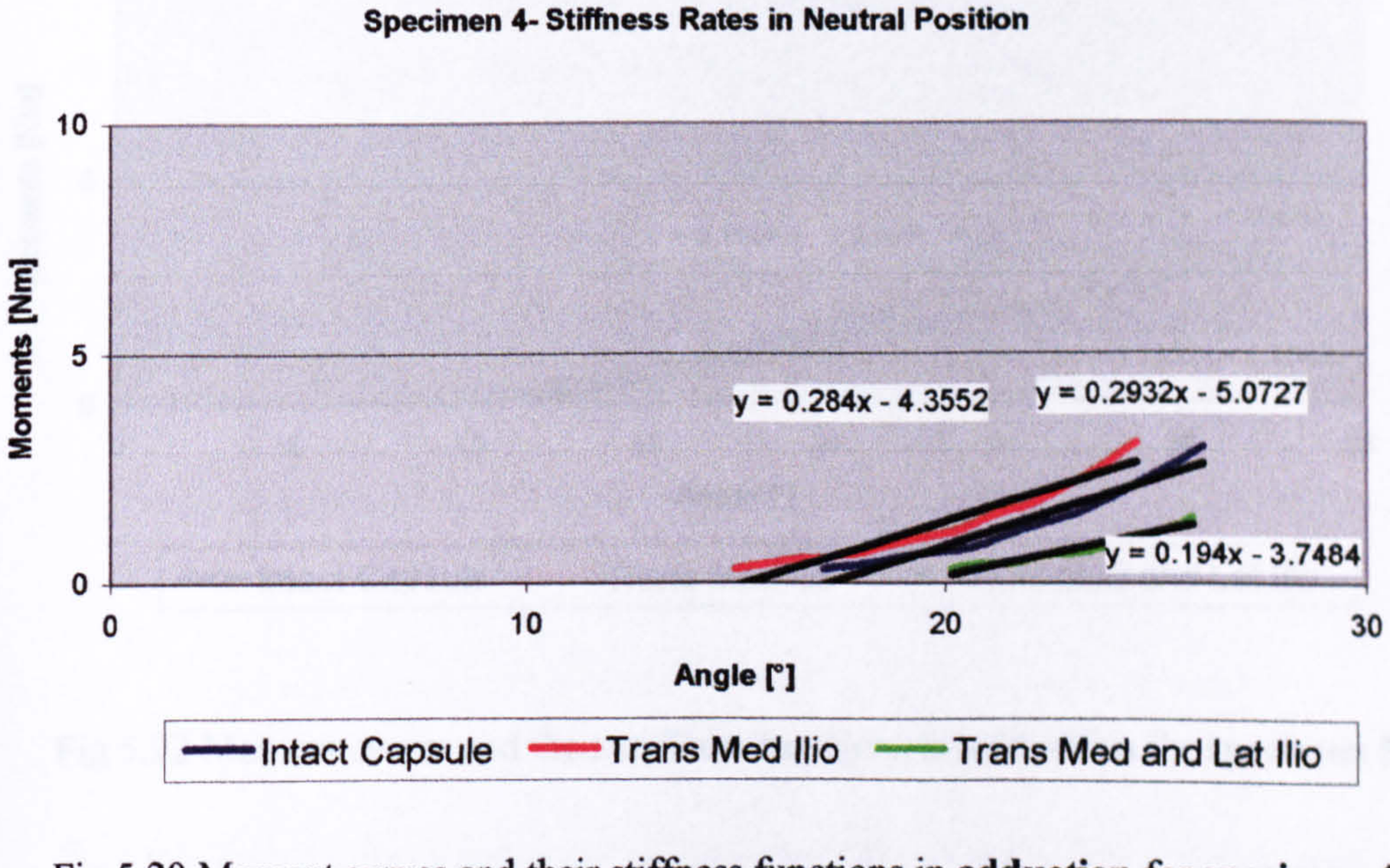

Fig 5.20 Moment curves and their stiffness functions in **adduction** for **specimen 4**.

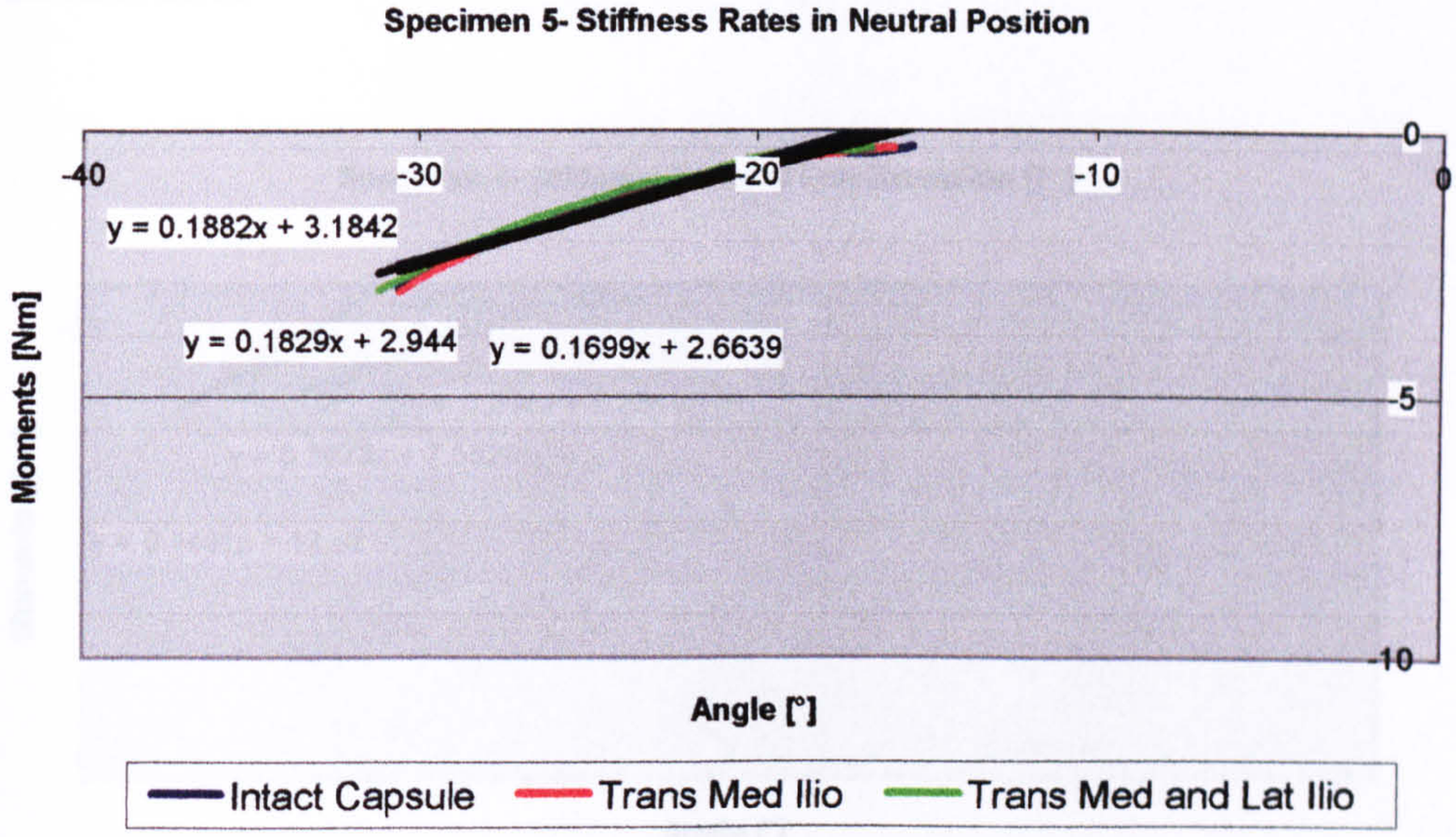

Fig 5.21 Moment curves and their stiffness functions in **abduction** for **specimen 5**.

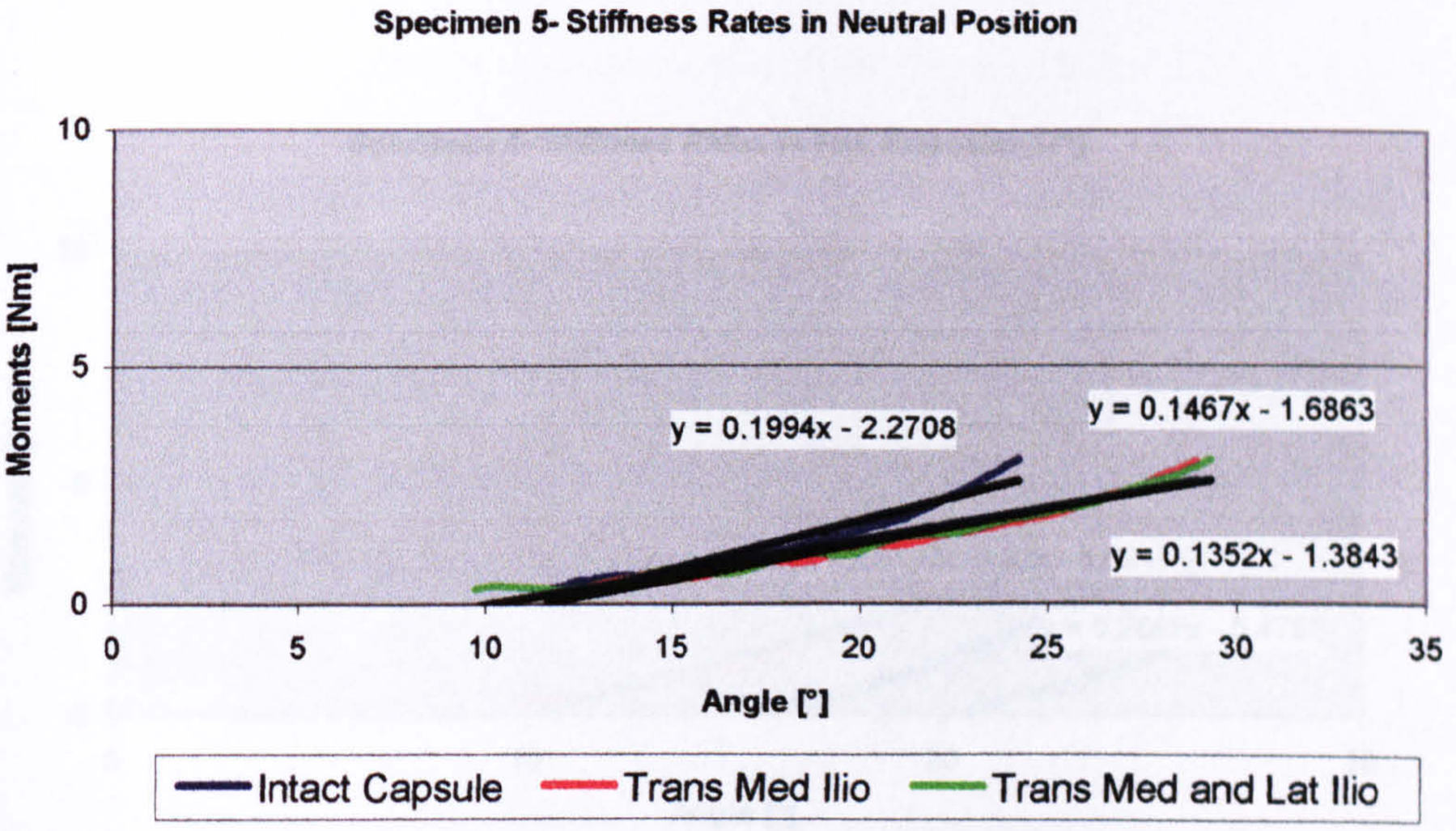

Fig 5.22 Moment curves and their stiffness functions in **adduction** for **specimen 5**.

Full Extension

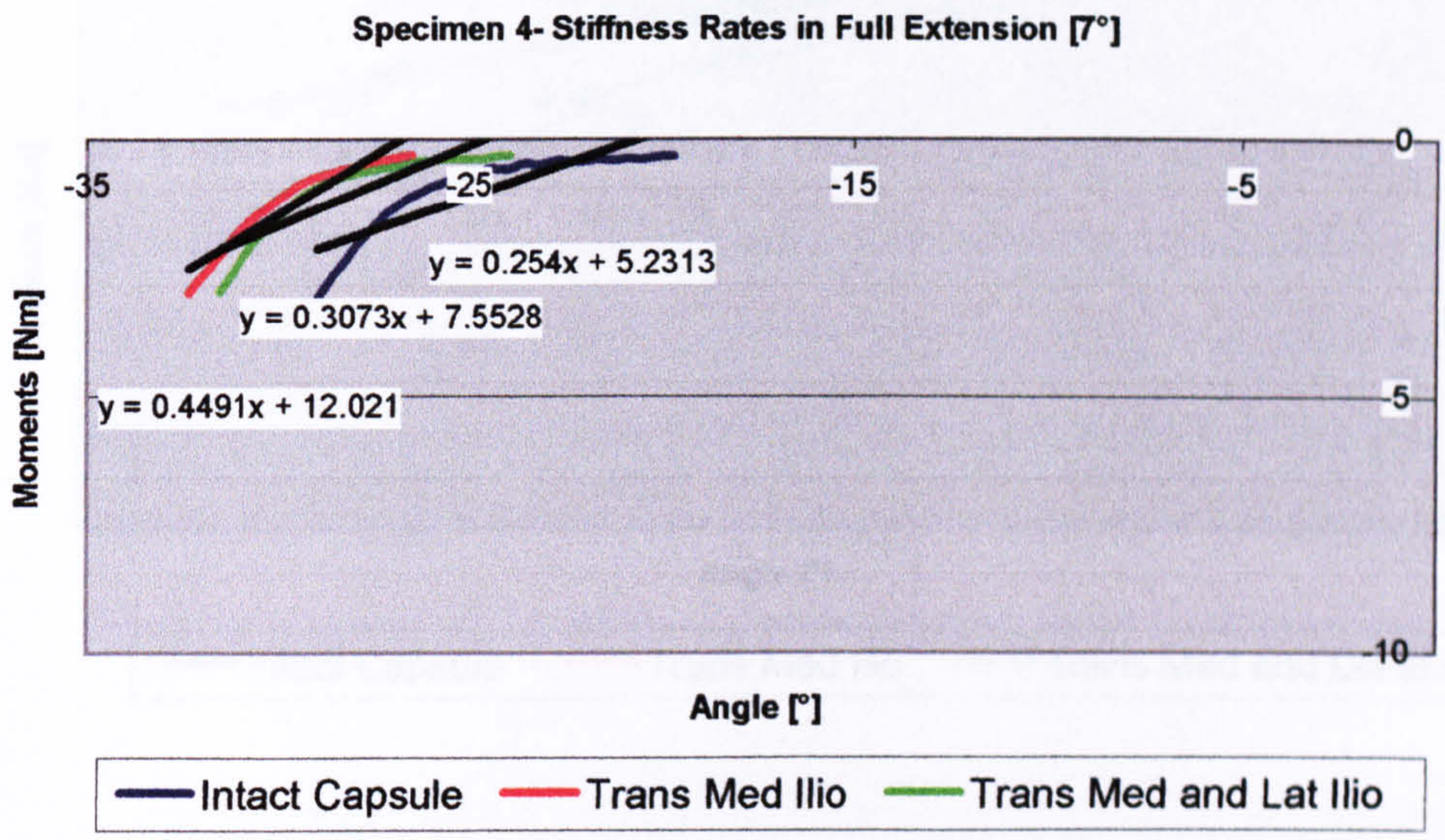

Fig 5.23 Moment curves and their stiffness functions in **abduction** for **specimen 4**.

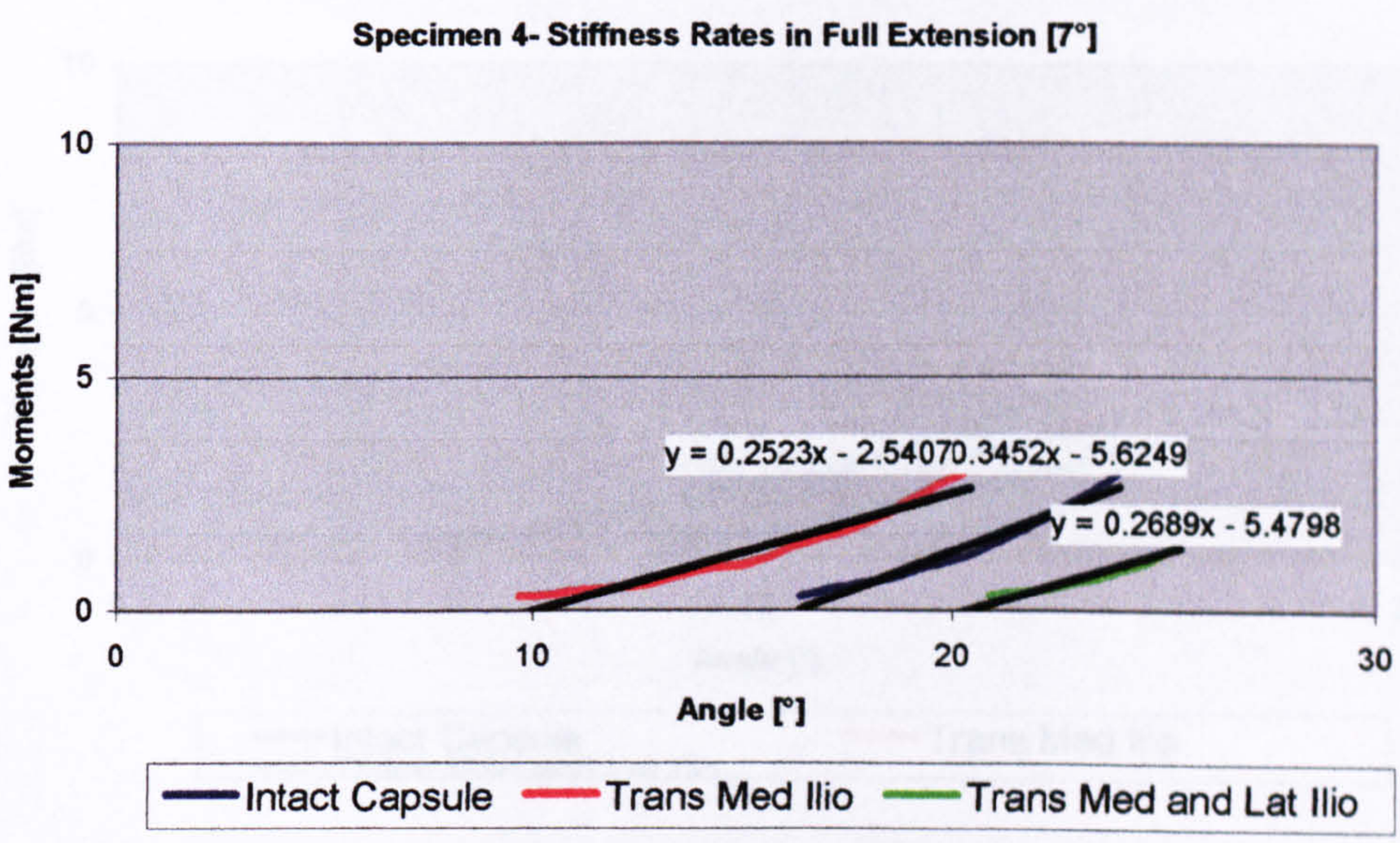

Fig 5.24 Moment curves and their stiffness functions in **adduction** for **specimen 4**.

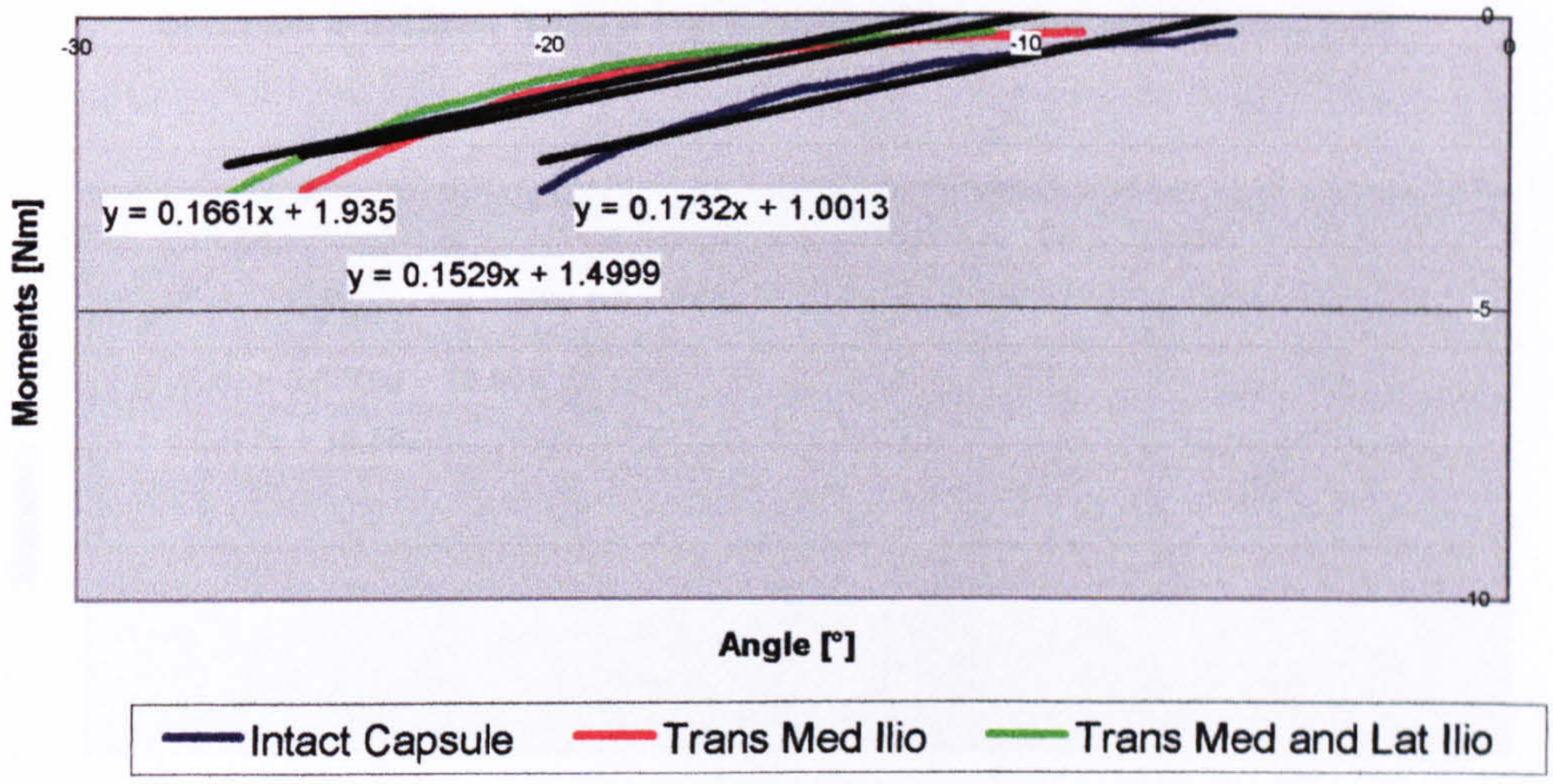

Fig 5.25 Moment curves and their stiffness functions in **abduction** for **specimen 5**.

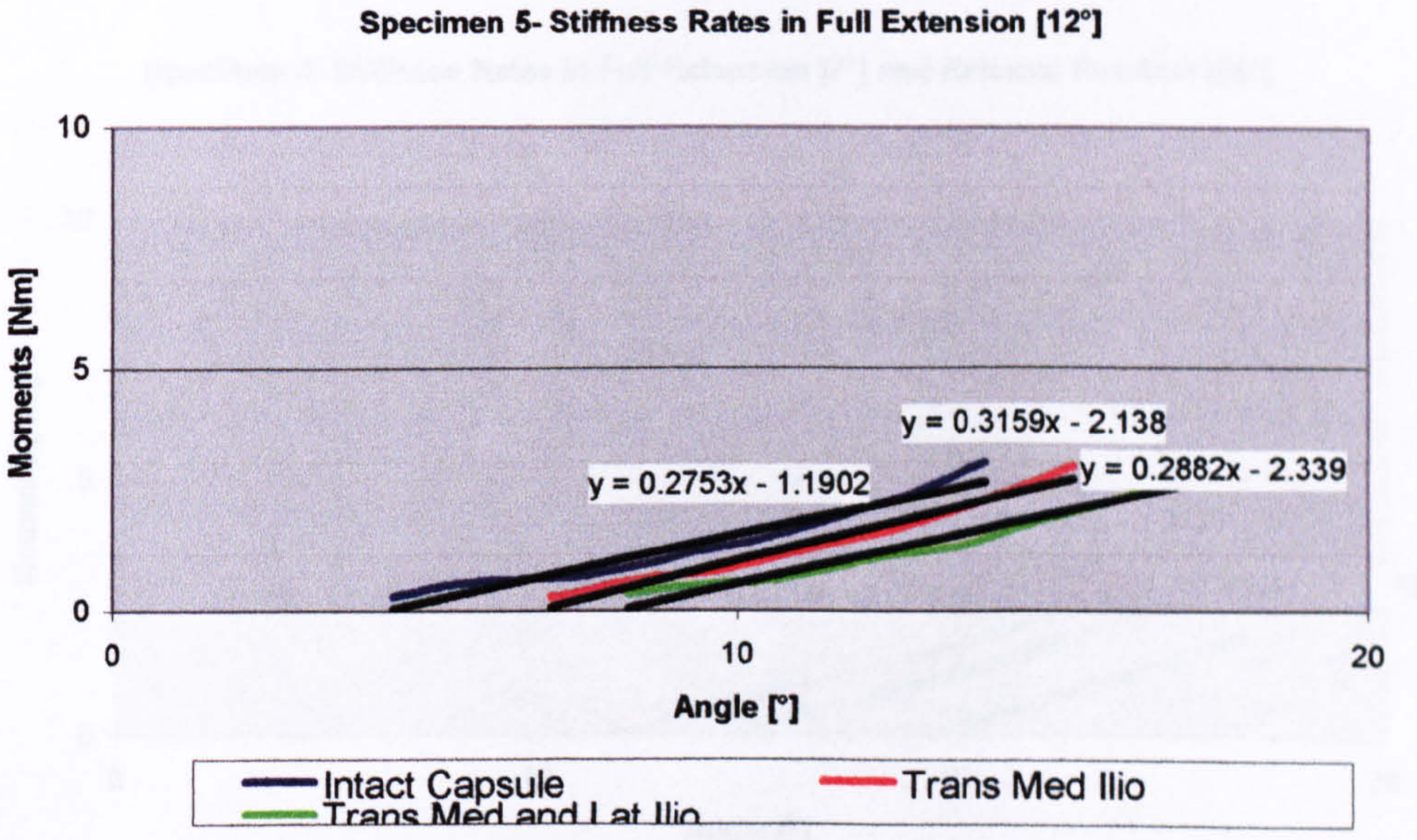

Fig 5.26 Moment curves and their stiffness functions in **adduction** for **specimen 5**.

Full Extension and External Rotation

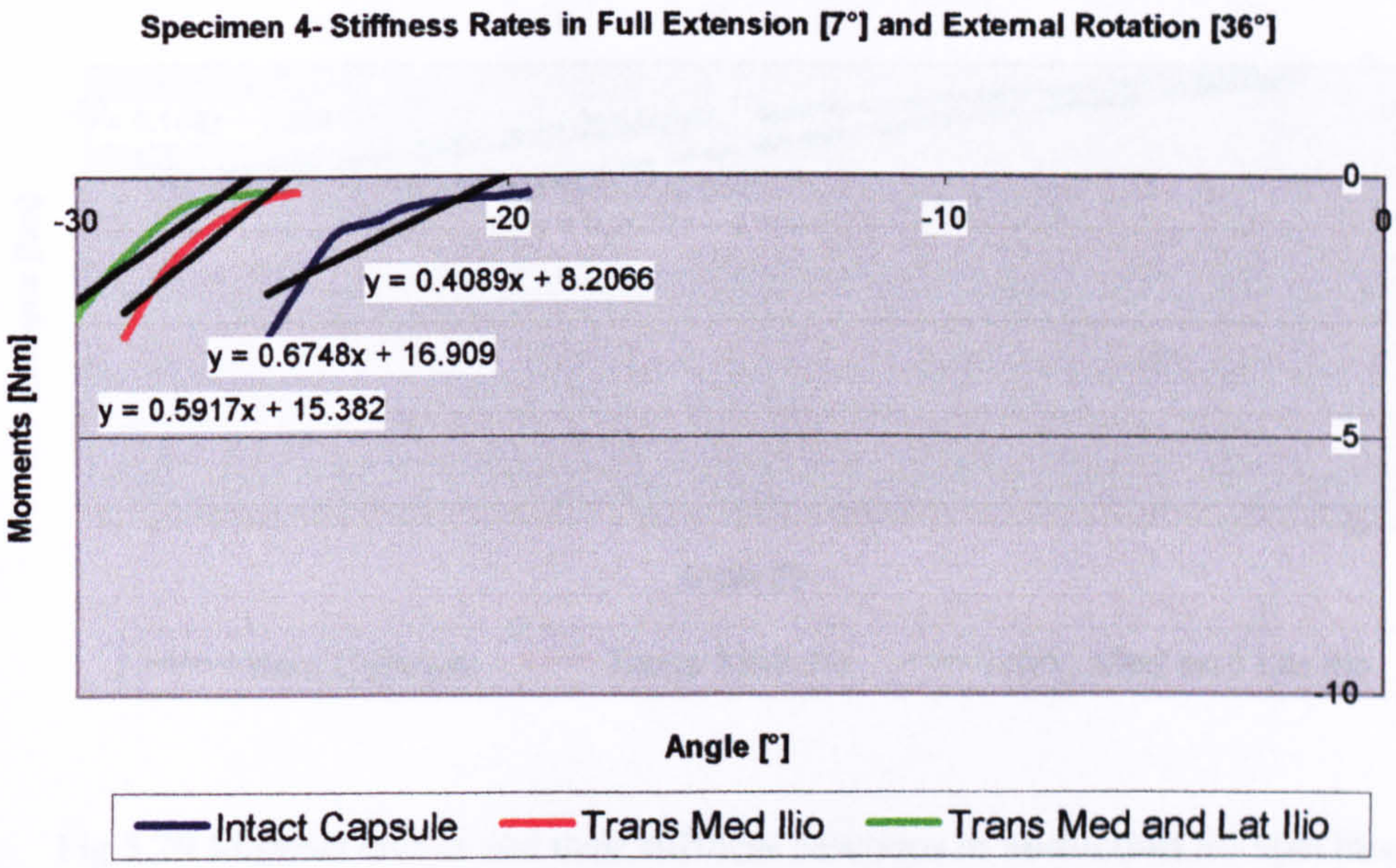

Fig 5.27 Moment curves and their stiffness functions in **abduction** for **specimen 4**.

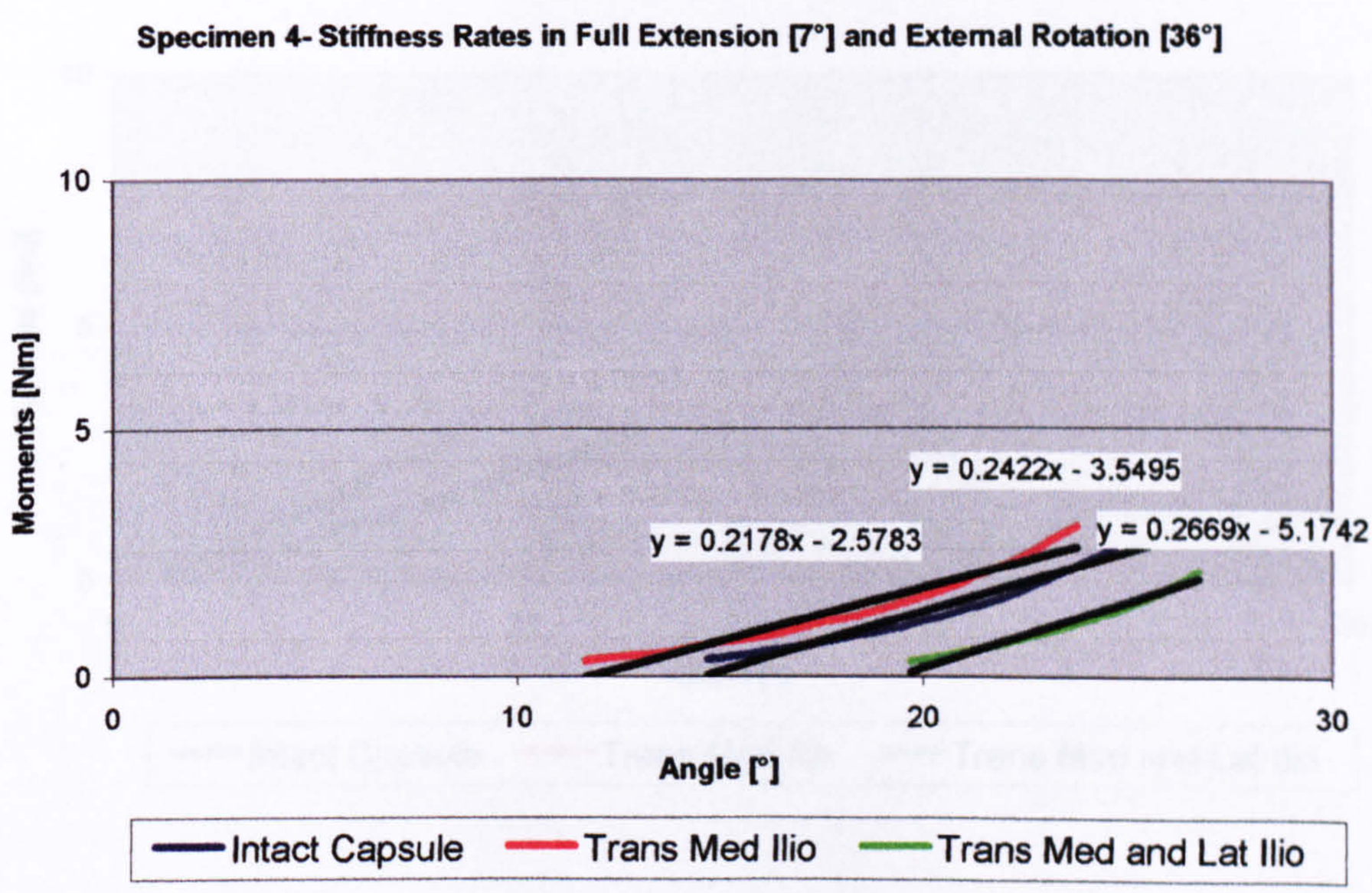

Fig 5.28 Moment curves and their stiffness functions in **adduction** for **specimen 4**.

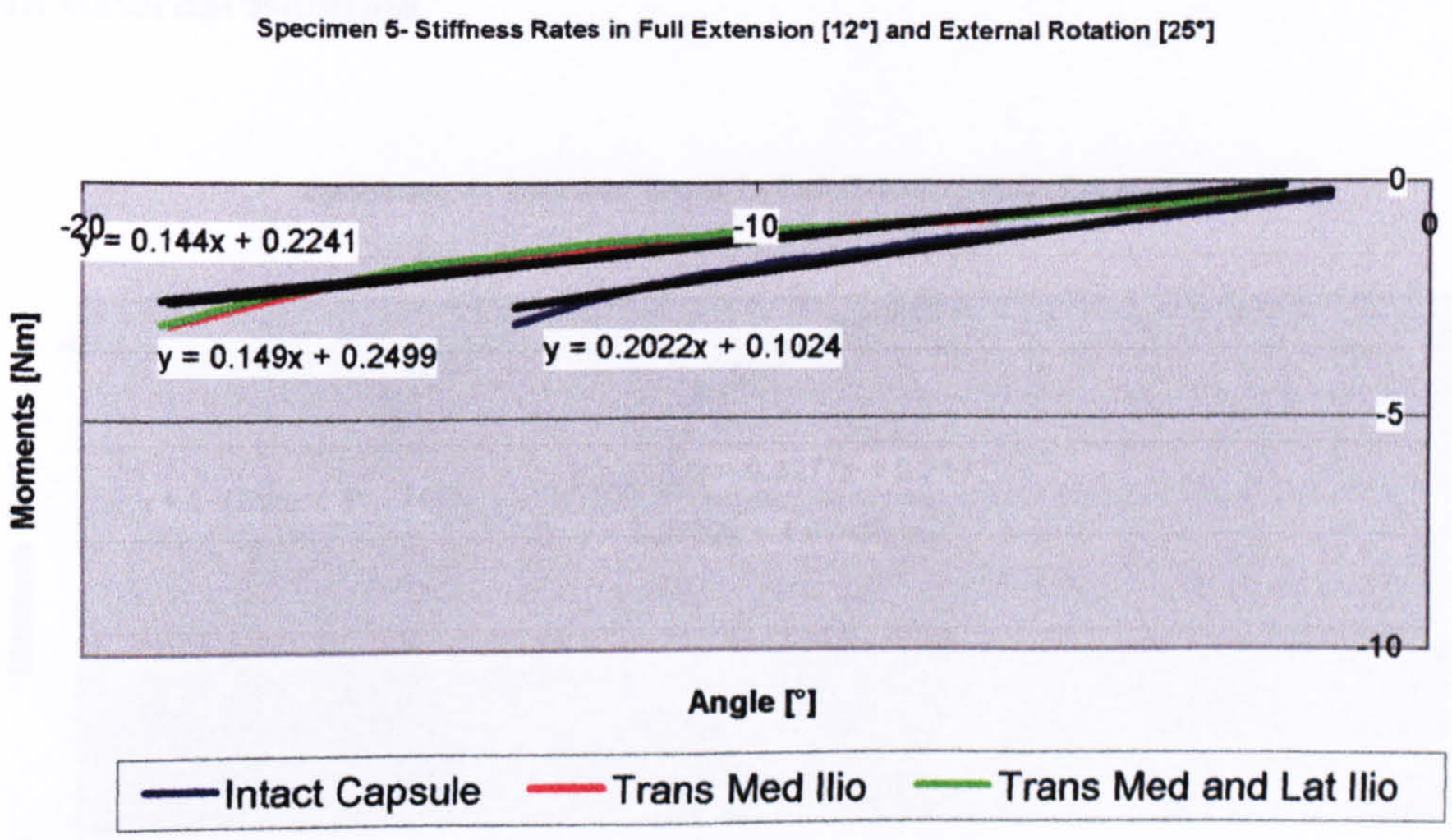

Fig 5.29 Moment curves and their stiffness functions in **abduction** for **specimen 5**.

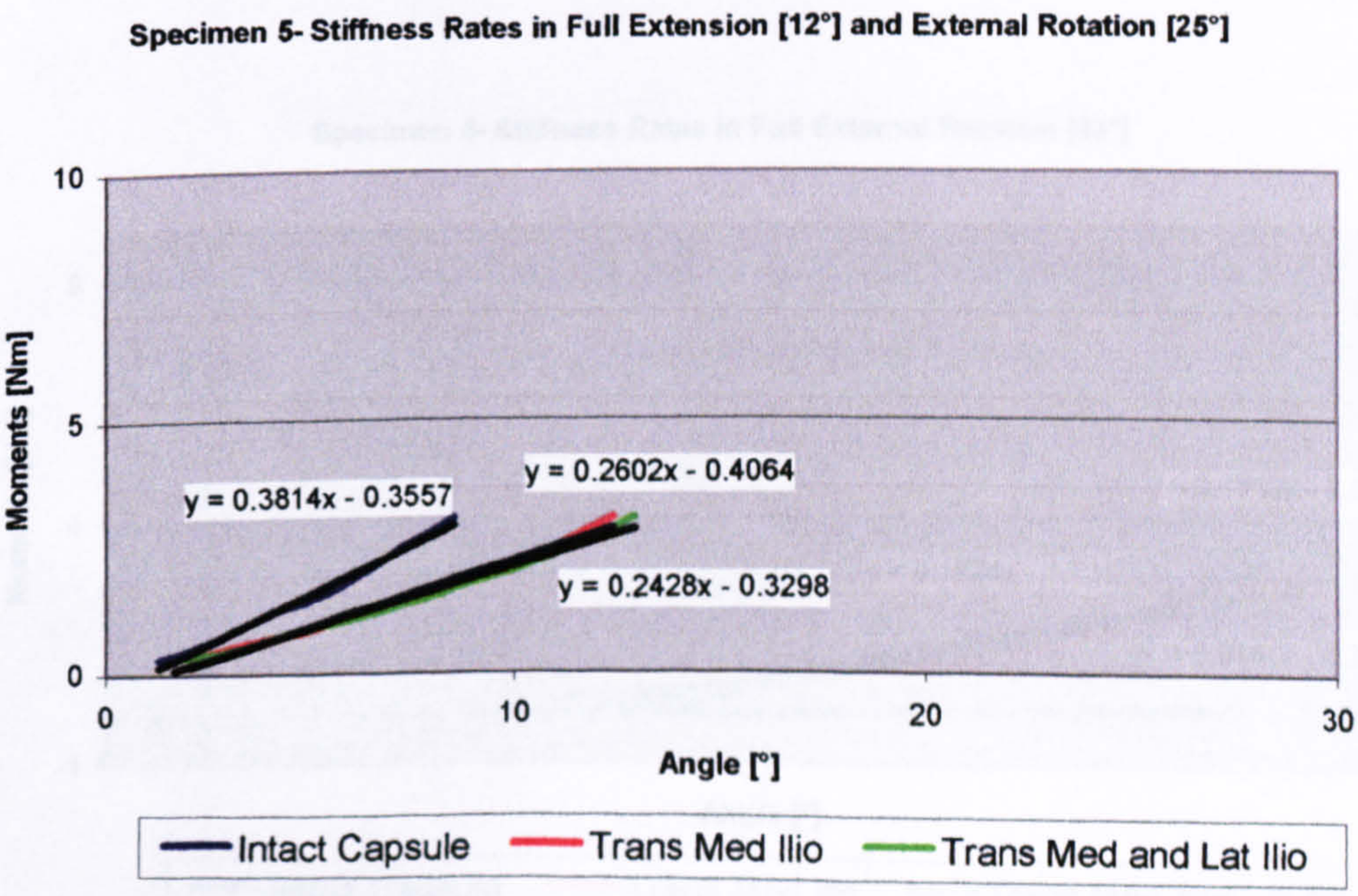

Fig 5.30 Moment curves and their stiffness functions in **adduction** for **specimen 5**.

Full External Rotation

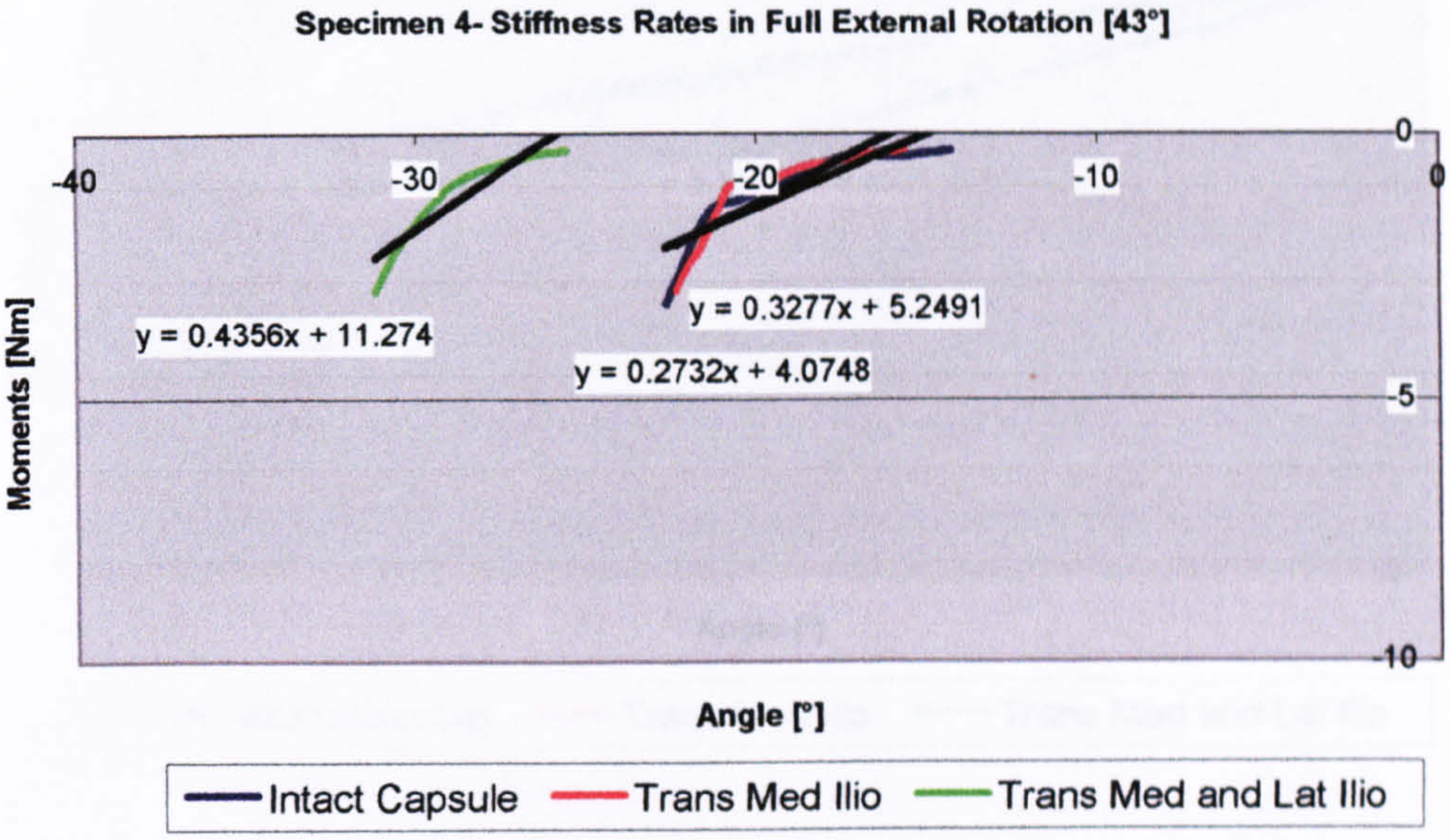

Fig 5.31Moment curves and their stiffness functions in **abduction** for **specimen 4**.

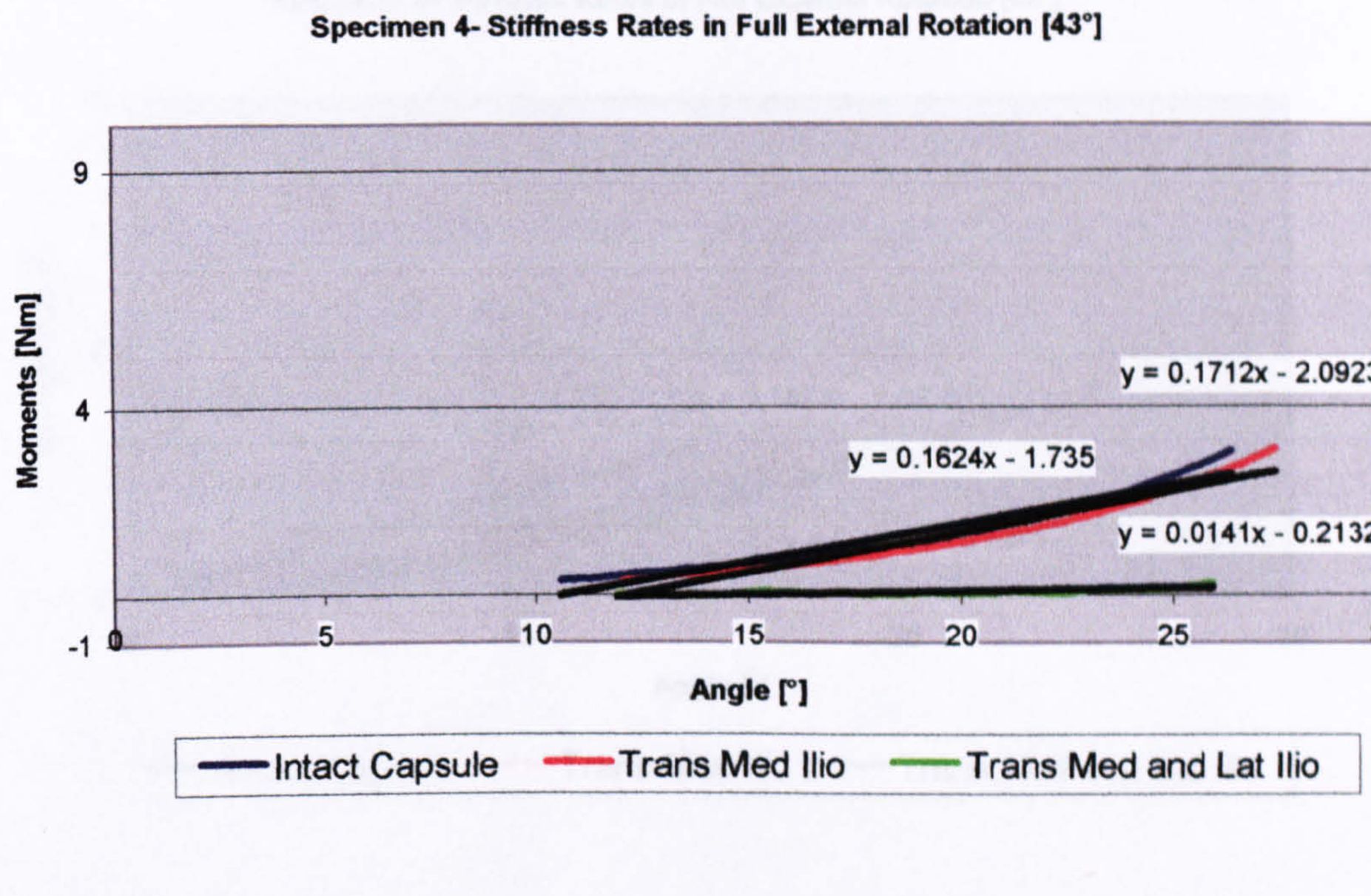

Fig 5.32 Moment curves and their stiffness functions in **adduction** for **specimen 4**.

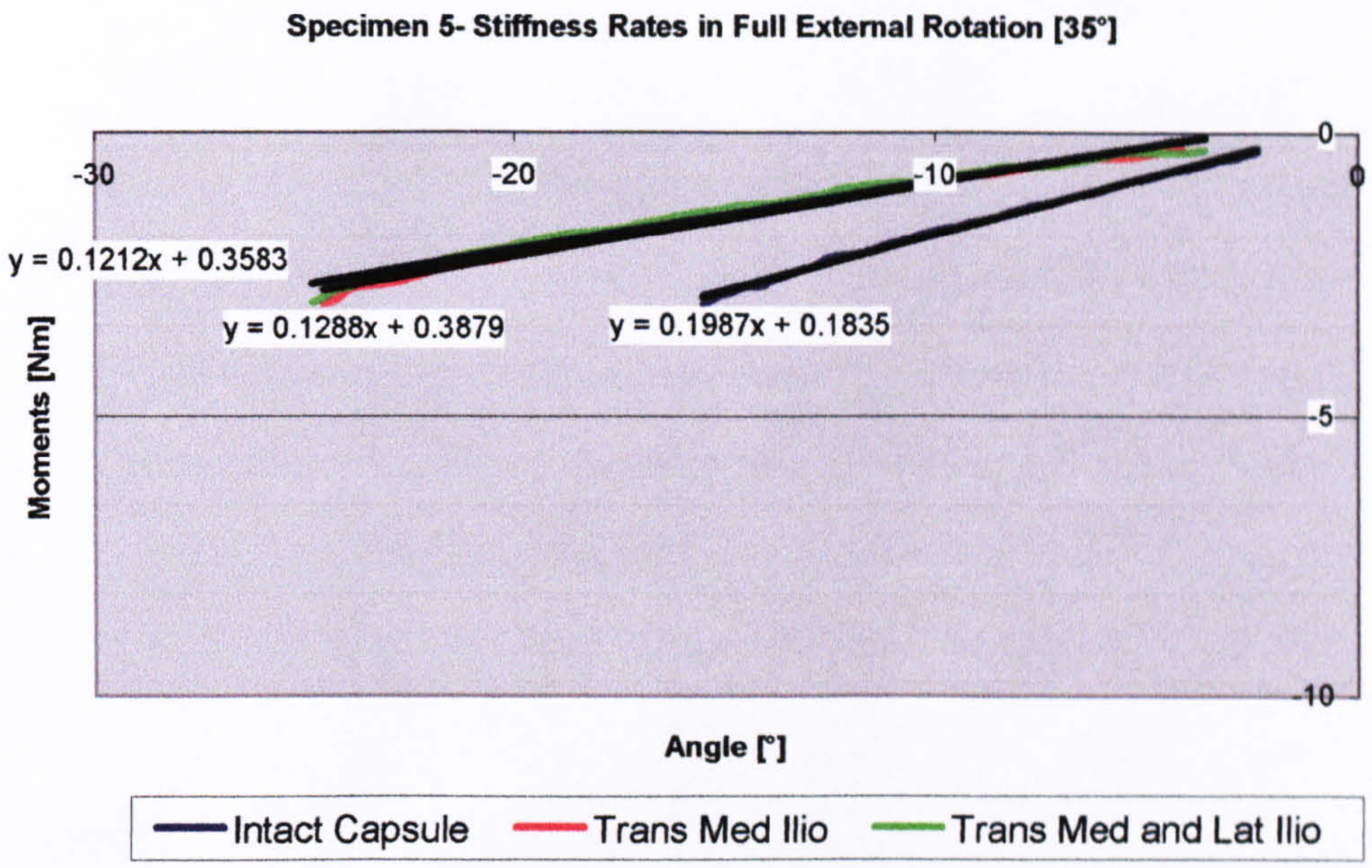

Fig 5.33 Moment curves and their stiffness functions in **abduction** for **specimen 5**.

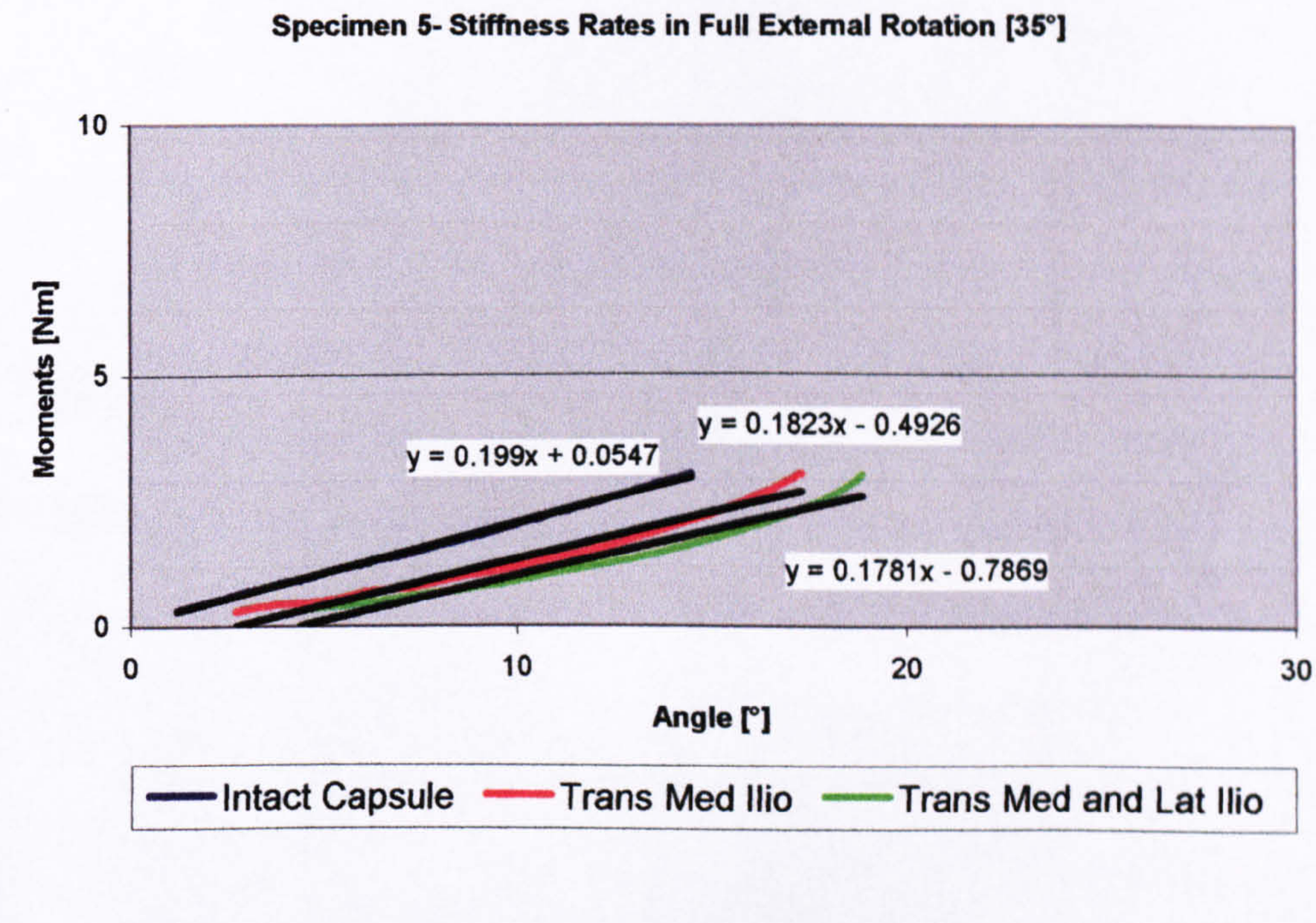

Fig 5.34 Moment curves and their stiffness functions in **adduction** for **specimen 5**.